

£1.50 net  
IN UK ONLY

# ELECTRONIC TIME MEASUREMENTS

EDITED BY BRITTON CHANCE  
ROBERT I. HULSIZER  
EDWARD F. MAC NICHOL, JR.  
FREDERICK C. WILLIAMS



CHANCE  
HULSIZER  
MAC NICHOL  
WILLIAMS

ELECTRONIC TIME  
MEASUREMENTS

DOVER

S1560

# DOVER BOOKS ON ENGINEERING AND ENGINEERING PHYSICS

- Supersonic Aerodynamics, E. R. C. Miles. \$1.45
- Fares Please! A Popular History of Trolleys, Horse-cars, Street-Cars, Buses, Elevators and Subways, John A. Miller, \$1.50
- Engineering Mathematics, Kenneth S. Miller. \$2.00
- Theory of Flight, Richard von Mises. \$2.95
- The Scientific Basis of Illuminating Engineering, Parry H. Moon. \$3.25
- Microwave Transmission Design Data, Theodore Moreno. \$1.65
- Principles of Mechanics Simply Explained, Morton Mott-Smith. \$1.00
- Heat and Its Workings, Morton Mott-Smith. \$1.00
- Concepts of Energy Simply Explained, Morton Mott-Smith. \$1.25
- Methods in Exterior Ballistics, Forest R. Moulton. \$1.75
- Introduction to Applied Mathematics, Francis D. Murnaghan. \$2.00
- Mathematical Engineering Analysis, Rufus Oldenburger. \$2.00
- Waterhammer Analysis, John Parmakian. \$1.65
- Spinning Tops and Gyroscopic Motion, John Perry. \$1.00
- Fundamentals of Hydro- and Aerodynamics, Ludwig Prandtl and O. G. Tietjens. \$1.85
- Applied Hydro- and Aerodynamics, Ludwig Prandtl and O. G. Tietjens. \$2.00
- Applied Elasticity, John Prescott. \$3.25
- The Theory of Sound, Lord Rayleigh. Two volume set \$4.70
- The Kinematics of Machinery, Franz Reuleaux. \$3.00
- Hydraulic Transients, George R. Rich. \$2.50
- Theory of Functions as Applied to Engineering Problems, R. Rothe, F. Ollendorff, and K. Pohlhausen. \$1.35
- Fluid Mechanics for Hydraulic Engineers, Hunter Rouse. \$2.25
- The History of Hydraulics, Hunter Rouse and Simon Ince. \$2.00
- Theory of Machines Through Worked Examples, G. H. Ryder. Cloth-bound \$5.00
- Structural Airplane Analysis and Design, Ernest E. Sechler and Lewis G. Dunn. \$2.25
- Weight-Strength Analysis of Aircraft Structures, F. R. Shanley. \$2.50
- Introduction to Relaxation Methods, Frederick S. Shaw. \$2.45
- Problems and Worked Solutions in Vector Analysis, L. R. Shorter. \$2.00
- Elementary Metallurgy and Metallography, Arthur M. Shrager. \$2.25
- Selected Papers on Human Factors in the Design and Use of Control Systems, edited by H. Wallace Sinaiko. \$2.75
- Microwave Transmission, John C. Slater. \$1.50

(continued on back flap)



# **ELECTRONIC TIME MEASUREMENTS**



# **ELECTRONIC TIME MEASUREMENTS**

*Edited by*

**BRITTON CHANCE**

**ASSISTANT PROFESSOR OF BIOPHYSICS, UNIVERSITY OF PENNSYLVANIA**

**ROBERT I. HULSIZER**

**DEPARTMENT OF PHYSICS, MASSACHUSETTS INSTITUTE OF TECHNOLOGY**

**EDWARD F. MacNICHOL, JR.**

**DEPARTMENT OF BIOPHYSICS, UNIVERSITY OF PENNSYLVANIA**

**FREDERICK C. WILLIAMS**

**PROFESSOR OF ELECTRO-TECHNICS, MANCHESTER UNIVERSITY**

**OFFICE OF SCIENTIFIC RESEARCH AND DEVELOPMENT  
NATIONAL DEFENSE RESEARCH COMMITTEE**

**NEW YORK**

**DOVER PUBLICATIONS, INC.**

Published in Canada by General Publishing Company, Ltd., 30 Lesmill Road, Don Mills, Toronto, Ontario.

Published in the United Kingdom by Constable and Company, Ltd., 10 Orange Street, London W. C. 2.

This Dover edition, first published in 1966, is an unabridged and unaltered republication of the work first published by McGraw-Hill Book Company, Inc., in 1949. It is made available through the kind cooperation of McGraw-Hill Book Company, Inc.

This book was originally published as volume 20 in the Massachusetts Institute of Technology Radiation Laboratory Series.

*Library of Congress Catalog Card Number 66-17129*

Manufactured in the United States of America

Dover Publications Inc.  
180 Varick Street  
New York, N. Y. 10014

# ***ELECTRONIC TIME MEASUREMENTS***

## ***EDITORIAL STAFF***

<b>BRITTON CHANCE</b>	<b>EDITOR</b>
<b>ROBERT I. HULSIZER</b>	<b>VOLUME EDITOR</b>
<b>E. F. MACNICHOL, JR.</b>	<b>VOLUME EDITOR</b>
<b>F. C. WILLIAMS</b>	<b>VOLUME EDITOR</b>

## ***CONTRIBUTING AUTHORS***

**BRITTON CHANCE**  
**RICHARD N. CLOSE**  
**DAVID GALE**  
**J. V. HOLDAM**  
**ROBERT I. HULSIZER**  
**HILLARD B. HUNTINGTON**  
**WILLIAM J. JACOBI**  
**WILLIAM B. JONES**  
**ROBERT C. KELNER**  
**ROBERT B. LEACHMAN**  
**E. F. MACNICHOL, JR.**  
**J. ROBERT ROGERS**  
**DAVID SAYRE**  
**WALTER SELOVE**

## *Foreword*

---

THE tremendous research and development effort that went into the development of radar and related techniques during World War II resulted not only in hundreds of radar sets for military (and some for possible peacetime) use but also in a great body of information and new techniques in the electronics and high-frequency fields. Because this basic material may be of great value to science and engineering, it seemed most important to publish it as soon as security permitted.

The Radiation Laboratory of MIT, which operated under the supervision of the National Defense Research Committee, undertook the great task of preparing these volumes. The work described herein, however, is the collective result of work done at many laboratories, Army, Navy, university, and industrial, both in this country and in England, Canada, and other Dominions.

The Radiation Laboratory, once its proposals were approved and finances provided by the Office of Scientific Research and Development, chose Louis N. Ridenour as Editor-in-Chief to lead and direct the entire project. An editorial staff was then selected of those best qualified for this type of task. Finally the authors for the various volumes or chapters or sections were chosen from among those experts who were intimately familiar with the various fields, and who were able and willing to write the summaries of them. This entire staff agreed to remain at work at MIT for six months or more after the work of the Radiation Laboratory was complete. These volumes stand as a monument to this group.

These volumes serve as a memorial to the unnamed hundreds and thousands of other scientists, engineers, and others who actually carried on the research, development, and engineering work the results of which are herein described. There were so many involved in this work and they worked so closely together even though often in widely separated laboratories that it is impossible to name or even to know those who contributed to a particular idea or development. Only certain ones who wrote reports or articles have even been mentioned. But to all those who contributed in any way to this great cooperative development enterprise, both in this country and in England, these volumes are dedicated.

L. A. DuBRIDGE



## *Preface*

---

THE preservation of the technical advancements represented by the precision circuits of the Radiation Laboratory was made possible through the foresight of Drs. Rabi and DuBridge. They appointed a committee consisting of Drs. L. J. Haworth, G. E. Valley, and the editor to consider the scope and content of a series of books on circuits, which resulted in Vols. 17-22 of the Series. At the termination of hostilities an intensive writing program was put into operation under the able leadership of Dr. L. N. Ridenour and resulted in the completion of the Series on an accelerated schedule. This schedule required the use of as many authors as possible and has inevitably resulted in discontinuities in the method of treatment and scope of material.

The object of this book is to present the method of approach to the problems of time and distance measurement by manual and automatic means, and the practical circuits employed for these purposes. In addition, important techniques of pulse data transmission and pulse-amplitude cancellation methods are included. The accurate measurement of short time intervals is not a new subject since many experiments have been devoted to the accurate determination of the velocity of light. The simplification and increased precision possible through the use of circuit techniques of Vol. 19 of the Series have led to time-measurement techniques that have resulted in practical and accurate radar distance-finding and data-transmitting systems. Since the characteristics of these circuits depend upon those of the radar system, the book is introduced by a survey of techniques for radio distance and speed measurement. The material then continues with a survey of basic techniques and methods in pulse time measurement, including the generation of fixed and movable timing markers and their applications to manual and automatic time measurements. The use of these techniques for precision data transmission and for the relaying of the radar PPI to remote points is next presented, and the book concludes with a discussion of the use of supersonic delay devices for the cancellation of recurrent waveforms.

Many of the developments described in this volume are contributions from other laboratories in this country or in the United Kingdom. It is a pleasure to acknowledge the excellent support to this project by the British Laboratories, and especially Telecommunications Research

Establishment. Through their generosity several experts have visited this laboratory and have contributed much useful information, and, in fact, this book has drawn heavily upon TRE reports. Our gratitude is due Sir Robert Watson Watt, Drs. W. B. Lewis and B. V. Bowden, and F. S. Barton for stimulating and authorizing this excellent exchange of information, which required several visits of Dr. F. C. Williams and others.

The foreword has indicated the difficulty of giving proper credit to all those who contributed to the writing or to the experimental developments that have made this work possible. However, references in the text have been made to journal papers on radar and associated subjects and declassified reports on radar.

Many of the contributors to this volume gave up industrial positions or academic fellowships in order to complete their contributions and much credit is due them for this sacrifice. The authors also wish to express their gratitude to those who contributed important background material from which the final manuscript was written, E. B. Hales, C. L. Longmire, F. Coffin, L. Bess, R. N. Close, I. Sudman, and J. R. Rogers. The speed of this program would have been impossible without the expert assistance of the production department under C. Newton. The efficiency of the typing pool under M. Dolbeare and P. Phillips and the drafting room under Dr. V. Josephson has been of great assistance. In addition, the Technical Coordination Group under Dr. Leon Linford has done much to ensure a coordination of style and a maintenance of standard. The authors wish to name specifically the following editorial assistants, production assistants, and secretaries whose aid has been invaluable in the preparation of this book: Nora Van der Groen, Joan Brown, Joan Leamy, Helene Benvie, Teresa Sheehan, Barbara Davidson, Helen Siderwicz, and Louise Rosser.

A few waveform photographs have been used to illustrate this volume. Nearly all these were taken by C. M. Connelly and the associated photographic work was carried out by P. D. Bales and credit to their work is gratefully acknowledged.

THE AUTHORS.

CAMBRIDGE, MASS.,  
May, 1946.

# Contents

---

FOREWORD . . . . .	vii
PREFACE. . . . .	xi
CHAP. 1. INTRODUCTION . . . . .	1
CHAP. 2. RADIO DISTANCE AND SPEED MEASUREMENTS . . . . .	4
DISTANCE MEASUREMENTS. . . . .	4
2-1. Introduction. . . . .	4
2-2. Definitions of Methods of Distance Measurement . . . . .	4
2-3. Time Modulation and Demodulation. . . . .	5
2-4. Phase Modulation and Demodulation. . . . .	7
2-5. Frequency Modulation and Demodulation. . . . .	13
2-6. Summary. . . . .	15
SPEED MEASUREMENTS. . . . .	16
2-7. Continuous-wave Systems. . . . .	16
2-8. Pulse Systems—Internally Coherent . . . . .	18
2-9. Pulse Systems—Externally Coherent. . . . .	20
SPEED AND DISTANCE MEASUREMENTS. . . . .	24
2-10. Phase and Rate of Change of Phase . . . . .	25
2-11. Time Demodulation and Differentiation. . . . .	26
2-12. Phase and Frequency Demodulation . . . . .	26
2-13. Time, Phase, and Frequency Demodulation. . . . .	28
2-14. Considerations Applying to Intermittent Data. . . . .	28
POSITION-FINDING. . . . .	29
2-15. Introduction. . . . .	29
2-16. Pulse-echo Systems. . . . .	31
2-17. Radar Beacons . . . . .	33
2-18. Hyperbolic Systems . . . . .	34
2-19. An Omnidirectional Beacon Using Time Modulation . . . . .	36
CHAP. 3. TECHNIQUES OF PULSE TIME MEASUREMENTS. . . . .	37
TRANSMISSION AND RECEPTION . . . . .	37
3-1. Transmission of Pulses . . . . .	37
3-2. The Reception of Pulses . . . . .	39

SYNCHRONIZATION . . . . .	42
3-3. Synchronization of the R-f Pulse Generator . . . . .	43
3-4. Control of the PRF by the Timing Waveform . . . . .	44
3-5. Synchronization by a PRF Generator . . . . .	45
3-6. Zero Calibration . . . . .	45
3-7. Remote Control of Synchronization . . . . .	46
TIME MODULATION . . . . .	47
3-8. Single-scale Time Modulation . . . . .	47
3-9. Multiple-scale Time Modulation . . . . .	48
<i>The Characteristics of Components</i> . . . . .	50
3-10. Timing Standards . . . . .	50
3-11. Vacuum Tubes . . . . .	51
3-12. Calibrated Subassemblies . . . . .	52
<i>Fixed and Modulated Timing Pulses</i> . . . . .	53
3-13. Fixed Pulses . . . . .	54
3-14. Single-scale Time-modulation Circuits . . . . .	55
3-15. Double-scale Time-modulation Circuits . . . . .	58
3-16. Multiple-scale Systems . . . . .	61
TIME DEMODULATION . . . . .	62
3-17. Time Selection and Discrimination . . . . .	62
SOME PROPERTIES OF CATHODE-RAY-TUBE DISPLAYS . . . . .	64
3-18. Time Selection and Discrimination . . . . .	64
3-19. Time Demodulation . . . . .	64
3-20. Time Modulation . . . . .	65
CHAP. 4. GENERATION OF FIXED INDICES . . . . .	69
SINGLE-FREQUENCY MARKER GENERATORS . . . . .	69
4-1. Sinusoidal Oscillators and Amplitude Comparators . . . . .	69
4-2. Regenerative Amplitude-comparison Circuits . . . . .	73
4-3. Class C Crystal Oscillator and Blocking Oscillator . . . . .	75
4-4. Gas-tetrode 300-cps Relaxation Oscillator . . . . .	76
4-5. Blocking Oscillators . . . . .	78
4-6. Multivibrators . . . . .	80
MULTIPLE-FREQUENCY MARKER AND TRIGGER GENERATORS . . . . .	81
4-7. Frequency Division . . . . .	81
4-8. Frequency Division and Pulse Selection . . . . .	87
4-9. Separate Oscillators and Pulse Selector . . . . .	89
4-10. Synchronization by Automatic Frequency Tracking . . . . .	95
4-11. Lightweight Direct-reading Loran PRF Generator . . . . .	100
4-12. Injection Feedback Divider for Oboe PRF . . . . .	103



GROUPED-MARKER GENERATION. . . . .	106
4-13. Single-frequency Grouped-marker Generators . . . . .	107
4-14. Multiple-frequency Grouped Markers. . . . .	109
CHAP. 5. GENERATION OF MOVABLE INDICES—SINGLE-SCALE CIRCUITS. . . . .	111
INTRODUCTION . . . . .	111
5-1. Applications of Time-modulated Indices . . . . .	111
5-2. System Requirements and Definition of Error. . . . .	112
VOLTAGE SAWTOOTH CIRCUITS . . . . .	114
5-3. A Gated Miller Integrator with a Multiar Comparator . . . . .	114
5-4. A Gated Multistage Miller Integrator with a Cathode-coupled Double-triode Comparator . . . . .	116
5-5. Self-gating Miller Integrator—The Phantastron . . . . .	118
5-6. Self-gating Miller Integrator—The Precision Sanatron . . . . .	124
5-7. Bootstrap Triangle Generator with Diode Comparator . . . . .	125
5-8. The Delay Multivibrator . . . . .	131
<i>Variable Delay Line</i> . . . . .	132
5-9. Supersonic Delay Tank. . . . .	132
SINUSOIDAL OSCILLATOR RANGE CIRCUITS . . . . .	135
5-10. LC-oscillator, Phase Modulator, and Comparator . . . . .	135
5-11. The Variable-frequency Oscillator. . . . .	137
5-12. A Comparison of Some Single-scale Circuits. . . . .	140
CHAP. 6. GENERATION OF MOVABLE INDICES—CIRCUITS. . . . .	142
PHASE MODULATION AND AMPLITUDE COMPARISON. . . . .	142
6-1. Meacham Range Unit . . . . .	142
6-2. Precision Ranging Indicator. . . . .	147
6-3. Scale Coordination by Frequency Division . . . . .	153
6-4. Sine-wave Tracking . . . . .	155
6-5. Three-scale Phase-modulation System . . . . .	157
CIRCULAR-SWEEP DISPLAYS AS A METHOD OF PHASE MODULATION AND AMPLITUDE COMPARISON. . . . .	161
6-6. Circular-sweep Time Modulators, SCR-584 . . . . .	161
STEP-INTERPOLATION TIME MODULATION. . . . .	164
6-7. AN/APS-15 Range Unit . . . . .	164
6-8. Lightweight Direct-reading Loran Indicator. . . . .	169
6-9. Summary. . . . .	174

CHAP. 7. MANUAL MEASUREMENTS. . . . .	176
GENERAL CONSIDERATIONS. . . . .	176
INTRODUCTION . . . . .	176
7-1. Uses . . . . .	177
CHARACTERISTICS OF DISPLAYS AND CURSORS. . . . .	178
7-2. General Considerations. . . . .	178
7-3. Indices. . . . .	180
7-4. Circular Sweeps . . . . .	184
7-5. Linear Sweep and Synchronized Presentation . . . . .	185
ACCURACY CONSIDERATIONS . . . . .	185
7-6. General Considerations. . . . .	186
7-7. Deflection-modulated Display and Deflection-modulated Index . . . . .	187
7-8. Deflection-modulated Signal and Mechanical Index. . . . .	190
7-9. Deflection-modulated Signal and Intensity-modulated Index . . . . .	190
7-10. Juxtaposition of Intensity-modulated Signal and Index . . . . .	190
7-11. Superposition of Signal and Index in Deflection-modulated Displays . . . . .	195
7-12. Reset Error with Intermittent Data and with Two-coordinate Controls . . . . .	198
7-13. Summary and Comparison of Methods . . . . .	199
TRACKING METHODS. . . . .	200
7-14. Continuous Data. . . . .	200
7-15. Intermittent Data . . . . .	206
7-16. Comparison of Methods. . . . .	213
FIXED INDICES FOR MANUAL TIME MEASUREMENT. . . . .	215
7-17. A-scope. . . . .	215
7-18. J-scope. . . . .	216
7-19. Plan-position Indicator with Mechanical Scale. . . . .	219
7-20. Electronic Time Marks. . . . .	219
MOVABLE TRACKING MARKS FOR MANUAL TIME MEASUREMENT. . . . .	220
<i>Direct Tracking.</i> . . . .	220
7-21. Introduction. . . . .	220
7-22. Movable Electronic Marks . . . . .	222
7-23. Detailed Circuit Description of Falcon . . . . .	225
7-24. A/R-scope . . . . .	231
7-25. A-scope Presentation Used in British CMH System . . . . .	238
7-26. Systems Using a J-scope with a PPI or B-scope . . . . .	243
<i>Tracking with Intermittent Data.</i> . . . .	247
7-27. Aided Tracking with Intermittent Data. . . . .	247
7-28. Two-coordinate Tracking. . . . .	251

<i>Especially Accurate Time-measuring Systems</i> . . . . .	261
7-29. Introduction. . . . .	261
7-30. Timing Sequence. . . . .	264
7-31. Circuit Details of Loran Indicator . . . . .	267
CHAP. 8. TECHNIQUES OF AUTOMATIC TIME MEASUREMENT . . . . .	275
INTRODUCTION . . . . .	275
8-1. Automatic vs. Manual Measurements. . . . .	275
8-2. General Technique of Automatic Time Measurement. . . . .	276
8-3. Nature of Data and Its Effect on Performance. . . . .	278
AUTOMATIC TIME MEASUREMENT WITH NORMALLY CONTINUOUS DATA. . . . .	279
<i>Design of Function Unit</i> . . . . .	279
8-4. General Theoretical Statement of the Problem. . . . .	279
8-5. Single-integrator Function Unit . . . . .	280
8-6. Double-integrator System. . . . .	282
8-7. Effect of Additional Smoothing . . . . .	286
8-8. Electrical Integrators. . . . .	291
8-9. Memory and Coast. . . . .	304
8-10. Mechanical Function Units . . . . .	305
<i>Time Discriminators</i> . . . . .	308
8-11. General Considerations. . . . .	308
8-12. Simple Time Discriminators. . . . .	309
8-13. Time Discriminators Consisting of Separate Time Selectors and Detectors. . . . .	314
8-14. Time Discriminators with Time Selectors, Pulse Stretcher, and Narrow-band Pulse Amplification . . . . .	317
8-15. Time Selection. . . . .	321
<i>Target Selection</i> . . . . .	325
8-16. General Considerations. . . . .	325
8-17. Practical Examples of Automatic Target Selection . . . . .	330
<i>Summary</i> . . . . .	337
8-18. System Planning. . . . .	337
CHAP. 9. SYSTEMS FOR AUTOMATIC TIME AND POSITION MEAS- UREMENT . . . . .	341
PRACTICAL SYSTEMS FOR AUTOMATIC TIME MEASUREMENT . . . . .	341
9-1. ARO Electrical System. . . . .	342
9-2. British Oboe Electrical System. . . . .	348
9-3. Electromechanical Systems. . . . .	357
POSITION ERROR DETECTORS AND INDICATORS. . . . .	367
9-4. General Considerations. . . . .	367

9-5. Design Requirements. . . . .	368
9-6. Manual Tracking Systems. . . . .	371
9-7. Automatic Tracking Systems. . . . .	376
TRACKING ON GROUPED OR PERIODICALLY INTERRUPTED DATA. . . . .	378
9-8. Introduction. . . . .	378
9-9. Automatic Time Measurement on Grouped Data. . . . .	380
9-10. Example of Automatic Range Tracking on Grouped Data. . . . .	386
9-11. Automatic Angle-positioning with Grouped Data. . . . .	389
CHAP. 10. SPECIAL DATA-TRANSMISSION SYSTEMS. . . . .	391
INTRODUCTION. . . . .	391
SHORT-DISTANCE WIRE DATA TRANSMISSION. . . . .	391
10-1. Telemetry. . . . .	391
10-2. Transmission of Continuous Rotation. . . . .	393
10-3. Follow-up Systems. . . . .	395
10-4. Characteristics of the Transmission Circuits. . . . .	397
RADIO DATA TRANSMISSION. . . . .	398
10-5. Introduction. . . . .	398
10-6. A Pulse Remote-control System. . . . .	400
10-7. Radiosonde. . . . .	408
10-8. A British Omnidirectional Beacon. . . . .	410
CHAP 11. RELAY RADAR SYSTEMS. . . . .	417
TIME-MODULATED SINE-COSINE SYSTEM. . . . .	417
11-1. Principle of Operation. . . . .	417
11-2. The Synchronizer. . . . .	424
11-3. Receiving Equipment. . . . .	426
11-4. Synchronizing-pulse Decoding Circuits. . . . .	426
11-5. Sequencing Circuits and Linear Delays. . . . .	429
11-6. Step-gate Tracking Circuits. . . . .	433
11-7. Modulators and Bidirectional Switch Detectors. . . . .	435
11-8. Arma Resolver and Servoamplifier. . . . .	438
11-9. Performance. . . . .	439
11-10. Later Developments in Receiving Equipment. . . . .	440
PHASE-MODULATED PULSE SYSTEM. . . . .	442
11-11. Introduction. . . . .	442
11-12. Pulse Representation of Phase-modulated Sinusoids. . . . .	442
11-13. Discussion of Phase-shifter System. . . . .	443
SIMPLIFIED RELAY RADAR SYSTEM FOR CONSTANT-SPEED ROTATION. . . . .	450
11-14. Introduction. . . . .	450
11-15. Details of the System. . . . .	451



C-W RELAY RADAR SYSTEM. . . . .	458
11-16. General Description of Transmitter Functions. . . . .	458
11-17. General Description of Receiving Equipment . . . . .	459
11-18. Details of the System. . . . .	461
11-19. Remarks and Comments on the System. . . . .	470

CHAP. 12. DELAY AND CANCELLATION OF RECURRENT WAVE TRAINS . . . . .	471
--	-----

12-1. Introduction. . . . .	471
-----------------------------	-----

THE DELAY LINE. . . . .	475
-------------------------	-----

<i>Design of Delay Line for Cancellation.</i> . . . .	475
---	-----

12-2. Introduction. . . . .	475
12-3. Echo Elimination . . . . .	476
12-4. Bandpass Shaping . . . . .	479
12-5. Equalization of Delay Time with Repetition Interval. . . . .	480

<i>Examples of Delay Design</i> . . . . .	481
---	-----

12-6. Mercury Lines. . . . .	481
12-7. Water Delay Line in System Use. . . . .	482
12-8. Possibility of Using Delays in Solids . . . . .	484

CIRCUIT CONSIDERATIONS IN DRIVING LINE. . . . .	487
---	-----

12-9. Required Nature of Signal . . . . .	487
12-10. Method of Obtaining Required Type of Signal. . . . .	489

<i>Carrier Generator and Modulator Unit</i> . . . . .	491
---	-----

12-11. Oscillator. . . . .	491
12-12. Modulation. . . . .	491
12-13. Amplification . . . . .	495
12-14. Output Circuit. . . . .	495

<i>Dynamic-range Compression.</i> . . . .	496
---	-----

12-15. Definition and Advantages of Compression . . . . .	496
12-16. Methods . . . . .	497

CANCELLATION AMPLIFIERS. . . . .	498
----------------------------------	-----

12-17. Introduction. . . . .	498
12-18. Cancellation Methods . . . . .	498

<i>Carrier-frequency Channels and Cancellation Circuit</i> . . . . .	499
--	-----

12-19. Pass Band . . . . .	499
12-20. Linearity . . . . .	501
12-21. Gain. . . . .	504

12-22. Detection. . . . .	506
12-23. Cancellation Circuit . . . . .	507
12-24. Coupling to Delay Line. . . . .	507
<i>Video Section.</i> . . . .	508
12-25. Requirements of Video Section. . . . .	508
12-26. Amplifier for Bidirectional Video. . . . .	508
12-27. Video Rectification. . . . .	510
REPETITION-RATE CONTROL. . . . .	511
12-28. Repetition-rate Requirements . . . . .	511
12-29. Manual Control of PRF . . . . .	514
12-30. Line Synchronized Methods. . . . .	515
12-31. Electronic Frequency Tracking . . . . .	522
12-32. Practical Circuit Details. . . . .	523
GLOSSARY . . . . .	527
INDEX. . . . .	529

# **ELECTRONIC TIME MEASUREMENTS**

## CHAPTER 1

### INTRODUCTION

BY BRITTON CHANCE

The resolution and measurement of extremely short time intervals and the precise measurement of much longer intervals are not new techniques; many devices were developed for measuring the extremely short times involved in electrical discharges.<sup>1</sup> These devices include rapidly rotating optical systems recording on photographic film, Kerr-cell devices,<sup>2</sup> and extremely high-speed oscilloscopes,<sup>3</sup> and have a resolution of roughly  $10^{-9}$  sec. On the other hand, methods for the precision measurement of approximately known time intervals have been studied exhaustively for determinations of the velocity of light<sup>4</sup> or radio waves.<sup>5</sup> In most recent and accurate measurements, a precision of approximately 5 parts in 100,000 has been obtained.<sup>6</sup> The problems of measurement of the height of the ionosphere,<sup>7</sup> the distance of a radar reflector, or the velocity of nuclear particles in physical instruments<sup>8</sup> require a technique combining the properties of both methods described above. In radar it is required to measure a variable time interval between  $10^{-6}$  and  $10^{-2}$  sec with a precision ranging from 1 part in 100 to 1 part in 10,000. In contrast with measurement of the velocity of light, the approximate value of the time interval is unknown; for example, the echo may correspond to an aircraft of unknown location. This device must, therefore, give immediate and unambiguous indications over the full scale. This has led to the use of multiple scales, which permit continuous measurements over a wide range of time with extremely high precision.

<sup>1</sup> C. V. Boys, "Progressive Lightning," *Nature*, **118**, 749 (1926).

<sup>2</sup> F. G. Dunnington, "The Electro-optical Shutter—Its Theory and Technique," *Phys. Rev.*, **2-38**, 1506 (1931).

<sup>3</sup> G. M. Lee, "A Three-beam Oscilloscope for Recording at Frequencies up to 10,000 MC," *Proc. I.R.E.*, **34**, 121W (1946).

<sup>4</sup> N. E. Dorsey, "The Velocity of Light," *Trans. Am. Phil. Soc.*, **34**, Part 1, (1944).

<sup>5</sup> F. T. Farmer and H. B. Mohanty, "The Velocity of Propagation of Wireless Waves over the Ground," *Proc. Phys. Soc.*, **52**, 456, (1940).

<sup>6</sup> N. E. Dorsey, *loc. cit.*

<sup>7</sup> G. Breit and M. A. Tuve, *Phys. Rev.*, **28**, 554 (1926).

<sup>8</sup> C. P. Baker and R. F. Bacher, "Experiments with Slow Neutron Velocity Spectrometer," *Phys. Rev.*, **2-59**, 332 (1941).



Another important requirement of time measurement in radar or nuclear physics is that of time selectivity. In radar a particular target must be selected to the exclusion of interfering echoes and in nuclear physics only those particles having a time of arrival corresponding to a particular velocity are to be counted. These problems have led to the development of cathode-ray-tube displays or electronic devices having appropriate time selectivity.

Another important requirement of radar is continuous measurement of variable time intervals by manual or automatic means. The characteristics of cathode-ray-tube displays and mechanical tracking aids for manual operation have been extensively studied and in addition a number of extremely important automatic devices have been developed to accomplish the same function with an equal precision. Both manual and automatic devices combine a high accuracy with a high degree of time selectivity. These devices rely upon a repetition of the phenomenon, and have not been tested for the measurement of a single transient event.

Although radar could take over the basic elements of the physicists' methods, an extremely large amount of circuit and component development was required before techniques capable of measuring 2 or 3 ft in 60,000 ft were reliable under military conditions.

Improvements in frequency dividers, rectangular pulse generators, and sawtooth generators were of tremendous importance in securing rapidly rising and yet stable timing waveforms. The development of improved phase-shifting condensers and precision linear potentiometers and the use of center-electrode cathode-ray tubes did much to permit the building of simple yet accurate ranging systems. An understanding of the minimum requirements for a satisfactory solution of the synchronization problem in radar systems led to a great increase in the economy of circuit planning and execution. In the later phases of the war, the development of small efficient pulse transformers and improved circuit designs, particularly in blocking oscillators, contributed much to the efficiency and compactness of radar timing equipment. Great progress was made in the standardization of the characteristics of vacuum tubes, resistors, and condensers through the introduction of the JAN specifications.

Highly precise timing techniques are an essential part of most radars. A number of systems for precision navigation embody no other function than time measurement: the American Micro-H, Shoran, and Loran systems, and the British Oboe, Gee, and Gee-H systems are examples. Precision timing methods, however, are useful for several other important functions. Transmission of intelligence by pulse time modulation and demodulation has already been used for identification, communication, and the transmission of linear and rotary motion. High fidelity and accuracy can be obtained by means of the linear modulation and demodu-

lation characteristics of timing circuits. The precision and rapidity of pulse methods have led to the use of these methods in computation, and all indications are that this use will greatly increase. The radar techniques of synchronization and display serve admirably for graphical indication and recording of the operation of complex electrical and mechanical devices and, in fact, have already been much used for the observation of bio-electric potentials.

The possibilities for the future development of timing methods of higher resolution and precision are excellent. The improvement of cathodes, permitting larger peak currents, is of fundamental importance to the whole field of pulse systems. At present, peak currents in excess of one ampere are obtainable in receiver-type tubes and it is likely that this can be improved by special designs. Such large peak currents are of importance in the generation of shorter pulses from blocking oscillators. For extremely short pulses short lengths of coaxial cable become much more practical for timing elements and their use should greatly facilitate circuit design and construction.

A significant reduction in circuit capacitance is obtained by utilizing baseless subminiature vacuum tubes. Furthermore the "solder-in" characteristic of these tubes encourages a new approach to the problem of component variation by the use of functional subassemblies that may be precalibrated to equal standards of performance during the manufacturing process. Thus subassemblies of precision circuits may be replaced without the need for recalibration. In this way a number of otherwise impractical circuit designs, previously limited to laboratory construction methods, may become a commercial reality.

## CHAPTER 2

### RADIO DISTANCE AND SPEED MEASUREMENTS

By BRITTON CHANCE

#### DISTANCE MEASUREMENTS

**2.1. Introduction.**—This chapter briefly presents characteristics of some systems for distance and speed measurements by continuous-wave (c-w) and pulse transmission from the standpoint of accuracy and not from the standpoint of economy or efficiency of r-f transmission and reception. For a full discussion of the general characteristics of these systems see Vol. 1.<sup>1</sup>

Experimental tests and quantitative results that are available are summarized. The discussion of untried methods is, of course, speculative.

**2.2. Definitions of Methods of Distance Measurement.**—The distance to any distinguishable object is measurable in terms of the time interval  $\Delta t$  required for a radio wave to travel from a transmitter to a reflector and back to a receiver. The velocity of propagation of radio waves is, as far as can be determined, equal to that of light. The distance is obtained from the product  $\Delta t \cdot c$ . Radar systems have been used to measure precisely distances from 50 ft to 1500 miles corresponding to a range of  $\Delta t$  from 0.1 to 15,000  $\mu\text{sec}$ . But the quantity  $\Delta t$  may be represented in a number of forms and may be measured by several methods:

1. Method (1) utilizes the fact that the time delay between a pair of radio-frequency pulses, one corresponding to the transmitted pulse and the other corresponding to the received echo, directly represents the interval  $\Delta t$  as  $\Delta t = 2d/c$ , where  $d$  = distance and  $c$  = velocity of light. This method is termed "time modulation" (Vol. 19, Chap. 13) because the time delay modulates the interval between the two pulses. The measurement is termed "time demodulation," (see Vol. 19, Chap. 14) and can be accomplished by the comparison of the interval between these two pulses with triangular or sinusoidal timing waveforms, or with the delay of a supersonic tank, or an electrical delay network. For a triangular waveform  $V = kt$ . The increment of voltage, corresponding to the interval  $\Delta t$ , is  $\Delta V = k\Delta t$  and  $\Delta V$  is a measure of distance.

<sup>1</sup> The references to other volumes of the Radiation Laboratory Series will appear in this form.

2. The second method utilizes the fact that the delay time corresponds to the phase shift by a number of oscillations  $n$  of the transmitted or modulating frequency;  $n = f\Delta t$ , where  $f$  is the transmitted frequency in megacycles per second and  $\Delta t$  is the time delay in microseconds. This method is termed "phase modulation" and occurs in pulse or continuous-wave systems. The measurement of the extent of this phase shift is termed "phase demodulation" and depends upon a comparison of the phase shift with that obtained from inductance or capacitance phase shifters. An important characteristic of phase modulation is that the rate of change of phase shift  $dn/dt$  indicates directly the radial velocity of the reflector with respect to the transmitter-receiver as a beat (or doppler) frequency.
3. The third method is a two-scale method that is a combination of Methods 1 and 2, where pulses are transmitted and distance is measured by phase and time demodulation. In pulse systems, phase demodulation requires the maintenance of r-f oscillations of the transmitted phase for the interval  $\Delta t$  and gives a precise but ambiguous value of the distance. Time demodulation gives an approximate value of the distance. Pulse transmission is often used to obtain target discrimination, and the doppler frequency obtained from phase demodulation may be employed to indicate target speed.
4. A fourth method utilizes the fact that the time delay  $\Delta t$  may be measured in terms of the amount of frequency modulation  $\Delta f$  of the transmitter occurring in this interval. If frequency modulation is linear with time, the frequency shift  $\Delta f$  occurring in the interval  $\Delta t$  is

$$\Delta f = \frac{df}{dt} \cdot \Delta t,$$

where  $df/dt$  is the rate of change of frequency. The measurement of  $\Delta f$  may be termed "frequency demodulation," and is carried out by frequency selection or metering.

The general characteristics of these four methods are discussed in the next sections from the standpoint of distance measurement and/or speed measurement.

**2-3. Time Modulation and Demodulation.**—In a pulse distance finder the measurement of distance involves the measurement of the time delay  $\Delta t$  between the transmission and reception of a radio-frequency pulse as indicated in the waveform diagram of Fig. 2-1. The principal requirements of this system are that the rise time of the transmitted and received pulses be no greater than 10 or 20 times the desired accuracy, and that the properties of the transmitting and receiving system have adequate

angular and time resolution to permit discrimination of the desired reflector. Some examples of radar systems are given in Secs. 2-15 to 2-19.

The block diagram of Fig. 2-1 shows a typical pulse radar system described in terms of the basic processes of Chap. 3 of this volume and of Chaps. 13 and 14 of Vol. 19. It is to be noted that the operation of distance measurement depends upon time modulation and demodulation. Modulation is accomplished by transmitting a radio-frequency pulse over the path from transmitter to reflector and back to receiver. The time delay of this pulse is given by  $2d/c$ , and the velocity of propaga-

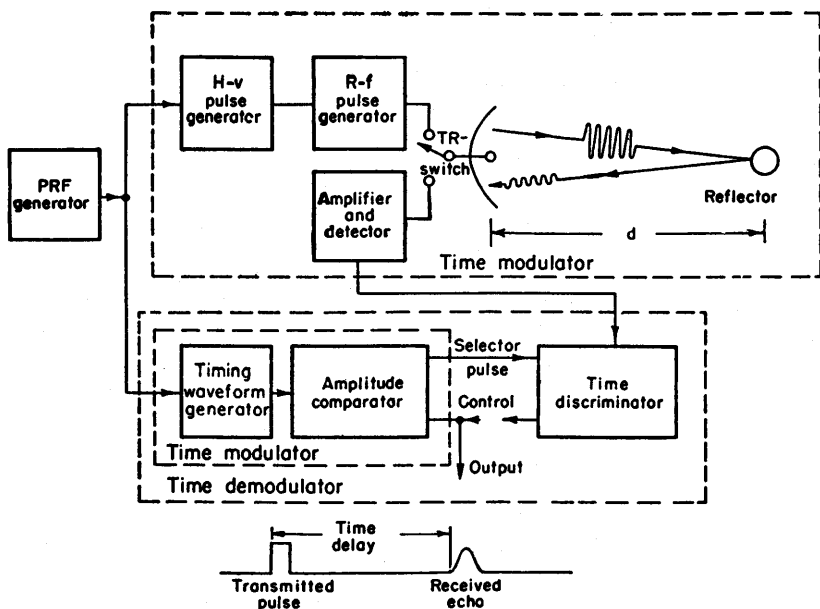


FIG. 2-1.—Pulse distance finder employing time modulation and demodulation.

tion of radio waves is assumed to be equal to the velocity of light. The factor of 2 arises from the fact that the radio wave travels twice the distance  $d$ . The measurement is, of course, independent of small variations of the transmitter frequency.

The radio system consists of a repetition-rate (PRF) generator of a period greater than that of the maximum value of  $\Delta t$  and a high-voltage pulse generator driven in exact synchronism with the repetition-rate generator. The pulse generator acts as a switch to initiate the operation of the radio-frequency pulse generator at precisely known instants. Another switch (TR), termed a "duplexer assembly" (see Vol. 14) makes possible the use of a single antenna for transmitting and receiving.

Most processes of time demodulation depend upon the generation of a waveform which rises linearly with time during the interval between transmission of a pulse and reception of an echo. An adjustable amplitude-comparison<sup>1</sup> circuit generates a pulse at a controllable delay relative to the transmitted pulse (time modulation) and a time-discrimination circuit indicates when the time of occurrence of the measuring pulse is equal to that of the echo. When they are not equal, an error signal is given which indicates the correction to be applied. Thus time demodulation consists of three processes: time modulation, time discrimination, and control. These are processes of considerable accuracy and sensitivity; the error of time modulation lies between one part in  $10^2$  to one part in  $10^5$  and the sensitivity is better than  $0.01 \mu\text{sec}$ . These processes are described in detail in Chaps. 3 to 9 and in Vol. 19, Chaps. 13 and 14.

The complexity of this system is obvious from the block diagram, and a consideration of the systems described in Sec. 2-4 will indicate clearly that pulse methods do not represent the simplest means of distance determination. But other considerations (see Vol. 1) make pulse systems the only practical ones for the determination of the distance of many types of reflector under a wide range of conditions.

**2-4. Phase Modulation and Demodulation.** *Continuous-wave System.* Figure 2-2 shows the essential elements of a continuous-wave distance finder employing phase modulation and demodulation. Continuous waves generated under the control of a frequency standard are amplified and transmitted to a reflector, received and amplified in a receiver. The time delay  $\Delta t$  produces a phase shift of  $n$  cycles of the transmitted wave and from the relations

$$n = f\Delta t$$

and

$$\Delta t = \frac{2d}{c}$$

we obtain

$$n = \frac{2fd}{c}.$$

Thus this measurement depends directly upon the transmitter frequency which may readily be maintained with an accuracy of one part in  $10^7$  or  $10^8$  by the use of crystal control and, if necessary, frequency multiplication to achieve the desired radio frequency.

For unambiguous measurements,  $f$  should be chosen so that the value of  $n$  is less than 1 at the maximum distance required. This is often impractical for long distances, as higher frequencies are desirable not only from the standpoint of efficiency but also for directivity. Where  $n$

<sup>1</sup> See Glossary.

is large, secondary means are employed to obtain the integral value of  $n$ . For example, if the approximate value of the distance is known, the exact value may be obtained by this method. On the other hand, small deviations from a known value of  $d$  due to movement of the reflector or transmitter-receiver are easily measured. In a method to be described shortly, time modulation and demodulation are employed to obtain the approximate value of  $d$ .

Phase demodulation is carried out by means of processes which are already well known and which have been described briefly in Vol. 19, Sec. 13-3 and 14-4. The waveform diagram of Fig. 2-2 indicates a typical phase shift between the transmitted and received signals. A reference

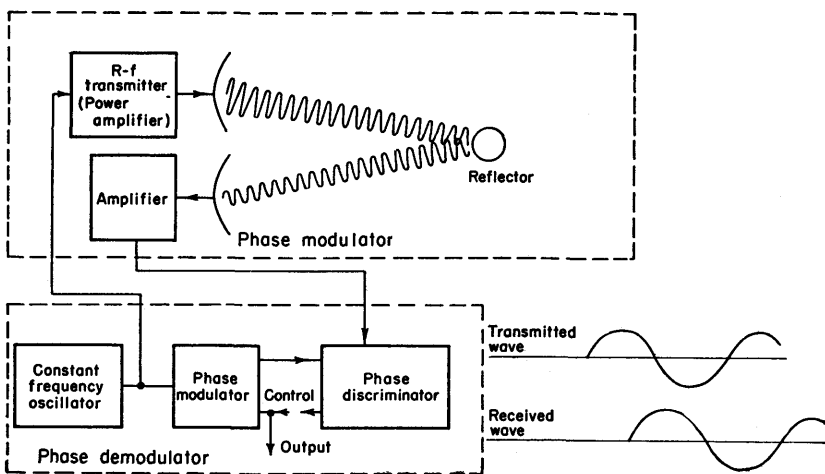


FIG. 2-2.—Continuous-wave distance finder employing phase modulation and demodulation.

signal obtained from the oscillator is phase-shifted by a phase shifter in response to a control. Phase-discriminating circuits similar to those described in Vol. 19, Sec. 14-4 detect the sense and the approximate magnitude of the phase shift between the phase-shifted and received frequencies. The output voltage is suitable for controlling a servomechanism that rotates the phase shifter to give zero output from the phase discriminator. A shaft position corresponding to the phase shift between the received and transmitted signal is then available at the output. This shaft position represents only the fractional part of  $n$ . Typical phase modulators are capacitance or inductance goniometers which are usually accurate to  $1^\circ$  (see Vol. 19, Sec. 13-3, and Vol. 17, Sec. 9-1).

If the value of  $d$  is known accurately to one wavelength by other methods, an indication of the fractional value may be obtained with high

sensitivity. This principle has been used in a low-frequency continuous-wave hyperbolic navigation system termed "Decca" (see Sec. 2-18 and Vol. 2). In this hyperbolic system the transmitter and receiver are separated, and the reference for the phase discriminator is transmitted at a separate radio frequency. The output reading is not the distance from a single transmitting station, but the difference in the distances from two transmitting stations. A wavelength of about one mile is employed, and the system is ambiguous and relies upon an approximately known position for determining the integral value of  $n$ . Deviations from a given reading can, of course, be followed with considerable accuracy, variously estimated as  $\frac{1}{50}$  to  $\frac{1}{1000}$  of a mile. The employment of a means of obtaining the integral value of  $n$  will greatly increase the utility of this system.

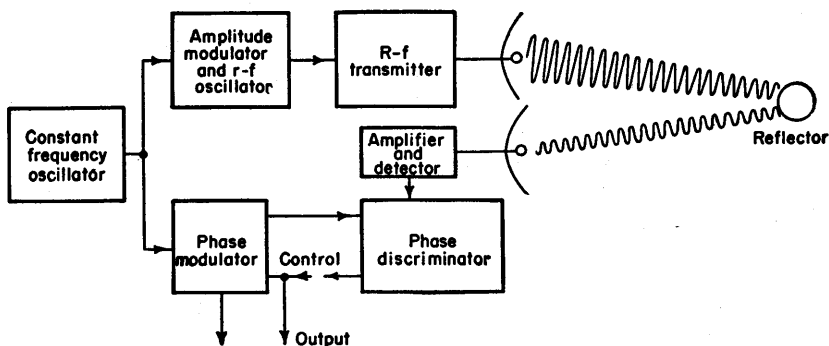


FIG. 2-3.—Continuous-wave distance finder employing phase modulation and demodulation of a low-frequency amplitude-modulated subcarrier.

The ambiguity due to the use of a high radio frequency is avoided in the system shown in Fig. 2-3. The r-f transmissions are amplitude-modulated, and phase demodulation at the lower frequency (subcarrier) gives a unique reading for all values of  $\Delta t$  less than the period of the modulating waveform. The accuracy of measurement is, of course, relatively poor. If, however, the accuracy of phase measurement at the lower frequency is equal to the ratio of this frequency to the radio frequency, identification of the proper cycle of the higher frequency may be achieved, and a combination of this system and that of Fig. 2-2 gives extremely precise and unambiguous distance measurements. This principle was used in a German bombing system. This combination system also appears to be very desirable for aircraft altimeters because not only is a small minimum distance indicated, but high accuracy at high altitudes may be obtained.

An interesting method of obtaining a low-frequency subcarrier is represented by a continuous-wave system (see Vol. 1, Chap. 5) using two



transmitters with a frequency difference of approximately 10 kc/sec. The phase shift of the beat note between the two transmitters is negligible for a reflector of zero distance. Up to a distance of 10 miles, the phase of the received beat note is proportional to the distance of the reflector, and phase-demodulation circuits similar to those indicated in Fig. 2-2 may be employed to measure the distance of the target.

*Pulse Methods.*—One of the most practical methods of determining the approximate distance of the reflector is the use of pulse techniques, which in effect, afford a subcarrier by which unambiguous measurements

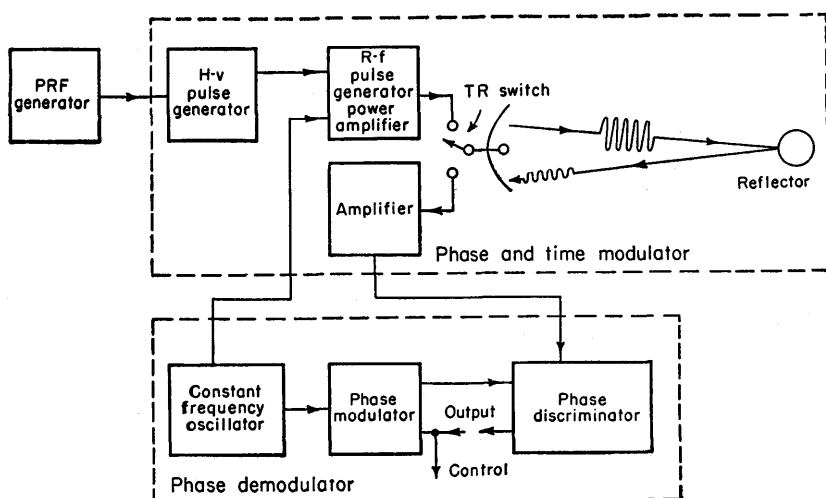


FIG. 2-4.—Pulse distance finder employing phase modulation and demodulation.

of distance may be obtained. In addition, the advantages of range discrimination are obtained and the possibility of large range errors due to the interference of unwanted reflections is greatly reduced.

The simplest application of pulse transmission to phase modulation and demodulation is indicated in Fig. 2-4, based upon components of Figs. 2-1 and 2-2. In spite of the fact that pulses are transmitted, the phase of the received energy is modulated in exactly the same way as in Fig. 2-2.

The phase shift between the constant-frequency oscillator and the received signal is demodulated in the same way as is indicated in Fig. 2-2. One may, however, obtain an additional advantage of pulse transmission since the phase discriminator need be operated only at the time of occurrence of the received pulse.

It is not always necessary to employ a constant-frequency oscillator and power amplifier; the transmitter may initiate a pulsed oscillator of the

same frequency, the output of which may be compared with that of the received signal at the end of the interval  $\Delta t$ . Such a pulsed oscillator is often called a "coherent oscillator," and its stability must be sufficient to prevent phase shift during the interval  $\Delta t$ . With every recurrence of the pulse transmission, this oscillator is restarted in phase with the transmitted oscillations. Phase demodulation is then carried out as shown in Fig. 2-4.

Figure 2-5 indicates a combination of the methods of Figs. 2-1 and 2-4 that makes a pulse distance finder of high accuracy. Phase demodulation is carried out in order to obtain a precise but ambiguous indication

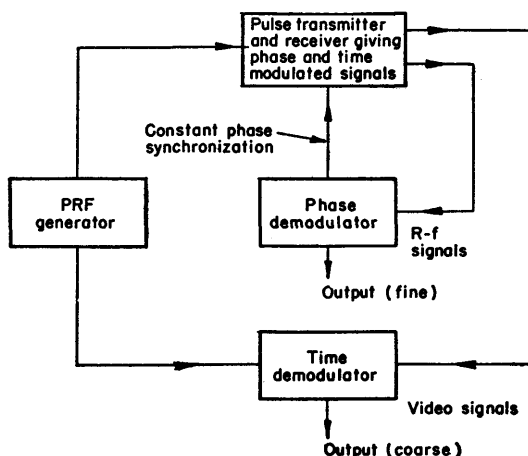


FIG. 2-5.—Pulse distance finder employing phase and time demodulation.

of the distance  $d$ . But this information is supplemented by a time-demodulation system of an accuracy exceeding  $2fd/c$ .

The principle shown here is related to that employed in experimental "cycle-matching" tests with Loran, a hyperbolic navigation system (see Sec. 2-18 and Vol. 2). Distance is not measured directly but the difference of distances is represented by the phase and time difference between two synchronized pulse transmitters. The transmitter frequency is approximately 1.8 Mc/sec and  $d = 200$  miles, corresponding to  $n = 4000$ .<sup>1</sup> The time demodulator must have a precision better than 1 part in 4000 ( $0.5 \mu\text{sec}$ ) in order to indicate unambiguously the proper value of  $n$ . A pulse rise time of roughly 100 times this value is satisfactory if the techniques of Sec. 7-11 are used and may easily be obtained with a reasonable value of transmitter and receiver bandwidth at this frequency. Loran represents a special case where the requirements for reliable day and night

<sup>1</sup> In the Loran system time may be computed on the basis of approximately  $10 \mu\text{sec}$  to the mile exactly the same as in radar systems. (See Vol. 1.)

coverage at great distances necessitate the use of a low frequency whereas the requirements of the navigation problem require the utmost accuracy of distance measurement.

Simple methods for coordinating the controls of the two measurement systems of Fig. 2-5 in order to obtain a single control operating continuously over the whole range are presented briefly in Sec. 3-16.<sup>1</sup>

At the present time it does not appear possible to obtain unambiguous distance measurements by phase modulation and demodulation in microwave radar systems. If the method of Fig. 2-4 were applied to microwave transmitters and receivers, certain difficulties would be encountered.

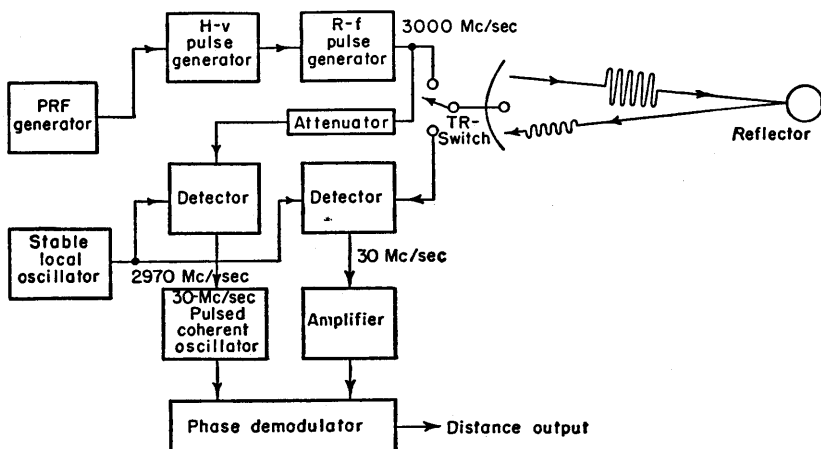


Fig. 2-6.—Heterodyne system for employing phase demodulation at a low frequency in a pulse system.

First, the synchronization of a pulsed magnetron with a continuous signal is not assured although preliminary experiments give promising results (see Vol. 6). Second, a microwave coherent oscillator must be initiated exactly in phase with the high-power transmission. Third, continuous phase modulators operating at these frequencies are not available.

On the other hand, it is possible to carry out phase demodulation at frequencies differing from the radio frequency, and advantage is taken of the fact that the phase of the transmitted and received waves is preserved even though they are heterodyned to a different frequency (see Vol. 1, Chap. 16). As indicated in the block diagram of Fig. 2-6, a 30 Mc/sec pulsed coherent oscillator is initiated exactly in phase with the heterodyne signal between the transmitted pulse and the stable local

<sup>1</sup> The similarity of the system of Fig. 2-5 to a multiple-scale range system using a pulsed oscillator and phase shifter is striking (see Chaps. 3 and 6). The pulsed oscillator used in time demodulation is analogous to the coherent oscillator of Fig. 2-6, except that lower frequencies are employed (0.1 to 1 Mc/sec).

oscillator. The frequency of the stable oscillator is maintained constant during the interval  $\Delta t$ , so that distance errors are avoided. The frequency stability of these oscillators is remarkable, and several types have been stabilized to an accuracy of 1 part in  $10^8$ , and in a special case, 5 parts in  $10^{10}$  have been obtained (see Vol. 14). Therefore, the phase of the heterodyne signal obtained from this stable oscillator and from the received echo gives an accurate although ambiguous indication of the distance. This heterodyne signal has, however, a frequency of 30 Mc/sec, and phase discrimination and demodulation may be carried out at this frequency by precise electromechanical devices (see Vol. 19, Sec. 13-13) in a manner similar to that indicated in the previous examples.

Since the phase of the stable local oscillator is not synchronized with its pulse-repetition frequency, it may vary through  $360^\circ$  from pulse to pulse. There is, however, a similar variation of the phase of the coherent oscillator because this phase depends upon the combined phases of the radio frequency and the local oscillator frequency. The phase of the received energy is varied correspondingly and thus the phase of the signal from a reflector at a fixed distance is constant.

Although the configuration of Fig. 2-6 may be extremely useful for indicating small increments in an accurately known distance, it does not yet appear to be feasible to select the proper cycle of the 30-Mc/sec received wave by time demodulation since a wave length of 10 cm requires an accuracy of roughly 0.3 ft or  $7 \times 10^{-4} \mu\text{sec}$  in time demodulation—corresponding to a pulse rise time of  $1 \times 10^{-2} \mu\text{sec}$ . In addition, the effects of echo interference upon the phase of the received signal are incompletely investigated.

**2-5. Frequency Modulation and Demodulation.**—Another method of introducing a subcarrier by which unambiguous measurements of the interval  $\Delta t$  may be obtained is the use of frequency modulation of the r-f transmissions. As indicated in Fig. 2-7, the transmitted frequency is varied in a continuous manner in accordance with the timing waveform. As far as is known, f-m systems are operated continuously and pulse techniques are not employed. The frequency-modulation system may be operated in three ways. In the first, the timing waveform is impressed upon the frequency-modulation system and, by a process of frequency demodulation, this waveform is recovered with a delay equal to  $\Delta t$ . Any of the methods mentioned previously for time-delay measurement may be employed to measure the delay between the transmitted and received waveforms.

A second method of operation is employed in some altimeters. Instead of demodulating the frequency-modulated wave to obtain a time delay as indicated in Fig. 2-7, the output of a phase discriminator is amplified and counted as indicated in Fig. 2-8. In addition, the counter

(beat-frequency meter) permits the use of a sinusoidal frequency modulation since it measures the average number of cycles in the recurrence period ( $T_r$ ) of this waveform. Since the recurrence period of the modulating waveform will contain both positive and negative values of  $df/dt$ , the total number of cycles counted in this interval is  $n = 2T_r\Delta f$ , where  $\Delta f$  is

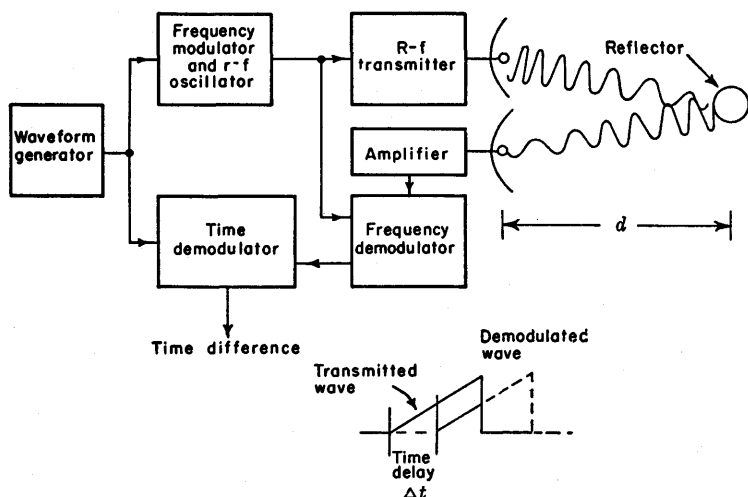


FIG. 2-7.—Continuous-wave distance finder employing frequency modulation and demodulation.

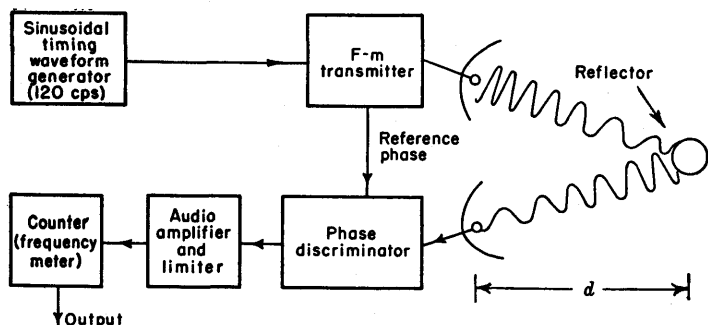


FIG. 2-8.—Continuous-wave distance finder employing frequency modulation and demodulation.

the frequency shift occurring in the time  $\Delta t$  and corresponds to the target range.

This counting technique does not, however, permit interpolation between cycles, and when some altimeters are used over a smooth surface—for example, the ocean—the measurement is discontinuous and the

indicated distance increases in integral values of  $n$ , that is, in steps of magnitude  $\Delta d = c/4F$ , where  $F$  is the total frequency deviation. In a particular system this may amount to as much as 6 ft.<sup>1</sup> On the other hand, this discontinuity causes little difficulty under usual conditions of operation over rough terrain, and accuracies of 1 per cent of full scale (5000 ft) and minimum distances of 1 ft are easily obtained with commercial designs.<sup>2</sup>

A third method depends upon control of the value of  $df/dt$  from the output of the phase discriminator. This output is, of course, a frequency shift  $\Delta f$  occurring in the interval  $\Delta t$  and, for a fixed target, is constant. Since  $df/dt$  usually has positive and negative values, there is a corresponding phase reversal of  $\Delta f$ . Usually this difficulty is avoided by shifting the modulated frequency by an amount  $\pm \Delta f$  depending upon the sign of  $df/dt$ , and in this way a constant phase of  $\Delta f$  is obtained for both signs of  $df/dt$  (see Sec. 2-12). Automatic frequency demodulation is carried out by variation of  $df/dt$  in two ways: first by variation of the repetition rate of the timing wave, and second by variation of the extent of frequency modulation at a constant repetition rate. The use of this technique in distance and speed measurements is given in greater detail in Sec. 2-12.

Target selection and discrimination in frequency-modulation systems must depend upon frequency selection.<sup>3</sup> The distance of any target corresponds to a particular value of frequency, and the total frequency shift corresponding to the maximum value of  $\Delta t$  must be sufficient to permit frequency selection with reasonable circuits, that is, bandwidths of approximately 10 cps or greater. But the problem of constructing 100 or more selective circuits to display targets, as on a PPI, is cumbersome compared with the simplicity of time selectivity in the cathode-ray-tube display (see Vol. 19, Sec. 10-6).

Existing frequency-modulation systems have not been used for precision distance measurements. Accurate frequency demodulation is possible with electronic counters.

**2-6. Summary.**—In most radar systems the need for target discrimination in range and azimuth has led to the use of frequencies and pulse durations that permit an ultimate range accuracy high compared with that actually required for military use. But there are several systems in which other requirements have dictated the pulse rise time, and with these the ultimate accuracy is required. An example of such a system is Loran, where a frequency of 2 Mc/sec is employed in order to achieve satisfactory propagation over great distances. There are already

<sup>1</sup> See D. G. Fink, "The F-m Altimeter," *Electronics*, **19**, No. 4, 130, (Apr. 1946).

<sup>2</sup> *Loc. cit.*

<sup>3</sup> Unless, for example, the duration of the timing waveform is short enough to permit time selection.

preliminary data that indicate the potential usefulness of the combination of phase and time demodulation for such a system.

Combinations of phase and time demodulation in microwave radar systems are not yet possible although phase demodulation may give a very sensitive indication of increments of distance.

At this point it is desirable to refer to the accuracy of time discrimination obtainable with special displays involving superposition of two video signals as in Loran. In an experimental test using synthetic signals free from noise, the accuracy of time discrimination approached that obtainable by phase discrimination of the r-f pulse carrier (see Sec. 7·11). In general, such accuracy would not be expected under practical conditions of operation where appreciable noise would be present.

The accuracy of time and phase modulators used in measurement of this type is discussed briefly in Sec. 3·14 and in considerable detail in Chap. 5. It is sufficient to mention here that accuracies of 0.3 per cent of full scale are readily obtainable with practical circuits. With certain arrangements, a cascade of a number of time- or phase-demodulation circuits increases the accuracy by the product of the accuracies of the two circuits that are cascaded (see Secs. 3·9 and 3·15 and Chap. 6). Considerably less has been done to develop precision frequency modulators that would be used for corresponding measurements in frequency-modulation systems. The usual accuracies obtainable are approximately 1 per cent and, as far as is known, no efforts have been made to cascade frequency-demodulation systems as is usually done in time- and phase-demodulation systems.

### SPEED MEASUREMENTS

In radar systems having inadequate range and angle resolution, moving objects are sometimes distinguished from fixed objects—rocks, trees, etc.—by speed measurements. The emphasis here is upon the means for determining target speed as supplementary information to target distance in order that prediction of future position of the target may be obtained. In a number of special cases, prediction along a radial line is sufficient, and the following discussion is confined to this subject. Rate information can, of course, be obtained upon differentiation of displacement measurements and this method is discussed in Sec. 2·11 and in Chaps. 7 to 9. In scanning radar systems, the interval between displacement measurements is often so great that a considerable time is required before sufficient information is available to permit satisfactory differentiation. Some aspects of this problem are reviewed in Sec. 2·14.

**2·7. Continuous-wave Systems.**—Figure 2·9 indicates a typical continuous-wave speed measurement system. It is based upon the elements of Fig. 2·2 and takes advantage of the fact that the rate of change of the

received phase due to motion of the reflector is given directly in the output of a phase discriminator as a doppler frequency.

The value of the output frequency may be calculated by the formula<sup>1</sup>

$$F_d = \frac{89.4V_r}{\lambda} \text{ cps/mph}$$

where  $V_r$  is the radial velocity of the target with respect to the transmitter-receiver system in mph,  $F_d$  is the doppler frequency or the rate of change of phase, and  $\lambda$  is the wavelength in cm. For example, at a wavelength of 3 cm,  $F_d$  is equal to 29.8 cps/mph.

A variety of frequency-metering circuits may be employed similar to those used in the measurement of distance in a frequency-modulated system (see Sec. 2-5).

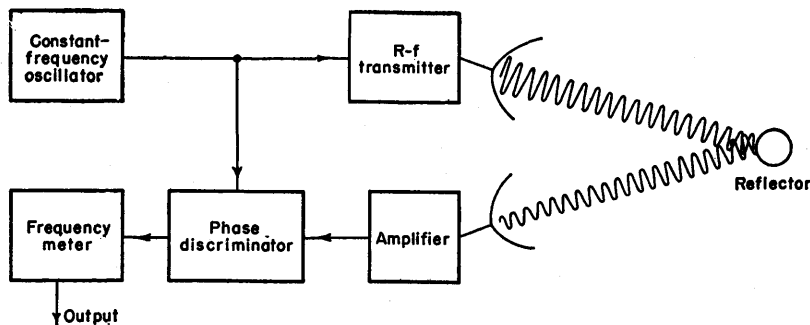


Fig. 2-9.—Continuous-wave speed measurement system.

The relative merits of a number of these systems used for aircraft detection are discussed in Vol. 1, Chap. 5. For most purposes the lack of range resolution has been a great handicap to continuous-wave systems used for speed measurement.

For isolated objects—for example, a bomb or projectile—accurate speed measurements are possible without the need for range resolution. In fact, continuous-wave systems would seem to be particularly useful for this purpose, and frequencies of 10,000 Mc/sec would be expected to give good results by direct recording of the doppler frequency. A reading accuracy of roughly one-quarter cycle at this frequency would give velocities accurate to a fraction of a per cent provided a reasonable number of cycles were recorded. In fact, such an accuracy would exceed that obtainable by time demodulation and differentiation by a factor of roughly 5 (see Sec. 2-11). The exact value of the distance may or may

<sup>1</sup> The factor 89.4 is twice the normal conversion factor for the doppler effect since both the transmitter and the receiver may be considered to be moving with respect to the reflector.



not be obtained in these speed measurements depending upon whether the zero point of recording the doppler cycles is accurately known. From that point onward distance measurement is obtained by simply counting the cycles and converting these into distance (for this frequency, one doppler cycle equals 1.6 cm).

**2-8. Pulse Systems—Internally Coherent.**—The doppler beat note derived from the rate of change of phase due to a moving target is readily obtained with the system shown in Fig. 2-4 by the alterations indicated in Fig. 2-10. As in Fig. 2-9, the phase-discriminator output is measured directly by a frequency meter. This method has been applied to several radar systems operating at 100 to 200 Mc/sec where audible indications

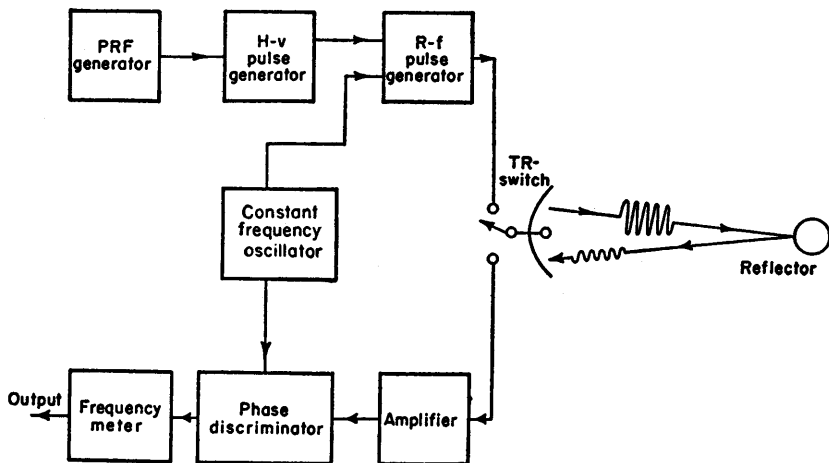


FIG. 2-10.—Pulse speed measurement system employing internal coherence.

of the speed of a moving target are required. It usually suffices to employ earphones for frequency estimation. The modification of the radio-frequency portions of this system as indicated in Fig. 2-6 is desirable when microwave frequencies are employed.

A qualitative indication of the speed of a large number of targets within the view of a scanning radar system is obtainable as indicated in the rudimentary schematic diagram of Fig. 2-11. This system is identical to that indicated in Fig. 2-10 with the exception that the frequency meter is replaced by a delay device of a delay that is exactly equal to the pulse recurrence interval. The input and output of this delay device are subtracted, and therefore targets moving more slowly than a given speed do not appear at the output of the subtraction circuit because they will have an inappreciable change of phase during the repetition interval. Some of the delay devices described in Chap. 12 are useful for these purposes.

The great usefulness of this system is that it gives a qualitative indication of the speed of a large number of targets. In the form indicated here, it does not, however, give accurate speed indications, and these are more appropriately obtained through phase demodulation. For microwave frequencies the heterodyne method of Fig. 2-6 is, of course, desirable.

If the doppler frequency in any of these systems is equal to or is an integral multiple of the repetition frequency of the transmitter, no modulation is observed. The radar then fails to detect the target and is said

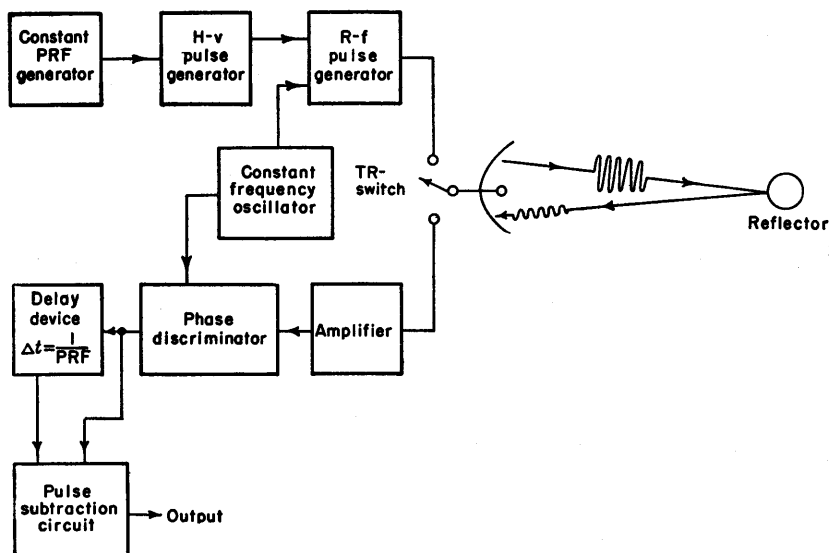


FIG. 2-11.—Pulse system for the qualitative indication of the speed of a large number of slowly moving targets by means of frequency selection at the pulse recurrence frequency.

to be "blind." The corresponding speed is the "blind speed." This may be stated more generally by the formula

$$V_{\text{blind}} = \frac{n \cdot \text{PRF} \cdot \lambda}{2}$$

where  $n$  is equal to 1, 2, 3, etc.

For the particular case, where  $\lambda$  is equal to 3 cm and PRF is equal to 2000,

$$V_{\text{blind}} = 67n \text{ mph.}$$

When this effect is objectionable, a slight variation of PRF increases the amplitude of the beat note to a measurable value. Usually fluctuations in the phase of the reflected signal that are due to the finite size of the target will cause this effect to be of small importance.

**2-9. Pulse Systems.—Externally-coherent Echo Interference.**—In the previously discussed systems the time delay between transmission and reception of the pulse requires the maintenance of the phase of the transmitted wave during this time interval in order to permit simultaneous comparison of the phase of the transmitted and received waves. The necessity for the coherent oscillator derives from the fact that the transmitted and received energies do not exist simultaneously at the transmit-receive point. On the other hand, the incident and reflected energy are coincident at the reflector for an interval equal to the pulse duration. Extremely important methods of relative speed measurement, which derive from this simple fact, are termed "external coherence."<sup>1</sup> External coherence may be employed to measure the relative rate of a moving vehicle with respect to a stationary background or the relative motion of portions of a large stationary object with respect to a moving transmitter-receiver.

*Relative Speed of Vehicle and Ground.*—The energy of the r-f pulse incident upon a moving reflector is also incident upon the stationary medium over which the object is moving. Experimental observations and theoretical calculations have indicated that the phase shift due to a large number of stationary scatterers is constant, even in the neighborhood of a distinctive moving reflector;<sup>2</sup> but the phase of the energy reflected from the moving object varies in accordance with the usual doppler formula. The reflected energy then contains a component equal to the sum or difference of the transmitted frequency and the frequency corresponding to the rate of change of phase (doppler frequency) caused by the motion of the object away from or toward the transmitter. Although the speed of the moving object may be determined by the doppler frequency, information on its range must be obtained by time demodulation.

Figure 2-12 shows the extreme simplicity of speed measurement by this means. All the elements are parts of a conventional radar system except the frequency meter. Since the energy reflected from the moving and stationary targets contains both the transmitted frequency and this frequency plus or minus the doppler frequency, phase discrimination is accomplished in a simple detector. Practical considerations in the design of these circuits are given in Vol. 19, Sec. 14-5, and in Vol. 1.

Time selection of the energy reflected from the desired target is, of course, important in order to secure minimum target confusion and

<sup>1</sup> External coherence is often termed "noncoherent" doppler detection. This term is not appropriate because the energy from stationary scatterers is *coherent* with the incident radiation.

<sup>2</sup> A. J. F. Siegert, "Fluctuations in Return Signals from Random Scatterers," RL Report No. 773, 1945.

optimum signal-to-noise ratio and also to provide measurement of distance. Other practical considerations, such as the removal of spurious modulation from the transmitter and receiver are also of importance.

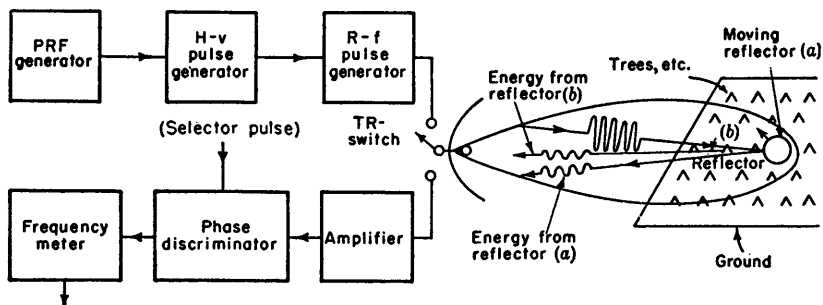


FIG. 2-12.—Pulse speed measurement employing external coherence (echo interference).

*Relative Speed of Portions of the Ground with Respect to Moving Transmitter-receiver.*—Two other extremely important measurements made with externally coherent-phase systems are applicable to airborne trans-

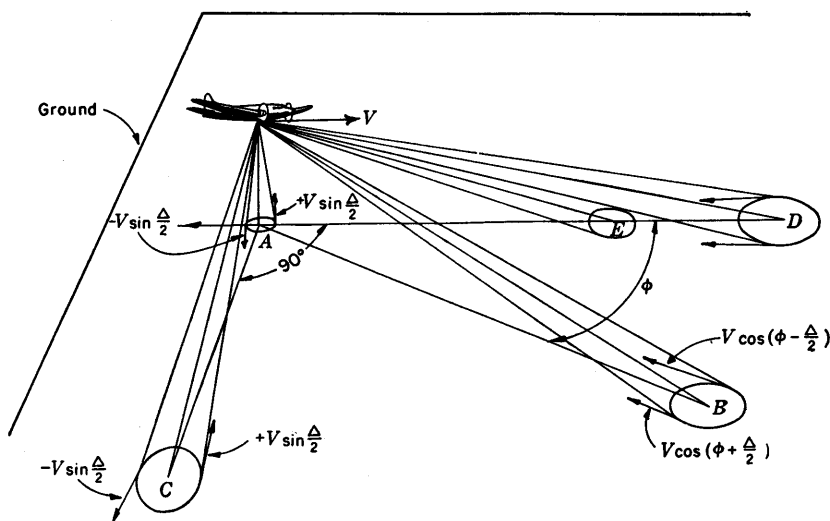


FIG. 2-13.—Geometry for determining echo interference effects. In positions A, B, and C doppler frequencies due to ground speed will be dominant. At D and E the doppler frequencies will be a minimum and the ground track of the aircraft may be determined.

mitter-receiver systems. The relative speed of portions of an illuminated patch of ground toward a moving transmitter-receiver gives indication of the rate and the direction of approach; this indication is due to echo-interference effects during the pulse. Figure 2-13 shows various positions

of the illuminating beam which emphasize various measurements of doppler beat frequencies. In *A* the beam is projected vertically downward from the moving airplane, and the relative motion of portions of the illuminated reflectors is toward the airplane if the reflectors are ahead and away if they are behind. The relative motion of the point of closest

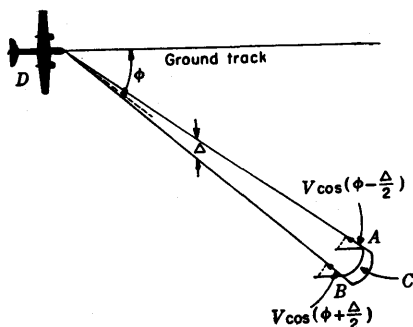


FIG. 2-14.—Differential doppler shift due to difference of motion of portions of reflector *A* and *B* toward the aircraft.

approach is, of course, zero. Particular reflectors at the extremities of the beam are approaching or receding from the airplane with a velocity denoted by  $\pm V \sin \Delta/2$  where  $\Delta$  is the beamwidth. The doppler beat note between these two reflectors is  $2V/\lambda \sin \Delta/2$ .

Actually the existence of two discrete reflectors at these positions is unlikely, but a frequency spectrum approaching the above expression as a maximum value is

obtained from the doppler beats of all the reflectors illuminated by the beam. The general form of this spectrum is indicated by Fig. 2-15.

Another possible geometry is indicated by position *B* in which the beam is directed at an angle  $\phi$  with respect to the ground path of the aircraft, and a portion of the ground at a considerable distance from the airplane is illuminated. Here the relative velocity of portions of the illuminated patch of ground is in the horizontal plane, the component in the vertical plane being negligible. Taking two points at the extreme lateral edges of the beam, their relative velocity of approach toward the aircraft may be computed as indicated in Fig. 2-14. This is

$$V \cos \left( \phi \pm \frac{\Delta}{2} \right)$$

where  $\phi$  is the azimuth angle of the antenna with respect to the ground track of the airplane, and the differential doppler frequency is multiplied by this geometric factor. As in the previous case, the doppler-frequency spectrum has a large energy at a small value of frequency and decreasing energy out to a frequency determined by the differential velocity of points at the extreme edges of the beam. An estimated spectrum for this differential doppler effect at two azimuth angles is indicated in Fig. 2-15. The amplitude of the high-frequency components increases as  $\phi$  increases and reaches a maximum where  $\phi$  is equal to  $90^\circ$ . When a radar frequency of 10,000 Mc/sec is used, the mid-frequency is centered

at approximately 1 cps for  $\phi = 0^\circ$  or  $180^\circ$ , and at 300 cps for  $\phi = 90^\circ$  or  $270^\circ$ .

If the antenna is oriented in position *C*, where  $\phi = 90^\circ$ , a reflector at the forward extremity of the beam will be moving toward the airplane, and one at the rear extremity will be moving away from it. Thus the differential speed is represented by

$$V \cos \left( \phi + \frac{\Delta}{2} \right) + V \cos \left( \phi - \frac{\Delta}{2} \right).$$

This expression reduces to  $2V \sin \Delta/2$ , since  $\cos \Delta/2$  at the rear extremity of the beam is negative. This value for the differential speed is the same as that obtained for a beam directed vertically downward as in *A*.

No practical application has been made of the differential doppler effect in positions *A* or *C* for the purposes of measuring ground speed. In the first place no single frequency is obtained corresponding to ground speed as observed from Fig. 2-15. The amplitude at any particular frequency is subject to large fluctuations due to variations of transmitted power, the character of the reflector, and the receiver sensitivity. It is conceivable that the ratio of the amplitudes at two frequencies  $f_1$  and  $f_2$  would give a measure of the ground speed. The practicability of this suggestion has, however, not been substantiated.

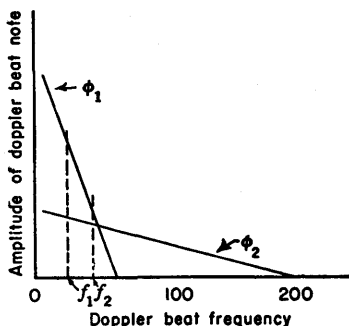


FIG. 2-15.—Estimated doppler spectrum for two values of antenna azimuth.

A most useful and practical result is, however, obtained by orientation of the radar antenna to position *D* of Fig. 2-13. In this position the differential velocities of points at the extreme edges of the pattern are equal. According to the simple formulas zero frequency would be observed, but actually a residual spectrum near 1 cps is obtained. A simple and highly sensitive method of locating the true ground track of an aircraft depends simply upon the observation of the angle  $\phi$  at which the differential-doppler frequency goes to a minimum value, and this minimum is easily observed. An experimental system taking advantage of this effect has indicated that when operating on a frequency of 10,000 Mc/sec with a beamwidth of  $3^\circ$  the ground track of the aircraft may be located with an accuracy of roughly  $\frac{1}{2}^\circ$ . The observations are made directly on the PPI display. A more detailed description of the method of measuring this effect is given in Vols. 1 and 2.

The doppler indications indicate the track of the aircraft along the line parallel to the plane from which echo-interference effects are obtained. If this plane is horizontal, the ground track is determined. But in mountainous terrain the doppler frequency null may not be observed since the beam may not illuminate a horizontal area. This effect has been observed in experimental flight tests and has caused some difficulty. In spite of this limitation, the doppler ground track is an extremely important navigational aid for airborne radar systems.

Two other methods of determining ground speed do not depend upon the relative motion of reflectors illuminated by the same pulse of r-f energy. If two antennas are used to project a continuous-wave beam directly forward and aft along the ground track, the doppler frequency may be measured to better than 5 mph. This method is not, however, immediately applicable to pulse radar systems.

A proposed system uses one beam but compares the energy at two different ranges. If, for example, the received energy from illuminated portion  $D$  is compared with that from  $E$  (Fig. 2-13), the following doppler frequency will be observed:

$$\Delta f = \frac{2V}{\lambda} (\sin \beta - \sin \alpha),$$

where  $\beta$  and  $\alpha$  are the vertical angles of  $D$  and  $E$ , respectively.<sup>1</sup> As there is an appreciable time delay between the reception of the energy from these two different portions of the ground, a delay device operating at the radio frequency or the intermediate frequency is employed in order to permit phase discrimination. Frequency measurement, of course, gives a value related to the ground speed as previously indicated. This method has two limitations: the angle  $\phi$  should be made zero; and suitable reflectors are required at two places on the ground rather than at a single place. A consideration of this method will indicate its similarity to coherent methods in which the phase of the transmitted pulse is compared with the reflected energy from  $D$ . It has the great advantage, however, that the required length of the delay element may be made short compared with that required if the transmitted pulse were to be delayed until the reception of a suitable echo.

#### SPEED AND DISTANCE MEASUREMENTS

Both rate and displacement information are required for the prediction of the time of arrival of a moving object at a particular point. In general, data in two or three coordinates are required, but a great many

<sup>1</sup> D. Sayre, "Pulse Doppler with Reference to Ground Speed Indication," RL Group Report, Mar. 20, 1944.

practical problems of prediction are satisfied by a knowledge of radial distance and speed.

The navigation problem is usually solved by establishing a "collision" course with the objective and by calculating the time of arrival on the basis of range and range-rate data.

The bombing problem is similar, for release is required at a distance from the target approximately equal to  $V_g t_f - T$  where  $V_g$  is ground speed,  $t_f$  is time of fall, and  $T$  is trail of the particular bomb. At low altitudes the slant range is approximately equal to ground range at the release point, but at high altitudes the slant range is converted to ground range by a computer (see Vol. 19, Sec. 8-5 and Vol. 21, Sec. 6-3).

A specialized navigational computer, which has been developed for the solution of these problems, presents a direct indication of course to and time of arrival at a destination (see Sec. 7.28 and Vol. 21, Chap. 7).

Associated equipment may often greatly decrease the accuracy requirements of prediction. For example, airborne radar simplifies the problem of Ground Control of Interception, GCI. Similarly, proximity fuses and guided missiles decrease the accuracy required of antiaircraft fire control and bombing systems.

The block diagrams of various methods of obtaining distance and speed are presented and are followed by a brief discussion of some of the problems of these measurements arising in scanning radar systems.

**2-10. Phase and Rate of Change of Phase.**—The problem of obtaining both distance and speed separately in phase-modulation systems has been discussed in Secs. 2-4, 2-7, and 2-8.

In a system in which it is desired to measure both distance and speed simultaneously, the measurement systems may operate independently. A typical block diagram of a c-w system is shown in Fig. 2-16 in which coherent oscillations establish synchronization between the phase demodulator and the transmitter (phase modulator). The received signals are phase-demodulated giving range information. In

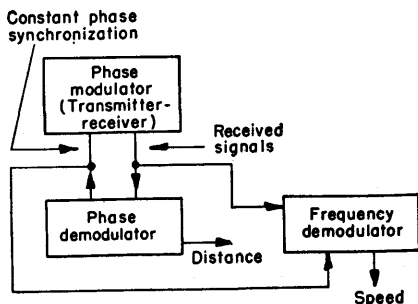


FIG. 2-16.—Distance and speed measurements by phase and frequency demodulation in a c-w system.

addition, the rate of change of range is obtained by phase discrimination and frequency selection using the transmitted phase as a reference.

This method has, of course, the advantage of extreme sensitivity in displacement and speed measurements, that is, it may respond to a fraction of the period of the radio frequency but will be subject to ambi-



guities in range as discussed in Sec. 2-4. There have been few practical applications of the method in this form although the two processes are used separately for a number of very accurate measurements (see Secs. 2-4 and 2-7). A more practical device would result from a combination of time demodulation for approximate range measurement and target discrimination as discussed in Sec. 2-13.

**2-11. Time Demodulation and Differentiation.**—The only feasible method of determining speed in a time-demodulation system is by differentiation of the distance. In fact, all pulse-radar systems so far used for distance-finding employ this method. A number of methods for differentiation by manual or automatic means are described in Sec. 7-14 and Sec. 9-3 and also in Vol. 21, Sec. 4-5. In general, manual methods consist

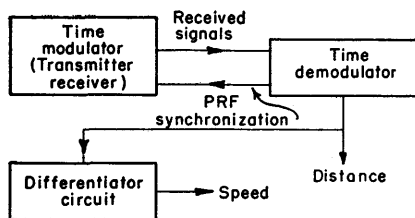


FIG. 2-17.—Distance and speed measurements by time demodulation and differentiation.

of various aiding devices for establishing continuity of the displacement information in the interval between displacement measurements. The speed of a motor or other device required to establish this continuity is then a measure of the rate. Automatic tracking methods of high sensitivity and rapid response are employed wherever practicable. A block diagram of a typical system is indicated in Fig. 2-17 where straightforward differentiation of the distance output of the time demodulator is indicated.

The properties and performance of a number of radar systems using these techniques are given in the next sections, especially Secs. 2-15, 2-16, and 2-17.

**2-12. Phase and Frequency Demodulation.**—In frequency-modulated distance finders the output information is obtained as a frequency shift  $\Delta f$  corresponding to the product of the time delay between transmission and reception of information and the rate of change of frequency with time. If there is relative motion of the transmitter-receiver system and the reflector, an additional frequency shift  $\pm \frac{2V}{\lambda}$  is added to  $\Delta f$ . A

method of distinguishing between the frequency shifts due to distance and speed depends upon the fact that  $\Delta f$  is subtracted from the doppler frequency for positive values of  $df/dt$  and added to it for negative values.

A block diagram of a possible system is shown in Fig. 2-18. In the initial condition the timing-waveform generator which controls the frequency modulation of  $A$  is disabled and the system operates by ordinary c-w doppler. If energy is reflected from an object moving within the

desired range of speeds, a phase discriminator operates and adjusts the frequency of a l-f frequency-modulated oscillator *B* to equal the doppler frequency. The output shaft represents the target speed. At this moment the timing-waveform generator is set into operation and frequency modulates the transmitter with a triangular wave. At the same time a rectangular wave is applied to the oscillator *B*. For increasing values of the transmitter frequency, the rectangular waveform reduces the frequency of the oscillator *B* by one-half the doppler frequency, and for increasing values of the transmitter frequency, it increases the frequency of the oscillator *B* by one-half the doppler frequency. If the rate of change of the transmitted frequency produces a value of  $\Delta f$  equal to

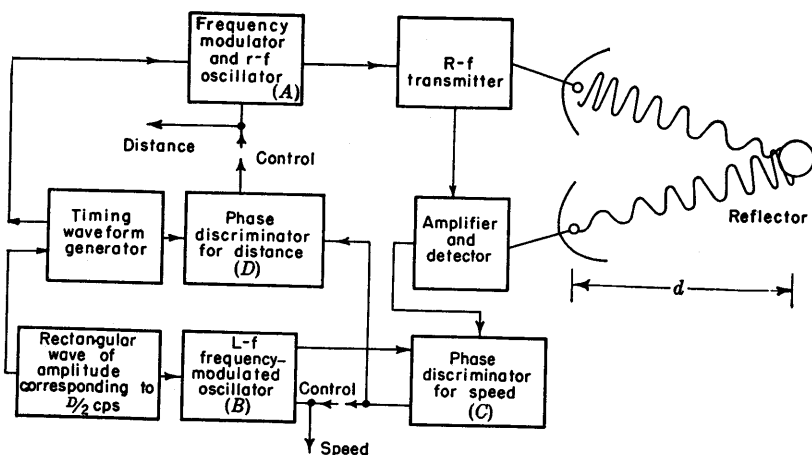


FIG. 2-18.—Distance and speed measurements in a continuous-wave frequency-modulated system.

one-half the doppler frequency, the resultant beat frequency applied to the phase discriminator *C* will be constant because  $\Delta f$  is subtracted from the doppler frequency for increasing transmitted frequencies, and vice versa. If the value  $\Delta f$  is not correct, the output of the phase discriminator *C* will be modulated at the frequency of the timing waveform. Phase discrimination of this signal with reference to the timing waveform in *D* gives a control signal that will adjust  $df/dt$  so that  $\Delta f$  is again equal to one-half the doppler frequency.

In another system, the total frequency shift was maintained constant, but the repetition rate of the timing waveform was varied. In this way a selector circuit operating at a constant frequency gives control signals varying the repetition rate of the timing-waveform generator so that continuous indications of the target range are obtained (see Vol. 1, Chap. 5).

**2-13. Time, Phase, and Frequency Demodulation.**—A possible pulse system is indicated in Fig. 2-19. An approximate value of the distance is obtained by time demodulation as indicated in Fig. 2-17 and is used to remove the ambiguities in the accurate value obtained by phase demodulation as indicated in Fig. 2-16. Rate information is obtained by frequency demodulation of the output of a phase discriminator.

At the present time this theoretically attractive system is impossible to apply to a microwave radar since the bandwidth of existing receivers and the accuracy of available time demodulators are inadequate to remove the ambiguity of the phase-demodulation system. Nevertheless, the possibilities of extremely accurate distance measurements combined with rapid determination of speed may warrant some consideration

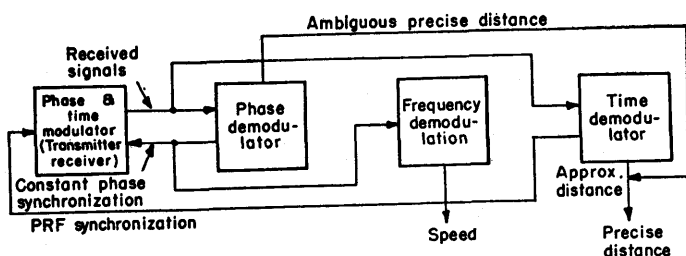


Fig. 2-19.—Distance and speed measurements by phase, time, and frequency demodulation in a pulse system.

of this method—especially in the case of slowly scanning radars giving intermittent data.

**2-14. Considerations Applying to Intermittent Data.**—Distance and speed determination in scanning radars presents some special problems. A particular radar employs a pulse length of 1  $\mu$ sec, a beamwidth of  $\frac{1}{2}^\circ$ , a scanning rate of 3 rpm, and maximum range scale of 300 miles in order to cover large areas and distinguish many targets. The amount of information obtained from each individual target is meager and infrequent because only 10 pulses are received at an interval of 20 sec, corresponding to an intermittency of 1 part in 3300 in range and 1 part in 720 in azimuth or a net intermittency of 1 part in 240,000.

In nearly all practical applications of radar of this type, the necessity arises for obtaining precise information on a few of the many targets detected, and special methods must therefore be employed to obtain distance and speed information in a reasonable amount of time. A few considerations of importance in determining distance and speed are outlined below. Similar considerations for the determination of angular position are given elsewhere (see Vol. 1 and Sec. 9-11).

**Distance Measurements.**—An electrically controlled time demodulator can give a satisfactory displacement measurement from several pulses

(5 to 10) provided the displacement error is not large. Mechanically controlled time demodulators are more sluggish and, hence, do not respond to a group of pulses immediately. Therefore, the mechanical systems assess the error during the reception of the pulse group and remove the error during the period between scans. A particular cathode-ray-tube display permits the same type of operation under manual control (Sec. 7-15). Similar considerations apply to mechanically controlled phase demodulators.

*Speed Measurements.*—Although a crude indication of target velocity is obtained in electrically controlled time demodulation systems during the reception of a few pulses, accurate rate information is only obtained by averaging the increments of displacement obtained on successive scans. It requires, therefore, several scan periods (equivalent to several minutes) to obtain accurate rate information. An even longer time may be required in mechanically controlled time demodulation systems.

It is often highly desirable to obtain the rate information as soon as the displacement information is obtained. This is difficult with time demodulation, but measurement of the doppler frequency appears to have several advantages. Since the time required for a speed measurement depends upon the sensitivity of the method employed, time and phase demodulation may be compared in this respect. A sensitivity of 5 ft is considered very good for most time-demodulation systems. On the other hand, a movement of the reflector less than a wavelength causes a perceptible doppler indication. For microwave radar, therefore, there is a theoretical factor of improvement in sensitivity of speed measurement of roughly one hundredfold, although this may not be obtainable with fluctuating echoes.

## POSITION-FINDING

**2-15. Introduction.**—The practical application of distance-finding is, of course, to position-finding, and a few of the methods by which position may be found by time-interval measurements are outlined. For the sake of completeness, a few types of angular measurements are included.

Range and angle measurements of an isolated reflector shown in Fig. 2-20*a* give good results at relatively short distances. For example, the tracking of an aircraft by microwave radar is accurate to better than  $\frac{1}{10}$  of a degree. Also, airborne navigation with simple types of scanning radar systems is accurate to a few hundred feet over distances of several miles.

A more accurate method is based upon the measurement of the distances to two accurately located objects. The intersection of the circular lines of position defined by the distance measurements gives the location of the radar station as in Fig. 2-20*b* and 2-20*c*. Using distinctive reflectors as beacons, this method is capable of high accuracy and is employed in

the precision beacon navigation systems, Shoran, Micro-H, and Gee-H in which reproducibilities of position-finding of roughly 25, 100, and 150 ft respectively have been obtained at distances of approximately 100 miles.

There are, of course, two possible arrangements, one in which the position of the transmitter-receiver is found with respect to the position of two known reflectors as in Fig. 2-20*b*, and one in which the position of a particular object is found with respect to the known positions of two transmitter-receivers as in Fig. 2-20*c*. The latter system is known as

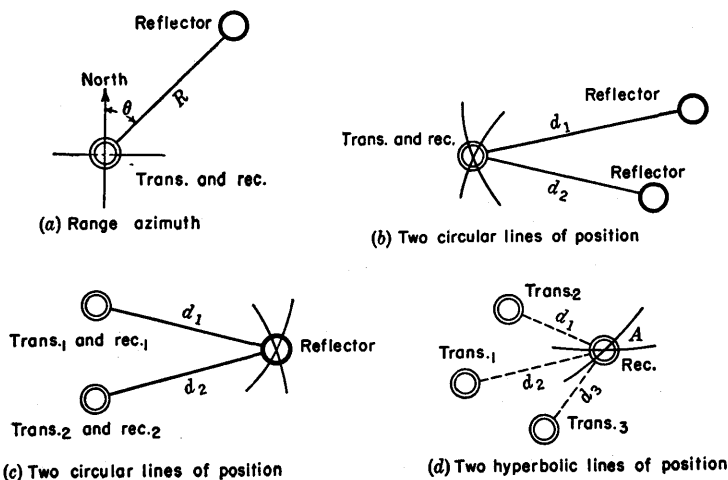


FIG. 2-20.—Some position-finding methods. The figure shows four basic position-finding methods. In (a) the position of the reflector is based on both the range and angle measurements made from a single transmitter and receiver. In (b) two circular lines of position are obtained from a pair of reflectors and a single transmitter-receiver. In (c) these lines are obtained from a pair of transmitter-receivers and a single reflector. In (d) two hyperbolic lines of position are obtained by a receiver at point A in combination with three transmitters and two receivers.

“Oboe” when a responder beacon is used at A; it has given reproducibility of roughly 50 ft at 200 miles.

Figure 2-20*d* indicates a system in which only the difference of the distances  $d_1$  and  $d_2$  is measured. For example, if the transmissions of Station 2 are synchronized with those of Station 1, the time difference in reception at A gives the difference of distances to the two stations. A constant difference of  $d_1$  and  $d_2$  defines a hyperbolic line of position having Stations 1 and 2 as its foci. The intersection of this line of position with another similarly derived from Stations 1 and 3 gives the position of A. Although this system has geometry that yields somewhat less accuracy than a system employing circular lines of position, it is of extreme importance because it permits the position of A to be found by receiving equipment alone. Examples of this system are Loran and Gee.

A brief discussion of the characteristics of a few practical position-finding systems follows.

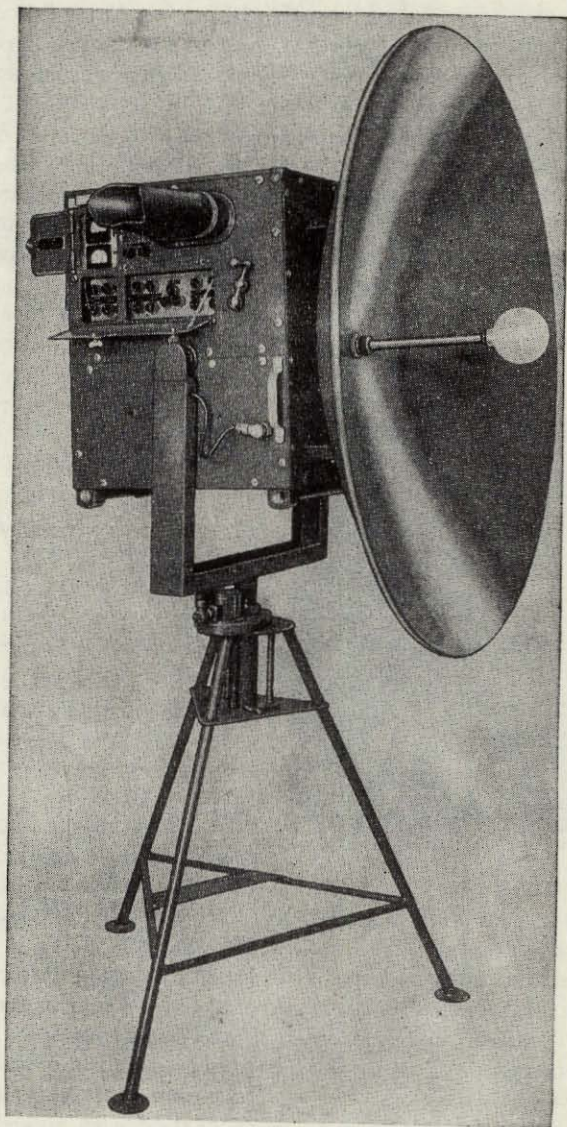


FIG. 2-21.—A microwave radar system specialized for accurate range measurement.

**2-16. Pulse Echo Systems.**—A simple radar system specialized for accurate range measurement is shown in Fig. 2-21. At a frequency of 3000 Mc/sec and with a 4-ft paraboloid, a beamwidth of  $4^\circ$  is obtained.



This beamwidth combined with a pulse length of  $1\ \mu\text{sec}$  gives satisfactory discrimination of shipping and some distinctive landmarks. Time demodulation is accomplished by a circular or type J oscilloscope, which provides an accurate time scale. A type B indication is provided for initial selection of the desired echo and for angular measurements (see Sec. 7-27).

With devices of this type, measurement of the range of isolated reflectors is accurate to between 15 to 50 ft depending upon the rise time of the received pulse, the accuracy of the timing circuit, and the character of the reflector. The accuracy of range measurement does not depend upon the distance measured (at least up to 10 miles) because of the character of the timing circuit employed (see Sec. 3-15).

Equal accuracy of position is obtainable by angular measurements using the type B indication but only at relatively small distances. For example, usual angular errors for  $4^\circ$  beams are  $\frac{1}{2}^\circ$ , giving errors of 50 ft at distances of one mile. The narrower beams used in 10,000-Mc/sec radar systems developed for airborne navigation and bombing give better accuracy ( $\sim \frac{1}{4}^\circ$ ). Figure 2-22 shows an electronic crosshair on a PPI display of a bombing radar. This crosshair may be set to any one of the visible targets for range and angle measurement. Although special indicators (see Sec. 7-28) and rapid angular scanning may increase the accuracy by a factor of 10, the accuracy of range measurement exceeds that of angular measurement at distances of about 20



FIG. 2-22.—PPI display showing crosshair for range and angle determination.

miles. For further discussion of the precision of angular measurements, the reader is referred to Vols. 1 and 2.

A critical test of the accuracy of distance and speed determination in pulse systems is afforded by measurements of the flight of the projectile since accurate calibration is afforded by existing techniques. In a particular case using photography of a 200-yard type J display (see Sec. 3-19) with SCR-584 and a special wide-band receiver (4Mc/sec), the track of a rocket was recorded over a distance of 2000 yd with an error of 4 yd; a corresponding value of the velocity accurate to 1 part in 500 resulted. Other experiments using less sensitive indicators and receivers of normal bandwidth (1 Mc/sec) gave velocity measurements accurate to approxi-

mately 1 per cent corresponding to an error of 30 ft/sec in a distance of 2000 yd. In this method the rate information is not immediately available, nor was it immediately needed. In systems used for tracking the fluctuating signal from aircraft when the rate information is needed immediately for fire control, the accuracy is not so good, and in a system comparable to the one employed above, errors of 2 or 3 times the values obtained for a projectile are observed. In a system having an intrinsic accuracy of about 10 ft, errors of range rate about 20 ft/sec with smoothing times of one-half second are observed in tracking a 300-mph aircraft.

**2-17. Radar Beacons.**—Isolated reflectors such as aircraft, ships, buoys, and abrupt points of land extending into water make relatively satisfactory objects for range-finding but it is often extremely difficult to find satisfactory objects overland. Even isolated reflectors, however, give inexact range readings since they have irregularities which result in considerable variation of the intensity of the reflected energy. Further-

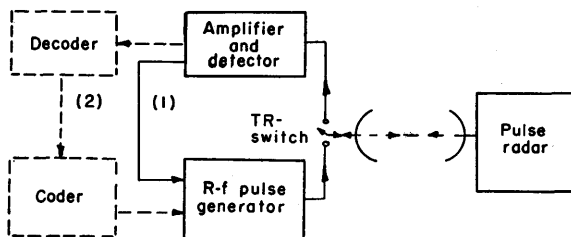


FIG. 2-23.—Block diagram of radar beacon.

more, moving objects result in additional intensity variations. A specially constructed reflector called a "corner reflector" (see Vol. 1, Sec. 3-2) is necessary for more reliable range readings.

For accurate overland distance measurement with microwave radar and for all types of measurements made with longer-wave systems, it is desirable to employ a precisely located beacon in place of a reflector. These devices, variously called "beacons," "responders," or "slave stations," are pulse relay systems that repeat the incident pulse with a known and constant time delay.

A beacon responding to the interrogations of the pulse system replies on a wavelength suitable for the receiver of the distance-measuring system and often in a manner characteristic of the particular beacon. For example, the system of Fig. 2-1 may interrogate the responder shown in Fig. 2-23. The beacon consists of an amplifier and detector suitable for generating a pulse of sufficient amplitude to initiate the operation of an r-f pulse generator which replies to the incoming pulses as in (1) of Fig. 2-23. Often the reply is in the form of a train of pulses, the number and spacing of which are determined by a coder as in (2). In certain cases



the beacons are arranged to respond only to a particular code in order that a particular transmitter may designate the beacon to reply.

The reply of the beacon is characterized by two faults in so far as accurate distance measurements are concerned. The first is the inevitable delay between the reception of the interrogation and the transmission of the response. This delay is due to a number of factors which are discussed in Secs. 3-1 and 3-2. The principal cause, however, is the delay of the receiver. In addition, the decoding of a coded interrogation pulse requires an interval equal to the length of the code. These delays introduce a fixed correction in the distance measured and the apparent distance of the beacon is always greater than its actual distance by several hundred yards. The second fundamental fault is due to the variation of the actual delay in the response with variations in the amplitude of the interrogating signal. This effect is due not only to the characteristic of the receiver discussed in Sec. 3-2 but also to the characteristic of the decoder. With careful design this variation may be reduced to  $0.1 \mu\text{sec}$  for a wide variation of signal intensity. A complete discussion appears in Vol. 3.

**2-18. Hyperbolic Systems.**—These systems, known as “Loran” and “Gee” navigational systems, permit distance-finding in a number of applications where weight or power restrictions prevent the use of transmitting equipment. In military operations requiring secrecy, these systems are advantageous in that no transmission is required. In other situations, for example, where a large number of mobile craft require distance information, no problem of mutual interference is involved. One serious drawback to their use as traffic control systems is that no indication of the position of the receiver is obtained at the transmitting stations.

A system has already been mentioned (see “Decca,” Sec. 2-4) in which synchronized continuous waves are sent from two stations to a remote receiver and increments of distance are obtained by phase demodulation. The Loran and Gee systems, however, employ a pulse subcarrier of sufficiently low frequency (25 and 500 cps, respectively), to permit unambiguous distance measurements over the entire range.

In these systems a simple beacon indicated by Fig. 2-23 is not employed because the bandwidth and signal-to-noise ratio are inadequate to permit direct synchronization of the responder. In addition, it is desirable to introduce very large coding delays to permit identification of master and slave stations. A block diagram of a possible system is indicated in Fig. 2-24 and it is seen that the system contains three synchronized timing oscillators. The PRF is set by the master station, and those of the slave station and the receiver are controlled by a process of frequency and phase demodulation which may be either manual or automatic.

The receiving station employs time demodulation for measurement of the interval elapsing between the reception of master and slave pulses. Accuracies of  $\frac{1}{2} \mu\text{sec}$  are achieved with 2-Mc/sec Loran under good conditions. For higher accuracy, some experimental systems employ a com-

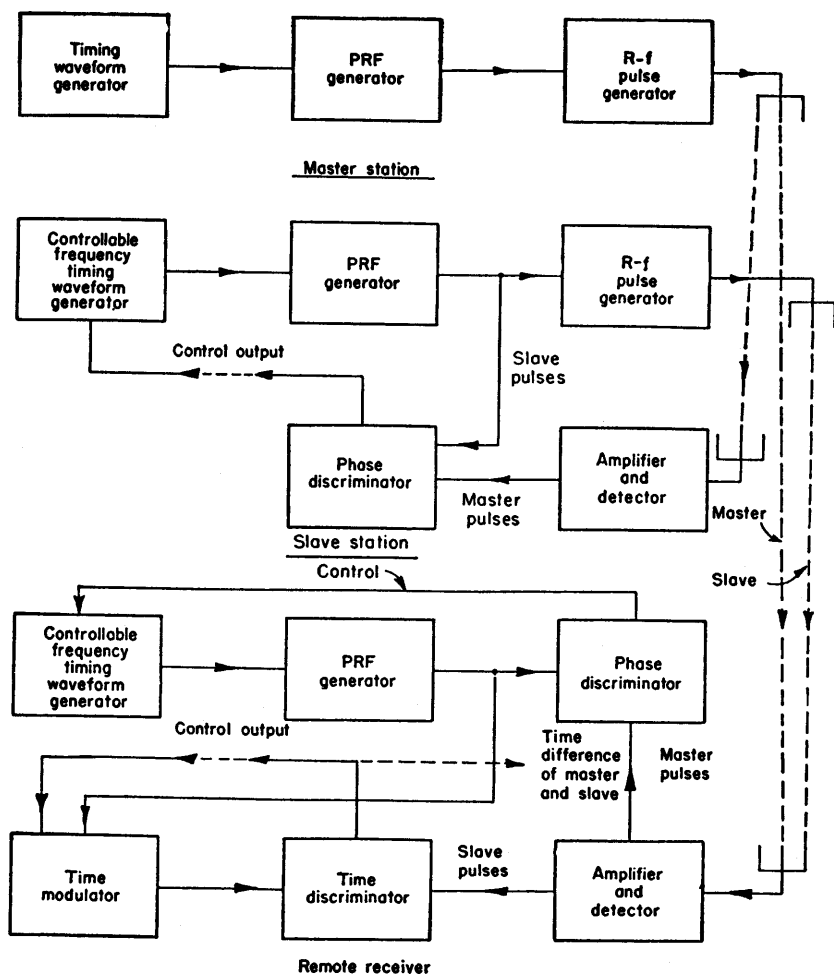


FIG. 2-24.—A hyperbolic system.

bination of time and phase demodulation as indicated in Fig. 2-5 and discussed in Sec. 2-4, and values of  $0.1 \mu\text{sec}$  may be obtained. Practical timing circuits are given in Sec. 7-31 and the whole system is presented in Vol. 4.

**2-19. An Omnidirectional Beacon Using Time Modulation.**—An interesting use of precision distance measurements for obtaining angular data is indicated in Fig. 2-25. In a hyperbolic system in which the base line is extremely short compared with the distance of the remote receiver, the time difference measured is proportional to the angular position of the receiver with respect to the antenna system. A master and slave combination similar to that used for position-finding is indicated in Fig. 2-25 except that the distances are so short that direct wire transmission from *D* to *A*, *B*, and *C* is possible and the transmitter is alternately switched from

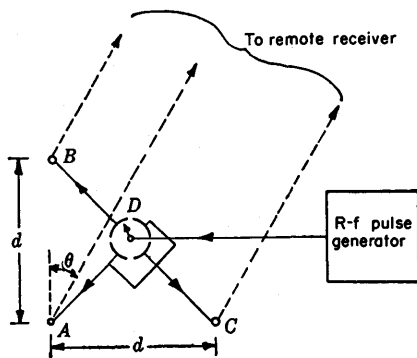


FIG. 2-25.—An omnidirectional beacon using time modulation.

*A* to *B* to *C*. The relative times of arrival of pulses from *A*, *B*, and *C* at a remote receiver varies, depending upon its angular position. For example, when a receiver is positioned as indicated in Fig. 2-25, pulses from *B* are received first—those from *C* second—and those from *A* last. The time difference of the received pulses, for example, on switching from antenna *A* to *B* is proportional to  $D \cos \theta$  where  $\theta$  is the direction of the receiver. In a typical system where  $d$  is equal to 500 ft, the maximum time difference is equivalent to  $\frac{1}{2} \mu\text{sec}$ <sup>1</sup> and a sensitivity of  $0.01 \mu\text{sec}$  or approximately  $1^\circ$  is obtained. Details of this system are given in Sec. 10-8.

<sup>1</sup> One-way transmission at approximately 1000 ft/ $\mu\text{sec}$ .

## CHAPTER 3

### TECHNIQUES OF PULSE TIME MEASUREMENTS

By BRITTON CHANCE

This chapter deals with the characteristics of the components and with their possible arrangements to make different types of systems. Methods of time measurement will be surveyed, and an attempt will be made to establish continuity between the treatment of the basic methods of waveform generation and manipulation discussed in Vol. 19 and the practical circuits to be described in later chapters of this book on manual and automatic time measuring systems. The transmitter and receiver are treated briefly and the time-measuring components in some detail. As stated in Sec. 2.3, precision time demodulation requires the processes of time modulation, time discrimination, and control.

#### TRANSMISSION AND RECEPTION

##### 3.1. Transmission of Pulses.

Common to all distance measuring systems using pulse time methods is the necessity for transmitting a rectangular waveform of short duration. Usually a high-voltage switch is used to connect the supply voltage momentarily to an r-f oscillator, for example, the magnetron. Figure 3.1 shows two typical circuits for generating a 1- $\mu$ sec pulse. Full details appear

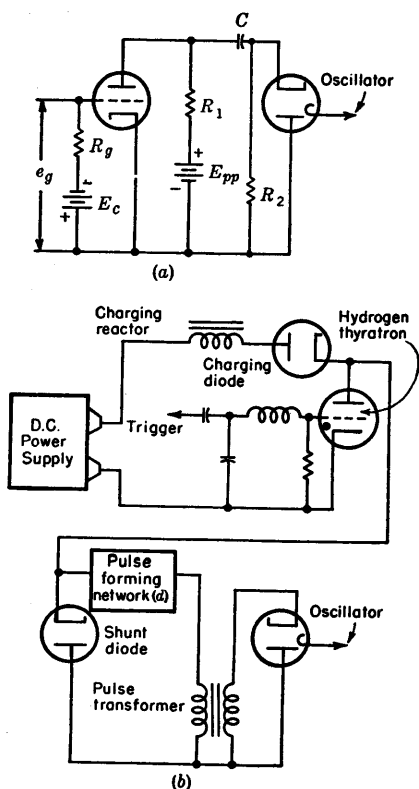


FIG. 3.1.—Two types of high-voltage pulse-generator circuits. In (a) vacuum tubes are used in the switch to discharge condenser  $C$ . In (b) a hydrogen thyatron is used to discharge the pulse forming network  $d$ .

in Vol. 5.

Accurate time measurements require exact reproducibility of the switching waveform and rapid rise of the transmitted pulse. The switching waveform and the rise of the oscillator current for a  $0.1\text{-}\mu\text{sec}$  pulse are shown in Fig. 3-2. More rapid rises ( $\sim 5 \times 10^{-9}$  sec) have been employed, but unstable operation of the magnetron is often observed (see Vol. 6). It is often desirable to employ as short a pulse as possible to obtain high discrimination in range. Durations of  $0.05$  to  $0.1\text{ }\mu\text{sec}$  have been used in experimental systems.

The actual buildup of oscillations in three types of oscillators, a  $3000\text{-Mc/sec}$  magnetron, a  $2\text{-Mc/sec}$  triode, and a  $16\text{-kc/sec}$  timing oscillator, is shown in Fig. 3-3. It is seen that the number of cycles required to reach full amplitude in the case of the two r-f oscillators is

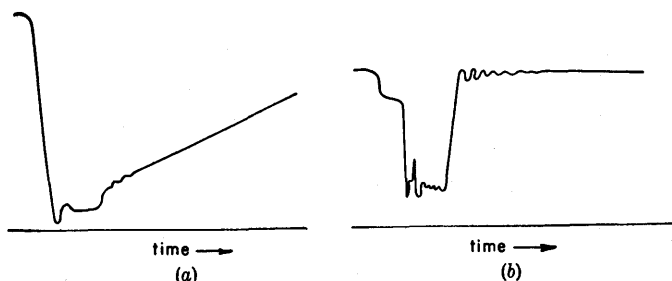


FIG. 3-2.—Voltage and current waveform in a magnetron oscillator. (a) shows the applied voltage waveform and (b) the oscillator current. The pulse duration is  $1\frac{1}{2}\text{ }\mu\text{sec}$ . In (a) the slow decay of the switching waveform is not typical of good modulator performance and could easily have been arranged to decay more rapidly. These pulses were generated by a circuit similar to that of Fig. 3-1a.

large compared with that of the timing oscillator. The rise of the oscillations in the magnetron (30 cycles,  $0.01\text{ }\mu\text{sec}$ ) is probably limited by the rise of the switching waveform but is sufficiently rapid for most distance measurements. The buildup of oscillations in the Loran transmitter is intentionally limited to 8 cycles or  $6\text{ }\mu\text{sec}$  in order to avoid an excessively wide spectrum and consequent interference with radio communication. To achieve reproducibility of time measurements, the shape of the transmitted pulse is carefully monitored and controlled. The initiation of oscillations in the  $16\text{-kc/sec}$  oscillator is obtained by interrupting the initial conditions either of maximum current through the inductance or of maximum voltage across the capacitance of the oscillating circuit (see Vol. 19, Sec. 4-14). Under these conditions starting times of a small fraction of a cycle are obtained. Similar performance has been obtained from oscillators operating at 30 to  $60\text{ Mc/sec}$ , but is rarely obtained in pulsed r-f oscillators where a switching wave usually supplies the plate power, and the buildup of oscillators is determined by the  $Q$  of the tuned circuits and the negative resistance of the oscillator.

Although the time delay between the rise of the switching waveform and the initiation of r-f oscillations in the magnetron is extremely small ( $< 10^{-9}$  sec), this interval may be appreciable in other oscillators, for example, the lighthouse-tube oscillators.<sup>1</sup> Figure 3-4 indicates 0.3- $\mu$ sec delay between the rise of the switching waveform and the initiation of oscillation in type 2C43. Not only does this factor have to be taken into account in the calibration of ranging equipment, but short- and long-period variations of this value must be kept at a minimum in order to avoid serious errors.

The short-time variations can be practically eliminated by the introduction of a low-level c-w signal at approximately the resonant frequency—and some reduction of the delay is also achieved. This method is particularly useful at frequencies of 200 Mc/sec.

### 3.2. The Reception of Pulses.—

As far as is known, the propagation of the transmitted pulse to the reflector and back to the receiver occurs at the velocity of light. The distortion of the leading edges of pulses reflected from some small stationary

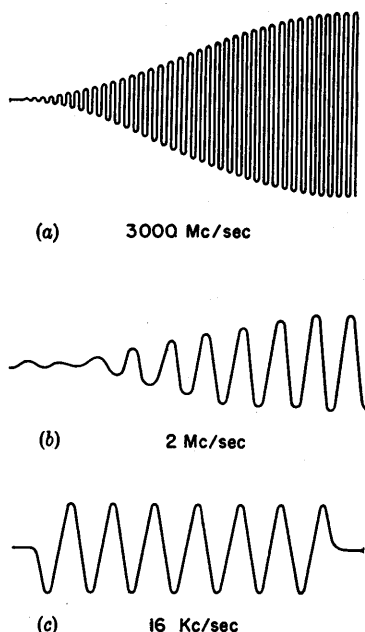


FIG. 3-3.—Tracings of oscillograms representing the starting times of various oscillator circuits. (a) represents the starting of a 3000-Mc/sec magnetron oscillator. To achieve full amplitude 30 oscillations are required. (b) represents the initiation of oscillations in a Loran transmitter operating at 2 Mc/sec. The buildup of oscillations here closely follows the rise of the switching waveform. (c) shows the initiation of oscillations in a 16-kc/sec timing waveform generator. Note that practically rapid starting is obtained.

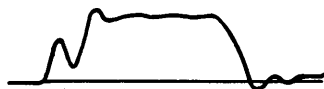


FIG. 3-4.—Delay between the switching waveform and the initiation of r-f oscillations. The buildup of oscillations in a lighthouse tube (2C43) operating with 1000 volts at the plate is shown, indicating a delay of roughly  $\frac{1}{2}$   $\mu$ sec. The duration of the current pulse is 1.16  $\mu$ sec.

objects is slight, but distortion of pulses reflected from other objects may be very serious and is due to the interference between rays reflected from various parts of the object (see Vol. 1).

**Bandwidth and Rise Time.**—An ideal receiver would exactly reproduce the transmitted waveform, and thus achieve optimum accuracy. Unfortunately, no receiver has been made to reproduce

<sup>1</sup> A microwave triode transmitter tube (see Vol. 7).

faithfully the shape of the magnetron pulse represented in Fig. 3-3a. At present, considerations of signal-to-noise ratio and the characteristics of available vacuum tubes set a limit to receiver bandwidths of 10 to 20 Mc/sec which restricts the accuracy of the distance measuring system. For optimum signal-to-noise ratio, the receiver bandwidth (see Vol. 18,

Sec. 7-1, and Vol. 23) is related to the pulse duration by the expression

$$t = \frac{1.2}{\mathfrak{B}},$$

where  $t$  is the pulse duration (microseconds) and  $\mathfrak{B}$  is the intermediate-frequency bandwidth (megacycles per second). Deviations from this optimum give only slight decreases of signal-to-noise ratio.

The rise time  $t_r$  obtainable with a given value of  $\mathfrak{B}$  is

$$t_r = \frac{0.7}{\mathfrak{B}}.$$

The output of a wideband receiver is shown in Fig. 3-5. The error of time measurement,  $\Delta t$ , will be roughly  $\frac{1}{20}$  the time of rise of the received signal for usual types of displays (see Sec. 7-13).

Some typical examples are given in Table 3-1:

TABLE 3-1.—CALCULATED VALUES OF ERROR OF TIME MEASUREMENT

System	$\mathfrak{B}$ , Mc/sec	$t_r$ , $\mu$ sec	$\Delta t$	
			$\mu$ sec	ft
Experimental radar.....	16	0.05	0.003	1.5
SCR-584.....	1.3	0.5	0.03	15
Loran.....	0.050	20	1	500

The figures in the last column are in good accord with the observed consistency of measurements on distinctive targets for the first two systems. For Loran the accuracy is intrinsically much greater than that indicated because of a more accurate method of pulse-matching.

*Delay Time.*—A second important characteristic of a receiver is its delay time, which adds a fixed correction varying from 50 to 200 ft

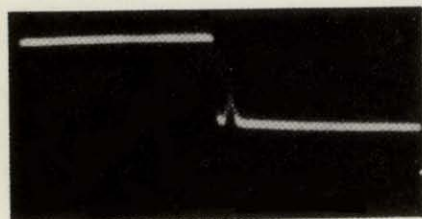


FIG. 3-5.—Output pulse of a wide-band receiver displayed on a cathode-ray tube. The sharp pulse following the abrupt drop of the range index has a duration of roughly 0.1  $\mu$ sec and is obtained from an experimental receiver of approximately 16 Mc/sec bandwidth. The steep drop of the range index (0.1  $\mu$ sec) can be set to the rise of the video pulse to an accuracy of better than 1 yd. The sweep duration is roughly 6  $\mu$ sec.

depending upon the bandwidth and number of stages of the receiver (see Vol. 18, Chap. 4).

This delay is expressed approximately as follows:

$$t_d = \frac{0.6}{\Omega}$$

for a six- or seven-stage single-tuned amplifier. The delay is roughly twice this value for a double-tuned amplifier of the same number of stages. In actual practice,  $t_d$  is measured for each particular radar system, and for a given radar it is found to be reproducible. The measurement of  $t_d$  is discussed briefly in Sec. 3-6.

*Variation of Delay with Signal Amplitude.*—A third practical consideration in the choice of receiver bandwidth is the effect of signal-amplitude fluctuations upon the time delay of the received pulse. In radar systems for tracking moving targets, such as ships or airplanes, interference effects give very large signal fluctuations. Also the echo is often amplitude-modulated by the angular scan of the radar. Figure 3-6 indicates variations of the time delay of an echo due to two types of receivers of inadequate bandwidth.

*Gain Control.*—The error due to signal-amplitude fluctuations is considerably reduced by automatic control of the gain of the receiver. Simple circuits that will maintain the average value of the signal amplitude constant are well known, and manyfold reduction of the range errors is readily obtained. Often the fluctuations of signal intensity are at a rate comparable to the pulse-repetition frequency—for example, fluctuations due to propeller modulation, slow changes of aspect, or angular scanning. Rapidly acting gain-control circuits may be used to remove amplitude changes due to these causes. Since some of these modulations may bear

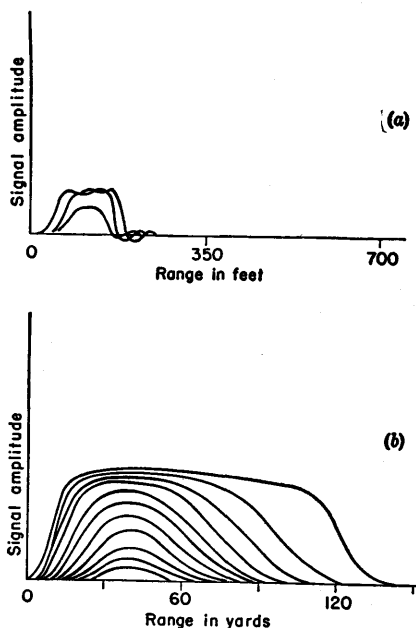


FIG. 3-6.—The effect of signal amplitude variation upon time delay in receivers of inadequate bandwidth. In both (a) and (b) the signal of smallest amplitude is delayed the most, and increasing amplitudes give an apparent decrease in range. The receiver of AN/APS-15 is represented by (a) and that of AN/APG-5 is represented by (b).



desirable information—for example, modulation due to angular scan—these voltages are recovered as a fluctuation of the control signal to the intermediate frequency amplifier and are suitable for directional control (see Sec. 9-5).

In hyperbolic navigation systems, the time difference between the reception of two signals is required. Since both these signals pass through the same amplifier, they are delayed an equal amount provided they are adjusted to the same amplitude. The Loran display is designed to permit the adjustment of the received signal amplitudes to equality. An electronically switched display and gain control are used so that the two received signals are alternately displayed and controlled in response to the setting of separate gain controls. If signal-intensity changes occur simultaneously for both waveforms, then the compensation for time errors occurs automatically. Otherwise, manual or automatic gain control may compensate for differential fluctuations of the signal amplitudes. In this way a high accuracy of time measurement is obtainable with a narrow-band receiver.

Since time-discrimination circuits are never perfectly balanced, their sensitivity to amplitude changes is minimized by satisfactory gain control. In addition, automatic gain control gives optimal immunity from smaller interfering signals, since the gain control is always held to the value relevant to the desired signal. In view of all these advantages, this feature is included in all receivers in which range accuracy is important.

Automatic gain control does not always ensure the elimination of receiver-delay variations due to signal-intensity changes, since alterations of the gain-control voltage itself may cause variations in receiver bandwidth and hence variations in time delay. In particular, gain control that depends upon variation of the transconductance of an amplifier tube must also vary the bandwidth of this stage to a certain extent. Quantitative data are available on this effect for SCR-584, where a 30-db signal-amplitude change resulted in a variation of receiver delay of 0.1  $\mu$ sec in spite of the maintenance of a constant output amplitude.

*Differentiation.*—Pulse-sharpening or pulse-differentiating circuits and large amplification have been used to increase the rate of rise of the receiver output; some typical circuits are given in Vol. 19, Sec. 9-8. No real increase in accuracy is obtained, however, that could not be achieved by more sensitive time-discrimination circuits. A differentiated pulse, however, may be convenient for manual range-tracking on a cathode-ray-tube display.

### SYNCHRONIZATION

Synchronization is the process of ensuring that the time reference for the time-modulation system and the time-demodulation system is the

same or differs by a known amount. The accuracy of range measurement depends upon the consistency of synchronization.

Various methods of synchronization are shown in Fig. 3-7 and are discussed individually in Secs. 3-3 to 3-5.

**3-3. Synchronization by the R-f Pulse Generator.**—Some high-voltage pulse generators generate their own recurrence frequency; for example, a motor-driven switch is often used. As indicated by (1) in Fig. 3-7, this provides a simple and straightforward method of synchronization, because the switching waveform or the oscillator current waveform may be used to initiate the operation of the time demodulator without the

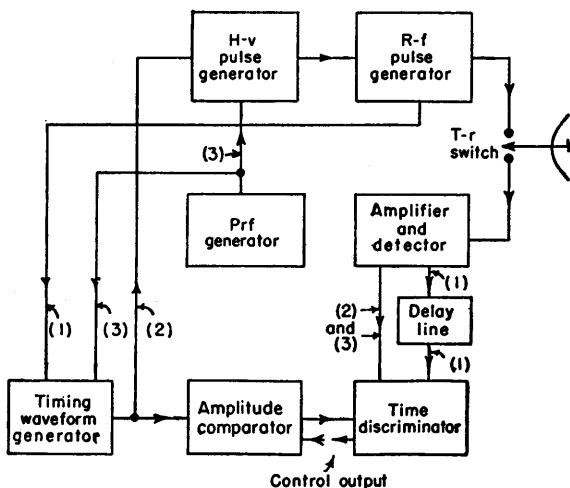


FIG. 3-7.—Three methods of synchronization. (1) Synchronization by the r-f pulse generator. (2) Synchronization by timing waveform generator. (3) Synchronization from the PRF generator. The numbers on each line indicate the path of the various signals in each system.

need for a separate PRF generator. This method imposes severe design restrictions upon the time-demodulation circuits. For example, the timing-waveform generator must be restarted with every transmitted pulse in order to maintain synchronism. Crystal, or *LC*, pulsed sinusoidal oscillators or *RC*-controlled triangular-waveform generators are therefore required. Variable delays in the initiation, and the termination of waveform before the next transmitted pulse represent serious design problems. In this respect *RC*- and *LC*-controlled timing circuits are much more satisfactory than pulsed crystal oscillators (see Vol. 19, Sec. 4-15). The stability of continuous oscillators is, however, closely approached in some designs of pulsed oscillators (see Sec. 3-10).

*Initiation of the Timing Waveform.*—Simultaneous initiation of the timing waveform by the transmitted pulse is not usually achieved even

in the most carefully designed circuits. As a result, each system has a correction to be applied to compensate for this delay. This correction varies from a fraction of a microsecond for *RC*-controlled triangular timing waveforms to several microseconds for pulsed crystal oscillators. The starting time of pulsed *LC*-oscillators is very small, and the transient response of associated phase-shifting networks usually determines the delay in operation. This, however, rarely exceeds  $\frac{1}{4}$  cycle of the timing wave. The necessary correction is usually determined by measuring the error in the range of a target at a known distance.

*Minimum Range.*—Another consequence of the delay in the initiation of the timing waveform is the inaccuracy of range measurements made a few microseconds after the transmitted pulse. This sets a limit to the minimum distance measurable. In many circuits this corresponds to a few per cent of the full range scale, and it is often desirable to insert a delay device between the receiver output and the time discriminator as shown in Fig. 3-7. This permits continuous range readings through zero. A delay line of 3 to 4  $\mu$ sec is required, and its temperature coefficient may cause additional errors (see Vol. 19, Sec. 13-7).

**3-4. Control of the PRF by the Timing Waveform.**—This method of synchronization, shown as (2) in Fig. 3-7, permits complete freedom in the design of the timing-waveform generator and usually results in a distance-measuring system of greater simplicity and accuracy than any other. One of the principal advantages is that a continuously oscillating time standard, such as a crystal-controlled oscillator, is employed. The reliability and stability of the quartz crystal remove the need for any other time standards. A chain of frequency dividers may be employed to generate a synchronizing pulse of a constant or adjustable PRF for the transmitter, as discussed in Secs. 3-13 and 3-15. Simple circuits are available for giving precise phasing between the sinusoidal oscillator and the trigger pulse. Finally, the essentials of simple and accurate multiple-scale range systems form an integral part of the oscillator frequency-divider system (see Sec. 3-15).

Another advantage of this type of synchronization is that continuous and accurate time measurements may be made before and after pulse transmission. Since the timing-waveform generator operates continuously, any errors due to its starting time are eliminated. In their place, however, other errors arise. In some designs the phase of the output of the frequency-dividing system may vary with respect to the timing waveform. This error may be almost completely avoided by the use of a frequency divider that incorporates time selection of a pulse generated at the frequency of the timing waveform (see Sec. 4-8). Another error may arise from a variation in the delay between the trigger to the high-voltage pulse generator and the transmission of the r-f pulse. In order

to minimize these difficulties, an extremely rapid trigger is used to initiate the high-voltage pulse generator that in turn must initiate the radio-frequency oscillations with extreme rapidity. The latter is accomplished satisfactorily in most cases (see Sec. 3-1).

If the given synchronizing waveforms are of equal rapidity, there is very little to choose between the accuracy of synchronization obtainable with this method and that described in Sec. 3-3. The main advantage of this method is the simplicity, economy, and accuracy of the time modulator built around the crystal oscillator and the frequency divider. The disadvantage is the regularity of pulse-recurrence interval.

**3-5. Synchronization by a PRF Generator.**—A separate PRF generator may be used to initiate the operation of the time demodulator and the r-f pulse generator as shown by (3) of Fig. 3-7. This connection is subject to the errors of both the previous systems since the starting times of both the r-f oscillator and time demodulator may vary. This connection is, however, often employed for medium-precision ranging systems having *RC* timing elements in the time demodulator and vacuum-tube switches in the high-voltage pulse generator. The operation of the time demodulator is usually started in advance of the r-f transmitter by a precisely known time interval to permit accurate zero calibration and to indicate the transmitted pulse on the cathode-ray-tube display.

A variant of this type of synchronization is one in which the function of the PRF generator is to select a train of timing waves from a continuous oscillator. The first member of this pulse train serves as the reference pulse of the time-demodulation system and also as the trigger for the r-f pulse generator. The other members of the selected pulse train are used in the timing circuits. The necessity for a frequency divider is avoided, and yet exact synchronism between the timing waveform and the r-f pulse is maintained. Also the average PRF is continuously variable (see Sec. 4-9).

**3-6. Zero Calibration.**—The existence of a number of fixed or variable delays between emission of the r-f pulse and initiation of the demodulation system has been indicated. If accurate time measurements are required, a zero-calibration procedure must be employed to determine the exact value of the delay and to correct for any variation which may occur because of the effects of time, temperature, or other variables upon the equipment.

The zero point for distance measurement is the moment of appearance, at the terminals of the time discriminator, of an echo from a target corresponding to zero range. This echo is, of course, never physically realizable because of the finite length of the transmitted pulse. A satisfactory substitute is a reflector placed at a known distance (approximately 1000 ft) that is large compared with the pulse length. The time-de-

modulation circuit is calibrated against some known standard such as the crystal-controlled oscillator. The difference between the reading of the time demodulator and the known distance of the artificial reflector then gives the proper zero correction for the system. This correction takes into account all errors. Particular care is needed when using time-demodulation circuits in which the calibration of the zero point interacts with the calibration of its slope.

Since the precise location of such a reflector is an extremely awkward operation under field conditions, any alternative proposal is preferable although the zero-calibration procedure becomes much more involved and much less accurate. One may assume that the signal of largest amplitude appearing at the output terminals of the receiver is the r-f pulse and that this pulse corresponds to an echo of zero range. This assumption is rarely justified since the energy of the high-voltage of r-f pulse may be sufficient to excite the later amplification stages of the receiver and in this way arrive in advance of energy which has traveled the same path as a received echo. Depending upon the shielding of the receiver and the energy of the transmitted pulse, the signal obtained in this manner may anticipate the true zero point of range by values indicated in the following table and must, therefore, be initially calibrated as described above. Such calibration is constant and holds true for a given type of radar.

TABLE 3-2.—APPROXIMATE ZERO CORRECTION FOR TYPICAL RADAR SYSTEMS

System	$\Delta t_0$ , $\mu\text{sec}$
Experimental radar.....	0.1
SCR-584.....	0.2
AN/APG-5.....	0.3

A practical difficulty in measuring the time of appearance of the pulse corresponding to zero range is due to possible nonlinearity of the characteristics of the time demodulator near zero range. If the time demodulator covers a range greater than the interval between transmitted pulses, the zero setting is made, not with respect to the transmitted pulse, but with respect to the pulse immediately succeeding it. For systems having a known and constant repetition interval, this eliminates the effects of any short-range nonlinearities of the time-demodulation circuit.

**3-7. Remote Control of Synchronization.**—Navigational systems in which a time demodulator is located remotely are synchronized by radio transmission of the reference pulse. This pulse may initiate the timing waveform of the remote receiver by direct triggering, or may be protected by pulse coding and decoding or pulse-recurrence-frequency demodulation. It is necessary to consider not only the rate of rise of the synchronizing waveform but also the effects of noise and interference on the reliability and accuracy with which the remote time demodulator is synchronized.

Since a single uncoded pulse is rarely satisfactory, the simplest systems employ coding and decoding circuits depending upon pulse duration or spacing. As shown in Vol. 19, Sec. 10-2, the earlier members of a multiple-pulse code permit unique time selection of the later members. The security of a code against interference increases much more rapidly than the number of pulses in the code. In a particular case the frequency at which a three-pulse code will be simulated by several interfering radars is but  $\frac{1}{1000}$  that of a two-pulse code.

If interference is heavy or the rise time of the synchronizing pulse is not sufficiently rapid to secure accurate triggering by pulse coding and decoding, pulse-recurrence-frequency demodulation is employed (see Fig. 2-23). This method has several advantages. If the transmitted PRF is crystal-controlled, the frequency-modulated oscillator of the frequency demodulator may also be crystal-controlled and have a stability permitting operation for appreciable intervals in the absence of synchronizing pulses. For example, in Loran ground stations synchronization loses accuracy ( $\frac{1}{2}$   $\mu$ sec) only after a 3-min interruption—corresponding to a loss of 4500 pulses. Another advantage of crystal-controlled PRF is that the oscillator may generate the timing waveform of the time demodulator.

Often initial selection of the correct PRF is made on the basis of pulse coding and decoding since instantaneous response to the correct code is obtained. This process is then combined with PRF demodulation.

## TIME MODULATION

### GENERAL DESCRIPTION

The subject of time modulation has been discussed extensively in Vol. 19, Chaps. 7, 9, and 13, and a number of practical single- and multiple-scale circuits are given in Chaps. 5 and 6 of this volume. Only the general properties of time-modulation devices are presented here.

**3-8. Single-scale Time Modulation.**—Time modulation is defined as the modulation of the time interval between two waveforms or between two portions of a waveform. The earlier waveform or portion of a waveform is termed the “time-reference” pulse while the latter is the “time-modulated” pulse. The interval over which time modulation may be expected is termed the “range of modulation.” This may be equal to the pulse-recurrence interval of the radar system, but is usually rather less than this value to permit the pulse-waveform generator to return to

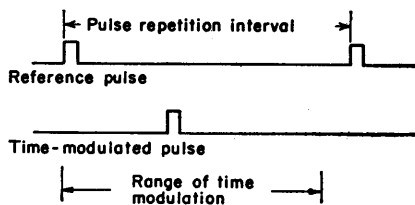


FIG. 3-8.—Single-scale time modulator.

its quiescent condition. The range of modulation, on the other hand, may be small compared with the pulse-recurrence interval as in pulse communication where the duration of the transmitted pulse is sometimes varied. A circuit is termed "single scale" if only one time modulator is used. It contains two timing waves, however, one for synchronization and the other for time modulation, but neither timing wave occurs more than once during the pulse-repetition interval, as shown in Fig. 3-8.

**3-9. Multiple-scale Time Modulation.**—The range of time modulation may be subdivided by a train of fixed pulses as shown in Fig. 3-9. If these pulses are generated from crystal- or *LC*-controlled oscillators,

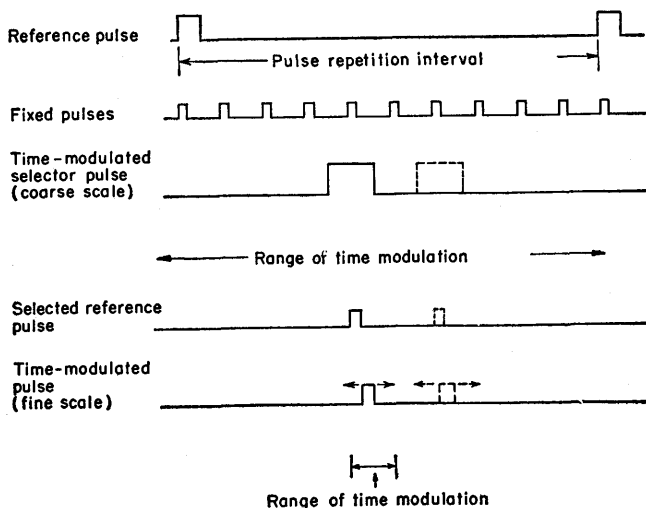


FIG. 3-9.—Two-scale time modulator employing selection of a fixed pulse and interpolation.

extremely accurate subdivisions are obtained and the pulse-recurrence interval may be set by accurately phased frequency dividers. With fixed pulses, there is no actual time modulation, that is, variation of a time interval in response to a control signal. When used on visual displays, interpolation between the fixed pulses is possible, but greater accuracy is obtained by using a time-modulation circuit that is initiated by one of the fixed pulses and has a range of modulation equal to the pulse spacing.

By the time selection of different fixed pulses to serve as the reference pulse for this "interpolating" time modulator, a range of modulation equal to the repetition interval is covered. Time selection of the desired fixed pulse is carried out by a "coarse" time-modulation circuit covering the full range and generating a selector pulse of duration less than the interval between fixed pulses. Mechanical or electrical coordination of the controls for the fine and coarse systems gives a single control of the

fine-scale pulse over the entire range. As shown in Fig. 3-9 this process depends upon two time modulators and a fixed pulse train generated by a precise timing waveform recurring many times during the full modulation interval. Three timing waves are involved, one for the fixed pulses and two for the coarse and fine scales. This combination is said to be "double scale." This arrangement is similar to double-scale synchro systems (see Vol. 19, Sec. 12-6), and the same accuracy increase is obtained.

The error of a time modulator may be considered a fixed fraction of the full range of modulation independent of the time scale. Thus the smaller the range of modulation in time units, the greater the accuracy in time units. Thus the accuracy is proportional to the number of times

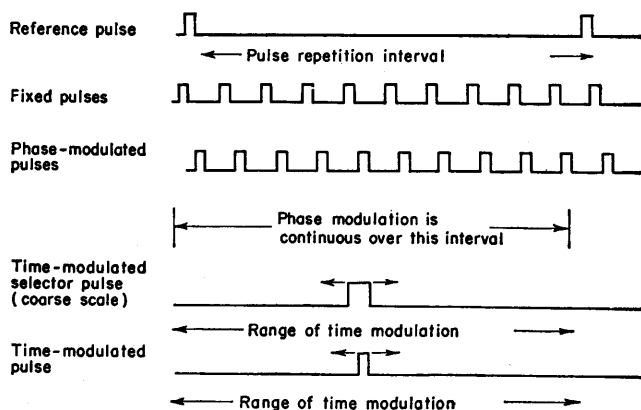


FIG. 3-10.—Two-scale time modulator employing selection of a phase-modulated pulse. the range of modulation is subdivided by the fixed pulses. The accuracy gain corresponding to Fig. 3-9 is 10-fold.

A different type of multiple-scale system depends upon phase modulation<sup>1</sup> (see Sec. 13-13, Vol. 19) of the timing waveform that is also used to generate the train of fixed pulses as shown in Fig. 3-10. Since phase modulation may be carried out by capacitance and inductance phase shifters that shift the phase continuously, effective interpolation over the interval between fixed pulses is immediately achieved, and the phase shifter replaces the interpolating delay.

In multiple-scale operation the extent of phase modulation may cover many cycles of the timing wave, and time selection of a particular member of the pulse train is carried out by a coarse time modulator. The mechanical or electrical connection between the coarse and fine scales is so arranged that a single control gives the same rate of change of time delay to both the phase-shifted pulse train and the selector pulse. A

<sup>1</sup> Frequency modulation of the timing waveform is rarely used.



particular phase-shifted pulse, once selected, is continuously selected over the entire range. The factor by which the accuracy is increased over a single-scale phase modulator is theoretically equal to the number of subdivisions of the range of modulation.

The next sections discuss the accuracy obtained with these timing systems.

### THE CHARACTERISTICS OF COMPONENTS

The precision of waveform generation and the stability of voltage measurements determine the accuracy of electrical timing. Before proceeding with a discussion of the employment of these methods, a brief review of the characteristics of available components will be presented. Greater detail is available in Vols. 17, 18, and 19.

**3-10. Timing Standards.**—Resistance-capacitance, inductance-capacitance, and quartz-crystal standards are used for the generation of precisely timed sinusoidal waves. The  $RC$ -standards are also extensively used for determining the slope of triangular, exponential, hyperbolic, and parabolic waveforms. The accuracy of the  $RC$ -standards for determining the slope of a wave is compared with the accuracy of quartz and  $LC$ -standards for determining the period of a sinusoidal wave.

*Accuracy of Specification.*—The perfection of methods of manufacture and quality control yields quartz crystals of an accuracy considerably in excess of one part per million—a simple and most accurate standard. The precision of manufacture of  $L$ -,  $C$ -, and  $R$ -components is negligible by comparison. Ordinary carbon resistors and paper condensers used in radio receivers are specified to within 5, 10, or 20 per cent depending upon the degree of selection which is specified. Mica dielectric condensers, wire-wound resistors, and permeability-tuned inductors are obtained within considerably closer tolerances, and specifications of 1 per cent are met by most manufacturers. The process analogous to the final grinding of quartz crystals may also be carried out with  $LC$ - and  $RC$ -standards since the period of sinusoids or the slope of triangular waves may be checked against quartz standards and adjusted to an equal precision. This is a more satisfactory procedure than direct measurement of the component values because variations of stray capacitance and tube characteristics usually necessitate a final calibration of the actual circuit.

The form of a sinusoidal or triangular wave may be accurately controlled by the characteristics of the associated amplifier. Negative-feedback circuits of extreme gain stability may be used to achieve a linearity of a triangular wave of a few parts in ten thousand (see Vol. 19, Sec. 7-11).

*Relative Stability of Similar Oscillators.*—The relative stability of crystal-controlled oscillators is outstanding. For example, the relative

drift of the PRF of the timers used in the Loran master and slave stations lies between 0.1 and 0.03  $\mu\text{sec}/\text{min}$ , or 100 and 30 ft/min. This corresponds to a relative stability of one part in  $10^8$  or  $10^9$ , equivalent to that obtainable from high-quality clocks. Greater relative stabilities are observed in cavity-stabilized microwave oscillators where values of five parts in  $10^{10}$  have been obtained (see Vol. 7).

*Temperature Coefficient.*—This characteristic of the timing element is extremely important, especially for airborne applications. Here again the quartz crystal excels since temperature coefficients of several parts per million per degree centigrade are readily obtainable. In *LC* and *RC* timing elements the components have appreciable temperature coefficients. In *RC*-combinations carbon resistors and paper condensers often give changes of 5 or 10 per cent in temperature intervals of  $40^\circ\text{C}$ . On the other hand, carefully selected combinations of mica condensers of negative temperature coefficient with wire-wound resistors of positive temperature coefficient give an over-all temperature coefficient of ten to twenty parts per million per degree centigrade.<sup>1</sup> By careful quality control *LC*-combinations having over-all temperature coefficients of five parts per million per degree centigrade are also obtained.

To obtain ultimate precision thermostatic control of all three types of timing standards is desirable. This practice has been employed for many years in communications transmitters. Relatively compact and simple temperature regulators are available for this purpose.

**3-11. Vacuum Tubes.**—Although the slope or duration of a wave is accurately determined by precision timing elements and negative-feedback amplifiers, the generation of accurate timing indices depends upon comparison of the amplitude of the timing wave to a reference voltage. At the moment of equality of these two voltages, a high-gain nonlinear vacuum-tube amplifier instantaneously responds and marks the equality by a sharp pulse. This process is termed "amplitude comparison" and the combination of circuit elements producing the pulse, an "amplitude comparator" (see Sec. 9-8, Vol. 19). Fluctuations due to the effect of time, voltage, etc., upon a particular vacuum tube or variations among different vacuum tubes of the same type may cause large errors in the indicated instant of equality of the two voltages.

*Accuracy of Specification.*—The thermionic vacuum tube is the least reproducible circuit element used in the processes described in this book. In the case of the popular 6SN7 double triode, the JAN Specification lists an allowable variation of the plate current at constant plate voltage, grid bias, and heater voltage of between 5.5 and 12.5 ma from tube to tube because of variables in the manufacturing process—a

<sup>1</sup> These coefficients unfortunately vary slightly with temperature, and the compensation is unsatisfactory over wide temperature ranges.

variation resulting in an error of time measurement roughly a million times greater than that of ordinary quartz crystals.

There is, however, a specially selected double triode, type 6SU7, in which a pair of triode elements is matched in such a way that the difference between their plate currents is very small. In terms of equivalent grid bias this amounts to less than 0.1 volt, roughly 3 per cent of the linear range.

The cutoff point of thermionic vacuum tubes is very poorly defined and variations between  $\frac{1}{2}$  volt and 10 or more volts (depending upon the type of vacuum tube and the cutoff voltage) may be expected. Diodes, on the other hand, are much more stable in this respect and stabilities of a few tenths of a volt may be achieved. Contact rectifiers, such as germanium crystals, are excellent in this respect, and variations considerably less than a millivolt are obtained. Other portions of their characteristic may, however, be very temperature-sensitive and unsuitable for this purpose.

The grid current of vacuum tubes, although often found to be in the region of a hundredth or a ten-thousandth of a microampere, is permitted to reach a few microamperes in nearly all vacuum tubes before they are rejected by the manufacturer. The type 6SU7 has, however, a specification requiring a grid current of less than 0.01  $\mu$ amp.

*Effect of Time and Mechanical Shock.*—The change of the characteristics of a thermionic vacuum tube with time is considerable, and variations corresponding to 10 mv of grid bias (at constant plate current) per week are obtained even under the most carefully controlled conditions. Diodes represent some improvement over this figure, and contact rectifiers are superior. Another variable in vacuum-tube circuits is the effect of mechanical shock which ranges from several hundred microvolts to complete destruction of the elements. In this connection it is interesting to note that "ruggedized" tubes apparently give little reduction of microphonics, although they undoubtedly withstand larger accelerations without failure. There is some evidence to indicate that the subminiature tubes, type 6K4 etc., have very small microphonic noise.

The stability of gaseous discharge tubes used for voltage standards is roughly 1 per cent of the nominal voltage if variations due to tube changes are excluded. For higher accuracy, electrochemical standards are preferable (see Vol. 21, Sec. 15-2).

**3-12. Calibrated Subassemblies.**—The largest variable of timing circuits based upon *R*-, *L*-, and *C*-components and thermionic vacuum tubes is the accuracy of their specification. Nearly all the difficulties of manufacture and maintenance of precision equipment may be attributed to this factor. This is due, in a large part, to the desire of consumers to replace vacuum tubes without recalibration simply because they may be

plugged into their sockets, as opposed to the replacement of "fixed" components, such as an inductor in an oscillator circuit where recalibration is recognized as essential.

A solution to this difficulty lies in the use of functional subassemblies in which the circuit components are adjusted to account for the variations in the characteristics of vacuum tubes. In fact, such functional subassemblies may be precalibrated to equal standards of performance during the manufacturing process. The replacement of a faulty subassembly can therefore be accomplished without loss of calibration provided the consumer is willing to discard the faulty unit.

This procedure is probably impractical with ordinary receiver tubes, but the "solder-in" subminiature vacuum tubes present new possibilities,

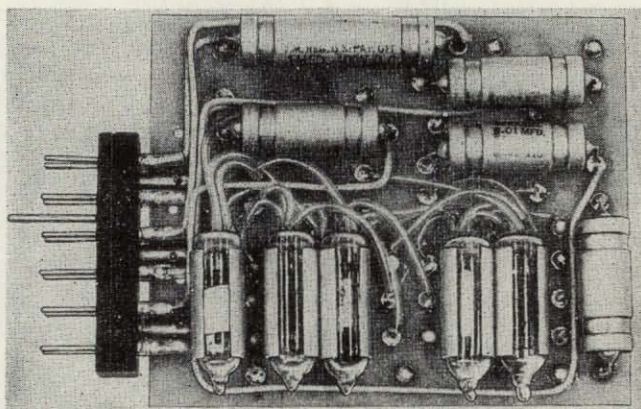


Fig. 3-11.—A calibrated subassembly used in an experimental model of a Loran indicator.

and an example of a calibrated subassembly using these tubes is shown in Fig. 3-11. The resistance elements of this circuit (not shown since they are mounted on the back of the card) are chosen with regard to the characteristics of the particular vacuum tube used in order that the performance of all subassemblies may be adjusted to the same standards with a very close tolerance. The success of this procedure must depend upon tubes of adequate life and freedom from drift and mechanical shock. At the present time, the life of these tubes under normal operating condition is in excess of 1000 hours and they are exceptionally insensitive to mechanical shock.

#### FIXED AND MODULATED TIMING PULSES

The generation of waveforms of precisely controlled slopes or periods and their comparison with fixed or variable reference potentials lead to the important methods of producing fixed or modulated pulses for time

measurement. The general types of circuits and the range of accuracy obtainable are outlined below. Circuit constants for practical designs are presented in Chaps. 4, 5, and 6.

**3-13. Fixed Pulses.**—An elementary example of the generation of a train of low-frequency pulses suitable for controlling the PRF of a timing

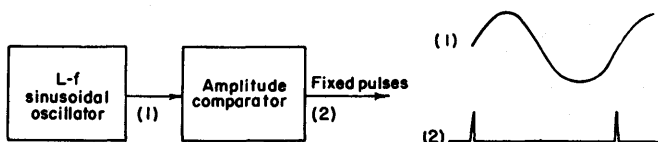


Fig. 3-12.—Fixed-pulse generator giving single-frequency markers.

system is shown in Fig. 3-12. The moment of equality of positive excursions of the sinusoidal waveform to zero voltage is indicated by a sharp pulse from an amplitude comparator. Other methods of PRF generation include the use of relaxation oscillators in which the sawtooth generation and amplitude comparison are carried out in the same circuit. They are, however, less stable than the circuits based upon Fig. 3-12.

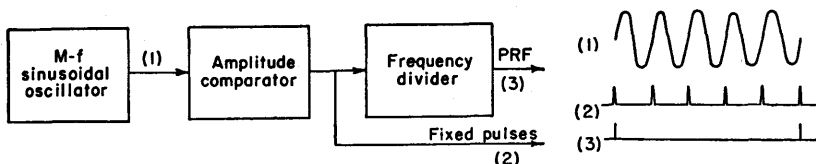


Fig. 3-13.—Fixed-pulse generator giving multiple-frequency markers.

The spacing of members of a train of pulses remains constant in spite of slow variations in the comparison circuit since the fluctuations vary all members of the pulse train equally.

If the pulses are generated at a higher frequency by means of a continuous oscillator, as shown in Fig. 3-13, frequency division is required to establish a PRF accurately synchronized with the high-frequency pulses.

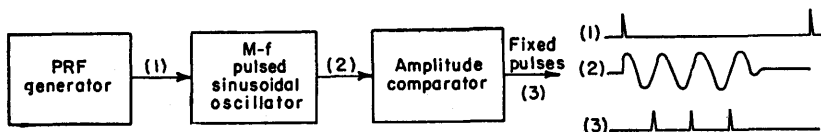


Fig. 3-14.—Fixed-pulse generator giving grouped markers.

A crystal oscillator operating at 80.86 kc/sec (one nautical mile) has usually been employed, and the frequency has been extended in either direction by multiplication or division over a range from 20 cps to 10 Mc/sec. Rectangular pulses as short as  $0.01 \mu\text{sec}$  have been obtained.

As in the case of single-frequency markers, voltage variations in the comparison circuit displace all timing pulses equally. Errors may arise

due to variations in the phase of the output of the frequency divider unless it operates to select a particular one of the fixed pulses (see Vol. 19, Chap. 15).

The third method of generating fixed pulses is indicated in Fig. 3-14, where a pulse-recurrence frequency generator (for example, that of Fig. 3-12) is employed to initiate the operation of the pulsed sinusoidal oscillator. This method is essential when the PRF is generated by a mechanical switch. The accuracy depends upon the rate of rise of the waveform initiating the sinusoidal oscillations. If this is sufficiently rapid, small fluctuations in the characteristics of the switching tube for the pulsed oscillator will have little effect. The objectionable features mentioned in Sec. 3-3 apply here.

**3-14. Single-scale Time-modulation Circuits.**—Two important methods of time modulation depend upon variation of the parameters in the processes of waveform generation and comparison. The reference potential of the comparison circuit is amplitude-modulated or the timing wave is phase-modulated in accordance with the desired signal. The instant of equality of the waveform and the reference potential is no longer fixed but is variable in accordance with the modulating signal. In the first method time modulation may be carried out by electrical means, but in the second method only mechanical signals may be employed (unless a servomechanism is used). The two types are therefore often classified as electrical and mechanical methods.

*Variation of the Reference Potential of the Comparison Circuit.*—Time modulation by waveform generation and amplitude comparison is shown in Fig. 3-15. The instant of equality of the triangular waveform and the control voltage applied to the comparison circuit is variable in response to changes of the control voltage. This produces a variation of the spacing of the delayed pulse in accordance with the control voltage as shown by the waveform. The process of amplitude comparison may occur externally as indicated in Fig. 3-15 or within the waveform generator as in the case of the multivibrator, phantastron, etc. (see Vol. 19, Sec. 13-12).

As already explained, the slope or shape of the waveform may be controlled to a high degree of precision by negative-feedback amplifiers and temperature-compensated timing elements to accuracies of one part in five thousand and 20 parts per million per degree centigrade, respectively. The level of the waveform and the performance of the comparison circuit are, however, subject to the voltage fluctuations of vacuum tubes. Since these fluctuations are likely to amount to a few tenths of a volt on changing tubes and a few tenths of a volt per week with time, over-all accuracies of single-scale time modulators of this type are limited to roughly  $0.3/V$ , where  $V$  is the amplitude of the timing waveform corresponding to the full range of modulation. Since reason-

able values of  $V$  obtainable with ordinary vacuum tubes are limited to a few hundred volts, their stability is the dominant factor in determining the error of this method.

Errors due to the level of the waveform may be compensated by the use of two similar comparison circuits, one for generating the trigger for the radar system and the other for the time-modulated marker as indicated by (2) in Fig. 3-15. Because of the substantial increase in the tube requirement, there has been little practical use of this method, which in any case is subject to differential variations between the two comparison circuits. Alternately, electrical or mechanical switching of the

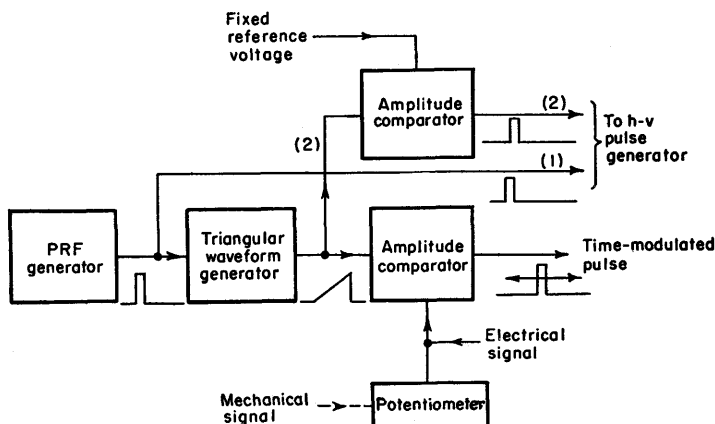


FIG. 3-15.—A single-scale electrically or mechanically controlled time modulator. The moment of equality of the triangular wave and the control potential is indicated by a sharp pulse and is adjustable in response to the control potential. Numbers on lines indicate alternative paths of signals in the two circuit configurations.

voltage to a single amplitude comparator between a fixed and a variable reference voltage may be used to reduce the error.

The control voltage for the comparison circuit may be derived from a potentiometer if mechanical signals are available. For a triangular waveform, a linear potentiometer gives a linear relation between time delay and shaft position. A number of accurately linear potentiometers are available for this purpose; the Beckman Helipot and the Gibbs Micropot (see Vol. 17) are especially suitable. These potentiometers have a winding about a 10-turn helical mandrel. They have high precision; many samples have been obtained in which the linearity approximates five parts in 10,000. Another type of potentiometer recently developed in the laboratory is termed the RL 270. These have a winding about a one-turn mandrel and have accuracies varying from one to five parts in 10,000.

A high-resistance potentiometer (approximately 20k) is desirable in order to have adequate resolution and to dissipate a small amount of power when supplied with a steady voltage equal to the full range of the timing wave (approximately 200 volts). The potentiometers listed above fulfill these requirements.

*Phase Modulation of the Timing Waveform.*—Phase shift of a symmetrical waveform by an inductance or capacitance goniometer varies the instant at which the waveform passes through zero amplitude as shown in Fig. 3-16. A comparison circuit responding to the zeros of the amplitude of the phase-modulated wave will give a train of pulses that are time-modulated with respect to the unshifted pulse train as shown in Fig. 3-16. The process of comparison is therefore the same as before, but the reference potential is constant, usually at ground.

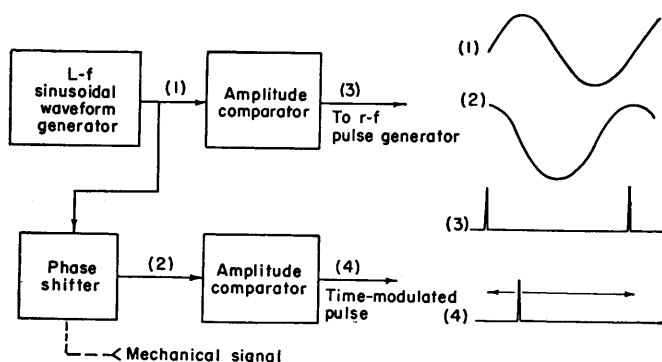


FIG. 3-16.—Single-scale mechanically controlled time modulator employing phase modulation of a sinusoidal waveform. The moment at which the sinusoidal waveform crosses the zero axis is indicated by the generation of a pulse. Variation of the time of occurrence of this pulse with reference to the unshifted sinusoid is accomplished by rotating the shaft of the phase shifter.

The purity of the sinusoid and the constancy of its frequency may be determined by the properties of negative-feedback amplifiers and precision-timing elements such as quartz crystals. The coupling of the symmetrical wave through a low-impedance transformer to a high-impedance amplitude comparator is often used to set the level of the wave without error; but the stability of the process of amplitude comparison limits the accuracy of pulse generation. As before, practical considerations limit the amplitude of the sinusoid to 100 or 200 volts, but, since the slope of the sinusoidal waveform at zero amplitude is  $\pi$  times that of a triangular wave of the same total amplitude and range of modulation, less difficulty is experienced with fluctuations of vacuum tubes.

Also, it is usual practice to employ two similar comparison circuits as shown in Fig. 3-16, one operating on the timing wave and the other upon the phase-shifted wave. This results in compensation of some errors.



The fractional accuracy of phase-shifter is much less than that of precision potentiometers and errors of one part in 360 are commonly observed. Since additional errors are introduced by imperfect balancing of the phase-splitting bridge, at best there exists an error of one part in 300, compared with about one part in 2000 for the linear potentiometer. This sixfold difference in accuracy is not maintained in practical circuits because of the error introduced by the amplitude comparator.

The choice between phase- and time-modulation methods is usually decided by the requirement for automatic control; where only electrical output data are required, electrically controlled time modulators are used. In double-scale systems mechanical control of phase modulation is much simpler as is shown in the next section.

**3-15. Double-scale Time-modulation Circuits.** *Pulse Selection and Interpolation.*—Figure 3-17 illustrates a two-scale electrical time modulator based upon interpolation between selected members of the train of multiple-frequency pulses generated in Fig. 3-13. With proper design the increase of accuracy over that obtainable in Fig. 3-15 may equal the number of times that the fixed pulses subdivide the desired range of modulation. The theoretical number of subdivisions is determined by the accuracy of the coarse scale which, if operating as indicated in Sec. 3-14, could be one part in 300, resulting in an over-all accuracy of one part in  $10^5$ . In practice, however, full advantage is rarely taken of the theoretical accuracy because faulty operation of the coarse scale causes an error equal to the period of the fixed pulses, and such a gross error is intolerable. Usually less than 100 subdivisions of the full range of modulation are made, and this has given accuracy compatible with the characteristics of the transmitter and receiver, and their synchronization, approximately one part in 30,000. (Usually 1- or 10-mile subdivisions are employed.)

In the actual design of such a timing system, the characteristics of the radar system usually determine the required repetition rate. The frequency of the fixed pulses is chosen not only with regard to the desired number of subdivisions of the scale, but also with regard to the units employed, for example, 1 nautical mile (80.86 kc/sec), 1 statute mile (93.11 kc/sec), 2000 yd (81.94 kc/sec), etc.

In some cases independent control of the coarse and fine scales is satisfactory, especially for navigation, etc., where continuous measurements are rarely needed. Considerable difficulty is encountered in coordinating the controls to achieve continuous modulation over the entire range. For example, when the fine control is increased to an interval exceeding that between two fixed pulses, the coarse control must be advanced to select the next pulse. This requires that the setting of the fine scale be simultaneously reduced from maximum to zero in

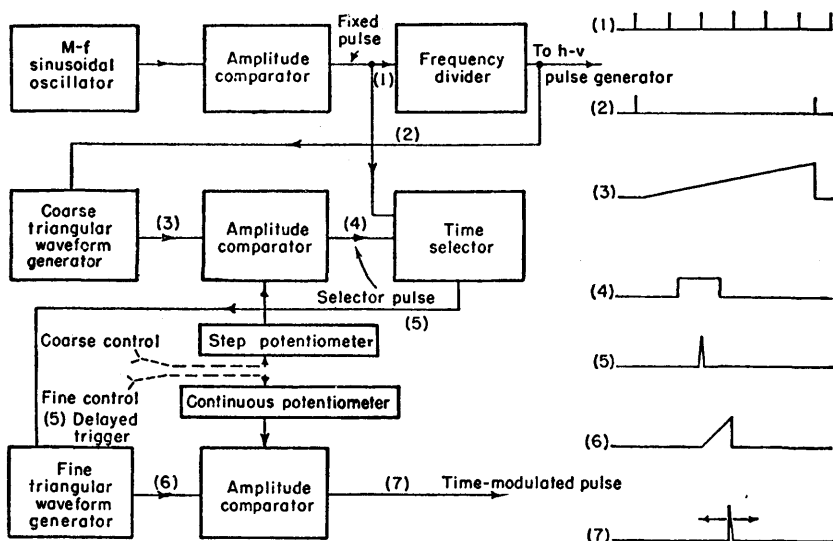


FIG. 3-17.—Two-scale electrically or mechanically controlled time modulator. The selection of any one of the fixed pulses lying within the range of modulation is accomplished by a single-scale circuit. This selected pulse operates a fine scale that serves to interpolate between a pair of fixed pulses.

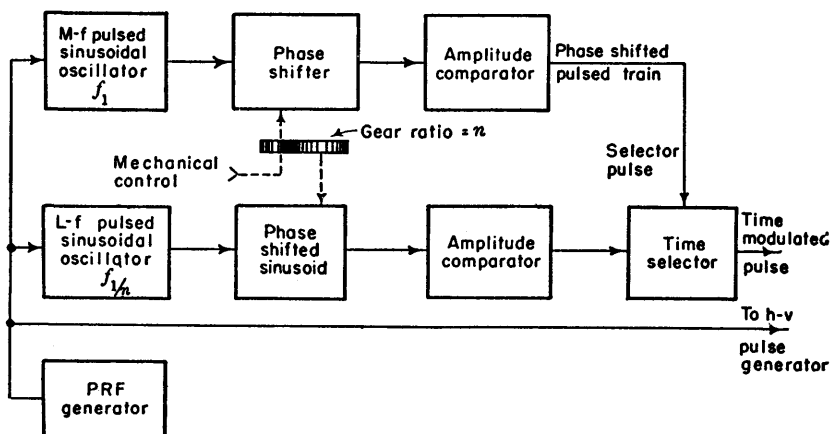


FIG. 3-18.—Two-scale mechanically controlled time modulator. A particular pulse derived from the phase-modulated sinusoids is selected by means of a selector pulse derived from a similar system operating at a lower frequency. The gear ratio  $n$  between the controls is chosen so that the rate of change of delay of the two circuits is identical and the same pulse is continuously selected.

order that approximately continuous movement of the time-modulated pulse be achieved. Although mechanical devices employing cams, switches, and potentiometers covering  $359\frac{1}{2}^\circ$  have been constructed to accomplish this, the apparatus is nearly impractical.

*Pulse Selection in Phase-shift Systems.*—Figure 3-18 represents a two-scale system based upon the method of Fig. 3-16, except that pulsed sinusoidal oscillators are shown instead of the continuous oscillator of the previous case to permit operation under control of the r-f pulse generator. Rotation of the control of the fine scale causes continuous phase modulation of the sinusoid and a train of phase-shifted pulses is produced, as in

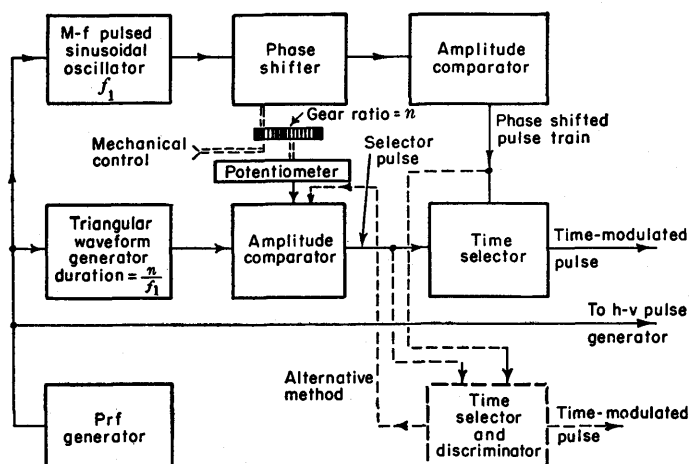


FIG. 3-19.—Two-scale time modulator with electrical and mechanical control. A particular member of the pulse train which is derived from the phase-modulated sinusoid is selected by means of a single-scale electrically controlled circuit. Equality of the rates of change of delay of the selector pulse and a member of the phase-shifted wave train is obtained by mechanical interconnection or, as shown in the dotted lines, by means of an electrical time discriminator automatically controlling the coarse scale to follow the pulse of the fine scale.

Fig. 3-16. A particular member of the pulse train is continuously selected by a coarse scale in which the rate of time modulation is made equal to that of the fine scale by appropriate gearing of the phase shifters. This method of obtaining continuous modulation is very straightforward compared with the cumbersome mechanism required in the previous case.

The repetition rate of this system is variable over a wide range, as long as the coarse scale has adequate time to recover. If, however, continuous oscillators and frequency dividers were employed, the repetition rate would be fixed to that of the coarse scale or a submultiple of it. Since the repetition rate, the fine-scale interval, and the number of subdivisions of the range of modulation are not independently variable, this system is often awkward to employ.

The ultimate accuracy that might be expected from this system would be roughly ten parts per million, but, as in the previous case, a considerable safety factor should be applied to the operation of the coarse scale.

In Fig. 3-19 is shown a combination of a phase-shift modulator for the fine scale and an electrically controlled time modulator for the coarse scale. Although a pulsed sinusoidal oscillator is shown, a continuous oscillator similar to that shown in Fig. 3-13 may be used. The pulse-repetition frequency of the coarse scale may be varied over a wide range provided the pulse-repetition interval is roughly 25 per cent greater than the range of modulation. This is a definite advantage over the version of Fig. 3-18, which uses a continuous oscillator for the coarse scale. Continuous time modulation may be obtained by connecting the potentiometer to the phase shifter with appropriate gear ratios and electrical scale factors so that the movement of the selector pulse and the phase-shifted wave train occurs at the same rate.

The possibility of electrical control of the fine scale permits a novel alternative indicated by the dotted lines of Fig. 3-19. If, for example, the selector pulse of the coarse scale and the phase-shifted pulse train are connected to a time discriminator (see Sec. 3-17) instead of to a time selector, an electrical signal may be obtained which will control the modulation of the coarse scale. This system has the advantage of simplicity since it does not require a potentiometer or associated mechanism for controlling the time delay of the coarse scale. On the other hand, momentary power failure or a transient mechanical shock might cause the time discriminator to operate upon a pulse other than the one initially selected and would result in a gross error of the reading. The accuracy would, of course, be regained by a simple reset mechanism.

**3-16. Multiple-scale Systems.**—Accuracies considerably in excess of those mentioned in the previous section may be obtained with systems employing a third or a fourth scale. The frequency stability of available sinusoidal oscillators would seldom warrant an increase beyond three where, for example, a potential accuracy of three parts in  $10^{10}$  is obtainable. There are, however, some mechanical difficulties in multiple-scale systems of high accuracy especially if a precise counter reading is desired, since the fine scale has a large number of turns for the full scale. A least count of nearly  $\frac{1}{310}$  of the fine scale may be desired for accurate reading. Most military applications require that the output be shifted from one end of the scale to the other in roughly 20 sec, which demands impossible shaft speeds in the counting mechanism. Although these difficulties are mitigated by dial indicators, they still remain serious in high-accuracy systems.

In a continuous-reading three-scale Loran indicator this difficulty is

avoided by employing an independent step control for the coarse scale; the intermediate and fine scales are operated very much as indicated by Fig. 3-19. Rapid transfer from high to low readings is obtained by operation of the coarse step control. Continuous indication is obtained because the step control alters the first two digits of the counter while the remainder of the count is indicated from the continuous system. These practical problems are discussed in more detail in Chaps. 6 and 7.

The possibility of employing a coherent oscillator for a timing standard has been pointed out in Sec. 2-4. This arrangement permits the fine scale to depend upon phase demodulation of the received radiation. This is a process of theoretically high accuracy, because radio frequencies up to several megacycles per second may be employed and the errors of phase modulators correspond to a small distance. The problem of scale coordination is similar to that of any multiple-scale system and the preceding methods are suitable.

### TIME DEMODULATION

The circuits of the previous section may be employed for generating pulses which are time-modulated with respect to certain reference pulses. These pulses may then be used as a component of a time-demodulation or precision data transmission system (see Chaps. 10 and 11).

**3-17. Time Selection and Discrimination.**—The process by which relative times of occurrence of an input pulse and a locally generated pulse are compared is termed "time discrimination." The output of a time discriminator is a signal indicating the sense and approximate value of the time difference of the two signals. The process consists of time selection and differential detection. A brief description of a typical process of time discrimination will be given in terms of a specific example in the next section.

The process of time selection is used to pick out a portion or portions of the time-modulated pulse. This results in sensitivity to small time differences and in an elimination of most interfering signals since the duration of the selection pulse or aperture is approximately that of the received signal. It is usual practice to employ two time selectors as a balanced time discriminator in order that the null point of the circuit be independent of variations of the amplitude of the time-modulated pulse. A simple form of time discriminator is shown in Fig. 3-20. Selector Pulse 1 is applied to the suppressor grid of pentode amplifier  $V_1$ . At the termination of this pulse, Pulse 2 of similar duration is applied to the suppressor grid of  $V_2$ . The second pulse is usually obtained by passing the first pulse through a delay line of delay equal to that of Pulse 1. The time-modulated input signal is applied to the parallel-connected control grids of  $V_1$  and  $V_2$ . Portions of the time-modulated signal which

overlap the selector pulses appear in the plate circuits of  $V_1$  and  $V_2$  as negative pulses. Condensers  $C_4$  and  $C_5$  are charged to potentials corresponding to the overlap of the signal and the selector pulses. The average potential difference at the plates of the two tubes is therefore proportional to the misalignment of the signal and the selector pulses.

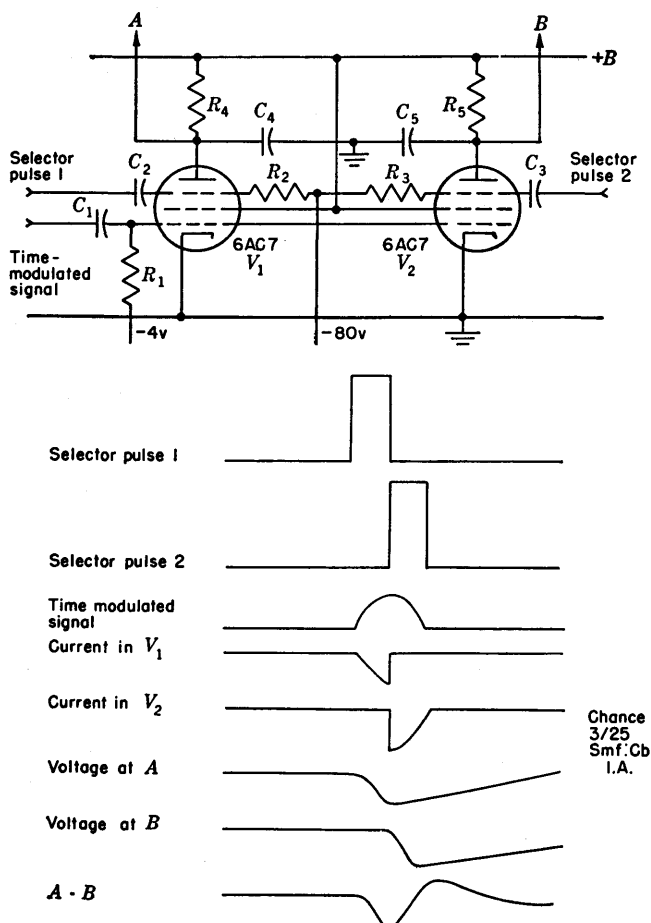


FIG. 3-20.—An elementary time-discriminator circuit.

With more elaborate circuits, sensitivities of  $\frac{1}{8}$  volt/ft are obtainable for the  $0.1\text{-}\mu\text{sec}$  pulses of Fig. 3-5.

The output of the time discriminator may vary the reference voltage of the amplitude comparator or it may operate an electromechanical servomechanism controlling a phase-shifting device and vary the time of

occurrence of the selector pulses so as to follow the time-modulated signal. In either case problems of stability and transient response are important (see Chap. 8).

### SOME PROPERTIES OF CATHODE-RAY-TUBE DISPLAYS

The cathode-ray-tube display has two important functions in time measurement by pulse methods: selection of the proper time-modulated signal and demodulation or measurement of a time-modulated signal.

These two processes will be discussed briefly, but the material is introductory to the discussion of Chap. 7. A more complete description of all uses of cathode-ray-tube displays appears in Vol. 22.

**3-18. Time Selection and Discrimination.**—The type A or linear-sweep oscilloscope is used mainly for the purpose of selecting a particular target on the basis of its range. Other types of displays such as the B-scope or PPI are used to select targets in range and azimuth or range and elevation. This selection process is, of course, an essential preliminary to accurate measurement.

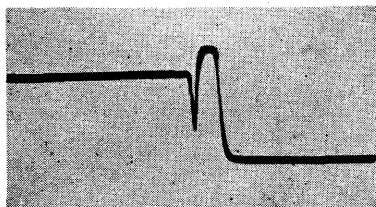


FIG. 3-21.—Photograph of step display for target selection using type A sweep.

Often the selection process involves manual adjustment of the selector pulse of an electrical time discriminator to the approximate range of the target. In this way the operation of an electric time demodulator is initiated and continuous tracking of the target may proceed.

An example of a cathode-ray-tube display for this purpose is given in Fig. 3-21. Manual control of the selector pulse, can, of course, be used for manual tracking of the target as discussed in the next section.

**3-19. Time Demodulation.**—The cathode-ray-tube display may be used in two ways for time demodulation. First, it serves simply as a time discriminator or null indicator; that is, it gives the operator visual indications of the displacement between the time-modulated signal and an electrical range index generated by the time-modulation systems of Secs. 3-14 and 3-15. In the second case, a mechanical index is used to represent a time-modulated pulse.

*Time Discrimination on Cathode-ray-tube Displays.*—This is the process of determining the position of a time-modulated pulse with respect to a given index; the accuracy with which it can be done is often termed the “resetability” of a display. The process may be crude or sensitive; Fig. 3-22 gives examples of both. Highly sensitive indications of the displacement of signal and index are afforded by the fine electronic cross-hair, and accurate time demodulation or range-tracking is possible. In

addition, the figure shows two additional echoes. The range of these is obtained by visual estimation and the accuracy may be considerably improved by the use of the transparent overlay over the face of the expanded type B oscilloscope. The position of crosshairs inscribed on the overlay is controlled by means of a joystick and may be set rapidly to the echoes.

The accuracy of time discrimination on cathode-ray-tube displays is considerable and, for the type B display shown in Fig. 3-22, the setting of the electronic index to a target may be repeated to an accuracy of  $\pm 12$  ft, roughly  $\frac{1}{20}$  the rise time of the received signal.

On other types of displays the accuracy of time discrimination is considerably greater; for example, in an experimental version of the Loran display (see Sec. 7-11) where two similar signals are superimposed, time discrimination accurate to  $\frac{1}{400}$  of their rise time is obtained under ideal conditions.

Time discrimination carried out on cathode-ray-tube displays usually implies manual control of the tracking index by means of direct or aided tracking (see Sec. 7-14). In one case, however, a pair of photocells has been used to measure the displacement of a target echo on a circular cathode-ray-tube display (see Vol. 19, Sec. 14-9).

Many other types of indices have been employed for the purposes of time discrimination on cathode-ray-tube displays. The detailed characteristics of a number of indices are discussed in Chap. 7.

**3-20. Time Modulation.**—In the previous discussion the use of a fast time base on a cathode-ray tube permitted the discrimination of the error between a controllable electrical index and a time-modulated signal. If a smaller accuracy is acceptable, an electrical index may no longer be needed, and the process of time demodulation is greatly simplified by employing a mechanical index on the face of the cathode-ray tube. If, for example, we apply a triangular waveform to the horizontal plates, the moments of arrival of the spot at various points on the face of the cathode-ray tube denote definite time delays with respect to the initiation of the triangular waveform. Movement of a mechanical cursor across

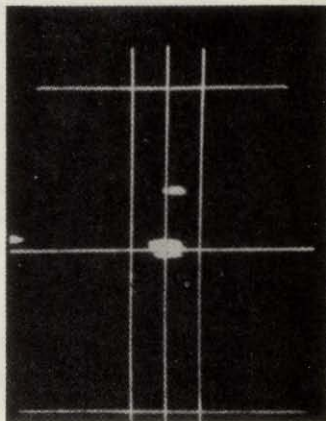


FIG. 3-22.—A type B cathode-ray-tube display indicating rough and precise range measurement. The range of the echo set exactly to the horizontal crosshair is exactly measured, although that of the two other echoes (one immediately preceding the target echo and the other some distance beyond it) is obtained by rough estimation of the displacement of these echoes from the crosshair. (Courtesy of McGraw-Hill Publishing Co.)



the face of the tube on which a triangular waveform is displayed thus creates an effectively time-modulated index with which the process of demodulation may be readily carried out.

It is profitable to compare this process to that used in the generation of electrical indices, where an electrical amplitude comparator indicates the equality of a timing waveform and a voltage by the generator of an index. The moment of displacement equality of the spot of the cathode-ray tube and the mechanical index represents the same process. As in the case of electronic indices, the mechanical indices may be fixed or movable; for movable indices the display serves not only to create the time-modulated index but also to permit time selection and discrimination by a human operator in order to give continuous time demodulation of a signal of variable range.

The lack of an electrical pulse corresponding to the mechanical index often causes difficulty in securing automatic operation of these methods without resorting to photocell pickoffs.

The accuracy of time modulation with a mechanical index on a linear sweep is low. The relation between spot deflection and applied voltage is no more accurate than 1 or 2 per cent in most cathode-ray tubes. In addition, a number of factors alter the position of the trace with respect to the index, especially variation of accelerating voltage and stray magnetic fields. Other practical difficulties are involved in avoiding parallax between the mechanical index and the trace. It is often desirable to project an illuminated grid directly upon the face of a cathode-ray tube (Chap. 7 and Vol. 22). The inaccuracy of the cathode-ray-tube display is usually so large that one encounters little difficulty with the variations in the properties of waveform generators.

The accuracy may be increased by subdivision of the range of time modulation by the use of fixed indices (Secs. 3-13 and 3-15) or by the use of phase modulation as discussed in the next paragraph.

*Phase Modulation.*—The circular or type J cathode-ray-tube display may be used as an electromechanical phase modulator very much in the fashion of those described in Sec. 3-14. The circular pattern is obtained by applying distortion-free two-phase sinusoidal voltages of appropriate amplitude to the deflecting plates of the cathode-ray tube. Since various points on the circle have a time delay which is proportional to their distance along the circumference, the angular position of a mechanical index rotating about the center of the display represents a linearly phase-modulated index. In circular-sweep displays the signal may be applied as a deflection modulation by means of a central electrode as shown in Fig. 3-23.

The stability of the circular sweep is somewhat better than that of the linear sweep because variations of accelerating voltage cause a negligible

error. The main errors of the display are due to decentering, ellipticity, and parallax. The employment of the mechanical cursor mounted very close to the face of the tube and including an inscribed circle makes these errors evident and easy to correct. A detailed analysis of the errors of the circular-sweep display is given in Vol. 22. One advantage of the circular-sweep phase shifter over inductance-capacitance goniometers is that the achievement of a circular pattern immediately indicates proper adjustment of the phase and magnitude of the applied voltages.

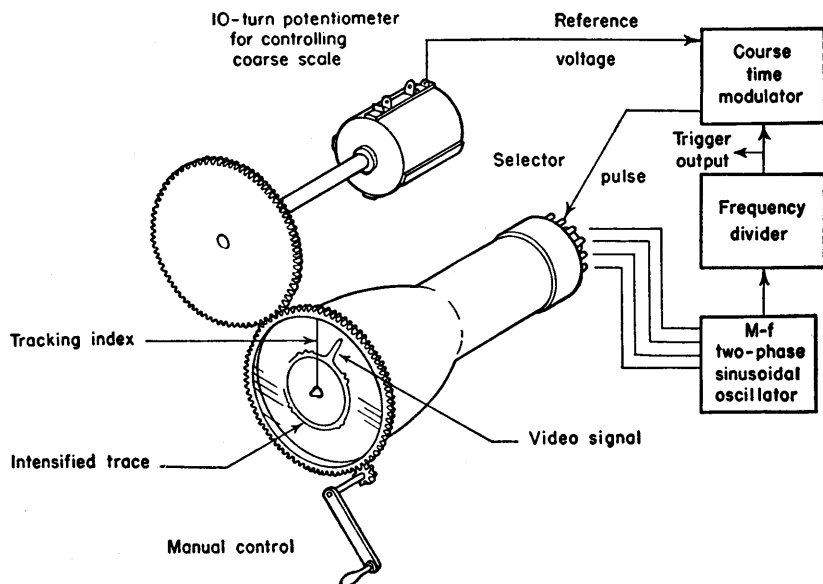


FIG. 3-23.—Circular-sweep range system.

The accuracy of a properly adjusted circular sweep is roughly  $1^\circ$ , comparable to that obtainable with other electromechanical phase shifters. One of the great advantages of this type of display is the fact that it may be converted to a multiple-scale system by employing a high-frequency sinusoid to generate the sweep and a single-scale electrical circuit to supply an intensifying pulse that will select the desired cycle of the high-frequency timing waveform as shown by the block diagram of Fig. 3-23.

This multiple-scale system has a number of advantages; the obvious one is simplicity and economy of vacuum tubes because the functions indicated in the block diagram may be carried out with as few as five double triodes. A less obvious but equally important advantage is gained by the employment of the mechanical time index that is equivalent to a marker pulse of accuracy equal to  $\frac{1}{4}$  per cent of the period of the tim-

ing waveform and of infinitely rapid rise time. This situation is preferable to that existing with an inductance or capacitance goniometer where the phase-shifted timing waveform must be amplified and passed through an amplitude comparator before an electrical marker pulse is obtained. On the other hand, no electrical pulse is available for electrical time selection or discrimination necessary for automatic tracking without the use of photocells. Circular-sweep displays operate satisfactorily at frequencies near 1 Mc/sec.

A type A display or type B display is usually included in the circuit of Fig. 3-23 for surveying simultaneously all targets within the desired range of modulation and for permitting initial target selection, as in the radar system (HR) mentioned in Chap. 2 and discussed further in Chap. 7.

Mechanical coordination of the coarse and fine scales is carried out in a manner similar to that of previous multiple-scale systems; the mechanical cursor and a potentiometer controlling the coarse scale are geared together at a ratio determined by the quotient of the full range of modulation of the coarse and fine scales.

The multiple-scale system corresponding to that of Sec. 3-15 employing several circular sweeps is not a useful system and has several basic limitations. If, for example, a low-frequency circular sweep is used in the coarse scale, one of the weaknesses of this type of phase shifter is immediately obvious; no selector pulse is generated by the display which may be used to select the desired portion of the fine scale, and it is necessary to use an electric circuit for the coarse scale. If the timing oscillator operates continuously and if the repetition rate is equal to the frequency of the sinusoid applied to the coarse scale, variations of the repetition rate are not permitted. If, however, pulsed oscillators are used, variations are permitted in the same way they are permitted in the circuits discussed in Sec. 3-15.

Pulsed sinusoidal oscillators may be employed to initiate the circular sweep. The minimum range of time modulation at which linear indications are obtained is slightly greater in this case than in the case of the pulsed-oscillator and condenser phase-shifter system of Sec. 3-14. This difference is due mainly to the necessity of applying large deflecting voltages to the cathode-ray tube to obtain a circle of adequate diameter as opposed to the relatively small voltages that can be used with the phase shifters. The pulsed sinusoidal oscillator system is undesirable because it lacks the simplicity and stability of the crystal-controlled continuous oscillator system; only one tube and a transformer are necessary for the latter system, but the former may require five or more vacuum tubes to generate pulsed oscillations and an accurate sweep.

## CHAPTER 4

### GENERATION OF FIXED INDICES

BY R. I. HULSIZER, D. SAYRE, AND R. B. LEACHMAN

In Chap. 3 it was pointed out that a sequence of fixed time markers is needed in time measurement to initiate operations periodically, to mark off time intervals on CRT displays, and to provide a coarse scale for multiple-scale time modulation. Some methods of generating fixed markers were also outlined and illustrated with block diagrams. The first method is to derive pulses from a sinusoidal oscillator with an amplitude comparator, as in Fig. 3-12. The second employs relaxation oscillators which perform the operations of sawtooth waveform generation and amplitude comparison in the same circuit. If markers of more than one frequency are desired, it is possible to employ frequency dividers (Fig. 3-13) or frequency multipliers. A somewhat more flexible, though more costly, method is to use low-frequency markers to initiate pulsed oscillators of higher frequencies to generate markers of any frequency desired (see Fig. 3-14).

The purpose of this chapter is to describe several useful circuits for generating fixed markers by these techniques. In general those circuits have been chosen for description which have been used enough to be considered reliable, although some of them represent techniques now considered to be inferior. The reader will find in Vol. 19 detailed treatments of the various component circuits that are used in marker generation—for example, crystal and relaxation oscillators, amplitude comparators, and frequency dividers and multipliers.

#### SINGLE-FREQUENCY MARKER GENERATORS

BY D. SAYRE AND R. I. HULSIZER

**4-1. Sinusoidal Oscillators and Amplitude Comparators.**—The following circuits were designed as PRF or range-mark generators to provide markers of good frequency stability. Often PRF triggers are required to be stable to 1.0 per cent either for coding purposes or because of r-f switch or indicator sweep-generator duty-ratio sensitivity. Range markers are usually required to be within 1.0 to 0.001 per cent of the desired frequency and furthermore must usually be accurately defined with respect to the phase of the reference sine wave.

*Circuit Using RC-oscillator, Squaring Amplifier, and Blocking-oscillator Pulse Generator.*—This type of circuit is typical of single-frequency pulse generators used to generate PRF triggers (see Fig. 4-1). A sine-wave oscillator was chosen because the frequency was specified to remain within 5 per cent even under severe operating conditions. There were no other special requirements.

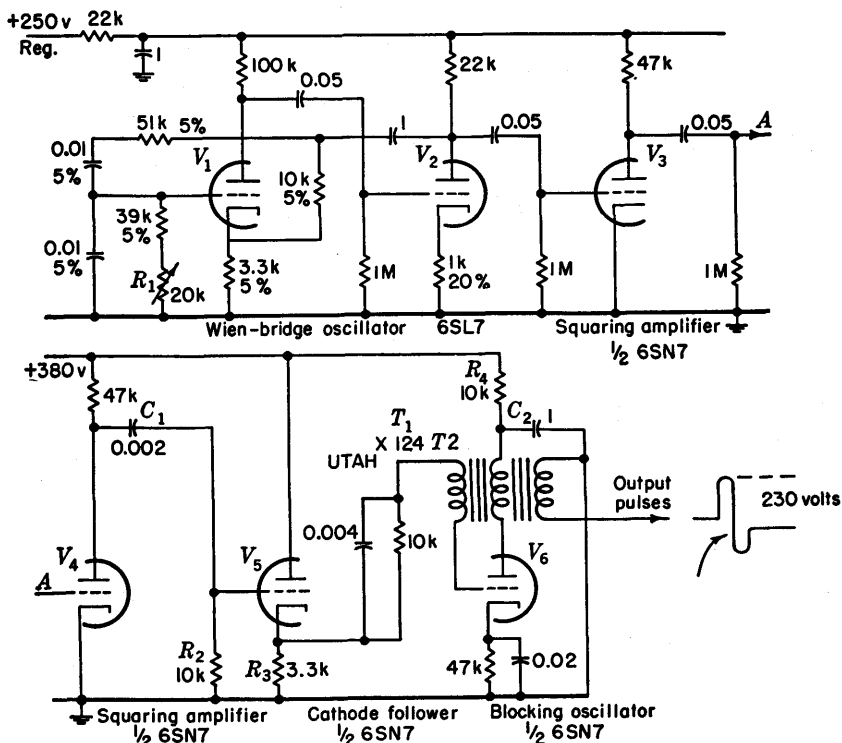


FIG. 4-1.—A 300-cps RC sine-wave oscillator, squaring amplifiers, and blocking-oscillator pulse generator.

Tubes  $V_1$  and  $V_2$  comprise a conventional Wien-bridge oscillator. Frequency control provided by the variable  $R_1$  compensates for manufacturing tolerances in the other components. From the plate of  $V_2$  is taken a distorted sine wave approximately 23 volts peak-to-peak. This is squared in  $V_3$  and again in  $V_4$ , from the plate of which is taken a square wave 300 volts peak-to-peak. After differentiation by  $C_1$  and  $R_2$  this is passed, via the cathode follower  $V_5$ , into the grid circuit of the blocking oscillator  $V_6$ . An alternative and satisfactory way of triggering the blocking oscillator would be to inject a negative pulse onto

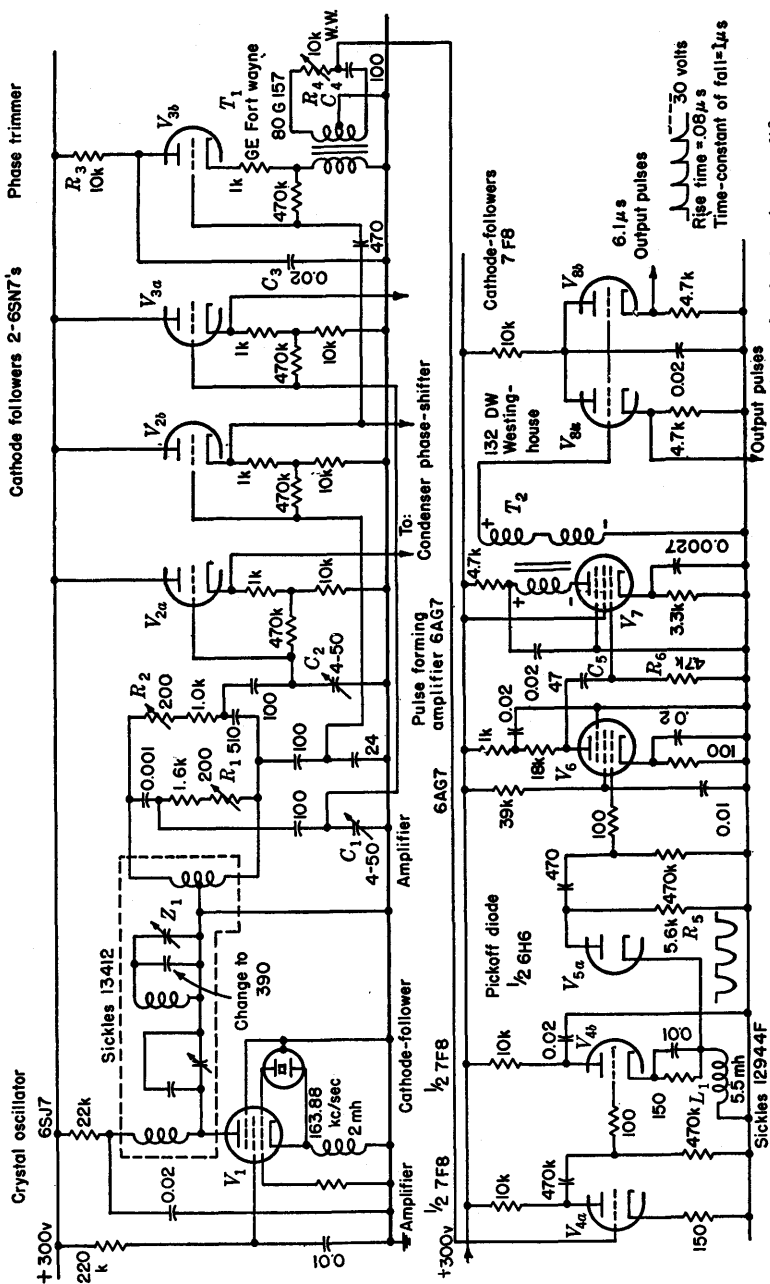
the plate of  $V_6$  by removing  $R_3$  and connecting the plate of  $V_6$  to the plate of  $V_5$  instead of to the plate supply. The decoupling network  $R_4$  and  $C_2$  prevents the large current pulse from getting onto the plate supply, from which it could get into other parts of the circuit. The output pulse of 230 volts is at an impedance level of 500 ohms. If greater frequency stability is desired it could be obtained by using a crystal oscillator in the 100-kc/sec range followed by stable frequency dividers, or for frequencies down to 2000 cps, by using a low-frequency crystal oscillator of the type described in Vol. 19, Chap. 4.

A further weakness of this circuit, which would become apparent if accurate phase lock between the sine wave and the pulses were required, is that inadequate provision is made for accurate determination of the exact point of the sine wave at which the pulse shall be generated. The amplitude comparison is performed by the cutoff and grid-current points of the triode control-grid characteristics of  $V_3$  and  $V_4$ . A much more accurate circuit in this respect will be described next.

*Crystal Oscillator and Diode Amplitude Comparator.*—The circuit of Fig. 4-2 is part of a radar synchronizer and two-scale time modulator. A series of fixed pulses is provided, one of which is selected as the PRF trigger every 330  $\mu$ sec. It also supplies 3-phase sinusoidal voltages to a condenser phase shifter. The phase-shifted output of the condenser is used to generate phase-shifted pulses. Thus it is important to maintain not only accurate frequency, but also accurate phase.

This circuit generates pulses approximately 6  $\mu$ sec apart whose time of appearance, relative to the sine wave which controls them, is stable to 0.01  $\mu$ sec. In order to maintain the phasing with that accuracy, the pulse must always be formed at precisely the same point of the sine wave. The zero point is the best, because there the rate of change of voltage is greatest. By taking the sine wave across the inductance  $L_1$  the zero point is always accurately at ground. Since the plate of the diode  $V_{5a}$  is held at ground by  $R_5$ , it will conduct on just exactly the lower half of the sine wave, the only possibility of error being a change in the diode cutoff potential. Such a change is not likely to affect the pickoff point by more than 0.1 volt, and by using a moderately large amplitude sine wave, perhaps 40 volts peak-to-peak, the resultant error amounts to about 0.003  $\mu$ sec.

The operation of the entire circuit is as follows. Balanced 163-kc/sec sine waves of very good quality are fed from the triple-tuned transformer  $Z_1$ . In addition to the train of pulses whose phase relative to these sine waves is fixed, it is desired to generate another similar train of pulses which can be continuously phase-shifted. The balanced sine-wave output, therefore, is fed into a phase-splitting network which provides 3-phase sine waves for a continuous phase-shifting condenser (see Chap. 5



and Vol. 19, Chap. 13). Controls  $C_1$  and  $C_2$  are provided for adjusting the amplitudes of two of the outputs to equality with that of the third, while  $R_1$  and  $R_2$  permit adjustment of their phases to  $\pm 120^\circ$  relative to the third. The three phase-shifted sine waves are fed out to the condenser phase-shifter via the cathode followers  $V_{2a}$ ,  $V_{2b}$ , and  $V_{3a}$ . The nonadjustable sine wave from  $V_{2b}$  is also fed into the cathode follower  $V_{3b}$ , from which it enters upon a series of amplifying and squaring circuits, finally emerging as the desired series of fixed pulses. The phase-shifted output of the condenser, after a stage of amplification to bring it up to its initial level again, goes through a similar circuit and ends up as a series of continuously phasable pulses.

Tube  $V_{3b}$  is a cathode follower with a transformer  $T_1$  in the cathode. The decoupling network  $R_3$  and  $C_3$  serves to lower the plate voltage so that a larger current can be passed through the primary of the transformer  $T_1$  without exceeding the rated plate dissipation of the tube. Similar networks are used in the plates of  $V_6$ ,  $V_7$ , and  $V_8$ . The transformer is used to obtain a balanced output to drive the adjustable phase-shift network  $R_4$  and  $C_4$  thus providing a zero adjustment on the phase shift between the two sets of pulses. The output of this network is amplified in  $V_{4a}$ . Tube  $V_{4b}$  is the cathode follower that drives the inductance  $L_1$ . The operation of the inductance  $L_1$  and the diode  $V_{5a}$  has already been described. The diode is arranged to pick off the negative half cycles rather than the positive ones so that  $V_6$  may be fully conducting and consequently in its region of highest  $g_m$ , at the moment of pickoff. After amplification in  $V_6$  the signal is differentiated in  $C_5$  and  $R_6$ , amplified once more in  $V_7$ , inverted and stepped up in  $T_2$ , and finally fed out through either of the cathode followers  $V_8$ . The shape of the output waveform is shown on the figure. The main weakness of the circuit lies in the expensive amplifier following the diode amplitude comparator. The transformer  $T_2$  used with  $V_7$  for inverting the pulse has excellent high-frequency response and might well have been connected with the diode  $V_{5a}$  and the amplifier  $V_6$  to form a regenerative amplitude comparator similar to the one described in Vol. 19, Sec. 9-14, and in the following section. It would also be possible to vary the quiescent plate potential of the diode  $V_{5a}$  to provide 0-phase adjustment rather than the more expensive phase-shift circuit of  $V_{3b}$  and the transformer  $T_1$ .

**4.2. Regenerative Amplitude-comparison Circuits.**—Regenerative devices are economical for generating a pulse at the instant a sinusoidal waveform passes through a particular potential, but nearly all such devices suffer from the fact that the point on the sine wave at which regeneration begins is subject to rather severe variation with a corresponding instability of the phase relations between the sine-wave input and the pulse output. Multivibrators, blocking oscillators, and other



regenerative devices can be used but all suffer from this fault. Gas-filled tubes likewise are economical but subject to variation of firing characteristics. The regenerative squaring amplifier to be described is therefore especially valuable because the moment of regeneration is determined by a diode and is quite well defined.

The fundamental circuit is shown in Fig. 4-3 and typical waveforms in Fig. 4-4. The action of the circuit is described in considerable detail in Vol. 19, Chap. 9. Briefly, a sine wave of the desired frequency up to perhaps 200 kc/sec and with an amplitude of 50 volts peak-to-peak is

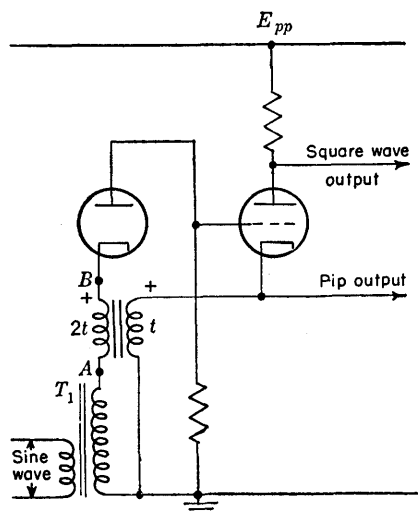


FIG. 4-3.—Regenerative amplitude comparator.

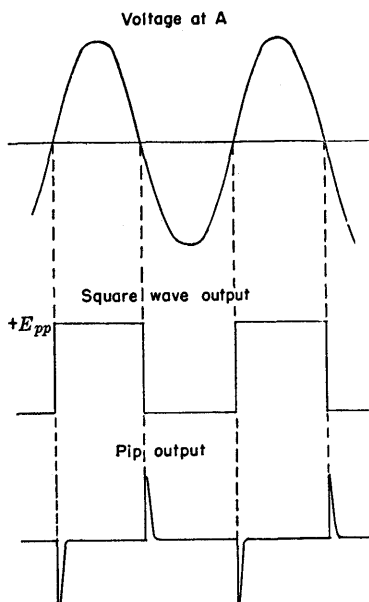


FIG. 4-4.—Waveforms from circuit of Fig. 4-3.

introduced through the low-resistance transformer  $T_1$ . The pulse transformer  $T_2$  is arranged to give about a 2-to-1 stepup to the grid, without reversal, from the cathode. When point A is positive the diode is cut off, the grid of the triode is at ground, and the triode is on. Point A moves downward; when point A reaches ground the diode conducts, the grid begins to move down, and the current in the primary of the transformer is decreased, inducing a larger negative signal on the grid. This action is regenerative and very quickly the triode is cut off. The plate voltage increases rapidly to the plate supply voltage, and a negative pulse is generated at the cathode. The sine wave now performs its negative half cycle, during which time the diode is on and the triode is off. When the



nique provides an economical method for controlling the frequency of a blocking oscillator with a crystal. Tube  $V_1$  is a Class C crystal oscillator which has a tank circuit and one winding of the pulse transformer (Utah X 124T3) of the blocking oscillator  $V_2$  in the plate. The current pulses through that winding, which occur accurately at 81.94 kc/sec, bring the blocking oscillator into synchronism.

Although the amplitude comparison is performed by the oscillator tube with reasonable accuracy, the pulses that are formed are not large enough to trigger the blocking oscillator without considerable error. At this frequency errors of  $0.4 \mu\text{sec}$  may be expected as the line voltage and oscillator amplitude are changed by  $\pm 30$  per cent. Changes in the tubes and the blocking-oscillator grid network may be expected to cause even larger errors.

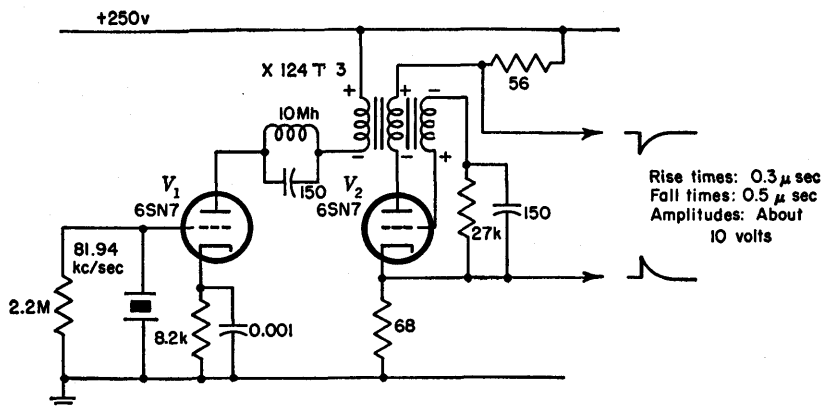


FIG. 4-6.—Crystal-controlled 81.94-kc/sec Class C sine-wave oscillator and blocking oscillator. Type 256-B, A/R range scope.

A very similar circuit, taken from the AN/APS-15 range circuit, is shown in Fig. 6-35.

**4-4. Gas-tetrode 300-cps Relaxation Oscillator.**—Though the previous sinusoidal-oscillator circuit performed its own amplitude comparison, in general the nature of sinusoidal oscillators does not lead to accurate performance of this function. On the other hand, relaxation oscillators by definition go through a very rapid change of state as a result of amplitude comparison at some time during their cycle of operation. Pulses derived from the rapid change of state mark the period of the oscillator and, in fact, the frequency depends upon the performance of the amplitude comparison process as well as on the slope of the timing waveform.

The exponential waveform of a gas-filled tube relaxation oscillator can be formed at any of its electrodes. In the customary "linear"

sweep generator built into oscilloscopes the timing waveform is on the plate, and the moment of firing is, therefore, determined by the plate firing characteristics. Much more accurate determination of the moment of firing is possible if the timing waveform is applied between grid and cathode instead of between plate and cathode, the factor of improvement being approximately the critical firing ratio  $\mu$  of the tube. In a type 884 gas-triode  $\mu$  is about 11; in a 2050 tetrode, it is about 250. Thus, for a 2050, the same change in tube characteristics which would cause the firing point to move 25 volts along an exponential in the plate will cause a 0.1-volt change when the exponential is in the grid circuit.

Such a circuit, employing a 2050, is shown in Fig. 4-7. Here the exponential waveform is on the cathode, and the grid is motionless; the tube fires when the cathode has dropped to within a few volts of the grid. Upon firing, the cathode rises very rapidly to within about 12 volts of the plate supply, remains there during the deionization time, and then falls along an exponential whose time constant is  $R_1C = \frac{1}{300}$  sec until the tube fires again. Each time

the tube fires, a narrow positive pulse is generated across  $R_2$ . The pulse rise time is less than 0.1  $\mu$ sec. Its fall is an exponential whose time constant is  $R_2C = 2.25 \mu$ sec, and the pulse amplitude is about 200 volts. A negative pulse could be obtained by inserting a small resistor in the plate. The frequency is controlled by varying the grid voltage with  $P$ . The severest fault of the circuit is the

large heater-cathode voltage, which reduces the life of the tube and affects the recurrence frequency by changing the cathode-to-heater resistance. If the heater voltage is supplied by a separate filament winding that is driven along with the cathode through an added cathode follower, both effects will be reduced.

Instability of the oscillator can be attributed to two causes in addition to changes in the time constant  $RC$ . One cause is change of the critical firing point and the other is change of clean-up time. If the exponential waveform is adjusted to fall to  $1/e$  of its initial value before firing, a change of 1 volt in the firing voltage will cause a 0.8 per cent change in frequency regardless of the operating frequency. Variations in cleanup time of 10  $\mu$ sec will cause an 0.3 per cent change in frequency at 300 cps. Variations of 1 volt and 10  $\mu$ sec in the firing voltage and cleanup time seem reasonable as tests show the frequency stability of this circuit to be

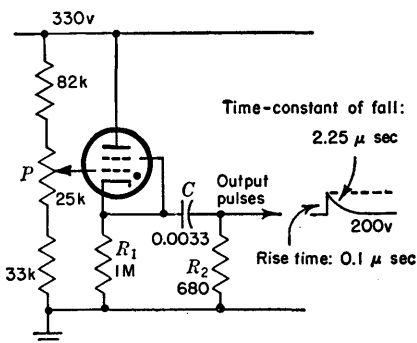


FIG. 4-7.—Gas-tetrode 300-cps relaxation oscillator.

about  $\pm 1$  per cent. This error increases with frequency. At high frequencies, gas triodes like types 884 or 6D4 are more suitable since they have cleanup times of only about 20  $\mu\text{sec}$ .

**4-5. Blocking Oscillators.**—Low-voltage blocking oscillators using receiver-type tubes, have much to recommend them for PRF and range-marker generation, for although their free-running frequency stability is only good to about 5 per cent, with considerable "jitter" (see Glossary), the pulse which they supply is useful. The voltage pulses from the pulse transformer windings are at impedances from 300 to 1500 ohms, either polarity, with amplitudes from 100 to 300 volts. Most blocking-oscillator voltage pulses have negative overshoots which are sometimes useful

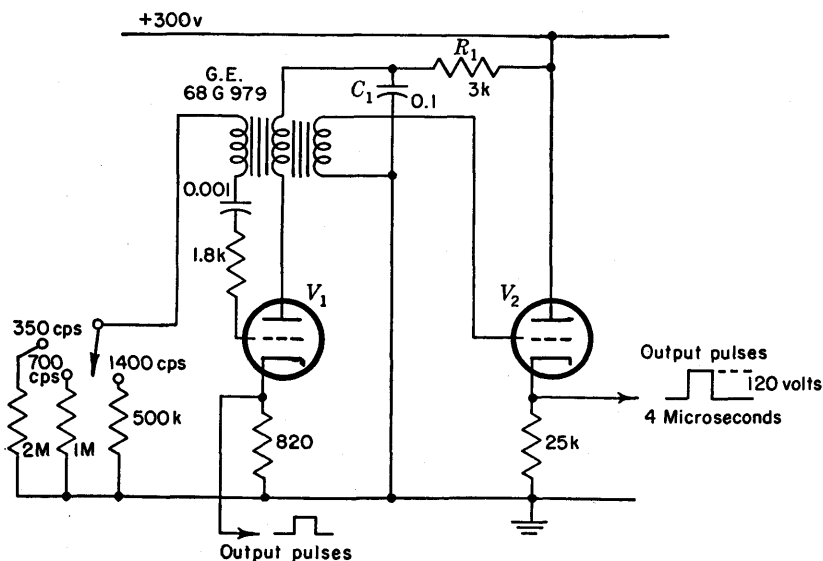


FIG. 4-8.—Blocking-oscillator PRF generator operating on 350, 700, or 1400 cps.

as delayed triggers. Furthermore, the pulse of current drawn during the regeneration period may be about one ampere. This permits large-amplitude pulses to be formed across series resistors of from 10 to 200 ohms, suitable for driving terminated cables. Blocking oscillators also have the property in common with gas-filled tube relaxation oscillators that current flows only for a very small percentage of the time, giving negligible average currents.

**Blocking-oscillator PRF Generator of AN/APS-3.**—This blocking oscillator, which is of perfectly conventional type, uses a GE68-G-979 pulse transformer and generates 4- $\mu\text{sec}$  pulses at a recurrence frequency of 350, 700, or 1400 cps, depending on the grid-leak resistor value (see Fig. 4-8). Components  $R_1$  and  $C_1$  decouple the circuit from the power

supply, a precaution which should always be observed. Two positive outputs are obtained, one across the cathode resistor of the blocking oscillator  $V_1$  and the other from the cathode follower  $V_2$ , which is supplied with a signal from a third winding on the pulse transformer.

*Quenching (Squegging) Oscillator with an Air-core Transformer.*—To avoid the "jitter" effect of an iron-core transformer (see Vol. 19, Chap. 6), the quenching (squegging) oscillator of Fig. 4-9, which uses an air-core transformer, can be used. The transformer itself consists of two six-

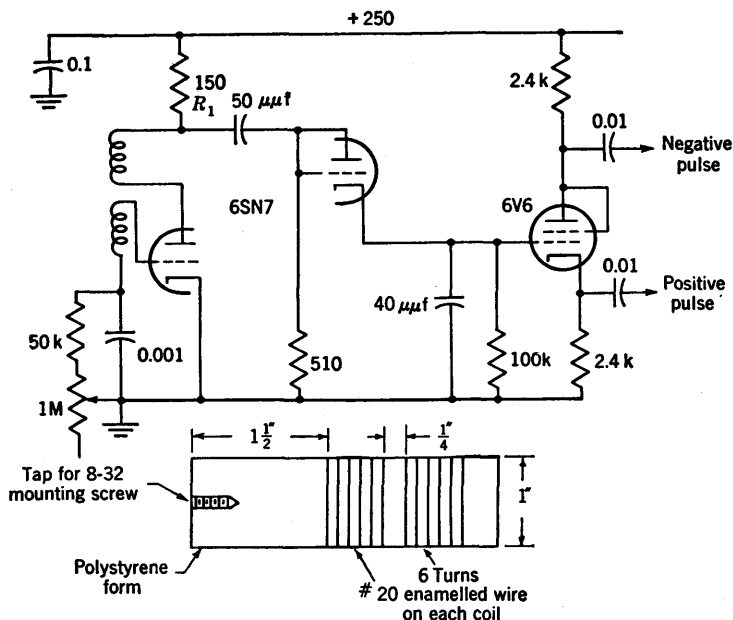


FIG. 4-9.—Quenching (squegging) oscillator.

turn windings, spaced 1 in. apart, on a 1-in. polystyrene rod. The train of oscillations, taken across a small resistor in series with the tube, is detected in the diode and filtered to obtain the output pulse, which may be of either polarity, depending upon which way the diode is facing. Rise time is about  $0.1 \mu\text{sec}$ , amplitude about 40 volts. The recurrence frequency is determined by  $RC$ .

An obvious simplification of this circuit is to bypass the r-f oscillations at  $R_1$  with a small condenser  $C$  (say  $0.001 \mu\text{f}$ ), to provide a low-impedance average-current pulse at  $R_1$ , allowing the oscillator tube to perform the detection. In some radar systems, the r-f oscillator is allowed to operate as a quenching (squegging) oscillator rather than the usual switched type, and may then define its own PRF.

**4-6. Multivibrators.**—The symmetrical multivibrator of Fig. 4-10, which oscillates at about 440 cps, shows a frequency change of  $-1$  cps for a 10 per cent increase of heater voltage and change of a  $-1\frac{2}{3}$  cps for a 10 per cent increase in plate supply voltage. Thus, a 10 per cent change in line voltage should cause about a 0.6 per cent change in frequency. Wire-wound resistors and good-quality condensers must be used to achieve this stability. Tube changes cause a further change of  $\pm 3$  per cent.

Compared with other types of PRF oscillators the multivibrator has the advantages of fairly high frequency stability as indicated by the data, low current drain (5 ma or less), and economy of space. The

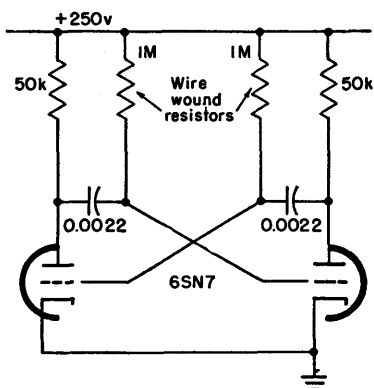


FIG. 4-10.—Symmetrical multivibrator as PRF generator.

blocking oscillator requires a pulse transformer which when hermetically sealed is almost as big as a tube. The *RC* sine-wave oscillator and squaring amplifiers are extravagant of parts and space and draw more current (19 ma). One drawback of the multivibrator PRF generator is that the positive output pulses are formed when the tube is cutting off and therefore when the impedance is essentially that of the plate load resistors. It is necessary, however, to keep the plate load resistance high for frequency stability. The negative pulse appears at the impedance

of the triode plate resistance. When a lower impedance is desired a cathode follower may be used.

A similar multivibrator design using 6AK5 pentodes rather than triodes was studied and found to have only slightly better frequency stability than the triode with high plate loads.

Work done at Rensselaer Polytechnic Institute led to some stabilization methods mainly effective against changes in plate supply voltages but also to a certain extent, against changes in heater supply voltages.<sup>1</sup>

A more effective refinement is the use of the double phantastron described in Chap. 7 of this volume and in Sec. 5-16 of Vol. 19, which should be as much better than the multivibrator as the phantastron time-modulation circuit is better than the delay multivibrator. Considerable thought has been given to the design of highly unsymmetrical multivibrators which would provide a short low-impedance pulse during one state of its operation, and remain in the other state for the remainder

<sup>1</sup> See NDRC Report 14-155, Project No. 18.07, Contract OEMsr-781.

of the recurrence interval. This subject is treated in Vol. 19, Secs. 5-10, 5.11.

## MULTIPLE-FREQUENCY MARKER AND TRIGGER GENERATORS

BY R. I. HULSIZER

Single-frequency marker generators are useful in providing triggers and time markers. If a trigger with an associated timing scale, or a system of time markers at various frequencies is desired, it is necessary to synchronize two or more single-frequency marker generators. There are five methods of synchronization: independent pulsed oscillators, frequency division, frequency multiplication, automatic frequency tracking, and pulse selection between two independent oscillators. The first three methods are standard practice and are described in detail in Vol. 19, Chaps. 4, 15, and 16. The fourth method involves frequency-modulating a slave oscillator according to the error signal from a phase detector that compares the relative phase of the reference oscillator and a pulse derived from each cycle of the slave oscillator. The fifth method generates a selecting gate from the low-frequency oscillator to select one of the high-frequency markers for each period of the low frequency. The resultant selected pulses will have an average period of the low-frequency oscillator but will differ from it by an amount up to one period of the higher frequency. The result will be a jittery time interval between selected pulses.

Examples of these types of synchronization appear in the following sections. The technique of generating markers at independent frequencies will be discussed under grouped markers in the last portion of the chapter.

Before discussing the electrical techniques of generating multiple-frequency markers it might be well to mention again a convenient electro-mechanical system for producing time markers. If a linear sweep is displayed on a CRT, time markers can be obtained by placing a linear scale along the display sweep. The circular sweep mentioned in Chap. 3 is a widely used method of obtaining a sweep of adequate linearity for this use. In this case the time markers are made by inscribing equally spaced radial lines on the CRT face.

Two quantities specify the performance of multiple-frequency-marker generators. One is the stability of the ratios of the several frequencies. The other is the stability of the phase lock between pulses of the separate frequencies which should normally occur simultaneously.

**4-7. Frequency Division.**—The following synchronizer represents a good example of a system in which exact frequency ratios are specified, but in which only moderate phase lock is required. As a result of this condi-



tion, very stable frequency dividers are used and the triggers and range marks are derived directly from the frequency dividers.

Pulse recurrence frequencies of 390 and 1170 cps are simultaneously provided. In addition, range marks were desired at 4000-, 20,000-, and 40,000-yd intervals with mixed 4000- and 20,000-yd marks. An unusual

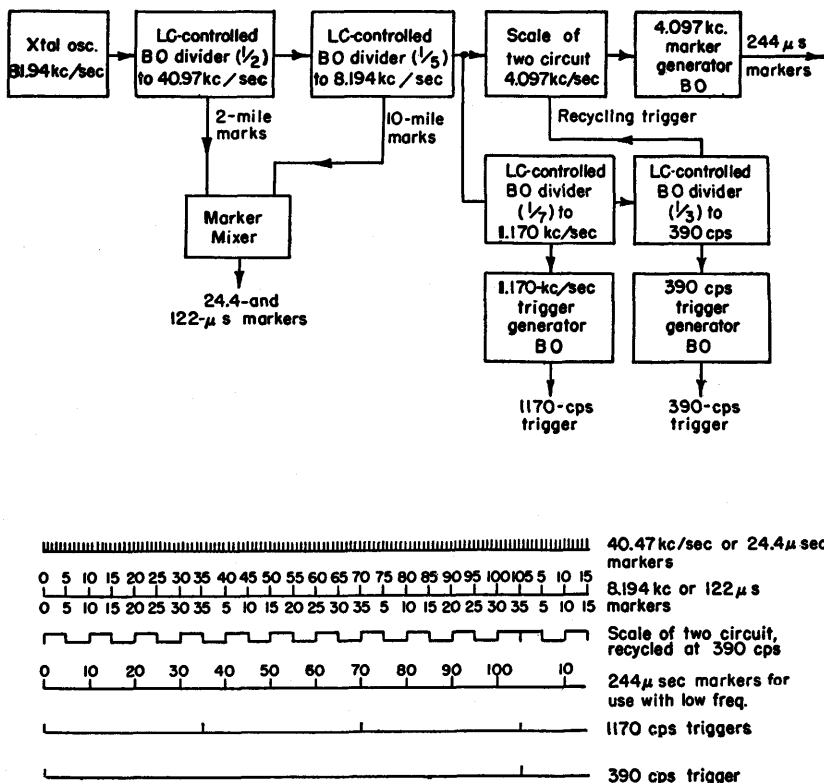


Fig. 4-11.—Timing and block diagram of special synchronizer for output at two simultaneous PRF's.

specification required that each trigger and range mark have four output circuits, any two of which might be short-circuited without interfering with the other two, or with the operation of the circuit as a whole. The block and timing diagram, Fig. 4-11, indicates the sequence of operations.

An accurate timing wave is generated by an 81.94-kc/sec crystal oscillator, a 40.97-kc/sec crystal being bulky and less procurable. The necessary division ratio of 2 to 1 from the oscillator to the 2-mile marks is unlikely to give rise to any frequency instability. The two frequencies, 40.97 and 8.19 kc/sec, are harmonics of both the PRF's and hence the

first two dividers operate continuously. The next frequency of markers, 4.097 kc/sec, is not a harmonic of either PRF. Since they are used only at 390 cps, it is only necessary to synchronize them with 390 cps as shown in the timing diagram; the method of recycling will be described shortly. Following the 10-mile marks there are two blocking-oscillator dividers dividing first by 7, and then 3, to produce the two PRF's.

Figure 4-12 shows the crystal oscillator, the first two dividers, and the 2- and 10-mile range mark mixer. A triode crystal oscillator is used since the specified range accuracy was only 0.1 per cent. Synchronizing

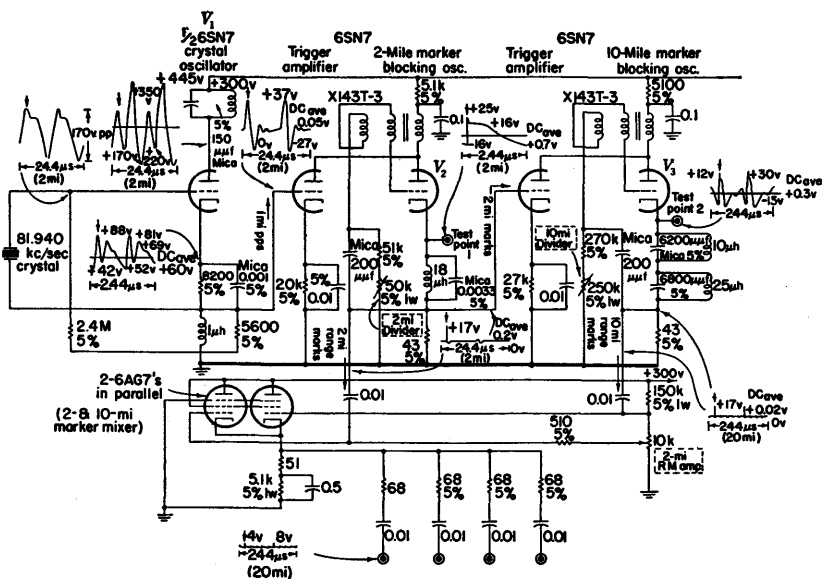


Fig. 4-12.—Crystal oscillator, 2:1 and 5:1 pulse frequency dividers, and mixer of special synchronizer of Fig. 4-11.

triggers were obtained from the crystal oscillator by passing the Class C current pulses through a damped choke to develop a pulse every 12.2  $\mu$ sec. Synchronization is applied to the first blocking oscillator, as to all the rest, through a triode trigger amplifier connected in parallel with the blocking-oscillator triode. The current pulses arising from the trigger triode induce synchronizing triggers in series with the grid waveforms. All the dividers save one are blocking oscillators operating at low division ratios and with *LC*-stabilization to insure constant frequency division for large variations of voltage and temperature and for tube changes. This technique is discussed in Vol. 19, Sec. 16-12.

The first blocking oscillator divides by 2, generating 40.970-kc/sec

marks. A 20-kc/sec ( $\frac{1}{2}f_r$ )<sup>1</sup> stabilizing resonant circuit in the cathode circuit effectively adds a one-half cycle cosine waveform to the exponential waveform in the grid return. Two-mile marks appear across a 43-ohm resistor in series with the cathode, developing a 17-volt positive pulse from the current surge of each blocking oscillation. Ten-mile markers are similarly derived in a 5-to-1 divider stabilized by two resonant circuits tuned to 20 kc/sec and 12 kc/sec ( $\frac{3}{2}f_r$  and  $\frac{5}{2}f_r$ ). To provide the required mixed marks at four terminals, the 2- and 10-mile

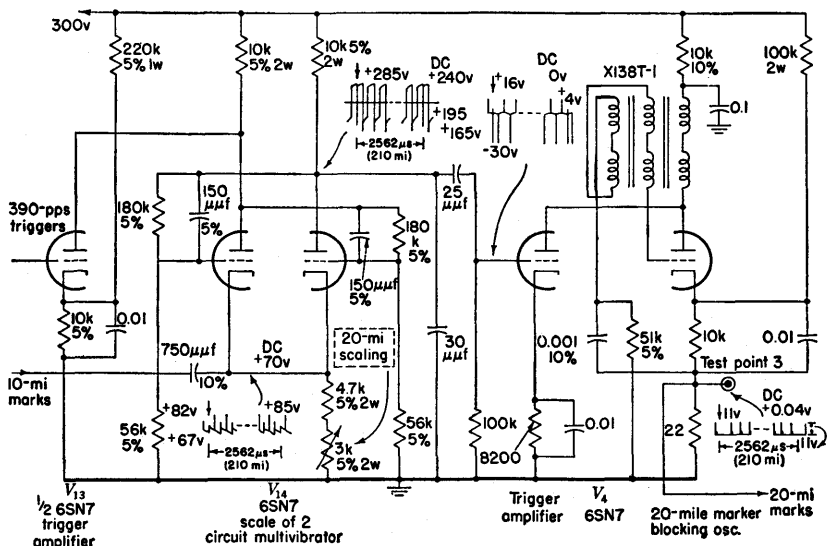
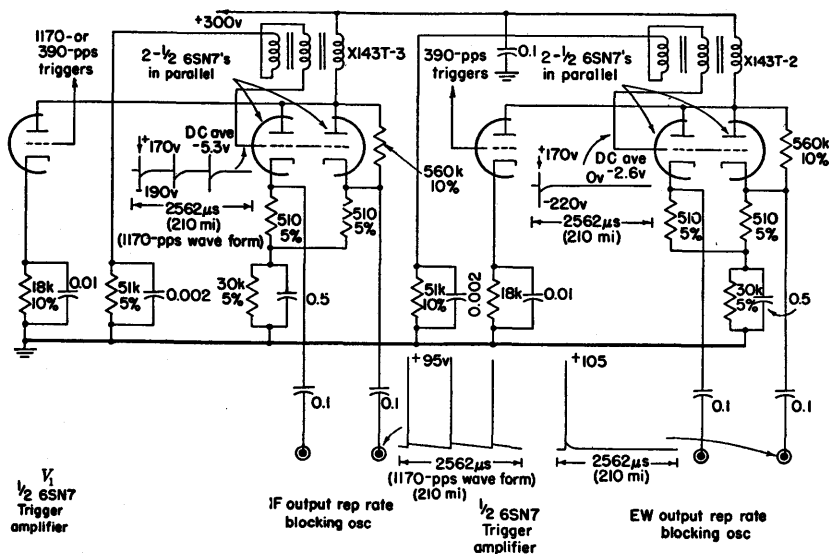
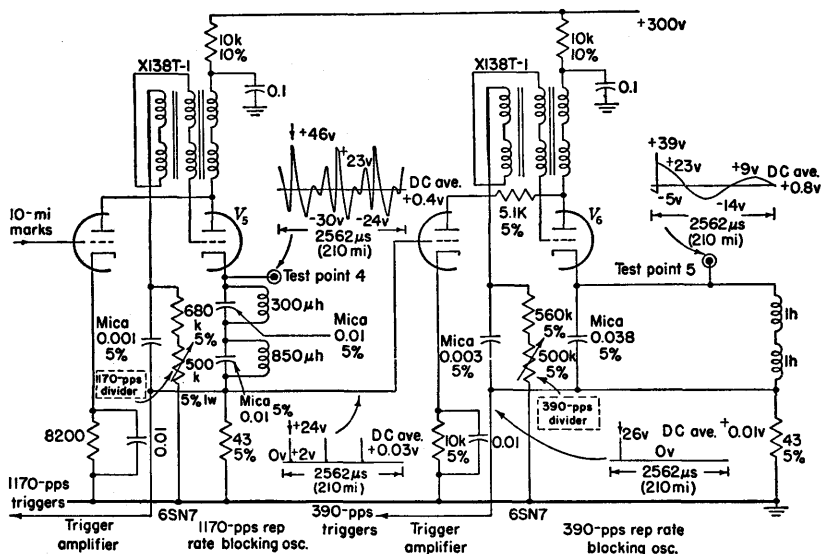


Fig. 4-13.—Scale-of-two multivibrator and blocking-oscillator pulse generator.

markers are mixed in a biased-off cathode-follower mixer using two 6AG7's, driving a 51-ohm load. The 2- and 10-mile markers add and accentuate every fifth mark as shown in Fig. 4-12. Each of the four 70-ohm range-mark cables are driven through 68-ohm resistors from the cathode follower. Short-circuiting any two cables changes the cathode load from 21 ohms to 15.3 ohms, a decrease which is acceptable. Of course, the rest of the circuit remains unaffected, since the cathode follower acts as a buffer.

The circuit of Fig. 4-13 counts the 10-mile marks in a scale-of-two counter circuit with the injected 390-pps trigger acting to make the counter inoperative for one of the 10-mile marks each recurrence interval. Therefore, the counter responds only to twenty 10-mile markers, thus providing only ten 20-mile markers in each 220-mile interval. The

<sup>1</sup> The symbol  $f_r$  will be used to represent the recurrence frequency of the output pulses of the stage being discussed.



recycling is accomplished by coupling the 390-pps trigger into the counter through a trigger amplifier which resets the circuit to the state it was in before the twenty-first 10-mile marker occurred.

The square wave from the second plate of  $V_{14}$  is differentiated in  $C_4$  and  $R_6$  and triggers a blocking oscillator  $V_4$  to form the 20-mile range markers. Its cathode is normally held at +27 volts and the grid time constant is only  $\frac{1}{20}$  of the recurrence interval. Pulses occur, therefore, every time the scale-of-two circuit counts. The four 70-ohm range-mark

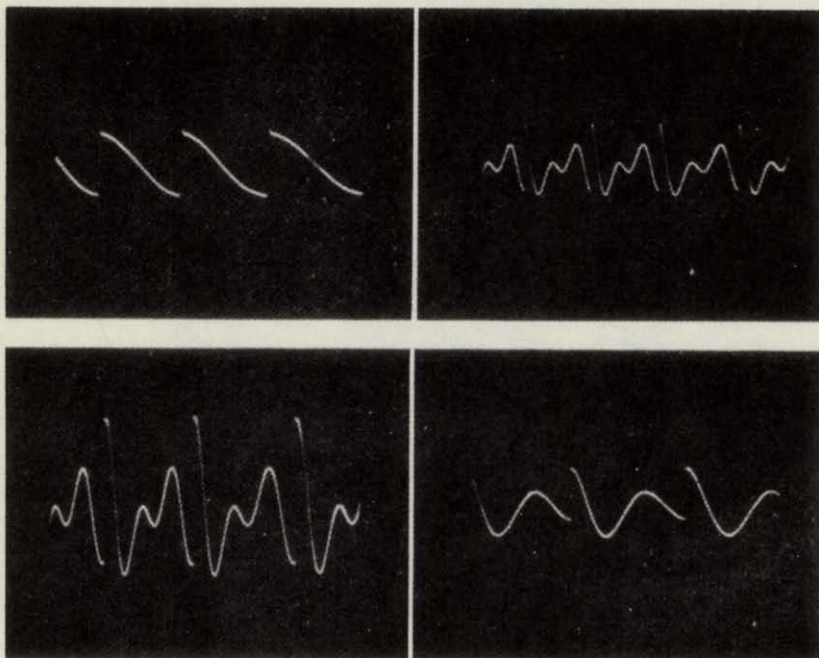


FIG. 4.16.—Cathode waveforms of frequency dividers. (a) Cathode of  $V_2$ ,  $f_r = 40.97$  kc/sec. (b) Cathode of  $V_3$ ,  $f_r = 8.194$  kc/sec. (c) Cathode of  $V_5$ ,  $f_r = 1170$  pps. (d) Cathode of  $V_6$ ,  $f_r = 390$  pps. ( $f_r$  is the output frequency of the divider stage.)

cables are each driven from the blocking-oscillator current pulses through 68-ohm resistors, as in the 2- and 10-mile mixer.

Also, following the 10-mile marker divider are the two PRF dividers shown in Fig. 4.14. The first divides by 7 to 1170 pps and is synchronized by tuned circuits at 1.750 kc/sec ( $\frac{3}{2}f_r$ ) and 2.730 kc/sec ( $\frac{5}{2}f_r$ ). The second PRF divider divides by 3 to 390 pps using a single resonant circuit tuned to 585 cps ( $\frac{3}{2}f_r$ ). The output circuit for the two sets of triggers, Fig. 4.15, is a pair of four-tube blocking oscillators, each tube having a separate cathode resistor thereby providing the required four

independent trigger sources for each trigger, any of which may be short-circuited without affecting the rest.

Figure 4-16 shows the cathode waveforms of the various dividers.

The complete system was found to operate without change of frequencies for JAN limit tubes and  $\pm 20$  per cent change in line voltage.

If more accurate phase lock of the triggers and the oscillator sinusoid were desired, pulse selection as described in the next section might have been applied.

#### 4-8. Frequency Division and Pulse Selection.

—In contrast to the previous synchronizer, the Model III calibrator has lax specifications on its PRF stability but very high specifications as to the accuracy of the

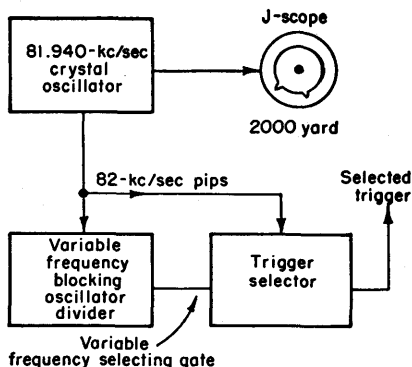


FIG. 4-17.—Block diagram of synchronizer for Model III calibrator.

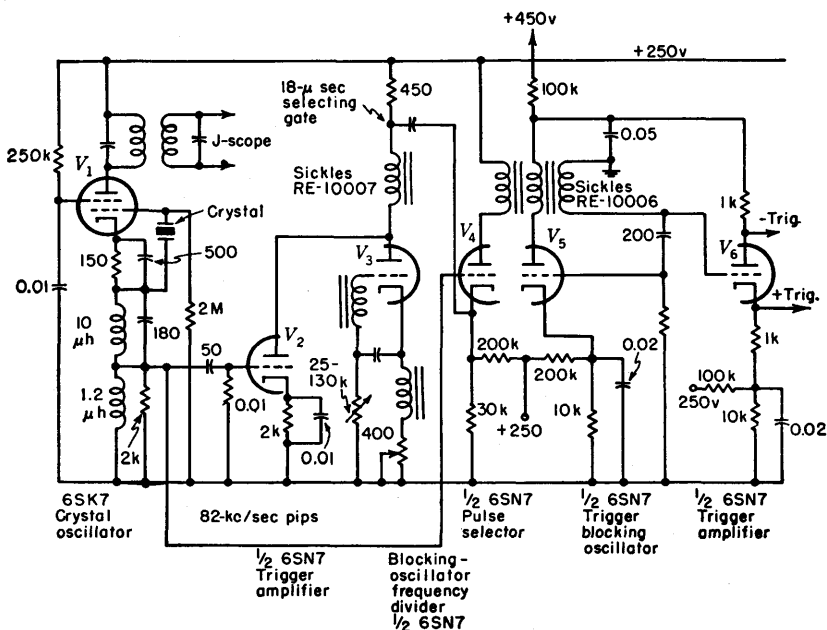


FIG. 4-18.—Schematic diagram of synchronizer portion of Model III calibrator.

time relationship between the PRF pulse and the crystal-oscillator sinusoid. The sinusoid is used to form a sweep for accurate time meas-

urements; hence the position of zero time—the PRF trigger—must be defined as closely as the time measurements are specified (about 0.03  $\mu\text{sec}$ ). A wide range of PRF's was desired, and it was necessary for the circuit to be simple to keep the size of the calibrator down to that of a useful bench instrument. Figure 4-17 shows the resulting design. The schematic diagram of the synchronizer is shown in Fig. 4-18.<sup>1</sup>

A tri-tet crystal oscillator  $V_1$  is used to maintain good frequency stability while the plate-load tuning is varied to control the desired circular-sweep amplitude. A damped choke in the cathode lead provides a pulse at the oscillator frequency. These pulses are amplified in  $V_2$  and trigger a variable-frequency blocking-oscillator frequency divider  $V_3$ . Since it is expected that the grid timing network will be varied, there will be large phase shifts between the blocking-oscillator pulses and the 82-kc/sec sinusoids. To provide a trigger whose phase does not vary relative to the sinusoid, the 18- $\mu\text{sec}$  pulse of the dividing blocking oscillator is used to select the 82-kc/sec pulse immediately following the one which triggered the blocking oscillator. The coincidence tube  $V_4$  is a triode with the 82-kc/sec pips applied to the grid and the repetition-frequency selecting gate applied to the cathode. The quiescent grid-to-cathode bias is 30 volts, and the 400-ohm variable resistor in the frequency-divider cathode return is adjusted to keep the selector gate below cutoff. Upon coincidence the sum of selecting gate and oscillator pip drives the grid above cutoff and plate current flows in the coincidence tube, firing the trigger blocking oscillator  $V_5$ . Positive and negative triggers at 1000-ohm impedance are provided by the trigger amplifier  $V_6$ .

The frequency divider might have been omitted and replaced by selection at random if a pentode time selector were used. In the Model III calibrator, time selection by waveform addition and amplitude selection is used. For this process it is desirable that the selecting pulse be of constant amplitude, or that the relative times or occurrence of the pulse and the selecting waveform be fixed. The latter alternative was chosen in the Model III calibrator and implemented by using a variable-ratio frequency divider whose output pulse is used as a selecting gate. This gate maintains a relatively fixed relationship with the pulse to be selected since it is initiated by the preceding pulse. On the other hand, if an occasional misfiring can be tolerated, a selecting gate occurring perfectly at random will cause poor trigger selection infrequently if its rise and fall are short compared with its duration.

The phase shift between the trigger and the sinusoid remained below 0.01  $\mu\text{sec}$  for all repetition frequencies. If the oscillator plate tuning is changed, the position of the trigger changes  $\pm 0.25 \mu\text{sec}$  for  $\pm 50$  per

<sup>1</sup> E. Gostyn, "Operating Data, Model III Calibrator," F. W. Sickles Co., March 1944.

cent change in sinusoid amplitude at the plate. Varying the line voltage with constant 82 kc sinusoid amplitude yielded the data in Table 4-1.

TABLE 4-1.—SHIFT IN TRIGGER PHASE WITH LINE VOLTAGE

Line voltage	Trigger displacement, $\mu\text{sec}$
75	0.10
85	0.05
100	0.00
115	0.10
130	0.15

Other examples of this technique are the TS-100 test oscilloscope and the Dumont 256-B A/R oscilloscope (see Vol. 21, Sec. 18-4). An example of a frequency-divider synchronizer system in which both accurate frequency and accurate phase were required is the SCR-584.<sup>1</sup>

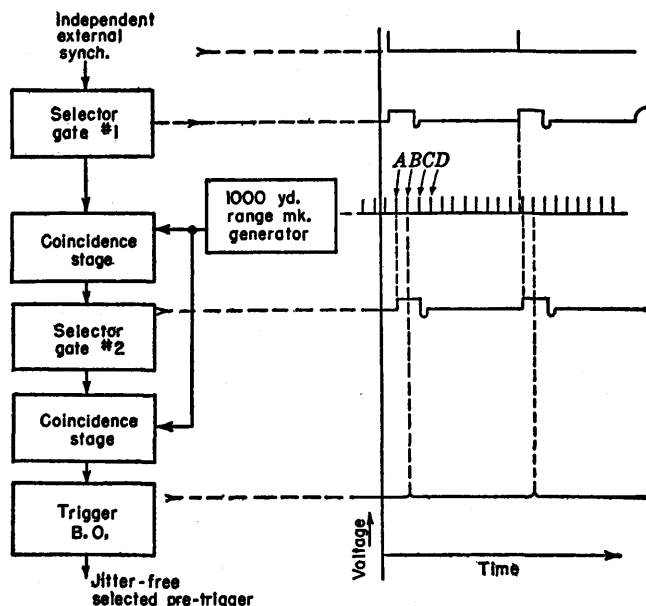


FIG. 4-19.—Trigger-selector block diagram of experimental radar synchronizer.

**4-9. Separate Oscillators and Pulse Selector.**—In some circuits an external sine wave oscillator is used to determine the recurrence frequency, but the crystal oscillator is desired as the time standard.

In contrast with the Model III calibrator where the alignment of the selecting gate with respect to the pulse is obtained by the use of a frequency divider as a PRF generator, the synchronizer of this section employs an external PRF oscillator (3 kc/sec) to select a pulse A at

<sup>1</sup> D. G. Fink, "The SCR-584 Radar," *Electronics*, 19, February 1946.



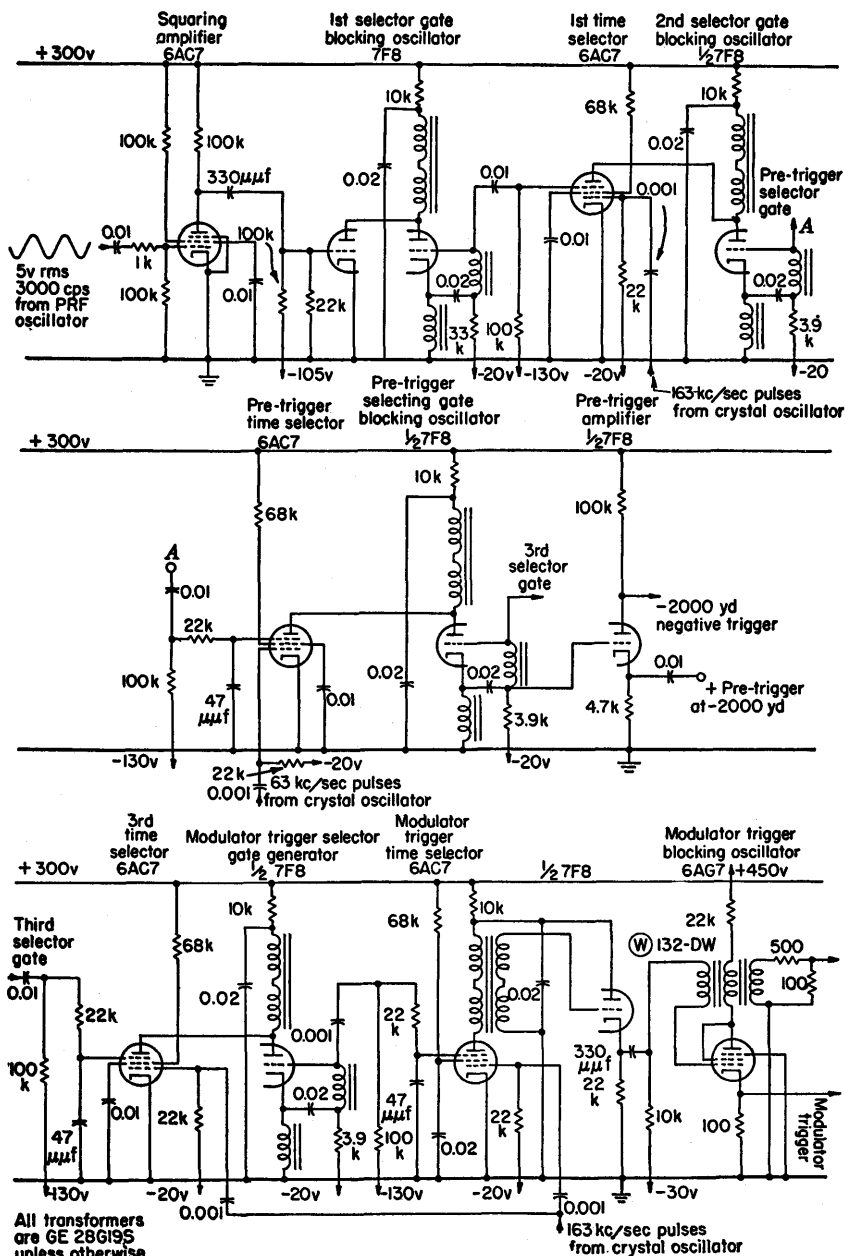


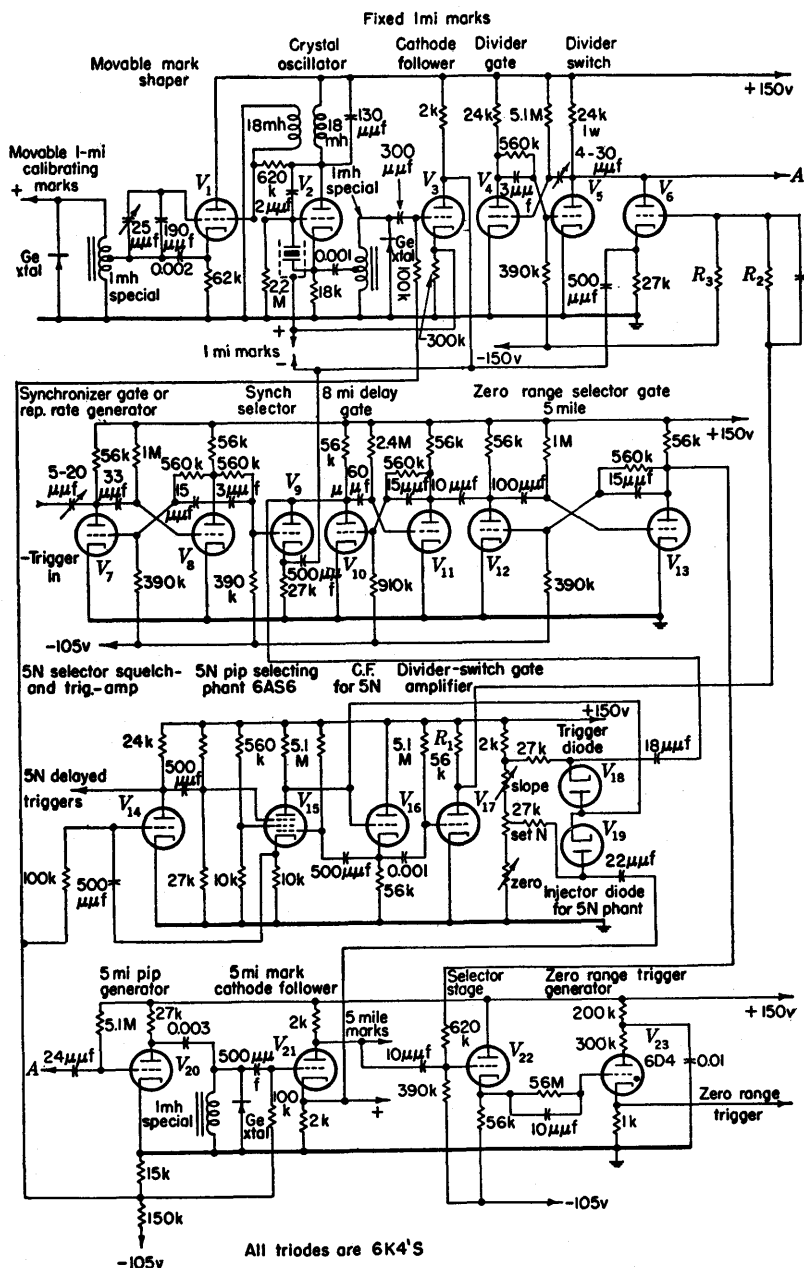
FIG. 4-20.—Synchronizer of experimental radar.

random that forms a selecting gate whose position with respect to the succeeding pulse *B* is thus adequately defined. As shown in Fig. 4.19, selection of pulse *B* results in a trigger which is stable with respect to the phase of the 163-kc/sec oscillator. Figure 4.20 shows the circuit. The first two rows of tubes perform the operations indicated on the block diagram. The third row uses the pretrigger to select a third pulse *C* which in turn triggers a selector gate to select the fourth pulse *D*, thus providing a trigger delayed exactly from the pretrigger by 2000  $\mu$ d. The selected pulse *D* drives a low-impedance blocking oscillator to supply the modulator trigger. The advantages of this type of synchronization are that it permits complete freedom of choice of the PRF and at the same time jitters, or phase-modulates, the triggers with respect to the PRF signal. The latter is an advantage in radar applications since it makes the radars less susceptible to mutual interference.

A proposed and as yet incompletely tested synchronizer was to be incorporated in a revised model of AN/APS-10 radar, and this circuit incorporates a number of good techniques and highly economical circuit practices. This design was made possible in part by the development of baseless subminiature triodes which permit very low stray capacitances, a powdered iron 1-mh choke having a high resonant frequency, and the germanium crystal rectifier which has a very low capacitance, about 0.5  $\mu$ f, and a forward resistance of less than 1000 ohms. Shunting the crystal across the choke provides an economical method of obtaining short pulses for triggers or markers since the crystal does not lower the choke-resonant frequency appreciably and yet offers severe damping after the first half cycle. The low-capacitance tubes and wiring permit the design of stable high-impedance multivibrators with reasonable output rise times.

One precaution that was observed as a result of large variations in the characteristics of the tubes was that when two circuits are direct-coupled the most significant value of the signal voltage should occur when the associated vacuum tubes are in a nonconducting state. A study of the schematic and block diagrams will illustrate the use of these special components and this philosophy of design.

One of the special requirements of the AN/APS-10 synchronizer was that it should operate on an external PRF source without introducing more than 2 per cent jitter. In addition the following markers were desired: positive and negative 1-mile markers; positive and negative 5-mile markers; positive 1-mile markers phasable with respect to the first set; a marker which would be movable in integral multiples of 5 miles, called the "5N-mile delayed trigger"; a PRF trigger accurately phased with respect to the above 1-mile markers; and a prestart trigger at the PRF preceding the zero range marker by 135  $\mu$ sec.



The value of plate supply was set at 150 volts for the following reasons: a simple 110-volt line-operated rectifier could be used, the average current consumption is in general proportional to the plate supply, and the low voltage permits the use of low-voltage condensers and low-wattage resistors. To supply synchronizing triggers from the external PRF without introducing more than the specified 2 per cent jitter, it was necessary to select one of the accurate 1-mile markers and to use a gated divider to supply the 5-mile markers.

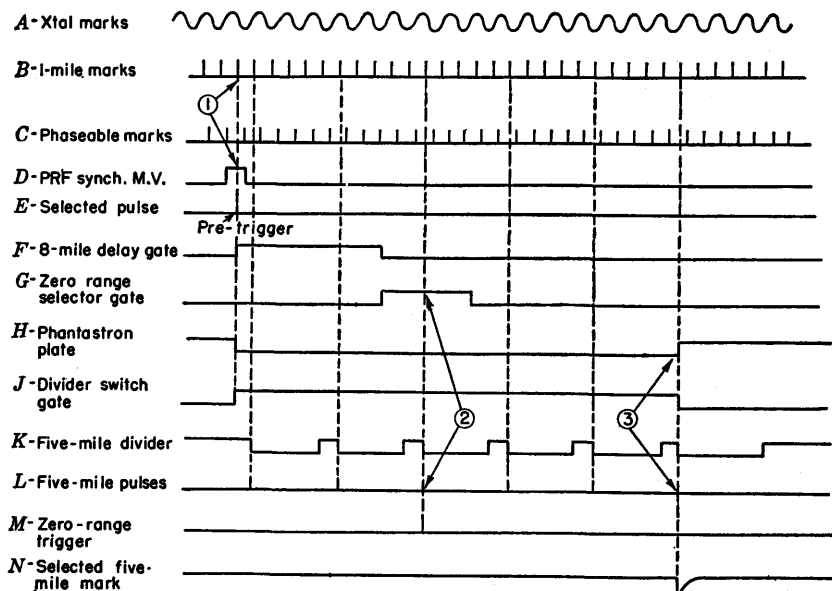


Fig. 4-22.—Timing diagram of proposed AN/APS-10 synchronizer. 1, 2, and 3 mark the three time-selection operations.

Referring to the diagrams, Figs. 4-21, 4-22, and 4-23, an 80.86-kc/sec triode crystal oscillator  $V_2$  generates sinusoids, waveform A, whose period corresponds to 1 nautical mile of radar range. The unusual features of this oscillator are the plate-to-grid coupling condenser necessary here because of the low interelectrode capacitances of the subminiature tubes and the combined resistive and inductive coupling into the movable mark shaper  $V_1$ . Tuning the secondary of the plate transformer provides the necessary variation of phase shift of the movable 1-mile calibrating marks, and the addition of the resistive coupling places the center of the phase-shift variation at the desired phase. The movable mark shaper  $V_1$  acts as a Class C amplifier, whose current surges shock-excite the damped choke in the cathode circuit, forming a short pulse, waveform C. The phasable pulses are required to permit the zero

correction of radar system (see Chap. 3). Pulses of fixed phase with respect to the crystal oscillations are formed from the current pulses in the crystal oscillator itself, and are developed across the damped choke in its cathode. The succeeding amplifier  $V_3$  supplies these marks at low impedance with both polarities to the rest of the synchronizer, and as range marks for the indicators, waveform  $B$ . As indicated in Fig. 4-23, the next operation on the sequence is the selection in  $V_9$  of the pretrigger by the PRF synchronizer pulse, waveform  $D$ , which is a positive gate slightly over 1 mile in duration. It is applied to the grid of a triode coincidence stage  $V_9$  whose cathode is driven by the 1-mile marker

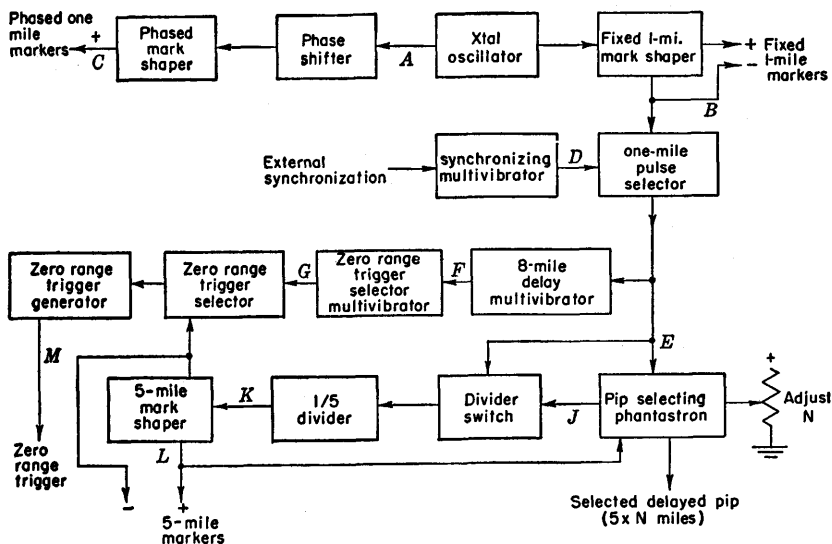


Fig. 4-23.—Block diagram of proposed AN/APS-10 synchronizer. Letters between blocks refer to waveforms of Fig. 4-22.

pulses. The resultant selected trigger  $E$  initiates an 8-mile delay gate  $F$  in  $V_{10}$  and  $V_{11}$  which in turn triggers the zero-range selector gate  $G$  in  $V_{12}$  and  $V_{13}$ . These three gates are generated from unsymmetrical monostable multivibrators (Vol. 19, Chap. 5) whose outstanding characteristics are the large plate resistors made possible by the low capacities of the tubes and the practice of using only the negative output when steep wavefronts are desired.

In order to follow the sequence of operations it is necessary to leave this train of operations at the generation of the zero-range selector gate waveform  $G$  and consider the generation of the 5-mile marks, since one of the 5-mile marks is to be selected by the gate  $G$  to form the zero-range trigger  $M$ .

The 5N pulse-selecting phantastron  $V_{15}$ ,  $V_{16}$  is triggered by the

selected pulse  $E$ . Its plate waveform immediately shuts off  $V_{17}$ , which in turn gates the 5-mile divider switch  $V_6$  with the waveform  $J$ . The voltage to which the grid of the divider switch tube  $V_6$  is brought by  $J$  is determined by a bleeder  $R_1$ ,  $R_2$ , and  $R_3$  between  $E_{pp}$  and the  $-105$ -volt supply at a time when  $V_{17}$  is nonconducting. With this arrangement, variations in characteristics of  $V_{17}$  do not affect the level to which the grid of the triode coincidence tube  $V_6$  is raised.

As a result of the divider switch action, the divider  $V_4$ ,  $V_5$ , starts to divide on the first 1-mile marker after the prestart trigger and continues to divide until the phantastron ( $V_{18}$ ) plate reaches a voltage sufficiently low to cause conduction in the injector diode  $V_{19}$ . As this happens, the  $N$ th 5-mile mark couples into the cathode follower  $V_{16}$  of the phantastron, driving the pentode grid more positive, generating a positive pip in the cathode of that tube. This is coupled to the 5N selector shutoff and trigger amplifier  $V_{14}$  which then provides a low-impedance 5N delayed trigger which shuts off the phantastron. As the phantastron shuts off, its plate rises, turning the divider-switch gate amplifier  $V_{17}$  on again and shutting off the 5-mile divider switch  $V_6$ , thus terminating the divider ( $V_4$ ,  $V_5$ ) action until the next repetition period. Since the zero-range trigger-selector gate does not turn on until after the 8-mile delay gate and is 5 miles in duration, it overlaps the third 5-mile pip which occurs 11 miles after the pretrigger. The coincidence of these two waveforms in  $V_{22}$  triggers a thyatron  $V_{23}$  to form the zero-range trigger for the radar modulator. It is interesting to note that although the coincidence between the externally synchronized selecting multivibrator will have occasional jitters when the overlap occurs on the rising edge of the selecting gate (about 1 per cent of the time), the zero-range selector gate maintains a constant time relationship to the 5-mile marker that it selects. Thus a stable PRF trigger is provided. The zero range trigger maintains a fixed time relationship to the fixed markers to within  $0.01\mu s$ .

One essential design practice required by the use of triode time selectors is that described in connection with the action of the time selector  $V_6$ ; the potential to which the grid is brought by the selecting gate is independent of variations in the characteristics of the gate-generating tube,  $V_{17}$ . This precaution is observed in the time selectors  $V_9$  and  $V_{22}$ .

**4-10. Synchronization by Automatic Frequency Tracking.**—Development of pulse techniques has led to a modification of the conventional frequency-tracking circuits that permits oscillators of two widely different frequencies to be synchronized. If, as indicated in Fig. 4-24, pulses are formed from each oscillator, the relative times of appearance of these pulses can be compared at  $A$ ,  $B$ ,  $C$ , etc. with a time discriminator.<sup>1</sup> If

<sup>1</sup> Secs. 3-17 and 3-18.

the two frequencies are fixed, but aligned at *A*, the error signal of the time discriminator would indicate an increasing time difference at *B* and *C*. When this error signal is applied to a reactance tube controlling either oscillator, the two oscillators will be made to operate at an integral frequency ratio with an accurately controlled phase relationship. If the limits of control of the reactance tube are such that it cannot change the frequency ratio by one integer, and the mean frequency of the controlled

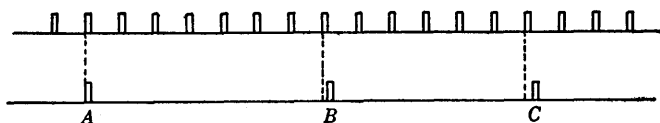


FIG. 4-24.—Frequency tracking by pulse time discriminator.

oscillator is within plus or minus one integer of the desired ratio, the system cannot synchronize at the wrong frequency ratio. Since the limiting factor to the frequency ratio obtainable with this system is essentially the stability of the two oscillators, one would expect to be able to work with frequency ratios from 100 to 10,000 depending upon the type of oscillator used. The distinct advantage of this technique is that in spite of large frequency ratios the time relationship of the pulses derived from the two oscillators is as stable as the time discriminator.

Figure 4-25 shows the block diagram of an automatic frequency-tracking synchronizer where a high-frequency oscillator is controlled by

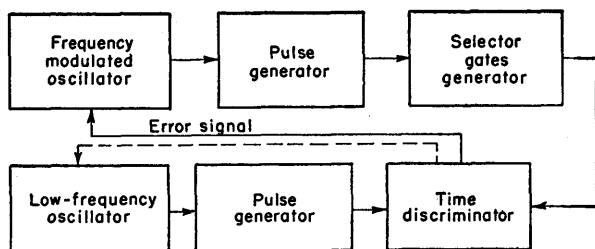


FIG. 4-25.—Block diagram of automatic frequency-tracking synchronizer.

reference to a low-frequency oscillator. The dashed connections indicate its use as a low-frequency oscillator controlled by reference to a high-frequency oscillator.

A design proposed for a lightweight direct-reading Loran indicator is a good example of pulse frequency tracking. The block diagram of Fig. 4-26 indicates that the frequency of the 20-kc/sec oscillator is adjusted so that its  $1/800$ th subharmonic agrees exactly with the PRF of the incoming video pulses received from the Loran ground stations.

The automatic frequency-control circuit is shown in Fig. 4-27. The 20-kc/sec LC-oscillator and pulse generator form 50- $\mu$ sec pulses which trig-

ger a multistage  $\frac{1}{800}$  divider that in turn triggers a 100- $\mu$ sec multivibrator to form the early gate for the time discriminator. The back edge of this gate triggers a similar multivibrator to form the late gate. These two gates turn on successively the grids of the top and bottom sections of a triode time discriminator  $V_2$  and  $V_3$  (see Chap. 3 and Fig. 4-28). The output controls the reactance tube  $V_1$ .

The grid of the reactance tube has full sine waves from the cathode of  $V_{12}$  impressed on it. The cathode is connected to the high-potential end of the tank coil through 24  $\mu$ f. If  $V_1$  conducts for the whole cycle of the sine wave, only a negligible voltage at 20 kc/sec appears across  $C_2$  and no detuning occurs. On the other hand, if  $V_1$  is so biased that it does

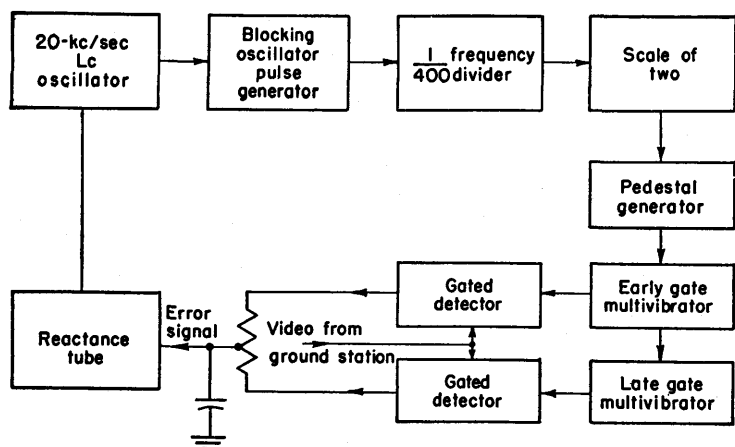


FIG. 4-26.—Block diagram of lightweight Loran automatic frequency-tracking circuit.

not conduct during any part of the cycle,  $C_2$  is essentially connected to ground through 10k from the high-potential side of the tank coil. These two conditions define the limits of frequency modulation by  $V_1$  as 0.24 per cent. Intermediate values of frequency result when  $V_1$  conducts for a portion of the cycle, as controlled by the bias produced by the time discriminator. The effect of switching a small condenser  $C_2$  across the tank circuit for a portion of the cycle apparently has little effect on the waveform of the oscillator since it was found not to affect the accuracy of the condenser phase shifter fed by the oscillator.

The application of this circuit to the more direct problem of synchronizing two oscillators can be accomplished by triggering the early- and late-gate generators from the low-frequency oscillator and feeding paraphased sine waves of the high frequency rather than paraphased video pulses into the time discriminator. The time discriminator thus becomes a hybrid time and phase discriminator. Circuits exemplifying this type





of time discriminator may be found in Chap. 6. A similar example of synchronization can be found in the British omnidirectional beacon described in Sec. 10-8.

*Precise Synchronization of Random Oscillators.*—The two examples of Sec. 4-8, that employ pip selection as a means of synchronizing two independent oscillators, are characterized by the fact that the selected

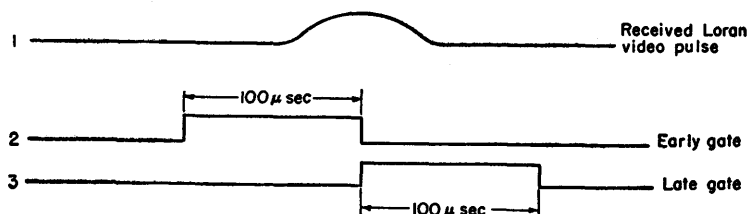


FIG. 4-28.—Loran time-discriminator timing diagram.

pulses can occur after the onset of the low-frequency synchronizing pulse by any amount up to one period of the high frequency. This is often undesirable and a method of obtaining high-frequency pulses accurately defined in time with respect to the low-frequency waveform has been developed and is illustrated in Fig. 4-29. The accurate timing oscillator is used to form a continuous circular sweep on the face of a storage tube.

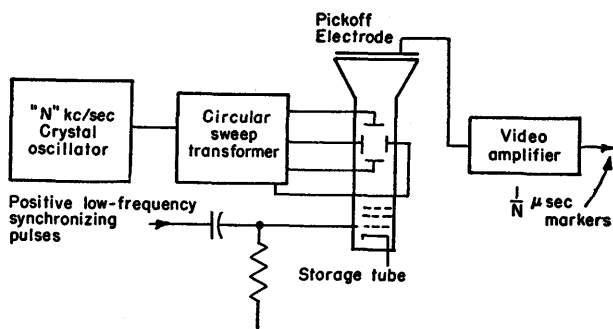


FIG. 4-29.—Block diagram of precise synchronization system for two independent oscillators.

The intensity of the electron beam is normally low. When the positive synchronizing pulse arrives at the storage-tube grid, the beam is momentarily intensified and charges up a short arc of the circular sweep. The succeeding sweeps of the electron beam around the tube face produce at the pickoff electrode a train of short pulses equally spaced at the period of the master oscillator but initiated at the exact instant called for by the external synchronizing pulse. This circuit may be very useful for physical measurements where there is no control over the time at which the interval to be measured commences. Complete details and actual

circuits are described in Vol. 19, Chap. 21 on the use of storage tubes. An alternative method of setting up an equally spaced train of markers starting at any random instant is to use a pulsed *LC*-oscillator and amplitude comparator. This is described in Secs. 4-13 and 4-14.

#### FREQUENCY DIVIDERS WITH INJECTION FEEDBACK

There are some applications where a pulse recurrence frequency is desired with a frequency ratio to the master oscillator that is not factorable into practical single-stage division ratios. It is also often desired to change the PRF by small increments without radically modifying the synchronizer circuit. Both of these problems may be solved with the use of injection feedback dividers.<sup>1</sup> In one form of this technique the last divider stage, in firing, effectively adds one or more extra triggers to the first stage of the chain. Fewer master-oscillator triggers are thus required to complete the next dividing period. In another form of feedback divider, the first divider stage is held off from dividing for a few triggers after the last stage fires. As a result, a complete dividing cycle takes a few more than the usual number of master-oscillator triggers. These methods will be illustrated with two examples.

**4-11. Lightweight Direct-reading Loran PRF Generator.**—In the previous section, the PRF divider circuit of the direct-reading Loran was indicated as a standard frequency-dividing circuit having a ratio of 800 to 1. Actually the Loran PRF's are given by the ratios  $\frac{20 \text{ kc/sec}}{2(300 - N)}$ ,  $\frac{20 \text{ kc/sec}}{2(400 - N)}$ , and  $\frac{20 \text{ kc/sec}}{2(500 - N)}$ , where  $N$  is any integer from 0 to 7 inclusive and corresponds to different stations. Variations in  $N$  give pulse recurrence periods which differ in steps of  $2 \times 50 \mu\text{sec}$ .

The method of providing these odd-valued PRF's from the frequency-controlled 20-kc/sec oscillator is shown in the schematic diagram, Fig. 4-30. Figure 4-31 shows the timing sequences drawn as though the 1-to-5 counter were missing and the last counter were set to count by 6, with  $N$  set for 2. To study the operation of the circuit, let us consider the action of the circuit without injection feedback. The counters are gas-filled tube step counters similar to those described in detail in Vol. 19, Chap. 16 of this series. Consider  $V_{16}$  just after it has fired. The cathode is held by  $V_{14}$  and  $V_{15}$  from going above +100 volts. Fifty microseconds after it fires, a negative pulse will come from the plate of the blocking oscillator  $V_{13}$ , causing the diode  $V_{14}$  to conduct, whereupon the voltage of the trigger pulse will be shared between  $C_7$  and  $C_8$ , lowering the cathode of  $V_{16}$  by about 6.4 volts. The succeeding pulse will

<sup>1</sup> Feedback in this sense does not have the connotation usually attributed to feedback in amplifiers.

find 6.4 volts bias across  $V_{14}$  which it must overcome before  $V_{14}$  conducts;  $C_7$  and  $C_8$  will share the remainder of the pulse voltage. This process

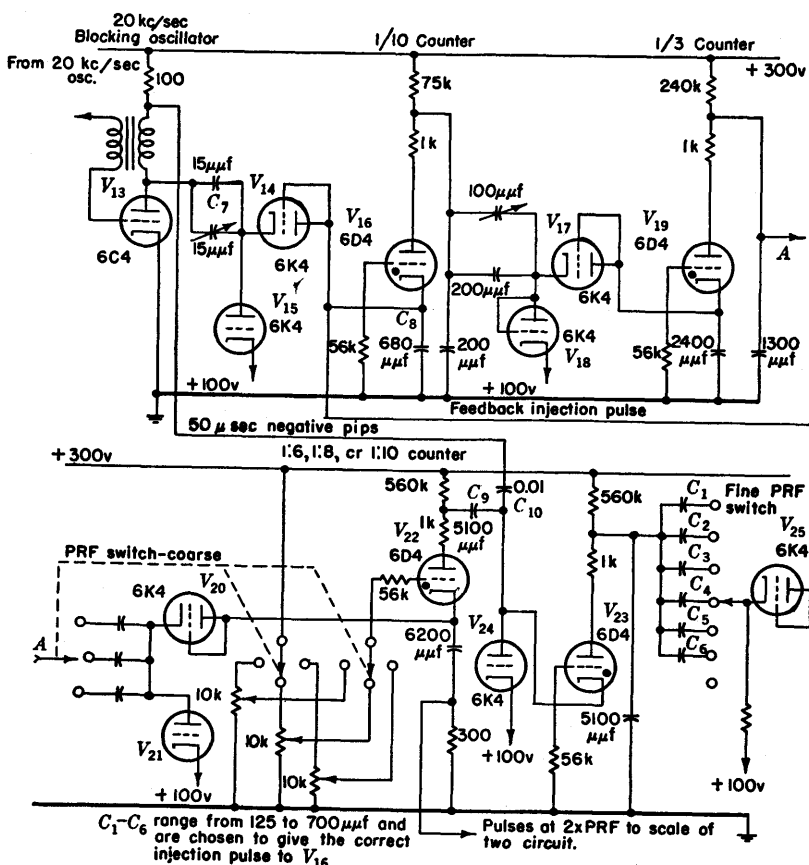


Fig. 4-30.—Schematic circuit of lightweight direct-reading Loran feedback PRF divider.

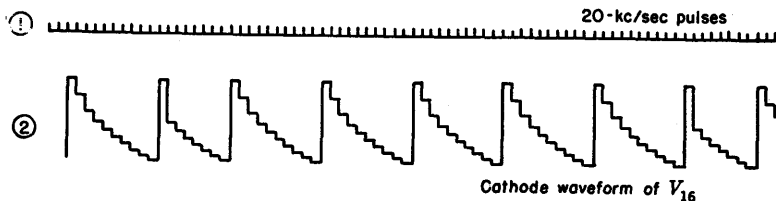


Fig. 4-31.—Abbreviated timing diagram of lightweight direct-reading Loran PRF generator. Dividing ratios are  $\frac{1}{10}$  and  $\frac{1}{3}$ ; injection feedback number,  $N$ , = 2.

continues for nine pulses from  $V_{13}$ , each one bringing the cathode of  $V_{16}$  closer to its firing potential. If  $C_7$  has been properly adjusted, the tenth

pulse will cause  $V_{16}$  to conduct. A similar process occurs in  $V_{19}$ , and  $V_{22}$ . In the absence of injection feedback, a total division ratio of 300, 400, or 500, will be produced.

When  $V_{22}$  fires, its plate drop appears across  $C_9$ ,  $C_{10}$ , and the 100-ohm plate resistor of  $V_{13}$  forming essentially a capacity divider. The fraction appearing at the junction of  $C_9$  and  $C_{10}$  is not quite large enough to fire  $V_{23}$ , but 50  $\mu\text{sec}$  later, when  $V_{13}$  fires, the pulse developed across the 100-ohm plate resistor adds enough to the cathode of  $V_{23}$  to trigger it. When it fires, its plate drop is coupled through one of seven condensers back to the cathode of  $V_{16}$  through the diode  $V_{26}$ . The size of the seven condensers is adjusted so that the voltage change on the cathode of  $V_{16}$  is equivalent to that which would be produced by zero to seven pulses from  $V_{13}$ . As indicated on Fig. 4-31, where  $N = 2$ , this decreases the number of pulses required to fire  $V_{16}$  by  $N$ , where  $N$  varies from zero to seven depending on the setting of the ground station selector. The net effect is to decrease the pulse recurrence interval by  $N \times 50 \mu\text{sec}$ , which after a division by 2 gives the PRF's described at the beginning of this section. The second and third counters are unaffected by the feedback except that the time between the PRF pulse and the next pulse which they receive is less by  $N \times 50 \mu\text{sec}$  than 500 and 2500  $\mu\text{sec}$  respectively.

The reason for employing  $V_{23}$  as a time selector, thus delaying the injection to  $V_{16}$  by 50  $\mu\text{sec}$ , is that  $V_{16}$  requires at least 20  $\mu\text{sec}$  to deionize. If a hard-tube regenerative counter of some type had been employed only a small delay would be necessary and the pulse from  $V_{22}$  could be coupled to  $V_{16}$  through a delay line.

It is obvious that counters are more advantageous for this purpose than conventional frequency dividers. First, the master-oscillator frequency might be subject to variations which would change the actual time between triggers to the dividers, but not their number.<sup>1</sup> Second, the time between triggers to the second and third dividers is not constant. Hence a divider that operates by virtue of a synchronized time base would be liable to change its division ratio if the time between synchronizing triggers changed appreciably. In contrast, counter dividers are relatively insensitive to the time spacing between the pulses that they count.

An interesting application of this fact is the use of counters as dividers in multiple-frequency marker systems in which it is desired to change the units of time without switching the time constants of each divider. If counter dividers are used it is only necessary to change the master-oscillator frequency. A good example of this situation is the design of a universal instrument to calibrate range units on radar systems. Three

<sup>1</sup> Actually the ground station PRF's in the Loran system are maintained with high accuracy.

units of time or distance are currently in use: the nautical mile, which corresponds to 80.86 kc/sec, the 2000-yd mile or 81.940 kc/sec, and the statute mile or 93.11 kc/sec. A test instrument to provide calibrating time markers for any of these three systems of units could easily be built using counter dividers to obtain the desired frequency ratios. The time scales then could be changed by switching master-oscillator crystals.

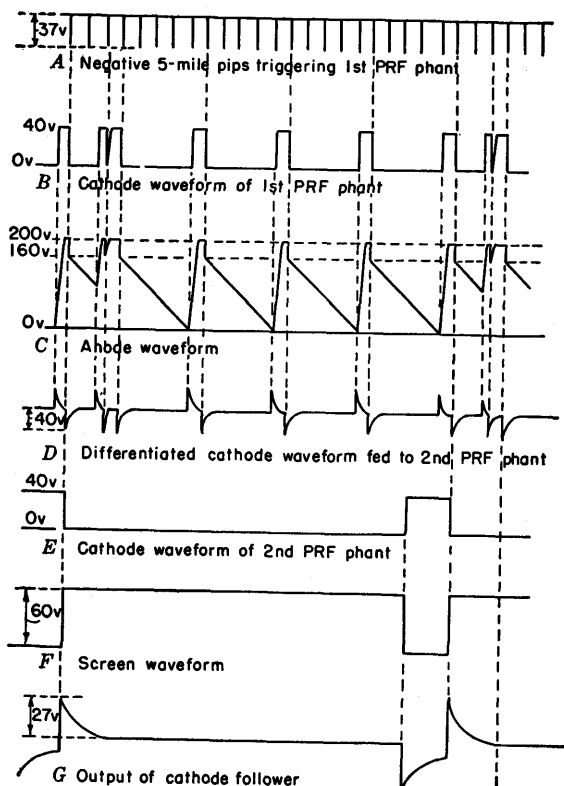


FIG. 4-32.—Waveforms of Oboe PRF divider.

**4-12. Injection Feedback Divider for Oboe PRF.**—Although time-base frequency dividers are less adapted to frequency division with injection feedback than counter dividers, it is perfectly possible to design such a system providing the number of injected pulses is not too large. Such a system is used to generate the PRF for the British Oboe ground station. The PRF pulses are obtained by dividing in two stages from 5-mile markers ( $53.75 \mu\text{sec}$ ) to produce recurrence frequencies between 90 and 150 cps. If it happens that the desired division ratio is a prime

number or is not the product of two small convenient factors, injection feedback is employed. In this system, the method of injection is that the

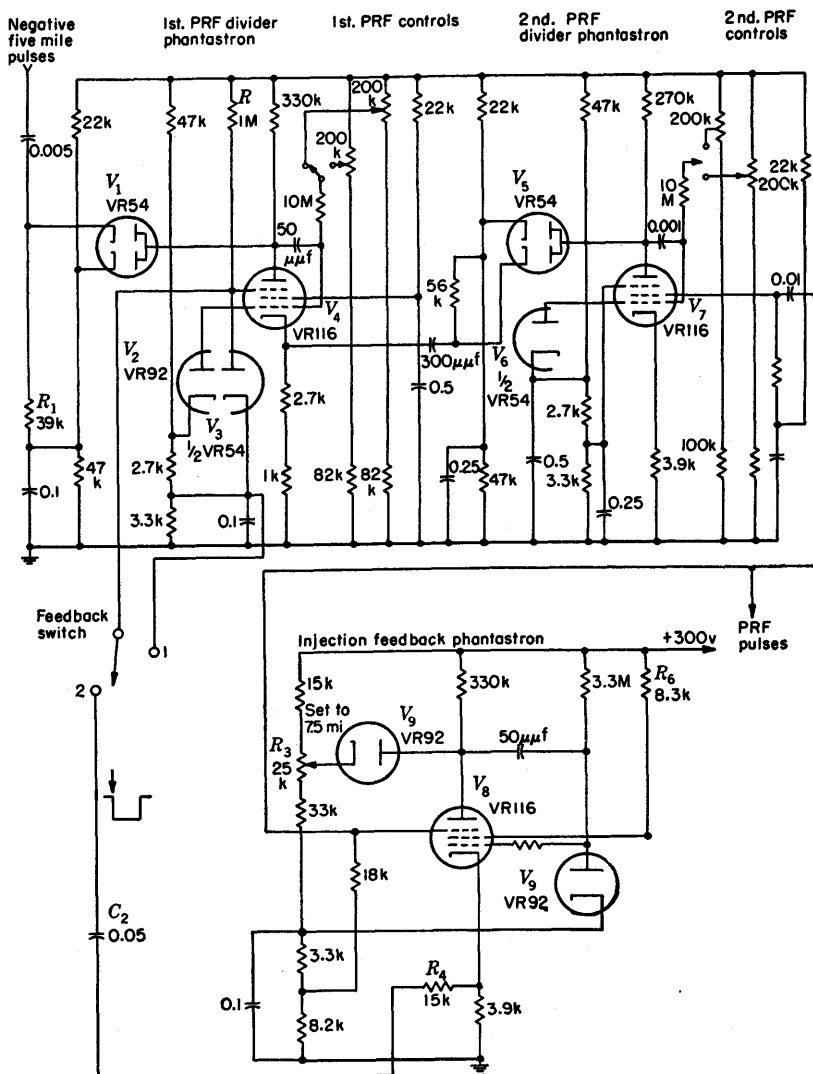


Fig. 4-33.—Feedback divider phantastron from Oboe calibrator.

trigger initiates a phantastron-gate generator which prevents the first phantastron divider from dividing for 0, 1, 2, or 3 miles, after which it divides in a normal fashion. In contrast to the Loran feedback divider,

the time interval between the PRF pulse and the first pulse fed to the second divider is increased by the feedback rather than decreased.

Figure 4-32 shows the timing sequences of the dividers set to divide by  $21 = 4 \times 5 + 1$ . The injection feedback is set to 1, the first divider divides by 4, and the second by 5. Figure 4-33 shows the circuit of the dividers. The negative 5-mile pulses are used to trigger the first PRF divider stage  $V_4$  on one cathode of the double diode  $V_1$ . The phantastron cathode waveform is shown in line *B* of Fig. 4-32. The negative edges are coincident with every  $n$ th 5-mile trigger pulse in the case of no feedback. The diode  $V_3$  is introduced in connection with

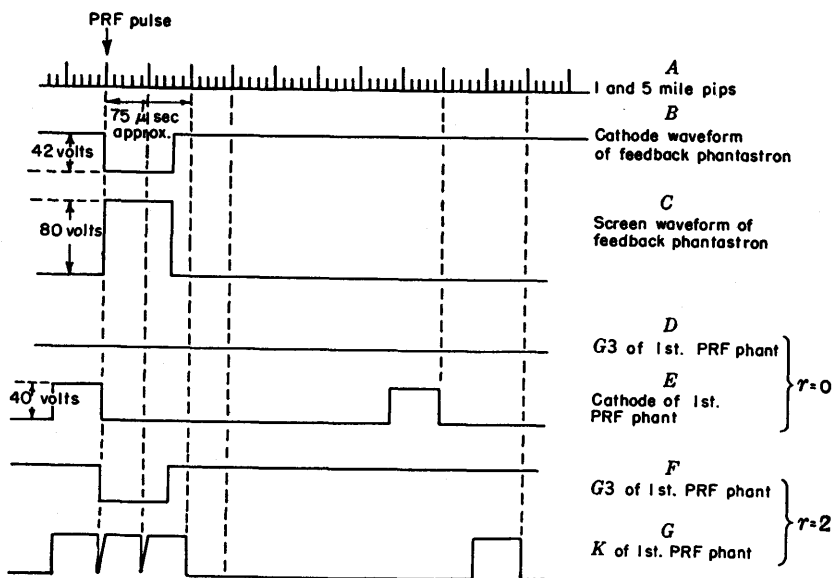


Fig. 4-34.—Feedback waveforms of Oboe PRF divider.

the feedback. With no feedback, which is the case to be considered first, the diode is short-circuited. The second half of the diode  $V_1$  is taken directly to  $+200$  volts on the bleeder and is employed to catch the plate of the phantastron as it rises on the flyback. The next 5-mile pulse developed across  $R_1$  pulls the phantastron plate down (cutting off the diode  $V_1$ ) and thus triggers the phantastron. The switch and potentiometers in the grid circuit of  $V_4$  allow the division ratio to be adjusted to either one of two numbers. The cathode and screen waveforms of the second PRF divider phantastron are shown on lines *E* and *F* of Fig. 4-32. The screen waveform *F* is differentiated and fed out through a cathode follower to form the PRF pulse *G*. It is also applied to the suppressor grid of the feedback phantastron  $V_3$ . The duration of the



waveforms from this phantastron is adjusted by  $R_3$  to be about  $7\frac{1}{2}$  miles for  $r = 2$ . The negative pulse fed to the suppressor grid of  $V_8$  has no effect, but the positive pulse triggers the phantastron. The cathode waveform is therefore as shown in Fig. 4-34, line  $B$  and the screen waveform as in line  $C$ . These two waveforms are used to obtain feedback as follows. The principle of the feedback is to apply to the suppressor grid of the first PRF phantastron a negative pulse  $F$  of sufficient amplitude to cause the phantastron to return to its quiescent condition. As indicated by the cathode waveform  $G$ , the negative pulse cuts off the plate which then rises towards  $E_{pp}$  until it is caught by the diode  $V_1$  at the +200 volt level. At the same time the cathode  $G$  and grid return to their quiescent voltages. The phantastron is then ready to be triggered off again by a 5-mile pip when the suppressor grid is allowed to return to its normal level. The gate fed back to obtain  $r = 1, 2, 3$  is obtained from the feedback phantastron  $V_8$ . The number of five-mile intervals to be added to the pulse recurrence interval by the feedback is  $r$ . The two cases of  $r = 0$  or 2 will be dealt with separately.

1. When  $r = 0$ , the suppressor of the phantastron  $V_4$  is held at a steady potential by short-circuiting the diode  $V_3$ .
2. When  $r = 2$ , the cathode waveform  $F$  of  $V_8$  is applied to the suppressor of  $V_4$ . The first PRF phantastron is thus caused to return to its quiescent state immediately after being triggered, and the suppressor voltage is held down while the next 5-mile pulse is fed to the plate. Hence the first PRF phantastron cannot retrigger at 5 miles. The negative feedback gate, however, is lifted from the suppressor before the second 5-mile pulse, and the phantastron is allowed to trigger at 10 miles (Fig. 4-34*h* and *j*). Thereafter it divides normally.

Little difficulty should be expected in this application from using time-base dividers with triggers of variable spacing since the maximum change of the PRF division ratio caused by feedback is only 15 per cent.

### GROUPED-MARKER GENERATION

BY R. B. LEACHMAN AND R. I. HULSIZER

Probably the majority of physical situations in which time measurements are to be made require that the time measurements start at a perfectly random instant. For this purpose circuits have been developed which will remain dormant until triggered externally, whereupon they provide a series of time markers of appropriate recurrence frequencies. After a suitable period, the markers are terminated and the circuits return to their quiescent condition, awaiting another triggering pulse.

Two methods exist for instrumenting this performance. One employs a storage tube fed with a continuous circular sweep from a stable oscillator as described in Sec. 4-9. The other employs pulsed oscillators which are turned on by the external pulse and provide markers of a particular frequency via an amplitude-comparison circuit. Several examples of the latter will be described in the following sections.

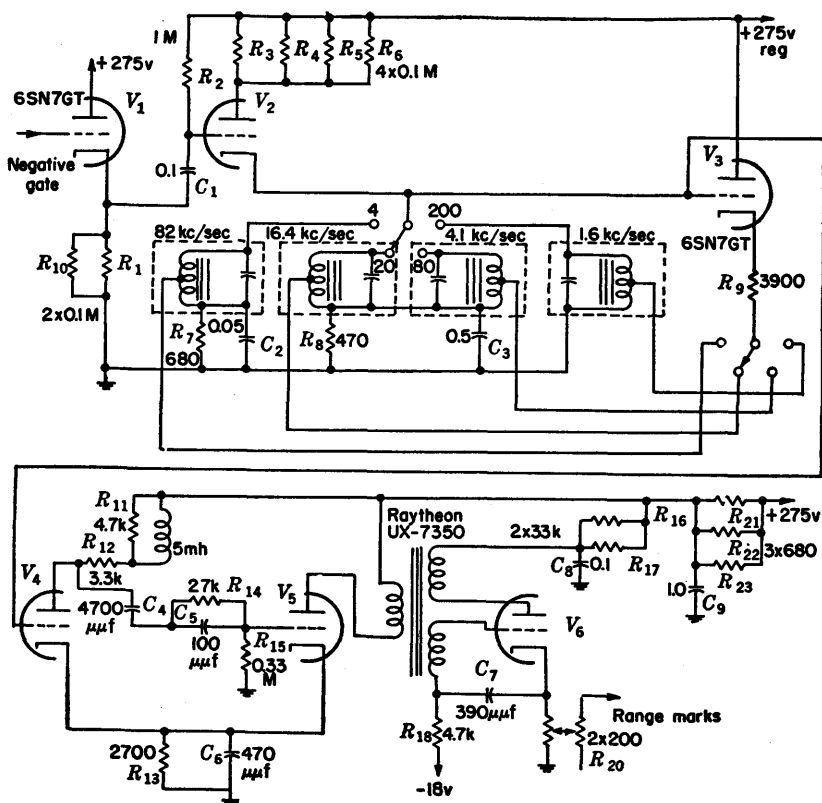


Fig. 4-35.—Pulsed range-mark circuit designed for a PPI indicator.

**4-13. Single-frequency Grouped-marker Generators.**—If a single-frequency marker is desired, techniques similar to those of Secs. 4-1 to 4-6 may be employed with the modification that the oscillators and amplitude-comparison circuits must be switched on and come to a stable operating condition quickly, and when switched off, they must return completely to the quiescent state before the next external pulse.

Although any type of oscillator may be used for this purpose, *LC*-oscillators were nearly always used and relaxation oscillators appear in few of the completed radar systems. A delay-line pulse generator was

employed in the preproduction AN/APG-5 range calibrator, but it was abandoned for a more stable pulsed *LC*-oscillator because the delay-line temperature coefficient was poor. Many synchrosopes simply pulse a tuned circuit to obtain a damped sinusoidal train for use in time calibration. The Germans used a supersonic delay-line time-marker generator to calibrate one of their height-finding systems. A pulse coupled into a glass rod produced a series of time markers by supersonic reflection.

*Pulsed LC Range-marker Circuit.*—Figure 4-35 shows the schematic diagram of a circuit for producing range marks of any one of four different frequencies for use on a radar indicator. Tube  $V_1$  is a cathode follower feeding a gate onto the grid of  $V_2$ . When  $V_2$  is on, it supplies a steady current at a very low impedance through one of the tank coils, maintaining heavy damping on the tank circuit. When  $V_2$  is cut off, the sudden change of current starts sinusoidal oscillations in the tank circuit. Examination of the initial conditions for the transient shows that a negative sine wave commences immediately with no distortion. With finite  $Q$ , the oscillations would die out rapidly, but  $V_3$  provides just sufficient positive feedback to maintain the oscillations at fairly constant amplitude. Tubes  $V_4$  and  $V_5$  amplify and distort the sine wave to trigger the blocking oscillator  $V_6$  which forms the range markers. Tube  $V_6$  is provided with a steady bias greater than cutoff. The grid-circuit time constant of  $2\ \mu\text{sec}$  is short enough to prevent any cumulative change in the point of triggering. It will be noticed that the point of amplitude comparison as performed by  $V_4$  depends on the grid characteristics and the bias provided by the average current of  $V_4$  and  $V_5$  flowing through their common cathode resistor. The stability of the bias depends on the symmetrical behavior of the two tubes which may lead to some error, either in long time stability, or as a transient error at the beginning of each marker group.

*Precise Pulsed LC Range-marker Circuit from Precision Ranging Indicator.*—The range-marker circuit just described provides range markers for the PPI where high accuracy is not required. This is reflected in the design of the amplitude-comparison circuit and the absence of temperature control on the resonant circuits. In the same indicator there is a precise pulsed range-marker circuit for use with the time-modulated range-marker circuit. This is described in Sec. 6-2 as an example of precision two-scale time modulation. The principle differences from the PPI range-marker circuit are that the *LC*-circuit and the feedback resistor of the oscillator are placed in a temperature-controlled oven, an oscillator circuit whose frequency is less sensitive to tube changes is employed, and the amplitude comparison of the sine wave to form the range marks is performed by a diode amplitude-comparison circuit. An inexpensive single-frequency grouped-time-marker circuit is described in Sec. 7-28.

**4-14. Multiple-frequency Grouped Markers.**—The most general solution to the problem of providing groups of multiple-frequency markers initiated by an external pulse and lasting for a fixed time is to employ

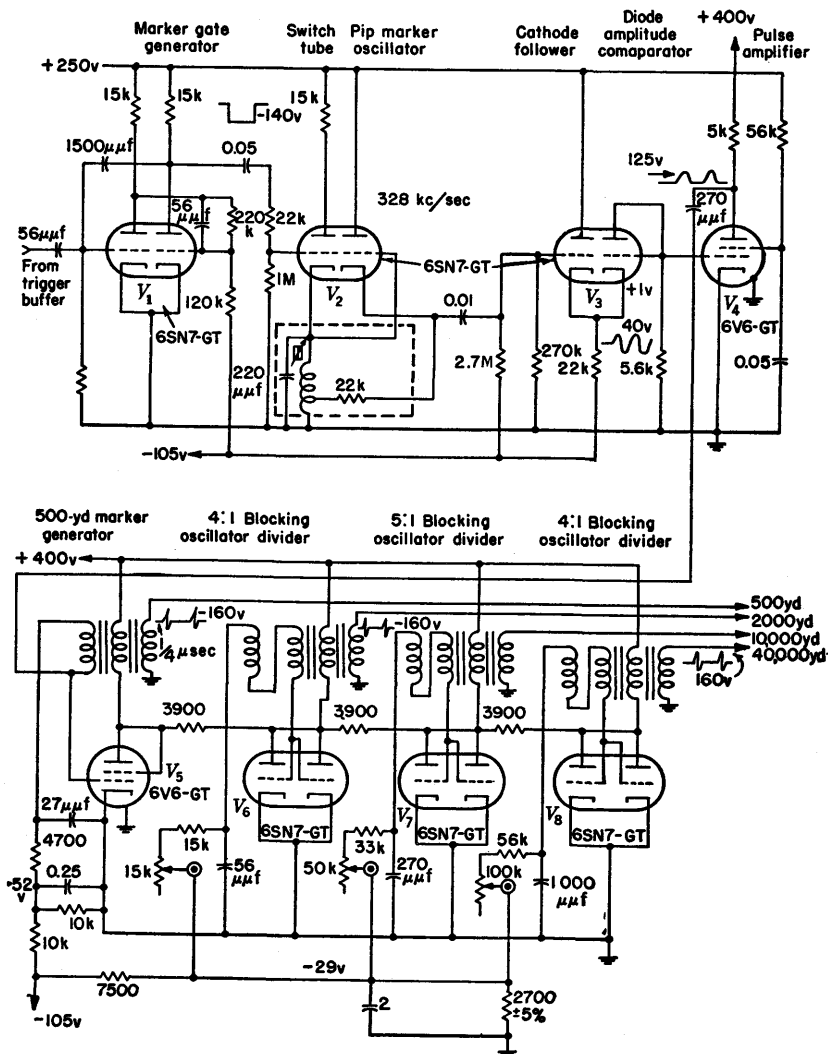


FIG. 4-36.—Multiple-frequency grouped-marker circuit using blocking-oscillator divider.  
All transformers are Raytheon UX8204.

several pulsed oscillators and amplitude-comparison circuits of the type described in Sec. 4-13. Each type of marker then is independent of the other and any desired frequency ratio may be easily obtained. Only

one of the oscillators need possess long-time frequency stability for the others may be calibrated against that one. A more economical, but less flexible solution is the use of a single-frequency marker generator and several pulse-divider circuits. The main precaution to be observed in the design of the dividers is that they remain inoperative except when receiving pulses from the gated oscillator, and that they should respond to the first few pulses of a group in exactly the same manner as to all the rest.

The circuit of Fig. 4-36 provides an example of this type of operation.<sup>1</sup> The external trigger initiates a multivibrator gate whose duration determines the length of time after the trigger that the markers will occur. It gates a 328-kc/sec *LC*-oscillator similar to the one described in Sec. 4-13. The amplitude comparison is performed by the diode half of  $V_3$  fed by the cathode-follower half. The cathode  $V_3$  is indicated as having a quiescent level of 1 volt. The point of conduction of the diode half of  $V_3$  will depend on variations of this potential. A better solution would be to replace the cathode resistor of  $V_3$  with a low-resistance grounded choke. A 10-mh choke would provide equivalent impedance at that frequency, and would provide an accurate reference potential, ground, when the sinusoid passes through zero amplitude.

Following the diode is a squaring amplifier and a 500- $\mu$ d (328-kc/sec) blocking oscillator employing a 6V6 biased to 52.5 volts, about 10 volts below cutoff. The use of a tube with a long grid base seems inadvisable at this point in the circuit where switching action at the instant the sine wave passes through zero amplitude is desired.

Plate-to-plate triggering is employed to synchronize the succeeding blocking-oscillator dividers. As in the 500- $\mu$ d marker blocking oscillator, each divider is normally biased below cutoff. Since the impedance of the Raytheon UX8204 pulse transformer is about 500 ohms, the effective triggering pulse appearing at the grid must be about 20 volts, which is perfectly adequate to overcome the quiescent bias. The division ratios are adjusted by varying the grid timing network resistance.

The requirement of maintaining the dividers nonoperative in the absence of an external trigger is certainly met by this circuit. In regard to assuring identical response to the first and last pulses of a train, there is some uncertainty. Because the grid timing networks are all very short compared with their operating frequency, little cumulative bias may be expected to develop there, but the bias bleeders have time constants which are neither short compared with the highest pulse recurrence interval (3  $\mu$ sec) nor long compared with the average external trigger recurrence interval. The saving feature may be that the average grid current might be too small to effect a change in bias during a pulse group.

<sup>1</sup> War Department Technical Manual TM11-1561, Aug. 31, 1944.

## CHAPTER 5

### GENERATION OF MOVABLE INDICES—SINGLE-SCALE CIRCUITS

By R. KELNER

#### INTRODUCTION

**5.1. Applications of Time-modulated Indices.**—A time-modulated index is a means for the identification of an instant of time that precedes or follows a reference instant by a controllable interval (see Sec. 3-8). The reference time instant may occur periodically or sporadically many times per second. The time interval (usually a delay) between the reference instant and the index is the useful variable of such arrangements. This interval is continuously or stepwise controllable and thus may be considered as an adjustable magnitude or a variable. This variable may be constrained so that a number is assigned to it by an automatic computer or an observer. Continuous variability is an essential property for most applications. The maximum delay of the indices discussed in this chapter is a fraction of a second. The index is usually a voltage pulse or step, or a mechanical index on a cathode-ray-tube display. Such a pulse can be used as a visible marker on a cathode-ray-tube display, as a trigger for starting the action of a circuit, or as the input to a demodulator.

The various methods for time modulation include the oscillator with phase modulator, the oscillator with frequency modulator, the sawtooth-waveform time modulator, propagation-time devices, and combinations of these methods (see Vol. 19, Chap. 13). The first three types utilize a comparator to derive a marker from the fundamental timing wave.

The circuits described in this chapter have, for the most part, been designed as components in time-demodulation systems, but there are numerous other applications. The transmission of data by time modulation is exactly analogous to data transmissions by frequency or amplitude modulation. In time modulation, a time interval is made proportional to the signal input. The transmitter emits a series of reference pulses at regular intervals; each is followed by a movable pulse, and a series of time intervals is defined. The frequencies of the data spectrum must be lower than the repetition frequency of the reference pulse<sup>1</sup> (see Chaps. 10 and 11).

<sup>1</sup> G. L. Fredendal *et al.*, "Transmission of Television Sound on the Picture Carrier, *Proc. I. R. E.*, **34**, No. 2, February 1946.

The relation between the control variable and the delay time (the transfer function of the time-modulation circuit) may be linear but also may be parabolic, hyperbolic, or some other shape. Means for achieving nonlinear functions are described in Vol. 19, Chap. 8.

Nonlinear time-modulation circuits are useful for automatic analogue computations (see Vol. 21). An example of this type of transfer characteristic is shown functionally in Fig. 5-1. In this case the delay time  $\Delta t$  is given by

$$\Delta t = k \sqrt{r^2 + h^2} \quad (1)$$

where  $r$  is proportional to the control variable and  $h$  to a constant. This equation is used for convert-

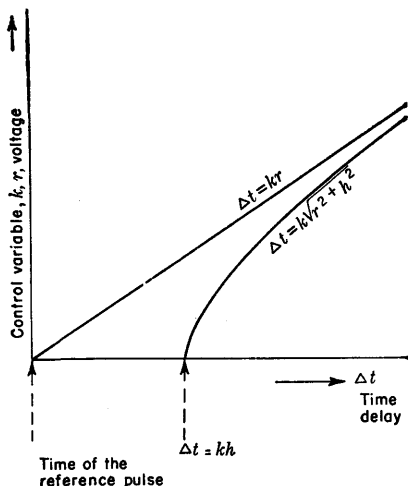


Fig. 5-1.—Transfer characteristic of a nonlinear time-modulation circuit.

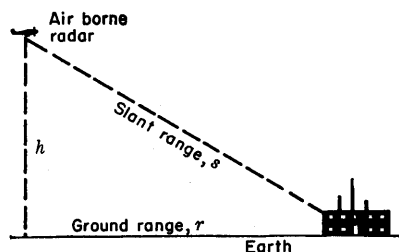


Fig. 5-2.—Distance measurement and triangulation.

ing a voltage that is proportional to ground range into a delay time that is proportional to slant range. These variables are identified for a practical distance-measurement problem in Fig. 5-2. The control variable of the time-modulation circuit is proportional to ground range if the altitude value is properly set in.

Time modulators of lesser precision may be used for controllable time delays. In order to obtain the proper sequence of events in a radar, a time-modulation circuit with a readily adjustable but comparatively unstable or unknown transfer characteristic may be used since this delay can be set by reference to some form of indicator. For example certain magnetic deflection coils for radar displays delay the start of a linear current in the coil from the start of the applied trapezoidal wave. Compensation is achieved by applying the time-base waveform before the sweep of the electron beam is to start. An adjustable delay is used to relate the triggering of the timing components and the radio-frequency components. Figure 5-3 is a timing diagram of these circuits.

**5-2. System Requirements and Definition of Error.**—From the standpoint of the system designer, the time-modulation circuit requires

or delivers a reference pulse, delivers an output pulse at a time later than that of the reference pulse, and accepts another input variable whose magnitude controls the duration of the interval between the pulses. The system designer ordinarily specifies the nature of the pulses and of the control variable and the relation between the control variable and the interval duration. Moreover, the pulse-repetition rate, the supply voltages, the permissible weight, size, complexity, power dissipation, the calibration procedure and the conditions of temperature, humidity, and acceleration to which the circuits will be subjected are more or less fixed. These external design factors are, of course, subject to control if extremely high accuracy is desired.

The *transfer characteristic* (relating control variable to delay time) is distorted by the drifts in component characteristics (see Chap. 3). Any deviation from the desired characteristic causes an error. In order to provide a basis for the comparison of the errors in various circuits, the following terms are useful:

1. The *limiting error* is the largest deviation from a normal characteristic that can ever be observed as long as each component value does not exceed its tolerances. Such a value exists because each component and input for a circuit must lie within a certain set of values.

Quality control insures the discard of components that are not within the required values. The normal transfer characteristic for a circuit is defined by the most probable of these values. The limiting error is caused by the worst possible combination of component values. Since each quantity can vary in either direction from its most probable value, the limiting error value is usually preceded by both the positive and the negative sign.

2. The *probable error* is that deviation which will be exceeded in half the cases of a statistical study of a large number of these circuits

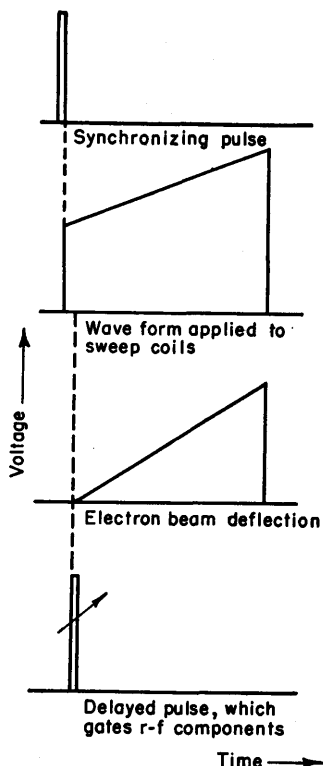


FIG. 5-3.—The prestating of magnetic CRT sweep coils. The arrow on the r-f trigger pulse indicates that it is adjusted to coincide with the start of the electron beam deflection.



operating under various conditions. The analysis by which this number is derived requires assumptions about the distribution of component values, the distribution of temperature variation, and other unpredictable quantities. The results, therefore, are subject to the validity of these assumptions. In most complex circuits, the verification of a probable error value is extremely difficult.

3. The *linearity* of a circuit is a criterion for those time-modulation devices that are designed to maintain a time interval proportional to the control variable. If the transfer characteristic is graphed and the straight line that best fits is superimposed, the differences in ordinates are the errors from linearity. The best fit is that which gives the smallest maximum difference of ordinates. The term "linearity" always has this connotation in this book. Since approximately linear circuits are common, slope and zero errors constitute convenient categories for linearity error analysis.

### VOLTAGE SAWTOOTH CIRCUITS

**5-3. A Gated Miller Integrator with a Multiar Comparator.**—The principle upon which all voltage-sawtooth time modulators depend is

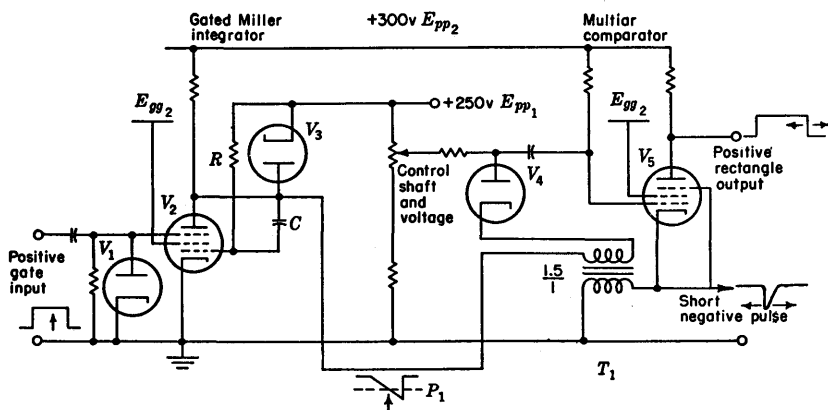


FIG. 5-4.—A simple Miller feedback time modulator. The pentode may be VR 91, 6AS6, VR 116, 6AC7, 6SA7 etc., or any other types in which plate current can be cut off by  $G_1$ . The diodes may be VR 92 or 6AL5. A pulse output may be taken from the cathode of  $V_4$ .

the identification of the instant at which a sawtooth wave reaches a certain amplitude. This amplitude is the control variable. The interval between the start of the sawtooth wave and the time when the wave reaches this amplitude is the delay that is modulated. The formation of a step or pulse at the instant when the waveform amplitude equals the control-variable amplitude is performed by a comparator such as those

of Vol. 19, Chap. 9. The generation of linear sawtooth waveforms or triangular waveforms is described also in Vol. 19, Chap. 7.

The circuit of Fig. 5-4 is an excellent example of a simple but accurate linear modulator. The circuit consists of a triangle generator—the gated Miller integrator—and a multar<sup>1</sup> comparator. The control variable is a potentiometer shaft rotation. When the linear rise reaches the voltage at the tap of this potentiometer, a diode conducts and the multar produces a step and a pulse marker. The delay produced by the circuit is the interval between the marker and the start of the gate for the sawtooth generator.

The circuit details may be understood by reference to Fig. 5-4. Ordinarily  $V_2$  is passing screen current but no plate current since the suppressor grid is held considerably below the cathode potential. The plate is caught<sup>2</sup> at  $E_{pp1}$  by the diode  $V_3$ . When the positive gate raises the suppressor sufficiently, plate current starts to flow and the plate rundown<sup>2</sup> proceeds after a small initial step. The fall of plate voltage is linear and is of slope proportional to  $(E_{pp1} - V_{g0})$ , where  $V_{g0}$  is the initial potential of the control grid of  $V_2$ .

The multar action is a regenerative cutoff of  $V_5$  when  $V_4$  starts to conduct, that is, when the plate rundown reaches the voltage at the tap of the potentiometer. The regenerative loop is completed through the transformer  $T_1$ . A positive step appears at the plate of  $V_5$  when  $V_4$  starts to conduct. The interval between the rise of the gate and the step in the output is approximately proportional to the difference between the quiescent plate voltages of  $V_3$  and  $V_4$  divided by the slope of the triangle. The diode biases and the slope are proportional to  $E_{pp1}$ . The time interval is therefore nearly independent of  $E_{pp1}$ .

The circuit of Fig. 5-4 accepts a gate and delivers a step; it may be followed by a blocking oscillator or a quasi differentiator if a pulse output is desired. Alternatively a pulse may be taken from the cathode. The addition of a multivibrator or the use of the screen current of  $V_2$  to provide a gate that may be applied to the suppressor grid of  $V_2$  will suffice to make the circuit sensitive to a pulse instead of a triangle.

In an experimental circuit using type VR-91 for  $V_2$ , a transfer characteristic that was linear to within  $\pm 0.05$  per cent of the maximum interval (36  $\mu$ sec) was obtained. A 5 per cent change of the supply voltages, including the filament supply, produced less than 0.04 per cent change in the zero and 0.1 per cent change in the slope of the characteristic. These data were taken with a slightly different comparator (a diode plus amplifier). The linearity could be somewhat improved by using an inductance in series with the plate load resistor and thus increas-

<sup>1</sup> See Glossary, and Vol. 19, Sec. 9-14.

<sup>2</sup> See Glossary.



Since the control voltage supplied by the computer occurs at a high impedance, it is necessary that the comparator circuit does not draw current from the control-voltage source. The maximum distance at which this radar receives useful signals is approximately 30 nautical miles. The lengths of the gate and the triangle are set at a delay corresponding to this distance. A positive trigger or reference pulse is supplied to the gate generator at a repetition frequency near 1000 cps.

After consideration of the accuracies of the radar and the computer, this circuit was assigned a probable error of about 20 yd at any point over the range of 60,000 yd. This figure cannot be achieved without the weekly resetting of a slope control and a zero control although the maximum errors are only slightly greater with only an initial calibration. These controls are not apparent in Fig. 5-5 since these operations are performed on the control voltage in the computer. An absolute standard is not required for the supply voltage that determines the slope of the triangle because the control voltage is supplied from the same source. Compensation of the drifts of  $V_{2b}$  would improve the stability of the zero. The linearity requirement for this circuit is somewhat higher than the requirement for absolute calibration since it is to be used for rate determination.

The gate generator is a multivibrator of conventional design except for the diode  $V_8$  which is used to stabilize the amplitude of the timing waveform and, hence, the duration of the gate. The rising grid of  $V_{1a}$ , acting through  $V_{2a}$ , lifts the grid of  $V_{3a}$  to its original level after the small fall during the sweep. The grid of  $V_{1a}$  stops its rise when grid current starts to flow. Thus the grid of  $V_{3a}$  is connected to ground through two diodes in series and of such polarity that the effects of changing heater voltage and of aging tend to cancel. In this way the slope of the triangle is accurately established. The chief variations arise through the replacement of the tube  $V_1$ .

The amplifier of the Miller integrator consists of two triodes and one pentode; hence a gain of 3000 is obtained. This ensures that the triangle shall have an exceedingly linear rise. Tests have shown that the departures from linearity of the entire modulator do not exceed 1 or 2 parts in 10,000. The limiting element is probably the comparator. The 6SU7 triode is used for the first stage of the amplifier because of its low grid current, thus eliminating nonlinearities and changes of slope due to variations in grid current. The triangle which appears at the output of the three-stage amplifier starts at a level that is determined entirely by the direct-current characteristics of the last tube. In order to avoid errors from this source a level-changing network and a diode  $V_{2b}$  are connected to start the linear rise accurately at ground. The behavior of the Miller integrator amplifier as a negative feedback amplifier is shown in Fig. 5-6.

The triangular wave is applied to one grid of a double-triode comparator circuit  $V_6$ , which is described in Vol. 19, Chap. 9. The output of the double-triode circuit is a selected portion of the input triangle which rises at approximately  $\frac{1}{3}$  volt/ $\mu$ sec. This is increased to 40 volts/ $\mu$ sec in the regenerative amplifier  $V_7$  and to more than 200 volts/ $\mu$ sec in the blocking oscillator  $V_{7b}$ . The delays in the starting of the sawtooth

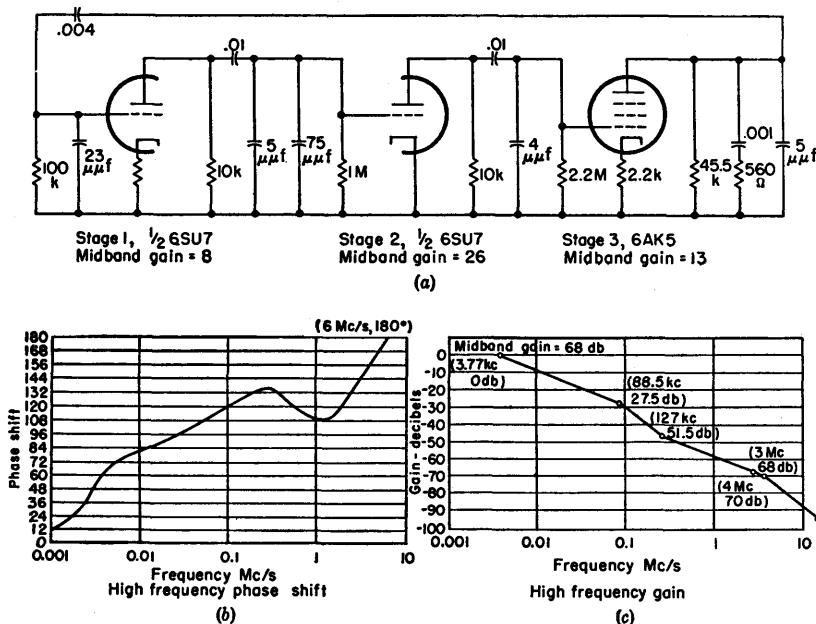


Fig. 5-6.—The feedback amplifier must be stabilized against undesired oscillations. The methods described in Vol. 18 are convenient. The frequency characteristics of the entire loop are shown in Fig. 5-6. (a) Equivalent circuit for gain calculations. (b) High-frequency phase shift. (c) High-frequency gain. Note: The effective input capacitance of the 6AK5 is negligible. The 4- $\mu$ f value was determined experimentally. The 75- $\mu$ f shunt in Stage (1) represents the Miller effect in Stage (2), and the 23- $\mu$ f shunt at the grid of Stage (1) also represents a Miller effect. The tubes may be considered as constant-current sources. Total gain is approximately 2700 for average tube characteristics. Series grid resistors are neglected.

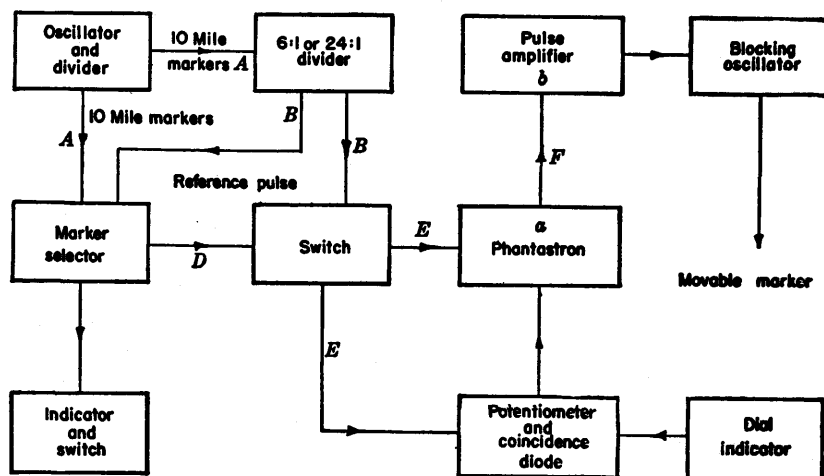
wave and in the pulse amplifiers cause the minimum range of the device to be about 1000 ft or 2  $\mu$ sec.

In an attempt to minimize the sensitivity to repetition-rate changes all the time constants in the circuit are made sufficiently small for the corresponding transients to decay to one thousandth of their maximum value in the allowable recovery time.

**5.5. Self-gating Miller Integrator.—The Phantastron.**—The phantastron<sup>1</sup> time-modulation circuit to be discussed here is the interpolating

<sup>1</sup> F. C. Williams, "Linear Time Bases, Ranging Circuits," I. E. E. Convention Paper, March 1946.

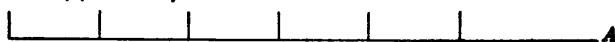
device in a two-scale time-interval measurement system (see Chap. 6). This system, as a part of the H<sub>2</sub>X airborne radar, aids in the accurate determination of distance (see Fig. 5-7).



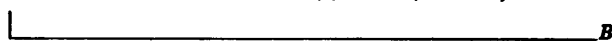
80.86 kc (1 naut. mi) pips from crystal oscillator and pip generator



80.86 kc (10 naut. mi) pips from 10/1 divider



1350 cps (60 naut. mi) or 340 cps (240 naut. mi) pips from 6/1 or 24/1 divider



Beacon phantastron delay gate



8 mile selector gate



Delayed selected trigger



Range phantastron delay gate (0.6 to 16 miles)

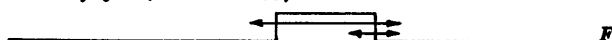


FIG. 5-7.—H<sub>2</sub>X system.

The results of the measurements are applied to the navigation of the airplane and to the indication of the proper range at which to release bombs. In this section, the system is briefly described and the time-modulation circuit is treated in detail.<sup>1</sup>

<sup>1</sup> See H. J. Reed, A. H. Fredrick, and B. Chance, "H<sub>2</sub>X Range Unit for Naviga-

*Time-measurement System.*—The range unit consists of a crystal-controlled oscillator (80.86 kc/sec), pulse frequency dividers supplying 1-, 10-, and 60- or 240-mile pulses, a cathode-ray-tube display, and a time modulator. The coarse-scale time modulator is triggered by the reference pulse selector. The whole range unit is a multiple-scale time-measuring circuit that includes the single-scale modulator that is discussed here. The interpolating delay (from the triggering marker) may be read from a dial on the shaft of the controlling potentiometer.

It is required that this precision ranging system have a probable error of approximately 100 yd out to slant range distances of 200 nautical miles.

The errors in the time-measurement circuits are those of the 10-mile markers (errors which may be as large as 0.05 per cent of the interval from the reference time) plus those of the time-modulation circuit. For the 40-mile marker, the total is a 40-yd limiting error. The probable error of the interpolating time-modulation circuit, therefore, can be nearly 100 yd. The maximum delay which the interpolation device is to produce must exceed the delay corresponding to 10 miles in order that any instant can be conveniently identified. This value is arbitrarily set at 15 miles. The delay circuit can therefore have a probable error of approximately 0.3 per cent of the maximum delay.

This accuracy can be provided by a phantastron if the transfer characteristic is adjusted by a resetting of slope and zero controls when the phantastron tube is changed. A simple calibration method is possible. An auxiliary type J oscilloscope is provided with a circular time base by the 80.86-kc/sec oscillator. This time base permits the interval between the reference time and the movable pulse to be determined to an accuracy that corresponds to ranging errors of  $\pm 20$  yd plus the errors in the oscillator frequency.

The temperatures, humidities, and accelerations that must be resisted by these circuits are those specified for aircraft equipments. A particular effort was made to reduce the size and power requirements of the H<sub>2</sub>X range unit. An unregulated plate-supply voltage can be used because the phantastron is insensitive to variations in the plate supply if the control potentiometer is supplied from the same source as the circuit. Since the duty ratio is at most 25 per cent, the recovery time is sufficiently short.

---

tion and Bombing," RL Report No. 342.

"Handbook of Maintenance Instructions for Model AN/APS-15 Aircraft Radar Equipment," CO-AN-08-30APS15-2, USN.

J. V. Holdam, S. McGrath, and A. D. Cole, "Radar for Blind Bombing," Part 1, *Electronics*, 19, 138 (May 1946).





the circuit reverts to its original condition (see the waveform diagram, Fig. 5-9).

*Choice of Constants.*—The  $H_2X$  range phantastron details are included in Fig. 5-8. The screen-potential divider is chosen as a fair balance between power consumption and permissible impedance. Also, the screen voltage cannot be too high if a large sawtooth voltage is to appear at the plate. The plate resistor value should be high relative to the potentiometer resistance in order that there shall be no small nonlinearities due to loading effects. The cathode resistor is chosen to maintain the quiescent state of the circuit with the grid connected to the plate

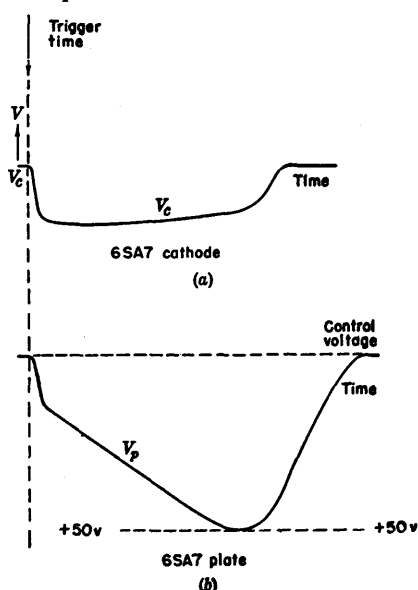


FIG. 5-9.—Phantastron waveforms.

The heater voltage changes the characteristic by about 2 yd per  $-1$  per cent change. These figures are very approximate and vary with the value of maximum delay and with the delay setting of a particular circuit. If a ripple of 6 volts rms is impressed on the plate-supply voltage, the delay variation amounts to approximately 100 yd. The effect is increased by connecting a large condenser between the potentiometer tap and ground.

The effect of repetition-rate changes upon this particular circuit is negligible because a maximum of 25 per cent of the period between triggers is used. Phantastrons may be operated to give a usable duty ratio of considerably more than 50 per cent; a modification of this circuit would usually be necessary (see Sec. 6-8). Undesirable transients are

supply through a large resistance. This grid resistance must be large enough to maintain the grid current at a low value. The grid time constant is chosen to give the proper maximum delay and the condenser is small enough to obtain rapid recovery.

*Phantastron Accuracy—Experimental Results.*—The accuracy tests of the  $H_2X$  phantastron have not been exhaustive, and where information is not available, data are sometimes given for very similar circuits. The insensitivity to plate-supply voltages which has been mentioned is such that a given delay will change by approximately  $+5$  yd per  $-1$  per cent change in supply voltage for the 30,000-yd maximum delay of this circuit.

reduced by plate-grid coupling through a cathode follower, direct-coupling to the pulse amplifier, and use of a screen divider without a bypass condenser.

The replacement of the 6SA7 tube has more effect upon the zero than upon the slope of the transfer characteristic. The average zero shift is between  $\frac{1}{2}$  and 1 per cent of the maximum delay, and the maximum shift may be 3 to 5 per cent. The slope shifts are all considerably smaller than 1 per cent.

Microphonic effects in the phantatron tube cause the delay to flutter or "jitter" over a small range. The effect is particularly noticeable in the  $H_2X$  range unit because a blower operates near the tube and vibrates it appreciably. Twenty different tubes were tested in one unit. The average jitter was approximately  $\frac{1}{2}$   $\mu$ sec or 100 yd for the phantatron of Fig. 5-8. This value is less than 10 yd if the blower is not operating.

The effect of changing various components by +10 per cent is given in Table 5-1, except for  $R_c$  and  $C_c$  to which the delay is directly proportional.

TABLE 5-1.—THE EFFECT OF COMPONENT VARIATIONS UPON A PHANTATRON DELAY

Component*	Resultant delay increment, %†
Plate resistor.....	-0.1
Cathode resistor.....	-1
Screen divider, top.....	+2
Screen divider, bottom.....	-2
$G_s$ divider, top.....	-0.25
$G_s$ divider, bottom.....	+0.25

\* A 10 per cent increase was made in all components.

† In all cases except the first, the error was mainly a zero error. In the first case, it was mainly a slope error.

The temperature compensation of the phantatron is complicated because the elements are all effective in determining the transfer characteristic. Fortunately, the temperature coefficients of the tube are not large enough to be of importance. The procedure used to fix the individual temperature coefficient so that the transfer characteristic is independent of temperature is primarily experimental. Each component is heated alone to determine its effect. The effectiveness of each voltage divider and other component is minimized and the remaining temperature coefficients are adjusted to compensate. The types of resistors given in Fig. 5-8 have the proper coefficients. Components  $R_c$  and  $C_c$  should have equal and opposite temperature coefficients. The usual wire-wound precision resistor has a small positive coefficient. In order to achieve a negative coefficient for the capacitor, a silver-mica condenser and a second unit with a smaller capacitance and a larger negative temperature coefficient (Ceramicon) are ordinarily used. The results that have been achieved indicate that the residual temperature coefficient

in the entire circuit need not exceed 0.005 per cent of maximum delay per degree centigrade and may be adjusted nearer to zero for particular units. This value represents a limiting-error rather than a probable-error value.

The linearity of the transfer characteristic depends upon many compensating factors. The plate-resistor value should be large with respect to the resistance of the control potentiometer. The screen and  $G_s$  biases must not vary from the proper values. The limiting errors from linearity of the arrangement in Fig. 5-8, as measured in the laboratory, are, for selected tubes, less than  $\pm \frac{1}{10}$  per cent of the maximum delay—exclusive of the potentiometer error. This value is approximately  $\pm 0.3$  per cent in the field with the potentiometer nonlinearities included.

If the heater- and plate-supply voltages vary by 10 per cent, if the circuit is recalibrated as often as tube drift and tube changes necessitate, if the phantatron nonlinearity (exclusive of the potentiometer) does not exceed  $\pm 0.1$  per cent, and if the potentiometer errors are also smaller than  $\pm 0.1$  per cent, the total errors from the calibrated transfer characteristic will not exceed  $\pm 0.4$  per cent. Temperature variations of  $50^\circ\text{C}$  increase this number by  $\pm 0.25$  per cent. If tube changes are not compensated by calibration, the limiting error is several per cent.

**5-6. Self-gating Miller Integrator—The Precision Sanatron.**—The capabilities of the sanatron as a generator of extremely linear and stable triangles are described in Vol. 19, Chaps. 5, 6, and 13. This section is intended to suggest means for realizing the accuracy of this waveform in a time modulator.

The simple sanatron yields a well-defined and linear triangular waveform which can be used with the multiar comparator of Vol. 19, Chap. 9. This use is similar to that described in Sec. 5-3. The present section describes a method for exceeding the accuracy of a sanatron circuit with internal comparison. The worst errors in the usual sanatron circuit arise from the variable duration of the interval between the end of the linear rundown and the start of the regeneration. This is the time required for the grid of the cutoff tube to rise to its grid base. This action is speeded by an additional circuit which is enclosed in dotted lines in the precision sanatron of Fig. 5-10.

The operation of the circuit except for the speedup network has been described in Vol. 19, Chap. 5. The speedup action is as follows. At the end of the linear rundown, diode  $V_2$  catches the anode of  $V_3$  and there is no further negative feedback to the control grid. This grid rises and increases the screen current. The differentiating transformer in the screen circuit provides a pulse that turns on  $V_4$  and  $V_6$  very soon after  $V_2$  starts to conduct.

The largest errors of the improved circuit are caused by poor defini-

tion of voltages by  $V_1$  and  $V_2$ , the loading of the control voltage by the plate resistor of  $V_3$ , the inconstancy of grid bias of  $V_3$  at the sweep start, the finite and variable gain of  $V_3$ , the instability of the product  $RC$ , and the variations of the supply voltages. The variation of the  $-250$ - or  $+300$ -volt supply by  $\pm 10$  per cent results in less than  $\pm 0.1$  per cent error at any point. If the heater supply is varied by  $\pm 10$  per cent, the delay increment is less than  $\pm 0.125$  per cent at all ranges. Replacement

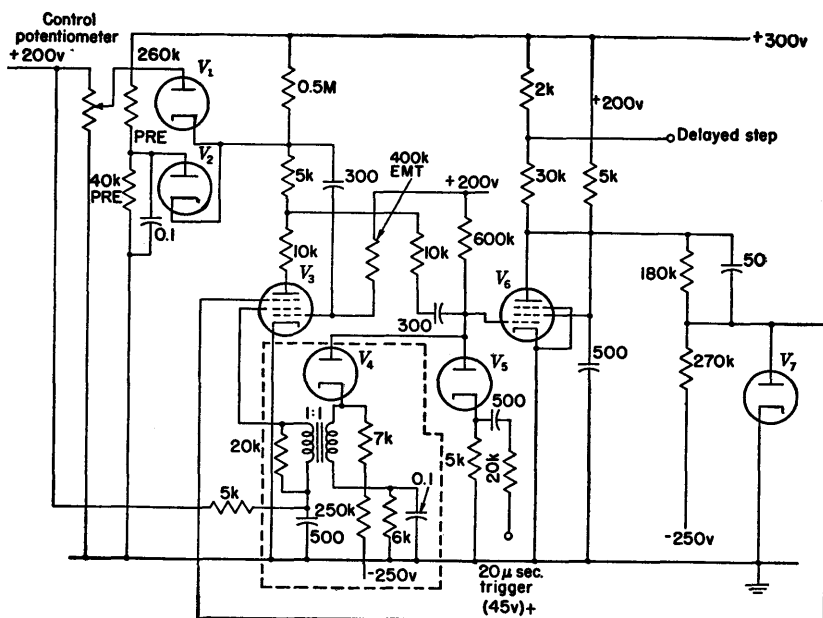


FIG. 5-10.—High-precision sanatron.

of either  $V_3$  or  $V_6$  may cause  $\pm 0.1$  per cent error; replacement of  $V_1$ , 0.15 per cent; and replacement of  $V_2$ , 0.2 per cent error at maximum and minimum ranges. The linearity of the circuit as shown is computed to be  $\pm 0.05$  per cent. By the use of an inductance as part of the plate load, the computed linearity may be increased to 0.0006 per cent (see Vol. 19, Chap. 7).

**5-7. Bootstrap Triangle Generator with Diode Comparator. Time-measuring System.**—This time-modulation circuit<sup>1</sup> consists of a gate generator, a triangle generator, a linear potentiometer and indicator, a comparator circuit, and a pulse amplifier. The functions performed and the relation of the time-modulation circuits to the other component

<sup>1</sup> G. Hite, "Medium-precision Range System" RL Report No. 579; V. W. Hughes, "A Range-measuring System Using an RC Linear Sweep," RL Report No. 540; and Vol. 19, Chaps. 7 and 13.

circuits in the range indicator are illustrated in Fig. 5-11. An oscillator provides a reference pulse at the rate of 2000 per second  $\pm 10$  per cent or 500 per second  $\pm 10$  per cent. Externally synchronized operation is also possible. In either case, the reference pulse triggers the radar transmitter, a time base extending from the reference time to either 240 or 960  $\mu\text{sec}$ , and also the time-modulation circuit. The time-modulation circuit provides a movable pulse delayed 15 to 240  $\mu\text{sec}$ .

A marker pulse is delayed from the beginning of the expanded sweep by an interval equal to half the duration of the sweep. The stability

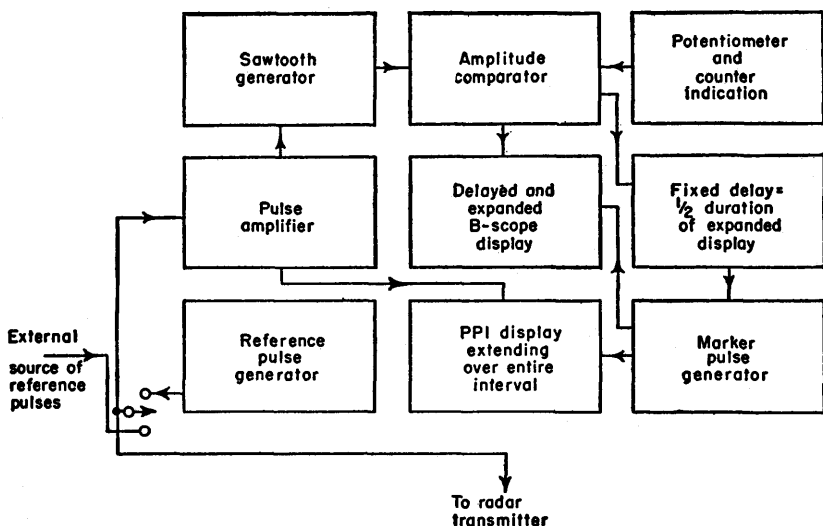


FIG. 5-11.—Block diagram of timing system.

of the expanded time base is unimportant because errors from this source tend to cancel. The counters that indicate the shaft rotation of the controlling potentiometer are set to indicate the time interval (actually, the corresponding distance in yards) from the reference time to the marker. The timing diagram shown in Fig. 5-12 illustrates the sequence of events.

In this radar system position is determined by turning the range-potentiometer shaft and the azimuth shaft until the center of the type B display coincides with the unknown echo. The counters which are coupled to the shafts can be arranged to read range and bearing of the object which corresponds to the echo.

The external design factors which affect the design of these circuits are those common to Navy equipment plus a few special requirements.

The time-modulation circuit is subject chiefly to the accuracy requirements for range determination. In this case the limiting errors must not exceed about  $\pm \frac{1}{2}$  per cent of the maximum range. This error is apportioned equally between the potentiometer and the circuits, although the circuits must be calibrated frequently to be satisfactory.

In Fig. 5-13, the time-modulation circuits of the range unit are shown schematically and in detail. The discussion of the detailed design of the circuit is clarified by the functional diagram Fig. 5-11 and by the timing diagram Fig. 5-12. The reference pulse or trigger, from a source either internal or external to the range unit, is amplified in tube  $V_1$ . This amplifier is a 6AC7 which is biased beyond plate-current cutoff by fixing the cathode at a potential a few volts above that of the grid. The trigger is positive and at least 5 volts in amplitude. Since a pentode is used, the trigger causes the tube to conduct strongly and a large negative pulse appears at the plate. This negative pulse is applied to a monostable multivibrator  $V_2$  that generates the 300- $\mu$ sec negative-gate pulse shown in Fig. 5-13. This circuit is less susceptible to changes of gate duration and amplitude caused by tube changes than are cathode-coupled circuits.

The negative gate at the plate of  $V_{2B}$  is direct-coupled to the grid of a switch tube. The direct coupling enables the start of the switch action to be independent of the repetition frequency. The triode switch  $V_{3a}$  is closed except during the 300  $\mu$ sec which follow the reference time. The triangle generator responds to the opening of the switch by producing a voltage that increases linearly with time. The circuit is a bootstrap circuit plus an integration network, which is analyzed in Vol. 19, Chap. 7. A linear rise occurs at the grid of tube  $V_{3a}$  and a rise which is less linear but which occurs at a lower impedance appears at the cathode. The grid waveform serves as the input to the comparator. The linear rise

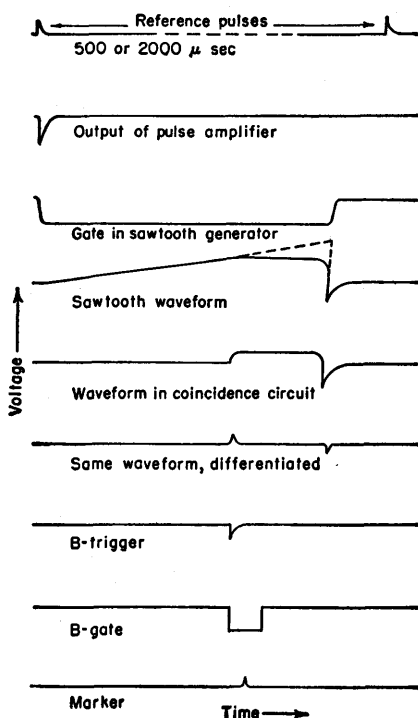


FIG. 5-12.—Timing diagram.



above the reference voltage is selected and amplified in the comparator amplifiers.

*Accuracy.*—The effects of changing the heater voltage, the regulated plate-supply voltage, the repetition rate, the temperature, various component values, and the vacuum tubes are represented by the data given in Table 5-2. When several tube specimens were tried in turn, the largest variation caused by any tube is given.

The transfer characteristic was linear during these tests to  $\pm 0.1$  per cent from 3 to 240  $\mu\text{sec}$ . The delay could be reduced to 2  $\mu\text{sec}$  or less. The linearity was checked whenever increments as large as 0.1 per cent appeared. No adjustment of the integrating resistor was required in order to maintain this linearity with tube change. Equation (12) of

TABLE 5-2.—ACCURACY TESTS ON THE DELAY CIRCUIT

Condition	Increment* in time interval at original interval of			Number of tubes tried
	3 $\mu\text{sec}$	120 $\mu\text{sec}$	240 $\mu\text{sec}$	
Filament voltage from 5.6 to 7.0 volts...	-0.05	-0.075	-0.075	2 sets
Regulated plate supply from 280 to 300 volts.....	<0.01	<0.01	<0.01	2 sets
Repetition frequency change from 300 cps to 2400 cps.....	<0.01	+0.05	+0.125	3 sets
Change of cathode-follower tube.....	+0.05	-0.05	+0.25	8
Change of switch tube and restorer diode across "integrating" resistor.....	-0.3	-0.2	+0.125	5
Change of other two diodes.....	+0.125	-0.125	-0.2	4
Change of all other tubes including gate and amplifiers.....	<0.02	<0.02	<0.02	8

\* In per cent of the maximum delay.

Vol. 19, Chap. 7 indicates that a change in  $g$  of 4 per cent, such as would be caused by a 40 per cent change in the  $g_m$  of the cathode-follower tube, would cause a deviation from the original linearity of 0.3 per cent. The experiments referred to in Table 5-2 probably did not include this extreme variation in  $g_m$ . Tube characteristics may be altered sufficiently by a light tapping on the tube to cause  $\pm 0.2$  per cent change in delay.

The temperature coefficient of the transfer characteristic depends upon the temperature coefficients of two resistances and two capacitances, to a first approximation. Some data that bear upon this point were taken with a circuit similar to that described in this section. Each resistance and capacitance in the circuit was varied by 10 per cent in turn, and the effect upon the transfer characteristic noted. The effect of changing  $R_1$  and the  $C_1, C_2, C_3, C_4$  combination was to change the slope of the transfer



characteristic proportionally to the parameter increment. The 10 per cent change in  $R_1$  also changes the zero by 0.15 per cent. The integrating resistor  $R_2$  causes 0.4 per cent change in the slope when it is changed by 10 per cent. Increasing the value ( $C_5 + C_6$ ) by 10 per cent decreases the slope of the characteristic by 0.1 per cent. Changes in the remainder of the components are less effective.

The circuit accuracy depends primarily upon a condenser, a resistor, a potentiometer, and the various vacuum-tube switches. The problem of temperature-compensation is practically that of maintaining constant values of two resistances and two capacitances. These circuits must be carefully designed to minimize stray capacitance, which may vary with temperature because of mechanical distortions.

Because of the characteristics of available components, the temperature compensation of circuits that depend upon the constancy of resistances and capacitances cannot be relied on to reduce the errors below 0.1 per cent of the maximum delay over a range of 50°C. In practice, this error may be several times larger because temperature coefficients of resistors and condensers are difficult to measure and control.

An estimate may be made of the limiting error of the circuit. If the heater voltage varies  $\pm 10$  per cent, the regulated plate voltage  $\pm 2$  per cent, and the repetition frequency from 400 to 2200 cps, the resultant errors are smaller than  $\pm 0.2$  per cent. Changing all tubes causes an error of 0.5 per cent, at worst. The effects of component changes with 50°C temperature change may add 0.2 per cent error. If the linearity errors are at most  $\pm 0.1$  per cent and the potentiometer errors  $\pm 0.25$  per cent, the over-all error cannot exceed 1.25 per cent. The errors encountered in practice are considerably smaller because there are many independently contributing factors. It is probable that the small numbers of tubes that were tried did not include limiting cases of tube characteristics. Although this estimate of the limiting error might be increased by a more careful study, the probable-error estimate would not be much affected.

To reduce the errors of this circuit appreciably would require a more accurate potentiometer, a large amplitude sawtooth waveform, or better switches, constant repetition frequency and supply voltages, and more precise temperature compensation. None of these requirements is exceptionally difficult to meet, particularly in the laboratory. Periodic calibration reduces the effects of some errors. This circuit is of value in applications where accuracies as great as  $\pm 0.1$  per cent are required.

A fundamental limitation is the variation of  $g_m$  of the cathode follower during the sawtooth wave. The tube nonlinearities of the feedback amplifier can be removed by increasing the gain of the feedback amplifier. Cathode followers are not the most convenient type of circuit for these

more linear amplifiers. When the Miller feedback principle is used, the residual errors from linearity are much smaller. The Miller circuits are therefore preferred for attaining good linearity.

**5-8. The Delay Multivibrator.**—The delay multivibrator (see Vol. 19, Chap. 5) is a simple self-gated two-tube time-modulation circuit of the sawtooth waveform type. The sawtooth waveform is exponential in shape but the transfer characteristic is linear. The output of the circuit is a square wave that rises at the reference time and falls after a variable duration. The fall is sufficiently sharp to identify an instant of time to within an error considerably less than  $1\ \mu\text{sec}$  for the maximum duration

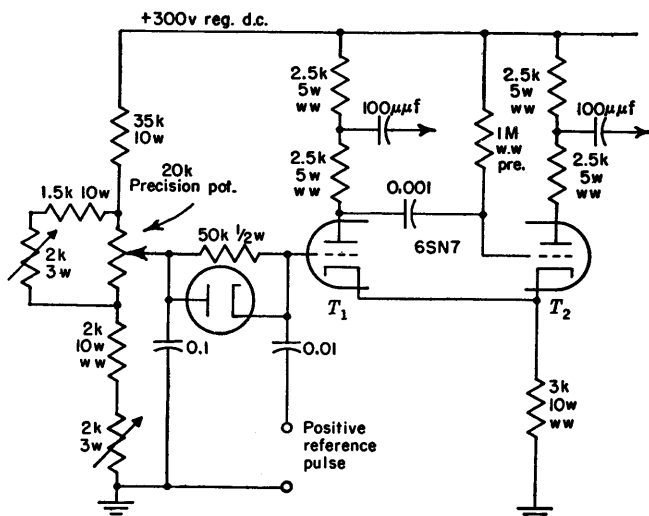


FIG. 5-14.—The SF delay multivibrator.

used in radar. The simplicity of the circuit is its greatest virtue and it is not now used as a precise time modulator although it was originally developed for this purpose. Other voltage-controlled circuits with more stable timing waveforms and more accurate comparators have supplanted it.

In one instance the circuit was used for the measurement of time intervals in a shipborne radar. The step at the end of the modulated interval was used as a step on a CRT display. The time-measurement system was therefore very economical, consisting of a potentiometer and dial, the delay multivibrator, and a cathode-ray tube. A crystal-controlled oscillator provided means for checking the transfer characteristic of the multivibrator.

The operation of the circuit is described in Vol. 19, Chap. 5. A circuit diagram is shown in Fig. 5-14. The means for triggering and the regula-

tion of the supply voltage must be good if satisfactory operation is to be achieved.

The linearity of the transfer characteristic is usually about 1 per cent, although careful adjustment of constants may give better results with selected tubes. Temperature sensitivity of the delay is large and compensation is not usually profitable. The coefficient of delay change with heater-supply variation has been observed to be approximately  $-0.2$  per cent per volt. A change of  $E_{pp}$  from 250 volts to 200 volts resulted in a 0.4 per cent change in delay. Tube changes result in variation of the transfer characteristic by as much as 10 per cent.

This circuit depends to a large extent upon the constancy of tube characteristics. The application of precision tubes, such as the 6SU7, to such circuits has not been sufficiently investigated. It is probable, however, that the development of more accurate voltage-sawtooth time-modulation circuits is most easily done with more complex circuits. Some increase in accuracy might be expected by the use of diodes to stabilize the initial amplitude of the timing waveform and the firing point of the regeneration.

#### VARIABLE DELAY LINE

**5-9. Supersonic Delay Tank.**—A delay-tank time-modulation system<sup>1</sup> consists of two crystals, a transmitter and a receiver, of supersonic oscillations mounted in a tank of liquid (see also Chap. 12). The delay is variable over a range of 2 to 240  $\mu$ sec by alteration of the distance between the transmitter and the receiver. A 240- $\mu$ sec delay is achieved with the transmitter and receiver approximately 20 in. apart.

The functional diagram of Fig. 5-15 shows the delay tank and the necessary circuits. The pulse generator accepts the reference pulse and produces a sharply rising high-voltage pulse that is applied to the transmitting crystal. The crystal oscillating at its natural frequency produces a short damped wave train of alternating compressional waves in the liquid surrounding the crystal. This wave train is propagated along the tank, and when it reaches the receiver, a voltage appears across that crystal.

The amplifier follows the receiver to raise the signal to a usable level since there are considerable losses in the tank. The amplitude-selector circuit accepts only signals that are greater than a certain magnitude. The automatic gain control ensures that only the largest signal from the receiver exceeds this level. The undesired signals are reflections from the tank walls. The amplitude selector produces a pulse that triggers a multivibrator whose output is a short low-impedance movable pulse.

<sup>1</sup> See "Instruction Book for Model SJ Radar Equipment," BuShips.

This system is capable of an extremely high degree of accuracy because the two crystals can be controlled in position to within 0.002 in. over the range of 20 in. The delays in the associated circuits may be made so small that normal variations in them are negligible. The rate of propagation of the supersonic waves through the liquid is a function of its temperature and composition. The tank normally contains 15.8 volumes of iron-free ethylene glycol to 100 volumes of water at 70°F. The velocity characteristic of the mixture has zero temperature coefficient at 135°F and is maintained at this temperature by a thermostatically controlled regulator. If the standard conditions are varied by 1 part of glycol in 100 parts of water or by 14°C, the transfer characteristic changes by  $\frac{1}{1000}$ .

The linearity of the system is nearly an order of magnitude better than that of voltage-sawtooth delay circuits. The slope and zero may be

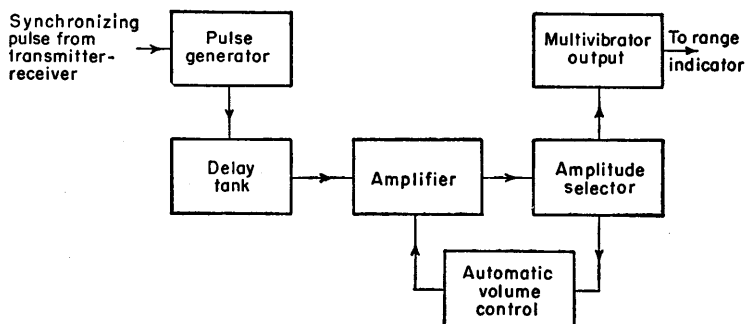


FIG. 5-15.—Model SJ radar range unit functional diagram.

maintained to this high degree of accuracy by specific-gravity and refractive-index measurements of the liquid and careful setting of the thermostatic control.

The device may be difficult to maintain for field operations and moreover weighs 60 lb. The difficulty of sealing the mechanical coupling between the movable crystal and the external crank against the leakage of liquid reduces the reliability considerably.

The various circuits are given in detail in Fig. 5-16. The pulse-generator circuit accepts a positive pulse that is stepped up about five times in the pulse transformer  $T_2$ . The amplifier  $V_4$  is biased below cutoff and does not respond to negative pulses. The positive pulse, however, produces a negative signal at the plate of  $V_{4a}$ . After being quasi-differentiated in  $C_{12}R_{20}$ , this negative pulse initiates a multivibrator  $V_{4b}-V_5$  which applies a 20- $\mu$ sec pulse to the transmitting crystal through  $C_{17}$ . The rapid rise of this 20- $\mu$ sec pulse causes supersonic oscillations in the crystal. These oscillations occur at the natural frequency of the

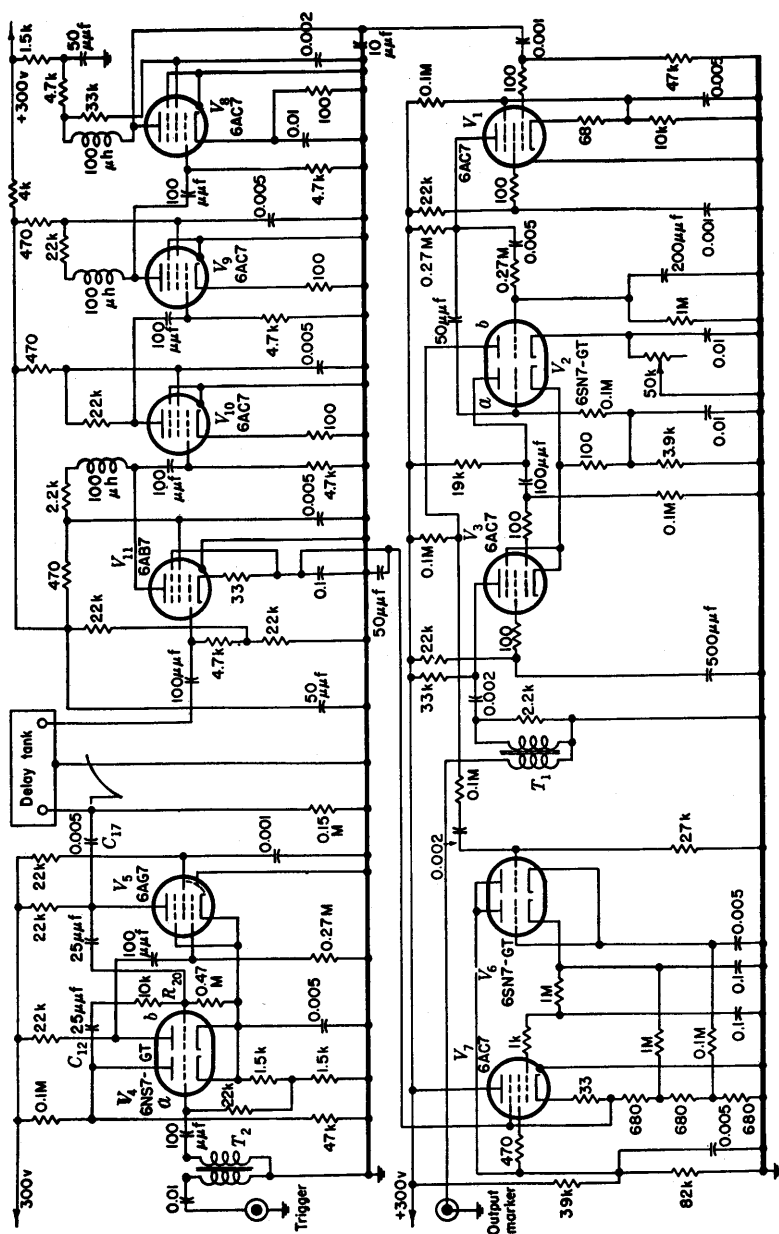


Fig. 5-16.—Model SJ radar range circuit using supersonic delay tank.

crystal, about 1.4 Mc/sec. The fall of the 20- $\mu$ sec pulse is not steep enough to produce oscillations in the crystal.

The transmitting and receiving crystals are flat plates about  $\frac{7}{8}$  in. square and 0.040 in. thick, mounted with their large flat faces directly facing each other. The voltage wave applied to the transmitter causes it to oscillate in a damped vibration at its natural frequency for longitudinal waves. This vibration is highly damped because of the contact between the crystal and the liquid and even more because of the mounting in which it is placed. In this mounting there is a brass "backing block" to which the whole back face of the crystal is tightly soldered. This block is used as one electrode. A grounded layer of solder applied to the front face of the crystal is the other electrode. The backing block is very effective in absorbing mechanical energy from the quartz and thus in damping out the vibration.

The faces of the crystals must be parallel to within about 0.01 in. if sufficient voltage is to be produced across the receiving crystal. The liquid in the tank is held at  $135^{\circ} \pm \frac{1}{2}^{\circ}\text{F}$  by the thermostat  $TD_2$  and is quickly raised to this temperature region by a high-heat element controlled by  $TD_1$ . Thermostat  $TD_1$  is set at a few degrees below  $TD_2$ .

The electrical connection to the moving crystal consists of a central conductor of several small wires surrounded by a layer of rubber which in turn is coated with Neoprene. This structure gives the wire low capacitance, high flexibility, and chemical resistance to the solution. The capacitance to ground, measured at 1 or 2 Mc/sec is about 55 to 85  $\mu\text{f}$ . The resistances to ground may be as low as 50,000 ohms although normally they are much higher.

The loss in the fluid itself is only 60 or 70 per cent, but the output that appears across the receiving crystal is about 5 mv peak amplitude. The amplifier accepts a 5-mv signal and produces about 15 volts at the output. The maximum gain is 75 db and can be reduced to about 65 db by automatic gain control. The automatic gain control maintains at a constant amplitude the signals to be applied to the amplitude selector. The amplitude selector is biased below cutoff so that only the highest peak of the highest wave train makes  $V_1$  conduct. Tubes  $V_{2a}$  and  $V_3$  make up a monostable multivibrator that is triggered by the amplitude-selector output and produces a movable marker pulse that is stepped down in impedance by transformer  $T_1$ .

### SINUSOIDAL OSCILLATOR RANGE CIRCUITS

**5-10. LC-oscillator, Phase Modulator, and Comparator.**—This circuit is of very early date and merits only the briefest description. The time measurement of the radar SCR-268<sup>1</sup> is accomplished with an oscil-

<sup>1</sup> *Electronics*, 18, 100-109, September 1945.

lator, a phase shifter, and pulse generators, with a cathode-ray-tube indicator. The basis of the time measurement is a stable oscillator that operates at a constant frequency of 4098 cps. The oscillation is distorted in a series of amplifiers so that a PRF trigger pulse is formed once each period. The sinusoidal output from the oscillator is phase-modulated by the rotation of the range handwheel and a movable pulse is derived from this wave.

The movable pulse is used as a trigger to initiate the time base for the cathode-ray tube. An approximately linear sawtooth waveform is applied to the horizontal plates of the tube. A vertical fixed hairline is placed at the center of the tube. The transmitted pulse and the target echo both appear as amplitude modulation.

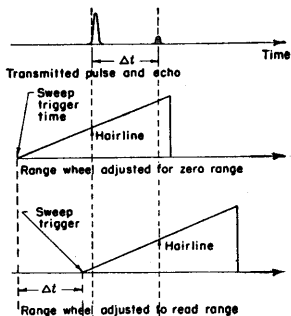


FIG. 5-17.—SCR-268 time-measurement circuit, timing diagram.

The sequence of events in a time measurement is presented in the timing diagram of Fig. 5-17. First the range handwheel is turned to bring the transmitted pulse to the hairline; next the echo is set to the hairline and the range is read in yards on the counter. The elements of this sys-

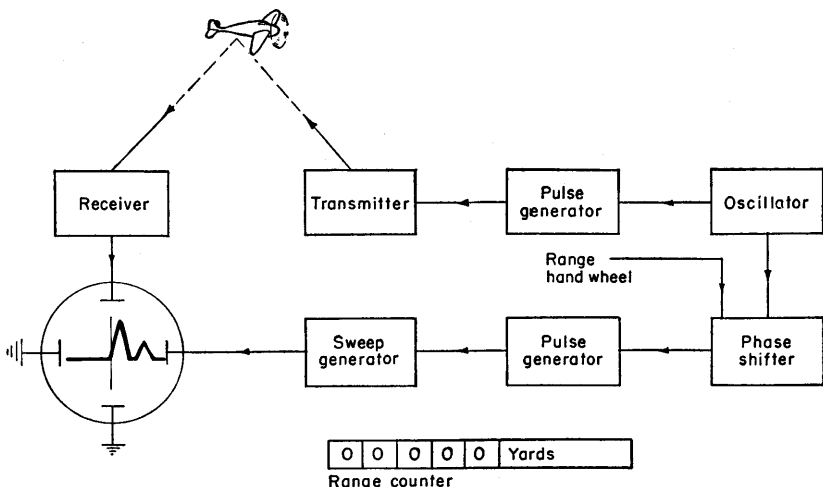


FIG. 5-18.—Time measurement with a single-scale oscillator (phase shifter).

tem are shown in Fig. 5-18. As shown, the reference pulse coincides with the hairline and the counter is properly zeroed.

The oscillator circuit is very simple and only of moderate accuracy in order to be consistent with the system accuracy. The radar operates at

205 Mc/sec and the transmitted pulse is 9  $\mu$ sec in duration. The accuracy is poor compared with that of later radars.

The oscillator circuit is shown in Fig. 5-19a. The tank circuit, which maintains the frequency of oscillation, is manufactured as a unit except for a trimmer condenser that serves as a frequency control. This condenser adjusts the slope of the time-modulation characteristic. By the use of a standard time interval, the slope can be calibrated.

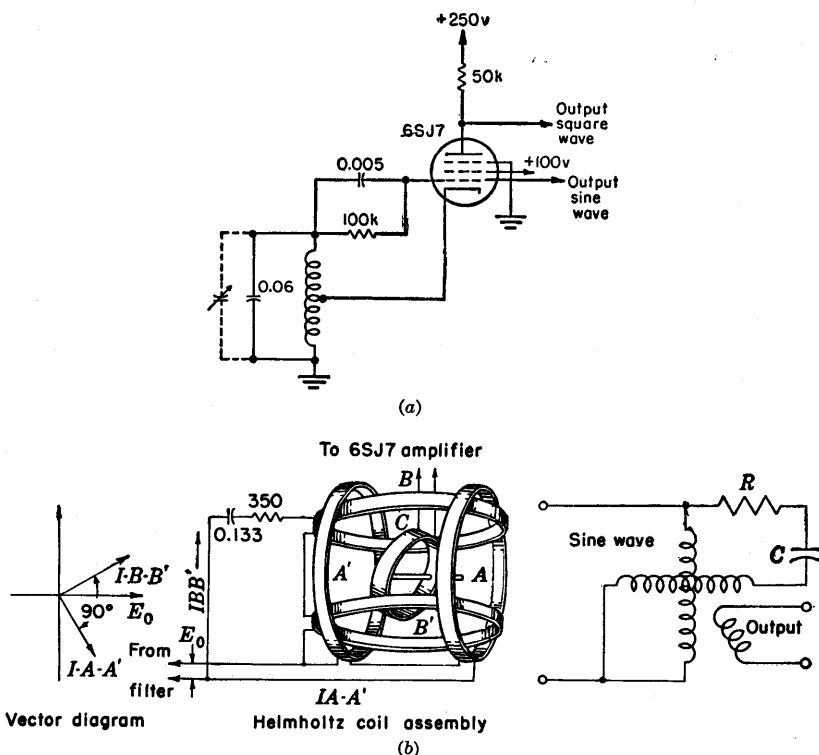


FIG. 5-19.—SCR-268 oscillator and magnetic phase shifter.

A pure sinusoid is derived by filtering and then is phase-shifted in an inductance goniometer (see Fig. 5-19b). This particular goniometer employs Helmholtz coils to give a uniform magnetic field. The accuracy is approximately  $\frac{1}{4}$  per cent of a full turn ( $360^\circ$ ).

A considerably improved system of this type could be made by minimizing the largest errors—in oscillator frequency, in phase modulation, and in amplitude comparison.

**5-11. The Variable-frequency Oscillator.**—If a variable-frequency oscillator is started at the time of a reference pulse by an oscillator gate,



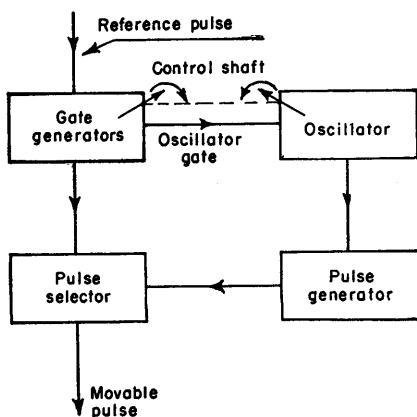


FIG. 5-20.—Variable-frequency oscillator time-modulator circuit.

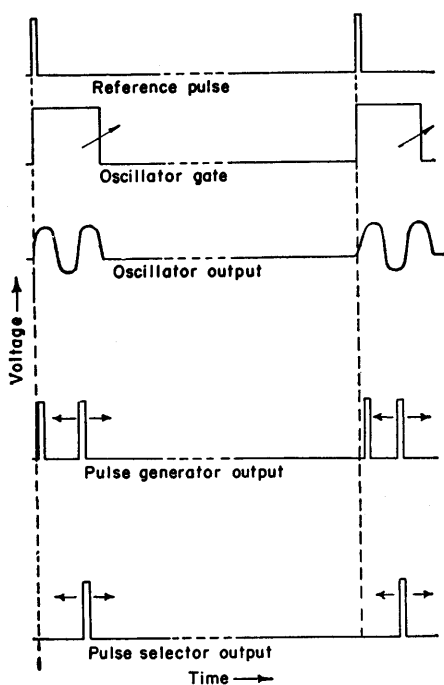


FIG. 5-21.—Timing diagram of the variable-frequency oscillator time modulator.

the first period of the oscillation constitutes a variable time delay. If a pulse is generated at the end of one period, the pulse will be time modulated. The block diagram of Fig. 5-20 shows a circuit of this type. Since the pulse generator operates on every period, it is necessary to eliminate the undesired pulses with the pulse selector. The oscillator is stopped shortly after one cycle by the oscillator gate which changes in duration with the control shaft.<sup>1</sup>

Some of the waveforms of a circuit of this type are shown in Fig. 5-21. Those which are shifted or expanded along the time axis as a function of the control variable are marked with an arrow.

The experimental circuit shown in Fig. 5-22 with additional gate generators, pulse generator, and pulse selector has been operated in the

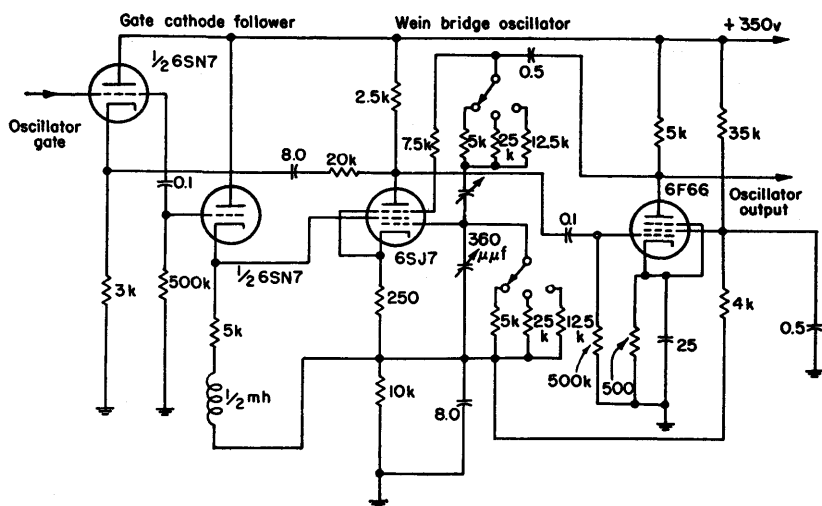


Fig. 5-22.—A variable-frequency oscillator for time modulation. The minimum delay is 3  $\mu$ sec; the maximum delay is 300  $\mu$ sec. The linearity is +2.6 per cent.

laboratory, but was never further developed. For an ideal Wien bridge oscillator, the period is proportional to the shaft rotation of the variable condensers if the bridge impedances are properly proportioned. The time intervals range from 3 to 300  $\mu$ sec in three scales obtained by switching the bridge resistance. The maximum errors from linearity are 0.03, 0.3, and 7.5  $\mu$ sec on the scales. The probable cause of the limiting error (2.5 per cent of the maximum time interval) is bridge asymmetry. The slope of the characteristic changes  $\frac{1}{4}$  per cent for a 1 per cent plate-supply voltage change. Heater-voltage changes within 10 per cent of the rated value

<sup>1</sup> See A. H. Frederick, RL Group Report No. 63-9/11/42.

had no appreciable effect. A temperature change from  $+20^{\circ}$  to  $-80^{\circ}\text{C}$  changes the slope of the characteristic by several per cent because of the lack of perfectly temperature-compensated resistance-capacitance elements. Somewhat better frequency stability (and linearity) is observed with the Hewlett-Packard oscillator.

The oscillator gate is applied to the screen grid of an oscillator tube by a cathode follower. Changes of the gate tube cause the oscillator to operate when it should be quiescent. The effect can be eliminated by capacitance coupling from the plate of the gate tube to the cathode-follower grid.

The second cathode follower of Fig. 5-22 is used to cancel the gate component partially in the oscillator output by applying the gate to the plate of the oscillator tube. It is desirable to have the alternating component swing about the quiescent level in order to square the waveform. The gate cannot be completely removed because a point is reached where the oscillation starts in the opposite phase. The gate should probably be removed at a point outside the oscillator feedback loop. The squaring amplifier may increase the time delay by 2 per cent—this increase is a function of the tube characteristics of several tubes. It is desirable to use a better method for synchronizing a pulse with the end of the period of a sinusoid. Such methods have been described in Chap. 9, Vol. 19. Differentiation of the squared waves produces signals of opposite signs at the  $180^{\circ}$  and  $360^{\circ}$  points of the sine wave. The  $180^{\circ}$  signal is discriminated against by a diode selector.

The frequency stability of the oscillator would be improved if an automatic amplitude control were used. Such a device would have to operate on voltage and not on power because the single period of oscillation does not permit thermal equilibrium to be established. The high frequencies necessary at minimum range increase the power requirements for the oscillator in order to maintain low-phase shift in the oscillator amplifier.

This method of time modulation has not proved reliable or inexpensive. The delay multivibrator is a much simpler circuit with approximately the same accuracy. The principle may be useful, however, for some special application.

**5-12. A Comparison of Some Single-scale Circuits.**—A brief comparison of some of the single-scale circuits may be of value if a choice for a particular application is necessary. The detailed studies on which these judgments are based are to be found in the earlier sections of this chapter, in Chap. 3, and in Chap. 13 of Vol. 19.

Without the repetition of a great deal of data, complete comparisons are not possible. The procedure here is to indicate which circuit possesses a particular virtue in the highest degree.

The best linearity is obtained with the supersonic delay tank and the

high-gain Miller integrator circuits. These single-scale circuits, which may be made nearly as linear as more complex multiple-scale circuits, have the additional advantage of freedom from cyclic error (see Chaps. 2, 7, and 8 and Vol. 19, Chap. 13).

The least sensitivity of the transfer characteristic to tube changes, tube drifts, and the vibrations occurs with the propagation-time circuits, the liquid and electric delay lines. The pulse amplifiers, which are the only necessary vacuum tubes, can be designed to introduce negligible delays into the circuit.

The least sensitivity to temperature changes is found in circuits whose fundamental element is a crystal-controlled oscillator. These are usually multiple-scale circuits. At the opposite extreme are the propagation-time circuits, for which the temperature coefficients are so great that control of the ambient temperature is often necessary.

Errors from changes in trigger-repetition rate are smallest for the propagation-time circuits, as are the effects of supply-voltage change. The range of modulating frequencies (speed of operation) is largest for the voltage-sawtooth circuits that accept a voltage as the control variable.

The voltage-sawtooth circuits are particularly useful where some sacrifice of accuracy can be made in order to save size, weight, complexity, expense, and power consumption. These have the further advantage of being relatively simple to construct and maintain as opposed to the liquid delay tank. Thus, they have been very widely used for medium-precision time measurement in radars.

## CHAPTER 6

### GENERATION OF MOVABLE INDICES-CIRCUITS

R. I. HULSIZER, R. B. LEACHMAN

#### PHASE MODULATION AND AMPLITUDE COMPARISON

This portion of the chapter describes several time-modulation circuits that employ a method outlined in Secs. 3-9 and 3-15: continuous phase modulation of the high-frequency timing waveform to form a movable train of pulses and selection of one of these pulses by a coarse-scale time-modulated pulse. By far the largest number of accurate range-measuring systems that were used in radar during the war employed this method. These systems fall into two classes: those actually using phase modulators, and those using circular-sweep indicators. The circular sweep is, in effect, a continuous phase modulator, since rotation of a radial index around the trace selects instants corresponding to all phases of the sinusoid from which the sweep is obtained. Selection of the correct cycle of the fine scale is provided by an intensifying gate, approximately centered on the index and time-modulated at the same rate as the index that moves around the sweep.

**6-1. Meacham Range Unit.**—One of the most straight-forward two-scale time modulators employing phase modulation is the following circuit used at the Bell Telephone Laboratories with several radars and intended as a replacement for the supersonic tank of Sec. 5-9. Its primary use was in fire-control radars where a continuous shaft rotation indicating range is required for ballistic computers. A block diagram of this unit is shown in Fig. 6-1, with a waveform diagram, Fig. 6-2. The system was designed to operate from an external trigger and hence employs a pulsed oscillator. Its tank circuit is tuned to 81.955 kc/sec and is mounted in a temperature-controlled oven for frequency stability. Quadrature voltages (Fig. 6-2*d-g*) drive the condenser phase modulator, whose output is amplified, squared (Fig. 6-2*i*), and differentiated as a method of amplitude comparison. The block labeled "Pulse Selector" performs the operation of generating an exponential sweep to which time-modulated pulses are added, as in Fig. 6-2*j*. Amplitude comparison with respect to a voltage from an exponentially tapered potentiometer selects one of the time-modulated pulses (Fig. 6-2*k*) which is then shaped (Fig. 6-2*l*) and made available at 120-ohm

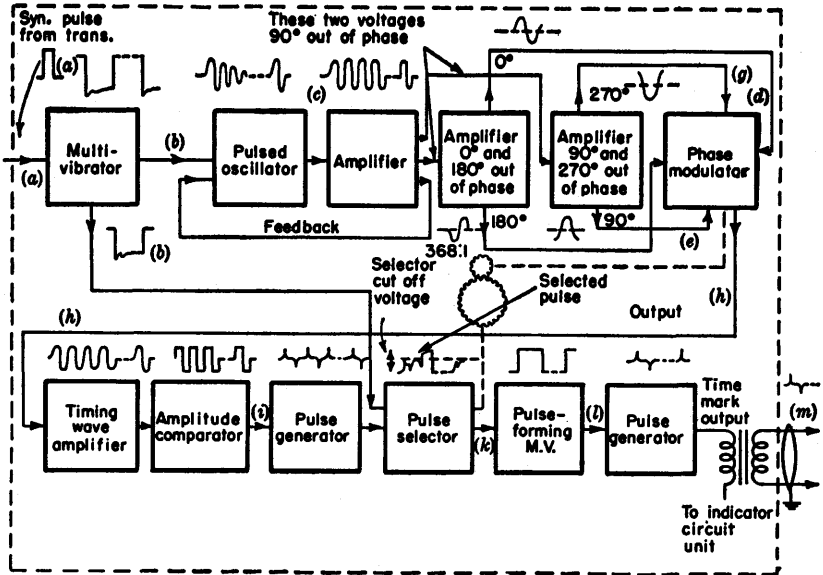


FIG. 6-1.—Block diagram of a two-scale phase-modulation range unit. Letters refer to waveforms on Fig. 6-2.

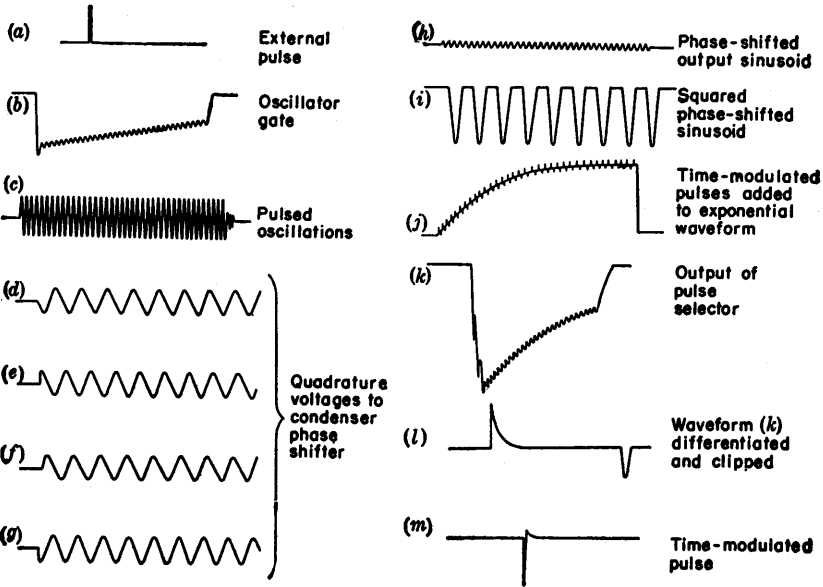


FIG. 6-2.—Waveforms of a two-scale range unit.

level (Fig. 6-2m). The circuit thus provides a single pulse, time-modulated with respect to the external trigger from zero to  $234\mu\text{sec}$ .

*Oscillator and Sawtooth Gate.*—The schematic circuit can be described in three parts. The first is the “wide-gate” monostable multivibrator (Fig. 6-3), which gates the pulsed oscillator and the exponential sweep generator. The left section is normally ON. The external trigger, applied to the left section, turns the multivibrator off for  $240\mu\text{sec}$ , generating a negative gate at the plate of  $V_2$ .

The second circuit section (Fig. 6-4) generates and phase-modulates the pulsed sinusoid. Normally the tuned circuit  $Z_1$  is clamped between the plate of  $V_3$  and the cathode of  $V_4$  is overdamped with an average cur-

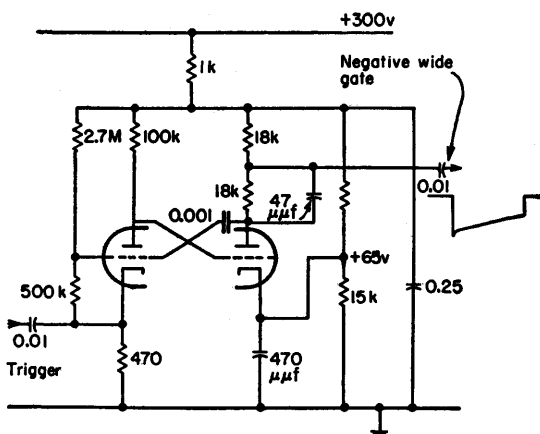


FIG. 6-3.—Wide-gate monostable multivibrator.

rent of about 12 ma flowing through it. Cutting off  $V_3$  and  $V_4$  with the wide gate starts oscillations in the tuned circuit which are coupled to the feedback and phase-shifting amplifier  $V_5$ . Feedback to sustain the initial amplitude of oscillations is provided through  $R_1$ . The  $RC$ -constants in the cathode circuit and the  $RL$ -constants in the plate circuit are adjusted to provide quadrature voltages at the plate and cathode. These are applied to two paraphase amplifiers  $V_6$  and  $V_7$  which in turn drive the condenser phase modulator.

*Amplitude Comparator.*—The phase-modulated output is amplified in  $V_8$  and  $V_9$ , which incorporate negative feedback to increase the input impedance seen by the condenser phase modulator (see Fig. 6-5). A high-resistance load on the condenser phase modulator is necessary to preserve its response to the PRF components of the pulsed sinusoidal waveform since its internal impedance is that of a very small capacitance. Tube  $V_{10}$  performs the amplitude comparison, since it has a large cathode





resistor, effectively unbypassed. When its grid is more negative than cutoff, the cathode rests at +6 volts. When the grid rises past cutoff, which with this arrangement is near ground potential, current will start to flow in the tube, and the plate voltage to start to fall. Thus the fixed potential to which the sinusoid is compared is the cutoff bias of  $V_{10}$ . The fall in plate voltage after the instant of equality would be slow were it not for the small cathode bypass condenser. The following tube  $V_{11}$  operates with its grid normally slightly positive. When the plate of  $V_{10}$  starts to fall, the plate of  $V_{11}$  starts to rise rapidly since  $V_{11}$  is then operating with maximum  $g_m$ . Differentiation in  $C_1$  and  $R_2$  forms short pulses for use in the pulse-selection circuit. The stability of the amplitude-comparison operation depends on the stability of the cutoff bias of a 6AC7. A shift of

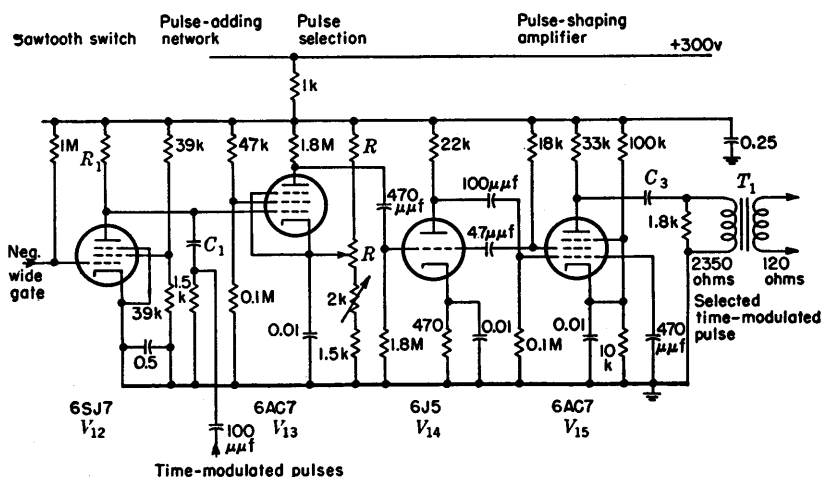


FIG. 6-6.—Coarse-scale time modulator and pulse selector.

this bias by 1 volt should introduce an error of about 3 yd, but experimentally a change of heater voltage from 5 to 6.6 volts shows less than 1 yd error; also, a change of plate supply voltage from 200 to 340 volts shows only 1 yd error.

**Coarse-scale Pulse Selector.**—Figure 6-6 shows the coarse-scale time modulator and pulse selector. Tube  $V_{12}$  is a switch tube operated by the negative wide gate. Its plate circuit contains an  $RC$ -element which forms an exponential waveform when the tube is cut off. A small resistor is inserted in the circuit by which the time-modulated pulses are added. Tube  $V_{13}$  acts as a part of an amplitude-comparison circuit, the reference voltage being applied to its cathode from an exponentially tapered potentiometer. Since the time-modulated pulses are larger than the amount by which the exponential waveform changes between pulses, a

pulse, rather than the exponential waveform, will initiate current in  $V_{13}$ . This action is analogous to that of amplitude-comparison multivibrator frequency dividers. The resultant negative pulse, whose leading edge coincides with one of the time-modulated pulses, is amplified and differentiated in the tubes  $V_{14}$  and  $V_{15}$  and the pulse transformer  $T_1$ .

Figure 6-7 shows the errors of the range unit from zero to 44,000 yd out of the maximum of 76,000 yd. The starting transient is negligible after

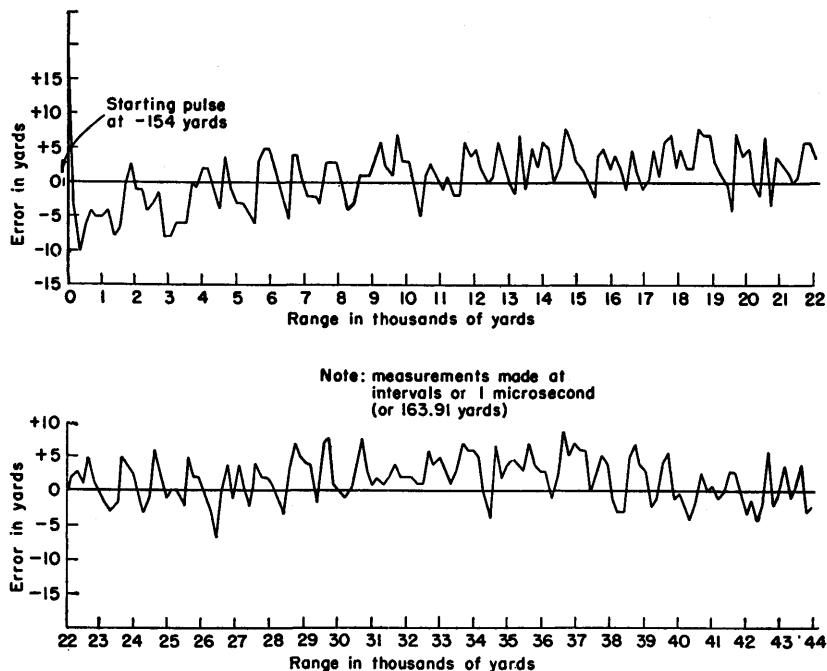


FIG. 6-7.—Results of laboratory test of two-scale range unit.

300 yd. The other errors are due to irregularities in the condenser phase shifter, improper frequency of the pulsed oscillator, and errors in the exponential potentiometer which vary the point of the time-modulated pulse at which pulse selection occurs.

**6.2. Precision Ranging Indicator.**—In contrast to the circuit of the previous section in which all of the fine-scale pulses are added to an exponential waveform and then one selected by amplitude selection, the circuit now to be described selects one of the fine-scale pulses by means of a pentode amplifier switched on by a pulse that is time modulated by the coarse scale. This method of pulse selection by multi-electrode vacuum tube switches is described in Secs. 3-9 and 3-15 of this volume and Chap.

10 of Vol. 19. The error to be expected in time selection by addition and amplitude selection is thus avoided. Figure 6-8 shows the block diagram. Figure 6-9 illustrates the timing relationships of the operations.

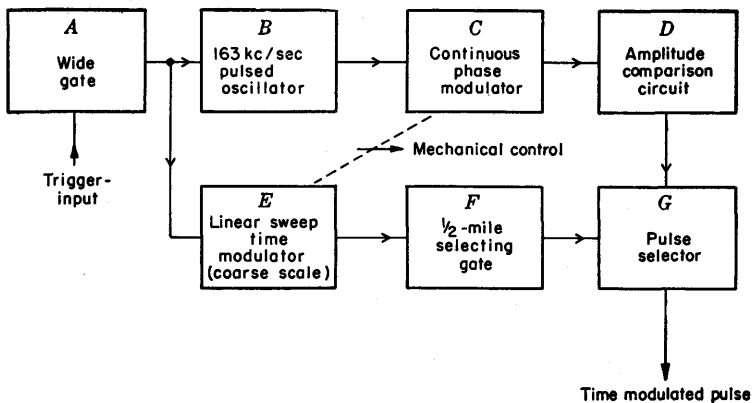


FIG. 6-8.—Block diagram of Precision Range Indicator.

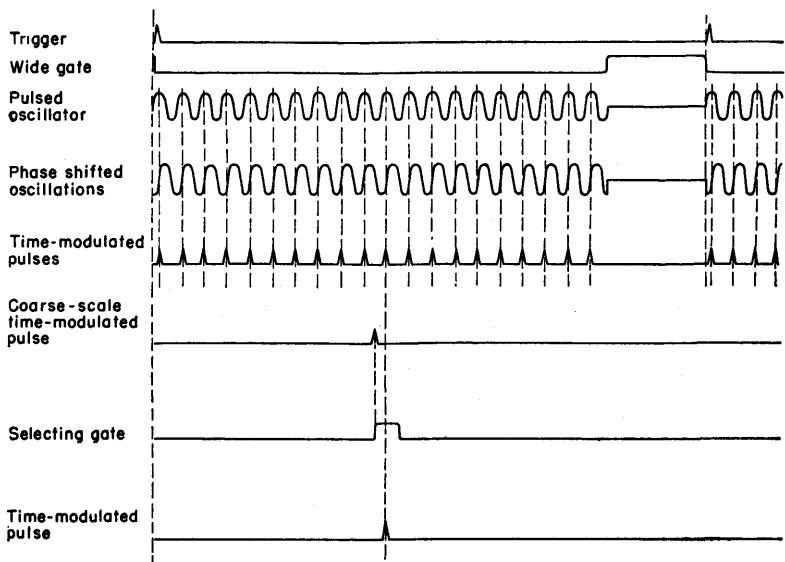


FIG. 6-9.—Timing diagram of Precision Range Indicator.

As before, the circuit has been drawn in sections for convenience. Figure 6-10 shows the wide-gate multivibrator. The pulsed oscillator  $V_5$  of Fig. 6-11 was designed for maximum frequency stability. The tuned circuit and feedback resistor are installed in a temperature-con-

trolled oven; the effect of heater-cathode capacitance variations in  $V_4$  is reduced by using a floating heater transformer connected to the cathode

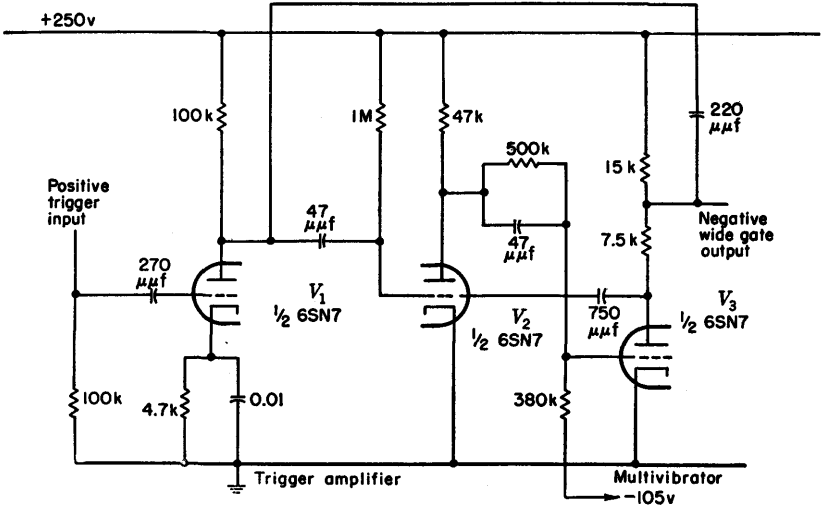


FIG. 6-10.—Wide-gate multivibrator of Precision Range Indicator.

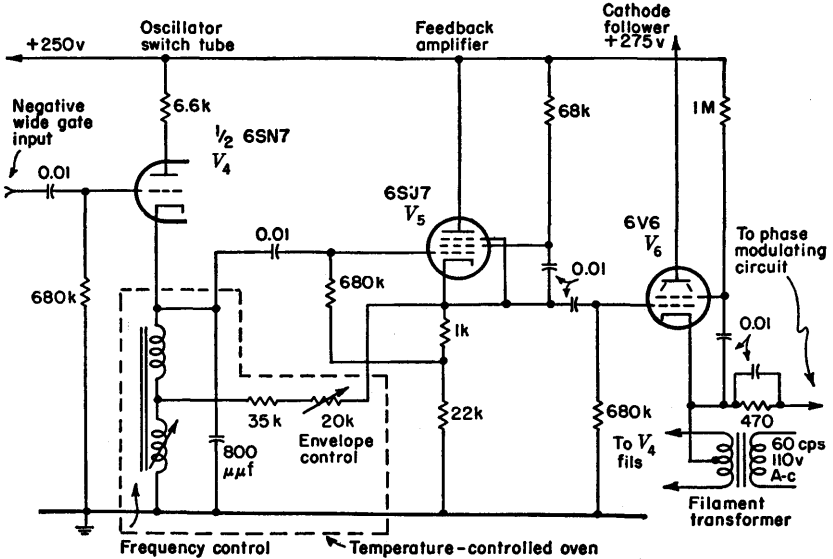


FIG. 6-11.—Pulsed oscillator of Precision Range Indicator range unit, 163 kc/sec.

follower  $V_6$  and a 6SJ7 was chosen as a feedback tube  $V_5$  because its characteristics are more stable than those of the 6AC7 used in the example

of Sec. 6-1. Data show a frequency variation with tube changes of  $\pm 0.025$  per cent for eight tubes of assorted manufacture for each of  $V_4$ ,  $V_5$ , and  $V_6$ .

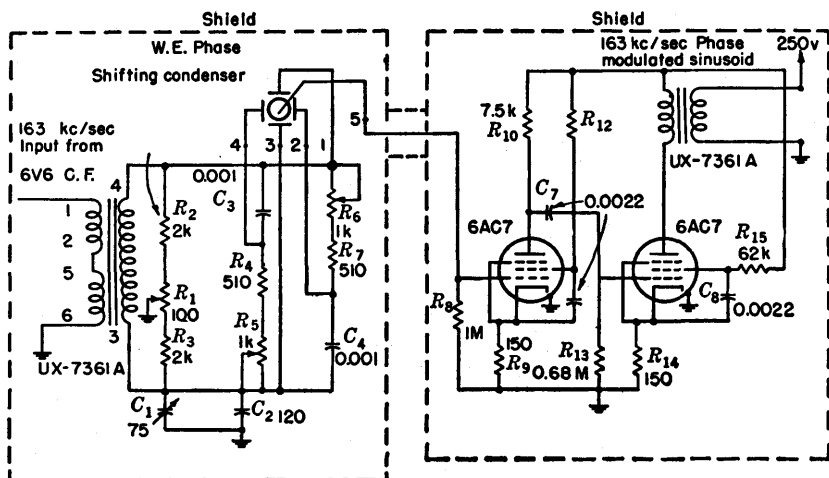


FIG. 6-12.—Precision Range Indicator phase-modulating circuit. See Table 6-1 for component specifications.

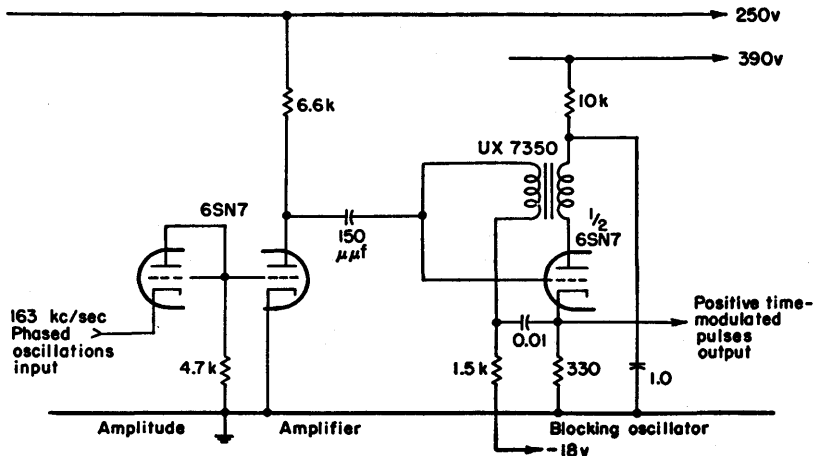


FIG. 6-13.—Precision Range Indicator amplitude-comparison circuit for generating time-modulated pulses from phase-modulated sinusoid.

Figure 6-12 shows the quadrature network for driving the condenser phase modulator, and a two-stage amplifier  $V_7$  and  $V_8$ . The input resistance of the amplifier is 1 megohm, compared with about 1.65 megohms for the more complicated circuit of Sec. 6-1. One precaution of considerable

importance is that the input and output circuits must be carefully shielded from each other since the output circuit of the phase modulator is at low voltage level and high impedance. Any stray pickup of sinusoid will introduce errors in the phase modulation.

The circuit for generating time-modulated pulses from the phase-modulated sinusoid is shown in Fig. 6-13. The amplitude comparison is

TABLE 6-1.—PARTS LIST FOR FIG. 6-13

Item	Value	Tolerance, %	Wattage	Miscellaneous
$R_1$	100 ohms	..	2	ww potentiometer
$R_2$	2 k	2	1	ww precision
$R_3$	2 k	2	1	ww precision
$R_4$	510 ohms	5	$\frac{1}{2}$	ww
$R_5$	1 k	..	2	Potentiometer
$R_6$	1 k	..	2	Potentiometer
$R_7$	510 ohms	5	$\frac{1}{2}$	ww
$R_8$	1 M	10	$\frac{1}{2}$	.....
$R_9$	150 ohms	5	$\frac{1}{2}$	.....
$R_{10}$	7.5 ohms	5	1	.....
$R_{12}$	62 k	5	1	.....
$R_{13}$	680 k	10	$\frac{1}{2}$	.....
$R_{14}$	150 ohms	5	$\frac{1}{2}$	.....
$R_{15}$	62 k	5	1	.....
$C_1$	75 $\mu\mu\text{f}$	..	..	Air trimmer, 180° balance
$C_2$	120 $\mu\mu\text{f}$	5	..	Silver mica
$C_3$	0.001 $\mu\text{f}$	2	..	Silver mica
$C_4$	0.001 $\mu\text{f}$	2	..	Silver mica
$C_6$	0.0022 $\mu\text{f}$	10		
$C_7$	0.0022 $\mu\text{f}$	10		
$C_8$	0.0022 $\mu\text{f}$	10		

performed by a diode whose output pulse is amplified and triggers a blocking oscillator.

To provide a time-modulated gate to select one of the accurately time-modulated pulses, a linear sawtooth waveform is generated that drives an amplitude-comparison circuit. This is shown in Fig. 6-14 and consists of a "bootstrap" linear sawtooth generator  $V_{12}$ ,  $V_{13}$ ,  $V_{17}$ , and  $V_{18}$ , and an amplitude-comparing diode  $V_{16}$ ; the latter is controlled by the linear range potentiometer that is geared to the condenser phase modulator.

The selecting gate is formed from the comparator output pulse by an amplifier and blocking oscillator, as shown in Fig. 6-15. The grid bias of the second amplifier is obtained from the grid of the blocking oscillator, which supplies a large negative exponential immediately following the blocking-oscillator pulse. The plate transformer of the first amplifier differentiates the amplitude-selected sawtooth received from the

diode to produce from its leading edge a positive pulse followed by a negative overshoot, and from its trailing edge a large negative pulse fol-

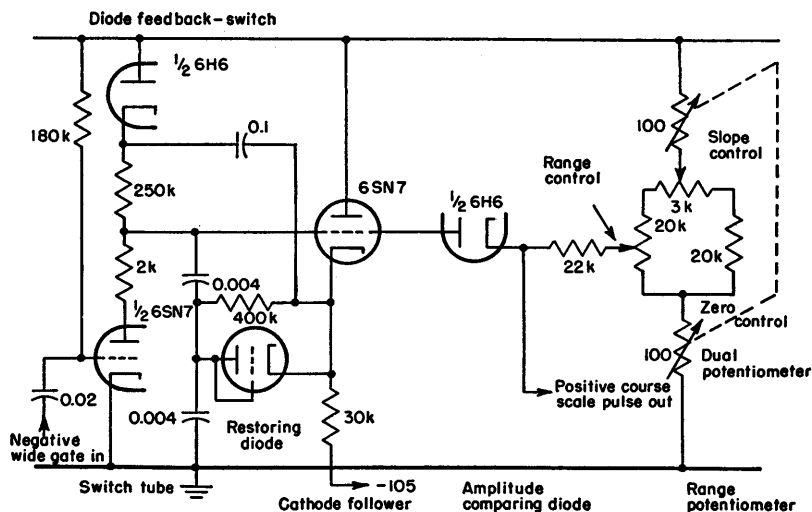


Fig. 6-14.—Precision Range Indicator linear-sweep time modulator.

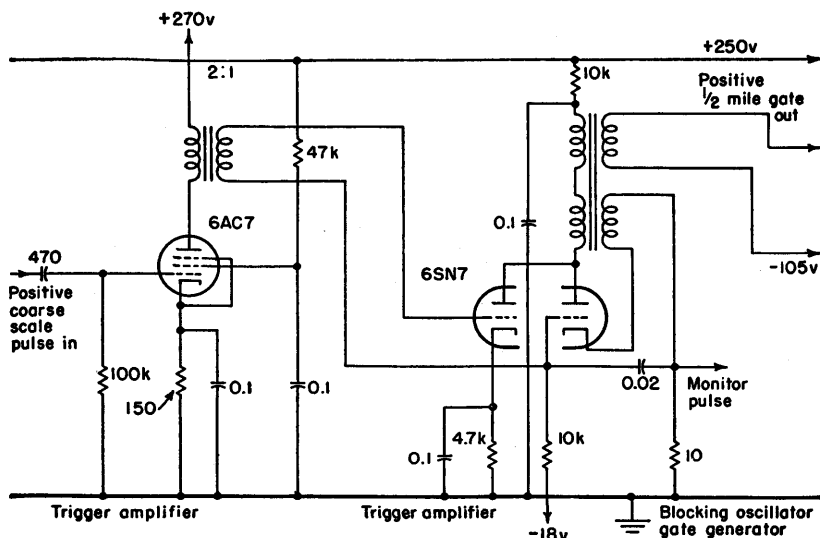


Fig. 6-15.—Precision Range Indicator 6-μsec pulse-selecting gate generator.

lowed by a correspondingly large positive pulse. The function of the special bias arrangement is to prevent the second amplifier from amplifying the second positive pulse. A later model of this circuit uses a diode

across the pulse transformer to absorb the undesired negative swings. A still later version employed the pulse-selecting gate to shut off the linear sweep generator, thus causing the undesired pulse to occur while the second amplifier grid was still at a large negative potential. Figure 6-16 shows the pulse-selecting circuit, a suppressor gated 6SJ7.

Although this circuit appears more complex than that of Sec. 6-1 because of the linear sweep generator, diode amplitude comparator, and separate pulse selector, nevertheless it requires only three more tube sections, and one less envelope, and does not require an exponentially tapered potentiometer. Furthermore the errors of amplitude comparison due to the exponential selecting waveform are eliminated. The sine-wave amplitude comparison is also better performed by the diode than by the pentode.

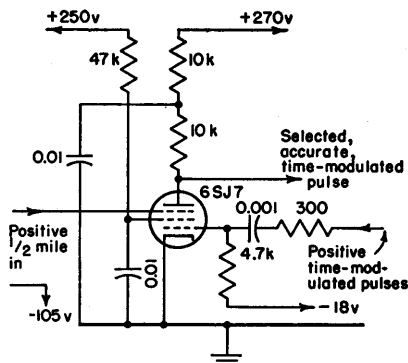


FIG. 6-16.—Precision Range Indicator pulse-selecting circuit.

In the circuit of Sec. 6-1, the fine-scale pulses are spaced at  $12.2 \mu\text{sec}$  and the total range is  $470 \mu\text{sec}$ , so the pulse-selection circuit has to be good to at least  $\pm 1.3$  per cent. In this circuit, the fine pulses are spaced at  $6.1 \mu\text{sec}$ , and the maximum range is  $244 \mu\text{sec}$ , giving a coarse-scale accuracy requirement of  $\pm 1.25$  per cent. The errors of the circuit of Sec. 6-1, as indicated in the graph of Fig. 6-17, do not exceed  $\pm 0.075 \mu\text{sec}$  in  $463 \mu\text{sec}$ , or  $\pm 0.016$  per cent. The errors of this circuit are about the same fraction of the total range, but the absolute accuracy would be higher because of the higher oscillator frequency, and should not exceed  $\pm 0.04 \mu\text{sec}$  over all.

**6-3. Scale Coordination by Frequency Division.**—One radar range unit is distinctive in that as a primary time standard it employs oscillations whose frequency is an order of magnitude higher than in the previous circuits. Furthermore, its method of coordinating the fine and coarse scales is unusual. Two identical sets of dividers generate a trigger and a time-modulated pulse from phase-modulated and reference-phase sinusoids, respectively. A change of  $360^\circ$  in phase of the high-frequency sinusoid time-modulates the output pulse an amount equal to one period of the high frequency. Thus the number of revolutions of the phase modulator required to traverse the recurrence interval is equal to the frequency division ratio. The arrangement of the functions is indicated in Fig. 6-17. The crystal oscillator of the first block is similar



to those previously shown. The phase modulator is of the inductive goniometer type and is coupled to the range driving motor.

Amplitude comparison is performed in this circuit by the grid-cutoff characteristics of a triode used as a squaring amplifier. This practice is

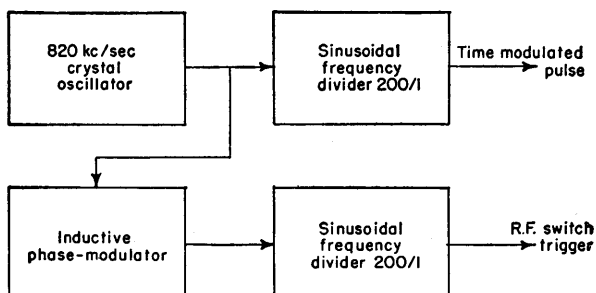


FIG. 6-17.—Block diagram of range unit using phase modulation and frequency division.

perfectly reasonable at this frequency since a whole cycle is only  $1.22 \mu\text{sec}$  and variations of 1 volt would cause a shift of only 0.6 yd.

Multivibrators are used as pulse-frequency dividers in the ratios of 4 to 1, 5 to 1, 5 to 1, and 2 to 1. The first three employ tuned circuits in

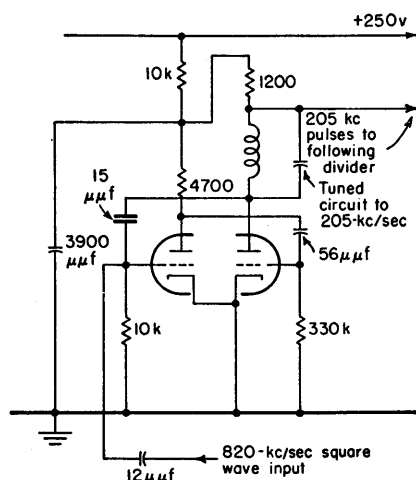


FIG. 6-18.—Multivibrator frequency divider designed to operate between 820 kc and 205 kc, with tuned plate load for stability of operation.

one plate of the multivibrator to increase the stability of division. Figure 6-18 shows a typical divider circuit. The last stage of frequency division is performed by a scale-of-two counter.

The unambiguity of the time-modulated pulse relies on the fact that when the power is first turned on the multivibrators are made to divide in isochronism with the range counter set to read zero range. Before this is done, there exists a random probability that any particular 820-kc/sec cycle will be the one that is isochronous with the 4.1-kc/sec time-modulated pulse. The method of calibrating is to set the range counter to zero and couple the first three

pairs of dividers together. If these dividers operate undisturbed after the coupling is removed, there will result a time modulation between the range-indicating pulse and system trigger which will be continuous and unambiguous for 200 revolutions of the phase-modulating goniometer.

In fact, the time modulation can be performed continuously from one recurrence interval into the next. The disadvantage of the system is that any temporary failure of the divider chains results in an error that is maintained until the system is reset; in this respect it is similar to the sine-wave tracking system of Sec. 6-4.

A consequence of time-modulating the system trigger rather than the range-indicating pulse is that the range index remains fixed on the circular-sweep indicators; if the time modulation matches that of a moving target,

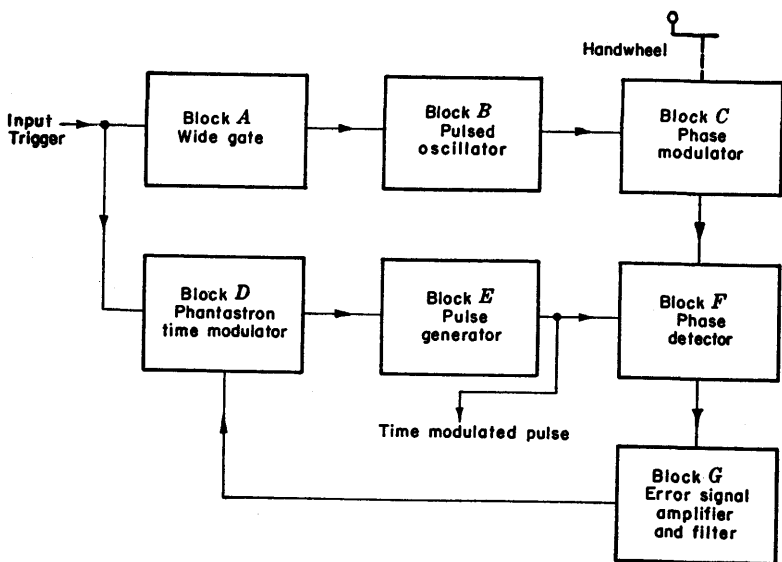


FIG. 6-19.—Proposed range-unit block diagram illustrating the technique of sine-wave tracking.

the target will remain fixed on the circular sweep rather than move around as it does in systems like the SCR-584 described in Chap. 7.

A dynamic range-tracking test showed that the errors, including those from the automatic range-tracking circuit, did not exceed  $\pm 0.0375 \mu\text{sec}$ .

**6-4. Sine-wave Tracking.**—An alternative method of eliminating the coarse-scale control in a multiple-scale time-modulation system is to cause a time-modulator of unspecified accuracy to follow the motion of one node of a train of phase-modulated sinusoidal oscillations. This can be instrumented with a phase discriminator, which compares the times of the node of the sinusoid and the time-modulated pulse to deliver an error signal that can be used to control the time modulator. The amount of time modulation is thus determined by the high-frequency sinusoid and is independent of the characteristics of the time modulator. The block diagram of Fig. 6-19 indicates the arrangement of operations. The dif-

difficulty with the system is that the phase discriminator cannot distinguish one node from another. Thus a momentary power failure or disturbance is liable to introduce a gross error. As in the system of Sec. 6-3, no indication of the existence of the gross error is provided.

A modification that would automatically remove gross errors can be described briefly by saying that an accurately linear time modulator is employed in the above system, and its control voltage as fixed by the sine-wave tracking operation is continuously compared with that of a linear potentiometer having the same voltage range. The potentiometer is geared correctly to the phase modulator so that its voltage is an approximate, but absolute, indication of the time modulation indicated by the dial. If the linear time-modulator control voltage differs from that of

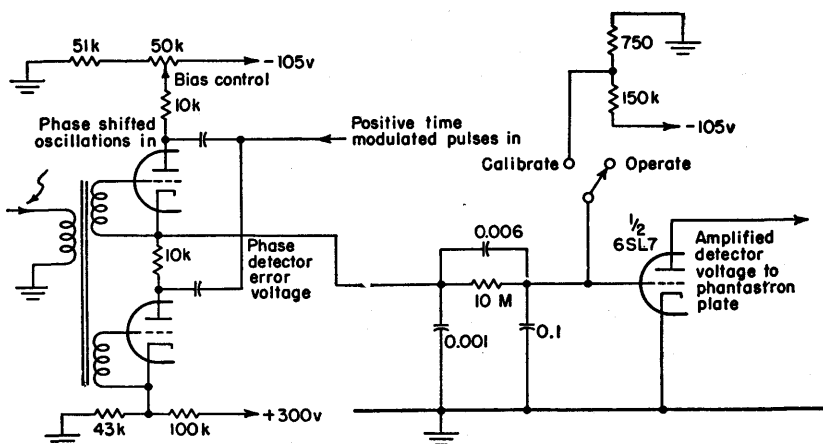


FIG. 6-20.—Phase detector and error-signal amplifier of proposed sine-wave tracking time modulator.

the potentiometer by an amount greater than that required to displace the time modulator by half a cycle of the sinusoid, a relay closes and connects the time-modulator control voltage momentarily to the potentiometer, thus bringing the pulse back to the correct node.

It is thus seen that the pursuit of this method to a point of reliable design yields a system closely parallel to the systems of Secs. 6-1 and 6-2. The accuracy of the pulse is limited in the latter systems by the stability of the operations of amplitude comparison and pulse selection, in the former by the stability of the phase discriminator. The only economy of sine-wave tracking is the elimination of the circuits for generating pulses from the sinusoid.

The two circuits required by this method of time modulation that have not been described previously are the phase detector and the error-signal amplifier and filter. They are illustrated in Fig. 6-20. A complete

discussion of automatic time-modulation systems is contained in Chaps. 8 and 9 in connection with automatic time measurements. Time discriminators are also treated in Chap. 14, Vol. 19.

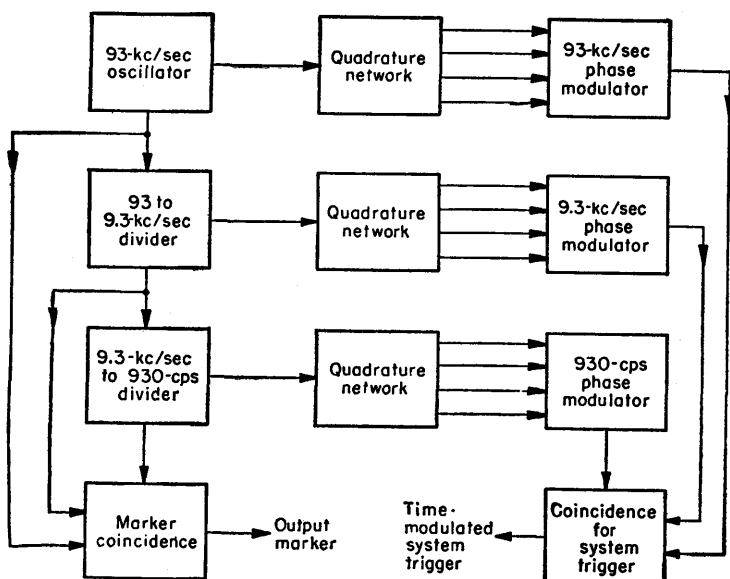


Fig. 6-21.—Block diagram of AN/APN-3, Shoran, time-measuring circuits.

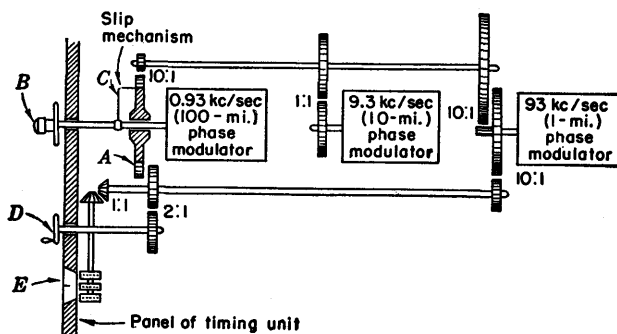


Fig. 6-22.—Gearing mechanism of AN/APN-3, Shoran.

**6-5. Three-scale Phase-modulation System.**—Shoran or AN/APN-3<sup>1</sup> is an example of a three-scale phase-modulation system. The coarsest scale covers 100 miles in a phase modulation of  $360^\circ$  to select one cycle of the second scale. The second scale of 10 miles per revolution in turn selects one cycle of the fine scale, which gives data at 1 mile per revolution.

<sup>1</sup> AN/APN-3 manual; RCA, Industry Service Division, Jan. 1944.

The combination provides continuous time modulation accurate to 13 yd in 100 miles with negligible possibility of gross error. Statute miles are used; hence the frequencies are approximately 0.93, 9.3, and 93 kc/sec,

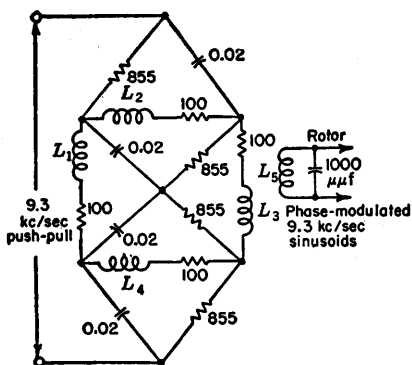


FIG. 6-23.—Phase-modulation network at 9.3 kc/sec using inductance goniometers.  $L_1$ ,  $L_2$ ,  $L_3$ ,  $L_4$  are the orthogonal stator windings.  $L_5$  is the rotor winding.

obtained from a crystal oscillator and two sinusoidal frequency dividers. Figure 6-21 shows the block diagram, and Fig. 6-22 shows the gear mechanism. The following discussion mentions the three distinctive circuits of this system.

This unit is unusual in that many of its electronic manipulations employ sinusoids rather than pulses.

*Inductance Goniometers.*—A typical quadrature network for driving the goniometer is shown in Fig. 6-23, where the values apply to the 9.3-kc/sec circuit.

The circuits for the other two frequencies are similar in arrangement and impedance. The goniometers are similar in construction for the

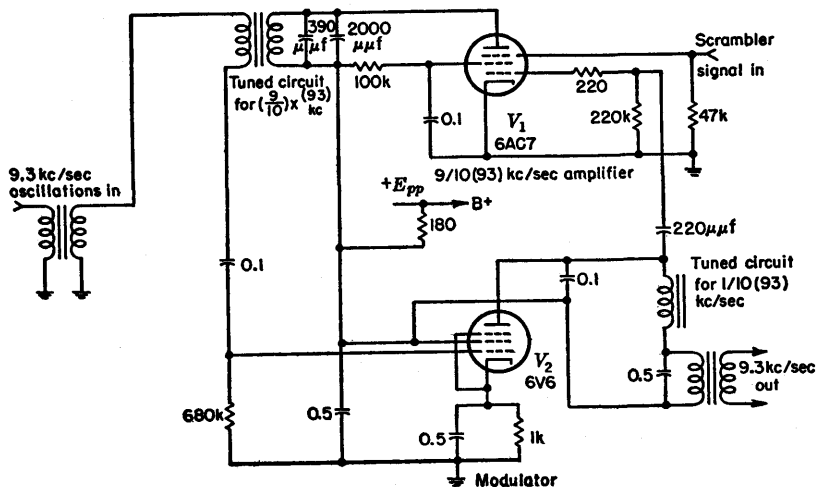


FIG. 6-24.—Sinusoidal divider circuit.

three frequencies except that electrostatic shielding is incorporated in the one operating at the high frequency. The number of turns required to match the quadrature network impedance of 855 ohms is, of course,

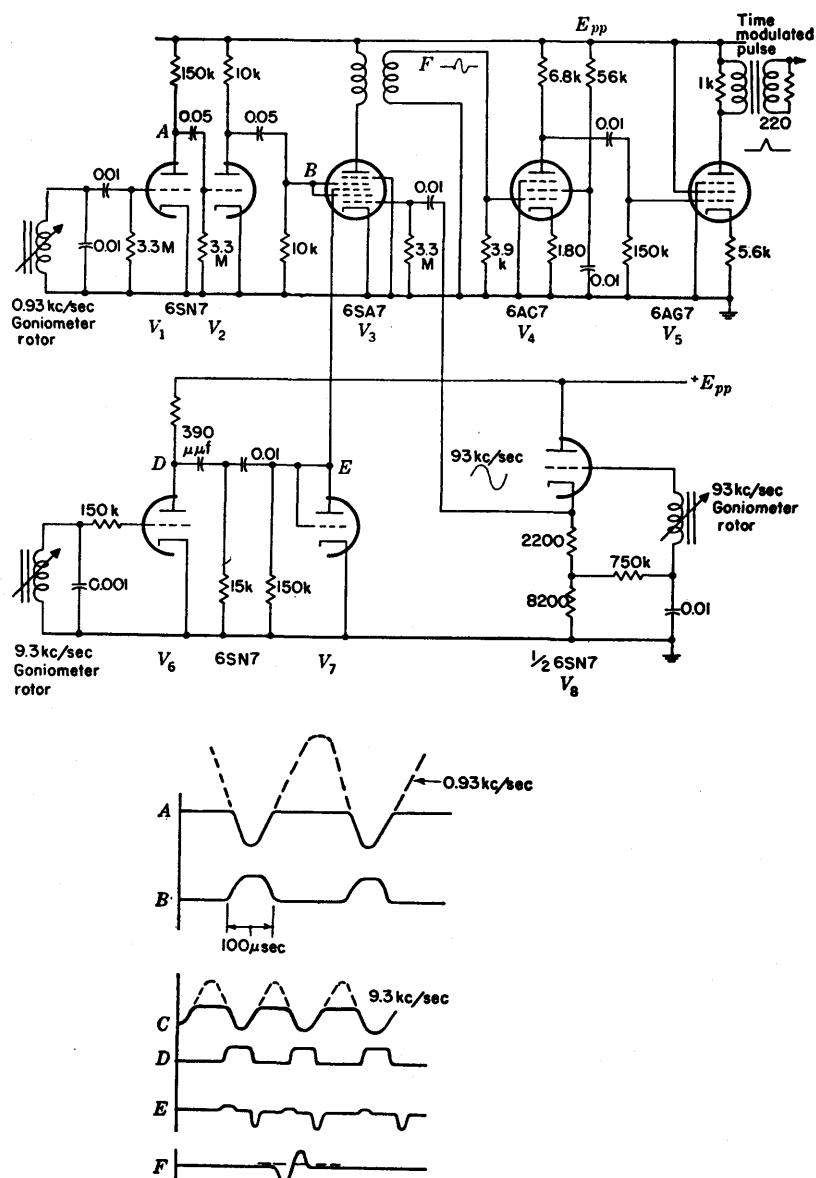


Fig. 6-25.—Amplitude-comparison and pulse-selection circuits of AN/APN-3, Shoran.

different at each frequency. Phase modulators of this type are described in detail in Chap. 13, Vol. 19.

*Sinusoidal Frequency Dividers.*—To obtain sinusoids at 9.3 and 0.93 kc/sec from 93-kc/sec crystal oscillator to drive the phase-modulator circuits, frequency division is performed by the well-known sinusoidal divider circuit. A typical circuit is shown in Fig. 6-24. Tube  $V_1$  is an intermodulator, and  $V_2$  is a multiplier. The scrambler signal is a slowly recurring pulse required because the divider is not self-starting. The operation of this circuit is described in detail in Chap. 15, Vol. 19.

*Amplitude Comparison and Pulse Selection.*—Figure 6-25 shows the circuits for coordinating the three time scales. The 930-cps sinusoids are fed to  $V_1$ , which by virtue of grid-leak bias conducts only on the positive peaks producing a plate waveform as shown in Line A of the timing diagram. The tube  $V_2$ , similarly biased, flattens the peaks and inverts them, forming positive square gates about 100  $\mu$ sec long. The width of the gates is dependent on the grid-cutoff potential and the amplitude of the 930-cps sinusoid. Amplitude comparison of the 9.3-kc/sec sinusoid to form a square selecting gate is performed by  $V_6$ . The large series grid resistor prevents the grid from being driven positive on each cycle, but allows the grid to go negative below cutoff. The resultant plate waveform is a rectangular positive gate, which is then differentiated in the output circuit to form positive and negative triangular pulses with a time constant of 6  $\mu$ sec. The positive pulses are slightly flattened by the diode  $V_7$  in the process of developing bias for the second control grid of the pulse-selector tube  $V_3$ . The tube  $V_8$  is merely a cathode follower to drive the grid of  $V_3$  with the 93-kc/sec sinusoids. The first grid of  $V_3$  is grid-leak-biased so that it conducts only on the positive peaks of the 93-kc/sec sinusoids. The second grid is biased by the rectified voltage developed at E by  $V_7$  and conducts on the positive 6- $\mu$ sec pulses from  $V_6$ . The screen is normally at ground and is driven positive with the 100- $\mu$ sec square wave from 930-cps circuit. Coincidence of these three waveforms produces in the plate transformer of  $V_3$  a negative pulse that represents the peak of the 93-kc/sec sinusoid. The transformer of  $V_3$  is a differentiating transformer and hence its output voltage represents the derivative of the peak of a sinusoid which goes through zero exactly at its peak. The positive portion, as indicated in line F, is amplified and is used as the time-modulated pulse.

The system trigger, or time reference, is formed by a similar pulse selector driven by the reference sinusoids of the three frequencies.<sup>1</sup> The

<sup>1</sup> The actual radar system employed the phase-modulated sinusoids to form the system trigger and the fixed sinusoids to form the time-modulated pulse. The particular advantage of this method, as in the circuit of Sec. 6-3, is that the time-modulated pulse remains fixed with respect to the circular-sweep display formed from the sinusoids.

resultant system has the advantage, similar to that of Sec. 6-3, of being able to time-modulate continuously from one recurrence into the next if the range-indicating dials are properly designed.

The Shoran system illustrates the ease of increasing the number of scales in order to achieve greater accuracy or greater reliability. In this circuit, the inductance goniometer has an accuracy of about  $\pm 7\frac{1}{2}$  parts per thousand, causing a  $\pm 0.08$ - $\mu$ sec error; the indicators provide resetability of 0.02  $\mu$ sec. This is slightly higher than the errors of the system of Sec. 6-1, but the use of three scales means that each of the coarse scales need only have an accuracy of 5 per cent. The resultant full-scale accuracy is  $\pm 7.5 \times 10^{-3}$  per cent. If the designer had wished, on the other hand, to work with closer tolerances and achieve higher accuracies, he might have employed frequency ratios of 50 to 1 and started at 930 kc/sec, dividing down to 370 cps. In this way he might have measured  $\pm 0.008$   $\mu$ sec out of 2640, or three parts per million, if the 930-kc/sec crystal oscillator and the receiver bandwidth were adequate.

#### CIRCULAR-SWEEP DISPLAYS AS A METHOD OF PHASE MODULATION AND AMPLITUDE COMPARISON

As is pointed out in Chap. 3 of this volume and in Chap. 13, Vol. 19 of the Series, the circular sweep or any linear display may become a time modulator if a mechanical index is moved along the display in a linear fashion. The processes of phase modulation and amplitude comparison are then performed by the rotation of the index and the passage of the electron beam past the point that the index marks. A single-scale circular-sweep system merely involves one revolution of the electron beam around the circle between each trigger. If the circular sweep is to be used in a multiple-scale system, the electron beam must traverse the circle several times. Pulse selection is carried out by intensifying, with a time-modulated gate, one of the several circles. The mechanical index defines the time-modulated instant in that selected circle.

**6-6. Circular-sweep Time Modulators, SCR-584.**—An example of this technique is the range unit of the SCR-584,<sup>1</sup> a widely used fire-control radar. This uses a two-scale time modulator with an 82-kc/sec (2000-yd) circular sweep as the fine scale, and a delay multivibrator (Sec. 5-10) to select one particular cycle of the sweep. The block diagram of Fig. 6-26 illustrates the arrangement. A crystal oscillator provides quadrature voltages for the circular sweep and 12.2- $\mu$ sec pulses for the multivibrator divider and trigger selector. The division is from 82 to 16 to 5.1 to 1.7 kc/sec. The output square wave from the 5.1-kc/sec multivibrator

<sup>1</sup> A description of the circuits of this system has been written in "Electronic War Reports," *Electronics*, 19, 2, (Feb. 1946).



drives a tuned Class C amplifier to form a 32,000-yd circular sweep as the long-range sweep. This sweep is not necessary in the time-modulation process, but aids the operator in finding which of the 2000-yd circles to intensify with the coarse-scale gate. A mechanical index appears in front of the 32,000-yd sweep and is rotated  $\frac{1}{16}$  as fast as the cursor on the 2000-yd sweep.

The 1.7-kc/sec divider provides a selecting gate at the PRF which selects one of the 82-kc/sec pulses to form a trigger that is well defined with respect to the 2000-yd sweep, a technique that is discussed in detail

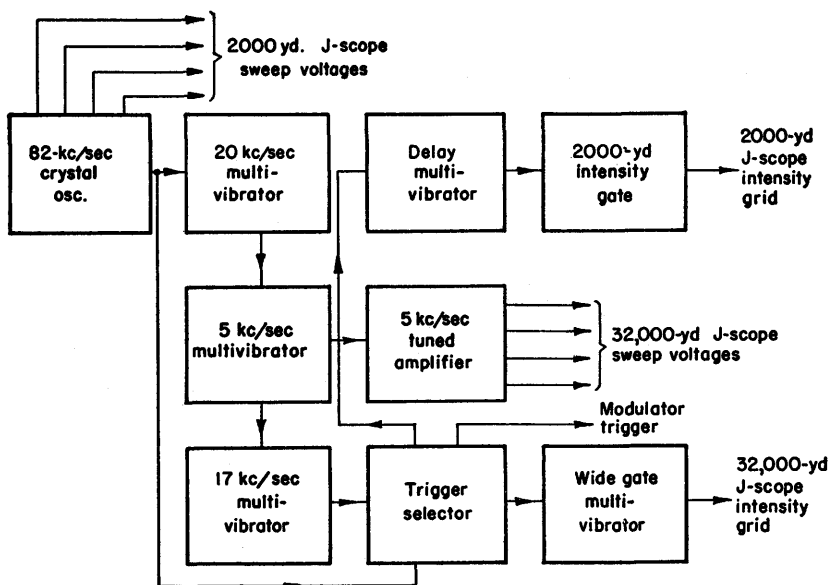


FIG. 6-26—Block diagram of SCR-584 circular-sweep time modulator. (Note: wide gate delay omitted for simplicity.)

in Secs. 4-8 and 4-9. The wide-gate multivibrator acts to intensify the first cycle of the 32,000-yd circular sweep, the remaining two cycles being blanked to avoid confusion.

The trigger also initiates the coarse-scale delay multivibrator that is controlled by a potentiometer geared to the cursors. Turning the range-tracking handwheel moves the cursor on the fine and coarse sweeps, and causes the intensity gate to move around the circular sweep continuously. The coarse scale need be accurate only to about  $\pm 800$  yd if its full width of 2000 yd is used. Since the intensity gate provides target discrimination by receiver gating, a shorter gate width is often used, whereupon requirements on the coarse-scale time modulation become more stringent. To overcome this weakness a field modification consist-

ing of a phase modulator driven by the 82-kc/sec sinusoid was connected to the range shaft to provide phase-shifted pulses, one of which is selected by the CRT intensity gate as a short receiver gate.

This addition removes the marked disadvantage of time modulation by circular-sweep phase modulation, that no pulse is generated at the instant corresponding to the position of the fine mechanical index. The HR radar system is very similar to the SCR-584 and is described in Sec. 7-26.

**Wurzburg Range Unit.**—Reports indicate that the German Wurzburg fire-control radar employed a type of time modulator very similar to the SCR-584. The basic difference is that in the Wurzburg the coarse-scale time modulation is provided by phase modulation and amplitude comparison at 3.7 kc/sec, instead of by a delay multivibrator. Both the PRF and the long-range circular sweep as well as the quadrature voltages for the phase modulator are formed from the 3.7-kc/sec sinusoids. This makes the wide intensity gate unnecessary since an r-f pulse is sent out each time the 3.7-kc/sec sweep n block diagram of the system.

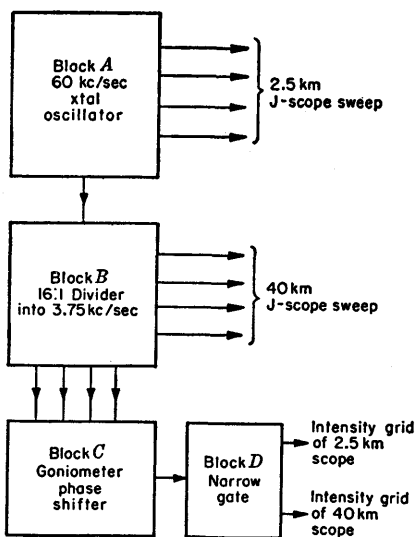


FIG. 6-27.—Block diagram of Wurzburg range unit.

*The SCR-718 Altimeter.*—Although not exactly a multiple-scale unit in the same sense as the SCR-584 and the Wurzburg, the SCR-718 altimeter offers a novel approach to the two-scale technique. This unit measures absolute altitude over the terrain below an aircraft by the same pulse technique as those used in ordinary radar sets. Its fine-scale range-measuring device is a J-scope; a completely independent instrument, the barometric altimeter, suffices as the coarse scale.

The sweep period of the J-scope is 5000 ft, and accordingly requires a 98.4-kc/sec crystal oscillator. Neither intensity gates nor moving hairlines are provided, only radial calibration marks. Reading only from the CRT scale would give ambiguities of 5000 feet. The barometer is accurate enough to resolve the ambiguities. Heights accurate to 30 ft should be obtainable with this combination of equipment. Another model of this altimeter provides a switch to change the sweep period

from 5000 to 50,000 ft in order to avoid reliance upon the barometric altimeter.

### STEP-INTERPOLATION TIME MODULATION

The following sections describe systems in which the time modulation is performed in large steps, with an interpolating time modulator to provide continuous modulation over the intervals between steps.

**6-7. AN/APS-15 Range Unit.**—This system represents an implementation of the step-interpolation method of multiple-scale time measurement outlined in Secs. 3-9, 3-14, and 3-15. The specifications call for time modulation over 2240  $\mu\text{sec}$ , accurate to  $\pm 0.38 \mu\text{sec}$ , and continuous time modulation over any 125- $\mu\text{sec}$  interval. Furthermore the PRF trigger must be supplied by the range unit.

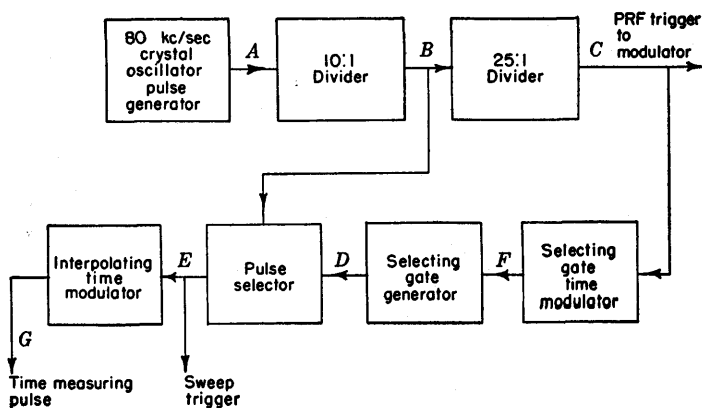


FIG. 6-28.—AN/APS-15 range-unit block diagram.

The phantastron circuit described in detail in Sec. 5.5 is used both for the step-delay and the interpolating time modulators, with appropriate circuit values.

The display used for time measurement is one in which the time-measuring pulse appears as an intensity modulation on an oscilloscope sweep of about 20 miles duration. This sweep is initiated by the same selected pulse as that which initiates the interpolating phantastron. Shown in Fig. 6-28 is a simplified block diagram of the AN/APS-15 range unit. Reference should be made to Fig 6-29 to consider the timing sequence in the various blocks of Fig. 6-28.

The circuit of the timing wave generator is Fig. 6-30. An 80.86-kc/sec crystal oscillator generates current pulses which trigger the blocking oscillator  $V_2$  through the pulse transformer. Blocking oscillator  $V_2$  then supplies negative pulses spaced at 10.75  $\mu\text{sec}$ , waveform A, across the 120-ohm plate resistor.

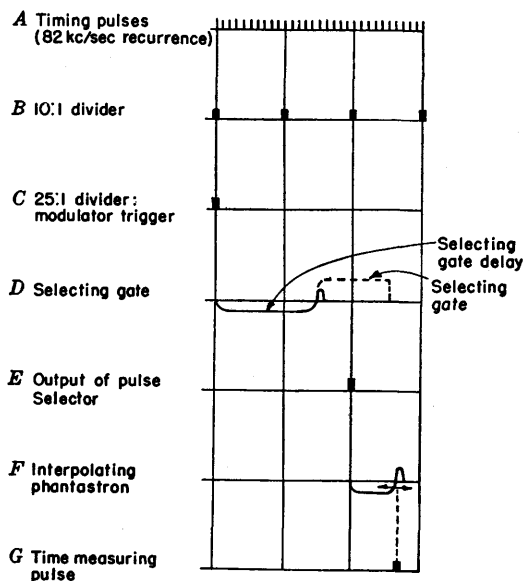


FIG. 6-29.—AN/APS-15 range-unit waveforms.

The subsequent circuit is the ten-to-one pulse divider of Fig. 6-31. The division is done in two steps, first a two-to-one division, in  $V_3$ , and then a five-to-one division in  $V_4$ . Two stages of division are used for greater stability, decreasing the need for calibrations. The output waveform is as shown in  $B$  of Fig. 6-29.

Pulses recurring at 10-mile intervals are obtained, one of which is selected to trigger the interpolating time modulator.

Since the maximum time to be measured by this system is  $2240 \mu\text{sec}$ , the interval between successive PRF triggers has been chosen to be about  $3000 \mu\text{sec}$  to allow the circuits in the radar system to return to the quiescent state before the next trigger occurs. A 25-to-1 blocking-oscillator divider synchronized by the 10-mile pulses is used to generate the PRF triggers. This circuit is

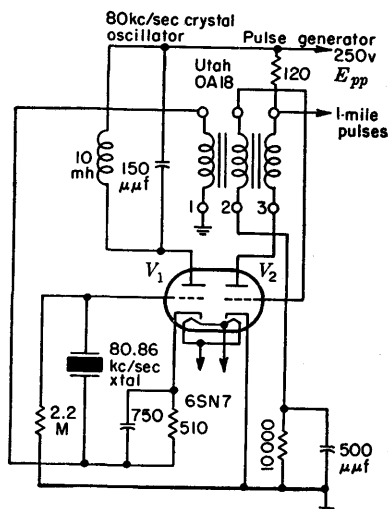


FIG. 6-30.—AN/APS-15 pulse generator, 82 kc/sec.



chronism with the 10-mile pulses is always maintained by the blocking oscillator as shown in *C* of the waveform diagram. By use of a

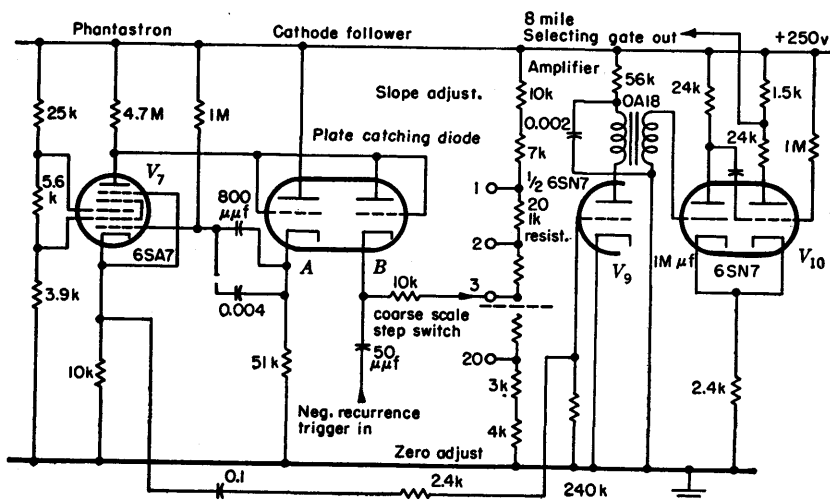


Fig. 6-33.—AN/APS-15 selecting-gate time modulator: phantastron.

cathode follower  $V_6$  the output impedance of the trigger is made about 500 ohms.

The step phantastron that time-modulates the selecting gate is initiated by the PRF trigger (Fig. 6-33). This circuit is of conventional phantastron design except that a step voltage control is used rather than a continuous potentiometer. The circuit is designed so that its steps are approximately 10 miles apart and so timed that the 8-mile gate, initiated by the termination of the step phantastron always embraces, in time, one of the 10-mile pulses, which is selected by the time-selector circuit of Fig. 6-34. The output of this tube triggers a blocking oscillator  $V_{12}$  whose output is the delayed coarse trigger that starts both the sweep presentation and the interpolating phantastron.

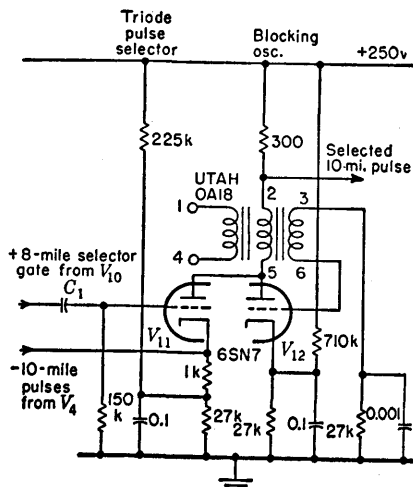


Fig. 6-34.—AN/APS-15 ten-mile pulse selector, and blocking oscillator.

This interpolating phantatron is as described in Sec. 5-7 and has a range of modulation of from 0.5 to 15.0 miles. The phantatron  $V_{13}$ ,  $V_{14}$  of Fig. 6-35 generates the waveform  $F$  of Fig. 6-29. Its trailing edge triggers the pulse generator  $V_{15}$ ,  $V_{16}$  to produce the fine-scale time-modulated pulse.

A limitation of this circuit should be noted. It is impossible for the selecting gate to embrace the PRF trigger since the gate itself is started simultaneously with the trigger. Therefore, for range measurements below 10 miles the coarse scale is eliminated, the interpolating phantatron being started by the trigger. This reverts the system to a single-scale

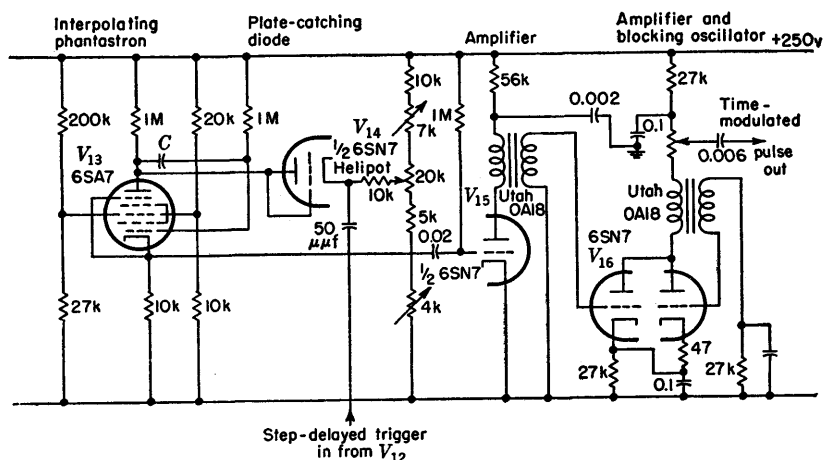


FIG. 6-35.—AN/APS-15 interpolating time modulator (phantatron) and blocking oscillator.

system. Zero-setting is conveniently performed by the procedure of Sec. 3-6.

In evaluating this technique as compared with the other methods of multiple-scale time modulation, there are several significant distinctions. Where the circular-sweep scope fails in not providing a pulse at the time corresponding to the position of the mechanical index, the step-interpolation method and the phase-modulation methods develop a time-modulated pulse that can be used on an indicator or in an automatic measuring circuit. Furthermore, this is the only multiple-scale system permitting electrical control of the time modulation, albeit only over a limited range. This feature is useful in automatic-range-tracking application where considerations of weight and size discourage the use of mechanical phase modulators. One system exemplifying this practice is the British Oboe, described in Sec. 9.2, wherein the fine-scale control voltage is used to indicate range to an electrical bombing computer.

A further example of this method, which illustrates the use of several interesting circuits, is the range unit that was designed for the revised AN/APS-10. This circuit is described in Sec. 4-9 with a complete circuit diagram.

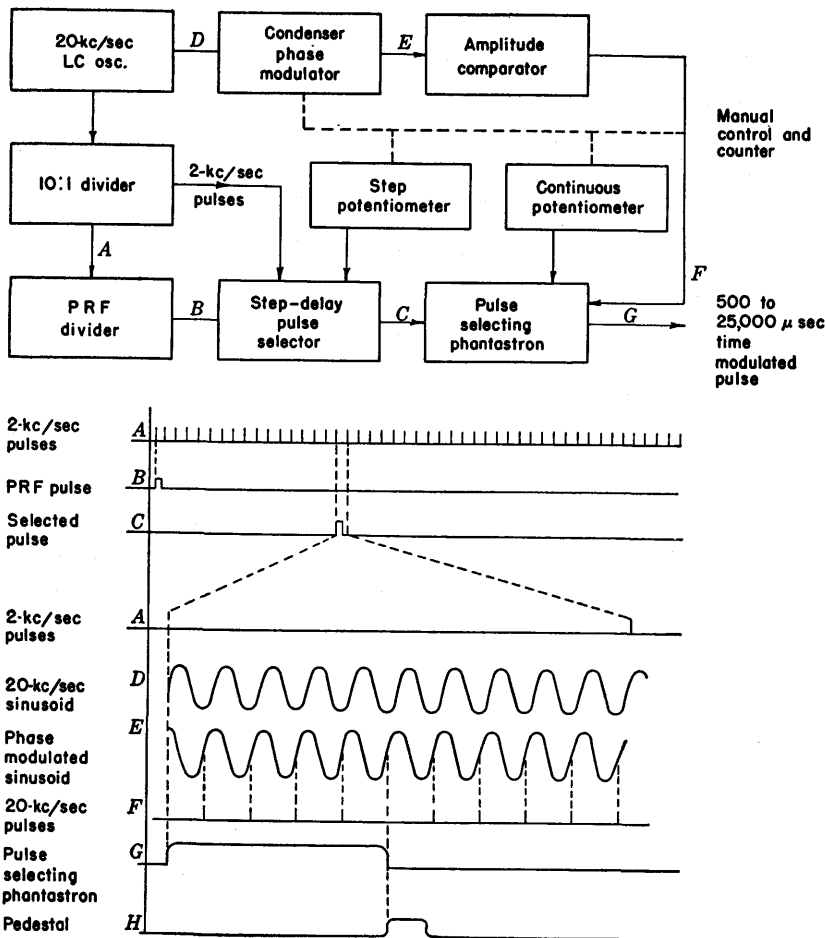


FIG. 6-36.—Block and timing diagram of the lightweight direct-reading Loran time modulator.

**6-8. Lightweight Direct-reading Loran Indicator.**—Certainly the best example to date of a three-scale time-modulation system is the lightweight direct-reading Loran indicator. Designed for airborne use and intended to provide time modulation from 500 to 25,000  $\mu$ sec with an accuracy of 1  $\mu$ sec, the system employs a step delay to select an



accurately time-modulated trigger to initiate a two-scale time modulator to interpolate between the steps. The two-scale time modulator employs phase modulation and pulse selection as in the circuits described in Secs. 6-1 and 6-2. The circuit technique represents the most recent practices and uses subminiature tubes and other components that allow the circuit to be built on small subassemblies, each representing a functional unit of the circuit. Repair of the time-modulation unit then involves only locating the faulty subassembly and replacing it in its entirety.

The block diagram and the timing diagram are shown in Fig. 6-36. The divider circuits are discussed in Sec. 4-11 and the use of the system

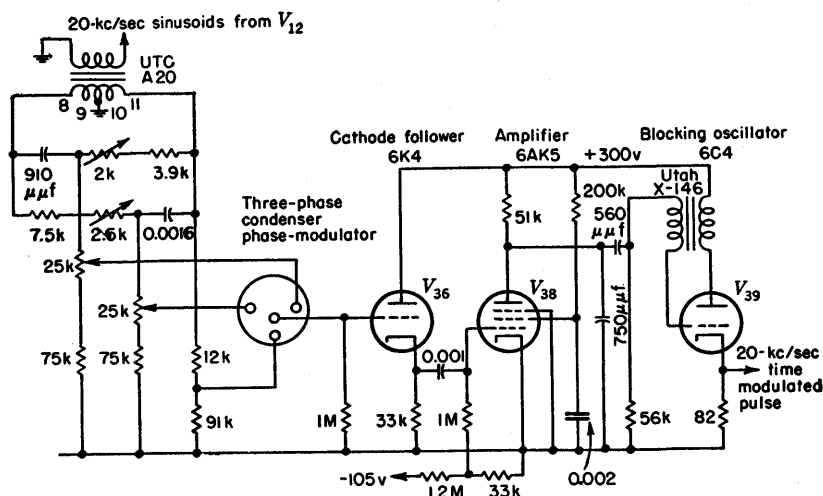


FIG. 6-37.—Phase modulator of lightweight direct-reading Loran time modulator. This circuit provides three phase voltages from a 20-kc single-phase sinusoid. A condenser-type phase modulator provides a phase-modulated sinusoid to the cathode follower and amplifier  $V_{36}$  and  $V_{38}$ , whose output synchronizes the blocking oscillator  $V_{39}$ .

as a time-measuring instrument is discussed in Sec. 7-30. The step potentiometer that picks one of the 500- $\mu$ sec pulses to initiate the interpolating time modulator, the continuous potentiometer that acts to select one of the time-modulated 50- $\mu$ sec pulses, and the condenser phase modulator that phase-modulates the 20-kc/sec sinusoids are all geared to one control and to the counter that indicates the total time modulation (see Fig. 6-40).

The first circuit to be considered is the 20-kc/sec phase modulator. The oscillator and driver circuits are described in Sec. 4-11 and are shown in Fig. 4-27. Figure 6-37 shows the network for producing 3-phase 20-kc/sec voltages, the 3-phase condenser phase modulator, and the

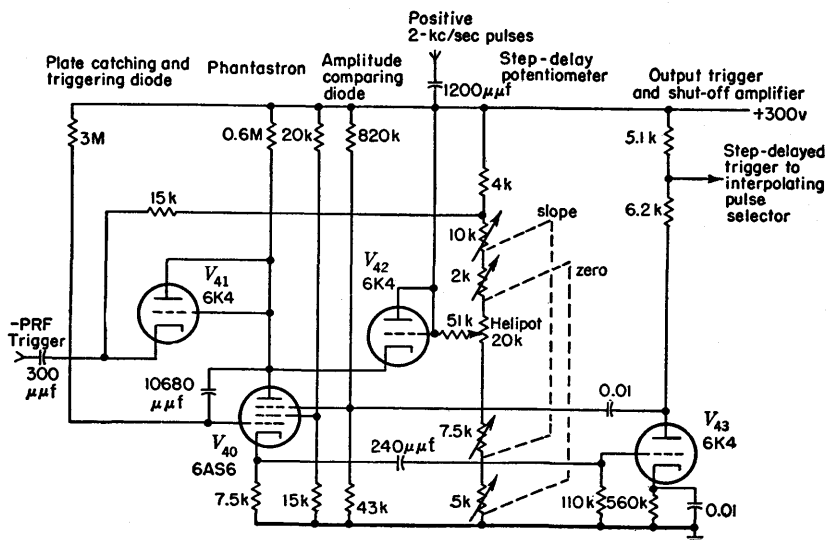


FIG. 6-38.—Step-delay time modulator and pulse selector. This circuit is triggered by the PRF pulse and generates a sawtooth waveform. 20-kc/sec pulses are added to the step-delay potentiometer voltage, enabling the diode to select one of them by amplitude selection. The resulting current pulse  $V_{42}$  shuts off the phantastron and generates a step-delayed trigger.

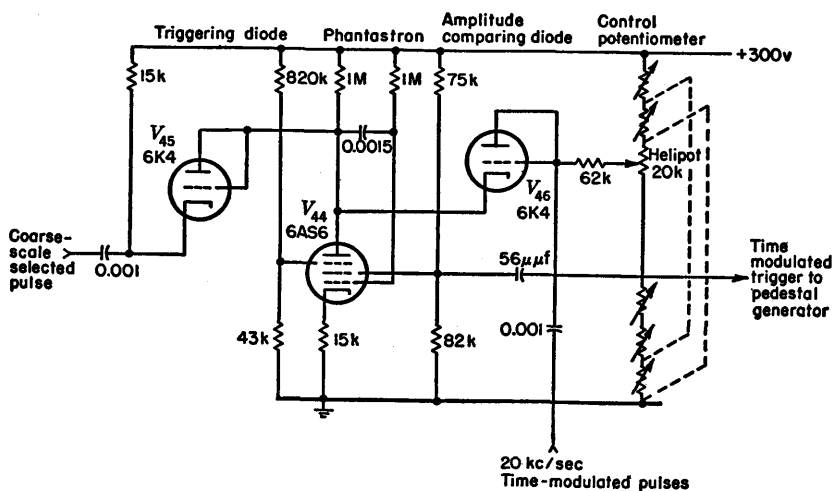


FIG. 6-39.—Interpolating time modulator, selecting one of several hundred time-modulated pulses, spaced at 50- $\mu$ sec intervals. The operation of the circuit, a pulse-selecting phantastron, is described in Sec. 4-9.

amplitude-comparison circuit. The 3-phase condenser system is used because it is possible to align the system with only a vacuum-tube voltmeter or a standard test oscilloscope. This procedure is described in Chap. 13, Vol. 19.

The output voltage from the phase modulator is amplified in a 6AK5 and directly synchronizes the blocking oscillator  $V_{39}$ . Amplitude comparison of the sinusoid is thus performed in  $V_{39}$  with reference to its

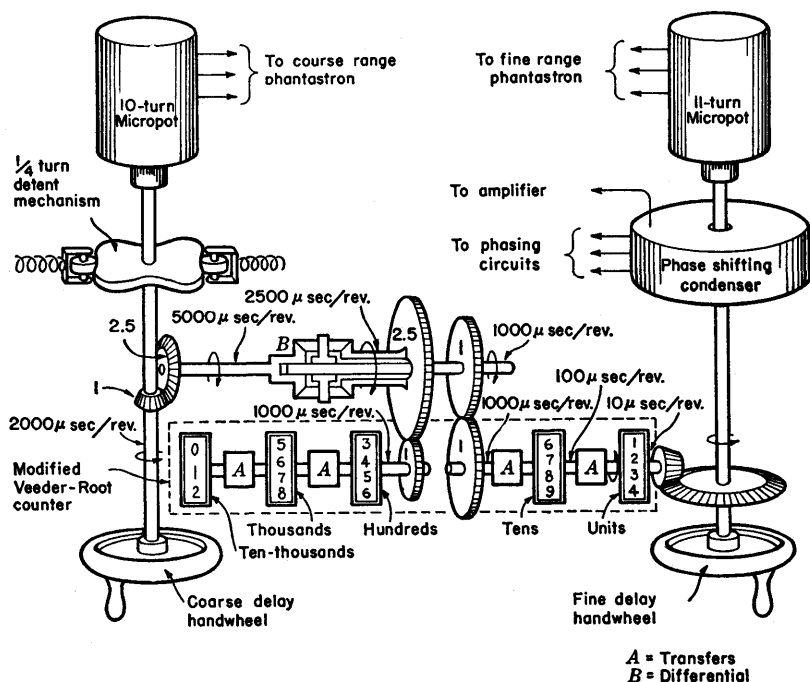


FIG. 6-40.—Schematic diagram of mechanical time-modulator control unit of direct-reading Loran indicator.

grid-cutoff potential. The time constant of the blocking-oscillator grid circuit is adjusted so that the regeneration commences as the sinusoid passes through zero amplitude.

The second circuit of interest is the pulse-selecting step delay, Fig. 6-38. The PRF trigger initiates the rundown of a 6AS6 phantastron, which continues until the plate voltage equals the sum of the step-delay potentiometer voltage and the amplitude of the 500- $\mu$ sec pulses. The first 500- $\mu$ sec pulse after the occurrence of this equality will cause conduction in the diode  $V_{42}$ , shutting off the phantastron and providing a step-delayed trigger in the same manner as the pulse-selecting phantastron described in Sec. 4-9 on the AN/APS-10 synchronizer.

The step-delayed trigger is supplied to the interpolating pulse selector. It should be noted that the event which directly initiates this trigger to the interpolating pulse selector is the flow of current in the amplitude-comparing diode  $V_{42}$  due to one of the 500- $\mu$ sec pulses. Thus the trigger to the interpolating pulse selector is truly the result of time selection of one of the 500- $\mu$ sec pulses. The 5-mile pip selector used in the British Oboe (Sec. 9-2, Fig. 9-12) is of similar design.

The interpolating time modulator, Fig. 6-39, employs exactly the same technique as the step time modulator except that the selected pulses are time-modulated rather than fixed, and the potentiometer voltage is varied continuously rather than in steps. The trigger to the indicator pedestal generator is obtained by differentiating the screen waveform.

The three scales of the time-modulator circuit are controlled by the mechanical unit, which operates as follows. Referring to Fig. 6-40, the coarse delay control turns in quarter-turn steps, one revolution being 2000  $\mu$ sec—that is, four 500- $\mu$ sec steps. Through bevel gears with a 1-to-2½ stepdown the input reaches the “output” shaft of a differential. Through the differential there is a 2-to-1 stepup which is geared to the hundreds wheel of the counter with a 2½-to-1 stepup. The gear on the differential is prevented from turning by ordinary counter construction.

The input from the fine delay control at 50  $\mu$ sec per revolution, reaches the units wheel of the counter through a 5-to-1 stepup. Transfer from the units wheel to the tens wheel is normal. From tens to hundreds the transfer is accomplished through the 1-to-1 action of the differential by having the transfer pinion drive the differential gear which also drives the hundreds wheel of the counter after going through the differential.

The counter then gives the total delay reading by adding the outputs of the coarse and fine delay circuits on the hundreds wheel by means of the differential.

The switching and various controls serve much the same function as in conventional Loran systems. All the controls and switches necessary for lining up the system and for taking a complete Loran fix are mounted on the control unit with the exception that the CRT controls, which are placed on the separate indicator unit.

It is interesting to compare this circuit with those of Secs. 6-1 and 6-2 on the basis of economy. By the use of pulse-selecting phantastrons, the complete operation of receiving a trigger and producing a time-modulated pulse is performed in 12 tube sections as compared with 15 for that of Sec. 6-1 and 18 for that of Sec. 6-2, in spite of the fact that this is a three-scale system whereas the others are two-scale. For perfectly fair comparison, an amplifier should be added to the Loran circuit to provide a sharper time-modulated pulse. A further reservation is that the amplitude comparison of the phase-modulated sinusoids is performed by

a blocking oscillator and hence is of questionable accuracy. A liberal allowance of 2 volts in the firing point of the blocking oscillator gives the required accuracy of  $\frac{1}{3}$   $\mu$ sec out of 25,000, or 0.001 per cent. Figures of this accuracy are justifiable since the frequency of the 20-kc/sec oscillator is controlled by automatic frequency control with reference to the ground station PRF, which is held to better than 1 part in  $10^7$  of the correct frequency.

An example of the construction technique permitted by this circuit design is discussed in detail in Chap. 17, Vol. 21 of the Series. Figure 6-41 shows the subassembly containing the circuit of Fig. 6-39 and the

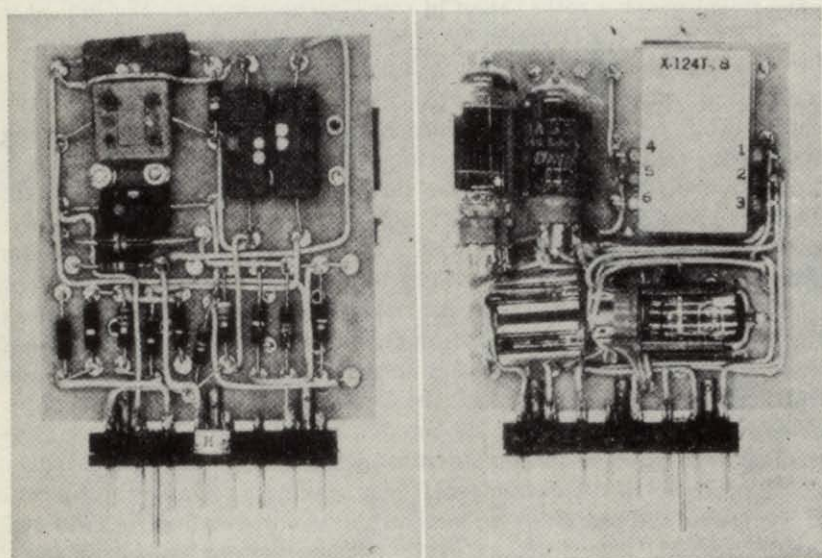


FIG. 6-41.—Subassembly containing interpolating time-modulator circuit of Fig 6-40 and the phase-modulated 20-kc/sec amplifier and blocking oscillator of Fig. 6-38.

circuit associated with  $V_{33}$  and  $V_{39}$  of Fig. 6-37. The bakelite portion of the card, on which the parts are mounted, is  $3\frac{3}{4}$  by  $3\frac{1}{8}$  in. The connector at the base of the card plugs into a socket in the chassis, and the card is supported by vertical slides. This is an example of a calibrated subassembly (see Chap. 3).

**6-9. Summary.**—In summary, the principal feature which characterizes the various multiple-scale time modulators is the method of coordinating scales. The highest accuracy is provided by the method of Sec. 6-2 in which pulses derived carefully from the crystal oscillator sinusoid are selected in a gated video amplifier. On the other hand, economy results from adding the coarse-and-fine-scale timing waveforms to operate a single instantaneous amplitude comparator as in the circuits of Secs.

6.1 and 6.8. Some economy is effected in the frequency-divider scheme of Sec. 6.3 and in the sine-wave tracking scheme of Sec. 6.4, but reliability is sacrificed. The only system described which can be controlled by an electrical rather than mechanical signal is the step and interpolation time modulator of Sec. 6.7. For time modulation in conjunction with an electrical computer this feature is valuable.

## CHAPTER 7

### MANUAL MEASUREMENTS

BY BRITTON CHANCE AND E. F. MACNICHOL, JR.

#### GENERAL CONSIDERATIONS

BY BRITTON CHANCE

#### INTRODUCTION

Manual measurements are extensively used in military applications. Extreme flexibility is often required to counter unexpected situations. Often it has not been possible to design or to maintain automatic equipment. Economy of manpower is sometimes not regarded as essential in military operations, and manual operators are often more available and more expedient than automatic equipment. In radar systems manual tracking of the variations of range of a moving target is an important procedure in plotting, interception, navigation, bombing, fire control, and many other applications.

The use of the cathode-ray-tube display for these purposes and the important factors affecting the accuracy of manual measurements are discussed here. The use of the cathode-ray tube for measurements of waveforms is discussed in Chap. 20, Vol. 19. The detailed design of all types of cathode-ray-tube displays and a number of two-coordinate displays are presented in Vol. 22. The general principles involved in time modulation and demodulation by means of cathode-ray-tube displays are given in Vol. 19, Sec. 14-9, and in this volume, Sec. 3-18-3-20.

Manual time-demodulation systems are negative-feedback systems in which an operator is an important part of the feedback loop. The properties of signal and index permit the operator to exercise visual time discrimination, and with this information he exerts suitable control over the time-modulation systems in order to follow continuously the variations of the input signal. In some operations the part played by the operator is a very simple one and he may be easily replaced by an automatic device. But in a number of operations he is irreplaceable. For example, target recognition is very difficult to describe in terms of operations that could be carried out automatically. Often the judgment and experience of the operator are of considerable value in avoiding the effects of interference and may achieve satisfactory results where available automatic devices fail completely.

This chapter therefore treats a number of methods for manually tracking time-modulated signals with special emphasis upon the suitability of these methods in adverse conditions in which noise interference or intermittency is present. In addition, some practical circuits are given for tracking in more than one coordinate.

The content of this chapter is also a logical extension of the discussion of methods for the determination of distance and speed presented in Sec. 2-11.

**7.1. Uses.**—Cathode-ray-tube displays are employed for two general types of measurements: (1) the measurement of a time interval, which may be regarded as unvarying, for the purpose of calibration, for plotting, and crude navigation, etc.; (2) the measurement of the range and rate of change of range of a target for the purposes of precise navigation, bombing, fire control, etc.

The design considerations involved in these two cases differ considerably, since the first case involves the static accuracy or resettability with which the time interval may be measured. The second case, however, includes in addition mechanical tracking aids that generate and maintain the rate of change of the range information in accordance with the operation of the manual controls. Practical examples of both cases are given in later sections.

*Fixed Time Intervals.*—The standardization and calibration of time-modulation circuits usually depend upon the use of cathode-ray-tube displays. Similarly the calibration of the zero point of a range-measuring system (see Sec. 3-6) involves this type of measurement.

Practically all the methods of rough position-finding for plotting aircraft position, for navigation by Loran, and for certain types of airborne bombing depend upon the measurement of range, which is assumed to be fixed at the moment of measurement. In certain systems where the range is varying, similar techniques are employed, but the time corresponding to a given range is noted.

*Variable Time Intervals.*—It is desirable to move an index in synchronism with the observed variations of the time-modulated signal. In radar systems in which the antenna continuously illuminates the reflector such as radar range finders or position-finding systems employing a rapid scan for angular data, the signal intensity never falls to zero for an appreciable time and the time-modulated signal is nearly continuously available to the observer. The tracking problem is relatively straightforward, and manually controlled mechanisms for generating the rate of change of range in response to observations of the displacement of the signal with respect to an index are effective in giving reasonably accurate rate information.

In many radar systems the excursion of the azimuth scan is equal



to 360° or at least greatly exceeds the width of the antenna pattern. Because of the limitations of mechanical scanning systems and because of scanning losses, the effective repetition rate (Vol. 1 of the Series) of the time-modulated information is often reduced, and special means are employed in order to assist in the generation of accurate rate and displacement data. One of the most effective methods calculates from expected characteristics of the time-modulated signal the probable rate of change of displacement. The manual operation then consists of readjusting the data entered into the computing device in view of discrepancies between the observed and calculated values. The computer and the tracking process are often called "regenerative." Other systems are less pretentious and employ simpler tracking devices.

Satisfactory demodulation of intermittent data usually requires a display that continuously indicates the error between the tracking index and the last value of the modulated signal (see Sec. 7-27).

#### CHARACTERISTICS OF DISPLAYS AND CURSORS

**7-2. General Considerations.**—The cathode-ray-tube display is the most effective method of data indication for the purposes of distance measurement. Its basic advantage is the large amount of information that it displays, as shown in the PPI display of Fig. 7-1 (see Vol. 22 of the Series). Range and azimuth indices are also shown set near a radar echo.

In usual practice, target selection and accurate range-tracking are carried out on separate displays. One display provides a view of all targets within range of the radar set and is used primarily for detection and target selection. This display preferably combines azimuth indication as in a B-scope or a PPI. Often, however, a simple linear time base or type A display is employed as in Fig. 7-2 where two targets are shown.

Final signal selection and accurate target-following are carried out on an expanded sweep as represented in Fig. 7-3. This display has a number of important uses. It permits discrimination against interfering signals and accurate selection of the desired one. In addition, any coding that may identify a particular signal is easily observed. Furthermore, the detectability of the signal will be optimal—that is, the pulse length is large compared with spot size of the cathode-ray tube (see Vol. 22). The tracking operation is greatly facilitated by the fast sweep, since it concentrates the operator's attention upon a particular target and increases the accuracy with which the tracking operation is carried out. Often a portion of a slow sweep may be expanded in the vicinity of the index, and the advantages of both types of sweep are obtained in one display, but this procedure is unsatisfactory in most cases.

The deflection-modulated linear or circular time base (see Figs. 7-4 and 7-5) is almost always employed for the fast sweep in radars where the

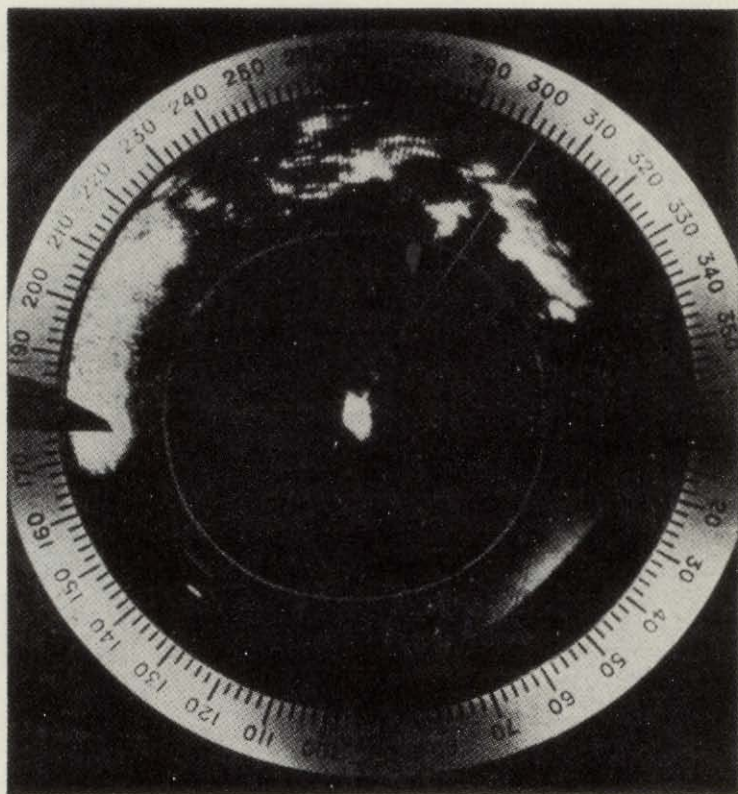


FIG. 7-1.—Range and azimuth index set near a radar echo on a PPI display.

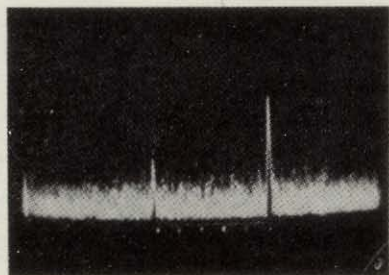


FIG. 7-2.—Type A display showing two signals and noise.

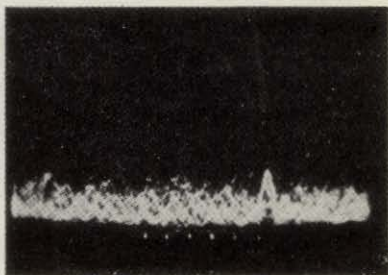


FIG. 7-3.—Expanded type A or type R sweep showing a signal and noise.

data are essentially continuous. On the other hand, the type B or PPI display is used when data are intermittent at a slow rate. When both

range and azimuth information is required the problem of the operator is complicated by the requirement for two-coordinate tracking (see Sec. 7-28).

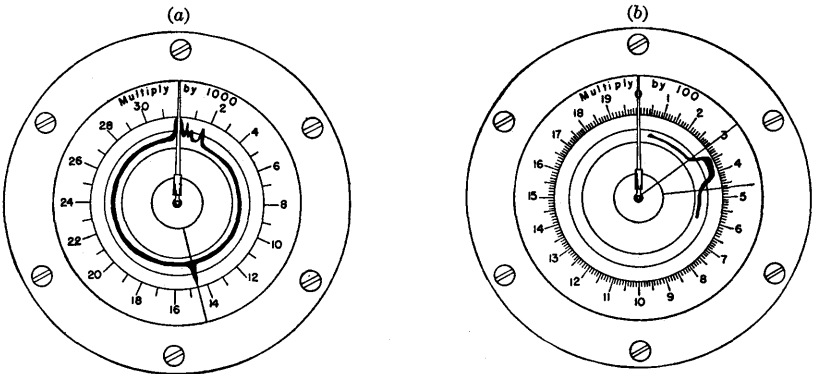


FIG. 7-4.—Type J display. The signal may be selected on the slow sweep (a) and accurately followed on the fast sweep (b).

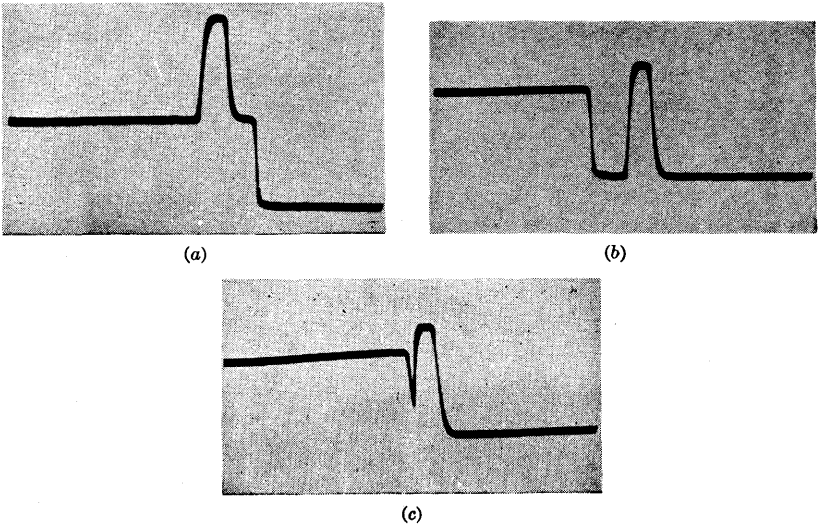


FIG. 7-5.—Type M display. The three oscillograms show the setting of a signal to a step type of marker. In (a) the step is set too late; in (b) it is too early. In (c) the step is set correctly so that the height of the notch between the fall of the signal and the rise of the marker varies rapidly with time difference.

**7.3. Indices.**—Although the range of a target may be crudely estimated by a simple display without an index, the provision of satisfactory indices greatly increases the accuracy and the ease of measurement. The three types are applicable: (1) intensity-modulated indices, (2) deflection-modulated indices, and (3) mechanical markers that are either

directly attached to the face of the tube or imaged upon it optically. Depending upon the type of measurements to be made, these indices may be "fixed" or "movable."

**Fixed Indices.**—Display of a train of fixed indices upon a linear time base is the most elementary method of time measurement by cathode-ray-tube display. Such displays are extensively used in all search radars and in many navigating instruments, especially the present models of

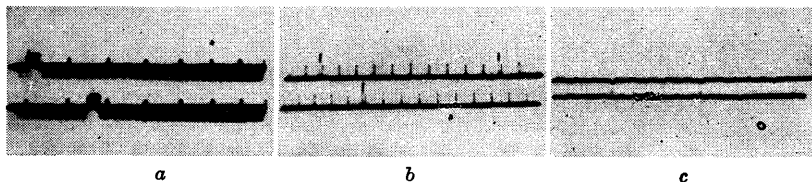


FIG. 7-6.—Time measurement by fixed pulses on a type A display (AN/APN-4). Three sweep speeds are required to resolve the time-difference reading between the upper and lower traces. In (a) the spacing of the pulses is 500  $\mu$ sec and a reading of 3500  $\mu$ sec is obtained. In (b) the spacing of the pulses is 50  $\mu$ sec and a reading of 350  $\mu$ sec is obtained. In (c) the spacing of the downward deflection is 50  $\mu$ sec and the small upward deflections, 10  $\mu$ sec. Interpolation gives a reading of 24  $\mu$ sec. The total reading is 3874  $\mu$ sec (Courtesy of McGraw-Hill Publishing Company.)

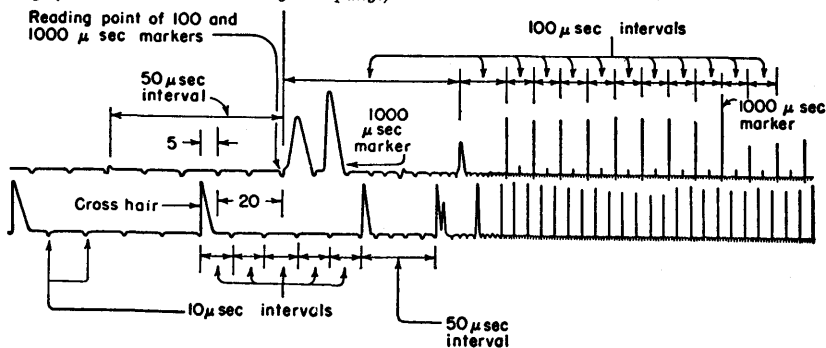


FIG. 7-7.—Display of fixed pulses on an exponential sweep (AN/APN-9). The time delay is measured between the pulse marked "cross hair" and the rise of the 50- $\mu$ sec pulse on the upper trace. The "fine" scale reading is 20 plus 5  $\mu$ sec as indicated. The integral number of 100- $\mu$ sec intervals is counted with respect to the 1000- $\mu$ sec marker and = zero  $\mu$ sec. The integral number of 1000- $\mu$ sec markers shown on this sweep is 2, but in the actual indicator the number is determined by switching to a slower display and, for this particular case, corresponds to 6000  $\mu$ sec. The total reading is therefore 6025  $\mu$ sec.

Loran (see Sec. 7-29). The methods become confusing and time-consuming when more than five similar indices appear upon any sweep.

Time measurement in Loran is somewhat more difficult since it is necessary to count several types of pulses distinguished on the basis of amplitude in order to obtain the final reading as is indicated in Fig. 7-6. Some attempts have been made to improve the situation by the use of roughly logarithmic sweeps as indicated in Fig. 7-7, but there is no conclusive evidence to indicate that a significant improvement is obtained.

The final reading in most pulse-counting systems is obtained by interpolation between the finest divisions of the scale. The problems here differ little from other problems of interpolation, and accuracies of 1 part in 5 are easily obtainable.

*Movable Indices.*—Even carefully trained operators make gross errors in pulse-counting systems, and continuously movable indices operating over the full range of measurement are preferable. Furthermore, this type of index is essential for continuous measurements.

The requirements for a continuously movable cursor for use with deflection- or intensity-modulated displays are as follows:

1. Primary requirements.
  - a. The cursor should be distinguishable through noise or interference.
  - b. The cursor should not deform the signal so that it is unrecognizable.
  - c. The parallax between the cursor and the signal should be negligible.
2. Secondary requirements.
  - a. The cursor should be continuously visible and movable even when signals are intermittent.
  - b. The display should be arranged to maintain the cursor and the signal at the center of a linear display.
  - c. A tracking mechanism should be provided to move the cursor continuously in accordance with rate and displacement controls.

Figure 7-8 gives the characteristics of mechanical and electrical indices which have been employed on cathode-ray-tube displays, and the degree to which they fulfill the requirements above are indicated. The simplicity of a mechanical index and the fact that it can be seen in spite of interfering signals make it the most attractive. The circumstances under which it can be used with a high degree of accuracy, however, are rather restricted; in fact, the circular display is at the present time the only feasible method by which a mechanical cursor can be used for precision measurements, although errors due to parallax and eccentricity are unfortunately appreciable (see Sec. 7-18).

On the other hand, the mechanical index has been used in a number of systems employing linear displays where a smaller accuracy is acceptable. In addition to the errors of the circular sweep, those due to the variation of the sweep amplitude must be taken into account. Also the errors due to sweep-centering are likely to be large.

If the video and the cursor are displayed alternately by electronic switching, the electronic cursor has the advantage of being visible in noise; however, the circuits may be power consuming.

The shape of the electronic index may be similar to that of the received pulse but should be easily distinguishable from it, as shown in Fig. 7-8. The step type of index is obtained when a rectangular waveform is applied to the vertical plates of the oscilloscope. The notch and pedestal type of index may be obtained from a shorter rectangular pulse in the same manner. The notch presentation is indicated in Fig. 7-9.

On intensity-modulated displays a waveform similar to that of the received pulse is almost always used for a range marker. However, it


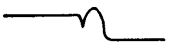

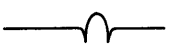
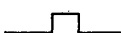

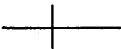
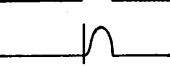
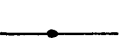



Type	Diagram	Correct setting	Chief faults
Step			Distorts signal
Notch			Signal seems to disappear in notch
Pedestal			Signal seems to disappear off pedestal
Mechanical			Parallax may be bad Accuracy depends on linearity of trace
Intensified			Rises of signal and noise elongate marker obscured by too high trace intensity
Blanked			Rises of signal and noise elongate marker

FIG. 7-8.—Types of tracking indices.

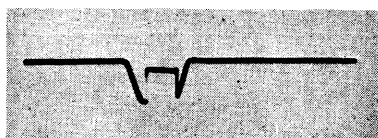
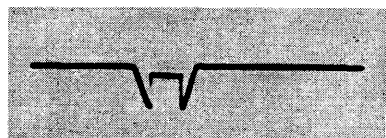


FIG. 7-9.—Cathode-ray-tube display of notch presentation. Although this gives a sensitive indication of the relative timing of signal and index, a weak signal may seem to "disappear" into the notch.

is desirable to have it rise and fall somewhat more rapidly than the received signal. In the case of range-angle display, the range marker is easily distinguishable from the received signal by the fact that the index consists of a circle or a line depending upon whether the display is polar (PPI) or rectangular (type B) (see Fig. 7-1).

With nearly all types of intensity-modulated displays and some types of deflection-modulated displays, a considerable time intervenes between successive renewals of the information on the screen because of the intermittency of the input data, and most of the time a persistent trace appears on the display. The effect of moving the range index, which is mixed with the video signals, cannot be compared with the desired echo until the next scan. In the case of very slow scans, it has been necessary



to provide a separate electronic index which may be moved to the position of a persistent echo as indicated by secondary Requirement *a*.

**7-4. Circular Sweeps.**—In deflection-modulated range-tracking displays, one has the choice of linear or circular traces, the former having perpendicular and the latter radial deflection. Both the technical and operational considerations differ considerably in these two circuits. In

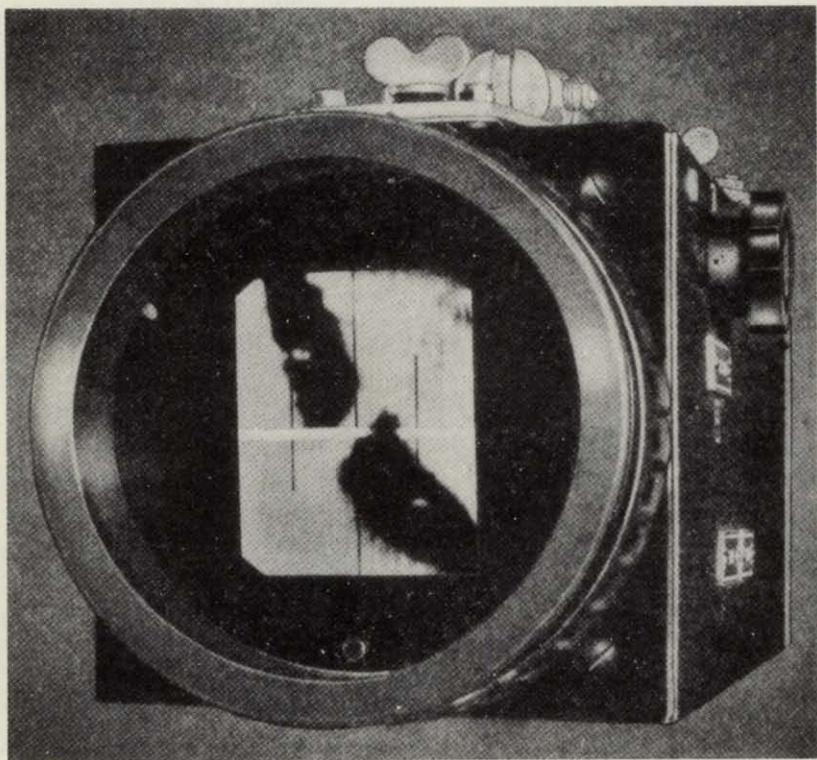


FIG. 7-10.—A delayed and synchronized type B display. The brighter horizontal line is the range index; the vertical dark line is the azimuth index. The oscilloscope photograph shows the range and azimuth index set to the George Washington Bridge, New York City. Because of the synchronization the target is maintained at the same position on the display as the aircraft approaches the target.

the circular sweep with radial deflection, one has a continuous circular scale which, when combined with a suitable selector pulse, may cover a full scale corresponding to a large number of cycles of the circular-sweep frequency. A mechanical cursor is readily employed, and although the problems of parallax are often serious, the distinctiveness and lack of ambiguity of the mechanical marker are to its advantage (see Fig. 7-4). In the circular trace the signal moves about its circumference, and

the tracking operation involves following the signal down one side of the circle and up the other side, a process that may be confusing to the uninitiated operator.<sup>1</sup> On the other hand, one advantage of the continuous movement of the signal with respect to the face of the cathode-ray tube is the additional information it gives—that is, the operator is continually informed of the approximate value of range rate by the motion of the echo past fixed points on the cathode-ray-tube face as shown in Fig. 7-4.

The circular trace is generated with great simplicity (see Sec. 7-18). The scale length obtained with a 3-in. circular trace, of course, is approximately equal to that obtainable from a 7-in. linear trace.

**7-5. Linear Sweep and Synchronized Presentation.**—Often the linear display and a step or other type of electrical mark is employed for range tracking. If this display is an expanded portion of the full scale over which range measurement is desired, the index is visible over a fraction of the required total range. This limitation is avoided if the delay of the sweep is varied with that of the tracking index so that the cursor always appears in the middle of the trace.

Figure 7-10 illustrates the use of a delayed synchronized linear sweep for range tracking in aircraft. In this particular case, a range-azimuth display is used, and the range index is an intensity-modulated horizontal line. The azimuth index is mechanical and is represented by the vertical black line in the center of the tube. The tracking process maintains the target stationary and at the center of the display in spite of the movement of the aircraft. These synchronized displays give a clear indication and hence accurate measurements.

#### ACCURACY CONSIDERATIONS<sup>2</sup>

The accuracy with which the time-modulated index may be set to a received pulse on a cathode-ray-tube display varies widely depending upon a number of simple geometric factors. For maximum sensitivity of this process of time discrimination, it is desirable to have a high rate of change of movement of the overlapping portions of the index and signal with respect to variation of the time interval between them. The accuracy with which the setting of index and signal may be made under static conditions is presented here; the tracking process involved in following a continuously moving signal is discussed in a later section.

It is required to set the index relative to the pulse so that the index represents the range of the pulse. This is done most accurately by defining as a coincident setting that setting from which there is the

<sup>1</sup> Phase modulation of the transmitted pulse gives a circular display in which the signal appears to be stationary (see Sec. 6-3).

<sup>2</sup> Mr. D. Gale assisted with the preliminary drafts of this material.



greatest rate of change of shape with relative position. To ascertain

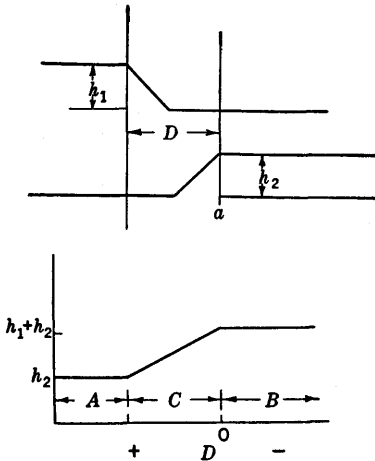


FIG. 7-11.—General relation of signal and index. The two signals of height  $h_1$  and  $h_2$ , separated by a distance  $D$ , give the amplitudes at  $a$  indicated in the graph below for various values of  $D$ . In regions  $A$  and  $B$  the amplitude is constant, but the length of the overlapping portion is variable; in  $C$  the amplitude of the overlapping portion is variable.

amplitude of the output is independent of the spacing of the two pulses.

On the other hand, the duration of their overlapping portion varies as indicated in Fig 7-12, where the pulses are shown complete and their overlapping portion is designated by  $c$ . A measurement may be made by estimating the duration of  $c$ , but it is insensitive since the accuracy does not depend upon the rise and fall of signal and index. This process of measurement is termed "addition."

The method of resetting becomes much more sensitive in zone  $C$  of Fig. 7-11, and measurements made in this region have been termed "juxtaposition." This may be defined as a resetting process in

this setting, the following discussion describes the shape changes that occur as the index is moved right through the echo. In addition, the reproducibility of the measurement with sweep speed is discussed.

#### 7-6. General Considerations.—

Figure 7-11 represents the fall of the index of amplitude  $h_1$  and the rise of a signal of amplitude  $h_2$  separated by a distance  $D$ . On variation of  $D$ , we obtain a characteristic plot of total amplitude vs.  $D$  if we take point  $a$  as a reference. Initially the amplitude is constant and equal to  $h_1$ , but on closer approach of the second pulse ( $D$  is decreasing), the height increases linearly until it reaches the sum of  $h_1$  and  $h_2$ .

For negative values of  $D$ , the amplitude is again constant as it was initially in region  $A$ . Therefore in these two regions ( $A$  and  $B$ ) the

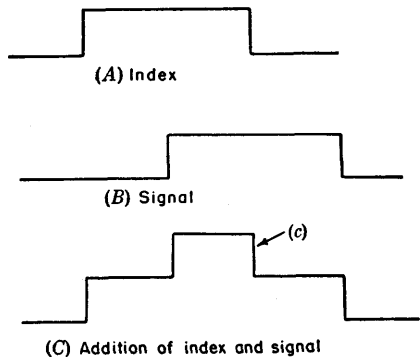


FIG. 7-12.—Addition of signal and index. This figure indicates the overlap of rectangular waveforms  $A$  and  $B$  to give pulse  $c$ , the length of which will indicate the amount of overlap.

which the amount of overlap of two pulses is observed in terms of the amplitude or intensity of their overlapping portions. Two types of juxtaposition of signal and index are indicated in Fig. 7-13. Furthermore, the amplitude or intensity of pulse *c* is constant regardless of the speed of the time base employed. Thus, juxtaposition may be considerably more sensitive than addition.

The most sensitive method of matching a signal and index is indicated in Fig. 7-14, and the measurement is made with completely overlapping pulses. The deflections do not add, however, since they are displayed separately either by electronic switching or by the use of a mechanical overlay or grid identical in size and shape with signal. If electronic switching is used, the persistence of the screen of a cathode-ray tube or of the eye may be relied upon to maintain the trace of the signal while the index is being displayed. The final setting may be made in terms of the brilliance of the rising edge of signal and index which will pass through the same configurations of addition or juxtaposition, but on a much finer time scale. This method is possible, of course, only with deflection-modulated displays and pulses of identical shape. It is, however, of considerable importance in obtaining extremely accurate measurements with pulses of slow rise and fall times.

The application of these methods of resetting to deflection- and intensity-modulated displays will now be taken up and, where feasible, formulas will be derived indicating the sensitivity or resettability in terms of rise and fall times of the pulses and speed of the time base upon which the pulses are displayed.

**7-7. Deflection-modulated Display and Deflection-modulated Index. Addition.**—The accuracy of resetting of two pulses under conditions where the length of their overlapping portion is employed as a criterion of the resetting is small compared with the accuracy of juxtaposition as described below.

The operator attempts to reproduce the length of pulse *c* of Fig. 7-12. Provided this pulse has a length greater than the spot size of the cathode-ray tube, the accuracy with which the length will be reproduced will be

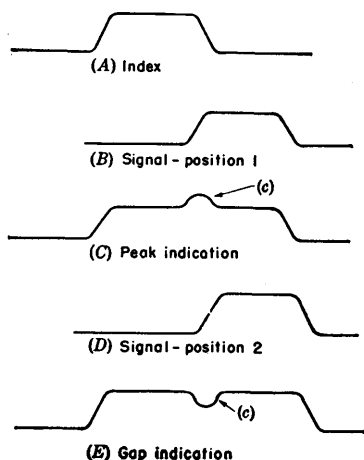


FIG. 7-13.—Juxtaposition of signal and index. The amplitude of the overlapping portion of the two pulses *c* is a sensitive indication of the separation of pulses (A) and (B). The amplitude of (c) may be positive or negative with respect to that of (A) or (B) giving a peak or gap indication.

relatively constant, and roughly 1 part in 10. The error of time measurement corresponding to a fluctuation of 1 part in 10 of  $D$  is  $0.1D/S$ , where  $S$  is the sweep speed in millimeters per microsecond and  $D$  is the length of pulse  $c$  in millimeters.

**Juxtaposition.**—A consideration of Fig. 7-13 indicates that the variation of amplitude of pulse  $c$  is from zero to the sum of the pulses  $a$  and  $b$  depending upon their overlap. A variety of adjustments may be made.

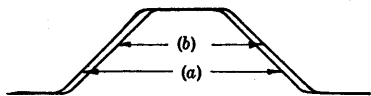


FIG. 7-14.—Electrical superposition of signal and index. Electronic switching of the inputs to the cathode-ray-tube display permits superposition of pulses (a) and (b).

For example, pulses  $a$  and  $b$  may be adjusted so that continuity between the two pulses is established. On the other hand, the setting may be made when the amplitude of pulse  $c$  is equal to a fraction of  $a$  or  $b$ . But the rate of change of the amplitude of pulse  $c$  with overlap of  $a$  and  $b$  will

be approximately constant regardless of the arbitrary criterion of measurement. A preferred method of adjustment is one in which the amplitude of pulse  $c$  is half that of signal and index, as is shown in Fig. 7-5c. If a criterion involving a large overlap is accepted, there is danger that a careless operator would make the setting in terms of the length of  $c$  and not its amplitude, with a consequent loss of accuracy.

A simplifying assumption applying to nearly all deflection-modulated displays is that the speed of the time base  $S$  is large enough so that the rise

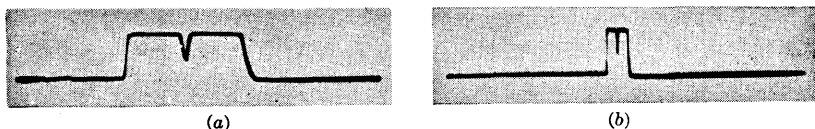


FIG. 7-15.—Juxtaposition at two values of sweep speed. The notch between signal and index is clearly seen in (a). Although the sweep speed has been decreased in (b) until the gap is confused with the spot of the cathode-ray tube, the height of the gap is still clearly indicated.

of pulse  $a$  and the fall of pulse  $c$  do not obscure the amplitude changes of pulse  $c$  which occur in the process of juxtaposition. A wide range of sweep speeds is possible, as shown in Fig. 7-15a and b. In fact the sweep speed may be so small that  $c$  has a length comparable to the spot size of the cathode-ray tube. This is not true, however, in the case of intensity-modulated two-dimensional displays (see Sec. 7-10). A second simplifying assumption is that pulses  $a$  and  $b$  are trapezoidal and have the same rise and fall times and amplitudes. This, of course, represents some deviation from the true shape of signal and index, especially at the initiation of the rise or near its completion. On the other hand, it is a good approximation when the amplitude of pulse  $c$  is roughly half the amplitude of signal and index.

In Fig. 7-16, where the geometry of juxtaposition is shown, similar triangles give

$$\frac{h}{h_r} = 2 - \frac{D}{d_r}, \quad (1)$$

where  $h$  = height of  $c$ ,  $h_r$  = height of  $a$  and  $b$ ,  $d_r$  = distance for  $a$  and  $b$  to rise to  $h_r$ , and  $D$  is the length of pulse  $c$ , plus the separation of the fall of  $a$  and the rise of  $b$ . The units are millimeters. But

$$D = tS$$

and

$$d_r = t_r S,$$

where  $S$  is the sweep speed (mm/ $\mu$ sec),  $t_r$  is the time ( $\mu$ sec)

required for the pulse to rise  $d_r$ , and  $t$  is time ( $\mu$ sec). Therefore,

$$t = \left(2 - \frac{h}{h_r}\right) t_r. \quad (2)$$

Differentiation of Eq. (2) gives

$$\frac{dh}{dt} = \frac{h_r}{t_r}.$$

The fractional rate of change of height of the pulse  $c$  is then inversely proportional to the speed of rise and fall of the index and signal.

Errors may be evaluated in terms of a fluctuation of  $t$ , ( $\Delta t$ ), due to an operator's error ( $\Delta h$ ) of reproducing  $h$ . Thus,

$$\Delta t = \frac{\Delta h}{h_r} t_r. \quad (3)$$

With careful setting,  $\Delta h/h_r$  would not exceed 5 or 10 per cent, although controlled measurements on this have not been made for cathode-ray-tube displays. On the other hand, a number of experimental data are available on the reproducibility of  $\Delta t$  obtained in measurements of the resettability of range of fixed targets using known values of  $t_r$  ( $= d_r/S$ ). We may, therefore, calculate typical values for the fluctuation of  $\Delta h/h_r$ . In a particular case,  $t_r$  is approximately 0.1  $\mu$ sec and  $\Delta t$  is about 0.005  $\mu$ sec, giving a value of  $\Delta h/h_r = \Delta t/t_r = \frac{1}{20}$ . These observations were based, of course, on the over-all resettability observed in a radar system, and the error with artificial signals may be somewhat less than is indicated by the figure  $\frac{1}{20}$ .

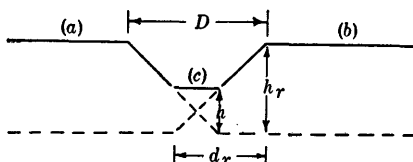


FIG. 7-16.—The geometry of juxtaposition of signal and index. It is assumed that pulses (a) and (b) have equal amplitudes, equal rates of rise and fall, and that their rises and falls are linear.

**7.8. Deflection-modulated Signal and Mechanical Index.**—The mechanical index represents an ideal index since it corresponds to a zero time of rise and fall of the index, and the accuracy of resetting depends solely upon the rise time of the signal pulse.

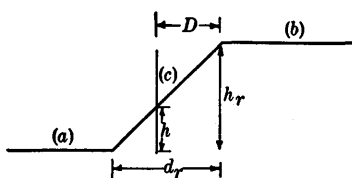


FIG. 7-17.—Geometry of electrical signal and mechanical index. The mechanical index is represented by (c).

As in the previous case of Fig. 7-16, we may obtain from Fig. 7-17 an expression for  $h$ ,

$$\frac{h}{h_r} = 1 - \frac{D}{d_r} \quad (4)$$

Substitution of  $D = St$  and  $d_r = St_r$  gives

$$t = 1 - \frac{h}{h_r} t_r \quad (5)$$

Likewise,

$$\Delta t = \frac{\Delta h}{h_r} t_r \quad (6)$$

In the case of SCR-584 (circular trace with mechanical cursor), the fluctuation  $\Delta t$  was observed to be roughly  $\frac{1}{30} \mu\text{sec}$  and the rise time  $t_r$  to be  $\frac{1}{2} \mu\text{sec}$ , giving values of  $\Delta t/t_r$  or  $\Delta h/h_r$  of approximately  $\frac{1}{15}$ , similar to that obtained in the previous case.

**7.9. Deflection-modulated Signal and Intensity-modulated Index.**—Three typical displays of signal and index are shown in Fig. 7-18*a*, *b*, and *c*. In all practical cases the duration of the marker is made short compared with the rise time of the signal. The resettability of these three types of display may therefore be evaluated by exactly the same formula as was used for the mechanical index above.

An intensifying pulse displayed on the rise of a rapid signal (as in Fig. 7-18*a*) must at the same time counteract the dimming of the trace due to the increase of sweep speed that is caused by the deflection-modulated signal. A distinguishable and clear mark is, therefore, difficult to obtain. Furthermore, noise and interference make it difficult to locate an intensifying pulse. A blanking marker shown in Fig. 7-18*b* and *c* is more effective since it cannot be obscured so easily by any reasonable value of sweep speed or by an incorrect adjustment of the bias of the cathode-ray tube.

**7.10. Juxtaposition of Intensity-modulated Signal and Index.** *General considerations.*—As in Sec. 7-7, juxtaposition of signal and index is the preferred method. The amplitude of pulse *c* of Fig. 7-13 is, however, represented by an intensity change instead of by a deflection.

By the use of a gap indication (see Fig. 7-13), the setting will be made in terms of the intensity of the dark gap between the signal and index. The setting is relatively independent of the bias adjustment of the cathode-ray tube as long as the intensity is low enough to give a reasonably dark space between the two pulses. A somewhat more distinctive indication is given by using peak indication (see Fig. 7-13), especially if the bias of the cathode-ray tube is adjusted so that the amplitude of pulses *a* or *b* give the maximum intensity obtainable without defocusing. The increase of intensity over this value due to pulse *c*

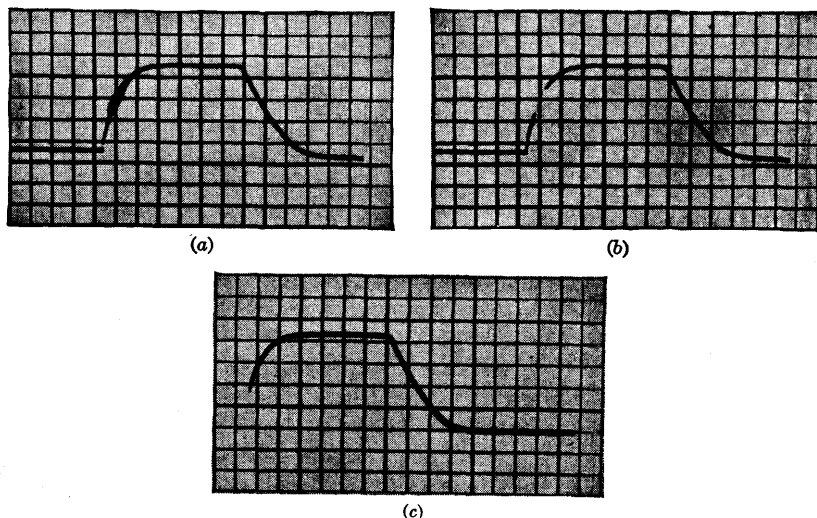


FIG. 7-18.—Three types of deflection-modulated signals and intensity-modulated index. In (a) the index intensifies the trace; in (b) and (c) the index is a blanking pulse and creates a gap in the signal. The latter two displays give a more sensitive indication of the time of occurrence of the signal.

will give a considerable defocusing, a phenomenon often termed "blooming." Thus the operator observes not only the increase of intensity but also the increase of spot size. This method is often objectionable because the distortion of portions of the signal overlapping the index may make them unrecognizable. Furthermore, the bias adjustment giving a pronounced blooming effect is likely to be more critical than that necessary for the dark-gap presentation. For these reasons the dark gap is considered to be the more suitable under operational conditions although no detailed experimental data on this point are available.

In airborne bombing of large cities with low-resolution radar,<sup>1</sup> the desired signal is poorly defined and large areas of the city may be displayed at nearly the maximum intensity of the cathode-ray tube. In

<sup>1</sup> S. McGrath *et al.*, "Blind Bombing Radar," *Electronics*, (May 1946).

this case an intensified index may be difficult to distinguish from the target unless it has an intensity greater than that of the signals. Sometimes a dark or blanking index is used for easier identification. This, however, leads to a considerable loss of accuracy since the setting is made in terms of the length of overlap of signal and index, of which there is no measure until the signal appears on both sides of the blanking index.

Most intensity-modulated displays are in two coordinates and serve the purposes of general survey in addition to precise time measurement. One method of meeting these two requirements is to increase progressively the speed of the sweep as the target is approached. During this period it is desired to make accurate measurements of the range of the target. It is, therefore, of considerable interest to determine the error of resettability over a wide range of sweep speeds. This range is so large that the length of pulse  $c$  (Fig. 7-13) is no longer large compared with the spot size for the slower sweeps. It is found that a very serious systematic error depending upon sweep speed arises because of the addition of the spot size to the length of the rise of signal and index.

*Reset Error.*—The same reasoning employed in the analysis of the amplitude-modulated display is applicable to intensity modulation providing some assumptions concerning the modulation characteristics of the cathode-ray tube are made. The first and most basic assumption is that the variations of intensity are small enough to be linearly related to the control-grid voltages over the range of measurement. This is approximately true where the variations of intensity are less than 10 per cent. Another simplifying assumption is that the distribution of intensity in the spot of the cathode-ray tube is roughly triangular and consists of a linear rise and fall of  $R$  millimeters. This is not strictly true, although in magnetic tubes the intensity variation approximates a Gaussian distribution. In electrostatic tubes, this assumption may not be justified as is pointed out in Sec. 7-11 (see Vol. 22, Chap. 17).

If spot size is neglected, the derivation of the relation between the variables is similar to that employed in deflection-modulated displays and the same formulas apply if we take intensity of the display to be equal to  $h'$  and  $h'_r$  over the required range,

$$h' = h'_r \left( 2 - \frac{D}{d_r} \right). \quad (7)$$

The effect of the spot size of the cathode-ray tube must also be considered. The quantity  $R$  is defined as the distance in millimeters required for the intensity of the triangular spot to fall from its maximum value to zero. If it is assumed that  $R$  adds linearly to the length of rise of the signal, it follows that

$$d_r = R + t_r S. \quad (8)$$

Then

$$h' = h'_r \left( 2 - \frac{St}{R + t_r S} \right), \quad (9)$$

or

$$t = \left( \frac{R}{S} + t_r \right) \left( 2 - \frac{h'}{h'_r} \right), \quad (10)$$

where  $h'/h'_r$  is represented as a light-intensity change.

The change in time corresponding to  $\Delta t'$ , a fluctuation of  $h'$ , ( $\Delta h'$ ), is given by

$$\Delta t = \frac{\Delta h'}{h'_r} \left( \frac{R}{S} + t_r \right). \quad (11)$$

The assumptions in this derivation have not been checked by direct experiment. The relation of the quantity  $R$  to other definitions of spot size has not been verified, and a figure for  $R$  of 0.4 mm has been arbitrarily assumed. The validity of direct addition of the quantity  $R$  to the length of the rise of signal  $d_r$  has not been verified experimentally. On the other hand, many data are available on the over-all accuracy obtainable in resetting on intensity-modulated displays for various values of  $S$  and  $t_r$ . In this way, the expressions are subject to over-all check. The accuracies will be compared by assuming the value of  $\Delta h'/h'_r$  to have a probable error of 5 per cent and comparing the calculated values with those observed experimentally. Formula (11) then reduces to

$$\Delta t = \pm 0.05 \left( \frac{R}{S} + t_r \right). \quad (12)$$

The experimental data obtained from synthetic signals displayed upon typical indicators of various radar systems are listed in the first two columns of Table 7-1. In addition, the display was repeated at intervals characteristic of the scan of the particular radar system mentioned. The measurements were made under laboratory conditions, however, and do not represent the performance that may be expected from an operator under battle conditions. Furthermore, the problems of target recognition were greatly simplified by the use of distinctive synthetic echoes.

The experimental and calculated values of the error in feet,  $\Delta \rho$ , are compared in Table 7-1. The agreement between the two sets of data is remarkably good in view of the differences in the character of the displays and the range of sweep speed over which data are available. Unfortunately the data were not all obtained by the same operator, and some part of the discrepancies may be due to this factor.



TABLE 7-1.—RESET ERROR OF VARIOUS DISPLAYS

Display	Expt.*	Type	$t_r$ , $\mu\text{sec}$	$R$ , mm	$S$ , mi/ 50 mm	$S$ , mm/ $\mu\text{sec}$	$\frac{\Delta h}{h_r}$ % (as- sumed)	$\Delta t$ , $\mu\text{sec}$ (calc)	$\Delta\rho$ , ft (calc)	$\Delta\rho$ , <sup>+</sup> ft (exptl.)	No. of exptl. obs.
AN/APS-3	ASD-1	B	0.1	0.4	1	5	5	0.009	5	7.5	16
AN/APS-15	GPI	PPI	0.1	0.4	2	2.5	5	0.013	7	~ 10	~ 10
AN/APS-15	GPI	PPI	0.1	0.4	5	1.0	5	0.025	13	15	80
AN/APS-15	M-H	PPI	0.1	0.4	20	0.25	5	0.085	43	50	70
AN/APS-15	M-H	PPI	0.25	0.4	4	1.3	5	0.028	14	5	10
AN/APS-15	M-H	PPI	0.25	0.4	4	1.3	5	0.028	14	23	5
AN/APS-15	M-H	PPI	0.25	0.4	11	0.46	5	0.057	29	27	17

\* These identify the particular equipment on which the measurements were made. In each case the data were intermittent at periods of from 1 to 3 sec.

<sup>+</sup> Data expressed as the probable error of a single observation.

*Reset Interval.*—Another significant computation is the expression for  $t$  as a function of  $S$  assuming that  $h'$  is adjusted to  $h'_r/2$ —that is, that the gap between the signal and index is just one-half the intensity of the two pulses. On substitution in Eq. (10) of  $h'/h'_r = 0.5$ , we get

$$t = 1.5 \left( \frac{R}{S} + t_r \right), \quad (13)$$

indicating that the time interval  $t$  (corresponding to the distance  $D$  between the fall of the index and the rise of the signal) is a function of the sweep speed  $S$  where  $R/S \geq t_r$ . We shall term this interval  $t$  the "reset interval."

TABLE 7-2.—RESET INTERVAL AS A FUNCTION OF SWEEP SPEED

$t_r$ , $\mu\text{sec}$	$R$ , mm	$S$ , mi/50 mm	$S$ , mm/ $\mu\text{sec}$	$t$ , $\mu\text{sec}$	$\Delta t$	$\Delta\rho$ , ft	$\Delta\rho$ obs., ft
0.25	0.4	5	1	1.0	...	...	....
0.25	0.4	10	0.5	1.6	0.6	300	400
0.25	0.4	15	0.33	2.2	1.2	600	....
0.25	0.4	20	0.25	2.8	1.8	900	1000

The next to the last column gives the calculated change of range reading which would be observed if the sweep speed were changed from 5 miles/50 mm to the other values. The last column give experimental figures from AN/APS-15 tests.

As already indicated, airborne search and bombing equipment require wide variations of sweep speed in order to facilitate target recognition. In Table 7-2 are shown representative values for the reset error of two radar systems used for these purposes, AN/APS-15 and AN/APQ-13. The quotient of  $R/S$  is greater than  $t_r$  over the range of sweep speeds

employed and the error is therefore roughly inversely related to  $S$ . Not only is the numerical value of  $\Delta\rho$  large but also the increment in going through successive values of  $S$  gives a variation of the reset interval 10 to 30 times that of the reset error of Table 7-1. In two cases where experimental data are available, fairly good checks with the calculated values are obtained. A significant error in the prediction of the time of fall of a bomb is involved when aided tracking methods are employed during the bomb run since the progressive decrease of  $\Delta\rho$  introduces a fictitious rate term.

**7-11. Superposition of Signal and Index in Deflection-modulated Displays.**—Superposition of signal and index of identical shape and size gives an extremely accurate method of resetting. Although mechanical overlays may be used for this purpose, electronic switching of two identical signals which are matched by superposition as in Loran has been most useful. In either case the two pulses must be adjusted to have similar amplitudes and shapes. An electronically switched differential gain control is employed in Loran for this purpose (see Sec. 3-2 and Vol. 5).

There are two criteria by which superposition may be judged. The pulses may be superimposed so that the traces completely overlap to give a summation of the intensity of the front edges of the two traces. On the other hand, the two traces may be juxtaposed and the intensity of the gap between the two deflection-modulated traces may be adjusted to reproducible values. Experimental data will indicate that the latter method is considerably more sensitive.

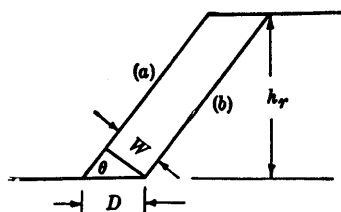


FIG. 7-19.—Geometry of electrical superposition.

The geometry of this method is shown in Fig. 7-19. From this figure

$$D = \frac{W}{\sin \theta}, \quad (14)$$

where  $W$  = the separation of the two traces, and  $\sin \theta = \frac{h_r}{\sqrt{d_r^2 + h_r^2}}$ .

Since  $D = St$  and  $d_r = St_r$ ,

$$t = \frac{W}{S \sin \theta}. \quad (15)$$

For an increment  $\Delta W$  we have a corresponding change of  $t$ ,

$$\Delta t = \frac{\Delta W}{S \sin \theta}. \quad (16)$$

*Addition.*—If the traces overlap completely, the maximum error an operator might make is  $\Delta W = \pm R$ , where  $R$  is defined as one-half the

trace width.<sup>1</sup> It is useful to represent the fluctuation as a fraction of the maximum excursion as in the previous equations, and we will define this fraction  $\Delta W/R$  as  $\Delta W'$ , from which Eq. (16) gives

$$\Delta t = \frac{R \Delta W'}{S \sin \theta}. \quad (17)$$

The accuracy of setting, therefore, increases with increasing sweep speed. However, with increasing sweep speed  $\sin \theta$  becomes much less than one and the trace is nearly horizontal.

$$\sin \theta = \frac{h_r}{d_r} = \frac{h_r}{St_r}.$$

The accuracy is then nearly independent of sweep speed and Eq. (17) may be simplified to give the expression

$$\Delta T = R \Delta W' \left( \frac{t_r}{h_r} \right). \quad (18)$$

Thus it is of no value to increase the sweep speed beyond a certain point.

*Juxtaposition.*—The reading may be taken by noting the gap in intensity between the traces *a* and *b* of Fig. 7-14 as in intensity-modulated displays.

From Eq. (7) we may compute the relation between the trace separation *W* and the intensity *h'* of the gap between traces *a* and *b* in terms of *h'\_r*, the maximum intensity of the two traces, and *R*, the distance for the trace intensity to fall linearly to zero.

$$\frac{h'}{h'_r} = 2 - \frac{W}{R} \quad (19)$$

or

$$W = R \left( 2 - \frac{h'}{h'_r} \right). \quad (20)$$

From Eqs. (20) and (15) we obtain

$$t = \frac{R}{S \sin \theta} \left( 2 - \frac{h'}{h'_r} \right), \quad (21)$$

and for an increment  $\Delta h'$

$$\Delta t = \frac{R}{S \sin \theta} \cdot \frac{\Delta h'}{h'_r}. \quad (22)$$

Equation (22) is similar in form to Eq. (16) with sweep speed being a determining factor in the accuracy. Similarly for  $\sin \theta \ll 1$ , Eq. (20)

<sup>1</sup> For a triangular intensity distribution, this is roughly equal to the value of *R* as previously defined.

reduces to

$$\Delta t = \frac{\Delta h'}{h_r'} \cdot \frac{R t_r}{h_r} \quad (23)$$

If the setting is made at  $h'/h_r' = 0.5$ ,

$$t = \frac{1.5R}{S \sin \theta} \quad (24)$$

But a continuous change of  $S$  is unlikely in deflection-modulated displays, and the dependence upon  $S$  is of no great importance.

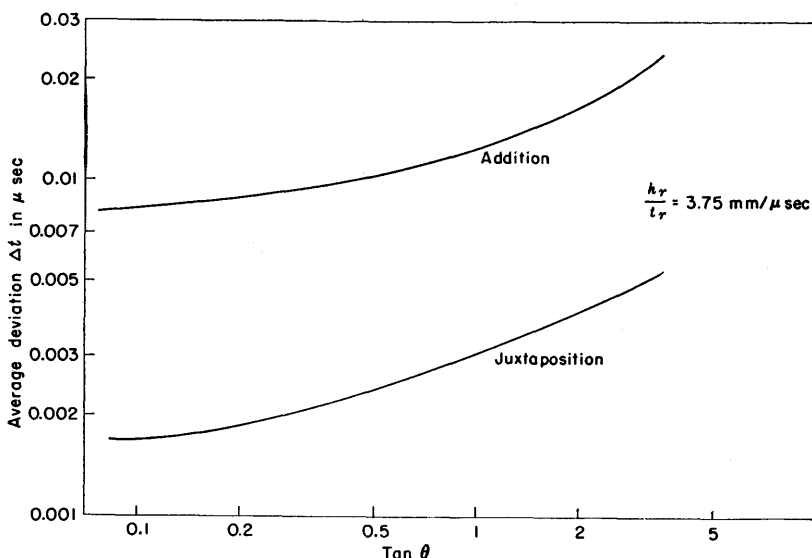


FIG. 7-20.—Experimental test of accuracy of electrical superposition of deflection-modulated signal and index employing an electronically switched display. The upper curve indicates the accuracy achieved by completely superposing the signal and index and employing as a criterion the maximum intensity obtained. In the lower figure the signals are juxtaposed and the intensity of the gap between them is observed. The signal employed in both cases had a rate of rise ( $h_r/t_r$ ) equal to 3.75 mm/ $\mu\text{sec}$ . The value of  $h_r/(t_r s) = \tan \theta$  is varied. The accuracy is amazingly good; in the lower diagram it is  $\frac{1}{2}$  ft with a pulse-rise time of approximately 20  $\mu\text{sec}$ . The curves represent solid lines drawn through the experimental points.

*Comparison of the Two Methods and Experimental Data.*—The values of  $\Delta W$  and  $\Delta h'/h_r'$  which may be achieved in practice are given in the two experimental curves of Fig. 7-20 representative of the Loran display. They correspond respectively to superposition by addition and juxtaposition. For the smallest values of  $\tan \theta$  available ( $\approx 0.08$ ),  $\Delta t$  is 0.008 and 0.0018  $\mu\text{sec}$ , respectively. The striking improvement in the accuracy obtained in these measurements is due to the term  $R/h_r$ , which is very small for these experimental conditions. We may calculate  $\Delta W'$

and  $\Delta h'/h'_r$  from Eqs. (17) and (22). Since these experiments were carried out with  $t_r/h_r = 1/3.75 \mu\text{sec}/\text{mm}$ ,  $\Delta W'$  is calculated to be  $\frac{1}{8}$  and  $\Delta h'/h'_r$  to be  $\frac{1}{80}$ , if it is assumed that  $R \approx 0.4 \text{ mm}$ . Resetting is, therefore, somewhat more precise if an intensity criterion is used.

The latter value is much less than that employed in Table 7-1 and the assumptions about the shape of the intensity distribution of the trace of the cathode-ray tube may be at fault. In electrostatic cathode-ray tubes using a mechanical aperture for obtaining a small spot size, the trace may have an intensity distribution including a flat top and rather steeply sloping sides.<sup>1</sup> Although no experimental data are available on this point, a slope approximately 3 times that assumed would give a value of  $\Delta h'/h'_r$  ( $\frac{1}{20}$ ) in accord with that used in Table 7-1 (see Vol. 22, Chap. 17). The nature of the intensity distribution of the cathode-ray-tube trace depends to a considerable extent upon the nature of the electron-optical system. Since this is not controlled in production, the abrupt intensity distribution may not be obtained in all tubes.

The extreme accuracy of resetting by superposition and intensity-matching is noteworthy; the reset error is approximately one foot. This approaches the values that might be expected from r-f cycle-matching in 2-Mc/sec Loran (see Vol. 5). However these tests were performed on a specially built indicator in which stable sweeps and accurate time-delay circuits and identical pulses were available. Furthermore, atmospheric and noise would distort the pulses and considerably reduce the accuracy of the setting. Also in the Loran system the accuracy of the synchronization and of the indicator circuits is no better than approximately 250 ft. A considerably improved indicator is described in Secs. 7-29 to 7-31.

**7-12. Reset Error with Intermittent Data and with Two-coordinate Controls.**—The operator is often required to make an accurate setting of signal and index even though they are displayed as infrequently as every 5 to 20 sec. This is especially true in scanning radar systems used for navigation, bombing, or fighter direction. A considerable amount of data was obtained in one particular case where the operator was required to set a two-coordinate index or crosshair to a radar echo in response to the operation of two controls in rectangular coordinates which adjusted the index on a PPI display. A detailed explanation of this system is given in Sec. 7-28. As the data were taken under conditions similar to those represented by Table 7-1, similar effects of sweep speed were noted. The most significant data of this experiment were the number of scans required to make a setting of ultimate accuracy. Since the interval between scans was appreciable, the number of tries necessary to make an accurate setting defined the rapidity with which the range was measured and a range rate established. This is illustrated in Fig. 7-21 where the

<sup>1</sup> In these tests a type 3BP1 operating at 2 kv was employed.

probable error of a single observation is plotted as a function of the number of times the signal and index are presented to the operator. It is clear from the errors observed that the difficulty of the process—that is, control of the index in two coordinates and the intermittency of the information—resulted in a setting which did not approach the accuracy obtained in the simpler experiments of Table 7-1. The best accuracy here is about 100 ft, whereas 27 ft was obtained under corresponding conditions with a single-coordinate control and somewhat more frequent data.

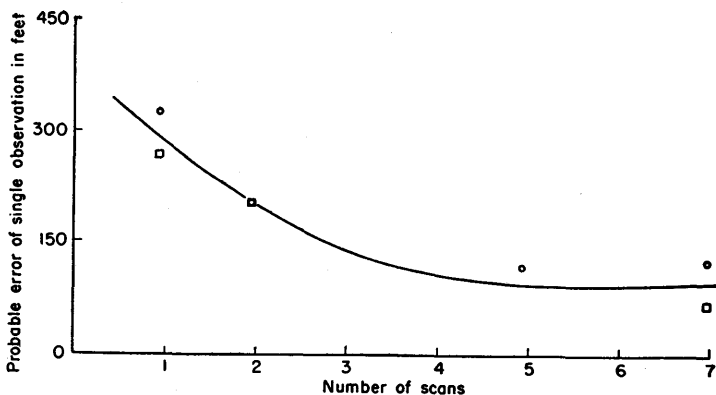


FIG. 7-21.—Static resettability with intermittent data using two-coordinate controls. The scan period is 5 sec. The curve indicates the required number of scans in order to make an accurate setting. The sweep speed of this experiment was roughly 15 miles/50 mm or 0.3 mm/ $\mu$ sec. Each point represents the average of several experiments.

**7-13. Summary and Comparison of Methods.**—Provided the sweep is rapid there is little to choose between deflection and intensity-modulated displays which employ juxtaposition of signal and index without superposition. The error of setting is represented by the product of the time of rise of the signal in microseconds and a factor  $\Delta h/h_r$ , which represents the accuracy with which an operator may reproduce a setting on the various types of displays. Experimental data indicate that this factor varies little depending upon whether a deflection or intensity-modulated display is used. Typical values lie between 1 part in 10 and 1 part in 20.

A significant advantage is obtained, however, by employing electrical superposition with deflection-modulated signals, especially where an intensity criterion is employed. The error of setting is likewise proportional to the product of the time of rise of the signal and a factor  $\Delta h'/h'_r$ , which represents the accuracy with which the operator may reproduce his setting. But here the error is multiplied by a factor  $R/h_r$ . Assuming that the expressions  $\Delta h'/h'_r$  and  $\Delta h/h_r$  are duplicated with equal accuracy, the accuracy of the method of electrical superposition

will exceed that of juxtaposition by a factor  $h_r/R$ . For example, if a 5-in. cathode-ray tube is employed,  $h_r$  may be as large as 100 mm and  $R$  as small as 0.2 mm, giving an increase of accuracy of roughly 500-fold.

Another conclusion of these sections regards the use of expandable sweeps. The employment of an intensity criterion for setting on intensity-modulated cathode-ray-tube displays of variable sweep speeds involves a systematic error which may be 20 or 30 times the error of resetting in the region where the spot size of the cathode-ray tube is comparable to the distance corresponding to the rise and fall of the signal and index.

### TRACKING METHODS

**7-14. Continuous Data.** *General Considerations.*—Continuous data are here defined as those recurring at an interval that is short compared to the response time of the operator during the tracking operation. Certainly any data that recur within the persistence of the operator's vision can be termed continuous, and perhaps data that recur as infrequently as once per second might be in this class. The data are classed as intermittent if the time of their presentation determines the moment at which the operator adjusts the tracking apparatus. With continuous data the operator may adjust his tracking control at any time. Thus other properties of the tracking devices may determine this time. On the other hand with intermittent data any inherent periodicity of the tracking mechanism must be adjusted to that of the data or eliminated.

A rigorous treatment of manual tracking methods is given in Vol. 25, Chap. 8 of the Series, and formulas are there derived indicating the optimum performance of aided tracking. The following material treats the tracking methods briefly and the special problems occurring in their use with oscilloscope displays of continuous or intermittent data.

The general methods of tracking are defined below and are shown in Fig. 7-22. The discussion of this chapter will be confined to the first five methods since the last is the subject of Chap. 8.

1. Direct tracking. The movement of the cursor is proportional to the movement of the tracking control.
2. Velocity tracking. The rate of movement of the cursor is proportional to the movement of the tracking control.
3. Aided tracking. This combines direct and rate tracking. The movement and the rate of movement of the tracking index are proportional to the movement of the control. The ratio of displacement to rate control has the dimensions of time and is called the "time constant." These two controls may be connected

directly or by adjacent knobs which may be grasped simultaneously by the operator by "double gripping."

4. Memory-point or linear-time-constant tracking. A single control adjusts rate and displacement but the time constant is varied

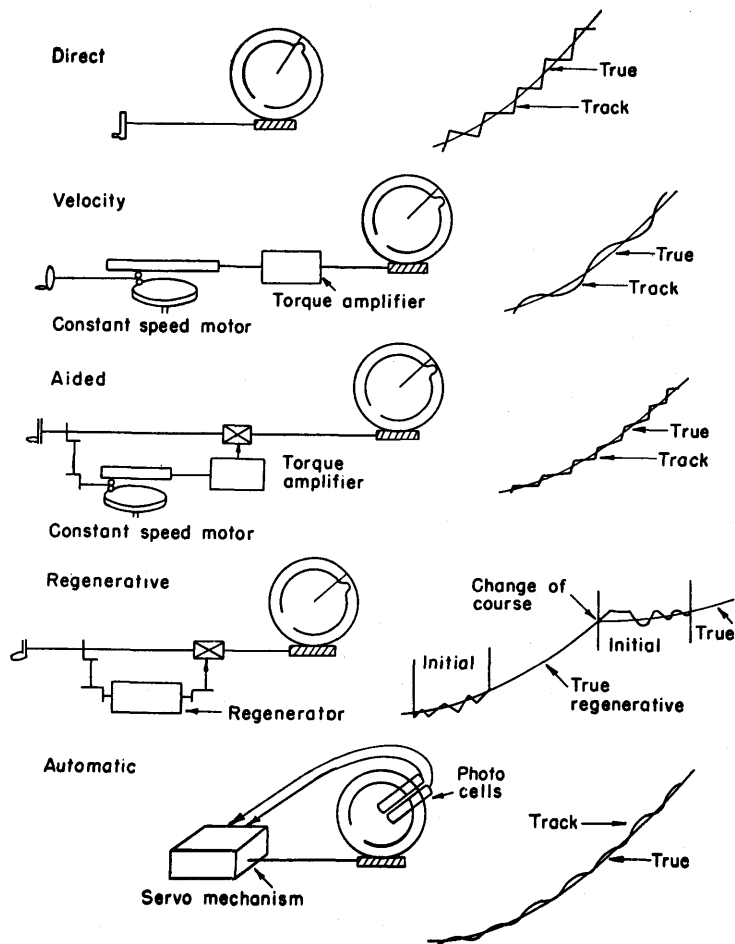


FIG. 7-22.—Pictorial display of various tracking methods—direct, velocity, aided, regenerative, and automatic.

automatically and in direct proportion to the time elapsed since initiating the tracking operation.

5. Regenerative tracking. In regenerative tracking a computer utilizes the known characteristics of the signal and any supplementary data that are available to generate trial values of rate,



which, after a period of initial tracking by manual operation of controls, is exactly corrected and the computer continues to track the target as long as the characteristics of the signal are unchanged.

6. Automatic tracking. Discrimination of the error between index and signal is automatic and a servomechanism causes the signal to be followed automatically.

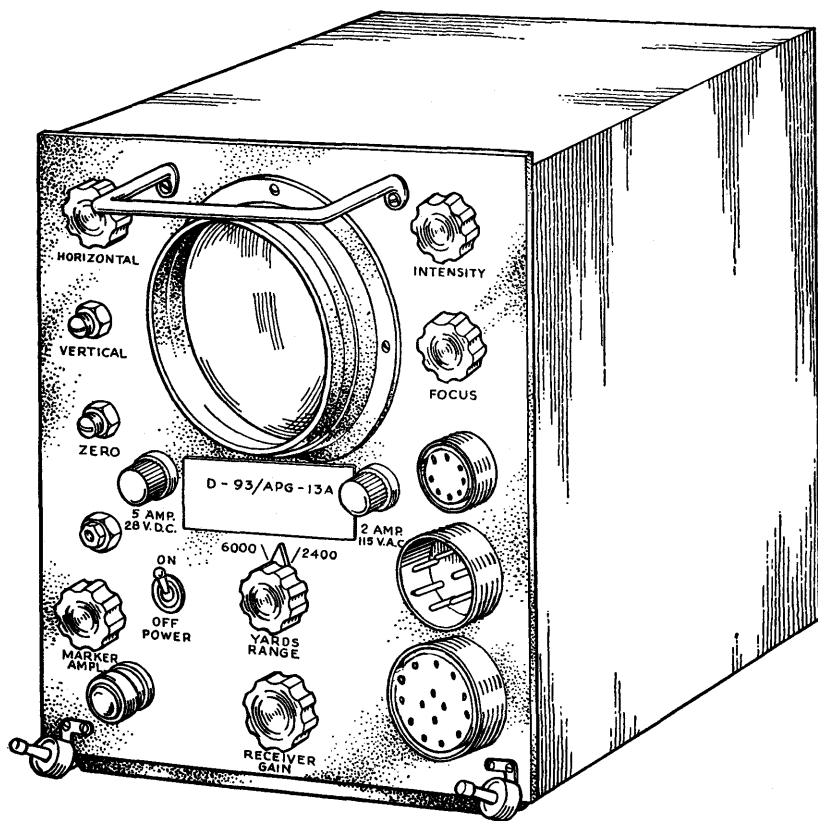


FIG. 7-23.—A type M display unit, Falcon AN/APG-13a. More details of this device are given in Sec. 7-23, especially Fig. 7-37.

*Direct Tracking.*—The simplest method of following a movable signal on a cathode-ray-tube display is by direct tracking where a movement of the operator's handwheel produces a proportional displacement of the tracking index. An advantage of this method is the rapidity with which the index may be set to a target and with which accurate measurements may be obtained. For example, this method is used for tracking ships or ground echoes at a short range ahead of a rapidly moving airplane. A

typical equipment for direct tracking is shown in Fig. 7-23. A complete description of this equipment is given in Sec. 7-23. The scale factor of the displacement control is proportioned to the characteristics of the input data and to the scale of the display. Usually the full scale of the displacement handwheel corresponds roughly to twenty turns to provide sufficient accuracy control and yet give a reasonably short time of slewing<sup>1</sup> from one end of the scale to the other. The excellent performance of direct tracking under certain circumstances is indicated in Fig. 7-29. Direct tracking is, however, fatiguing for the operator if it must be sustained for long periods of time. Furthermore, it is very unsatisfactory for use with intermittent information since as it does not sustain the rate in the interval between input signals (see Sec. 7-16). More accurate information on the rate of change of target range is obtained from the following methods.

*Velocity Tracking.*—Velocity control has been used in place of displacement control in order to obtain more accurate rate information. The velocity of the index is varied to equal that of the signal. The usual procedure for reducing displacement errors consists of arbitrarily increasing the velocity of the index and, when the displacement error has been reduced to zero, returning the velocity control to the estimated correct rate. Although this method affords a satisfactory solution for a target moving at a constant velocity, it is rather difficult to use, because of the lack of a displacement control to get the cursor initially set to the target and moving at the proper rate.

*Aided Tracking.*—This method has the advantage of smooth rate information, obtained with velocity tracking, and the facilities of getting on target rapidly and of adjusting the rate for new conditions. The properties of the system are simply expressed below.

The scale factor of the displacement handwheel is defined as  $D$  yd per turn and the scale factor of the rate control as  $R$  yd/sec per turn. It is assumed that both these quantities are constant and that the input signal has a constant velocity  $V_s$ . At some instant  $T = 0$ , the tracking index and the input signal are set into coincidence and the tracking mechanism is started at an arbitrary rate  $V$ , which will probably be different from that of the input signal. If, for example,  $V$  is too small, the tracking index will fall farther and farther behind the target. After  $T$  sec, it will be  $(V_s - V)T$  yd behind, and a displacement of the handwheel equal to  $\left(\frac{V_s - V}{D}\right)T$  will be required to set the index back to the target. A corresponding increase of  $V$  equal to  $(RT/D)(V_s - V)$  is produced. If the time elapsed between resetting is  $D/R$  sec, then the

<sup>1</sup> Altering the position of the index.

increase of rate is exactly the required amount,  $V_s - V$ . The quantity  $D/R$  is called the "time constant" of the aided-tracking system. In this system  $D/R$  is constant; in others, it will vary according to a definite law.

With continuous data the time constant may be adjusted to suit the characteristics of the operator, the fluctuations of the input data, and the accuracy and speed with which the rate data are required. In practice it is found that a time constant between 2 and 10 sec is quite satisfactory for most range-tracking systems. A typical record of aided tracking of an aircraft echo on a circular sweep display is shown in Fig. 7-24.

In some cases, the rate and displacement controls are not directly geared but are available separately to the operator, as in Fig. 7-25. They are usually concentrically mounted so that gripping both controls at the same time gives the designed time constant. This is termed "double grip" tracking and has been found desirable in cases where it is necessary to use large values of displacement to move the cursor close to the target before initiating the tracking process.

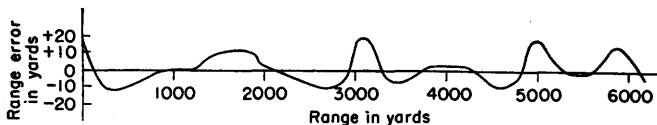


Fig. 7-24.—Aided tracking of an aircraft echo using SCR-584, 2000-yd circular sweep.

Double-grip controls are of considerable importance in cases where the characteristics of the input data or changing geometrical conditions render the designed time constant unsatisfactory. In this case, accurate tracking can be done by training the operator to allow slippage between the rate and displacement knobs when a setting is made. This process, though difficult to teach, has actually been used extensively in tracking with the Norden bombsight, the controls of which are shown in Fig. 7-25. Little training is required if memory-point tracking is used (see Fig. 7-29).

The controllable speed may be provided by a ball-and-disk mechanism or a variable-speed electric motor. The details of several types of aided-tracking systems are given in Vol. 25, Chap. 8. Many of the speed-controlled servomechanisms of Vol. 21, Sec. 14.4 are suitable for these purposes.

Various methods of combining rate and displacement outputs of an aided-tracking unit have been employed. Usually a mechanical differential is used for adding the outputs of the speed-control device and the mechanical handwheel, but there are a few ways to avoid this. For example, one system employs push buttons that momentarily speed up the motor and enter a total displacement that is equal to the product of the time for which the push button is depressed and the speed of the

motor. This also serves as a slewing mechanism which can be used to reduce the displacement errors to zero before adjustment of the velocity control is attempted. In electric speed-control systems the output of a tachometer generator is compared with the adjustable speed-control voltage. If the speed-control servomechanism responds linearly to voltage input, the displacement of the output shaft will be equal to the

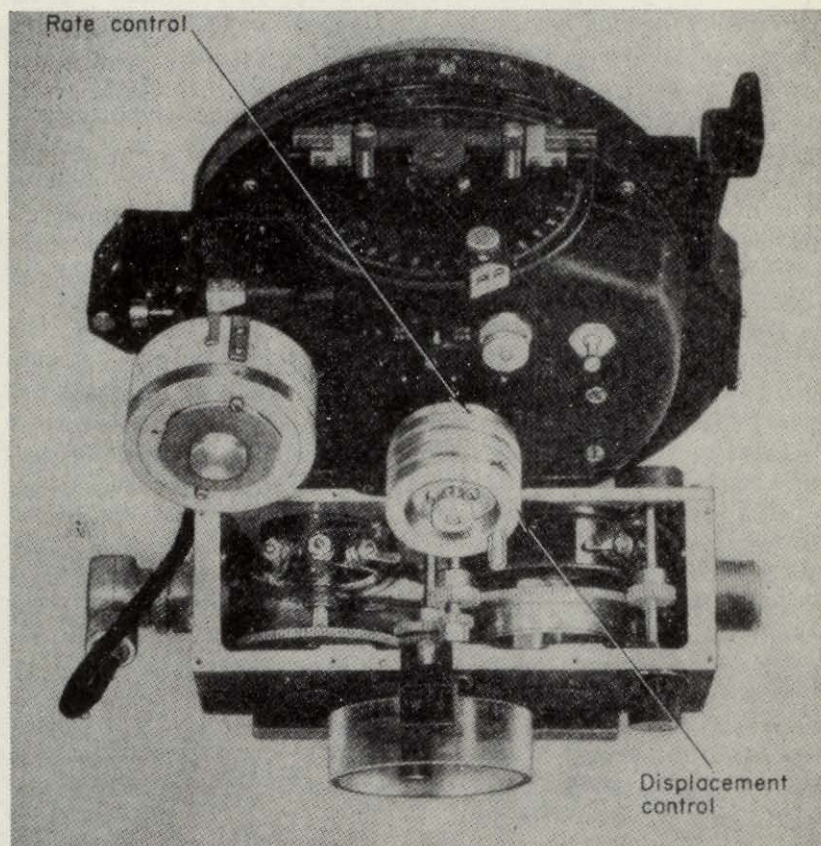


FIG. 7-25.—Aided-tracking mechanism of Norden bombsight modified for range-tracking on radar displays.

time integral of the voltage output of a manually controlled generator, which is proportional to the number of the turns of its generator shaft. Thus the displacement and rate controls consist of a potentiometer and a generator and are very convenient where remote control of the aided tracking mechanism is required (see Sec. 7-27). These circuits are based on methods given in Vol. 21, Sec. 14-4.

**7-15. Intermittent Data. General Considerations.**—The data of a scanning radar system are presented for a time (roughly  $\frac{1}{30}$  sec) which is too short to permit anything more than a displacement measurement, and yet the recurrence interval of the information is so large, 3 to 20 sec, that a long time is required before a range rate of reasonable accuracy may be obtained. If, however, the target is moving so slowly that several thousand observations may be obtained while it traverses the full range of the radar system and a reasonable number of the measurements may be averaged to obtain the rate information, the tracking methods of the previous section are suitable. But radar systems for tracking rapidly moving aircraft from the ground or vice versa may give only 30 to 60 observations of a target in the entire range. For example, a ground radar having a range of 200 miles and a scan period of 30 sec gives at best only 60 observations of a 400-mph airplane. Although the amount of information available for airborne bombing may be increased by rapidly scanning antennas, the limitation in long-range ground radar employing a narrow beam is fundamental (see Vol. 1).

Direct or velocity tracking is of little use for intermittent data. It is extremely difficult to maintain the correct rate during the intervals when no data are available, and it is equally difficult with velocity tracking to estimate the increase of rate which will cause the displacement error to become zero at a time when the data recur. Therefore, special methods must be employed in order to obtain accurate rate information.

In a few special cases, however, the interval between displacement measurements may be employed for approximate rate measurements. In a moving vehicle—for example, an airplane—some choice of the range at which the displacement measurement is made is permissible. The echo from a fixed object is allowed to approach and to coincide with the first of a series of fixed range markers. A stop watch is then started and it is stopped when the echo touches the next fixed index which represents a distance, for example, of 5 miles nearer the aircraft. The average rate over this interval is obtained from a simple slide rule shown in Fig. 7-26. Not only does this slide rule convert the time interval into speed along the line of sight but it also corrects for the altitude of the airplane giving the desired quantity, ground speed.

**Aided Tracking.**—If the intermittent data recur at a constant rate, the time constant of an aided-tracking mechanism may be made equal to this interval or to any integral multiple of it. Therefore, the displacement and rate controls may be double-gripped in synchronism with the scan period or a multiple of it and the setting will have been made in accordance with the requirements of the time constant. Depending upon the type of cursor employed, the amount of correction may be entered in accordance with an estimate of the error at the time of appear-

ance of the index and the signal, or may be entered with a high degree of accuracy by moving a continuously controllable cursor (obtained by electronic switching or a mechanical overlay) to the echo displayed on a persistent screen. A display adapted for this purpose is described in Sec. 7-28.

*Memory-point Tracking.*—The operation of the memory-point tracking system is similar to that of aided tracking except that the time

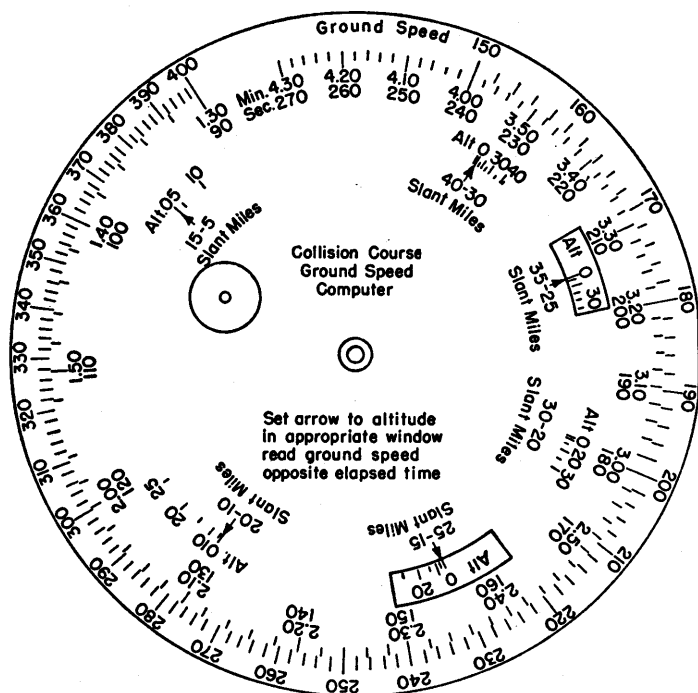


FIG. 7-26.—A ground-speed computer. The time required for an echo to pass between two fixed range markers (spaced at 5 miles) is measured on a stop watch and entered on the inner dial of the computer, giving ground speed by conversion from slant speed in view of the known altitude.

constant is a linear function of time. The displacement error is initially made zero by appropriate displacement settings, and this is usually done when using a control that introduces no rate corrections. The operation of the time-constant varying mechanism is immediately set into operation at what is called the "memory point." Initially the time constant is zero; thereafter it is a linear function of time. At any time later, the control knob varies both rate and displacement with the appropriate time constant, and the cursor is reset to give zero displacement error whenever the data recur. The appropriate rate correction is entered as

shown below. The setting of the rate control gives, ideally, the mean rate of the index over the interval since the start of tracking. Usually such devices have a limit to the maximum time constant and for a number of purposes five or ten minutes have been adequate. A functional block diagram is given in Fig. 7-27.

Memory-point tracking also has important advantages for tracking with continuous data, and the computations of Sec. 7-17 indicate that a considerably more accurate rate is obtained than with aided tracking. In memory-point tracking systems the velocity obtained represents the average value of the velocity over the entire tracking interval. The

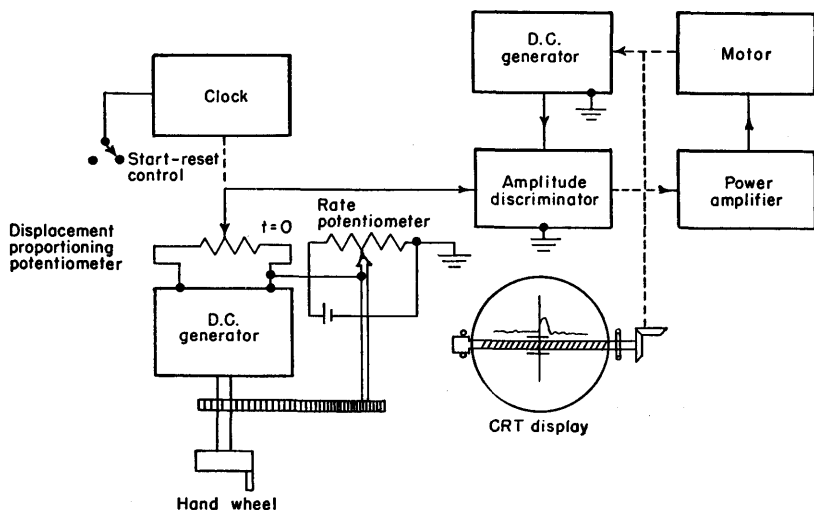


FIG. 7-27.—Block diagram of a memory-point tracking system. The handwheel controls rate and displacement of the tracking index through the clock and proportioning potentiometer.

influence on the measured rate of individual displacement errors at the beginning or end of the interval is reduced proportionately as the interval is increased. There are, however, two important considerations that must be observed in memory-point tracking. First, if an object traveling at a constant velocity has been tracked well for a long initial period, and the memory point has been reset, the rate should not be readjusted for a tracking period equal to the duration of the previous one; otherwise, the accuracy achieved in the previous tracking period may be lost. Second, the memory-point tracking system is specifically designed for obtaining the rate on collision courses. A change in the velocity of the signal requires that the memory point be reset immediately and that the tracking operation be restarted or a considerable error will be involved.

Time constant<sup>1</sup>  $T$  is defined as the ratio of an increment of displacement of the tracking index to the corresponding increment of velocity. The time constant is equal to the time  $t$  elapsed since the start of the tracking operation. It will be shown that this feature enables the operator to track out a velocity error regardless of how he makes corrections, provided that he ultimately reduces the displacement error to zero.

If the velocity of the tracking index is  $V$  and the displacement  $x$ , then the time constant is  $T = dx/dV$ . This definition applies to a tracking system regardless of the independent variable of the tracking operation. In the aided-tracking system described in Sec. 7-14, the independent variable is shaft rotation  $\theta$ , and the scale factors of the respective handwheels are  $R = dV/d\theta$  and  $D = dx/d\theta$ , so that the time constant is  $D/R = dx/dV$ . Since  $\theta$ ,  $V$ , and  $x$  are all changed proportionally it makes little difference which is considered the independent variable. But in memory-point tracking, where the ratios are not constant, there are several choices for the independent variables: the tracking control may vary displacement directly, in which case  $x$  or  $\theta$  is an independent variable; it may vary  $V$  directly, in which case  $V$  or  $\theta$ , is the independent variable; or it may be a push-button type of control, in which a control may allow velocity to be corrected at a constant rate  $dV/dt$ , so that time is the independent variable. In the first two cases either  $R$  or  $D$  is variable, and in the third the variable  $\theta$  is absent, so that  $R$  and  $D$  cannot be defined. The definition of memory-point tracking  $T = dx/dV = t$  can, however, be applied to any of these systems.

In order to show that the result of tracking is independent of the way in which the operator brings the index to the signal, an equation may be written which gives the displacement error in any tracking operation as a function of the corrections that have been made.

Let  $x_s$  = displacement of signal being tracked,

$x_i$  = displacement of index,

$x_c$  = total displacement correction applied to the index up to time  $t$ ,

$V_s$  = velocity of signal (assumed constant), and

$V_i$  = velocity of index at the time  $t$ .

If the velocity of the signal is constant, the displacement of the signal is given by

$$x_s = x_s(0) + V_s t. \quad (25)$$

The displacement of the index is given by

$$x_i = x_i(0) + x_c + \int_0^t V_i dt.$$

<sup>1</sup> This derivation was written by Duncan MacRae, Jr.



If in this equation the condition for memory-point tracking,

$$\frac{dx_i}{dV_i} = \frac{dx_e}{dV_i} = t, \quad \text{or} \quad dx_e = t dV_i,$$

is substituted, the result is

$$x_i = x_i(0) + \int_0^t (t dV_i + V_i dt).$$

The integrand is  $d(V_i t)$ , so the integral may be evaluated:

$$x_i = x_i(0) + V_i t. \quad (26)$$

Subtracting Eq. (26) from Eq. (25),

$$(x_s - x_i)_t = (x_s - x_i)_0 + t(V_s - V_i). \quad (27)$$

Thus if the displacement error at time  $t$  is the same as that at  $t = 0$ , then  $t(V_s - V_i) = 0$ ; and if this condition is satisfied at  $t \neq 0$ ,  $V_s = V_i$ , and the velocity error is completely removed, regardless of the nature of the function  $V_i(t)$ .

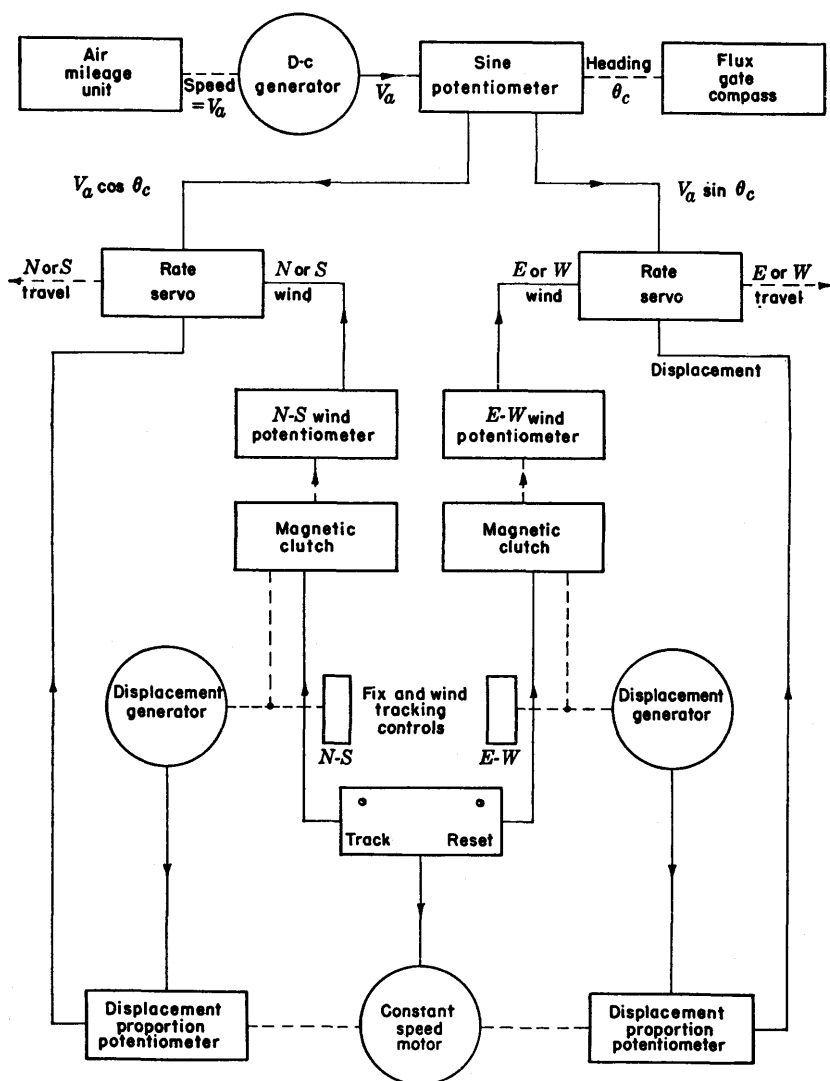
Equation (27) relates the velocity error of a memory-point tracking operation to the displacement errors at times 0 and  $t$ . For if  $E = x_s - x_i$ , then the velocity error is

$$V_s - V_i = \frac{E(t) - E(0)}{t}. \quad (28)$$

*Regenerative and Memory-point Tracking.*—Where the characteristics of the target velocity are predictable—for example, in tracking an object on the ground from a moving aircraft—most of the velocity is due to the motion of the aircraft. A tracking system that adds the proper components of the aircraft velocity to the data obtained from a memory-point tracking system is indicated in Fig. 7-28. In the particular case described the tracking operation consists of accounting for the wind and residual errors in the computing mechanism by memory-point tracking. If the wind is zero and the computer errors are zero, only displacement corrections are required. Since the computer errors vary little with the aircraft heading and airspeed, memory-point tracking may be continued even though these quantities alter (see also Sec. 7-28).

*Comparison of Methods.*—An experimental comparison of manual, aided, and memory-point tracking methods has been carried out, and results indicating the superiority of memory-point tracking are included here. An interesting difference between the accuracy obtainable with memory-point and aided tracking is also shown.

The tests were made using 5-in. type B displays (similar to that of AN/APS-3) having a sweep speed of 1.3 mm/ $\mu$ sec and a scan period of 2 sec. A simulation of the radar display was made by a range- and



**Fig. 7-28.—Combination of regenerative and memory-point tracking. Electrical connections solid—mechanical connections dashed.**

azimuth-gated 30-Mc/sec oscillator. The output of this oscillator was connected to a high-gain amplifier giving an amplitude- and time-modulated 1- $\mu$ sec pulse of adjustable signal-to-noise ratio. The waveforms of the receiver output and the tracking marker had rises of 0.3 and 0.1  $\mu$ sec, respectively. The time delay of this pulse was varied at a constant rate of 120 yd/sec by a synchronous motor. A range-tracking index of duration approximately 0.3  $\mu$ sec was used. The range error

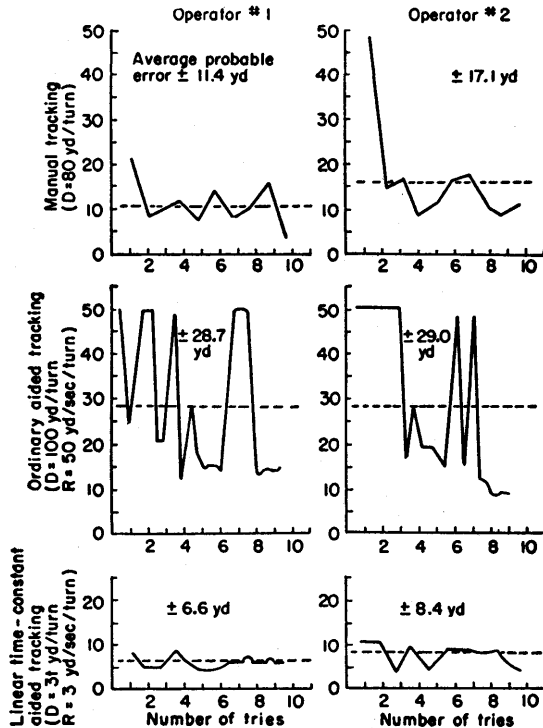


FIG. 7-29.—Comparison of direct, aided, and memory-point tracking. These results were obtained using an intensity-modulated signal and index displayed on a type B indicator having sweep speed corresponding to 2 miles/50 mm or 1.3 mm/ $\mu$ sec. These data represent the first attempts of inexperienced operators.

was automatically recorded on an Esterline-Angus meter by subtraction of the control voltages for the time-modulated signal and the time-modulated index.

The results of tracking tests with two inexperienced operators are given in Fig. 7-29. The performance with memory-point tracking is outstanding; the performance with aided tracking is poor.

With experienced and intelligent operators under the same conditions much more accurate results were obtained, especially with aided track-

ing: (1) manual tracking, average probable error— $\pm 10$  yd; (2) aided tracking, average probable error— $\pm 8$  yd; (3) linear time-constant aided tracking, average probable error— $\pm 5$  yd. In these tests the tracking with (1) and (3) was easy as was the damping of errors. In (2) the tracking required concentration. However, the accuracy was better than that obtained with manual tracking.

A number of tests were made with a practical memory-point tracking system operating in two coordinates and supplied with intermittent data of a 3-sec period displayed on a 5-in. PPI. The time required for an operator to set up the correct velocity with memory-point tracking varied from 4 to 16 scans depending upon a number of factors, among them the difference of velocity between the tracking system and the moving signal. In addition, some preliminary estimates of the resettability were obtained during the tracking operation. When the differential velocity between the cursor and signal was 200 knots, the average error of the first setting was 200 ft compared with 90 ft for static conditions. Although the absolute values of resettability obtained are not significant because of the certain imperfections of the index and signal, the effect of the velocity differential is significant. As soon as the correct rate was established, the reset error dropped to the static value.

**7-16. Comparison of Methods.**<sup>1</sup>—The properties of several types of tracking systems employed for high-altitude bombing have been analyzed in order to determine the theoretical error of their operation. In all cases it is assumed that the data are substantially continuous or at least recur at the period of the aided-tracking mechanism.

The time of fall has been assumed to be 40 sec and the time allowed for tracking the radar echo is taken as twice this value. Taking  $E_n$  and  $V_n$  as the displacement and velocity errors at the last fix, the error in fall of the bomb will be  $E_n + T_f V_n$ , where  $T_f$  is the time of the fall of the bomb. Assuming that the error in the next to last measurement is equal to the error in the last measurement and that the time constant  $T$  of the tracking mechanism is equal to 10 sec, the rms value of the miss is six and a half times the rms value of the last measurement. For a value of  $T = 40$ , however, the multiplier is reduced to 2.2.

In the Norden bombsight  $T = 10$  sec in order to accommodate operation at low altitude. The accuracy at high altitude would be greatly increased by increasing the time constant—for example, to the value of 40. This has been done by waiting an increasing interval between resetting as the end of the bombing run approaches. On the last setting a time approximately equal to the time of fall is allowed to elapse, and, instead of double-gripping the rate and displacement knobs of the aided-tracking mechanism, the rate knob is slipped so that it turns only  $\frac{1}{4}$  the

<sup>1</sup> These formulas and the computations are the work of Mr. J. Irving.

amount that the displacement knob was reset. This is a difficult procedure but results in one-third the error if properly done.

A serious error, however, may be involved if the rate and displacement knobs are corrected equally after waiting a time long compared to the time constant. For example, errors as large as three or four times the value of 6.5 mentioned above might be involved (see Table 7-4). In no case is the error of the miss reduced to a value comparable to that of the error of the last observation. In memory-point tracking a much closer approach to this ideal is achieved. Making the same assumptions as previously with regard to the error of the next to last measurement being equal to the error of the last measurement, we obtain the rms error of the miss, which is

$$\sqrt{\left(1 + \frac{T_f}{T_n}\right)^2 (E_n^2) + \left(\frac{T_f}{T_n}\right)^2 E_0^2} \quad (29)$$

where  $E_0$  is the initial displacement error of the memory-point tracking system, made at the time when the tracking was initiated and  $E_n$  is the error of the final measurement as in the previous case. The time of tracking is  $T_n$ . Taking, for example, conditions similar to those of the previous problem—that is, a time of fall of 40 sec and bombing run of 80 sec—the rms value of the miss is equal to 1.6 times the rms error of the last observation; a considerable improvement over the factor 2.2 obtained under best conditions in the previous case. If, however, the initial value of the rate is approximately known, this factor is somewhat reduced—for example, to 1.5.

Table 7-4 indicates some comparative values for aided and memory-point tracking.

TABLE 7-4.—RELATIVE MERITS OF VARIOUS TRACKING SYSTEMS

Name of system and conditions of use	$T$ (time constant, sec)	Miss of bomb rms error (to be multiplied by error of last observation)
1. Norden bombsight—range-tracking fixed double-gripping ratio.....	10	6.5
2. Same as (1).....	40	2.2
3. Norden bombsight reset at twice the time constant.....	10	19.0
4. Memory-point tracking for 80 sec.....	80	1.6
5. Memory-point tracking for 80 sec (initial value known).....	..	1.5

## FIXED INDICES FOR MANUAL TIME MEASUREMENT

BY E. F. MACNICHOL, JR.

**7.17. A-scope.**—The simplest type of manual measuring device consists of a cathode-ray tube with a linear or exponential time base applied between one pair of deflecting plates while the video signals are applied to the other pair. If the deflection sensitivity of the CRT is known and if the sweep speed is defined by letting a known time constant charge through a known voltage, the time of occurrence of a signal may be measured by means of a ruled scale printed on the face of the CRT. Such a simple device is shown in Fig. 7-30. The grid of the switch tube is initially positive drawing current through  $R_1$  and the plate is clamped to within a volt or two of the cathode (assuming  $R > 100\text{ k}$ ), and  $C$  is dis-

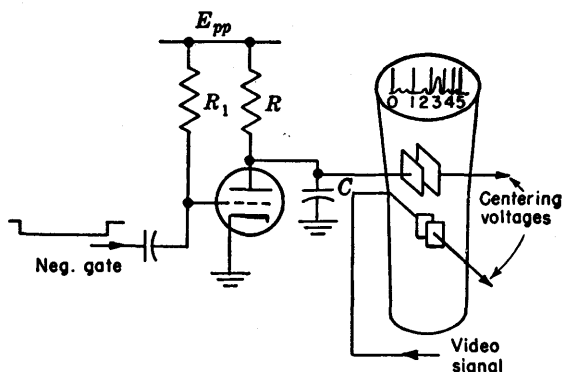


Fig. 7-30.—Simple time-measuring system using exponential sweep and fixed mechanical timing marks.

charged. The spot on the CRT is adjusted to the zero index by means of a centering voltage applied to the free horizontal plate. At the instant measurement starts, a negative gate is applied to the control grid of the switch tube cutting it off and holding it off for the total time interval to be measured. The condenser  $C$  charges exponentially toward  $E_{pp}$  according to the well-known law

$$E = E_{pp}(1 - e^{-\frac{t}{RC}}).$$

If the deflection sensitivity of the CRT is  $ds/dE$  (in./volt), the distance in time  $t$  traveled is  $s = E ds/dE$ .

$$\therefore s = \frac{ds}{dE} E_{pp}(1 - e^{-\frac{t}{RC}}).$$

It is then a simple matter to mark off values of  $s$  on a scale on the face of the cathode-ray tube showing convenient values of  $t$ . The edge of the

vertical deflection marking the time of occurrence of the signal may be compared with the fixed time marks by means of visual interpolation. If a linear sweep is used equal sensitivity is obtained over the whole scale (see Vol. 19, Chap. 7).

In practice such a simple system is open to a number of objections. In the first place the CRT will not focus over the whole sweep length if the time base is applied to only one plate. A unity-gain phase inverter may be used to apply an inverse potential to the other plate as indicated in Vol. 19, Chap. 7. Another objection is the variation of  $ds/dE$  from tube to tube over limits as great as  $\pm 20$  per cent. This can be allowed for by adjusting  $E_{pp}$  so that the total sweep always covers the distance between two fixed indices.

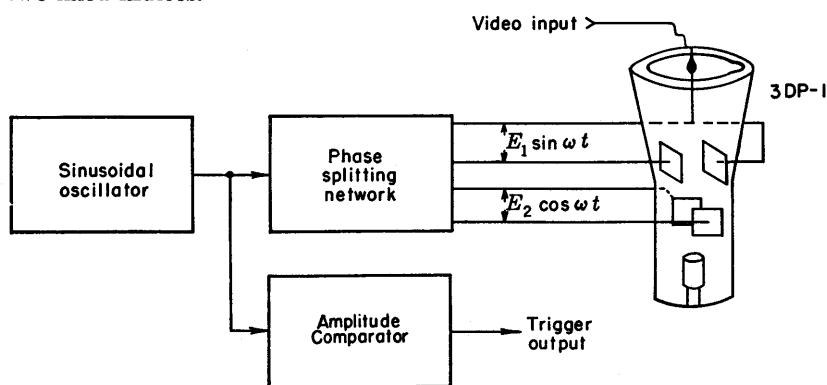


FIG. 7-31.—Elementary J-sweep.

More serious objections arise from the fact that  $ds/dE$  is not constant or accurately predictable and varies with the accelerating potential. Also, mechanical indices give parallax and are difficult to see unless the scale is ruled on edge-illuminated plastic. This type of display, however, is used with some refinements in most of the early radars such as the British Mark II ASV and U. S. Navy Radar ASB. It is probably adequate for measuring time intervals with an accuracy of  $\pm 10$  per cent.

**7-18. J-scope.**—As stated in Chap. 3 and Sec. 7-4, one type of device in which a time base can be compared with fixed or movable mechanical indices with considerable precision is the circular-trace indicator or type J oscilloscope, shown in the block diagram Fig. 7-31. This method of phase measurement was presented in Vol. 19, Chap. 20 and in Vol. 21, Chap. 17. The deflecting plates are supplied with two-phase sinusoidal potentials. Since the deflection sensitivities of the two pairs of plates are different, the amplitudes of the sinusoids are adjusted until both have the same effect on the beam. If the phases of the voltages are in quadrature the spot will then move in a circular orbit with constant angular velocity.

The angle traversed by the spot in a given time interval is equal to the phase change of the timing wave. For sinusoids of frequency  $\nu$ , the time interval  $t$  corresponding to an angle  $\theta$  is

$$t = \frac{\theta}{360\nu}$$

This relation is only true for a trace that is exactly centered with respect to the protractor for measuring  $\theta$ . If, however, harmonics are present in the sinusoids, appreciable errors are present in circular patterns (see Chap. 1, Vol. 22).

One advantage of the circular sweep for high-speed traces is that the stray capacitances of the deflecting electrodes become part of the tuned circuit generating the sweep and therefore do not set a limitation to the sweep speed (see Vol. 19, Chap. 4). The adjustments for circularity are straightforward, and the shape of the circle gives immediate indication of any errors; therefore, adjustable phase-shifting circuits may be employed.

The most satisfactory fixed scale is applied directly to the face of the tube and consists of radial lines indicating fractions of an orbit, and a circular line to aid in centering the trace. It is, of course, of utmost importance that the trace and the scale be accurately concentric. Photographs of a typical scale are shown in Fig. 7-32.<sup>1</sup>

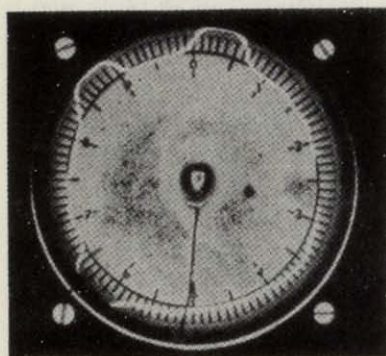
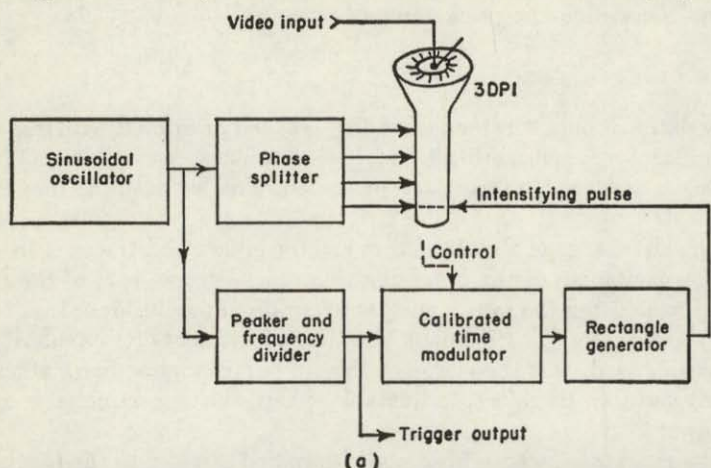
Video signals are applied to a deflecting electrode (see Vol. 22) which consists of a wire that passes through the center of the face of the CRT toward the center of the electron gun. The effect of a potential applied to this wire is to deflect the spot radially inward or outward regardless of its position along its circular path. The display may be thought of as a polar coordinate analogue to the A-scope in which  $R$  indicates amplitude and  $\theta$  time. Because of the geometry of the tube, distortion occurs if large signals are applied to the central electrode. This distortion is small if the radial deflection is less than  $\frac{1}{4}$  in. in the 3DP-1 tube. Although the input capacitance of the tube is low (about  $2 \mu\text{mf}$ ) its deflection sensitivity is also low (roughly 100 volts/ $\frac{1}{4}$  in. at 2 kv accelerating potential) so that large video voltages are required.<sup>2</sup>

<sup>1</sup> A convenient scale is formed by applying India ink directly to the face of the CRT with a ruling pen. The ink will adhere if the tube had previously been cleaned with a slightly abrasive cleaning powder. A ruling "jig" for holding the CRT, a straight edge, and a circular protractor can be readily constructed. Scales may also be printed on thin collodion films (decal type) that are applied to the CRT face.

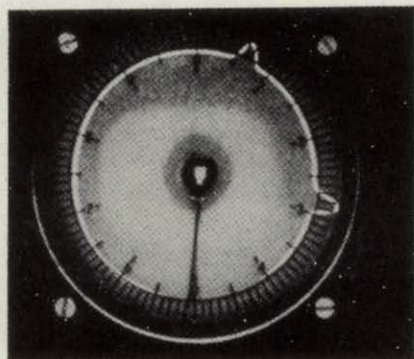
<sup>2</sup> The low capacitance of the deflecting electrode may be utilized to best advantage by minimizing the output capacitance of the last video stage. This has been accomplished by mounting the tube and plate resistor concentrically with the deflecting electrode on a transparent disk placed in front of the face of the CRT. Tubes that have been found satisfactory for this purpose are 6AK5's and 6K4's. The latter are connected as grounded-grid amplifiers to minimize  $C_{gp}$  and to terminate the input cable correctly.



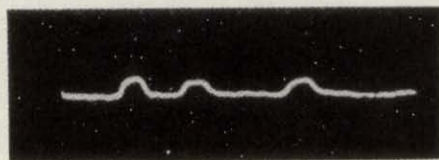
A number of methods have been used to synchronize the trace with the video signals. If the phenomena to be observed are externally synchro-



(b)



(c)



(d)

FIG. 7-32.—TS-100 scope with signal and transfer scale. (a) block diagram, (b) typical echoes from 1- $\mu$ sec radar pulse (c) 0.2- $\mu$ sec pulses 2.4  $\mu$ sec apart on 12.2- $\mu$ sec sweep, (d) echoes of (b) as shown on conventional linear display.

nizable, the oscillator generating the circular trace may be crystal-controlled and run continuously. A basic timing pulse may then be obtained by squaring and differentiating the sinusoid from the oscillator

(Chap. 6; Vol. 19, Chap. 4; and Vol. 21, Chap. 18). An example of a single-scale J-scope is the SCR-718 altimeter.<sup>1</sup>

If the phenomena to be studied cannot be synchronized externally a pulsed oscillator and a phase splitter having good transient response must be used to generate the circular trace (Vol. 19, Chap. 4). Since the deflection sensitivity of  $x$ - and  $y$ -axes is usually quite low (220 volts/in. for 3DP-1 at 2 kv accelerating potential), deflecting amplifiers must give a large output voltage with good transient response. The complexity and current consumption of such amplifiers usually cause designers to choose other systems.

A great advantage of the J-scope is its adaptability to multiple-scale systems. A typical example has already been shown in Fig. 7.32a. A single-scale time-modulation circuit delays a rectangular pulse a variable amount with respect to the trigger. The CRT grid is normally biased beyond cutoff so that no circular trace appears. The rectangular pulse which is controlled by the coarse-scale delay permits time selection of a particular cycle of the circular fine scale. If the coarse scale is uncalibrated the number of cycles can be counted by turning the control slowly from zero range to the desired cycle, since the brightened portion of the trace will travel around the tube once for each cycle (see Fig. 7.45).

**7-19. Plan-position Indicator with Mechanical Scale.**—Fixed range and angle marks are applied to edge-illuminated plastic screens fixed in front of the face of the type B or PPI display. These methods, although simple and convenient, are subject to the limitations mentioned in the discussion of their use with type A displays. Frequently the illuminated screen takes the form of a map overlay of the region in which the radar is operating. This facilitates the recognition of shore lines, islands, or other landmarks and makes navigation simpler. (For details of overlays and photographic map projectors see Vol. 22.)

**7-20. Electronic Time Marks.**—Accurately spaced, fixed timing marks may be generated by any of the methods discussed in Chap. 4 and applied as deflection or intensity modulation to the CRT. The position of the video signal with respect to the fixed indices may be estimated by visual interpolation. The advantages of electrical marks over mechanical marks are that the sweep speed does not have to be known or constant; nor does the trace have to be accurately centered, and parallax is non-existent. On the other hand a complex video signal may obscure the marker pulses.

A combination of electronic and mechanical marks may frequently be used to good advantage. If the sweep speed is adjustable, electronic marks may be adjusted to coincide with marks on a mechanical overlay. The mechanical marks may then be relied upon for a short time. Since

<sup>1</sup> Albert Goldman, "Pulse-type Radio Altimeter," *Electronics*, June, 1946.

the video signals will not obscure them a large number of very narrow marks may be used to facilitate interpolation.

The use of electronic indices for PPI displays is completely discussed in Vol. 22.

## MOVABLE TRACKING MARKS FOR MANUAL TIME MEASUREMENT

### DIRECT TRACKING

**7-21. Introduction.**—The simplest device for direct tracking is a mechanical index moved across the face of a type A display by a crank turned by the operator (see Sec. 7-9). A dial attached to the crank mechanism is calibrated to read range. Because of the limitations of the cathode-ray tube, errors of the order of magnitude of  $\pm 10$  per cent will be involved unless regular calibration is carried out. The type J display

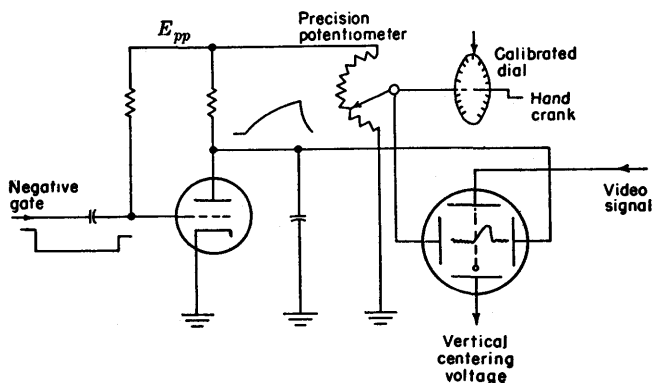


FIG. 7-33.—Elementary continuous-tracking time-measuring device using CRT as a null-measuring device.

with movable index is, however, more accurate. If care is taken to reduce parallax the edge of the signal may be followed with an accuracy of  $\pm 1$  per cent.

The following methods will illustrate how the accuracy of the type A display with mechanical index may be improved by amplitude selection of a portion of the time base instead of using the whole time base. In this way, the effect of variables of the display are reduced by a factor corresponding to the fraction of the total trace which is displayed. This, of course, assumes that the timing waveform is linear and that the amplitude selector is stable.

In Fig. 7-33 the cathode-ray tube itself is used as an amplitude selector (see Vol. 19, Chap. 3). The timing waveform is applied to one plate of the cathode-ray tube, and the reference potential for amplitude selection to the other plate. In this case the cathode-ray tube functions as a null indicator since the spot is centered when the instantaneous sweep voltage

is equal to the centering potential. A single index is inscribed in the center of the CRT and the signal is moved to this index by means of a calibrated horizontal-centering control. When the potentiometer voltage is made equal to the sweep voltage at the time of occurrence of the signal, the signal will appear coincident with the index and this setting will be independent of the scale of the sweep. Tolerances in the alignment of the CRT gun may be allowed for by moving the index until the start of the sweep is on the index when the potentiometer is set to zero. In the simple circuit shown the sweep is exponential so that the potentiometer must be wound with an exponential function if a shaft rotation directly proportional to range is required. If the shaft rotation is not to be used to transmit the range data elsewhere, the dial can be calibrated exponentially and a linear potentiometer used.

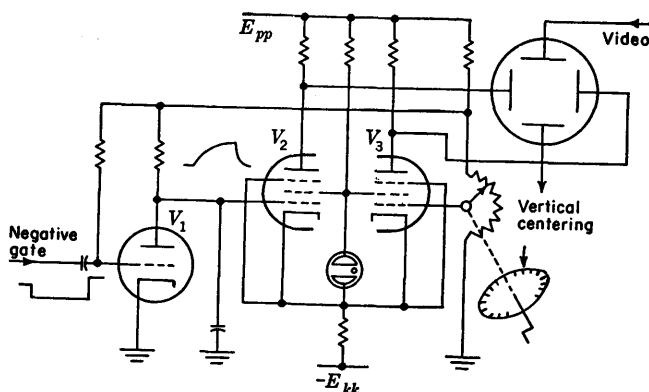


Fig. 7-34.—Continuous-tracking device using a movable expanded sweep with CRT and a differential amplifier as a null device.

In the simple circuit shown, the potential applied to the deflecting plates with respect to the second anode of the CRT varies with the setting of the potentiometer so that defocusing of the trace will take place for large excursions. This objection could be overcome by using a CRT power supply that has its positive terminal fixed with respect to the potentiometer arm instead of to ground.

The second method of reducing the effects of the instability of the cathode-ray tube is shown in Fig. 7-34. Amplitude selection is accomplished previous to the display of the waveforms on the cathode-ray tube. In the particular circuit shown, preliminary amplitude selection is accomplished by a biased differential amplifier consisting of  $V_2$  and  $V_3$ . In this circuit with  $V_1$  conducting  $V_2$  is cut off and  $V_3$  is acting as a cathode follower. The plate of  $V_2$  is at  $E_{pp}$  while that of  $V_3$  is somewhat negative. The spot is therefore deflected off the left-hand edge of the CRT. The

sweep rises until  $V_2$  starts to conduct. As the cathodes rise the current is increased in  $V_2$  and decreased in  $V_3$ , causing the spot to sweep across the CRT. Eventually  $V_3$  will be cut off and the sweep will continue to rise to the available supply potential. Pentodes are used because their gain and cutoff characteristics are nearly independent of the plate-supply voltage which varies with the potentiometer setting. A fixed screen supply is obtained by means of a gaseous voltage-regulator tube. The advantage of this display is that the errors of the CRT are further reduced by the increase of sweep speed that causes a given distance on the tube face to represent a shorter time. With sufficient amplification the onus for the stability rests wholly with the electrical amplitude selector. An alternative method of generating expanded sweeps of this type is to initiate the sweep from a delayed trigger obtained from an accurate time modulator.

**7-22. Movable Electronic Marks.**—Time-modulation devices are frequently used to provide accurately movable electronic indices for

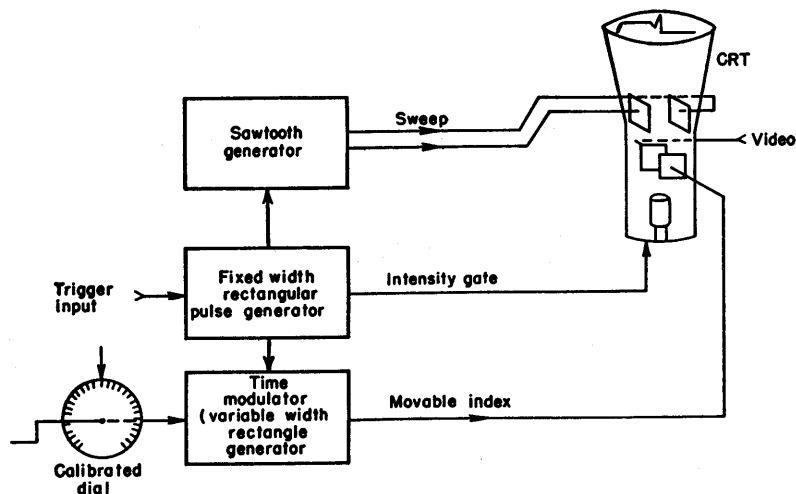


FIG. 7-35.—Use of variable-width rectangle generator to produce time-modulated tracking index.

tracking the video signal. One of the simplest methods used is the comparison of the time of occurrence of the signal with that of the edge of a variable-width rectangular pulse. An accurate variable-width rectangle is generated directly in the phantatron, sanatron, and cathode-coupled multivibrator. This waveform is added to the video signal and both are applied to the vertical deflection system of a type A oscilloscope as shown in Figs. 7-35 and 7-36. The width of the rectangle is varied until the edge of the rectangle merges with the desired signal as shown in Fig. 7-5.

It is possible to use a single linear-sawtooth generator to produce the sweep, the tracking index, and the intensity gate. The type M indicator of the Falcon radar, AN/APG-13A, is an example of this type of device. This is a radar used for the purpose of measuring the range of fairly well-isolated targets on the surface of the water. The range information is applied to an optical sight that corrects the aim of an airborne cannon to allow for the drop of the projectile during its flight.

As shown in the block diagram, Fig. 7.37, the transmitter produces  $\frac{3}{4}$ - $\mu$ sec pulses at a PRF of 1200 cps. High-level pulses plate-modulate the lighthouse-tube transmitter producing  $\frac{3}{4}$ - $\mu$ sec pulses at 2500-Mc/sec energy with a pulse power of 1 to 2 kw.

The transmitter also produces a 100-volt negative pulse that starts the sawtooth generator in the indicator, as shown in Fig. 7.38. The saw-

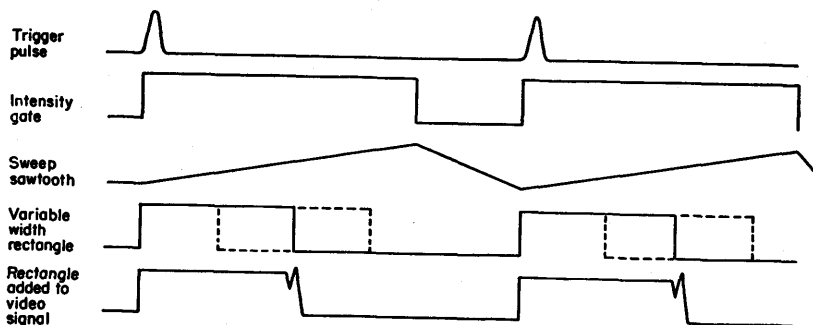


FIG. 7.36.—Timing diagram of indicator using variable-width rectangle for time measurement.

tooth is paraphased and the push-pull output is applied to the horizontal deflecting plates of the CRT. Since the sawtooth generator is self-sustaining, a rectangular pulse which is used to brighten the trace on the CRT and to gate the fixed range-mark generator is produced by the sustaining circuit. The range-tracking step is produced by an amplitude-selection circuit that selects, amplifies, and limits a portion of the sawtooth wave to form a rectangular step. This is mixed with the output of the receiver and applied through a push-pull amplifier to the vertical deflecting system.

A potentiometer on the gun sight provides the reference voltage of the amplitude comparator and thereby determines the instant at which the rectangular step occurs. The potentiometer is turned through a gear-reduction unit by means of a flexible shaft driven by a hand crank. Since the potentiometer and sweep are both linear, a linear variation of range with shaft angle is produced. This range can be read on a dial but is used mainly to turn a cam which deflects a mirror, which in turn deflects the

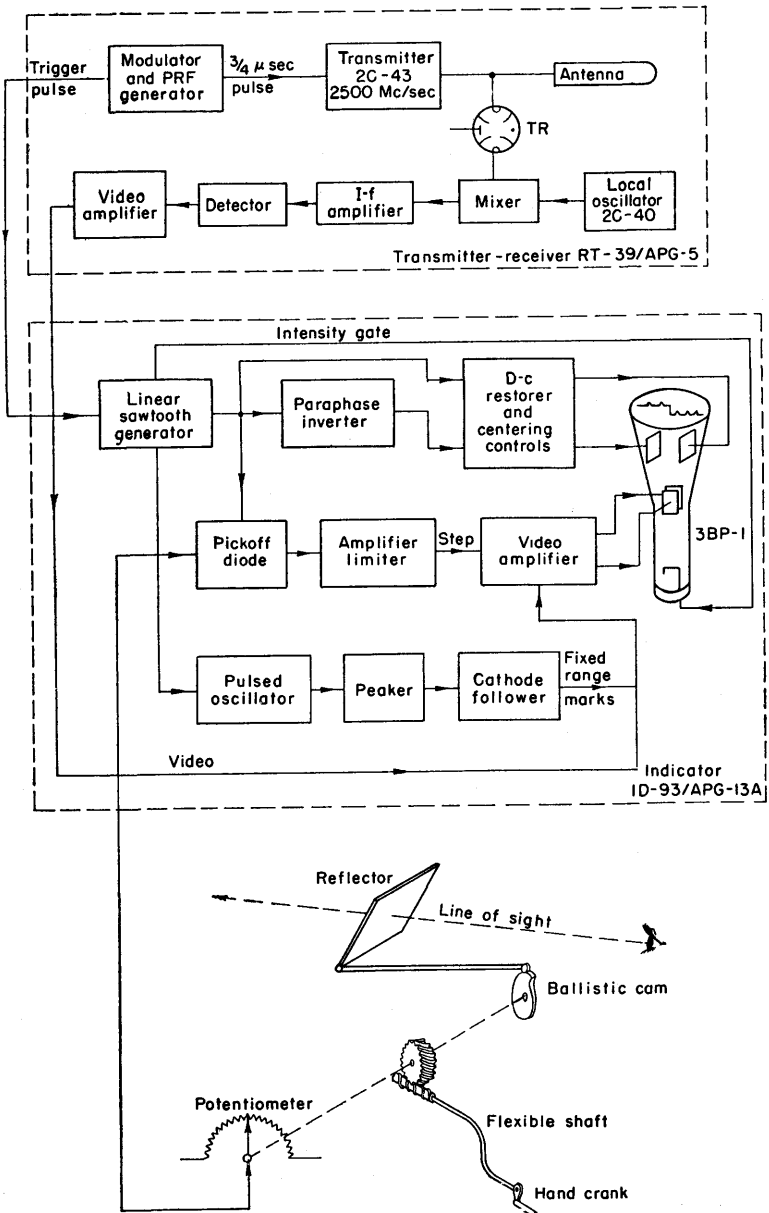


FIG. 7-37.—AN/APG-13A radar system.

line of sight for aiming the cannon. The cam is cut with a ballistic function to give the correct superelevation to the gun.

**7-23. Detailed Circuit Description of Falcon.**—A complete circuit diagram of the Falcon indicator is shown in Fig. 7-39. A positive-feedback linear-sawtooth generator (Vol. 19, Chap. 7) is formed by  $V_{1b}$ ,  $V_{2a}$ , and  $V_{3a}$ . The plate of  $V_{1b}$  clamped at about +1 volt and the sweep is started when plate current is cut off by the trigger introduced through  $C_1$ .

A positive step is produced across  $R_1$  of amplitude  $E_{bb} \left( \frac{R_1}{R_1 + R_2} \right) = 16$  volts. This step overcomes the fixed bias on the grid of  $V_{1a}$  causing the

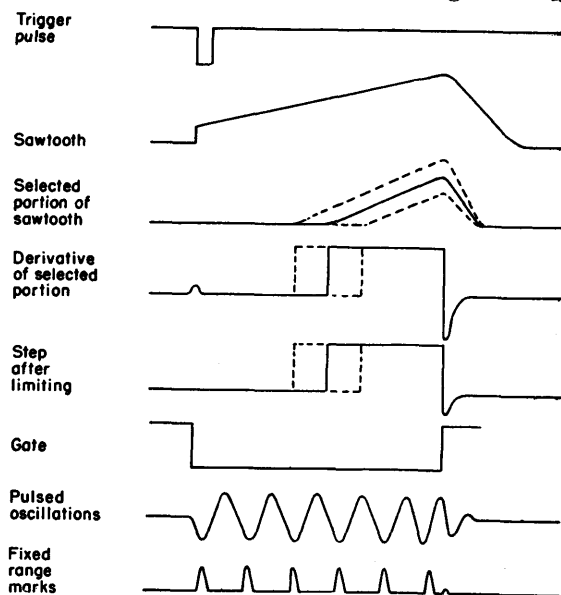


FIG. 7-38.—Timing diagram of Falcon M-scope.

plate to fall. The negative amplified step is applied to the grid of  $V_{1b}$  through  $C_2$  holding the tube cut off after the termination of the trigger pulse. Since the charging current for the sweep condensers  $C_3$  and  $C_4$  flows through  $R_1$  the step persists as long as the sweep continues. The positive feedback from the cathode follower  $V_{3a}$  through  $C_5$  to the positive end of  $R_2$  serves to keep the voltage across  $R_2$  nearly constant and hence the sweep nearly linear. Further compensation is introduced by the network  $C_4$ ,  $R_3$  so that the sweep is linear from +17 to +280 volts within  $\pm 0.2$  per cent (see Chap. 5). When the sweep has reached +280 volts the grid bias on  $V_{3a}$  will have reached -0.5 volt so that grid current will commence and the sawtooth will become slower and exponential. Eventually the charging current in  $C_3$  and  $C_4$  will have decreased sufficiently



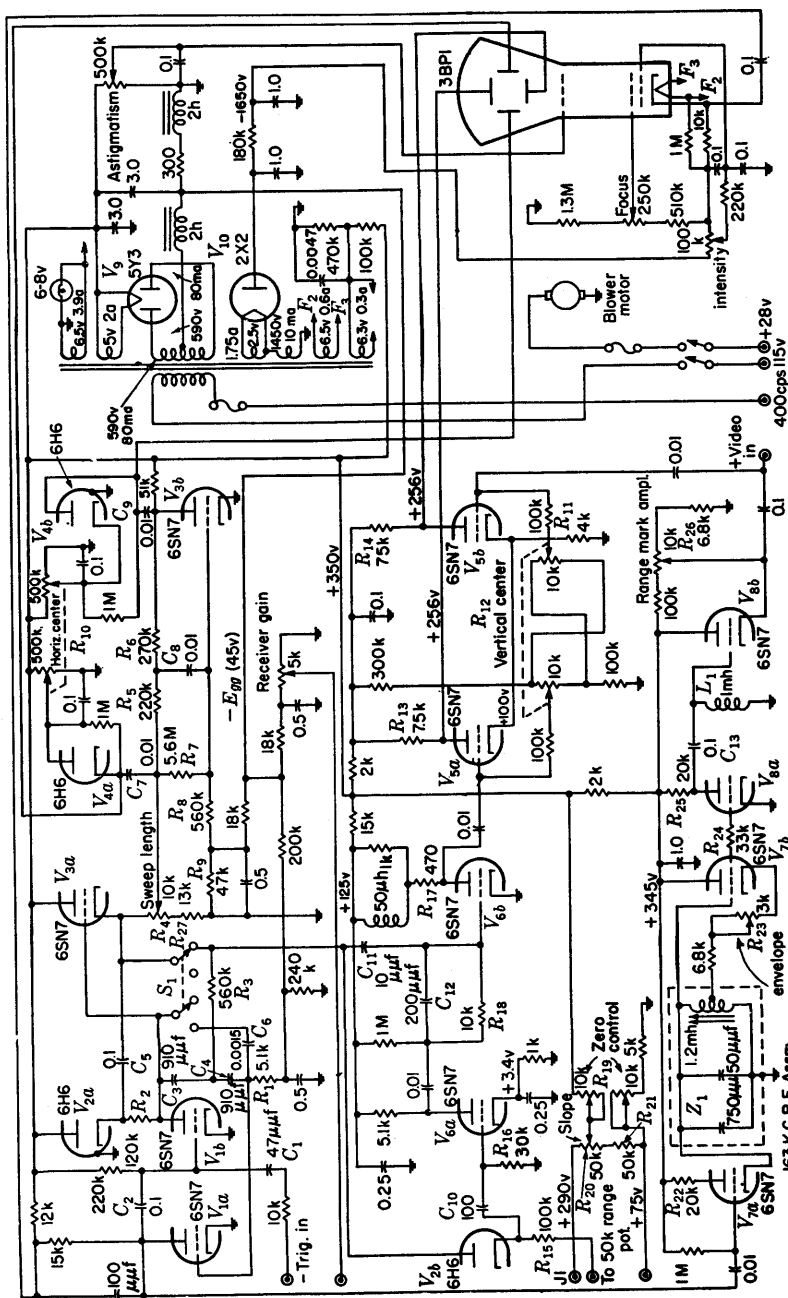


Fig. 7-39.—Circuit diagram Falcon M-scope (1D-93/APG-13A).

to cut off  $V_{1a}$  so that its plate rises again causing  $V_{1b}$  to conduct discharging  $C_3$  and  $C_4$  to their original state. The time constant  $R_2 \left( \frac{C_3 + C_4}{2} \right)$  is chosen so that the 263 volts of linear sawtooth will cover 36.6  $\mu\text{sec}$  or 6000 yd radar range as given by the formula  $dE/dt = E_{pp}/RC$  since  $E_{pp}$  is constant due to feedback.

$$\therefore C = \frac{E_{pp}}{E} \frac{t}{R} = 470 \mu\text{f.}$$

The sweep will stop at about 55  $\mu\text{sec}$  or 9000 yd. The control  $R_4$  is adjusted so that 49  $\mu\text{sec}$  or 8000 yd covers the face of the CRT. With  $S_1$  in the 24,000-yd position the tracking mark is removed and  $C_5$  switched in to give a 150- $\mu\text{sec}$  or 24,000-yd trace across the CRT. Part of the negative rectangular pulse on the plate of  $V_1$  is applied to the CRT cathode to turn on the beam during the sweep time. The sweep from  $R_4$  is applied to  $D_2$  of the CRT through  $C_7$ . It is also applied to the grid of  $V_{3b}$  through  $R_5$  and  $C_8$ . Feedback through  $R_6$  reduces the gain of  $V_{3b}$  to unity. Bias is provided by the resistance network  $R_7$ ,  $R_8$ , and  $R_9$ . This path also divides the signal applied to the grid of  $V_{3b}$  by an amount approximately equal to its gain so that only a small correction need be applied via  $C_8$ . This network keeps the biasing condition on  $V_{3b}$  nearly constant and independent of duty ratio since negligible voltage is built up across  $C_8$ . The output wave from  $V_{3b}$  is exactly the inverse of that appearing on  $D_2$  of the CRT. It is applied to  $D_1$  through  $C_9$  to give push-pull deflection. The diodes  $V_{4a}$  and  $V_{4b}$  are d-c restorers and prevent the shift in horizontal centering which would otherwise occur when the PRF changes or  $S_1$  is thrown. A dual potentiometer  $k_{10}$  is used to derive the centering voltages. The potentials applied to the two d-c restorers change in opposite directions when the control is moved. This produces a deflection of the trace and still keeps the mean potential of the deflecting system constant so that correct focus is maintained.

The video amplifier  $V_5$  is directly coupled to the vertical deflecting system ( $D_3$  and  $D_4$ ) and produces push-pull output by virtue of the large, common cathode resistor  $R_{11}$  when signals are applied to either grid. Vertical centering adjustment is obtained by  $R_{12}$  which inserts a differential bias between the two grids keeping the common cathode current constant. This produces a vertical displacement of the trace without altering the mean potential of the deflecting system. Each half of  $V_5$  draws 12.5 ma and produces a cathode voltage of +100 and a plate voltage of approximately +256 volts. Each plate resistor has a mean voltage drop of 94 volts. By reference to the published tube curves of the 6SN7 using a 7.5-k load line starting at +250 volts it is evident that 120 volts of deflecting potential are available from each tube and that

the differential gain between plates will be approximately 11. Since a large video deflection ( $\sim 2$  in.) is desired a push-pull video amplifier is necessary to prevent defocusing of the trace near the limits of deflection. The time constant of the video amplifier is given approximately by  $[C_{gp}(4\mu\text{f}) + 2 \times \text{capacity between deflecting plates } (10\mu\text{f}) + \text{strays } (10\mu\text{f})] \times R_{13}(7.5 \text{ k}) = 2.5 \times 10^{-7} \text{ sec}$ . The time of rise to 90 per cent  $\approx 3RC = 0.75 \mu\text{sec}$  which is barely adequate for the 0.75- $\mu\text{sec}$  pulse. (It is assumed that the grids are driven from a low-impedance source and that their motion is negligible.)

The section of the sawtooth producing the tracking step is selected by the diode  $V_{2b}$  which is biased by means of the 50-k range potentiometer at  $J_1$ . The plate of the diode is supplied from the cathode of  $V_{3a}$  rather than the grid. This introduces an additional uncertain potential in series with the clamped plate voltage of  $V_{1b}$  and the emission potential of the diode but it cannot be avoided since the loading imposed by  $R_{15}$  in parallel with  $(R_{16} + 1/pC_{10})^1$  would terminate the sweep on the CRT shortly after the appearance of the step. The selected portion of the sawtooth is "differentiated" by the 3- $\mu\text{sec}$  time constant  $R_{16}C_{10}$ . The drop across  $R_{16}$  during the rise of the selected sawtooth will be approximately  $E_R = RC dv/dt = 3 \times 10^{-6} \frac{260 \text{ volts}}{37 \times 10^{-6} \text{ sec}} = 21 \text{ volts}$ . Since  $V_6$

has approximately 3 volts of grid bias it is driven rapidly into the grid-current region so that the plate drops abruptly cutting off  $V_{6a}$ . The current in the plate resistor is cut off rapidly producing a step on the grid of the video amplifier  $V_{5a}$ . The speed with which the step rises is limited by the 0.25- $\mu\text{sec}$  time constant of the video amplifier which is slower than the rest of the circuit. Unfortunately the early portion of the sawtooth is also differentiated by the 4- $\mu\text{f}$  plate-to-cathode capacitance of  $V_{2b}$  before it conducts. This produces a step of

$$RC \frac{dv}{dt} = 3 \times 10^4 \times 4 \times 10^{-12} \times \frac{260}{37} \times 10^{-6} = 0.8 \text{ volts}$$

at the grid of  $V_{6a}$ . As the over-all gain is  $6 \times 0.6 \times 11 \approx 40$  a step of 32 volts would appear between  $D_3$  and  $D_4$ . Also the initial step of 16 volts at the start of the sawtooth would be nearly unattenuated, driving the video amplifier to saturation. A neutralizing condenser  $C_{11}$  differentiates the whole sawtooth and applies it to the grid of  $V_{6a}$  in opposite phase to the amplified signal due to the diode. The values of  $C_{11}$  and the mixing network  $C_{12}R_{18}$  are chosen experimentally to neutralize the effect of the diode capacity. It is not practical to calculate these values as their magnitudes depend upon the stray capacitance of the wiring. The step amplitude is given by

$$(I_p \text{ of } V_{6b}) \times R_{17} \times (\text{Gain of } V_5) = 14 \text{ ma} \times 470 \text{ ohms} \times 11 = 72 \text{ volts.}$$

<sup>1</sup> This notation is explained in Vol. 19, Chap. 2.

The CRT has a vertical-plate deflection sensitivity of 132 volts/in. at a voltage of  $-1800$ . It will be apparent that the total deflection is, therefore,

$$72 \text{ volts} \times \frac{1 \text{ in.}}{132 \text{ volts}} = 0.55 \text{ in.}$$

The system is normalized by the "zero" potentiometer  $R_{19}$  which adjusts the potential at the negative end of the range potentiometer and by the "slope" potentiometer  $R_{20}$  which adjusts the current through it. The zero potentiometer removes resistance from the top of the resistance network while adding it at the bottom so that the current in the resistance network is unchanged. Thus an adjustment of the zero does not change the slope. The slope control will change the total current although using  $R_{20} + R_{21}$  as a potentiometer reduces the effect. Therefore the zero control will have to be readjusted every time the slope control is changed.

Fixed range marks are provided by the pulsed oscillator. Normally 12.5 ma is flowing through the switch tube  $V_{7a}$  and the tuned circuit, being limited by  $R_{22}$ . The current is rapidly cut off by the negative gate from  $V_{1a}$ . The peak voltage of the first half cycle developed by the tuned circuit is given by

$$V = i \sqrt{\frac{2L}{C}} = 12.5 \times 10^{-3} \text{ amp} \times \sqrt{\frac{2 \times 1.2 \times 10^{-3} \text{ henries}}{8 \times 10^{-10} \text{ farads}}} = 21 \text{ volts.}$$

The feedback tube  $V_{7b}$  supplies a negative resistance that is adjusted by  $R_{23}$  to neutralize the damping due to the resistance of the coil and  $R_{24}$ , so maintaining the initial amplitude. The signal applied to the grid of  $V_{8a}$  consists of negative half cycles since the positive excursions of the sinusoid are limited by grid current drawn through  $R_{24}$ . The value of 33 k was chosen to be large compared to the diode impedance of the grid ( $\approx 500$  ohms) but small enough to introduce negligible time delay when shunted by the tube input capacitance. On positive half cycles 12.5 ma flows through  $V_{8a}$  being limited by  $R_{25}$ . The current is abruptly reduced at the start of the negative excursion of the sinusoid producing an overdamped oscillation in  $L_1$  which is tuned by stray capacitance. These pulses are about  $\frac{3}{4} \mu\text{sec}$  wide at one-half amplitude and are roughly symmetrical. The cathode follower  $V_{8b}$  applies the pulses to the grid of the video amplifier. The cathode follower has negligible effect on the video since it is biased near cutoff and the video input is positive. The amplitude of the range marks is adjusted by changing the bias of  $V_{8b}$  by means of  $R_{26}$ . Unfortunately moving this control produces a variable delay in the start of the range marks since it changes the portion of the mark selected.<sup>1</sup> The condenser  $C_{13}$  is made very large so that the average

<sup>1</sup> Better results would be obtained if the tube was always conducting slightly and  $R_{26}$  was inserted across  $L_1$  as a variable shunt.

plate voltage of  $V_{sa}$  changes negligibly during the time the pulsed oscillator is operating. If it were small the plate voltage and hence the pulse current would increase causing an increase in the amplitude of successive marker pulses. The tuned circuit  $Z_1$  is ruggedly made and temperature-compensated. The leads to the associated tubes are made as short and direct as possible. A change of  $5 \mu\text{mf}$  in the self-capacitance of  $V_7$  or in the stray capacitance (an extreme value) would produce a change of  $(\sqrt{805} - \sqrt{800})/\sqrt{800} = 0.3$  per cent in the oscillator period. This is the same order of magnitude as the expected change in the delay circuit with tube and wiring changes so that the fixed range-mark circuit cannot be considered to be a primary standard; it must be initially calibrated against a crystal-controlled circuit. The output pulses from the oscillator are brought into coincidence on successive cycles of the circular-sweep oscilloscope—for example, the TS-100/AP (see Vol. 21, Chap. 18). It is possible then to calibrate accurately this step.

It has been found by experiment that the properly spaced marks have a fixed error with respect to true radar range. This error is mainly introduced by the transmitter and receiver delays (see Chap. 3). It is removed by adding the magnitude of the error to the reading on the sight dial when setting the step on the 1000-yd mark during zero adjustment.

The power supplies used are unregulated as nearly perfect compensation is obtained for changes in line voltage. The voltage across the range potentiometer increases in direct proportion to the change in the slope of the sawtooth so that no slope error is introduced. The change in emission potential of the sweep-clamp and pickoff diode are in opposite directions and tend to cancel.<sup>1</sup> As all the tubes that draw heavy current are triodes and as grid bias is supplied from a series resistor in the negative lead of the power supply the change in grid bias just compensates the change in  $E_{pp}$ . The result is a change of less than 10 yd indicated range over a range of line voltage of 100 to 130 volts. The change in sweep length is also compensated by a corresponding change in deflection sensitivity of the CRT since the CRT supply voltage changes in direct proportion to line voltage. However, the trace length will change somewhat with the waveform of the a-c supply since the CRT supply has a condenser input filter and hence its d-c level is proportional to the peak of the input wave while  $E_{pp}$  is supplied from a choke-input filter so that it will be proportional to the average value of the input wave.

The range of pulse recurrence frequencies is from 20 to 1400 cps and negligible changes are produced in the functioning of the circuit. Above 1400 cps the sweep and gate circuit will divide frequency, because  $C_3$  and  $C_4$  will not have time to discharge and because  $C_5$  will not have time to

<sup>1</sup> Unfortunately the drift due to change in  $g_m$  of  $V_{sa}$  with  $E_A$  and  $E_{pp}$  is uncompensated but its effects are small, as the performance data show.

recharge through  $R_4 + R_{27}$ ,  $V_{3a}$  being cut off during this time. The extra charge in  $C_4$  due to the linearizing resistor  $R_3$  will not have time to leak off completely.

*Performance.*—The performance of the system is indicated by the following data:

- A. Linearity of delay  $\pm 0.2$  per cent limiting error
- B. Maximum change in indicated range (6000-yd scale)
  - 1. Line voltage changed 100 to 130 volts.  $\Delta R < 10$  yd
  - 2. Tubes changed in time modulator  $\Delta R \pm 60$  yd
- C. Peak tracking errors of average operator on well-defined target
  - 1. Stationary resetability  $\pm 5$  to 10 yd
  - 2. Steadily moving target (200 mph)  $\pm 15$  to 30 yd

**7-24. A/R-scope.**—A delayable expanded A-sweep, commonly known as an R-sweep is often used when it is necessary to measure the range of a moving signal with an accuracy greater than that obtainable on a full-range display. It may also be used to examine critically the amplitude and shape of a delayed signal. As mentioned previously it is possible to produce such a sweep by amplifying a portion of a slow time base. Instead of selecting a portion of a linear sawtooth covering the entire range of modulation, some circuits employ amplitude comparison to generate a movable pulse and then initiate a delayed fast sweep with this time-modulated pulse. The Dumont 256-B A/R Oscilloscope<sup>1</sup> is an example of this type of device. It was originally designed as a precision ranging attachment for the SCR-582 search radar but is now more generally used as a precision test and calibrating device.

As shown in the block diagram Fig. 7-40 either an internal or an external trigger may be used. The internal trigger is derived from a 81.94-kc/sec crystal oscillator. The output of the oscillator is peaked to produce 2000-yd range marks. These marks are also used to synchronize a blocking oscillator that divides by 5 to produce 10,000-yd marks. By suitable switching the marks may be applied, separately or mixed, to the CRT as deflection or intensity modulation along with the video. A further blocking oscillator divides the 10,000-yd marks to an adjustable PRF. As only simple division ratios are possible the PRF will vary in steps that are simple fractions of 16.4 kc/sec as the control is moved. Since a large division ratio is used (the PRF is adjustable from 80 to 2000 cps) the divider cannot be expected to count stably but may skip from one submultiple of 16.4 kc/sec to another. A coincidence between the divider pulse and one of the 2000-yd marks forms the actual trigger. The internal trigger generator therefore forms a series of very accurate range marks that are accurately locked in phase with a trigger of adjusta-

<sup>1</sup> A commercial model of this instrument is now available from the Allen B. Dumont Laboratories.

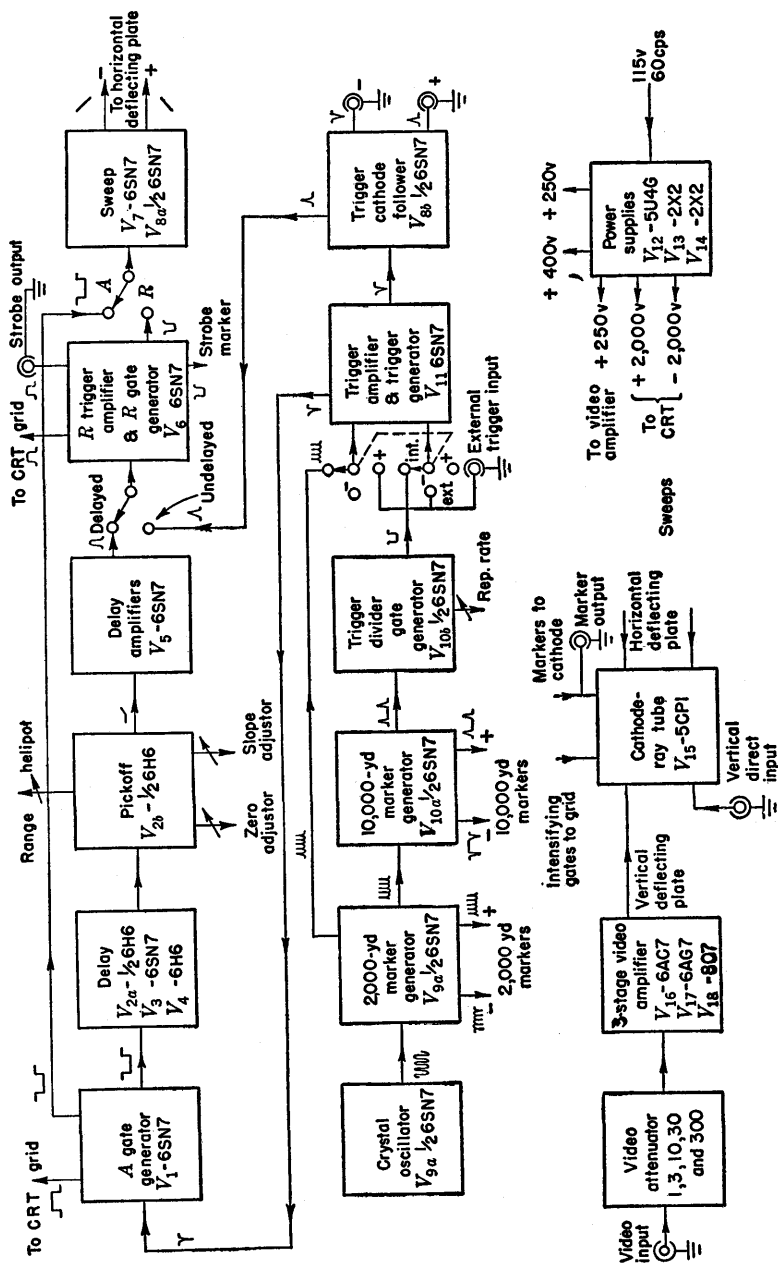


Fig. 7-40.—Block diagram of Dumont 256-B A/R oscilloscope.

ble PRF. The trigger and range marks are also available externally for synchronizing and calibrating other devices.

The internally or externally generated trigger is applied to the wide-gate multivibrator that is adjustable to cover the full range of 20,000 to 200,000 yd. The rectangular pulse from this multivibrator initiates the delay sawtooth that is formed in a "bootstrap" sawtooth generator. The sawtooth is picked off by an amplitude selector, is amplified, and triggers the 4000-yd R-gate blocking oscillator. This gate is available externally as an accurately delayed pulse and is also used to produce a bright mark or strobe on the A-sweep to facilitate in setting the R-sweep on a signal.

The push-pull sweep for the CRT is generated by another bootstrap sawtooth generator followed by a paraphase inverter. The time-base sawtooth is initiated and terminated by the wide gate when on the A-sweeps and by the R-gate when on the R-sweep. A-sweeps of 20,000, 200,000, and 400,000 yd and R-sweeps of 800, 2000, and 4000 yd are available. Part of the rectangular pulse generated by the A- or R-gate is used to intensify the CRT beam during the sweep.

A 3-stage video amplifier is included which has a rise or fall time of  $0.08 \mu\text{sec}$  and a 10 per cent drop at the end of a rectangular pulse of  $1000\text{-}\mu\text{sec}$  duration. An attenuator is provided which gives a deflection of  $\frac{3}{4}$  in. for 0.2, 0.6, 2.0, 6.0, and 20 volts input. (For complete specifications of this oscilloscope see Vol. 21, Chap. 18.)

Where used in conjunction with a radar set the R-gate or strobe is used to intensity-modulate the PPI producing an illuminated band which can be readily set on a selected signal. This signal will then appear on the R-display for critical examination.

As the A/R-scope has been normally used, measurement of the delay of the signal with respect to the trigger is made by setting the edge of the signal at the very beginning of the R-sweep. This method is not entirely satisfactory since the early part of the signal is not visible. If the video pulse is complex a view of the early part is most desirable when making a setting. An alternative method consists of placing a ruled grid or ink mark on the CRT and adjusting the delay with respect to this mark. The stability of this method is not very good since the horizontal centering may be changed by accident or by changes in PRF or line voltage since no d-c restoration or voltage stabilization is provided. A better method of measurement would be obtained if the R-gate were delayed 3 or  $4 \mu\text{sec}$  by means of a delay network and applied to the free vertical plate of the CRT. The leading edge of the gate would then appear as a step on the trace which could then be used for setting by juxtaposition.

The slope adjustment of the delay circuit may readily be made by reference to the crystal-controlled markers. If the radar system is triggered from the A/R-scope a  $4\text{-}\mu\text{sec}$  delay line can be inserted into the





trigger lead to make the transmitted pulse appear on the sweep. If the system supplies the trigger pulse, the delay line may be inserted in the video lead to delay the video until the timing circuits have started. By this means the zero delays of the radar system and the nonlinearity at minimum range may be calibrated out.<sup>1</sup>

*Detailed Circuit Description of the A/R-scope.*—A complete circuit diagram is shown in Fig. 7-41. A conventional triode crystal oscillator  $V_{9a}$  is operated biased in the Class C region so that pulses appear in the plate circuit. These pulses are separated from the sine wave appearing in the plate circuit by means of the transformer  $T_3$  that has an inductance that is small compared to that of the resonant circuit  $L_1C_{42}$ . The other two windings in the transformer are used as a blocking oscillator in conjunction with  $V_{9a}$ . Positive 2000-yd marks of about 50 volts amplitude and 1- $\mu$ sec duration are produced across the 68-ohm cathode resistor. These marks are used to synchronize the 10,000-yd-mark generator  $V_{10a}$ , which is a cathode-feedback blocking oscillator. The cathode-feedback type appears to be more stable than the conventional type (see Vol. 19, Chap. 6). The positive output from the 33-ohm cathode resistor is used to synchronize the trigger-divider blocking oscillator  $V_{10b}$ . This is of the grid-plate-cathode-coupled variety since it was found that pulses of sufficient duration could only be generated by this connection (see Vol. 19, Chap. 6). A negative 15- to 20- $\mu$ sec pulse is obtained from the 220-ohm resistor in series with the plate and is applied to the cathode of the trigger amplifier (time selector)  $V_{11a}$ . This pulse alone is not sufficient to permit plate current to flow. Positive 2000-yd marks from the cathode of  $V_{9a}$  are applied to the grid. The first mark appearing during the cathode pulse is selected and applied to the blocking oscillator  $V_{11b}$ . The output of  $V_{11b}$  is decoupled from the output circuit by the cathode-follower-phase-inverter  $V_{8b}$  that produces positive and negative triggers of about 100-volt amplitude and 1- $\mu$ sec duration.

The division ratios of the dividers are adjusted by the potentiometers  $R_{50}$  and  $R_{57}$  which form part of the grid time constants of the blocking oscillators.  $R_{50}$  is factory-preset while  $R_{57}$  is controlled from the front panel to produce PRF's from 80 to 400 pps when the 200,000-yd delay is used and from 80 to 2000 pps when the 20,000-yd delay is in use. Positive and negative range marks are both produced by the 2000-yd and 10,000-yd blocking oscillators and are selected by  $S_4$  for application to an external circuit and to the cathode of the CRT. When the positive 2000-yd marks are switched on, the 10,000-yd marks appear as negative overshoots on every fifth mark. This is due to back coupling through  $C_{46}$ .

<sup>1</sup> A suitable delay line in the General Electric type YE4B which in lengths of less than 4  $\mu$ sec produces negligible distortion of signals produced by receivers of less than 2 Mc/sec. video bandwidth. (See Vol. 17, Chap. 6 and Vol. 19, Chap. 22).

The first 10,000-yd mark appears at 8000 yd, the next at 18,000, etc. This is due to the fact that the trigger selector is synchronized by a 10,000-yd mark while the trigger is formed from the next 2000-yd mark.

When an external trigger is used, the trigger amplifier must be supplied with a sufficiently large positive pulse on its grid or negative pulse on its cathode to fire the blocking oscillator  $V_{11b}$ . The trigger must also rise steeply enough to induce sufficient voltage in the small inductance of  $T_6$  to initiate regeneration. An amplitude of 15 volts with a rate of rise not less than 100 volts/ $\mu$ sec. is the minimum permitted for stable operation.

The wide-gate generator  $V_1$  is a conventional monostable multivibrator with plate-to-grid coupling. This type of multivibrator was chosen because it is stable, is capable of rapid recovery, and gives a large negative rectangle with a fast leading edge to insure rapid cutoff of the sawtooth clamp  $V_{3a}$ . The wide gate is initiated by a negative trigger having a steep fall and a slow recovery from the grid time-constant circuit of  $V_{11b}$ . This trigger is coupled via  $C_5$  and insures reliable operation since the tail of the pulse rises too slowly in turn off the multivibrator. The "bootstrap" sawtooth generator ( $V_{2a}$ ,  $V_{3a}$ ,  $V_{3b}$ ,  $V_4$ ) producing the delay sawtooth uses a carefully temperature-compensated sweep network with manganin resistors and a combination of silver mica and negative-temperature coefficient condensers. A compensating network is used to make up for the lack of gain of  $V_{3b}$  and the loss of charge in  $C_{21}$  during the sweep. A resistor  $R_{11}$  is provided in the plate circuit of the clamp tube  $V_{3a}$  to adjust the quiescent voltage on the grid of the cathode follower  $V_{3b}$  so that this tube does not cut off during the recharging of  $C_{21}$ . Restoring diodes  $V_4$  are connected across the sweep-compensating resistors  $R_{12}$  and  $R_{13}$  to stabilize the voltage between the condensers and increase the permissible duty ratio. The amplitude selector  $V_{2b}$  is a diode biased by the range potentiometer. Although the same potentiometer is used on both range scales separate zero and slope controls are provided for each range. They are factory-preset and very rarely need adjustment although they should be checked if  $V_2$  or  $V_3$  is changed. The selected portion of the sawtooth is differentiated, amplified, and limited by  $V_5$  and  $V_{6b}$  and applied to the blocking-oscillator R-gate generator,  $V_{6a}$ . Like the trigger divider, this blocking oscillator uses a transformer  $T_2$  with grid, plate, and cathode windings since it must produce a 4000-yd pulse and yet use a transformer capable of giving reasonable rates of rise. When an undelayed expanded sweep is desired, the R-gate blocking oscillator can be triggered directly from the trigger input through  $S_2$ . A positive gate is applied to the grid of the CRT through  $S_{1c}$  from the positive-going plate of the wide-gate generator or from the cathode of the R-gate blocking

oscillator. The negative pulse from the blocking oscillator  $V_{6a}$  is used to cut off the sweep clamp  $V_{7b}$  and to produce the negative marking pulse (strobe) on the A-sweep or external PPI. The sweep generator is similar to the delay-sawtooth generator except that special provisions have not been made to insure accurate level setting and good linearity. The compensating network has been omitted and the recharging diode has been replaced by a resistor  $R_{38}$ . As a result the sweep speed will change with duty ratio but the effect is unimportant since the accuracy of measurement does not depend directly upon the speed of the CRT trace. The grid of the paraphase inverter  $V_{7a}$  is supplied by a signal from the sweep generator through  $C_{41}$  and feedback is supplied through  $C_{42}$  to hold the gain exactly equal to unity. Bias is supplied through a resistive divider that passes the low-frequency components of the sweep waveform since it has a d-c attenuation approximately equal to the gain of the tube.

Video is applied directly to one of the CRT deflecting plates or through the video amplifier depending upon the position of  $S_6$ . The video attenuator is switched by means of  $S_6$  and is of the resistance-capacity type so that its characteristics are independent of frequency. It presents a nearly constant load of approximately 1 megohm. Video input may be supplied through a properly terminated cable of any length without impairing the frequency response. If the cable is not terminated it must be used in conjunction with a capacity-divider probe or must be an open wire line. The amplifier is conventional, using shunt compensation in the first and second stages and series-shunt compensation in the output. The frequency response is flat from about 100 cps to several megacycles. It is down 3 db at 7 Mc/sec and 6 db at 10 Mc/sec. Bias for the video amplifier is obtained from part of the CRT-supply divider.

Since the timing circuits are self-compensating for changes in supply voltage, unregulated power supplies are used. The indicated range varies less than 0.1 per cent of full scale for a  $\pm 10$  per cent change in supply voltage. As bleeder bias is used in all circuits but the video amplifier some economy in power consumption might be brought about by the use of a negative supply.

The sawtooth delay circuit will operate with less than 0.1 per cent change in indicated range up to about a 50 per cent duty ratio after which errors appear since  $C_6$ , the sweep network, and  $C_{21}$ , do not have sufficient time to discharge. When the internal PRF generator is used, the duty ratio is limited to a safe value. On external triggers when duty ratio becomes greater than about 90 per cent the wide-gate multivibrator divides the frequency. This is particularly convenient as it permits the viewing of the next trigger pulse on the 400,000-yd sweep.

*Accuracy.*—A pulse rising in  $0.5 \mu\text{sec}$  may be reset at the start of the 800-yd delayed sweep within  $\pm 10$  yd. The delay circuits are linear to

within  $\pm 0.1$  per cent of the total delay and the zero point is stable to within  $\pm 0.1$  per cent of total delay for several days after calibration in spite of line voltage changes of  $\pm 10$  per cent. For accurate following of moving targets the range control should be operated by the aided or regenerative methods.

**7-25. A-scope Presentation Used in British CMH System.**—This device produces a normal type A presentation covering 40 miles on the CRT.<sup>1</sup> The display, however, contains a continuously variable expanded portion that covers about two tenths of the tube face and has a duration of about 4  $\mu$ sec. In the center of the expanded portion is an accurate range mark consisting of a notch of 2- $\mu$ sec duration having a leading edge with a fall of 0.2  $\mu$ sec. The signal is matched with the leading edge of the notch by juxtaposition. The expanded sweep and notch are moved continuously by means of a two-scale range circuit having an accuracy of about  $\pm 15$  yd.

The system is externally synchronized, and the timing waveform is obtained by use of a pulsed crystal oscillator and phase shifter so that external calibration is unnecessary.

*Circuit Description of CMH A-scope.*—Referring to Fig. 7-42, a positive trigger is amplified by  $V_3$  cutting off the sweep clamp tube  $V_5$ . The screen circuit of  $V_5$  and  $V_4$  form a multivibrator that holds  $V_5$  cut off for the duration of the sweep. Condenser  $C_1$  recharges through  $R_1$  and causes  $V_5$  to conduct after a time equivalent to 40,000 yd, cutting off  $V_4$  and returning the multivibrator to its initial condition. The time constant  $R_2C_2$  is long enough to hold  $V_4$  off during the waiting period associated with any expected PRF.

Initially when  $V_5$  is bottomed,  $V_6$  is drawing current through  $V_5$  and through the range potentiometer from the +1.2-kv supply. When  $V_5$  is cut off the cathode degeneration in  $V_6$  causes it to draw constant current charging  $C$  at a constant rate and producing a linear sawtooth. The impedance presented by the cathode circuit  $V_6$  is about 50 megohms. Only 100 volts of sweep is used before  $V_5$  is again switched on. This sweep is accurately linear but of small amplitude compared with current practice, since it must be stable to within better than 1 part in 120 (120 cycles of the oscillator represent full range). The bottoming of  $V_5$  may vary  $\pm 0.5$  volt (1 part in 200) with age and heater variation which leaves a very narrow margin of safety.

The sweep is amplified by  $V_7$  and  $V_8$ , applied to one horizontal plate of the CRT, and gives the slow sweep. The sweep amplitude is stabilized by cathode degeneration in  $V_7$  and  $V_8$ . The 300- $\mu$ f condenser in the cathode of  $V_8$  is used to compensate stray capacities in the anode circuit

<sup>1</sup> A Pulsed Crystal Oscillator Circuit for Radar Ranging J. D. Mynall, I.E.E. Convention Paper, March, 1946.

Fig. 7.42.—British CMH range circuit, type A presentation.

permitting rapid starting of the sweep. Part of the screen pulse of  $V_5$  is used to intensify the trace on the CRT.

The start of the expanded portion of the sweep is determined by the amplitude selector  $V_9$ ,  $V_{10}$ . This is a differential amplifier having a very large cathode resistor drawing current from the  $-5$ -kv CRT supply. Thus the two tubes are supplied from a nearly constant-current source and the current drawn by each tube is dependent only on the difference between their grid potentials and not upon the common level of both grids. The output of the range potentiometer is applied to the grid of  $V_{10}$  while the sawtooth from  $V_6$  is added to square waves derived from the output of the phase shifter in the fine scale and the sum is applied to the grid of  $V_9$ . When the voltage on the grid of  $V_9$  becomes nearly equal to that of the grid of  $V_{10}$  current shifts from  $V_{10}$  to  $V_9$ . This action is speeded by condenser coupling from the plate of  $V_9$  to the grid of  $V_{10}$  causing the two tubes to behave as a cathode-coupled multivibrator. The positive step on the plate of  $V_{10}$  causes  $V_{11}$  to conduct, cutting off the fast-sweep clamp  $V_{12}$ . The plate potential of  $V_{12}$  rises exponentially toward  $+1.2$  kv and is caught by  $V_{13}$  after rising to  $+250$  volts. This 250-volt sawtooth is applied to the other horizontal plate of the CRT causing the rapid sweep. To assist in target selection the sweep may be slowed by a factor of 10 by depressing a push button which inserts an additional capacitor in the sweep circuit.

Considering now the generation of the timing wave for the fine scale, part of the negative gate produced in the plate circuit of  $V_4$  is applied to the grid of  $V_{14}$ . Cutting off  $V_{14}$  produces a transient in the crystal driving transformer. The transient excites the crystal which oscillates at 279.43 kc/sec or 3 cycles per mile. The oscillations of the crystal are amplified by  $V_{15}$ , the initiating transient being balanced out by applying an adjustable portion of it to the grid of  $V_{15}$  in opposite phase. At the end of 120 oscillations the gate pulse ends causing  $V_{14}$  to conduct and closing the negative-feedback path from  $V_{15}$  back to  $V_{14}$ . The negative feedback stops the crystal after several cycles. The pulsed oscillations in  $V_{15}$  are amplified by  $V_{16}$  which produces a current in the transformer proportional to the voltage on its grid since it has cathode degeneration. The output of the transformer drives the stator windings of the goniometer through phase-splitting networks. Since the goniometer is inductive, resistance is inserted in series with one stator coil to produce a  $45^\circ$  lagging current. Enough resistance and capacitance is inserted in series with the other coil to produce a  $45^\circ$  leading current. Thus the two fields are in quadrature. The transient response is sufficiently good that steady-state conditions are reached well within the minimum range (3 cycles).

The goniometer is geared to the coarse range potentiometer with a 144





to 1 ratio so that the wave train from the goniometer and the picked-off sawtooth voltage advance in synchronism as the range handwheel is turned. The sinusoidal output of  $V_{17}$  is converted to a square wave on the grid of  $V_{19}$  by the limiting action of grid current in  $V_{19}$  and the diode  $V_{18}$ . The waveform at the cathode of  $V_{19}$  is added to the coarse range sawtooth waveform and the combined waveform used to actuate the amplitude selector  $V_9$ ,  $V_{10}$ . Tubes  $V_{19}$  and  $V_{20}$  form a parallel coincidence circuit (time selector). The step produced by  $V_9$ ,  $V_{10}$  is amplified by  $V_{11}$  and shock-excites a critically damped tuned circuit in the grid circuit of  $V_{20}$ . This pulse is timed to select the ensuing negative half cycle on the grid of  $V_{19}$  when current is cut off in both  $V_{19}$  and  $V_{20}$  causing the plate potential to rise until caught by the diode  $V_{21}$ . This pulse is inverted by  $V_{22}$  and forms the range "notch" on the CRT. It is also used as a gate for the angle-following circuits.

*Modification including sine-wave tracking.*—Since it was not possible to obtain coarse range potentiometers of sufficient accuracy during the early part of the War the sine-wave tracking circuit shown in Fig 7-43 was adopted for the production equipment. (For a complete discussion of sine-wave tracking see Chap. 6.) The positive range mark from the cathode of  $V_{22}$  is applied to the anode of the time discriminator  $V_6$ . The step produced in the plate circuit of  $V_{11}$  shock-excites a tuned circuit in the grid of  $V_6$  producing a 4- $\mu$ sec negative pulse. The positive overshoot of this pulse permits plate current to flow if the marker is applied simultaneously to the plate circuit. The rectified current resulting from the overlap of these pulses is applied to the Miller integrator  $V_7$  through a phase-advance network. The output of  $V_7$  is then applied to the grid of  $V_{10}$  in place of the output of the coarse range potentiometer. The feedback loop then holds this voltage so that the two pulses partially overlap. The sawtooth pulse is synchronized with the desired cycle of the phase shifter by cranking to zero range, when a switch automatically operates to raise the cathode potential of  $V_6$  bringing the selector pulse into zero range. Momentary failure of power which might cause the selector to lock on the wrong cycle also opens a latching relay which interrupts the CRT supply. The trace on the CRT can be restored only by cranking to zero range which resets the range circuit and reapplies the CRT potential.

Although far advanced for its time the equipment does not represent the best current design practice in that rather excessive potentials are applied to receiving-type tubes. By use of the present types of sawtooth generators 150 to 200 volts of accurately linear sawtooth voltage can be obtained from a 250-volt supply without recourse to + 1.2 kv. A diode amplitude selector would eliminate the use of the - 5-kv supply for anything but the CRT. The type A presentation with an expanded section is somewhat confusing to use and separate A- and R-traces would be prefer-

able. These may be obtained on separate CRT's, or on a single CRT, by using electronic switching or a double-gun tube.

**7-26. Systems Using a J-scope with a PPI or B-scope.**—Several systems have been developed which use a J-scope with a movable mechanical mark for accurate following and a B-scope or PPI to give angular information and to present the full range scale. The J-scope gate is used to produce an illuminated band on the full range display to permit target acquisition. These systems are distinguished for their electrical simplicity and reliability. A typical example is provided by the indicator circuit of the Hand Radar Set. (See Sec. 2-16.)

The indicator circuits of this equipment are shown in Fig 7-44. The timing standard is a crystal oscillator  $V_{1a}$  using a reactive load ( $L_1, C_1$ ) in the cathode circuit which maintains oscillation over a wide range of adjustment of the plate-tuned circuit. The tuning of the plate circuit adjusts the diameter of the circle on the J-scope. The secondaries of the plate transformer  $T_1$  are much less than critically coupled to the primary and tuned to obtain quadrature voltage for the CRT deflecting plates.

Since the oscillator operates in Class C, pulses of plate current appear in the primary of the pulse transformer  $T_2$ . The other two windings of the transformer in conjunction with  $V_{1b}$  form a blocking oscillator which divides the original 81.94 kc by five and produces 10,000-yd range marks. The plate waveform of  $V_{1b}$  is used to synchronize the PRF divider blocking oscillator  $V_{2a}$ . This divider counts down to an adjustable PRF in the neighborhood of 400 pps. Unlike the A/R-scope the output of this divider is used directly to form the trigger for the system. Since no trigger selection circuit is used the trigger may drift phase  $\pm \frac{1}{4} \mu\text{sec}$  with respect to the circular sweep if the divider adjustments,  $R_1$  and  $R_2$ , are changed. The cathode follower  $V_{2b}$  is used to prevent loading of the blocking oscillator.

The trigger from  $V_{2b}$  is used to key the radar transmitter and to initiate the wide gate produced by the cathode-coupled multivibrator  $V_3$ . The negative-going rectangle produced by this multivibrator is used to initiate and to terminate the 50,000-yd linear sweep for the B-scope. This sweep is produced by cutting off plate current in  $V_{6a}$  which interrupts the current in  $L_2$  which is tuned by  $C_2$  and  $C_3$ . The sweep consists of a small portion of the damped oscillation produced by this circuit and is quite linear. (For discussion of the LCR-sweep see Vol. 19, Chap. 7.)

This sweep is applied to one of the vertical plates of the B-scope  $V_9$  and is inverted by  $V_{6b}$  and applied to the other vertical plate to give symmetrical deflection. The capacity divider ( $C_2, C_3$ ) is used to attenuate the sweep by an amount equal to the gain of  $V_{6b}$ . This arrangement is not so satisfactory as the feedback sweep inverters used in Falcon and the



A/R-scope since the sweep output will be directly proportional to the gain of  $V_{6b}$ . A horizontal sweep proportional to the azimuth or elevation angle of the antenna is supplied to the horizontal plates of  $V_9$  from the potentiometer  $R_3$  or  $R_4$  via the deflecting amplifier  $V_7$ . The azimuth and elevation potentiometers are mounted directly on the antenna axes. The azimuth potentiometer is driven by a mechanism that causes it to repeat its reading for each quadrant of azimuth.

Part of the positive-going wave at the plate of  $V_{3b}$  is applied to the grid of  $V_9$  to illuminate the trace. The positive gate is also differentiated and used to trigger the narrow-gate delay multivibrator  $V_4$  which is also of the cathode-coupled type. This multivibrator must be triggered from a pulse of greater duration than its own to avoid being triggered back by the termination of the trigger pulse. Care has been taken in the design of the delay multivibrator to secure maximum stability and linearity of its pulse width as a function of the voltage supplied by the range potentiometer  $R_5$ .

The narrow gate that illuminates the J-scope is obtained from the cathode-coupled multivibrator  $V_5$ . This multivibrator is normally triggered by differentiating the end of the rectangular pulse produced in the plate circuit of  $V_{4a}$ . The gate is connected to the grid of  $V_8$  and should remain symmetrical about the position of the mechanical cursor within  $\pm \frac{1}{4}$  circle throughout the tracking range. This means a stability of the multivibrator  $V_4$  of  $\pm 1$  per cent is required. The narrow-gate pulse is initiated by the rise of the positive wide-gate pulse from the plate of  $V_{3b}$  when approaching zero range. This is accomplished by throwing  $S_1$ . The band marking the position of the narrow gate on the B-scope is produced by mixing part of the narrow-gate pulse with the wide-gate pulse in the common plate resistor.

Negative video is applied directly to the radial deflecting electrode of the J-scope through the condenser  $C_4$  and to the cathode of the B-scope through  $C_5$  and the attenuator  $R_7$ ,  $R_8$ ,  $R_9$ . Mixed 2000- and 10,000-yd range marks are obtained from the common plate resistor of the blocking oscillators ( $R_{10}$ ) through  $S_2$  and  $C_6$  and mixed with the video across  $R_9$ .

An exploded view of a mechanical tracking system similar to that used in the HR is shown in Fig. 7-45. A ring gear containing a transparent plastic dial is mounted in front of the J-scope. This gear is driven through a one-to-one gear by the handwheel which also drives the range potentiometer  $R_5$  through a 25 to 1 gear reduction. The total range is indicated on a counter geared to the handwheel. The zero and slope controls  $R_{11}$  and  $R_{12}$  are used to adjust the illuminated portion of the trace so that it is correctly centered with respect to the scribed cursor on the Plexiglas disk. The microswitch  $S_1$  is operated by a cam on the

50,000-yd-per-turn shaft and sets the gate at zero range when the minimum range of the delay multivibrator is approached.

Several features of the circuit are worthy of note. All tubes used are of a single type, the 6SN7 dual triode. One type of blocking oscillator and one type of multivibrator are used to generate all pulses. All necessary adjustments can be made by observation of the J- and B-scopes.

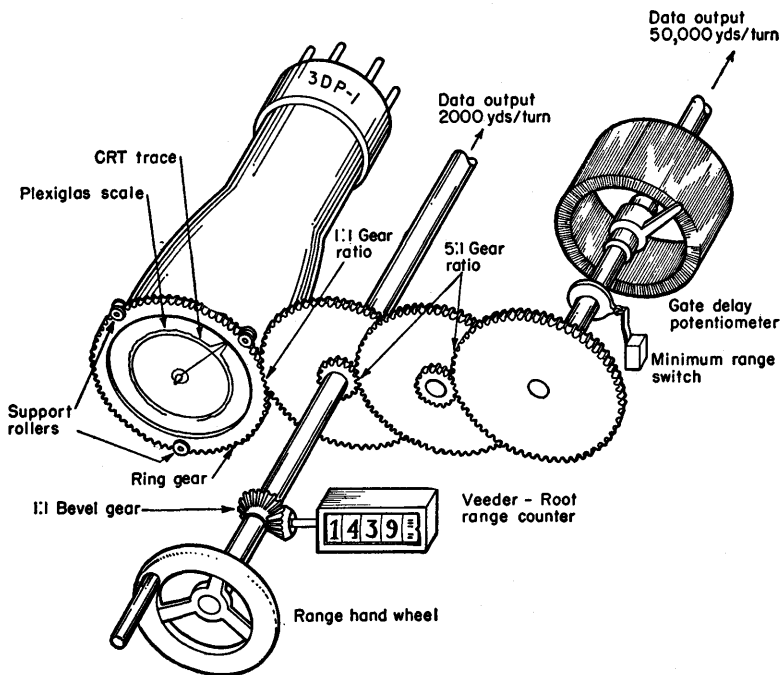


FIG. 7-45.—Mechanical drive used with J-scope.

An improvement would be a replacement of the coarse scale by a more stable circuit and the inclusion of time selection of the PRF trigger.

The accuracy of the system can be summarized in the following manner.

1. The drift in the crystal oscillator frequency should not exceed  $\pm 15$  cps. This amount would produce an error of  $\pm 10$  yd at 50,000 yd.
2. The  $\pm 0.25$ - $\mu$ sec phase drift in the frequency divider can produce an error of  $\pm 40$  yd.
3. An operator can reset the cursor a 2000-yd circular sweep to  $\pm 10$  yd on stationary targets and  $\pm 15$  to 20 yd on a target moving at a constant rate.

## TRACKING WITH INTERMITTENT DATA

**7-27. Aided Tracking with Intermittent Data.**—A very simple device that moves a range mark on a range-angle display is the ballistic computer, AN/APA-30. Like the AN/APG-13A it is used to deflect a gun-sight as a function of slant range. It is used as an attachment to the

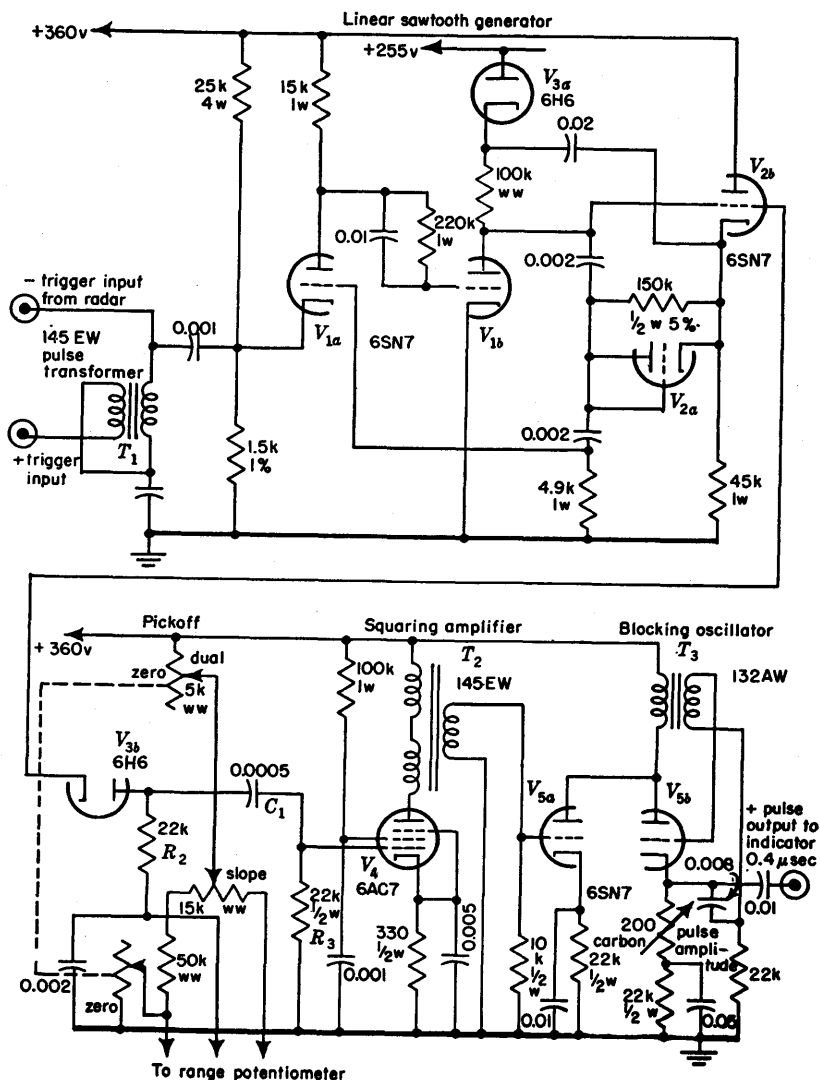


FIG. 7-46.—Aided-tracking mechanism, AN/APA-30. (Range circuits.)

search radar (AN/APS-3, AN/APS-4, or AN/APS-10). The tracking is done on the indicator furnished with the radar, a B-scope or PPI. The range line is produced by mixing a  $\frac{1}{2}$ - $\mu$ sec-delayed pulse derived from the tracking device with the radar video. Figures 7-46 and 7-47 show a schematic diagram of the device. A trigger from the radar operates the self-sustaining linear sawtooth generator,  $V_1$ ,  $V_2$ ,  $V_3$  which operates in a manner identical with that of AN/APG-13. A 250-volt sawtooth can be produced of which about 200 volts are linear and represent

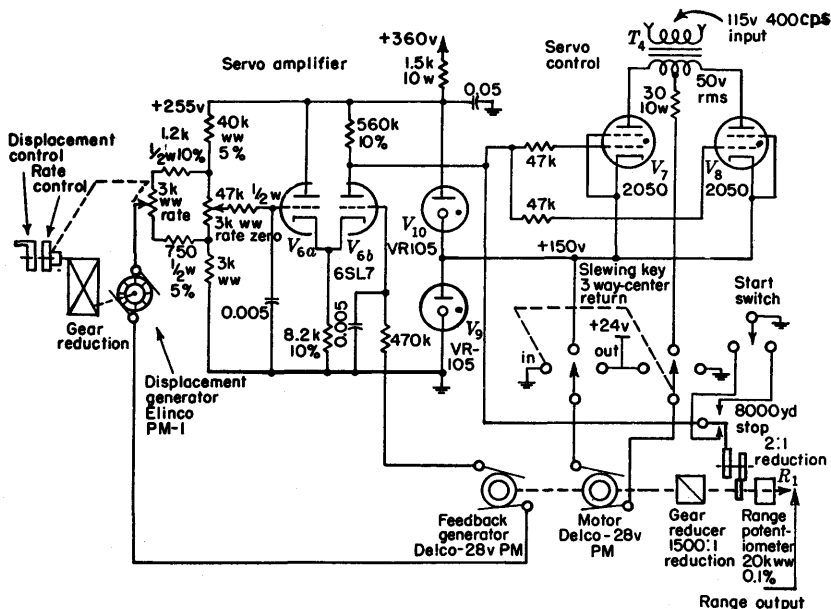


FIG. 7-47.—Aided-tracking mechanism, AN/APA-30. (Speed servomechanism.)

10,000 yd. The amplitude-selector diode  $V_{3b}$  is biased by the range potentiometer which is connected to the aided-tracking mechanism. The loading imposed by  $R_2$ ,  $C_1$ , and  $R_3$  terminates the sweep soon after selection has been accomplished. The selected portion is partly differentiated by  $R_3C_1$ , amplified by  $V_4$ , inverted by  $T_2$ , and applied to the driver amplifier  $V_{5a}$  which fires the blocking oscillator  $V_{5b}$ . A positive 0.4- $\mu$ sec pulse having a maximum amplitude of 50 volts is produced in the cathode of  $V_{5b}$  and is mixed with the radar video in the radar indicator. The cathode current pulse is used because it has no overshoot which would cause blanking of the indicator trace and consequent obscuration of the video signal.

The gun-sight and control unit are shown in Fig. 7-48. The range-tracking potentiometer is mounted in the gun sight and turned through a

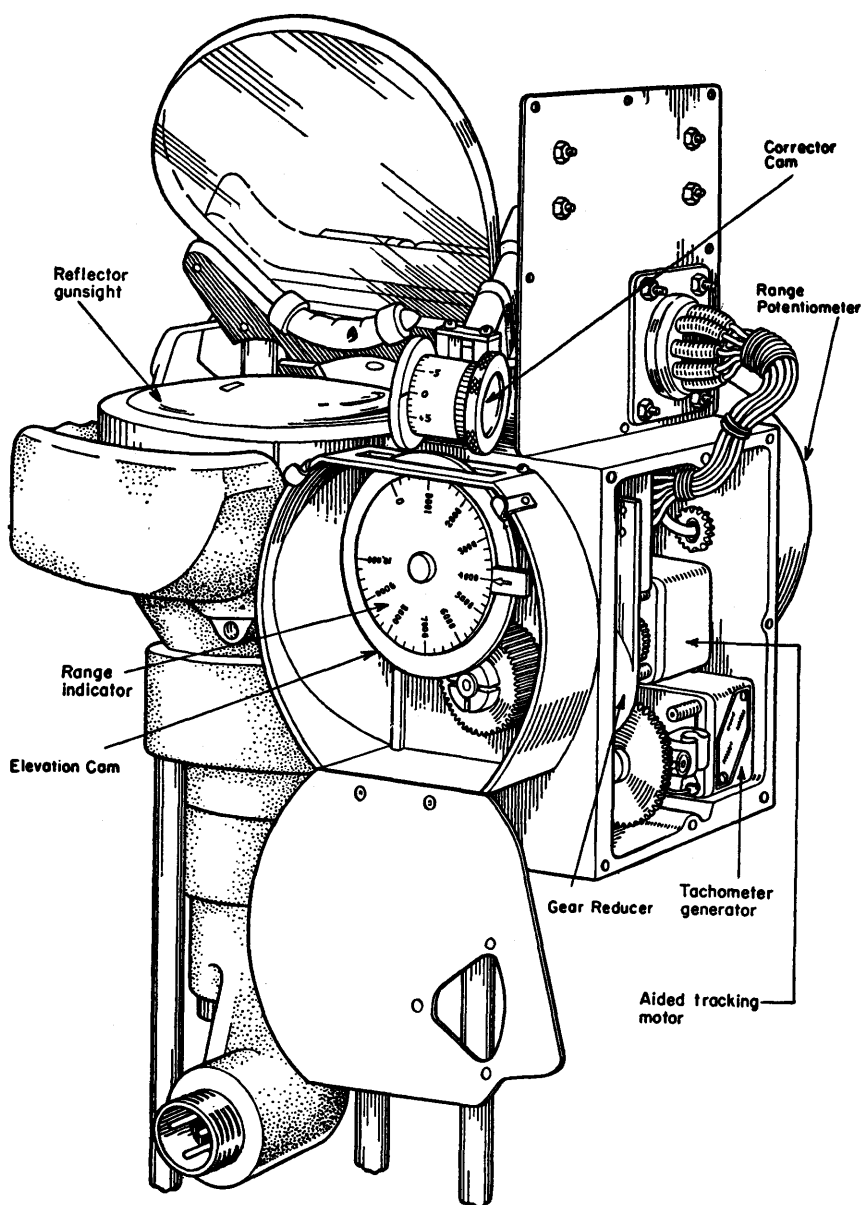


FIG. 7-48a.—Gun-sight unit of AN/APA-30.



large gear reduction by means of a miniature 28-volt permanent-magnet field motor. Power for the motor is supplied from the full-wave thyatron grid-controlled rectifier  $V_7$ ,  $V_8$  (see Fig. 7.47). The thyatrons are capable of supplying 0.5 amp d-c to the motor. The speed of the motor is controlled by the grid voltage applied to the thyatrons which changes the average amount of time during which they conduct. The grid voltage is supplied from the d-c amplifier  $V_6$  which is driven by the difference between the potential supplied by the rate potentiometer and that supplied by the two tachometer generators. The velocity feedback loop

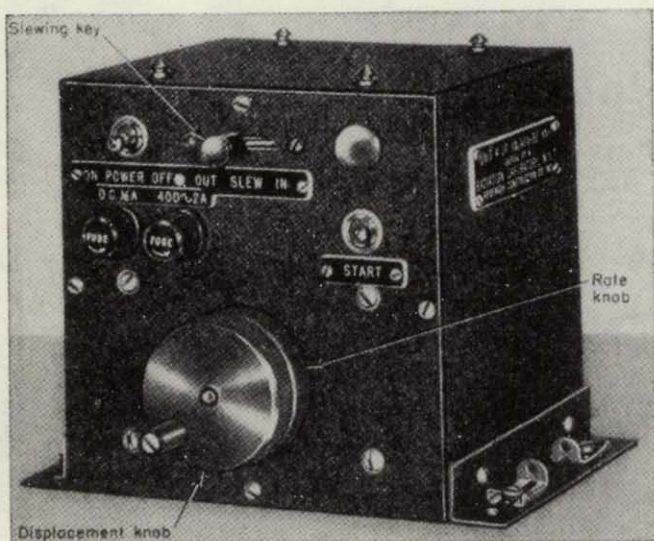


FIG. 7.48b.—Control unit of AN/APA-30.

operates in the following manner (see also Vol. 21, Chap. 14). A voltage difference between the grids of  $V_6$  is produced by the rate potentiometer. This voltage, when amplified, causes the thyatrons to conduct and energizes the motor. The motor drives the feedback generator which produces an output potential proportional to velocity. When this potential is nearly equal to that produced by the rate potentiometer, the thyatrons are cut off, slowing the motor. The motor then runs at such a speed that the thyatrons are conducting only part of the time. Since the rate potentiometer and the feedback generator are both linear, the speed is a linear function of the potentiometer position.

The displacement generator produces a voltage proportional to the rate of change of the hand-crank displacement. The feedback generator produces a voltage proportional to the rate of change of the range-shaft displacement. These two voltages are added algebraically, causing the

motor to run to hold them equal. The displacement of the range shaft is therefore proportional to the displacement of the hand crank. The displacement generator and rate potentiometer are driven by coaxial knobs which may be "double-gripped." The ratio of displacement to rate is chosen to give a time constant of about 2 sec which is the scanning period of the radar. Thus a correction can be made every scan while getting on target. To achieve this time constant with reasonably small displacements of the tracking controls, speed of slewing has been sacrificed. A slewing key is provided for easy target acquisition. The key has three positions with center return. The center position causes normal operation. The other positions apply 24 volts to the motor causing it to run inward or outward at full speed. An additional aid to the operator is the automatic stop switch. When tracking is complete the motor continues to run until the slide of the potentiometer has passed over the end of the winding and has brought the mark out again to the extreme range. At 8000 yd a cam opens a switch, grounding the grids of the thyratrons and stopping the motor. When the next target approaches, the operator has only to wait until the target touches the tracking mark and throw the start switch. The tracking mechanism starts immediately with nearly the correct displacement and rate.

The design of the equipment is simple and it could easily be modified to fit other applications in which smooth following and an accuracy of  $\pm 0.25$  per cent of full scale are desired.

**7-28. Two-coordinate Tracking. Ground-position Indicator.**—Often the target has characteristic or predictable motion, and a great simplification of the difficulties of two-coordinate tracking may be achieved by taking advantage of this information in a regenerative tracking system. For example, if one is flying in an airplane and it is desired to track an object located on the ground in two coordinates, for example, north-south and east-west distances, one can make use of the approximately known north-south and east-west components of its position which can be obtained by integrating the components of its instantaneous velocity. This information is readily available in air-position indicators (for example, the Bendix Air-position Indicator). This information may then be added to the output of two aided-tracking mechanisms in order to indicate continuously the position of a particular object (see Vol. 21 Chap. 7).

In other applications it is desired to stabilize the PPI display against the motion of the aircraft to give a representation of a stationary ground with the origin of the sweep representing the moving aircraft instead of the usual picture which indicates at its center the stationary aircraft with the earth moving past it. An example of a practical system for accomplishing this is shown in Fig. 7-49.

A d-c generator is turned by a Bendix air-mileage unit at a speed

proportional to true airspeed. The air-speed potential derived from it is resolved by means of a sine-cosine potentiometer into north-south and east-west components of air speed. Since the N-S and E-W channels are identical, only the N-S channel will be described. A manually controlled potential is added to the N-S component of air speed as a velocity correction. If the equipment is correctly calibrated this potential representing the difference between air speed and ground speed is equal to the

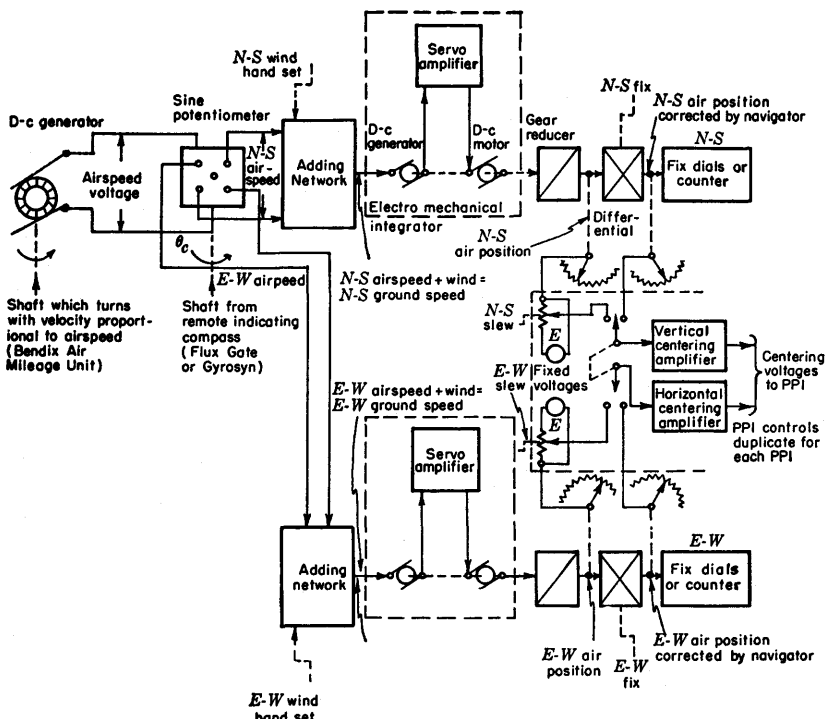
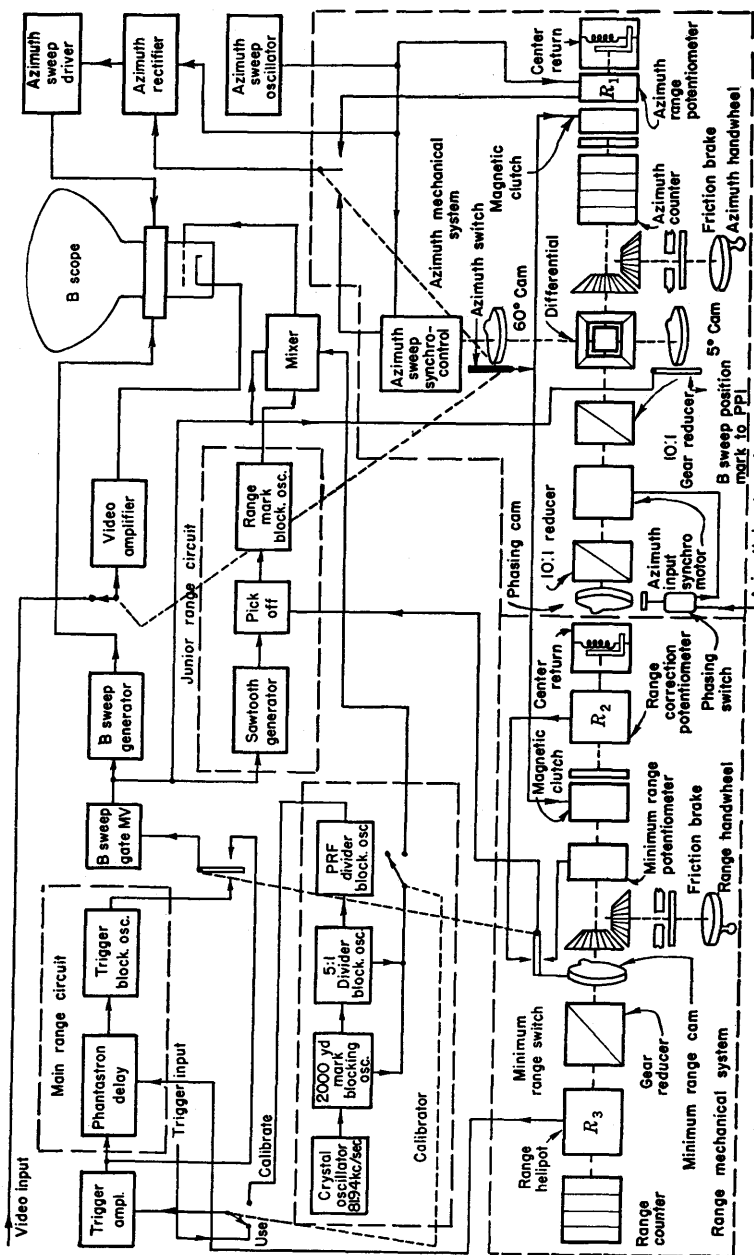


Fig. 7-49.—Simplified GPI used to stop motion of ground on airborne PPI's.

N-S component of wind. The sum of N-S air speed and N-S wind is then integrated by means of an electromechanical integrator (velocity servomechanism) to give N-S ground position. The constant of integration in the form of a fix on some identifiable object is added through a differential. The navigator's fix dials read N-S and E-W distance with respect to some convenient reference point in the area to be patrolled. As the plane changes speed or direction, the N-S and E-W components of ground speed change accordingly, so that if position and wind have been entered into the computer, the fix dials will read the position of the plane from the reference point at all times. Position data are taken from poten-



**data (10 speed) from antenna synchro**

tiometers on the outputs of the air-speed integrator. Two sets of potentiometers are provided.

In some cases it may be desirable to stabilize a number of PPI patterns with respect to different geographical points, and, as the diagram indicates, it is possible for the different PPI's to have individual constants

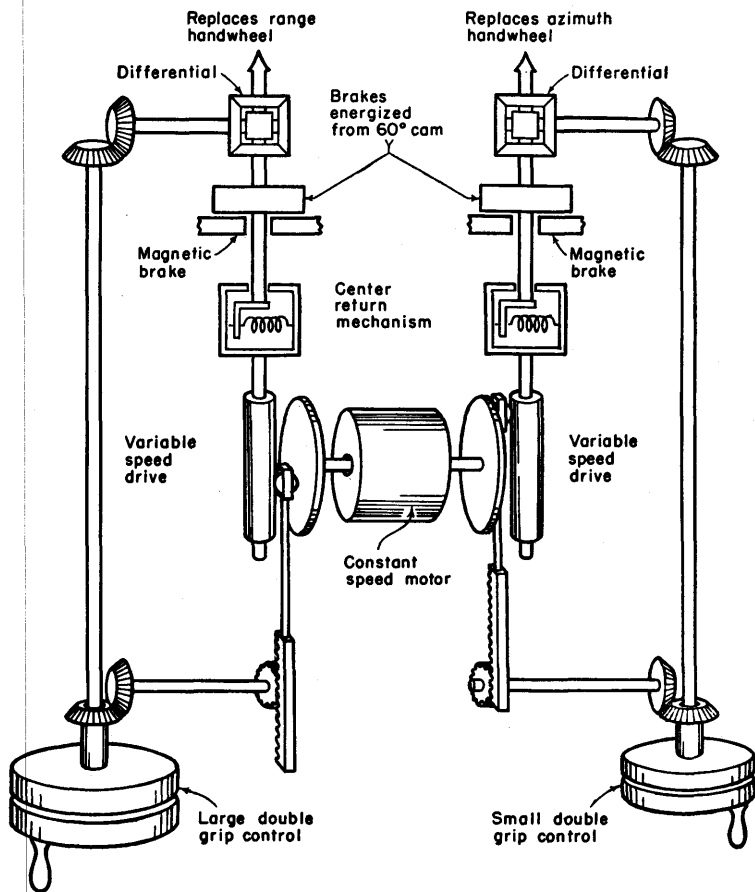


FIG. 7-51.—Aided-tracking machine suitable for precision B-scope.

of integration added by means of a pair of potentiometers which will then refer the displays to particular geographical points. Another set of potentiometers is driven on the same shaft as the fix dials, and in this way any recent correction to the navigational data may be added to all the displays.

The outputs of the potentiometers are amplified, changed to the correct impedance level, and applied to the horizontal and vertical centering

controls of the PPI's. The PPI's themselves then convert the data back to polar coordinates by the influence of the deflecting fields upon the spot.

Much higher accuracy may be achieved by avoiding the use of the cathode-ray tube for conversion from rectangular to polar coordinates, and systems relying upon the use of electrical resolvers for this purpose are described in Vol. 21, Part I.

*Precision Type B Indicator.*—In some radar systems the interval between successive groups of echoes from the same target may be as great as 20 or 30 sec. As indicated in Sec. 7-16, it is necessary to provide a cursor which may be moved to the persistent echo in this interval and the following circuit satisfies this requirement. This unit is designed to convert a search radar (SCR682A) into an accurate fire-control device against surface targets. A block diagram<sup>1</sup> is shown in Fig. 7-50 and a circuit schematic in Fig. 7-51. This device presents an expanded type B display which is continuously movable in range and azimuth and which presents a sector  $40^\circ$  in azimuth by 4000 yd in range. After calibration the accuracies are  $\pm 0.3^\circ$  in azimuth and 0.1 per cent of full scale in range. Two range scales are available, the short scale from 300 to 20,000 yd and the long scale from 6000 to 200,000 yd. The unit is triggered externally from the radar system and contains a crystal calibrator for adjusting the range circuits.

As shown in the block diagram the range sweep is triggered from the phantastron time modulator (main range circuit), which is in turn triggered by the system or by the calibrator. The time of the start of the sweep is accurately determined by the range helipot  $R_3$ , which is controlled by the range handwheel. A range mark is placed on the range sweep by means of an interpolating time modulator, the "junior" range circuit. During the PPI scan a 2000-yd index is produced in the middle of the sweep by the delayed pulse from the junior range circuit, which is then operating as a fixed 2000-yd delay triggered by the time modulator and controlled by the potentiometer  $R_2$ . At this time  $R_2$  is held at the center of the winding by a center-return device. The video is switched on to the cathode of the CRT during a selected  $60^\circ$  azimuth sector. The azimuth sweep occupies the center  $40^\circ$  of this sector. The echo pattern of the signals is painted during this time. After the  $60^\circ$  interval the signals are removed, the azimuth sweep is recentered and a magnetic clutch connects the correction potentiometer  $R_2$  (which was previously centered) to the range gearing so that the spot which formerly marked the center of the CRT may be moved across its face and adjusted in coincidence with a persistent echo. Motion of the handwheel also changes the main range potentiometer  $R_3$  so that the start of the range sweep is shifted by the same amount of time as the junior delay has been changed. When

<sup>1</sup> See Army Report BC-1365, Indicator-Tracker Unit.

the antenna has again reached the start of the selected  $60^\circ$  sector, the magnetic clutch is opened and the range mark springs back to the center of the CRT. Since the sweep start has been shifted by the correct amount, the selected echo should now appear coincident with the range mark half way along the range trace on the B-scope.

Azimuth marking is achieved in a similar manner. The position of the antenna is transmitted from a synchro generator geared to the radar antenna to a synchro motor which drives the azimuth gearing. The synchro system operates at ten times the antenna speed to minimize errors and furnish more torque. Phasing switches mounted on the antenna and in the azimuth gear train prevent ambiguity in the data which might otherwise result. The antenna motion is applied through a differential to the sweep synchro and to a  $60^\circ$  cam which operates switches to select the operating sector. These switches put the video on the B-scope and operate the magnetic clutches. The rotor of the azimuth sweep synchro is supplied from a 2000-cycle oscillator. Only one stator winding is used which gives an output which changes in magnitude with angle and reverses in phase when going through zero amplitude. During the scan the output of the synchro is applied to a phase-sensitive rectifier which converts the output of the synchro into a d-c voltage proportional to the cosine of the shaft angle (see Vol. 19, Chap. 12). Only a  $60^\circ$  interval centered at zero amplitude is selected by the azimuth switch. In this interval the rate of change of voltage with angle is sufficiently constant to produce an approximately linear sweep in the middle  $40^\circ$  of this interval ( $\sin \theta \approx \theta$  for angles  $< \pm 20^\circ$ ). The azimuth sweep driver converts the voltage change into a current change in the deflecting coils. The gain of the amplifier is adjusted to drive the sweep from one side of the CRT to the other during a  $40^\circ$  rotation of the synchro. Outside the  $40^\circ$  sector the synchro is disconnected from the rectifier and the azimuth correction potentiometer substituted. A magnetic clutch connects the azimuth handwheel, which also drives one shaft of the differential, to the correction potentiometer ( $R_1$ ) which is supplied symmetrically with alternating current. The potentiometer slider is normally held in the center of the winding by means of a center-return mechanism. When the alternating voltage from the potentiometer ( $R_1$ ) is connected to the rectifier, motion of the azimuth handwheel moves the spot horizontally on the face of the tube. If the spot is superposed upon the persistent image of an echo, the azimuth synchro is rotated through by an angle appropriate to the motion of the spot so that when the synchro is again connected to the sweep circuit the echo will be centered horizontally upon the CRT. When the sweep commences the magnetic clutch opens, causing the return mechanism to recenter the azimuth-correction potentiometer.

In a particular case regenerative tracking (see Sec. 7-15) has been

combined with this display to obtain very accurate aircraft tracks from a slowly scanning radar. If the target motion is rapid compared to the scanning rate of the radar, the rate-generating mechanism must be disconnected from the range and azimuth inputs when the displacement corrections are entered; otherwise, the tracking mark will drift while the persistent image of the echo remains stationary. If the rate-generator mechanisms are connected through center-return mechanisms similar to those used to recenter the potentiometers and if magnetic brakes are used to remember the integrated rate during the reset time, the desired result may be accomplished as shown in Fig. 7-50. The results of this interconnection were gratifying.<sup>1</sup>

*Detailed Circuits.*—Referring to Fig. 7-52, the trigger is applied through an inverting switch to  $T_1$  which permits either polarity of input to be used. Amplifier and sharpener  $V_{1a}$  drives the blocking oscillator  $V_{1b}$ . The phantastron delay uses a 6SA7,  $V_2$ , with feedback through a cathode follower  $V_{3a}$  to improve recovery time. Time constants in the Miller feedback circuit are temperature-compensated and are switched to change ranges. The cathode waveform from the phantastron  $V_2$  is amplified, differentiated and fires a blocking oscillator  $V_{4b}$ . The plate-current pulse of the blocking oscillator  $V_{4b}$  forms the trigger for the type B display. At minimum range this display and the junior range circuit are triggered from  $V_1$ , the phantastron delay being bypassed. An extra potentiometer  $R_1$  geared to the range handwheel is automatically connected to the junior range unit and used to move the tracking mark at minimum range. When the minimum delay of the phantastron is reached (less than 4000 yd from the trigger), the sweep jumps into zero range and tracking is accomplished by moving the tracking mark across the face of the CRT. If it were possible to pretrigger the phantastron

<sup>1</sup> Tests in tracking ships with an antenna producing a beam of  $7^\circ$  in azimuth scanning at 7 rpm and mounted on a moving platform rolling  $\pm 20^\circ$  with a 14-sec period gave the following typical results:

	Average position errors		Average difference between successive errors	
	Range, yd	Azimuth, degrees	Range, yd	Azimuth, degrees
Aided.....	35 at 6550	0.59	4.1	0.20
Unaided.....	39 at 9931	0.68	15	0.285

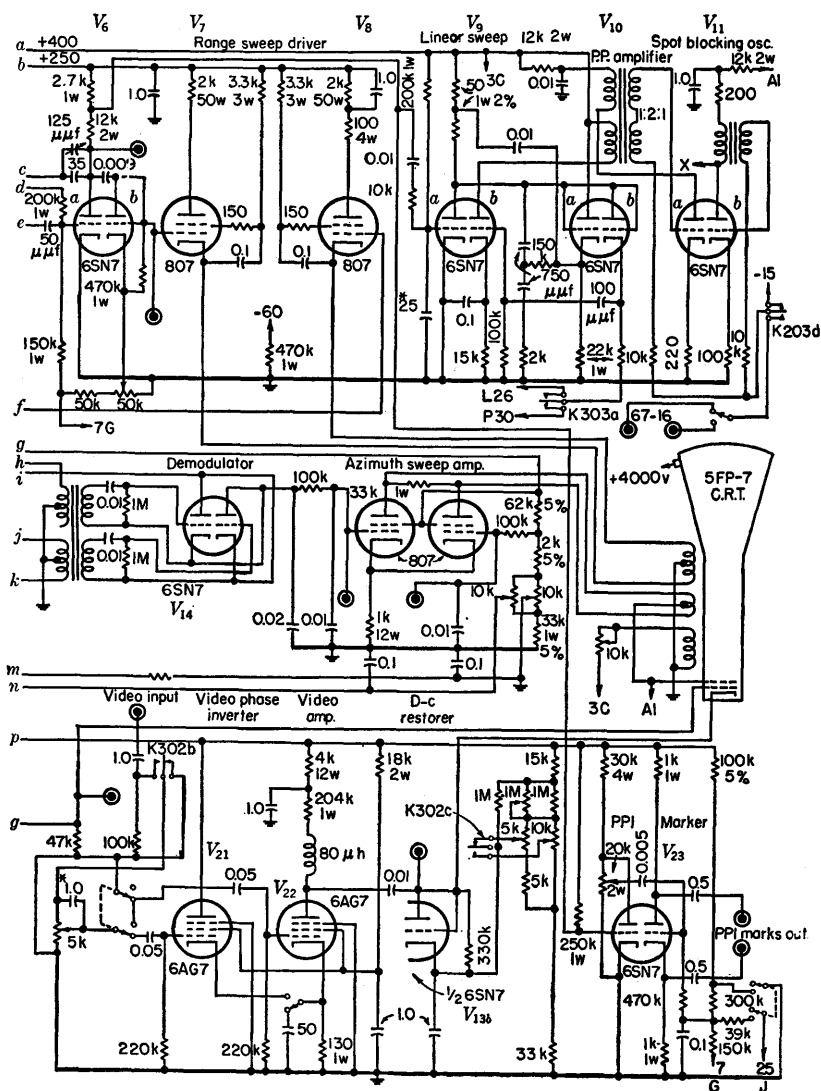
It was concluded that aided tracking was the more accurate under all conditions; that it gave fairly good tracking under conditions in which direct tracking was impossible; and that it was less fatiguing to the operator.





necessary to force current in the large inductance of the deflecting coils. Vertical centering voltage is inserted through the d-c restorer  $V_{6b}$ .

The junior range circuit consists of a bootstrap sawtooth generator  $V_{9a}$ ,  $V_{10a}$ , which is initiated by the negative B-gate waveform and a diode amplitude selector  $V_{10b}$  and amplifiers  $V_{9b}$  and  $V_{11a}$ , driving the blocking



\*  $\mu\mu\text{f}$   
of precision B-scope.

oscillator  $V_{11b}$ . Care has been taken to make the minimum delay of this unit as short as possible. The mixer  $V_{20}$  adds the tracking mark, the calibration marks, and the B-gate. The sum is then applied to the grid of the CRT. The tracking mark for an external PPI display is obtained by passing the B-gate through the limiter-amplifier  $V_{23}$ .

The video amplifier consists of  $V_{21}$  and  $V_{22}$ . When positive video is used, only  $V_{22}$  is connected. When negative video is used,  $V_{21}$  drives the cathode of  $V_{22}$  so that the output is in phase with the input. The d-c restorer  $V_{13b}$  is used to stabilize the zero-signal level applied to the cathode of the CRT. Two intensity controls are used to adjust the cathode bias of the CRT and are switched by the 60° cam. These two controls are necessary to make the radar video and the tracking spot appear equally bright.

The 2000 cps a-c for the azimuth sweep is generated in a two-stage feedback oscillator  $V_{12}$ . The frequency is determined by resonating the rotor of the azimuth sweep synchro. A loading network is connected across the stators of the synchro to prevent changes in the oscillator amplitude as the synchro rotates. The angle sweep rectifier (demodulator)  $V_{14}$  is a triode bidirectional switch (Vol. 19, Chap. 14). A filter removes the residual a-c component from the sweep waveform. The azimuth-sweep driver is a cathode-coupled push-pull amplifier. As the azimuth sweep waveform is very slow no special provisions are necessary to compensate for the inductance of the deflecting coils.

The calibrator is conventional. A crystal oscillator  $V_{13a}$  operates Class C producing pulses in the transformer connected in its cathode circuit. The other windings in conjunction with  $V_{13b}$  form a blocking oscillator. This is synchronized at 1-to-1 ratio. The 10,000-yd-mark divider  $V_{19a}$  is of the plate-cathode-coupled variety, the synchronizing signal being injected in the grid circuit. The PRF divider  $V_{19b}$  is triggered on an extra winding from the plate-current pulse of the 10,000-yd divider and operates at about 400 cps. The calibration marks are mixed through small condensers and applied through an attenuator to the grid of  $V_{20a}$ . Plate-current pulses are used because they have no overshoots which would blank the PPI.

The indicator has given excellent performance. It is possible to reset the tracking spot on small, isolated targets to at least 5 per cent of the rise time of the video pulse and 5 per cent of the antenna beamwidth of the associated radar set.

The design of the circuits is straightforward but not particularly economical of parts. There seems to be no particular good reason for using a phantatron time modulator for the main range unit and a bootstrap sawtooth generator for the junior time modulator. Instruction of

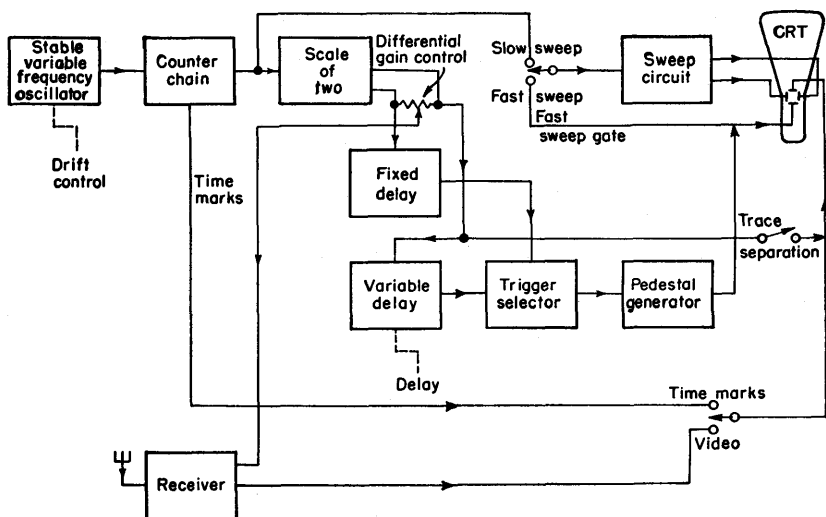
maintenance personnel could be considerably simplified if both circuits were of the same type.

### ESPECIALLY ACCURATE TIME-MEASURING SYSTEMS

**7-29. Introduction.**—In hyperbolic navigation systems such as Loran and Gee it is necessary to measure time differences with an extremely high degree of precision. Measurement of times as large as 20,000  $\mu\text{sec}$  with an accuracy of  $\pm \frac{1}{2} \mu\text{sec}$  is frequently desirable. In order to conserve r-f channel space, pulses rising as slowly as 10 to 90 per cent in 100  $\mu\text{sec}$  are used. Measurement of these pulses with the requisite accuracy can only be accomplished by superposition methods (see Sec. 7-11). In Loran the "master" station transmits at a PRF of about 25 cps. The "slave" station receives the pulse delayed by the time of propagation from one station to the other, waits  $\frac{1}{2}$  period (10,000  $\mu\text{sec}$ ) and transmits a pulse. The receiving equipment located in the vessel being navigated must synchronize its timing circuits with the master pulse and accurately measure the delay between the master and slave received pulses.

A simplified block diagram illustrating the basic method of accurate time-difference measurement is shown in Fig. 7-53. A stable oscillator serves as the timing standard. This oscillator is controllable over a narrow frequency range by manual or automatic means. A counter chain is synchronized with the oscillator to produce a PRF of twice the frequency transmitted by the ground stations. A bistable multivibrator circuit divides this frequency by 2, producing the fundamental PRF of the transmitter stations. Since the slave station waits  $\frac{1}{2}$  period after receiving the pulse from the master station the two received pulses will appear during alternate half cycles of the scale-of-two. The slow type A sweep is started with each trigger from the counter and lasts for nearly all the time between triggers. A square wave from the multivibrator is applied to a vertical deflecting plate of the CRT so that the trace appears alternately on two lines as shown in Fig. 7-54a. An accurate fixed-delay produces a pedestal near the beginning of the upper trace. The master station pulse is placed upon this pedestal by adjusting the frequency of the oscillator until the master pulse drifts onto the pedestal. If the master pulse remains stationary, the frequency of the timing system is then accurately synchronized with that of the master station. A variable delay (time modulator) produces a pedestal on the lower trace. By means of a delay control this pedestal is placed under the slave station pulse. The long sweeps do not provide sufficient time discrimination for accurate time measurement. Accordingly expanded sweeps are provided which are only slightly longer than the received pulses. These sweeps are initiated alternately by the fixed and the movable pedestals. If the master pulse

is near the rising edges of the fixed pedestal and the slave pulse is near the rising edge of the movable pedestal, changing to the expanded sweeps will still present both pulses. (See Fig. 7-54b.) The pulses can be super-



Marks from oscillator

Trigger from divider chain

Scale of two

Slow sweep

Pedestals

Fast Sweeps

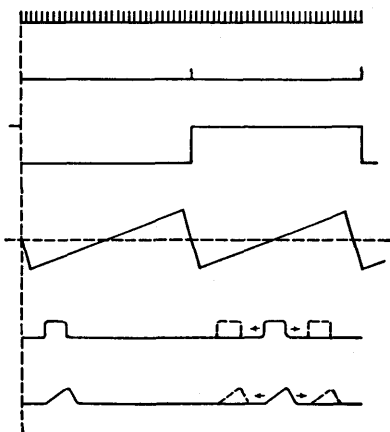


Fig. 7-53.—Simplified block diagram and timing diagram of Loran receiving system.

posed by disconnecting the square wave which separates the traces and by adjusting the delay of the movable pedestal. The position of the pulses on the pedestal does not affect the measurement and they may even drift slowly.

To accomplish accurate superposition the received pulses must be of equal amplitude. Since they are received over different paths the incoming signal amplitudes may be unequal. Therefore, the receiver gain must be varied selectively for the two pulses. This is accomplished by applying a square wave of variable amplitude (derived from the scale-of-two) to the grid returns of the i-f stages of the receiver. The amplitude of the square wave is adjusted by a control (called the differential gain control) until the displayed pulses are of equal amplitudes after which superposition is readily accomplished by adjustment of the delay control.

The time difference between the pulses is measured by determining the time difference between the start of the two pedestals. In the conventional Loran equipment (AN/APN-4 and AN/APN-9) this is accomplished by applying 10- $\mu$ sec, 50- $\mu$ sec, 100- $\mu$ sec, 500- $\mu$ sec, 1000- $\mu$ sec, and 2500- $\mu$ sec time marks derived from the several stages of the counter circuit to the sweeps, and by counting the number of marks on the lower trace to the right of the pedestal on the upper trace. The time between the pedestal on the upper trace and the start of the lower trace is always constant. The time modulator which varies the position of the lower trace pedestal consists of a step delay synchronized by the 500- $\mu$ sec marks plus a variable delay which interpolates between the 500- $\mu$ sec intervals. Both delays are uncalibrated and they need only be stable for a long enough period to count the number of fixed marks in the delay interval.

The above method has made possible very accurate navigation by the Loran<sup>1</sup> and Gee systems. The counting methods, however, are difficult to teach and there is considerable possibility of error under difficult operational conditions. To overcome this difficulty a direct-reading Loran indicator could be used in which the time modulator is accurately calibrated so that it is only necessary to match the pulses and read the time difference directly from a counter geared to the delay controls. A system of this sort on which circuit design has been completed but which is not in production at the time of writing is now to be described.

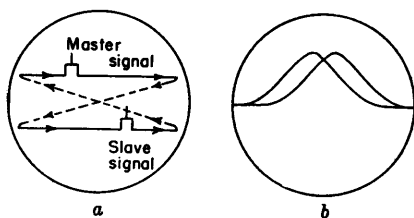


FIG. 7-54.—Typical Loran displays. (a) Appearance of slow sweeps with signals superposed on pedestals. (b) Appearance of fast sweeps with signals nearly superposed. Arrows indicate direction of traces.

<sup>1</sup> Complete circuit details of the currently used Loran devices are available in the instruction manuals for the AN/APN-4 and AN/APN-9 equipments as these devices have been released for general use and are no longer considered to be solely military devices. The Loran method is further described in Vol. 5 of the Series and in *Electronics* for November and December, 1945.

**7-30. Timing Sequence.**—The basic Loran<sup>1</sup> repetition frequencies may be given by the formulas  $\frac{20}{2 \times (300 - n)}$  kc,  $\frac{20}{2 \times (400 - n)}$  kc or  $\frac{20}{2 \times (500 - n)}$  kc where  $n$  is any integer from 0 to 7 inclusive and corresponds to the station number. These three formulas give the exact repetition frequencies for the 20-, 25-, 33 $\frac{1}{3}$ -cps bands. The oscillator frequency is chosen to be 20 kc/sec because this is twice the lowest common multiple of all the pulse repetition frequencies employed. The reason for the factor of 2 will be apparent later. It should be noted here that the repetition-frequency formulas give frequencies whose periods vary in steps of  $2 \times 50$   $\mu$ sec in each case.

The two Loran signals will be referred to as the master and the slave signal. Starting with the master and going to the slave signal, the time difference must always be greater than  $P/2$  and less than  $P$  where  $P$  is the repetition period. These signals are displayed on the Loran sweeps. The slow sweeps are triggered at the repetition frequencies given above and display the full cycle. The first half cycle of the complete period appears as an upper trace and the second half cycle as a lower trace. (For convenience the first half cycle will be referred to as  $P_1$  and the second half as  $P_2$ .) This then means that if the master station appears near the beginning of the upper trace, the slave station must appear somewhere on the lower trace. "Zero" time difference will be referred to as a time difference of exactly  $P/2$ ; that is, the master station will appear on the upper trace directly above the slave station on the lower trace. This implies that the time duration of the upper sweep must, for all values of  $N$  be of exactly the same as that of the lower sweep, and since the various repetition rates in any one band are obtained by removing  $2 \times 50 \times n$   $\mu$ sec from the period of the 20-, 25-, or 33 $\frac{1}{3}$ -cps repetition frequencies, this implies that  $50 \times n$   $\mu$ sec must be removed from  $P_1$  and  $P_2$  to maintain this symmetry. This explains the reason the formulas in the first paragraph are written with a 20-kc/sec rather than a 10-kc/sec basic timing rate. This removal of  $n \times 50$   $\mu$ sec is accomplished at the beginning of  $P_1$  and  $P_2$  because of circuit considerations. The final matching of the Loran signals is accomplished on fast sweeps. The fast sweep on which the master station pulse appears occurs near the start of  $P_1$ , and is fixed in time. The fast sweep on which the slave station appears, however, may be located in time any place in  $P_2$ , provided, that is, that this

<sup>1</sup> This device was developed at the Radiation Laboratory for airborne use. An electrical working model had been built and tested, and a final model suitable for flight test was in the process of construction at the end of the war. A direct-reading indicator of quite different design for shipboard use is in production at the Sperry Gyroscope Co.

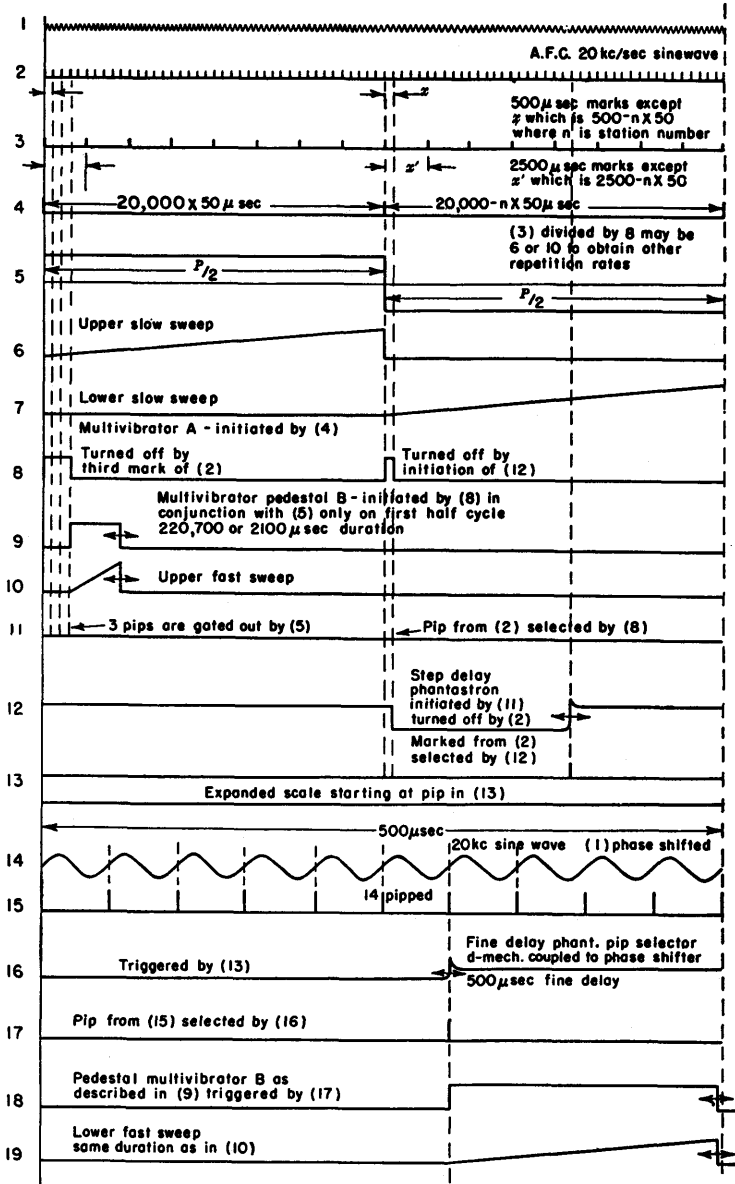


FIG. 7-55.—Timing diagram for direct-reading Loran indicator.



time, measured from the beginning of  $P_2$ , is not less than the time from the beginning of  $P_1$  to the beginning of the first fast sweep. It is more convenient to use timing marks as a time reference than the beginning of each sweep (the generation of these timing marks will be explained later). Therefore, the first fast sweep is originated at a time  $1500 - n \times 50 \mu\text{sec}$  after the start of  $P_1$ , and the delay circuits which eventually initiate the second fast sweep, are started at a time of  $500 - n \times 50 \mu\text{sec}$  after the start of  $P_2$ .

Referring to Fig. 7-55, line 1 indicates the 20-kc sine wave which is used as a master-timing reference. The frequency of this sine wave is controlled by an AFC circuit with reference to the incoming pulse from the master station (see Chap. 4). Line 2 represents division by 10 yielding 500- $\mu\text{sec}$  range marks except the first mark after the start of each half period of the repetition rate, this time being equal to  $500 - n \times 50 \mu\text{sec}$  in each case that is, a division of  $10 - n$ . The marks shown in line 2 are now divided by 5 in a counter that gives an output for every fifth mark of line 2. This is shown in line 3. These are then applied to a circuit which gives an output for every sixth, eighth, or tenth mark shown in line 3. This is indicated in line 4. These marks are then used as triggers for a scale-of-two circuit. This gives a square wave as an output whose recurrence frequency is equal to the Loran repetition frequency desired and is indicated in line 5. It should be noted that this square wave has half-cycle symmetry. This circuit accounts for the factor of 2 in the denominator of the formula for the repetition frequencies. It should be kept in mind that any of the range marks mentioned previously are uniformly spaced except the first one occurring after the start of each half period. Here the time interval is  $n \times 50 \mu\text{sec}$  less than the rest of the series. By the means of these various frequency divisions, we have now obtained all the repetition frequencies required.

Line 6 indicates the upper slow sweep as being started at the beginning of  $P_1$ . Line 7 indicates the lower slow sweep being started at the beginning of  $P_2$ . Line 8 indicates the fixed delay of  $1500 - n \times 50 \mu\text{sec}$  which initiates the first fast sweep. This is actually a multivibrator which is turned off on the third 500- $\mu\text{sec}$  mark after the start of the first half cycle. On the second half cycle, the step-delay circuit shown in Line 12 is turned on by the first 500- $\mu\text{sec}$  mark, that is,  $500 - n \times 50 \mu\text{sec}$  after the start of  $P_2$ . This is accomplished rather indirectly. A coincidence tube is included in the circuit which will give an output only during  $P_2$  and when a 500- $\mu\text{sec}$  mark and the rectangular pulse shown in line 8 are coincident. This means a trigger will be obtained with the first 500- $\mu\text{sec}$  mark on the lower sweep. This trigger then initiates a coarse delay which in turn terminates the delay rectangle shown in line 8 on second half cycle to prevent further coincidences. Line 9 indicates the upper sweep

pedestal being started at the time  $1500 - n \times 50 \mu\text{sec}$  after the start of the upper slow sweep. The duration of this pedestal is 220, 700, or  $2100 \mu\text{sec}$ . Line 10 indicates the actual upper fast sweep which coincides in time to the pedestal. Line 11 shows the selected trigger from 2 which is selected by the waveform of Line 8 in conjunction with that of Line 5 as explained. Line 12 indicates the coarse phantastron delay. This delay is started at a time  $500 - n \times 50 \mu\text{sec}$  after the start of  $P_2$ . This delay is made to select any of the  $500\text{-}\mu\text{sec}$  marks in the  $P_2$  interval after the one originating it. This constitutes a selection of one out of 39,500- $\mu\text{sec}$  marks. The output of the coarse phantastron-delay circuit, see Line 13, is used to initiate the fine delay circuit. The 20-kc/sec sine wave is made continuously phasable and is then used to generate  $50\text{-}\mu\text{sec}$  timing marks. This is indicated in Lines 14 and 15. The fine delay circuit, after being initiated by the coarse phantastron, then selects one of the phase-shifted  $50\text{-}\mu\text{sec}$  timing marks, the control for this delay circuit being coupled to the phase shifter in such a manner that as the delay is increased it will always select the same  $50\text{-}\mu\text{sec}$  timing mark. The selector pulse is indicated on Line 16, and Line 17 indicates the selected pulse. It should be noted that this delay is continuous and may introduce any time delay from very nearly 0 to over  $550 \mu\text{sec}$ . Line 18 indicates the lower sweep pedestal which is originated by the continuously time-modulated pip of Line 17. This in turn originates the lower fast sweep as shown in Line 19. The lower pedestal and fast sweep are identical to those during  $P_1$ . Since the delay circuit is initiated  $1000 \mu\text{sec}$  sooner after the start of  $P_2$  than the upper fast sweep is initiated after the start of  $P_1$ , the lower fast sweep can be brought into what corresponds to "zero" time delay; that is, it occurs exactly  $\frac{1}{2} P$  after the upper fast sweep.

**7-31. Circuit Details of Loran Indicator.**—Figure 7-56 is a simplified block diagram of the indicator. The basic time reference is a 20-kc/sec LC-oscillator, with automatic frequency control. (For details see Chap. 4, Sec. 4-11.) There are two 20-kc/sec output signals supplied by a combination buffer-amplifier and cathode follower. One of these outputs is fed into a pulse generator, a blocking oscillator, which generates  $50 \mu\text{sec}$  markers. The output of the pulse generator is fed into the counter circuit. In the block diagram it is marked as a Frequency Divider dividing by 400. The divider consists of a step counter chain with feedback, the first counter dividing by 10, the second by 5 and a third stage by 6, 8 or 10 depending upon whether the selected PRF is in the 33-, 25-, or 20-cps group. The counter chain is described in detail in Sec. 4-11.

The output of the counter chain triggers a bistable multivibrator, which produces a symmetrical square wave at the repetition frequency. This is used for trace separation on the CRT and as a switching arrangement in the trigger-selector and pedestal-generator circuits.

The pedestal generator supplies the two pedestals for the sweeps and a trigger to the automatic-frequency-control circuit.

The sweep generator supplies all the sweep function necessary in the unit. It requires two different triggers; one for the slow sweeps and one for the fast sweeps. The triggers for the slow sweeps are derived from the last stage of the counter chains. The triggers for the fast sweeps are provided by the delayed pedestals which are used to mark the position of the received pulses. The sweeps are applied to the horizontal plates of the cathode-ray tube.

The complete 3-scale time modulator comprising a phantatron pip-selector that selects 500- $\mu$ sec marks, and a fine delay which is in reality

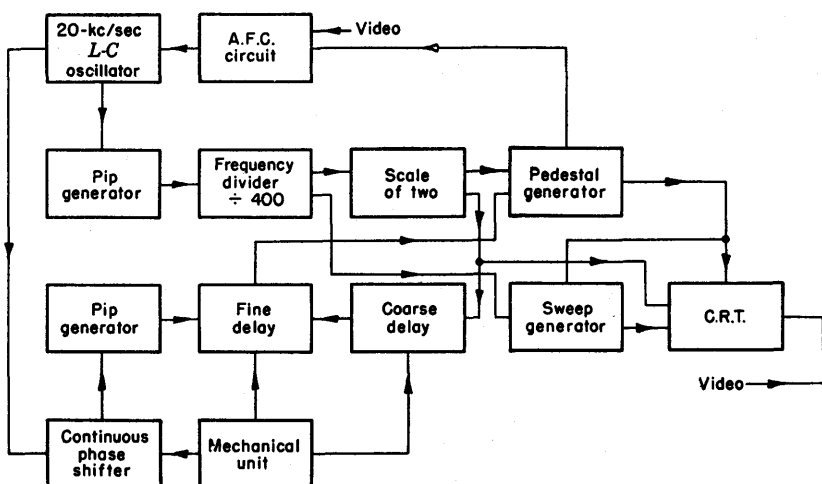


FIG. 7-56.—Loran direct-reading indicator; simplified block diagram.

a 2-scale system comprising phase shifter and a phantatron pip selector is described in Sec. 6.8.

Figures 7-57 and 7-58 are the detailed block diagram and the circuit diagram respectively. Only type 6K4, 6D4 and 6AS6 tubes are used.

The frequency of the  $LC$ -oscillator  $V_{11}$  is controlled by the reactance tube  $V_1$  which obtains a control signal from the time discriminator which consists of the time-selective detector  $V_2$ ,  $V_3$  and the early gate generator  $V_8$ ,  $V_9$  and the later gate generator  $V_6$ ,  $V_7$ . The early gate generator is triggered from the pedestal generator,  $V_{49}$ ,  $V_{50}$ , and the AFC circuit functions to hold the master pulse on the upper sweep pedestal. The scale-of-two circuit  $V_{36}$ ,  $V_{37}$  produces a bias on the cathode of the triggering diode  $V_{10}$  to prevent the gate from being triggered by the lower sweep pedestal.

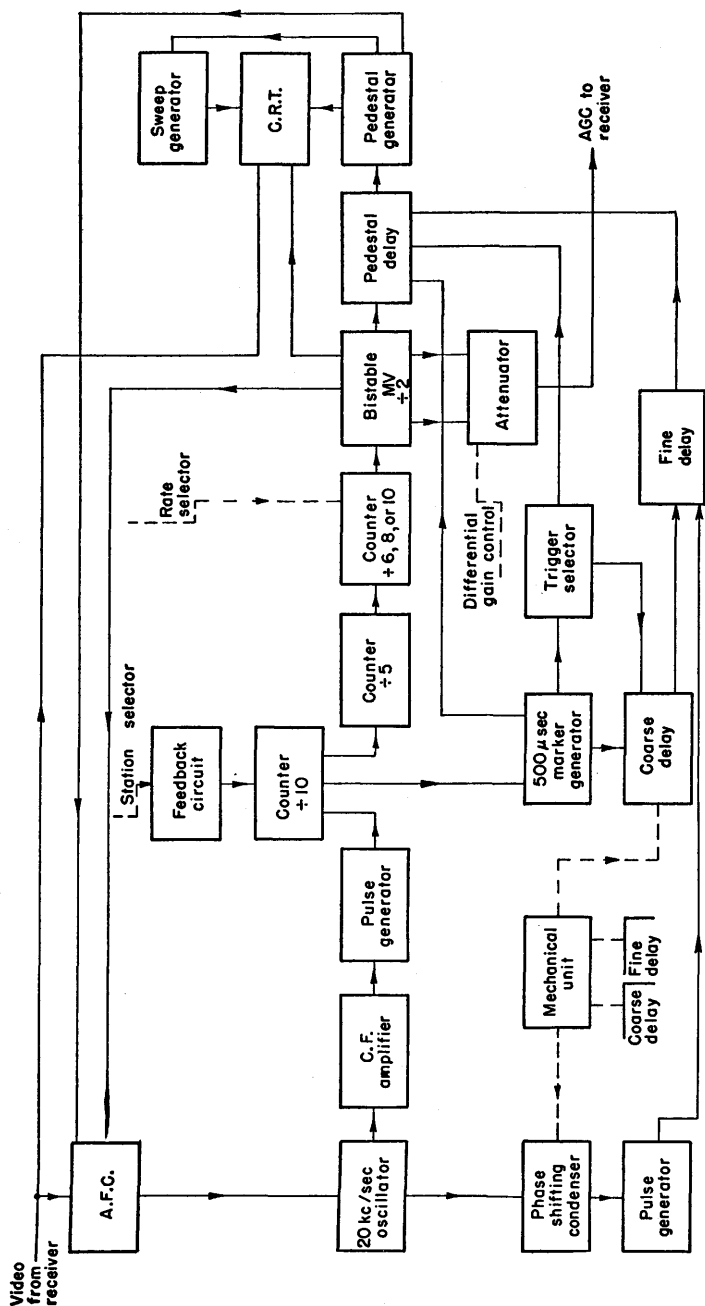
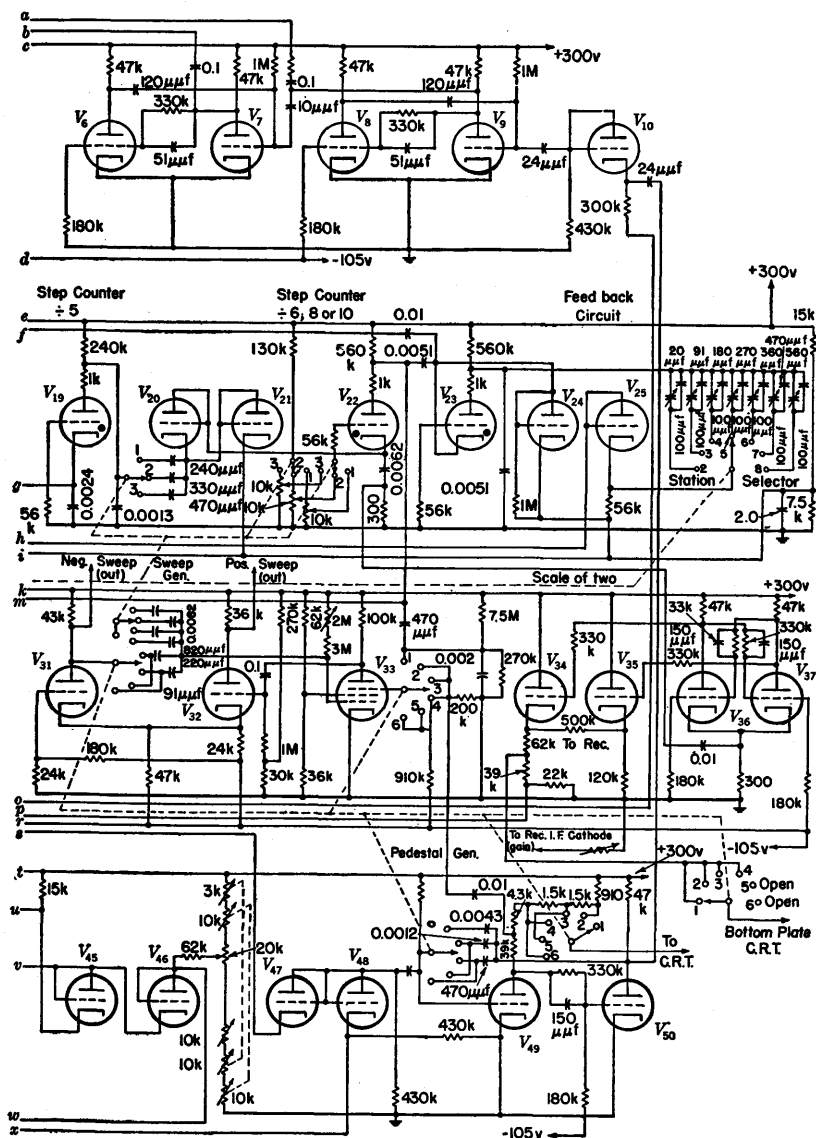


FIG. 7-57.—Detailed block diagram of direct-reading Loran indicator.





indicator circuit.

To prevent loading the oscillator a buffer-amplifier  $V_{12}$  is used following the oscillator. This stage supplies two sources of 20-kc sine waves, one to the pip-generating circuit and one to the continuous phase-shifter network.

The pulse-generating circuit, which receives its synchronizing signal in the form of a sine wave from the buffer-amplifier, is a conventional grid-coupled blocking oscillator. Large negative pulses are obtained on the plate of the blocking oscillator which are used as the initiating triggers for the counter chain, and as 50- $\mu$ sec markers.

The counter chain following the blocking-oscillator pip generator consists of three divider stages, their count being 10, 5, and 6, 8, or 10, respectively. The first stage produces 500- $\mu$ sec markers except "X" (referring to timing diagram) which is  $500 - n \times 50$  where  $n$  is the station number. This variation is due to the feedback circuit, the operation of which is explained in Sec. 4-11 and in Vol. 19, Chap. 17. The second stage produces 2500- $\mu$ sec markers except "X" again which occurs at  $2500 - n \times 50$   $\mu$ sec. The third stage produces repetition-rate triggers of 66 $\frac{2}{3}$ , 50, or 40 pps. Again the first count contains the "X" function which is dependent upon the station number selected.

The design of the gas-filled tube counters is discussed in Vol. 3, Chap. 17, and in Sec. 4-11. The feedback circuit which is an integral part of the divider chain is used to obtain the repetition rates necessary to correspond to the various station rates. It results in division by  $300 - n$ ;  $400 - n$  or  $500 - n$  when  $n$  is the station number. The operation of the counter chain is described in detail in Sec. 4-11.

In order to obtain a double-trace sweep on the cathode-ray tube a bistable multivibrator  $V_{36}$ ,  $V_{37}$  (scale-of-two) is used, which generates a square wave at the repetition frequency. This square wave is applied to the vertical deflection plates of the cathode-ray tube. In this application triggering is done on the cathode.

Cathode followers are used to prevent loading of  $V_{36}$  and  $V_{37}$ . They supply outputs to the differential receiver gain control, pedestal delay, trace separation, and AFC circuits.

The pedestal delay generator  $V_{29}$ ,  $V_{30}$  performs several functions. It delays the start of the upper-trace pedestal until after the occurrence of three 500- $\mu$ sec markers. It generates a gate to operate the trigger selector which selects the first 500- $\mu$ sec mark on the lower trace to trigger the coarse delay.

It is a monostable multivibrator which receives its initial trigger from the output of the last counter stage. On the first half cycle corresponding to the upper trace, the pedestal delay generator terminates its action on the third 500- $\mu$ sec range mark; this termination is accomplished by the following operation:  $V_{30}$  is normally conducting and  $V_{29}$

nonconducting, a negative trigger on the grid of  $V_{30}$  starts regeneration. The grid of  $V_{30}$  is held negative for a time determined by the time constant  $C_{51}, R_{70}$ . The value of this time constant is such that when the 500- $\mu$ sec marks are applied to the grid of  $V_{29}$ , amplified, and applied to the grid of  $V_{30}$ , the grid recovers sufficiently to return to the conducting region when the third range mark actuates the grid. The late edge of the pedestal delay generator triggers the pedestal generator hence supplying the pedestal for the upper trace.

In the second half cycle, regeneration is initiated by the same means but the pulse is terminated after the first 500- $\mu$ sec mark by the negative cathode waveform of the coarse delay which only operates during  $P_2$ .

Two amplitudes of 500- $\mu$ sec marks are employed in this process because as the stations are selected the 500- $\mu$ sec marks move in 50- $\mu$ sec steps. In order to keep the top pedestal three 500- $\mu$ sec marks from the start of the sweep the amplitude of the markers applied to the multi-vibrator is changed.

The trigger selector  $V_{28}$  initiates the coarse delay.

Three pulses are applied simultaneously to different electrodes of  $V_{28}$ . The 500- $\mu$ sec marks are applied to the cathode, the pulse from the pedestal delay generator is applied to the control grid and the square wave is applied to the suppressor.

The square wave on the suppressor prevents any output during the first half cycle corresponding to the upper trace. During the second half cycle it permits the tube to conduct during coincidence with the other pulses. An output signal from the plate is obtained when a coincidence between the pedestal delay generators and a 500- $\mu$ sec mark occurs, this signal output triggers the coarse delay which terminates the pedestal delay generator to prevent further coincidence.

The pedestal generator  $V_{49}, V_{50}$  performs two functions. It generates three different lengths of pedestals for the upper and lower traces. These are the rectangles which actuate the sweep generator for the fast sweeps. A portion of the output of  $V_{49}$  is used to intensify the trace on the CRT during the fast sweeps. The pedestal generator is a monostable multi-vibrator which is triggered in the following manner. On the upper trace the pedestal generator is triggered by the falling edge of the pedestal delay generator pulse. To prevent this trigger from firing it on the lower trace, the square wave is applied to the trigger selector diode  $V_{47}$ . Triggering on the lower trace is accomplished by a trigger from the fine delay through diode  $V_{48}$ .

The sweep circuit consists of three tubes,  $V_{31}, V_{32}$ , and  $V_{33}$ . The same circuit generates the slow and fast sweeps. It is a Miller feedback circuit comprising a pentode amplifier coupled to a triode differential amplifier.

For slow sweeps the recovery is accomplished by a negative voltage



pulse from the last divider stage which cuts off the pentode suppressor. The sweep condenser is rapidly recharged by the plate resistor of the differential amplifier. The circuit provides push-pull sweeps which are capable of a very high duty ratio.

Switching of the sweep circuit is accomplished in a different manner during the fast sweeps. The suppressor of  $V_{33}$  is pulsed into the conducting region by the pedestals from  $V_{49}$ . The rate of rise of the sweep is changed by switching the sweep condenser. The durations of the sweeps are governed by those of the pedestals.

The time-modulator circuit which delays the lower pedestal is a three-scale system which produces a continuously variable delay. Unlike the time-modulator circuits in the conventional Loran system this time modulator is calibrated to read in microseconds directly on a Veeder-Root counter with an accuracy  $\pm 0.5 \mu\text{sec}$  of a maximum delay of 20,000  $\mu\text{sec}$ . It is described fully in Sec. 6-8 and comprises the following units.

1. A coarse-delay step phantastron  $V_{40}$ ,  $V_{41}$ ,  $V_{42}$ , and  $V_{43}$ , which is started by the trigger selector  $V_{28}$  and stopped by a selected 500- $\mu\text{sec}$  mark from  $V_{27}$ . The delay is variable in steps of 500  $\mu\text{sec}$  which correspond to the spacing between the 500- $\mu\text{sec}$  marks.
2. A fine delay which interpolates between the 500- $\mu\text{sec}$  marks. This is a two-scale time modulator comprising a step phantastron which is started from the end of the coarse delay. Its action is terminated by a selected, phase-shifted 500- $\mu\text{sec}$  mark. The phase-shifted mark is derived from the 20-kc/sec sine wave from the cathode of  $V_{12}$ , shifted in phase by a phase-shifting condenser the output of which is amplified by  $V_{38}$  and converted into a pulse by  $V_{39}$ . The phase-shifted 50- $\mu\text{sec}$  mark selected by the step phantastron actuates the pedestal generator through  $V_{48}$ .

Details of the mechanical unit that controls the time modulator are given in Sec. 6-8. This unit is one of the most important features of the direct-reading system in that although the coarse scale is controlled by one handwheel and the fine scales by another their readings are algebraically added in such a way that the counter reads the correct total time interval.

## CHAPTER 8

### TECHNIQUES OF AUTOMATIC TIME MEASUREMENT

By R. I. HULSIZER, AND F. C. WILLIAMS

#### INTRODUCTION

**8-1. Automatic vs. Manual Measurements.**—Many arguments have been advanced, particularly at the beginning of radar history, on the relative merits of manual and automatic measurement. Some of the objections to automatic tracking result from the inferior performance of the early automatic tracking equipment. Further argument arises from the extremely undesirable characteristics of radar signals. In pulse-echo systems the signals often fade into thermal noise; furthermore, undesired signals from interfering objects and other radars demand from the tracking mechanism, either human or automatic, discrimination, alertness, and judgment. Nevertheless there are several advantages to be listed for automatic tracking which have justified its inclusion in many radars, particularly those designed for fire-control use.

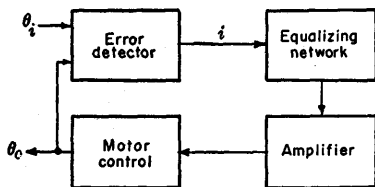
The rapidity of response and higher-accuracy characteristic of automatic control are of value especially for high-accuracy anti-aircraft radars. Response times of  $\frac{1}{4}$  to  $\frac{1}{10}$  sec are realizable with automatic tracking loops, whereas normal operator tracking shows response times of one second or greater. It might be argued with considerable justification that short response times are not requisite for tracking most radar targets because of low accelerations, but it is preferable to employ a fast-acting tracking device followed by a consistent and reliable smoothing device rather than to rely on erratic smoothing by the operator. Time-measurement operations started near the end of the war on high-velocity projectiles indicate the inadequacy of human tracking to follow accurately such high velocities and accelerations.

A second favorable aspect of tracking automatically is the advantage in weight provided by electronic time measurement as opposed to visual measurement, since visual measurement implies at least a meter presentation and usually a cathode-ray tube and certainly a man. A prime example of this feature is the ARO radar AN/APG-5, which has automatic searching and tracking, and indicates the approach of a target within a certain range simply by a warning light.

The following two reasons for automatic tracking are more general and apply significantly to the design of apparatus for measuring time

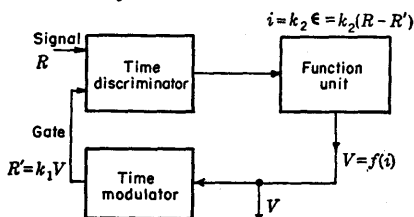
duration of various phenomena in which the signal-to-noise ratio is large enough to require less attention and discrimination on the part of the operator. These are (1) that automatic tracking is less fatiguing for the operator, particularly when high accuracies are demanded over long periods of operation, and (2) that under favorable conditions, one operator might monitor several simultaneous automatic-tracking operations. Such a situation might arise with an air-traffic-control radar where each plane carries a beacon to be triggered by a zenith search set. As each plane comes into the area of control, tracking gates are set to track its beacon response until the plane leaves the area or lands. One operator could handle several such tracking machines, from which data would be fed automatically to a central control station.

Numerous applications in research or industrial control can be imagined



(a) Conventional servomechanism diagram

$\theta_i$  = input signal or motion  
 $\theta_o$  = output motion



(b) Block diagram of time-measuring system

FIG. 8-1.—A block diagram of a conventional servomechanism and an automatic time-measuring system.

where automatically recorded data is desired simultaneously on the time duration of several phenomena, yet where the cost of engaging a separate operator for each measurement might be prohibitive.

## 8-2. General Technique of Automatic Time Measurement.

The two basic methods of manual time measurement have automatic analogues. The first, that of converting the time dimension into a space dimension on a cathode-ray-tube display and measuring time in terms of distance, has been successfully performed with the aid of a pair of adjacent photoelectric cells whose difference output is made to drive them along the direction of the time base in

accordance with the motion of the signal (see Vol. 19, Chap. 14).

The second method, the discriminate-remodulate technique (Chap. 3), is usually employed. The process of comparing the time modulation of the echo and the locally modulated pulse is known as time discrimination (Chap. 3) and yields a voltage or current which is operated upon to convert it into a form suitable for controlling the local time modulator. One immediately recognizes the ubiquitous automatic control mechanism or servo, where a detector measures the difference between an unknown quantity and the "following" or servoed quantity to generate an error

signal which acts through a control device to make the "following" quantity equal to the unknown. Figure 8-1 illustrates this similarity as well as indicates the elements of the time-demodulation system.

The box labelled "Function unit" performs the operation of converting the time-discriminator output into a form suitable for controlling the local time demodulator and may be an amplifier, electrical integrator, rate servo, or a complex combination of such elements. This unit defines the external properties of the system. Sections 8-6 to 8-10 will discuss the design of these electrical or electromechanical operators.

Since the method of control has such a marked effect upon the design of the function unit, they will be treated separately depending upon whether electrically or mechanically controlled time modulators are employed.

Electrically controlled time modulators are all substantially single-scale, although they may be combined with an accurate fixed-delay device to make a multiple-scale time modulator that is continuous over a small interval. Good examples of this practice are the AN/APS-15 and the British Oboe. As single-scale devices, these modulators are at present limited in accuracy from 0.1 to 2 per cent of their maximum excursion. Completely electrical tracking loops are possible which are lighter, smaller, less expensive than their mechanical analogues, and are capable of following very high speeds and accelerations, and usually of supplying more accurate rate data.

Mechanical time modulators have the advantages of enabling the use of multiple scales for high accuracy and of supplying data as a mechanical motion directly rather than from a voltage-follow-up servo.

One difference between mechanical and electrical time modulators that may be of importance in future time-measurement problems in which high accelerations are expected is their comparative rate accuracies. The rate errors introduced by the nonlinearities of time modulators are proportional to the slope of the range error plotted against range. The mechanical time modulators, such as the phase shifter, are accurate only to about 0.3 per cent of a complete revolution whereas the electrical time modulators are capable of linearities ten times better, and should therefore be expected to introduce only one-tenth as much error into the target-rate data.

It has been pointed out in Chap. 15 of Vol. 19 that with a multiplicity of signals a time discriminator must have only a limited region of sensitivity. The consequence of this restriction is that time-measuring systems that must track one pulse in a complex group must include some means for moving its sensitive region or time aperture into coincidence with the pulse to be tracked. In radar practice this is termed target-selection; it is usually achieved by a search display on a cathode-ray tube

to indicate the relative locations of the time aperture and the target signal, and an on-target indicator. Automatic search circuits may be substituted for the display whereupon an automatic target indicator would perform the function of stopping the search action and locking on target. The problems of target selection are discussed in Secs. 8-13 and 8-14.

Another function which the time-measuring system must perform is that of remembering the last velocity and position of a signal that has faded and of keeping the tracking gates and data output moving at the last velocity without severe transients until the signal reappears. Such ability is called "velocity memory." Memory time is often limited by the quality of electrical components, and hence an auxiliary function called "coast" has been developed whereby the operator can throw a switch disconnecting the signal to enable the tracking system to continue moving indefinitely at the last measured rate. This is particularly useful in radar applications where the operator can observe on suitable indicators the approach of interfering signals and "coast" through them. If the function has been performed properly he should be able to reconnect the tracking loop when the signal again comes into the clear and find the signal still in the time aperture. Memory provides no immunity from interfering signals, only from fades; coast gives immunity from both.

**8-3. Nature of Data and Its Effect on Performance.**—This topic has been treated in Chap. 2 and need only be summarized herein. If the data consists solely of a synchronizing pulse and a time-modulated pulse it is only necessary for the simplest form of automatic time-measuring circuit to trigger a scale-of-two circuit once with the transmitted pulse and later with the received echo. Measurement of time can then be made by measuring the average current for a fixed recurrence interval, or by any of several available methods. The immediate objection to this technique is that it would be completely confused by multiple signals. A technique one step more complex is the method of the AGL-(T), Sec. 8-17, in which a range gate is made to increase in duration until it includes part of an echo. This method has discrimination to the extent of selecting only the first of several pulses. Further methods of selecting any one of many signals are discussed in Secs. 8-16, 8-17, and 8-18.

A second characteristic of the data that affects the time-measuring accuracy is the receiver bandwidth and the pulse rise time, for the data of Chap. 3 show that range errors of appreciable magnitude can result from amplitude modulation of the signal if the receiver bandwidth is inadequate. Signal modulation often results from fading, which can last as long as several seconds and result in errors both in range and range rate. Automatic gain control improves this situation. Rapid gain

control reduces not only the errors in range but also the rate errors introduced by fades. Furthermore, automatic gain control improves the range-tracking performance since the signal amplitude and hence the time-discriminator sensitivity will remain constant.

A most serious consideration is the nature of the reflector. For example, if one were measuring the range to a mountain with a radar set, there would be no indication as to what part of the mountain is responsible for the leading edge, or the center, of the received pulse. Even in measuring the distance to an island in which the leading edge of the pulse is liable to be fairly well defined, the circuits must measure the distance to the leading edge and not to the center of area of the pulse as many time discriminators do. If the target is a complex moving target, such as a ship, considerable fluctuations will occur in the apparent range due to specular reflection from particular surfaces and interference between the waves reflected from various surfaces. The range-tracking gates of an experimental radar set employing 0.1- $\mu$ sec pulses to give 27-in. resettability were found to wander over the whole length of the signal received from a freighter since the circuit was seeking the point of maximum amplitude. Even differentiating the signal to track the leading edge is not wholly satisfactory since with rapid AGC the appearance of the leading edge of the pulse from a ship wanders more than half the length of the ship.

## AUTOMATIC TIME MEASUREMENT WITH NORMALLY CONTINUOUS DATA

### DESIGN OF THE FUNCTION UNIT

**8-4. General Theoretical Statement of the Problem.**—In the introductory description of the elements of the automatic tracking loop, nothing was said about the transfer characteristics of the individual elements. If, as indicated in Fig. 8-1, the time discriminator and the time modulator are linear over a reasonable range and have frequency and phase responses good enough to be neglected compared with the rest of the system, it is the function unit that is called upon to meet the requirements for stable tracking and to provide the functions of memory, coast, and target selection. In addition, it must operate on the error signal  $E$  to convert it into a form suitable for controlling the time modulator and supplying data to a computer or indicator. These operations are symbolized by the expression

$$V = f(i) \quad (1)$$

and the laws of the time discriminator and the time modulator are expressed as

$$i = k_2 \epsilon = k_2(R - R') \quad (2)$$

and

$$R' = k_1 V \quad (3)$$

over their linear region of operation. The symbol  $R$  represents the range or instantaneous value of the time modulation of the signal being measured, and  $R'$  similarly represents the time modulation of the locally time-modulated comparison pulse. The control signal of the local time modulator is represented by  $V$  and may be either a voltage or a shaft rotation. The error signal current  $i$  is usually in the form of a current that flows only for the duration of the signal being tracked and hence consists of pulses of current at the PRF. Since an average current can be obtained by smoothing, its discontinuous nature is not important provided the period of the PRF is very short compared with the periods of fluctuation of the time modulation. Quite apart from its discontinuous nature the current is not immediately suitable for controlling  $R'$ . For example, if  $i$  is made to flow through a resistance to generate a voltage  $V$  for controlling an electrical time modulator, the discriminator current could be zero for only one value of  $R'$ . For all other values of  $R'$  the current  $i$ , and hence the difference  $R - R'$  would have to be different from zero and  $V$  would not indicate the true time modulation  $R$ . It can be argued that if  $k_1 k_2$  is sufficiently large this error would be negligible, but it is also true that this condition renders proper stabilization of the tracking loop possible only with a very slow response. Therefore a function unit that relates  $i$  and  $V$  in direct proportion is unsatisfactory.

We deduce from this argument that one property which the function unit must have is that the output  $V$  can have any value while its input  $i$  is zero. Furthermore, as was mentioned in Sec. 8-3, the properties of position or velocity memory are desirable. These two requirements and the knowledge that the data must be reasonably smooth suggest the use of one or more integrators in the function unit. Further restrictions on the function unit are that  $\epsilon$  must not differ from zero by an amount larger than the dynamic accuracy specifications, and that the tracking loop be stable.

In the ensuing sections, the quantities  $R$  and  $R'$  will be regarded as distances rather than times since it is much easier to discuss velocity as the rate of change of distance with time than as the rate of change of time modulation with time.

**8-5. Single-integrator Function Unit.**—By an argument similar to the one wherein the weakness of the proportional function unit was demonstrated, it can be seen that a function unit performing the operation

$$V = \frac{1}{C} \int_i i \, dx \quad (4)$$

will allow  $V$  to take any fixed value when  $i$  is zero, but will require  $i$  to be different from zero by an amount proportional to the desired rate of change of  $V$ . In this operation  $C$  has the dimensions of capacitance.

Differentiating Eq. (4) and using the operational notation  $p = d/dt$ ,  $1/p = \int dt$ , discussed in Vol. 19, Chap. 2, we have

$$pV = \frac{i}{C}. \quad (5)$$

Using this equation as defining the performance of the function unit, and combining it with Eqs. (2) and (3) to give the equation of motion of the system, we have

$$pR' = \frac{k_1 k_2}{C} (R - R') \quad (6)$$

The circuit of Fig. 8-2 obeys a similar equation, for there

$$i = \frac{(V_1 - V_2)}{r}$$

and  $i = pCV_2$  giving

$$pV_2 = \frac{1}{rC} (V_1 - V_2) \quad (7)$$

which is identical with Eq. (6) provided

$$\left. \begin{aligned} V_1 &= R \\ V_2 &= R' \\ r &= \frac{1}{k_1 k_2} \end{aligned} \right\} \quad (8)$$

Thus the behavior of the single-integrator system can be deduced from this circuit.

The general behavior of this circuit is so well known that it remains only to note a few salient properties of the system, namely:

1. In the steady state,  $R' = R$ .
2. If  $R$  suffers a unit function change,  $R'$  will approach equality with  $R$  exponentially with a time constant

$$S = \frac{C}{k_1 k_2}. \quad (9)$$

3. If  $R$  is changing at a constant rate  $dR/dt = \alpha$  then  $R'$  in the steady state will exhibit a lag behind  $R$  of

$$R - R' = S\alpha. \quad (10)$$

If  $R$  is regarded as position, this system may be said to exhibit velocity lag.

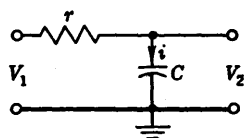


FIG. 8-2.—Equivalent circuit for single-integrator system.



In applying the above discussion to the automatic tracking system, there are a few remarks that can be made concerning a single integrator system. If there is actually only one integrating element, the equation of the system has no oscillatory terms and hence needs no additional components for stabilization. An interesting concept can be derived from the fact that the time constant of the system is  $C/k_1k_2$ , since  $1/k_1k_2$  then has the dimensions of resistance. Now  $k_1$  and  $k_2$  are the factors of proportionality of the time modulator and the discriminator respectively and may be called the gains of those elements. Developing the concept further,  $1/pC$  may be regarded as the gain of the integrator. Hence the factor  $k_1k_2/pC$  may be called the over-all gain of the three elements, and, referring to Fig. 8-1, the system may be regarded as an amplifier with negative feedback where the entire output is fed back to the input ( $\beta = 1$ ). Much has been written on the stabilization and design of feedback amplifiers and on the application of feedback amplifier theory to automatic control systems. This treatment is used in Vol. 21, Chap. 9, on automatic control systems where earlier references are indicated. A high gain factor produces a short time constant and fast response. In addition high gain provides "tight tracking," for the velocity lag is  $S\alpha$  from Eq. (10). This is in accord with the conclusions of negative-feedback-amplifier practice where high internal gain results in wide bandwidth and a large reduction in over-all gain variations.

The conclusion that such a system is unconditionally stable also agrees with feedback amplifier theory, because the loop gain factor  $k_1k_2/pC$  has an attenuation vs. frequency curve that never exceeds  $-6\text{db/octave}$ , a sufficient condition for stability.<sup>1</sup>

The system possesses position memory, for, if the incoming signal fails, the function unit cannot distinguish whether this is due to the equality of  $R$  and  $R'$  or to inoperation of the circuit in the absence of a signal; hence,  $k_2$  in Eq. (6) is effectively zero and  $pR' = 0$ —that is, the position of the tracking gates  $R'$  become stationary at its last value.

Since the input signal usually moves continuously, it appears that position memory in itself is of little value unless the fades are so short that the misalignment between signal and gates will not exceed the range aperture. Even then, the fades or interruptions introduce large errors in the position and rate data. Velocity memory is obviously required if fades are expected.

**8-6. Double-integrator System.**—Just as by making  $V$  proportional to  $\int i dt$ ,  $V$  was enabled to assume any fixed value without demanding any input current  $i$ , so by adding to  $V$  a component proportional to  $\int \int i dt dt$ , it is enabled to assume any steady rate of change without

<sup>1</sup> H. W. Bode, "Relation between Attenuation and Phase in Feedback Amplifiers," *Bell System Tel. J.*, **19**, 421-455, July 3, 1940.

demanding any input current  $i$ . Thus if the function unit obeys the equation

$$V = \frac{1}{C} \int_i dx + \frac{1}{SC} \int_i \int_x i ds dx, \quad (11)$$

which can be rewritten operationally as

$$p^2 V = \frac{1}{CS} (1 + pS)i, \quad (12)$$

then with  $i$  zero,  $p^2 V$  will be zero—that is, the rate of change of  $V$  can be constant at any value. In this equation as before, the constant  $S$  has the dimensions of time.

To see whether the constants for the solution of the above equation can be chosen to give stable tracking of  $R$  by  $R'$ , we combine Eq. (12) with Eqs. (2) and (3) to give the equation of the system in terms of  $R$  and  $R'$ ,

$$p^2 R' = \frac{k_1 k_2}{CS} (1 + pS)(R - R'). \quad (13)$$

Once again, an equivalent circuit (Fig. 8-3) will help in making clear the general properties of the system. In this circuit

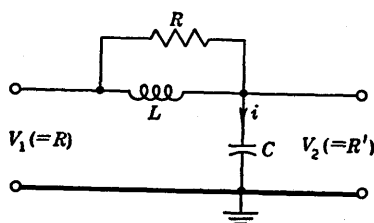


FIG. 8-3.—Equivalent circuit of double-integrator system.

$$i = \frac{R + Lp}{RLp} (V_1 - V_2) \quad (14a)$$

and

$$i = pCV_2. \quad (14b)$$

Hence

$$p^2 V_2 = \frac{1}{LC} \left( 1 + p \frac{L}{R} \right) (V_1 - V_2), \quad (14c)$$

which is of the same form as Eq. (13) with

$$\left. \begin{aligned} V_1 &\rightarrow R \\ V_2 &\rightarrow R' \\ \frac{L}{R} &\rightarrow S \\ \frac{1}{LC} &\rightarrow \frac{k_1 k_2}{CS} \end{aligned} \right\} \quad (15)$$

The complete integral of Eq. (13) is

$$R' = Ae \left( -\frac{k_1 k_2}{2C} + \sqrt{\frac{k_1^2 k_2^2}{4C^2} - \frac{k_1 k_2}{CS}} \right) t + Be \left( -\frac{k_1 k_2}{2C} - \sqrt{\frac{k_1^2 k_2^2}{4C^2} - \frac{k_1 k_2}{CS}} \right) t + f(R) \quad (16)$$

It follows from the well-known behavior of the equivalent circuit that a control system which has a function unit obeying Eq. (12) will behave in general as a damped resonant circuit of resonant frequency (undamped)  $f_n$  given by

$$\omega_n^2 = (2\pi f_n)^2 = \frac{k_1 k_2}{CS}. \quad (17)$$

The damping will be critical when

$$S\omega_n = 2, \quad (18)$$

the circuit being underdamped for lower values of  $S$ . Equation (13) can now be written as

$$p^2 R' = \omega_n^2 (1 + pS)(R - R'). \quad (19)$$

This is also the equation of the circuit of Fig. 8-3 using Eq. (17) and the equivalences (15).

The salient features of the system can be deduced from the behavior of the circuit of Fig. 8-3 and the solutions of Eq. (14c) by substituting  $R$  and  $R'$  for  $V_1$  and  $V_2$ .

If  $R'$  is constant, then in the steady state (i.e., when  $t \rightarrow \infty$ )  $R' = R$ ; therefore, there should be no error in  $R'$  for any static values of  $R$ .

If  $R$  performs a unit function change,  $R'$  will follow this change with an overshoot and a number of oscillations of decaying amplitude, the rate of decay being dependent on the damping, and therefore the system is theoretically capable of stable operation. Figure 8-4 shows typical examples.

If  $R$  takes on a rate of change  $\alpha$ , then in the steady state,  $i$  will be constant and  $R - R'$  will become zero as in Fig. 8-5. This predicts zero velocity lag—i.e., zero position error—as a function of target velocity. The behavior of  $(R - R')$  during the settling-down period is shown by the curves of Fig. 8-5.

If  $R$  has a constant second derivative (acceleration) equal to  $\beta$ , then by solving Eqs. (14) for  $V_1 - V_2$  in terms of  $V_1$ , we find for  $t \rightarrow \infty$ ,  $V_1 - V_2 = \beta LC$ ; that is, the system exhibits acceleration lag equal to  $(k_1 k_2 / CS)\beta$ .

The final question to be considered is whether or not the system possesses velocity memory. The condition for velocity memory is that if the signal fails,  $pR'$  shall be constant. It is necessary at this point to abandon the equivalent circuit since in the absence of a signal, Eq. (2), basic to the analysis, is no longer valid. The disappearance of the signal is equivalent to rendering  $k_2 = 0$ . Equation (13) for the automatic control system, then reveals the behavior, for with  $k_2 = 0$ ,  $p^2 R' = 0$ , which is the criterion for velocity memory.

In review we find that the double-integrator system has an acceleration lag but no velocity or position lag, that it is capable of stable opera-

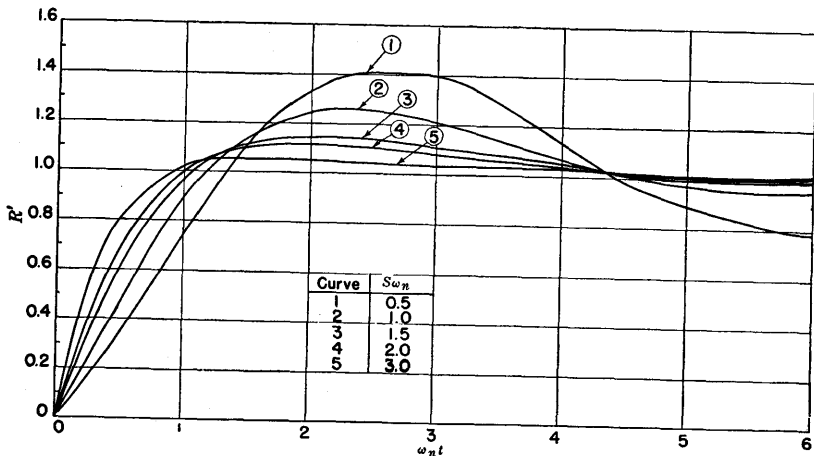


FIG. 8-4.—Transient response of double-integrator system to a step function in position for several values of damping. Curve 4 shows critically damped response.

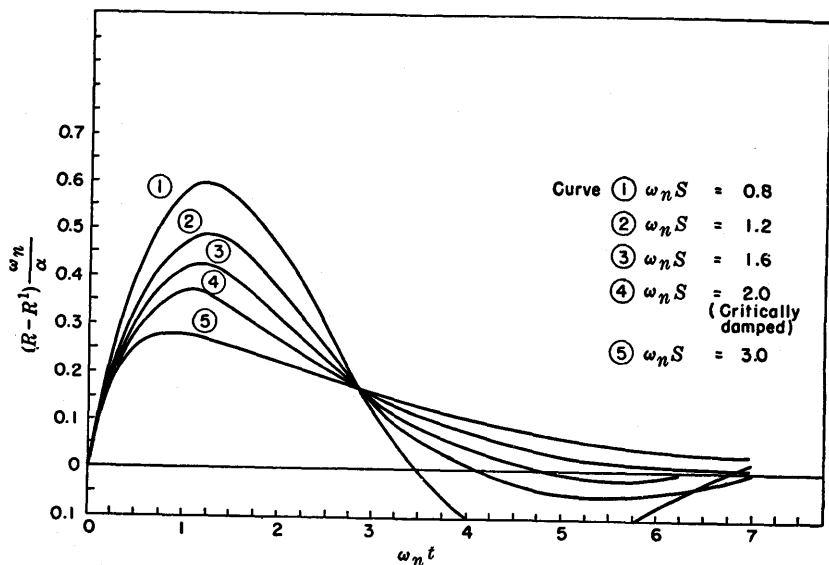


FIG. 8-5.—Behavior of  $R-R'$  in response to an instantaneous change  $\alpha$  in the value of  $dR/dt$  ( $pR$ ) for various values of  $\omega_n^2$ . This is the response of a double-integrator system characterized by Eq. (19).

tion, and that it possesses velocity memory. (This is sometimes referred to as "position and velocity memory.")

As in the discussion of the single-integrator system, the useful negative feedback amplifier theory can be applied as an alternative approach to the solution. The system can be seen to correspond to two amplifiers of gain  $k_1$  and  $k_2$  in series with a device of gain  $(1/pC) + (1/p^2CS)$ . The over-all gain without feedback has two components,

$$\frac{k_1 k_2}{pC} \quad \text{and} \quad \frac{k_1 k_2}{p^2 CS}.$$

The term  $k_1 k_2 / pCS$  gives 12 db/octave; the addition in the above solution of a component  $k_1 k_2 / pC$ , which attenuates at 6 db/octave only, brings the attenuation slope to less than 12 db/octave, a condition for stability.

In the transition from a single-integrator to a double-integrator system it would have been perfectly natural to propose a function unit in which the current  $i$  is simply integrated twice to form the quantity  $V$ —that is,

$$V = \frac{1}{CS} \int_i \int_x i \, ds \, dx. \quad (20)$$

The equation of motion for a system having a function unit of this type is equivalent to that of an undamped resonator. The immediate conclusion is that it would be impossible to stabilize such a system. Alternatively, in terms of feedback amplifier theory, each integration introduces a phase lag of  $90^\circ$ . Hence there would be no region in which the feedback would be negative.

Satisfactory control of  $R'$  can be achieved with many other forms of function unit, but the two so far described form the basis of most automatic tracking systems.

**8-7. Effect of Additional Smoothing.**—Since the information (current) supplied by the discriminator is essentially discontinuous at the PRF, some smoothing of the PRF components will usually be necessary. The smoothing usually consists of one or more simple  $RC$ -smoothers of the type shown in Fig 8-2 for which

$$\frac{V_2}{V_1} = \frac{1}{1 + pT},$$

where  $T_s = RC$ , the circuit time constant. If a single circuit does not provide sufficient smoothing, additional circuits with the same time constants may be used. The effect of introducing such circuits is to multiply the function unit equation by a factor  $\left(\frac{1}{1 + pT_s}\right)^n$ , where  $n$  is the number of smoothing circuits. In the presence of such circuits,

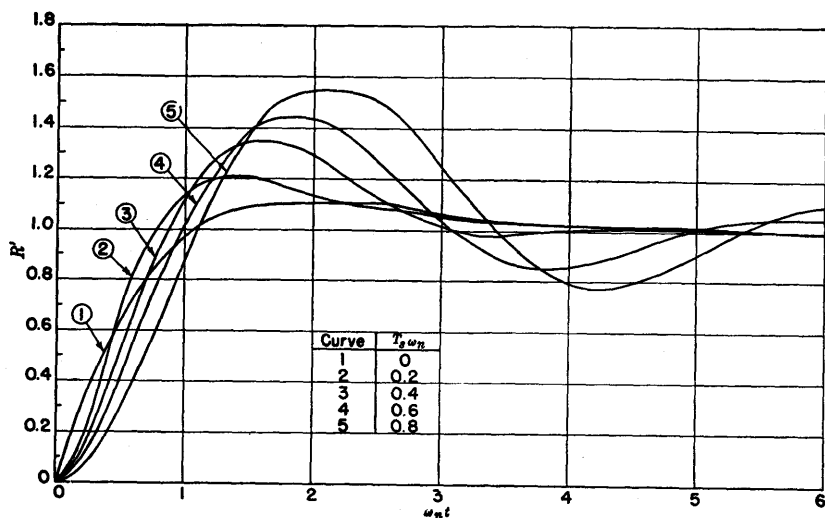


FIG. 8-6.—Response of a double-integrator system with one smoothing network to a unit function change in  $R$  for various values of  $\omega_n T_s$ . Damping critical for all curves ( $\omega_n T = 2$ ) and  $n = 1$ .

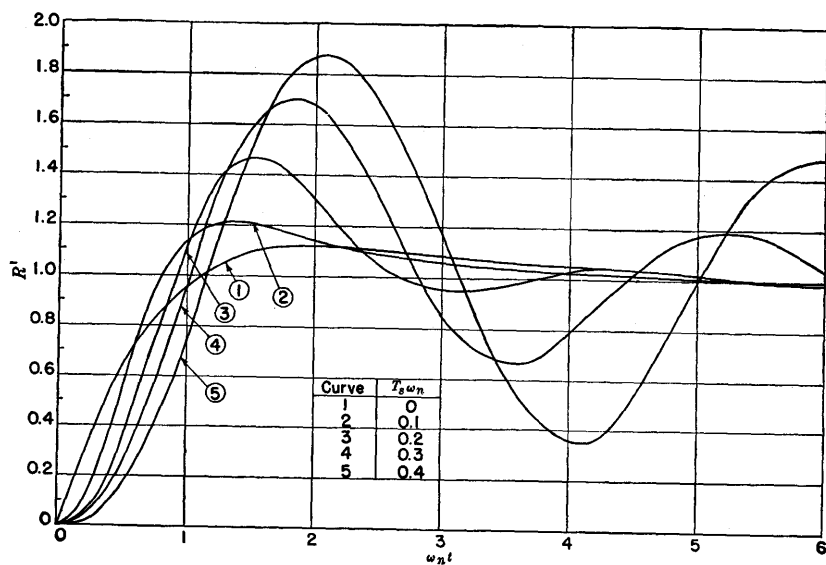


FIG. 8-7.—Response of double-integrator system with two smoothing networks to a unit function change in  $R$  for various values of  $\omega_n T_s$ . Damping critical for all curves ( $\omega_n T = 2$ ) and  $n = 2$ .

Eq. (12) becomes

$$p^2V = \frac{1}{CS} \frac{(1 + pS)}{(1 + pT_s)^n} i, \quad (21)$$

and Eqs. (13) and (19) become

$$p^2R' = \frac{k_1k_2}{CS} \frac{(1 + pS)}{(1 + pT_s)^n} (R - R') \quad (22)$$

and

$$p^2R' = \omega_n^2 \frac{(1 + pS)}{(1 + pT_s)^n} (R - R'). \quad (23)$$

The effect that these smoothers have on the behavior of the system is shown in Figs. 8-6 and 8-7, which show the response to unit step function with  $n = 1$  and  $n = 2$  for various values of  $\omega_n T_s$ . The value of  $\omega_n$  is given by Eq. (17). In these curves the damping is critical, i.e.,  $S\omega_n = 2$ , and it may be seen that the response is not seriously spoiled provided that

$$\text{and} \quad \left. \begin{array}{ll} T_s \omega_n < 0.4 & \text{with } n = 1 \\ T_s \omega_n < 0.2 & \text{with } n = 2. \end{array} \right\} \quad (24)$$

For single-integrator systems whose behavior is expressed in Eq. (6), additional smoothing may conveniently employ different time constants for the smoothers since an additional feature can thus be obtained. Equation (5) is replaced by

$$pV = \frac{i}{C} \frac{1}{(1 + pT_1)(1 + pT_s)^n}, \quad (25)$$

and Eq. (6) becomes

$$pR' = \frac{k_1k_2}{C} \frac{1}{(1 + pT_1)(1 + pT_s)^n} (R - R'), \quad (26)$$

where  $T_1$  is the smoother with a different time constant from its fellows. Equation (26) can now be written

$$p^2R' = \frac{k_1k_2}{CT_1} \frac{pT_1}{(1 + pT_1)(1 + pT_s)^n} (R - R'). \quad (27)$$

With  $n = 0$ , this equation corresponds with that of the series damped oscillatory circuit of Fig 8-8, for which

$$\begin{aligned} i &= \frac{V_1 - V_2}{r + pL} \\ i &= pCV_2 \\ pV_2 &= \frac{1}{RC \left(1 + p \frac{L}{R}\right)} (V_1 - V_2). \end{aligned}$$

Since constant  $dV_2/dt$  demands constant  $i$ , the system will exhibit velocity lag, but the presence of  $L$  will introduce a certain amount of velocity memory.

Equation 27 with  $n = 0$  may be rewritten as

$$(1 + pT_1)pR' = \frac{k_1k_2}{C} (R - R'),$$

for which, when  $k_2 = 0$ ,  $(1 + pT_1)pR'$  remains. The solution for this is

$$R' = A + Be^{-\frac{t}{T_1}},$$

from which  $pR' = \frac{B}{T_1} e^{-\frac{t}{T_1}}$ . Thus any velocity existing at  $t = 0$  decays exponentially to zero with a time constant  $T_1$ . This may be called transient velocity memory.

The resonant frequency of the circuit is given by

$$\omega_n^2 = \frac{k_1k_2}{CT_1^2}, \quad (28)$$

and damping is critical when

$$T_1\omega_n = \frac{1}{2}, \quad (29)$$

the damping increasing with *decreasing*  $T$ , as shown in Fig. 8-9.

When  $n = 1$ , the response is as indicated in Fig. 8-10, which shows the unit function response with critical damping for various values of  $\omega_n T_1$ , and in Fig. 8-11 for  $m = 2$ .

The preceding presentation has the advantage of having equations of motions of automatic tracking loops in a form that indicates clearly the type of function unit necessary to perform the desired operations.

Examples of synthesizing electrical function units for several systems will be given in the next section. Feedback amplifier theory is probably more lucid on the matter of stabilization but does not indicate directly the electrical operations that are necessary to synthesize the equations.

Furthermore, in the simple electrical systems that are frequently used, stabilization is a secondary consideration usually investigated after the more fundamental operations of memory and target selection have been obtained. It might be advisable in complex systems to use differential equations to indicate the desired operations and then to obtain the conditions for stability by treating the system as a feedback amplifier.

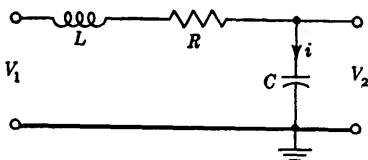


FIG. 8-8.—Equivalent circuit for single-integrator system with one smoothing network.



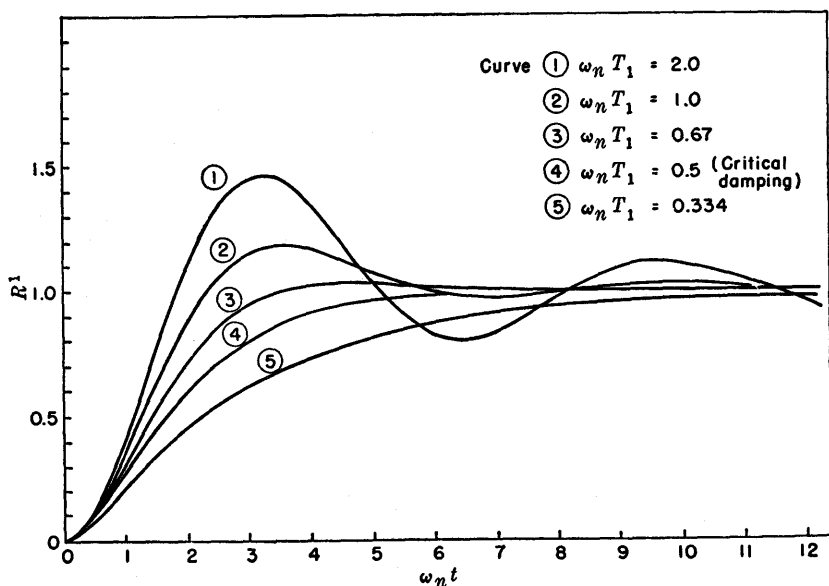


FIG. 8-9.—Response of single-integrator system with one smoothing network to a unit function change in  $R$  for various damping factors. This response is described by Eq. (27) with  $n = 0$ .

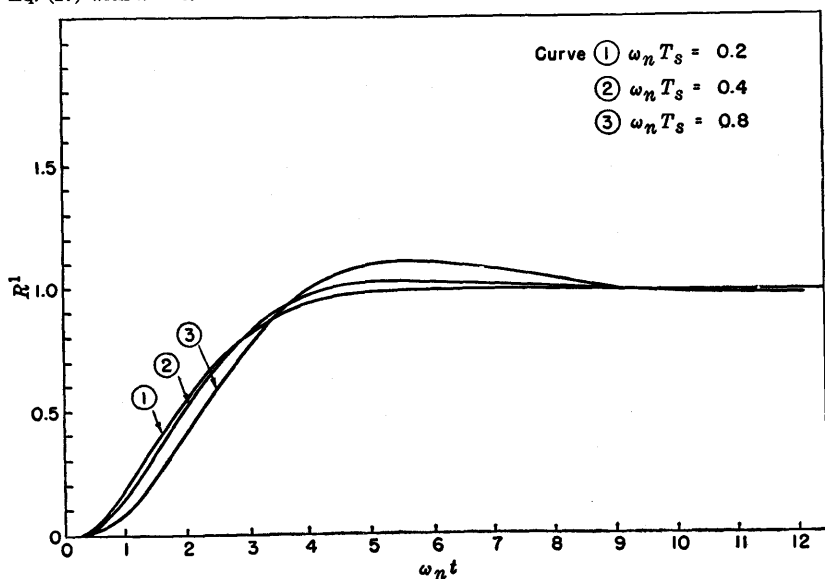


FIG. 8-10.—Curves showing response of single-integrator system with two smoothing networks to a unit function change in  $R$  for various values of  $\omega_n T_s$ . Damping is critical for all curves ( $\omega_n T_1 = \frac{1}{2}$ ) and  $n = 1$ .

This might be particularly advantageous in the design of electromechanical systems, in which the primary functions can be predicted fairly easily, but in which the factors leading to instability are more subtle and yield most easily to feedback amplifier methods.

It should be noted in addition that the major design considerations of most wartime-designed automatic tracking systems were meeting the military requirements and the designs were frequently achieved by intuitive methods. Work on a useful theory progressed during the war, but a complete treatment awaited the additional time available in the reporting and terminating activities. Hence, widespread variations in

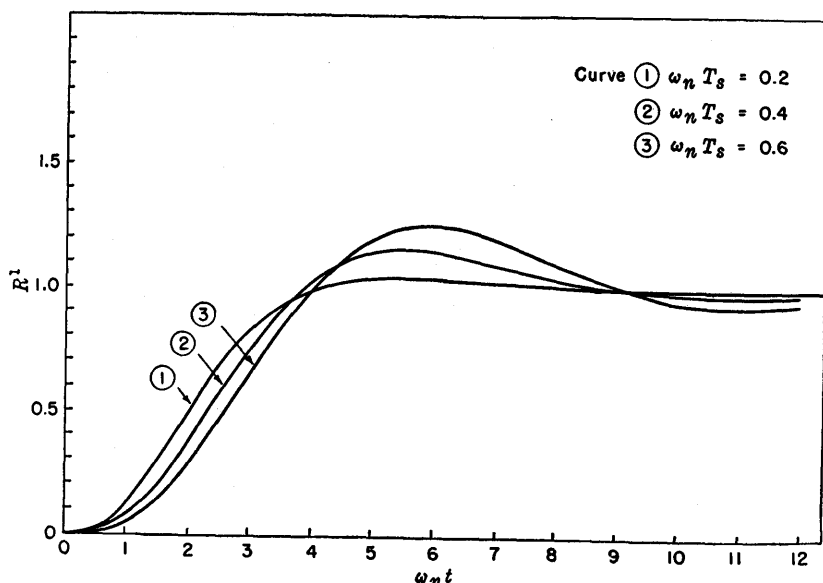


FIG. 8-11.—Curves showing response of single-integrator system with three smoothing networks to a unit function change in  $R$  for various values of  $\omega_n T_s$ . Damping is critical for all curves ( $\omega_n T_1 = \frac{1}{2}$ ) and  $n = 2$ .

practice will be observed in the section of this chapter that describes actual systems.

**8-8. Electrical Integrators.**—It follows from the previous section that the error signal must be smoothed and integrated and thereby rendered suitable to control the time modulator. Using only passive elements smoothing operations can be obtained exactly with components of reasonable value, but only very approximate integration can be thus achieved. Chapter 12 of Vol. 19 describes feedback amplifiers used to perform integration, differentiation, and combinations of these operations. The electrical function units can be synthesized from these amplifiers.

TABLE 8-1.

<p>1.</p> <p><math>v_1 = E_{(1)}</math></p> <p>Admittance = <math>\frac{1}{R_1}</math>      Impedance = <math>R_2</math>      Virtual ground</p> <p><math>v_2 = \frac{1}{R_1} \times R_2 E_{(1)}</math></p>	<p>2.</p> <p><math>v_1 = \frac{a}{p}</math></p> <p>Admittance = <math>pC</math>      Impedance = <math>R</math>      Virtual ground</p> <p><math>v_2 = CRa</math></p>
<p>5.</p> <p><math>v_1 = E_{(1)}</math></p> <p>Admittance = <math>\frac{1}{R}</math>      Impedance = <math>\frac{1}{pC}</math>      Virtual ground</p> <p><math>v_2 = \frac{1}{pCR} E_{(1)}</math>      Slope = <math>\frac{1}{CR} E_{(1)}</math></p>	<p>6.</p> <p><math>v_1 = E_{(1)}</math></p> <p>Admittance = <math>pC_1</math>      Impedance = <math>\frac{1}{pC_2}</math>      Virtual ground</p> <p><math>v_2 = \frac{C_1}{C_2} E_{(1)}</math></p>
<p>9.</p> <p><math>v_1 = E_{(1)}</math></p> <p>Admittance = <math>\frac{1}{R_1}</math>      Impedance = <math>\frac{1}{pC_2} (1 + pR_2C_2)</math>      Virtual ground</p> <p><math>v_2 = \frac{(1 + pR_2C_2)}{pC_2R_1} E_{(1)}</math>      Slope = <math>\frac{1}{R_1C_2} E_{(1)}</math></p>	<p>10.</p> <p><math>v_1 = \frac{a}{p}</math></p> <p>Admittance = <math>pC_1</math>      Impedance = <math>\frac{1}{pC_2} (1 + pR_2C_2)</math>      Virtual ground</p> <p><math>v_2 = a \left( \frac{C_1}{C_2} + pR_2C_1 \right)</math>      Slope = <math>\frac{C_1}{C_2} a</math></p>
<p>13.</p> <p><math>v_1 = E_{(1)}</math></p> <p>Admittance = <math>\frac{1}{R_1}</math>      Impedance = <math>\frac{R_2}{1 + pC_2R_2}</math>      Virtual ground</p> <p><math>v_2 = \frac{R_2}{R_1} \frac{1}{(1 + pC_2R_2)} E_{(1)}</math>      <math>T = R_2C_2</math>      <math>\frac{R_2}{R_1} E_{(1)}</math></p>	<p>14.</p> <p><math>v_1 = E_{(1)}</math></p> <p>Admittance = <math>pC_1</math>      Impedance = <math>\frac{R_2}{1 + pC_2R_2}</math>      Virtual ground</p> <p><math>v_2 = \frac{pC_1R_2}{1 + pC_2R_2} E_{(1)}</math>      <math>T = R_2C_2</math>      <math>\frac{C_1}{C_2} E_{(1)}</math></p>

TABLE 8-1.—(Continued)

<p>3.</p> <p><math>v_1 = E_{(1)}</math></p> <p>Admittance = <math>\frac{pC}{(1 + pCR_1)}</math></p> <p>Impedance = <math>R_2</math></p> <p>Virtual ground</p> <p><math>v_2 = \frac{pC}{(1 + pCR_1)} \times R_2 E_{(1)}</math></p> <p><math>T = R_1 C</math></p>	<p>4.</p> <p><math>v_1 = \frac{a}{p}</math></p> <p>Admittance = <math>\frac{1}{R_1} (1 + pCR_1)</math></p> <p>Impedance = <math>R_2</math></p> <p>Virtual ground</p> <p><math>v_2 = \frac{aR_2}{pR_1} + aCR_2</math></p> <p>Slope = <math>\frac{R_2}{R_1} a</math></p>
<p>7.</p> <p><math>v_1 = E_{(1)}</math></p> <p>Admittance = <math>\frac{pC_1}{(1 + pC_1R_1)}</math></p> <p>Impedance = <math>\frac{1}{pC_2}</math></p> <p>Virtual ground</p> <p><math>v_2 = \frac{C_1}{C_2} \frac{1}{(1 + pC_1R_1)} E_{(1)}</math></p> <p><math>T = C_1R_1</math></p>	<p>8.</p> <p><math>v_1 = E_{(1)}</math></p> <p>Admittance = <math>\frac{1}{R_1} (1 + pC_1R_1)</math></p> <p>Impedance = <math>\frac{1}{pC_2}</math></p> <p>Virtual ground</p> <p><math>v_2 = \frac{1}{R_1} (1 + pC_1R_1) \times \frac{1}{pC_2} E_{(1)}</math></p> <p>Slope = <math>\frac{E_{(1)}}{C_1R_1}</math></p>
<p>11.</p> <p><math>v_1 = E_{(1)}</math></p> <p>Admittance = <math>\frac{pC_1}{(1 + pR_1C_1)}</math></p> <p>Impedance = <math>\frac{1 + pC_2R_2}{pC_2}</math></p> <p>Virtual ground</p> <p><math>v_2 = \frac{pC_1}{(1 + pR_1C_1)} \times \frac{(1 + pC_2R_2)}{pC_2} E_{(1)}</math></p> <p><math>T = C_1R_1</math></p>	<p>12.</p> <p><math>v_1 = \frac{a}{p}</math></p> <p>Admittance = <math>\frac{1}{R_1} (1 + pC_1R_1)</math></p> <p>Impedance = <math>\frac{1 + pC_2R_2}{pC_2}</math></p> <p>Virtual ground</p> <p><math>v_2 = \frac{a}{p} \frac{(1 + pC_1R_1)}{R_1} \times \frac{(1 + pC_2R_2)}{pC_2}</math></p> <p><math>T = \frac{C_1R_1}{C_2} a</math></p>
<p>15.</p> <p><math>v_1 = E_{(1)}</math></p> <p>Admittance = <math>\frac{pC_1}{1 + pC_1R_1}</math></p> <p>Impedance = <math>\frac{R_2}{1 + pC_2R_2}</math></p> <p>Virtual ground</p> <p><math>v_2 = \frac{pC_1R_2}{(1 + pC_1R_1)(1 + pC_2R_2)} E_{(1)}</math></p> <p>Assuming <math>C_2R_2 &gt; C_1R_1</math></p> <p><math>T = C_1R_1</math></p>	<p>16.</p> <p><math>v_1 = E_{(1)}</math></p> <p>Admittance = <math>\frac{1 + pC_1R_1}{R_1}</math></p> <p>Impedance = <math>\frac{R_2}{1 + pC_2R_2}</math></p> <p>Virtual ground</p> <p><math>v_2 = \frac{R_2 (1 + pC_1R_1)}{R_1 (1 + pC_2R_2)} E_{(1)}</math></p> <p><math>T = C_2R_2</math></p>

In summary, the feedback amplifier of Fig. 8-12 is shown there to be similar to the circuit shown in Fig. 8-13. The "virtual ground" is a ground only in that the action of the feedback amplifier is to hold that point fixed by supplying a current through  $Z_2$ . Within the limits over which this assumption is valid, the output voltage can be calculated

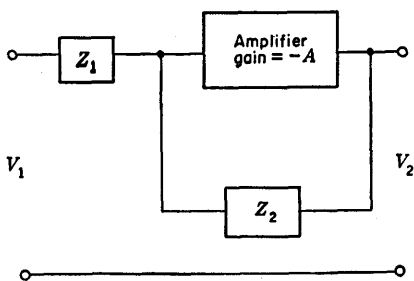


FIG. 8-12.—Feedback-amplifier block diagram.

by assuming that the current which flows from  $V_1$  to the virtual ground is equal and opposite to the current which flows to the virtual ground from  $V_2$ . The transformation performed by the circuit is the negative of the product of the admittance of the input branch and the impedance of the output branch. Table 8-1 shows the transformations that can be set up using the more common

combinations of resistance and capacitance to replace  $Z_1$  and  $Z_2$ . The input admittance and the output impedance are shown in operational notation, as well as the response of each circuit to unit functions of  $V_1$  or  $dV_1/dt$ . Where the input is in the form of a current, as it is in most time discriminators, the diagrams of column (1) are relevant with  $R_1$  omitted and  $i$  replacing  $V_1/R_1$ .

There are numerous other possible arrangements in which the network has one or more components with one terminal grounded, two of which are shown in Fig. 8-14. The output voltage of the circuit in Fig. 8-14a, in which current feed is used, can be determined by calculating  $i$ , the current entering the virtual ground, and the output can be obtained as before by assuming that the same current flows in opposite sense through the output impedance. These steps are as follows for Fig. 8-14a:

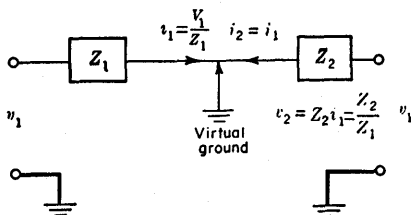


FIG. 8-13.—Equivalent circuit of feedback amplifier using general impedances  $Z_1$  and  $Z_2$ .

$$i_3 = \frac{i_1}{1 + pC_1R_1}$$

$$V_2 = \frac{i_1}{pC_2(1 + pC_1R_1)}$$

In Fig 8-14b it is the feedback which has a component grounded; here, the process is to calculate  $i_2$  in terms of  $V_2$ , and  $i_1$  in terms of  $V_1$ , and

equate them as follows:

$$i_2 = \frac{V_2}{R_2(2 + pR_2C_2)} = i_1 = \frac{V_1}{R_1}$$

$$V_2 = \frac{V_1 R_2}{R_1} (2 + pR_2C_2).$$

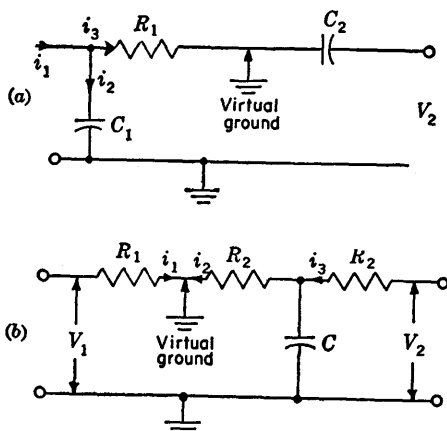


FIG. 8-14.—Two feedback function units having one component grounded.

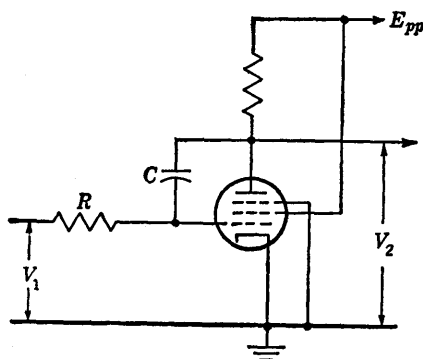


FIG. 8-15.—Simple integrator circuit.  $V_1 = -RCpV_2(1 + \frac{1}{A}) - \frac{V_2}{A}$

The assumption that the point labelled virtual ground remains fixed is valid only for infinite amplifier gain. In the simple integrator circuit of Fig. 8-15, two effects result from finite gain. These can be observed easily by determining to what extent the input is the derivative of the output. This is expressed as

$$\left. \begin{aligned} V_1 &= -\frac{Z_1}{Z_2} V_2 \left(1 + \frac{1}{A}\right) - \frac{V_2}{A} \\ \text{or} \\ V_1 &= -RCpV_2 \left(1 + \frac{1}{A}\right) - \frac{V_2}{A} \end{aligned} \right\} \quad (30)$$

The first effect is that the desired operation, integration, is in error by a factor  $(1 + 1/A)$ . Furthermore, the output is related at all times to the input by the addition term  $-V_2/A$ . The following example will show to what extent these errors can be neglected.

*Synthesis of Double Integrator with Smoothing.*—These methods will now be used to synthesize a circuit of a function unit that obeys Eq. (21),

$$p^2V = \frac{1}{CS} \frac{(1 + pS)}{(1 + pT_s)^n} i, \quad (21)$$

or substituting  $k_1k_2/\omega_n^2$  for  $CS$  from Eq. (17),

$$p^2V = \frac{\omega_n^2}{k_1k_2} \frac{(1 + pS)}{(1 + pT_s)^n} i. \quad (22)$$

Rewriting Eq. (22) for  $n = 1$  in a form suitable for synthesis, one form is

$$\frac{i}{1 + pT_s} \times \frac{1}{pC} \times \frac{(1 + pC_1R_1)}{R_1} \times \frac{1}{pC_2} = V. \quad (31)$$

This equation can be synthesized by the circuit of Fig. 8-14a, and Circuit 8 of Table 8-1 operating in series. Figure 8-16 shows this network for

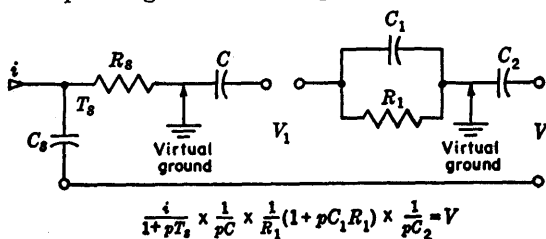


FIG. 8-16.—Equivalent circuit for Eq. (22) with  $n = 1$ .

$n = 1$ . Each term in the equation is arranged to be below the component that supplies that term. Equations (31) and (22) provide that

$$\left. \begin{aligned} CR_1C_2 &= \frac{k_1k_2}{\omega_n^2} \\ R_1C_1 &= S. \end{aligned} \right\} \quad (32)$$

An alternative form of Eq. (22), this time with  $n = 2$  is

$$V = \frac{1}{1 + pT_s} \times \frac{1}{p(C + C')} \times \frac{1 + pCR_1}{1 + p \frac{C'CR_1}{C + C'}} \times \frac{1}{R_1} \times \frac{1}{pC_2}.$$

Here requirements for identity are (see Fig. 8-17)

$$\left. \begin{aligned} (C + C')R_2C_2 &= \frac{k_1k_2}{\omega_n^2} \\ CR_1 &= S \\ \frac{C'}{C + C'} CR_1 &= T. \end{aligned} \right\} \quad (33)$$

The important difference between these two circuits that may influence a choice between them is that in the one of Fig. 8-16,

$$V_1 = \frac{pC_2R_1}{1 + pC_1R_1} V,$$

and in Fig. 8-17,

$$V_1 = pC_2R_2V.$$

Consequently in Fig. 8-17,  $V_1$ , which is the output voltage of the first feedback amplifier, is the differential of  $V$  and is, therefore, proportional

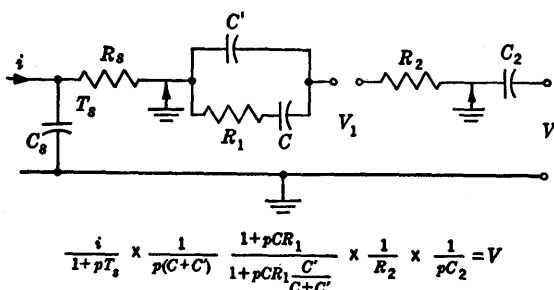


FIG. 8-17.—Equivalent circuit for Eq. (21) when  $n = 2$ .

to velocity, whereas in Fig 8-16  $V_1$  is proportional to velocity smoothed by a time constant  $R_1C_1$ . A choice between the circuits will be based on the desire for either instantaneous or smoothed velocity. In general, smoothed velocity is required since instantaneous velocity is liable to have superposed on it a spurious fluttering caused by signal amplitude modulations. A further advantage of Fig 8-16 is that the smoothing tends to prevent overloading of the second feedback amplifier caused by flutter of large amplitude.

Note that if condenser  $C'$  in Fig. 8-17 is omitted,

$$\left. \begin{aligned} n &= 1, \\ CR_2C_2 &= \frac{k_1k_2}{\omega_n^2}, \\ CR_1 &= S. \end{aligned} \right\} \quad (34)$$

and



*Synthesis of Single-integrator System.*—Another synthesis of interest is that for Eq. (25), the single-integrator system with  $n + 1$  smoothers:

$$pV = \frac{i}{C} \frac{1}{(1 + pT_1)(1 + pT_s)^n}, \quad (25)$$

which can be rewritten

$$p^2V = \frac{i}{T_1C} \times \frac{pT_1}{(1 + pT_1)} \times \frac{1}{(1 + pT_s)^n}, \quad (35)$$

or, substituting  $k_1k_2/\omega_n^2$  for  $CS$  from Eq. (17),

$$p^2V = i \frac{\omega_n^2}{k_1k_2} \times \frac{pT_1}{(1 + pT_1)} \times \frac{1}{(1 + pT_s)^n}. \quad (36)$$

The network for this equation with  $n = 1$  is shown in Fig 8-18. The equation on Fig. 8-18 is identical with Eq. (36) provided that

$$\left. \begin{aligned} \frac{\omega_n^2}{k_1k_2} &= \frac{1}{CC_2R} \\ S &= CR. \end{aligned} \right\}$$

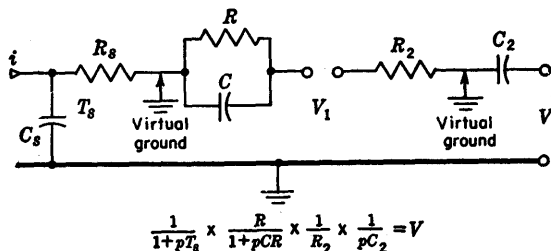


FIG. 8-18.—Equivalent circuit for a single-integrator system with two smoothers.

*Practical Circuit Design for Double Integrator.*—Returning now to Fig. 8-16, this circuit has been chosen as an example because it has many practical applications. If it is assumed that the discriminator provides  $55 \mu\text{a}$  per  $\mu\text{sec}$  of misalignment ( $k_2 = 55 \text{ amp/sec}$ ) and that the time modulator circuit sweeps over the range of 0 to  $100 \mu\text{sec}$  as  $V$  changes by 100 volts, then  $k_1 = 10^{-6} \text{ sec/volt}$ . If in addition it is assumed that the gain of a single pentode stage may be treated as infinite, the circuit will then be as shown in Fig. 8-19, where the key components of Fig. 8-16 are denoted by heavy lines. The first difference between the two circuits is the potential divider  $R_2$ - $R_3$ , needed after the first tube  $V_A$  to enable the potential  $E_1$  at the junction point of  $R_2$ - $R_3$  to move positively and negatively with respect to ground in response to variations of the plate potential of  $V_A$ . A similar potentiometer would be needed after the second tube  $V_B$  were it not for the fact that the particular time modulator requires only positive voltages to operate it. Since the potential divider

is actually needed to supply only  $R_1$ , the condensers  $C$  and  $C_1$  may be taken to the plate of the first tube, at the expense of losing direct comparison with Fig. 8-16 but with considerable practical advantage. The advantages are twofold: (1) since potential variations at the plate exceed those at  $V$ , smaller condensers can be used, and (2) as the excursions of plate potential to produce a required rate of change of  $E_2$  will be

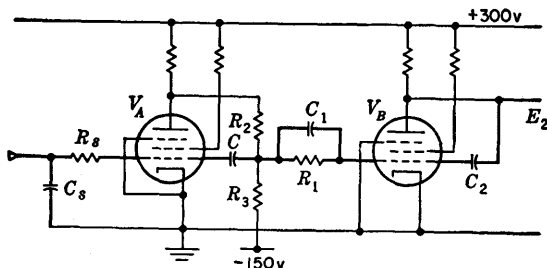


FIG. 8-19.—Actual circuit equivalent to circuit of Fig. 8-16.

greatly reduced, there will be a reduction in any tendency for  $V_A$  to overload.

The modifications to the circuit of Fig. 8-19 are shown in Fig. 8-20. In this figure the primes indicate components whose values require modification—that is,  $C'$ ,  $C'_1$ , and  $R'_1$ . Thus if  $C'$  is kept equal to  $C$ , and  $V_1$  is now redefined as the voltage of the first plate (due allowance being made for its steady direct component of about 150 volts) then  $C'_1 = C_1$ ,

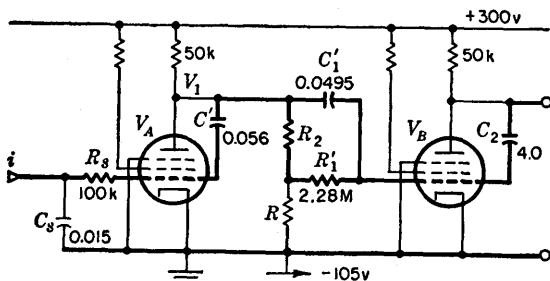


FIG. 8-20.—Modification of circuit of Fig. 8-19.

but  $R'_1$  requires alteration. Voltage  $V_1$  is now effectively halved by the two resistors  $R_2$  and  $R_3$  and the current due to  $V_1$  flows through an equivalent resistance  $R'_1 + R_2$  hence for equal current through  $R_1$  and  $R'_1$  of Figs. 8-19 and 8-20, with  $R = R_2$ ,

$$\frac{V_1}{2} \times \frac{1}{R'_1 + \frac{R_2}{2}} = \frac{V_1}{R_1}$$

or

$$R'_1 = \frac{R_1 - R_2}{2}.$$

Bearing in mind that this adjustment will be needed, Fig. 8-19 is the easiest figure to use when evaluating components.

The resistance  $R_s$  that may be placed in series with the output of a practical discriminator is limited because the circuit will not operate properly if the product of the misalignment current and output resistor amounts to more than a few volts (Vol. 19, Chap. 14).

As the misalignment  $(R - R')$  increases, the misalignment current from the discriminator increases linearly at first until a maximum value  $i_{\max}$  is reached. Any further increase in  $(R - R')$  then produces a fall in output current. With the maximum d-c back voltage that may be applied to the discriminator as  $\pm 4$  volts and the maximum misalignment current as  $40 \mu a$ ,  $R_s$  should not exceed  $4 \text{ volts}/40 \mu a$  or 100 k. The largest value of  $C_s$  that may be used is determined by  $\omega_n$ , and the smallest value depends upon the amount of PRF ripple that may be tolerated on  $i$ . If  $i_{\max} = 40 \mu a$ , the charge entering  $C_s$  per pulse is  $40 \mu a/650 = 0.0616 \mu \text{coulombs}$ , where 650 pps is the PRF. Allowing a further  $\pm 4$  volts of discriminator voltage output to accommodate the ripple voltage that this charge will produce on  $C_s$ ,  $C_s \geq 0.0616 \mu \text{coulombs}/4 \text{ volts} \geq 0.015 \mu f$ . Hence the minimum value of  $C_s R_s$  with  $R_s = 100 \text{ k}$  is 0.0015 sec. Since  $T_s \omega_n$  should be equal or less than 0.4 for stability,

$$\omega_{n\max} = \frac{0.4}{T_s} = 265 \text{ radians/sec.}$$

The lag time constant  $T_s$  will not affect the stability of the system for values of  $\omega_n$  less than  $\omega_{n\max}$ . Since smooth operation is usually desired in spite of the presence of noise and random fading of the signal, much lower values of  $\omega_n$  are usually employed. In a particular case the gates were to track an aircraft echo and to provide rate measurement in the range of  $\pm 500 \text{ mph}$  with a total change of  $\pm 30$  volts. A value of  $\omega_n = 6(f_n = 1 \text{ cps})$  was chosen. To provide the correct scale of rate measurement,  $R_1 C_2$  must be such that when

$$pR' = pk_1 V = 1.53 \mu \text{sec/sec} \approx \frac{500 \times 11}{3600},$$

then  $V_1 = pR_1 C_2 V = 30 \text{ volts.}$

Hence  $R_1 C_2 = \frac{30}{pV} = \frac{30k_1}{1.53},$

and with  $k_1 = 1.38 \mu \text{sec/volts},$   
 $R_1 C_2 = 27 \text{ sec.}$

The largest convenient value for  $C_2$  is 4  $\mu\text{f}$ ; hence

$$R_1 \approx 6.75 \text{ M.}$$

On converting this value to  $R'_1$  as in Fig. 8.20, where  $R_2 = R = 2.2 \text{ M}$ , it is found that

$$R'_1 = \frac{1}{2}(R_1 - R_2) = 2.27 \text{ M.}$$

With

$$CR_1C_2 = \frac{k_1k_2}{\omega_n^2}$$

derived from Eq. (32), and with  $k_2$  equal to 55  $\mu\text{a}/\text{sec}$ ,

$$C = \frac{10^{-6} \times 55}{27 \times 36} = 0.056 \mu\text{f.}$$

The condenser  $C_1$  is now chosen to give appropriate damping. For critical damping [from Eqs. (18) and (32)]

$$C_1R_1\omega_n = 2.$$

Hence

$$C_1 = \frac{2}{R_1\omega_n}$$

or

$$C_1 = \frac{2}{6.74 \times 10^6 \times 6} = 0.0495 \mu\text{f.}$$

These values are pertinent to Fig. 8.20; the remaining components (i.e., the two plate load resistors) are each 50 k. It now remains to check the assumption that single-stage amplifiers have sufficient gain. Tube  $V_6$  is a high- $g_m$  pentode with a plate load of 50 k, whose gain  $A$  will thus be about 100. The term  $Z_1/Z_2$  in Eq. (30) expresses the desired operation, and  $Z_1/Z_2(1 + 1/A)$  differs from this only by 1 per cent. In addition the term  $1/A$  introduces what might be called a position error in this circuit. In Fig. 8.20, for a particular value of  $V$ ,  $V_1$  can be called zero, but as  $V$  varies,  $V_1$  must also vary by  $(1/A)V$ , and hence the indicated velocity is in error by  $1/A$  times the indicated range voltage. In the system described,  $V$  goes from +50 volts to +150 volts. If the value of  $V_1$  for which  $V = 100$  volts is designated zero velocity, then in the steady-state tracking of a fixed target, the limiting departures of  $V_1$  from zero will be  $\pm 0.5$  volt. Since the swing  $V_1$  for  $\pm 500$  mph is  $\pm 30$  volts, the velocity may be in error because of this term by

$$(0.5/30) \times 100 \text{ per cent} = 1.6 \text{ per cent.}$$

Similar errors will occur while tracking a moving target, the error in velocity varying with range.

*Alternative Integrators.*—Synthesis of time-measuring systems employing either the difference integrator or the bootstrap integrator described in Vol. 19, Chap. 19 and shown in Figs. 8-21 and 8-22 can be accomplished by methods similar to those used in the feedback amplifier integrator. Since the equations for the three types of integrator are identical except in the terms expressing the errors of operation, the choice of any one for

a particular system can be based on the convenience afforded by particular circuit arrangements. For example, the feedback amplifier integrator is certainly the most simple to employ, for the input voltage may be referred to ground or a fixed point, and the equivalent circuit using the con-

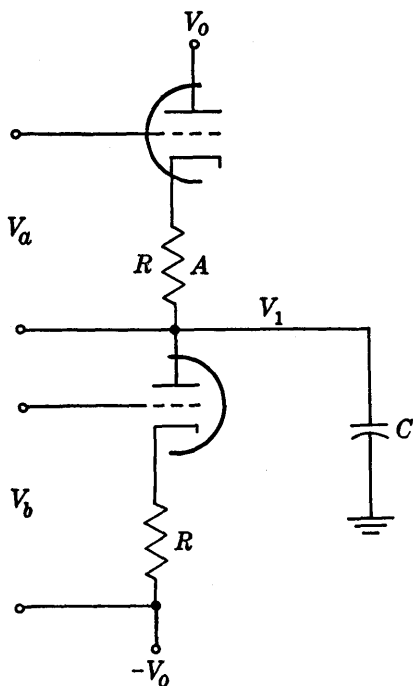


FIG. 8-21.—Difference integrator.

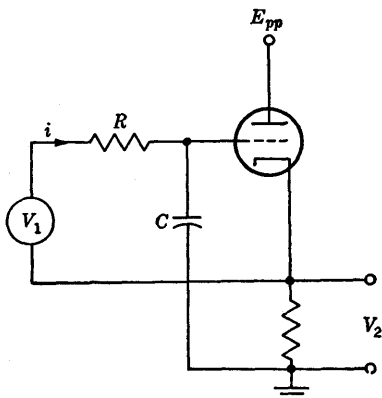


FIG. 8-22.—Bootstrap integrator.

cept of a virtual ground is very suitable for the “electron-chasing” type of reasoning. The difference integrator has the advantage of performing a subtraction or comparison at the same time that it integrates or smooths, but both it and the bootstrap integrator require a floating error-signal generator. For this reason, no particular advantage can be seen for the bootstrap integrator, since it offers no compensating feature. It was argued at one time that a “cathode-follower” integrator could be operated at lower grid current,<sup>1</sup> but this is a fallacy, for the circuit is

<sup>1</sup> The advantage that a straight cathode follower has over a d-c amplifier for grid current is that large input voltages can be accepted with a small change in grid-to-cathode bias. The bias can then be chosen as that associated with minimum grid current. This argument does not hold here for in fact more grid swing is required with the triode than with the pentode integrator.

nothing more than a d-c amplifier. General considerations of grid current are considered in Vol. 18, Chap. 11. A limitation of the difference integrator is that the value of  $R$  is limited by cathode-to-heater leakage current and the cathode-to-plate current that flows independent of grid bias. The resistive elements in the bootstrap integrator and the feedback integrator are limited only by grid current, which is usually small.

The equation for the difference integrator is

$$R_e C_p V = \frac{\mu}{2} (V_a - V_b) - V,$$

where

$$R_e = \frac{1}{2}[r_p + (\mu + 1)R].$$

If we call  $R = Z$ ,  $1/pC = Z_2$ , and assume that  $R_e \approx (\mu/2)R = (\mu/2)Z_1$  and if we let

$$\frac{\mu}{2} = A,$$

then

$$A \frac{Z_1}{Z_2} = \frac{A V_a - V_b - V}{V}$$

Hence

$$\frac{V_a - V_b}{V} = \frac{Z_1}{Z_2} \left( 1 + \frac{1}{m} \right).$$

This is identical with Eq. (30) for the feedback integrator except for the position error terms that dropped out in letting  $R_e \approx (\mu/2)R$ . The design of a time-measuring system using this type of integrator will be discussed in Sec. 9-10. It will be noted that  $Z_1$  and  $Z_2$  cannot take all forms in this integrator—for example,  $Z_1 = 1/j\omega C$  is impossible.

The equations for the bootstrap integrator are similarly equivalent to those for the feedback amplifier, if  $1/pC = Z_2$ ,  $R = Z_1$ , and if we remember that  $\mathcal{G}$ , the gain of a cathode follower, is very nearly unity,

$$V_1 = \frac{V_2}{\mathcal{G}} (pRC + 1 - \mathcal{G}) = V_2 pRC \left[ \frac{1}{\mathcal{G}} + \frac{(1 - \mathcal{G})}{\mathcal{G}} \cdot pRC \right]$$

Making the above substitutions,

$$V_1 = \frac{Z_1}{Z_2} \left( \frac{1}{\mathcal{G}} \right) V_2 + \frac{(1 - \mathcal{G})}{\mathcal{G}} V_2.$$

This equation is identical in nature with Eq. (30), since  $\mathcal{G}$  is nearly unity. Hence all the integrators are seen to have similar characteristics and errors.

**8-9. Memory and Coast.**—Before completing the discussion of electrical function units, a few remarks will be made on methods of obtaining memory and coast using the circuits described previously. In discussing the feedback-amplifier integrator the remark was made several times that, if the signal faded, the current from the discriminator went to zero; then, depending upon the type of circuit, either position or velocity memory was obtained. This implies two things: (1) that if there is noise present, the discriminator must be perfectly balanced so that the presence of noise will not create an error signal current which would produce either a velocity or an acceleration; and (2) that in the absence of noise, the undesired currents in the discriminator due to insulation leakage or current associated with vacuum-tube electrodes must be small.

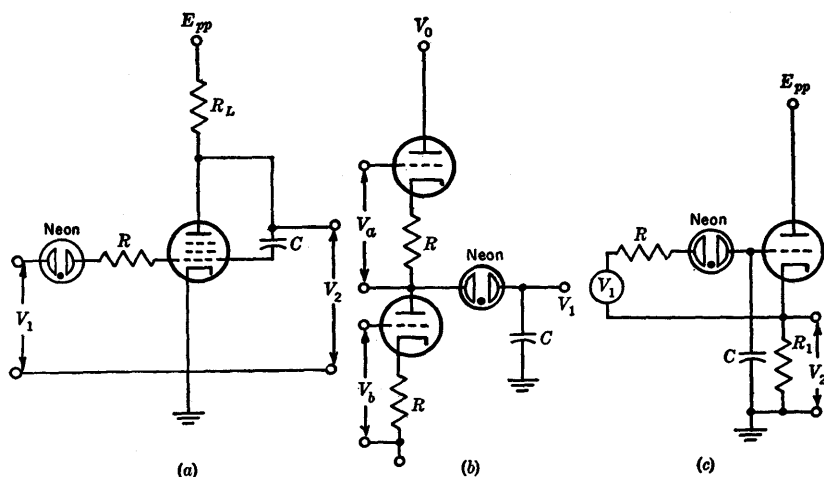


FIG. 8-23.—Integrators showing method of inserting a neon-tube disconnecter.

Since it is difficult to maintain balance in the error signal discriminators and to keep leakage currents small, it has been suggested that a neon tube of low operating voltage be placed in series with the integrating condenser so that current will flow into it only when the error signal multiplied by the gain of the stage becomes large enough to break down the neon tube. In the absence of a signal, the unbalance current and leakage current can usually be kept small enough so that the neon tube will not strike. The circuit arrangements for this addition are shown in Fig. 8-23.

It is at once evident that the only circuit in which the insertion of a neon tube is really appropriate is the difference integrator, for in the other two circuits the time discriminator must provide adequate voltage to overcome the neon-tube striking voltage. If the difference integrator circuit is not appropriate and yet the circuit demands a disconnecter, a

pair of back-to-back biased diodes can be used, with the precaution that the leakage currents associated with the electrodes of the diodes be kept very much smaller than the unbalance currents of the discriminator. The biased diodes are particularly advantageous when small leakage currents are tolerable and when large unbalance currents require an automatic disconnecter without the large backlash associated with a neon tube.

According to our definition of coast, a switch or relay may be provided for interrupting the discriminator current either at the discretion of the operator or in response to some device that detects the presence of interfering signals. By this definition, the neon tube disconnecter is indeed a coast device since it disconnects the time discriminator circuit when the *error signal* lies below a threshold value as it should with only noise present or when locked accurately on a signal. One precaution that needs to be taken is that the insulation resistance of the switch be high so as not to allow any spurious currents that might flow into the integrator condenser and change the rate voltage. An additional provision is usually to insert simultaneously a large properly charged condenser in parallel with the normal feedback condenser. The Oboe automatic range-tracking circuit described in Sec. 9-1 is a good example of this technique.

**8-10. Mechanical Function Units.**—Ideally, an identical approach to the design of function units can be made by employing mechanical

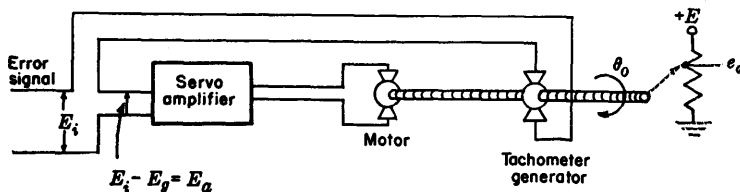


FIG. 8-24.—Mechanical integrator.

elements in the place of vacuum-tube amplifiers. There exist numerous types of mechanical integrators but the one most appropriate for the purpose of synthesizing function units is the velocity-controlled servo-mechanism employing tachometric feedback as illustrated in Fig. 8-24. This integrator has the advantages over other mechanical types, such as the ball-and-disk, of being constructed of standard components, of possessing high gain, of delivering abundant torque for computers and data transmitters, and of being sensibly independent of torque loading. Moreover, the loop containing the servoamplifier, the motor, and the tachometric generator can be regarded simply as a voltage amplifier. The act of connecting the output of the tachometric generator in series



with and opposing the input error signal ensures that the generator voltage is always approximately equal to the error signal, for indeed this is the function of the servoamplifier and motor. If the servo loop is stable, it is analogous to the feedback amplifier described in Table 8-1, circuit 1, having resistance input and resistance feedback elements. Integration is performed by virtue of the relation between the generator shaft and its output voltage—namely, that the shaft position is the integral with respect to time of the generator voltage. Provided always

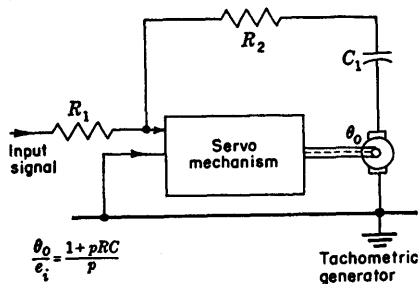


FIG. 8-25.—Servomechanism with tachometer feedback modified to perform a more complex operation.

that the requirements of loop stability are met, the mechanical integrator may be modified in the same manner as the electrical integrator to perform the functions of smoothing and loop stabilization. This modification involves inserting in series with the tachometric generator resistive and capacitive elements to perform the desired functions. A simple example is shown in Fig. 8-25, in which an  $RC$  circuit is

placed in series with the tachometric generator voltage, being fed back to the input of the servomechanism. The performance of a velocity servo with this modification is described in detail in a British Report<sup>1</sup> on velocity servomechanisms, the velodyne.

The equations for this modification show that the transfer function becomes  $\theta_0/e_i = a(1 + pRC)/(p)$  where  $a$  is the scale factor of the tachometer generator in volts per rpm. Further modifications in accordance with Table 8-1 are likewise possible, though one should bear in mind always the restriction that the servomechanism must be capable of stable operation under the modified conditions and that the output quantity illustrated in the table is shaft speed. The remark made in Sec. 9-7 about the relative merits of the differential equation solution and the method of feedback amplifier analysis in designing the automatic time-measuring systems is especially pertinent with mechanical function units. The recommended procedure is to make the simplifying assumptions of the previous paragraphs in determining the general nature of the mechanical function unit, and then to work out the detailed design, including stabilization, according to established automatic-control-mechanism practice. In the particular case of the velodyne this last step has not been found necessary where the natural period,  $1/f_n$ , is long.

The three specifications that an automatic time-measuring system

<sup>1</sup> I.E.E. Convention paper, F. C. Williams and A. U. Uttley, March 1946.

must meet and that thus determine the specific design of the mechanical function unit are: (1) the system must possess sufficient gain to keep the range-tracking gate aligned with the tracked signal to within the desired range accuracy; (2) the tracking must be sufficiently sluggish and stable to prevent noise components in the signal from causing large fluctuations in the output data or even pulling the tracking pulse away from the target signal; and (3) the sluggishness must not be so great as to limit the ability of the system to lock onto a moving target quickly, or to cause appreciable velocity error.

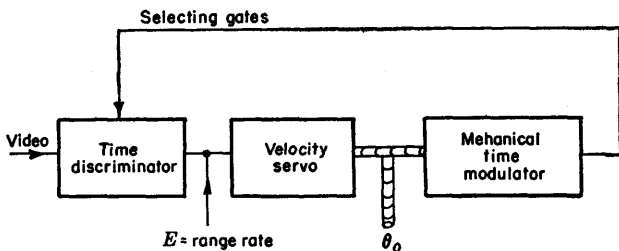


Fig. 8-26.—Single integrator mechanical time-measuring device.

The complexity of mechanical function units is such that they are used only when the requirements of the system demand either mechanical data output, or the use of a mechanical time modulator. Even then it is of course possible to use an electrical tracking system together with a mechanical voltage- or time-follow-up mechanism, as discussed in Sec. 8-15. Such an arrangement involves some duplication of equipment, which is costly unless the separate electrical signal tracking loop is exploited for rapid target selection or automatic search. This situa-

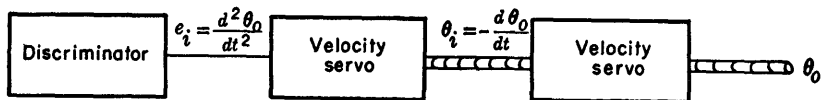


Fig. 8-27.—Double-integration system employing two velocity servomechanisms.

tion occurs in range-tracking systems in which mechanical output data and an accurate mechanical time modulator are used.

A fundamental advantage of mechanical function units, is that mechanical integrators are free from the position error term  $-V_2/m$  of Eq. (30). Well-designed servomechanisms can be balanced with great stability and the conditions for good velocity or position memory then rest solely on the balance on noise of the time discriminator. If adequate time-discriminator balance cannot be obtained through careful design, the technique discussed in Sec. 8-9 of introducing a neon tube or biased diode disconnecter is appropriate here, providing the backlash introduced

does not disturb the stability of the system. Figure 8-26 shows the block diagram of a single-integrator mechanical time-measuring system, which possesses position memory only. As is pointed out in Sec. 9-2, it possesses some velocity memory by virtue of the smoothing networks preceding the velocity servomechanism.

Figure 8-27 shows the block diagram of a double-integration system with velocity memory employing two velocity servos. Such systems have been used for angle-tracking but not, to the author's knowledge, for range-tracking. This system has the advantage of providing range and range-rate data directly as shaft rotations. An alternative method is to use a mechanical integrator to integrate range rate and a feedback-amplifier integrator to integrate acceleration, as illustrated in Fig. 8-28.

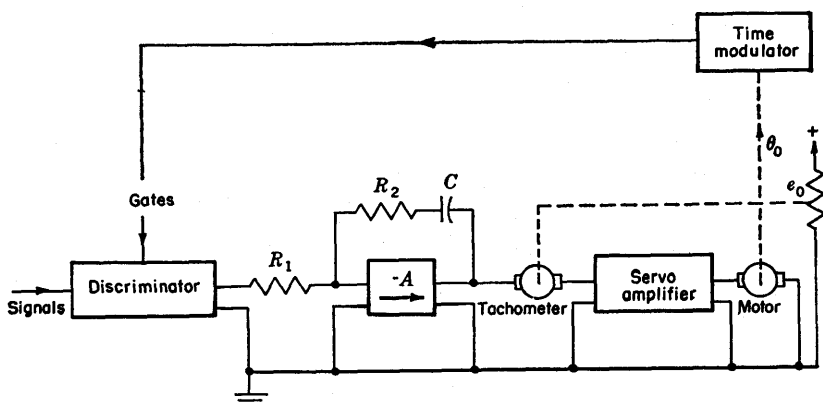


FIG. 8-28.—Typical combination of electronic and mechanical integration.

The objection to this scheme is that range rate is not obtained as a shaft rotation.

### TIME DISCRIMINATORS

**8-11. General Considerations.**—In the complete time-demodulation scheme employing discrimination and remodulation as described in Sec. 8-2, the basic process of time demodulation in its simple form is performed by the time discriminator. Its function is not to indicate the absolute value of time modulation of the received signal but to indicate only the magnitude and sense of the time difference between the locally generated selector-waveform and the received signal.

Some time-discrimination circuits are contained in Chap. 10 of Vol. 19. The following sections will give several circuits that were used in radar automatic range-tracking systems.

The first operation is that of time selection—that is, two adjacent portions of the signal to be tracked must be isolated from each other and

from the remainder of the video information. This is usually performed by a pair of time selectors (see Chap. 10, Vol. 19). The selecting waveforms or gates are time-modulated by the local time modulator. The two outputs from the time selectors are then detected and compared in a difference detector (see Chap. 14, Vol. 19). The difference current or voltage is operated upon by the function unit to control the local time modulator. The two selecting waveforms are thus made to divide the video signal equally. The value of the time-modulator control voltage that locates the waveforms symmetrically on the signal is then the desired indication of the time modulation of the signal.

The properties desired of a time discriminator are that the output signal (microamperes per microsecond of misalignment) should be large compared with the noise level at this point in the circuit and that the balance should be stable. There are two conditions for balance in the time discriminator. First, the output voltage or current in the absence of any signals must be zero, and second, the output voltage in the presence of equal signals in the selector gates must be zero for various amplitudes of signals. The latter requirement applies to both noise and intelligible signals. Balance is required on noise to avoid change of velocity or position during fades of the signal; balance on signals is required to prevent shifting of the tracking point with fluctuations of signal amplitude. Unbalance on noise might also shift the tracking point in the presence of a signal if the signal-to-noise ratio were low. If the system is to have position or velocity memory in the presence of noise without the use of an error signal disconnecter (such as a neon tube) noise balance is necessary; otherwise, the function unit will take a position or velocity or acceleration indicated by the amount of unbalance in the time discriminator. If a disconnecter is not used, the time discriminator should operate on video signals of large amplitude, and should be followed by as little gain as is necessary. If this is done the effects of either zero or dynamic unbalance in the time discriminator can be minimized.

Since the generation of square selecting waveforms (Vol. 19, Chaps. 5 and 6) or gates is not particularly stressed elsewhere, the circuits for generating them are included occasionally in the following circuit descriptions of time discriminators.

**8-12. Simple Time Discriminators.**—A simple discriminator is one in which the time selection, amplitude comparison, and the operations of the function unit are all performed in an essentially indivisible circuit. The principal advantages of such circuits are their economy in size, components, and power consumption; hence their frequent use in airborne radar systems. The possible disadvantages of sensitivity to interference and imperfect balance on noise are not often serious limitations for the particular use for which they are designed.

**AGL (T) Discriminator.**—The first circuit of this kind to be described is the time discriminator from the AGL (T) Mark I British Radar.

In this discriminator the output from a single time selector is detected and compared against a reference voltage to tell how much of the target signal is coincident with the tracking gate. Although two gates are employed in the time discriminator only one ever coincides with the echo (see Fig. 8-29). The waveform of line *a* is a pre-pulse lasting 20  $\mu$ sec, at the end of which the r-f pulse goes out. Waveform *b* shows the output of a phantastron which is triggered first at  $t_1$ , recovers after a time  $t'$ , and

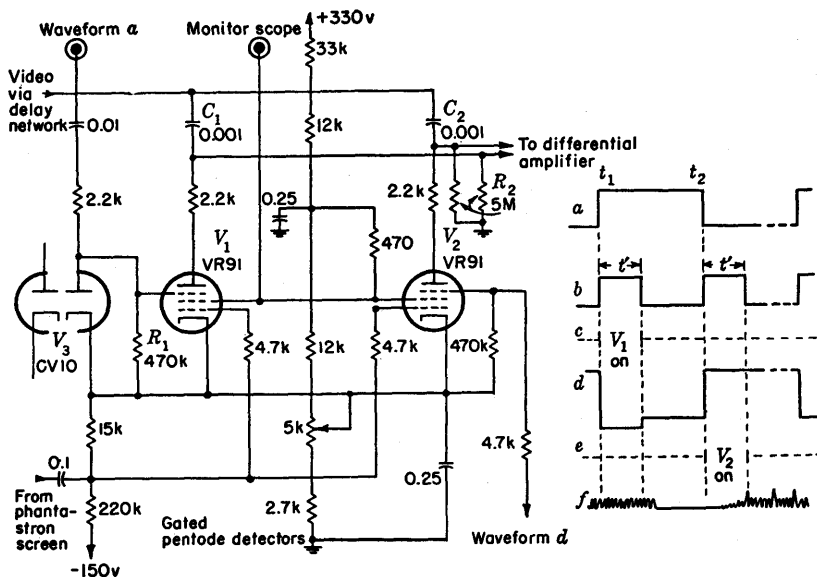


FIG. 8-29.—AGL-(T) time-discriminator circuit and waveforms.

is triggered again at  $t_2$  to stay on again for a time  $t'$ . The length of the interval  $t'$  is determined by the position of the range control. Waveform *d* is the output of an amplifier driven by waveform *a*. Waveform *f* shows the output of the receiver. The blank space in the vicinity of  $t_2$  results from a gain-suppression action that removes the transmitted pulse from the receiver output. The circuit of Fig. 8-29 shows two gated pentode detectors  $V_1$  and  $V_2$ . These tubes are both gated on their control grids by waveform *b* from the range phantastron, so that space current flows during the two intervals  $t'$  of each recurrence interval. The suppressors are gated positive respectively by the waveforms *a* and *d* so that during the interval  $t'$  following  $t_1$ ,  $V_1$  has both its control grid and suppressor grid on and acts as a pentode-switch detector (strobed diode,

Vol. 19, Chap. 14) having 100 volts of screen potential, zero grid and suppressor bias. During this interval  $V_2$  has its suppressor cut off. On the other hand, during the interval  $t'$  following  $t_2$ ,  $V_1$  is off and  $V_2$  is conducting. The control grids are normally biased off to  $-10$  volts and are prevented from going positive by the series grid resistor. The suppressor is biased by current drawn on positive swings flowing through  $R_1$ , so that it will also automatically adjust itself to a bias of zero volts while the gates are on. The plate current that flows in  $V_1$  on the coincidence of the waveforms  $a$  and  $b$  is determined by the plate voltage that is supplied from the video output of the receiver. As indicated in line  $f$  the receiver output during the first gate is purely noise since it occurs at the extreme end of the previous recurrence interval. When the two gates on  $V_1$  go off the condenser  $C_1$  is left charged with a voltage proportional to the average noise during the interval  $t'$ . This voltage decays exponentially through  $R_2$  to ground with a time constant of  $4700 \mu\text{sec}$ . The PRF is 670 pps. Tube  $V_2$  operates in a similar manner. In the condition shown,  $C_2$  will charge up to a voltage representing the average of the noise and that portion of the video echo which is included in the interval  $t'$  following  $t_2$ . If the two circuits are identical, the negative voltage on  $C_2$  will be greater than that on  $C_1$  due to the presence of a signal in the second gate. In the absence of a signal the difference will be zero except for the unbalance caused by the time-varying gain. With zero output the time modulator is arranged to creep out in range. Unbalance in the output due to variations of  $V_1$  and  $V_2$  are reducing by adding  $2.2 \text{ k}$  in series with the plate. The charging time constant thus becomes at least  $2.2 \mu\text{sec}$  for a  $0.5\text{-}\mu\text{sec}$  pulse, ensuring that the detector is an average detector.

The two outputs are connected to a differential amplifier which feeds a relay servomechanism whose output shaft controls the range potentiometer to adjust the interval  $t'$  to terminate on the front edge of the closest signal. The circuit may be said to possess the simplicity of a single-gate system and the advantages of a balanced double-gate system. In the original conception of the system in which time-varying gain was not used, noise in one gate balanced the effects of noise in the other. But in this circuit changes in signal amplitude would cause the tracking point to shift although AGC would minimize this effect.

*Oboe Time Discriminator.*—The second simple time discriminator is the one used in the British Oboe Ground Station that automatically tracks the aircraft response in range and uses the range voltage either to keep the aircraft on a constant range course or to provide a bomb-release signal, depending upon which of the two ground-station functions the set is performing. A complete discussion of this tracking unit will be given later in Sec. 8-22. The discriminator is shown in Fig. 8-30. The

beacon response from the aircraft is fed to the time discriminator from the cathode follower  $V_2$  with a maximum amplitude of 90 volts, and is represented as waveform  $d$  on Fig. 8-30. The selecting waveforms are shown as waveforms  $b$  and  $c$ , and are formed in the gate generator circuit of  $V_1$ . The gates are not equal in length: the second gate  $c$  overlaps the

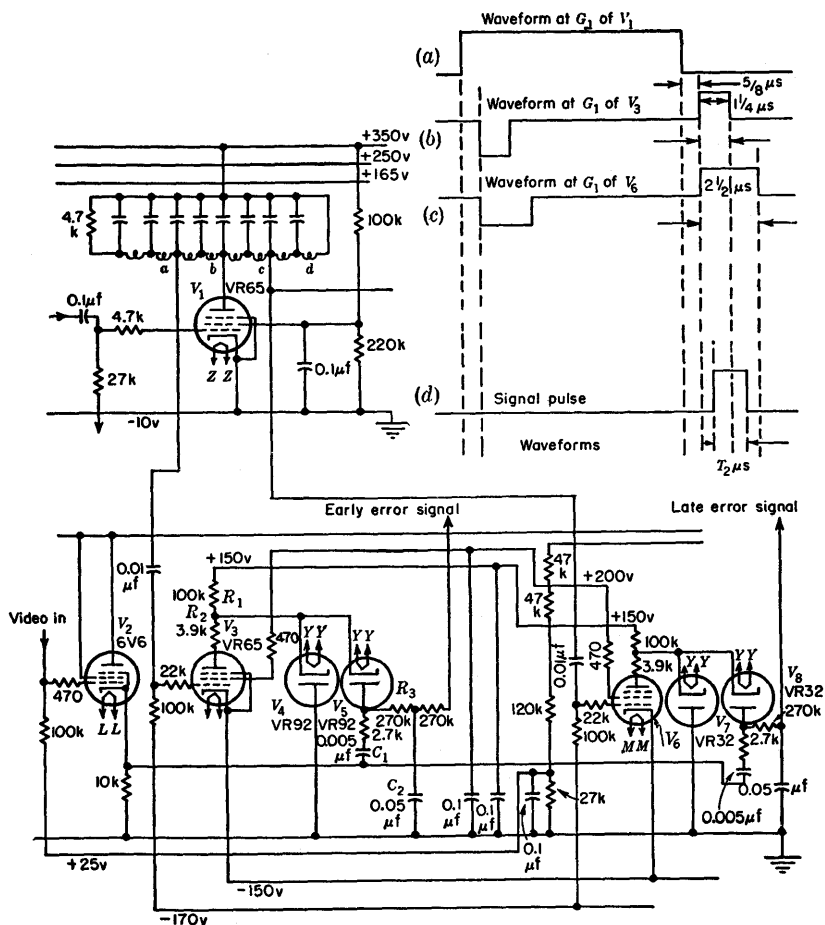


Fig. 8-30.—Oboe time discriminator.

signal completely and the short gate overlaps the first half of the long gate as indicated. The desired discriminator characteristic is obtained from two average detectors gated by these pulses by combining half of the output of the long gated detector with that of the short gated detector. The output of the long gated detector can be employed directly for

signal amplitude indication and AGC. The circuit for accomplishing this is shown in Fig. 8-30. The short gate is applied to the control grid of  $V_3$  driving it positive from  $-170$  volts until it draws grid current at  $-150$  volts. Its plate drops until the cathode of  $V_4$  comes to ground, at which time  $V_4$  conducts and holds the junction of  $R_1$  and  $R_2$  near ground. During the time this condition holds, the video pulses applied to the plate of the diode  $V_5$  can draw current and charge  $C_1$ . When the gate turns off, the plate of  $V_3$  rises again and brings the cathode of  $V_5$  up to  $+150$  volts, shutting off the diode. This design aims at making the current due to the video pulse independent of the gate amplitude and of tube characteristics. This is realized by using a resistor in series with the diode and by using the gated tube only as a means of bringing the cathode of the detecting diode from cutoff to ground. The charge collected on  $C_1$  from rectification of the video pulses flows through the smoothing network  $R_3C_2$  to provide a smoothed current. The tube  $V_6$  and the associated diodes  $V_7$  and  $V_8$  operate in the same manner, gated by the long gate and creating a smoothed current proportional to signal amplitude. This current is later inverted, halved, and mixed with that from the short gate to provide a discriminator error signal.

*SCR-784 Time Discriminator.*—A third simple discriminator is one that was used in the automatic range-tracking circuit for the SCR-784.<sup>1</sup> Here again gating and detecting are done in the same circuit. One difference between this circuit and the previous examples is that, whereas previously two separate detector currents were derived to be compared in a subsequent circuit, in this circuit advantage is taken of the fact that the difference between two currents is desired, and the gated rectifiers act to charge and discharge a single condenser simultaneously, forming a difference detector. The error signal is the net charge on the condenser at the end of this competitive process and no discharging resistor is required. This process is similar to the bidirectional detector action described in Chap. 14 of Vol. 19. At each occurrence of the gates, the voltage of the output condenser is adjusted to the relevant value, and between pulses it is left charged, thus effectively converting pulse amplitude directly into d-c voltage of the same value. The action is shown in the circuit of Fig. 8-31. The cathode follower  $V_1$  feeds shortened video signals directly onto the grid of  $V_2$  and to the grid of  $V_3$  through a short delay line. The tubes  $V_2$  and  $V_3$  are connected as triodes and are plate-gated by the narrow tracking gate. Normally  $V_2$  and  $V_3$  are biased off by voltage derived from a cathode follower which follows the output error signal and keeps the plate voltage on the gated tubes approximately independent of output voltage. The presence of a

<sup>1</sup> War Department Technical Manual TM11-1554, "Radio Set SCR-784 Service Manual," Mar. 1, 1945.



signal coincident with the gate on  $V_2$  causes current to flow to charge  $C_1$  and  $C_2$ , whereas a signal on the grid of  $V_3$  coincident with the gate acts to discharge  $C_1$  and  $C_2$ . The sensitivity is about 150 volts/ $\mu$ sec of misalignment. In the absence of gates and signals,  $C_1$  and  $C_2$  have only leakage paths to ground and hence remain charged. A negative bias is applied to the cathodes of  $V_2$  and  $V_3$  by a bias gate and is adjusted to keep them cut off for the duration of the plate gate unless a video signal appears. This was necessary to prevent unbalance currents in the presence of noise, but it has the disadvantage of placing small signals at

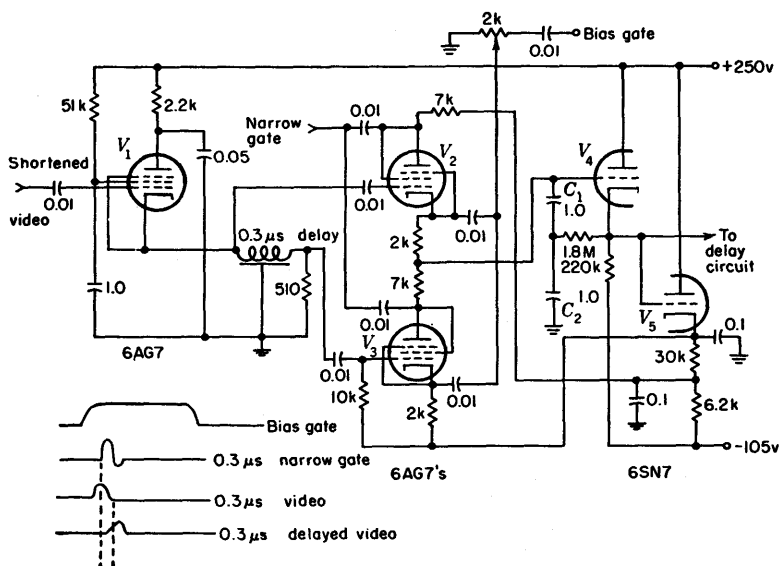


FIG. 8-31.—Time discriminator of Radio Set SCR-784.

the low- $g_m$  portion of the gated tube characteristics, and furthermore if AGC is used it fails in its purpose entirely, for the AGC brings the noise up to average signal height. A more logical approach would have been to put a gain-balance control in the circuit to keep the average charge delivered to  $C_1$  and  $C_2$  zero for noise, leaving the grid bias smaller.

The cathode follower  $V_4$  provides a high-impedance input to connect the error signal to the delay circuit. A similar time demodulator is described in Vol. 19, Chap. 14.

**8-13. Time Discriminators Consisting of Separate Time Selectors and Detectors.**—In the following circuit the actions of time selection and detection are separated. One consequent disadvantage is that the additional stages increase the variations in zero and gain balance with tube changes. It offers the advantage of the same type of competitive charg-

ing of the output condenser as that in the SCR-784 and provides an inexpensive source of the sum of the output of the two gates without resorting to the long and short gate device of the Oboe. Unlike the SCR-784, the output of this discriminator is used as a current. The circuit is shown in Fig. 8-32. The video amplifier  $V_1$  supplies  $V_2$  with video pulses of 20 volts peak. The cathode of  $V_2$  is approximately at  $-300$  volts and in the absence of gates, its plate current flows through the diode  $V_5$  to ground. When the early gate comes on  $V_3$  its cathode rises,

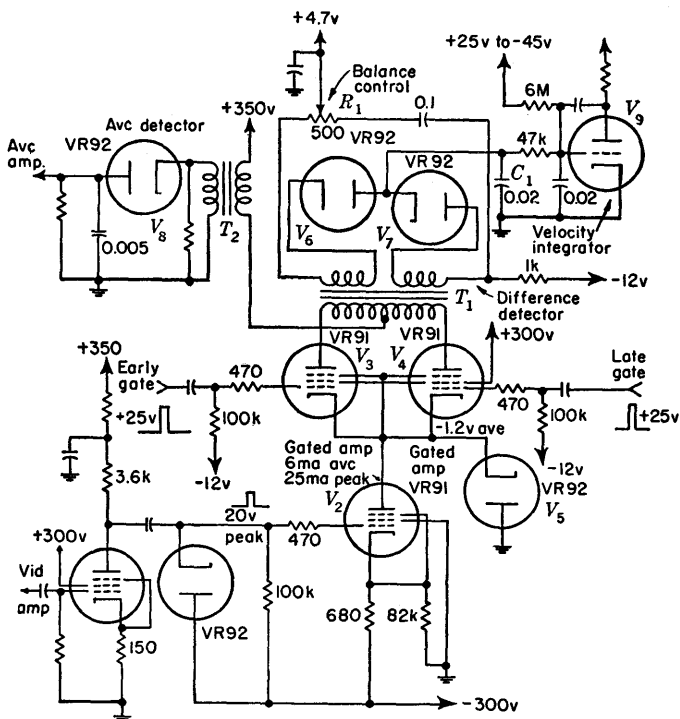


FIG. 8-32.—Time discriminator of British radar set.

cutting off  $V_5$ . Since  $V_2$  is a pentode, the current is substantially independent of the plate load, and the same current that was flowing through  $V_5$  will flow through  $V_3$  and through the plate-circuit pulse transformer  $T_1$  and cause a negative current to flow in  $C_1$  through the diode  $V_6$ . When the early gate goes off and the late gate comes on, the plate current of  $V_2$  is switched from  $V_3$  to  $V_4$  and causes a positive current to flow into  $C_1$  through the diode  $V_7$ . If the average current during each gate is the same,  $C_1$  will receive no net charge. If the average voltage on the grid of  $V_2$  is larger or smaller during the first gate interval than during the



A second discriminator that performs the two functions of time selection and detecting separately and also uses difference-taking in a condenser directly is the time discriminator of the ARO (AN/APG-15, AN/APG-5) shown in Fig. 8-33. Tubes  $V_1$  and  $V_2$  are suppressor-gated pentodes with the video signal applied to the control grids and inverting pulse transformers in the plate circuits. The secondaries of the inverting transformers feed triode detectors of the type shown in Chap. 14, Vol. 19. The net charge in  $C_1$  is the difference between the charge that flows in  $V_3$  and  $V_4$  due to the early- and late-gated video pulses. A difference detector using high impedance triodes of the 6SL7 type to charge  $1.0 \mu\text{f}$  for  $0.5 \mu\text{sec}$  is certainly operating as an average detector. The output signals from the secondaries of  $T_1$  and  $T_2$  are mixed to provide a combined pulse for the AGC detector which represents the signal amplitude during the whole of the gating interval. The bias of  $V_4$  is fixed, and the bias of  $V_3$  is maintained nearly constant by the cathode follower  $V_5$  operating with a pentode as a cathode load as the potential on  $C_1$  moves up and down over a range of 15 volts. A balance control in the cathodes of the gating amplifiers provides balance on equal signals so the voltage on  $C_1$  will not change in the absence of signals or in the presence of noise alone.

**8-14. Time Discriminators with Time Selectors, Pulse Stretcher, and Narrow-band Pulse Amplification.**—An example of this type of discrimination on which considerable data is available is the circuit used to supply automatic range tracking for an experimental radar. Two aims were prominent in the time-discriminator design: minimum sensitivity to interference, and accurate position memory and coast.

The first item was achieved by decreasing the range aperture to  $0.4 \mu\text{sec}$  and employing rapid-charging peak detectors in the time discriminator. Unfortunately the short range aperture requires wide receiver bandwidth and thus decreases the receiver sensitivity and increases the cost of amplification.

The second aim was achieved by designing a time discriminator that would remain balanced on all amplitudes of noise up to receiver saturation.

The principal method of achieving good balance on noise is to maintain extreme linearity in the amplifiers and detectors, which operate separately on the early- and late-gated video.

As is shown in Fig. 8-34, the selecting gate is formed in  $V_1$ , a blocking oscillator using a Westinghouse 132-DW pulse transformer to generate a  $0.12\text{-}\mu\text{sec}$  pulse. A  $0.1\text{-}\mu\text{sec}$  delay line is employed to provide a late gate from the early gate. The spacing of the gates is chosen to keep the additive output of the two gated-video stages constant over as wide a range of misalignment as possible. It turns out that this condition



provides the maximum slope of range-error signal vs. range error. The video signals of +1-volt level are amplified to +8 volts in a two-stage 20-Mc/sec video amplifier to drive the grids of the two suppressor-gated 6AC7 amplifiers,  $V_2$  and  $V_3$ . A d-c restorer  $V_4$  is supplied. In order to obtain the maximum gain from the gated amplifiers, the screens are gated from +75 to +150 volts for a 6- $\mu$ sec period centered on the tracking gates. This is necessary because during the time that the suppressors are held at -130 volts the total space current flows to the screens, which would burn up if maintained constantly at +150 volts.

When the screen is at +75 volts the cathode bias is small and large video signals cause grid current to flow, which passes to ground through the low resistance of the diode  $V_4$ . The gating amplifiers are fairly highly degenerated to minimize gain variations between the two stages.<sup>1</sup> The net stage gain is about 0.5. The plate loads of these amplifiers are designed with shunt and series compensation to provide a pulse rise time (10 to 90 per cent) of 0.02  $\mu$ sec in the stray capacitance of the output circuit of the 6AL5 diodes  $V_5$  and  $V_6$ . It is unnecessary to provide low-frequency response after the gating stage because there can be no signals longer than the gate width, hence the small coupling condensers which permit lower capacity wiring, a factor highly important in wide-band video construction practice. The type 6AL5 diodes were used because each section has a resistance of 200 ohms, giving 100 ohms for the pair as the series resistance through which the stray capacitance from plates to ground must be charged with a time constant of 0.02  $\mu$ sec. The decay time of this detector is about 10  $\mu$ sec through the 1-megohm resistors  $R_1$  and  $R_2$ . The output of the peak detectors are negative 10- $\mu$ sec triangular pulses whose initial amplitudes represent the peak amplitude of the gated video signals and may now be amplified in narrow-band amplifiers. This completes the desired operation of rapid peak detection.

Tubes  $V_7$  and  $V_8$  are the narrow-band amplifiers, having a gain of six. Their bandwidth was chosen as  $\frac{1}{2}$  Mc/sec to allow the plate to rise to an appreciable fraction of the peak of the triangular input pulse and still provide reasonable gain. Degeneration is employed again to reduce the differential gain variations and to allow the amplifiers to handle the maximum possible grid signals without departure from the linear portion of the grid characteristics. The cathode followers  $V_{9A}$  and  $V_{9B}$  provide low-impedance output to the pulse transformers  $T_6$  and  $T_7$ , which drive the detector diodes  $V_{10A}$  and  $V_{10B}$ . The diodes respectively discharge and charge  $C_1$  through the smoothing resistors  $R_3$  and  $R_4$ . The net charge on  $C_1$  is the range-error signal which is fed to the integrator and range-

<sup>1</sup> The degeneration of this stage is actually so high that it would probably have made little difference to the gain if the screens had been operated steadily at +75 volts.

tracking servo. Figure 8-35 shows the range-error voltage plotted against range error; the slope is 164 volts/ $\mu$ sec and the aperture is 0.4/ $\mu$ sec.

The gated amplifiers  $V_2$  and  $V_3$  are biased Class A during the gating interval. This implies an average plate current of about half of peak. Hence when the gate comes on the suppressor, the plate drops to the zero-signal level. This pedestal lasts as long as the gate is on and is largely removed by biasing off the peak-detecting diodes. A differential bias control determines the balance of the range-error signal in the absence of signal and noise. In the presence of noise, the balance is determined by the differential gain control in the cathodes of  $V_{17}$  and  $V_{18}$ .

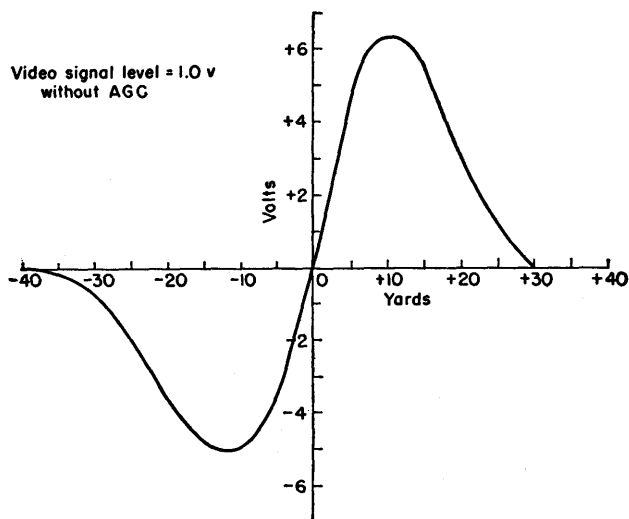


FIG. 8-35.—Error signal curve of pulse-stretching time discriminator.

The high gain of the servo amplifier following the time discriminator makes balance conditions very critical. For example the maximum error signal is  $\pm 5$  volts but in order for the drift velocity on noise to be less than 20 yards/sec, the range-error signal on noise must be less than 0.1 volt, thus requiring balance to 2 per cent. This was obtained over periods of several hours and with values of noise from zero to twice AGC levels. The pulse output from the cathode followers  $V_{9a}$  and  $V_{9b}$  is added to provide for AGC a single pulse representing the sum of the peak amplitudes of the two gated videos.

The reasoning behind the choice of the two time-constant detectors is that, since rapid peak detection is desired, it is economical to detect at low level in a very small capacitance whose exponentially decaying output can be amplified with reasonable gain in narrow-band amplifiers

and redetected at high level to provide a d-c error signal. One alternative would have been to amplify the direct-current component of the output of diodes  $V_5$  and  $V_6$ . At such a low level, 5 mv/yard, balance errors due to drifts of the d-c amplifiers would have been introduced. To increase the level at this point would require additional video amplification, which for 20-Mc/sec bandwidth and voltages above a few volts is very expensive.<sup>1</sup>

Review of the circuit shows that its real value is the pulse stretching of the peak-detector stage which provides a long voltage pulse from a short one. More effort might well have been put into increasing the resistance of the diode output circuit than into providing narrow-band gain since the subsequent average detection is benefited as much by increasing pulse duration as by increasing pulse amplitude.

**8-15. Time Selection.**—In the absence of interfering signals, the time selection operation could simply divide the recurrence interval into two periods, time before the signal and time after the signal, each period including half the signal as in Figs. 8-36 and 8-37.

In the presence of multiple signals, the time-selection process must reject information from all but the desired signal. In fact, since a 3° radar beam has an angular aperture of about 600 yd at 10,000 yd, scanning radar range finders rely on time selection or range discrimination to provide most of the target discrimination. An advantage of discriminating in time more finely than in angle is that it is a very simple matter to extend the time aperture for searching either by scanning in range or by presenting the whole time interval on a CRT display, whereas the problem of expanding an angular aperture from a very narrow beam is a complicated mechanical problem involving either high-speed scanning or some sort of beam defocusing.

If the output of the time selector shown in Fig. 8-36 were put into an amplitude comparison and memory circuit the output error signal would have the form shown in Fig. 8-37. If only one gate were used, say the early gate, the output would appear as in Fig. 8-38, and is identical with that from the double-gating system except that its amplitude is halved and it has a different d-c level. The single-gate system has been used for light-weight airborne fire-control radars where only one target

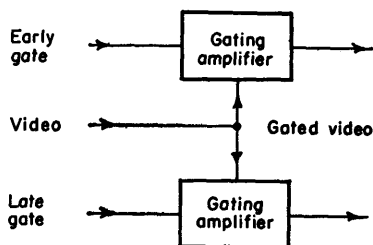


FIG. 8-36.—Block diagram of the time selector of a time discriminator.

<sup>1</sup> A rough calculation assuming video amplifier design consistent with the rest of the system shows a cost of 140 ma for first stage of 11 db and 410 ma for second stage 11 db, which would bring the error signal up to a reasonable value of 50 mv/yard.



was expected—for example the AGL-T in Sec. 8-12. The obvious advantage of the gating systems of Figs. 8-37 and 8-38 is that no matter where the gates are with respect to the video signal there exists a significant error signal: hence no search problem exists for a single target.

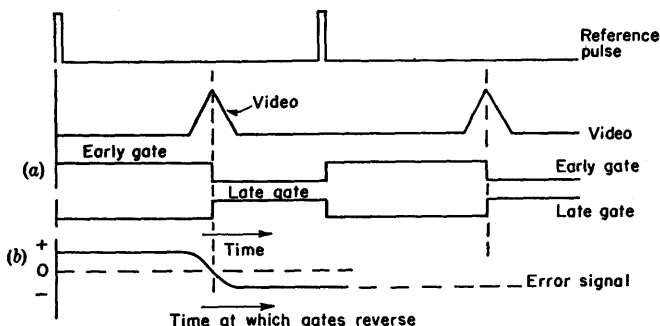


FIG. 8-37.—Time-selector waveforms and error-signal curve of a time discriminator.

The disadvantage of the system of Fig. 8-38 is that the time-discrimination technique involves matching the output of a single detector against a d-c level, so that the output of the single detector is a function of signal amplitude as well as of its time modulation; hence the tracking point varies with signal strength.

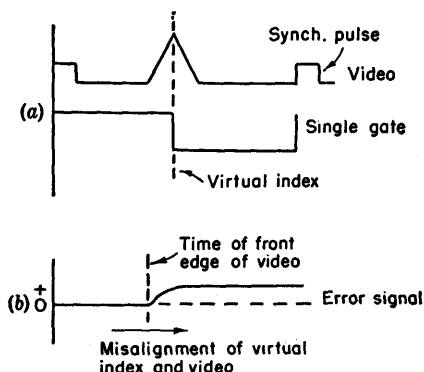


FIG. 8-38.—Waveforms and error-signal curve of single-gate time discriminator.

Multiple signals require narrow selecting gates, the gate width and pulse width being determined by estimated signal width, separation, and the desired resolution. In radar applications the undesired signals are ground echoes, sea clutter, pulses from adjoining radar sets, and interfering targets near the desired one. Decreasing the range aperture

more than necessary increases the difficulty of locating the gates on the signal in the search process and the probability of losing the target during a fade.

Measurements taken on power required for minimum detectable signal in noise as a function of gate width show that the power required increases with the gate width for values of the ratio of gate width to pulse width greater than unity. For gates narrower than the signals the signal-to-noise ratio is fairly constant.<sup>1</sup> Hence most radar systems are designed with each gate approximately equal to half the signal width. Reducing the gates of Fig. 8-37 to half the signal width gives the discriminator curve of Fig. 8-39. The range aperture is the region from  $a$  to  $b$  on line 6 of the drawing. Signals outside this region will not affect the tracking, and in fact, tracking will not be lost even if a signal of equal amplitude comes within about one gate width of the desired signal. Conversely, the signal must be brought within one pulse width of the virtual index for tracking to commence.<sup>2</sup>

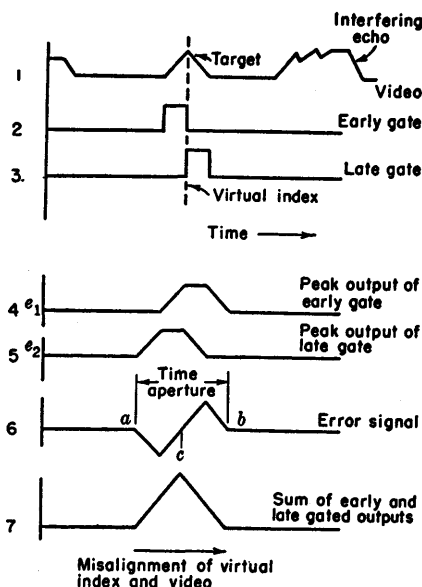


FIG. 8-39.—Discriminator waveform and error signal with gates reduced to half signal width.

The separation of the gates is determined by two factors. First, two separate outputs indicated by lines 3 and 4 of Fig. 8-39 should combine to provide a smooth curve at point  $c$  on line 6 since this is where normal tracking occurs, and the slope at this point is a factor in the gain of the tracking loop. Large variations in gain will lead to either possible instability in the tracking loop or sluggish tracking. Second, the outputs of the two time selectors are often mixed additively to give a signal representing the average pulse height for AGC and amplitude demodulation, indicated in line 7 of Fig. 8-39. The plot of this term vs. misalignment should have a flat portion to avoid interaction between slight movements

<sup>1</sup> Data from W. H. Jordan taken by listening for PRF note out of receiver as a function of gate width.

<sup>2</sup> In the diagrams for this section, triangular signals, square gates, switch-type gated amplifiers, and peak detectors are assumed for simplicity in graphical construction. Results for average detection, etc. are easily obtained by the same method.

of the tracking gate and the amplitude of the signal representing pulse height (see Fig. 8-40).

The gate separation shown in Fig. 8-40a provides the maximum possible slope of the error-signal curve in the region of the tracking point, and at the same time provides the maximum length of flat portion in the curve plotting the sum of the gated outputs vs. misalignment although giving considerably smaller output than the arrangement of Fig. 8-39.

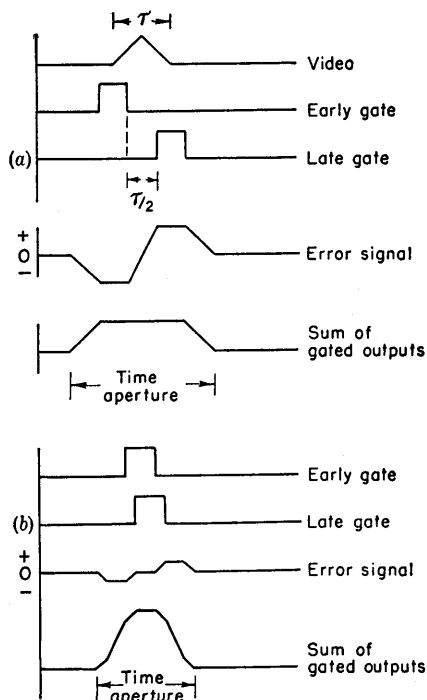


FIG. 8-40.—Effect on time selection of varying gate separation.

The situation is different for average detectors. The arrangement of part (b) produces a flat portion in the sum curve but gives a very small nonlinear range-error curve. If the video pulse width is  $\tau$ , and the gates are  $\tau/2$  wide, the time apertures associated with the three gate spacings shown are:

1. No overlap: 2 gate width + video pulse width =  $2\tau$
2.  $\frac{2}{3}$  overlap:  $1\frac{1}{3}$  gate width + video pulse width =  $1\frac{2}{3}\tau$
3. Separate by one gate width: 3 gate widths + video pulse width =  $2\frac{1}{2}\tau$ .

An alternative to generating two adjacent gates is to delay the video and apply the same gate to both gating amplifiers as in Fig. 8-41. The video spacing of Fig. 8-41 has been arranged to provide the maximum slope of the error-signal curve and maximum flat portion in the sum

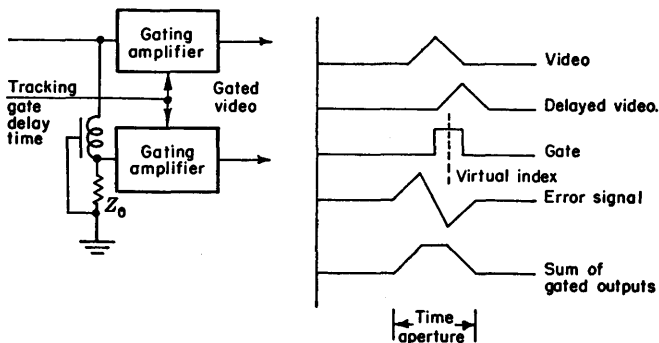


FIG. 8-41.—Delayed video time discriminator.

curve. The associated time aperture is the video width plus the gate width or  $\frac{3}{2}r$ , which is considerably smaller than the double-gate arrangement for the same conditions.

It is often desirable to obtain a warning of interfering signals approaching the tracking gates. Methods for accomplishing this with out-rigger gates will be discussed in Sec. 9-17.

One interesting but untried possibility is to increase the range aperture during search. One simple possibility employs a multiple-valued rather than a switch characteristic for a time selector. If this is done, the early and late gates could have sloping front and back respectively to extend the range aperture without seriously affecting

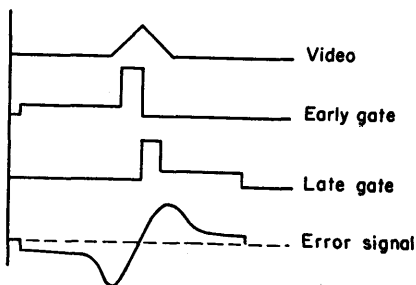


FIG. 8-42.—Time selector with sloping gates.

the interference rejection of the narrow square gates (see Fig. 8-42).

## TARGET SELECTION

**8-16. General Considerations.**—In any automatic time-measurement system whose time-selecting waveforms do not cover the whole recurrence interval, there exists the problem of bringing some portion of one of the selecting waveforms into coincidence with the desired signal. When this has been done, the time discriminator by definition will produce an error signal of the correct sense to make the selecting wave-

forms move to exact coincidence with the target. The latter process will be called "locking on target." If the process is to be done manually there are five steps in the operation.

1. *Search* visually over the displayed range to find a target.
2. *Identify* the target as the one desired.
3. *Slew* the selecting gates toward the target.
4. Note *indication* of their *coincidence*.
5. *Switch* to automatic tracking and allow the circuit to lock on.

Of these five operations only the last three will be discussed in this chapter since the first two belong in the treatment of displays in Vol. 22.

The procedure of automatic target selection is similar to the manual process but differs in the following ways. In general, searching is combined with slewing—that is, the method of search is to slew the range gates through the range interval of interest at a convenient speed until a target occurs in the gates.<sup>1</sup> In automatic target selection, target identification and indication of coincidence are identical processes, for the circuit that detects coincidence simultaneously examines the target for any electrically distinguishable characteristics. Upon coincidence with a suitable signal, target indication is given and the tracking circuits are connected to "lock-on."

There are two applications of automatic time-measuring systems where it is almost imperative for automatic search to be included. One occurs when the operator employing the automatic time-measuring system has many other duties—for example, the pilot of a single-seater fighter plane who is relying on automatic range measurements in his radar to superelevate his gunsight. Another example of the need for automatic search is a radar system which functions to report the presence of an approaching target. The target selecting circuit would have to find the target, lock on, measure the sense of its range rate, and either sound a warning or reject it and continue the searching.

*Conditions for Automatic Search.*—The question to be answered by the designer is, "When is it possible to exchange an elaborate CRT display for an automatic search circuit?" The answer depends on whether the desired target can be identified electrically and whether the range gates can be made to scan without missing the targets.

Regarding automatic identification, frequently it is sufficient that the target desired be always closer in range than any other. The obvious procedure is to search *out* in range until a target is found; if none is

<sup>1</sup> It is interesting to note that the inherent speed of the range scan is the speed of light, because as the electron beam traces out the display, it is actually presenting the course of the r-f pulse through space. Persistence of vision or of CRT screens allows the scan to be examined visually in retrospect at a lower speed.

encountered, then return from maximum to zero range rapidly with the lock-on circuits inhibited.

Pulse decoding offers more elaborate automatic target identification. With this method, a decoder located before the automatic search circuits will eliminate undesired signals, permitting tracking only on satisfactorily coded signals. Target selection may also be made with respect to the angular position of the target. Amplitude modulation of the echoes may be utilized for target selection in a conical scanning system. The antenna scans conically, and the pilot of the plane keeps the antenna axis pointed at the desired target by means of an optical sight. The automatic search circuit then locks only on targets with zero amplitude modulation—that is, on the axis of the antenna. Since the antenna looks down at the earth from the plane, there is only one point on the ground which is on the axis of the antenna. Many other methods of automatic target identification may be suggested by the particular need.

The second condition, that of ensuring that the range gates will cover the desired range interval without missing a target, is somewhat like an impatient boy trying to mow a lawn rapidly without leaving any uncut strips. First, since the signal pulses appear only at the PRF, the rate of searching in range should not be so large that the range gates will move more than one range aperture at each recurrence interval. Second, if there is some likelihood of signal fading, the range gates should overlap each point in the range interval long enough to allow the signal to recover from a fade during the time that the range aperture includes that point. Third, if the antenna is being scanned in angle, the range search either should move so slowly as to move out less than one range aperture during each complete angle scan, or should move so rapidly as to search out the whole range interval while the beam moves one beamwidth. The second alternative conflicts with the first two points, especially since most radar systems are designed to search in angle so rapidly that only a few (say five) pulses are received from a small target per angular scan. The fourth point that causes the rate of range search to be decreased is that the coincidence detector is often designed to require more than one pulse to build up enough signal to override or disconnect the search circuit. This prevents noise pulses or randomly occurring interfering pulses from stopping the search. If the time delay involved in switching by relays to track from search is appreciable, the gates should not move away from the target. An equation could be written showing exactly the fastest rate of range search scan in terms of these five factors, but the definition of symbols would take more space than the equation would save.

As a practical example, the AN/APG-15 is of interest. It has a PRF of 1400 pps and a conical scanning rate of 35 cps, relays with

0.01-sec closing time to disconnect the search sweep, and a  $0.7\text{ }\mu\text{sec}$  pulse with two adjacent  $0.7\text{-}\mu\text{sec}$  range gates. The range aperture is thus about  $2.0\text{ }\mu\text{sec}$ , or 320 yd; the maximum search range is 1800 yd. If there were no conical scanning, the range gates might move out 320 yd each recurrence interval, covering the 1800 yd 318 times per second if negligible flashback time is assumed. With conical scan, a range scan of 320 yd in  $\frac{1}{318}$  sec, or 11,000 yd/sec would just give complete coverage of the volume swept by the conical scan. If the disconnect relay takes  $\frac{1}{160}$  sec to close, the gates will have moved 110 yd or one-third the range aperture between the time of detecting a target and starting to lock on. In the actual system a more conservative rate of 4000 yd/sec was employed.

Nonlinear search rate or synchronized range search scans might be used in particular situations to emphasize particular portions of space or to skip portions of space.

Rapid search of the type indicated in the above example is easily accomplished in *electrical* tracking systems where the only limitation to scanning speed and particularly to the speed of flashing back to initial range at the end of the scan is the fact that a large condenser to ground usually exists at the point at which the range control voltage is found. The low impedances available in thyratrons or pulsed hard tubes provide flashbacks of about  $100\text{-}\mu\text{sec}$  duration even with several microfarads capacitance. In addition, the presence of a large condenser favors the practice of discharging small condensers into the range condenser for introducing a "kick" in range to remove the gates from an undesired signal. Several methods of scanning and disconnecting will be shown in examples to follow.

Mechanical tracking systems offer a quite different picture. The greatest obstacle to range search in these systems is the wear on the gears and moving parts that would follow from continuous scanning in range. If wear is not objectionable, it is still usually impossible to scan the whole search range in fractions of a second and decelerate to target velocity without losing the target unless the search range is very limited.

*On-target Indication.*—The target-detecting circuit is that one which should possess the maximum possible discrimination since it most closely simulates the action of the operator in choosing or rejecting a target. The simplest method of detecting the presence of a target signal in coincidence with the tracking gates is to connect a biased detector to the output of the time selector and set the bias so high that only signals large enough to track will cause current to flow. The resulting voltage can be used to operate the search-disconnect device and the on-target indicators. The major disadvantage of this system is the practice of comparing the signal level from a receiver without constant level AGC

with a fixed threshold voltage. A method which overcomes this shortcoming is that of comparing the output of the tracking-gate time selector with that from a time selector operating on the output of the receiver during a time in which only noise is present. The criterion of comparison is thus the signal-to-noise ratio and not the absolute signal level. This technique is used in the British AGL-(T). Some circuits employ in addition sensitivity to the misalignment of the target and the gates, pulse width, and presence or absence of other echoes near enough to interfere with the tracking.

In addition to stopping the search and indicating to the operator that a target is in the gates visually or audibly, the target indicator must often connect auxiliary follow-up servos, stop the angle search operation, or perform other switching functions. These may be done with relays or electronically depending upon the speed of action required. It is probable that the demand on radars to track high-speed projectiles in the

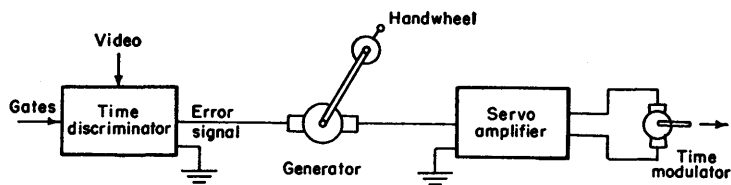


FIG. 8-43.—Target selector of mechanical range-tracking system permitting insertion of manual slewing without disconnecting the automatic range-tracking loop.

future will require that all these operations to be done electronically, to prevent loss of the target during the switching interval.

If visual indication of the target is available on a CRT display, or if the operator is able to see the target and know that its true range differs from the range indicated by the automatic tracking circuit, it may be helpful to provide manual methods of displacing the range gates in supplement to the automatic search. Methods of introducing a "kick" into an electrical tracking system were previously mentioned. A drift in either direction may also be introduced by manually connecting the range voltage condenser to a higher or lower potential through a large resistance.

A convenient trick for manual target selection that has been used in some mechanical range-tracking systems is to introduce a hand-driven generator in series with the lead to the mechanical range integrator as shown in Fig. 8-43. After the operator has slewed rapidly to the region of the target, he can turn the generator in such a direction as to move the gates toward the target. As soon as coincidence occurs, the time discriminator will add a voltage to the generator voltage, causing the gates to lock on the target. From then on, as long as the operator does



not turn the generator violently, the gates will remain on the target. If the operator finds he has selected the wrong target and wants to move on, he can give the generator a quick turn which will overcome the time-discriminator signal and take the gates away from the undesired target. This was used in the Automatic Radar produced by General Electric.

*Precautions.*—If the receiver gain is controlled by a “slow” (0.1 sec) AGC circuit, this should be disconnected during search and the gain set manually at the desired level. This is not necessary if the AGC time constant is much shorter than the times involved in the range scan.

Precautions must be taken to keep the automatic-search circuits from endeavoring to lock on to the transmitted pulse, which can be done by limiting the minimum range of the range search scan, or blanking the receiver during the transmitted pulse. For many applications it may be advisable to apply temporal gain control to prevent locking-on insignificant nearby targets such as birds or on side-lobe echoes.

**8-17. Practical Examples of Automatic Target Selection.**—The following section will discuss several useful circuits for accomplishing the operations described in the previous section. One method for picking up an approaching target automatically is simply to adjust the quiescent position of the range-tracking gates at the desired range leaving the automatic tracking circuits connected. As soon as an echo reaches the gated interval, the automatic tracking circuits should lock on and start tracking. This does not take care of the possibility that a target might approach (or be approached) in such a manner as not to appear until it was at a range closer than the gated range interval.

*AGL-(T).*—A system one degree more complex is the British AGL-(T) previously mentioned in Sec. 8-12. In brief, the output of the receiver is examined by a detector for an interval  $t_1$  just before the transmitted pulse, and a second interval  $t_2$  of equal duration immediately following the transmitted pulse. The duration of the two intervals is controlled by a relay-controlled motor and a phantastron. If the content of the two intervals is the same (noise), the motor is made to increase the duration of  $t_1$  and  $t_2$ . If there is a signal in  $t_2$ , the motor is made to run in until only a small portion of the signal is included in  $t_2$ , at which time the motor stops until the signal moves. If no signal appears, the motor increases the duration of  $t_1$  and  $t_2$  until the maximum width of 1400 yd is reached. The gates will remain at this width until a signal appears, within 1400 yd. which the motor will follow. This is a simple arrangement involving no switching of functions and could be converted to a completely electrical system to provide an inexpensive automatic search and tracking system that is independent of receiver gain.

Figure 8-44 shows the sequence of gating waveforms in a typical target acquisition.

AN/APG-5.—Figure 9-2 shows the complete automatic search and range-tracking circuits of the AN/APG-5 and AN/APG-15. The automatic search and lock-on circuits of these systems will be described here. The normal operation of the circuit is that of searching by scanning the gates out in range at 4000 yd/sec. A symmetrical infinite-impedance detector  $V_{10}$  detects the highest output of either of the two time selectors  $V_4$  and  $V_5$ , biasing  $V_{9a}$  to conduct for all signals of amplitude greater than that set by the "clamp" adjustment  $R_5$ , which determines the lock-on threshold. When  $V_{9a}$  conducts,  $C_2$  is discharged through the plate resistance of  $V_{9a}$ , finally cutting off  $V_{9b}$  and starting in less than 300  $\mu$ sec to close relay  $K_1$ . If the signal is lost,  $V_{9a}$  is cut off and  $C_{25}$  charges toward +250 v through  $R_1$  (10 megohms). On the average, this point will rise in about 0.3 sec, enough to start opening the relay  $K_1$ . In the absence of a signal,  $K_1$  connects the search sawtooth generator  $V_{12}$  to the range integrator condenser  $C_1$ . When the relay  $K_1$  is energized by



FIG. 8-44.—Gating waveforms in a typical target selection with the AGL-(T) time discriminator.

coincidence between a signal and the gates,  $V_{12}$  is disconnected, the on-target lamp is lighted, and the range follow-up servomechanism is turned on.

The searching is done by connecting the range integrating condenser  $C_1$  to the plate circuit of  $V_{12}$ , which operates as a thyatron relaxation oscillator. Condenser  $C_1$  charges exponentially toward +400 volts through  $C_3$  and  $R_2$ . The double-diode limiter  $V_{20}$  is connected to set adjustable limits to the maximum and minimum voltage through which the unit searches. The reverse sweep during conduction of  $V_{12}$  is sufficiently fast to prevent lock-on for the largest signals encountered.

Provision is made for manual rejection of the signal being tracked, with subsequent drift in the desired direction. The circuit will lock-on to the first target then encountered. Relays  $K_2$  (in) and  $K_3$  (out) control this action and are energized by push buttons. Either of these relays disconnects the sawtooth generator and disconnects  $C_2$ , reducing the time constant of the target detector circuit. It then connects a charged condenser across the range integrating condenser  $C_1$  so as to force the gates completely off the signal and at the same time connects a bleeder resistor to give drift of the gates in the desired direction. The shunt condenser and bleeder are disconnected at lock-on and the normal

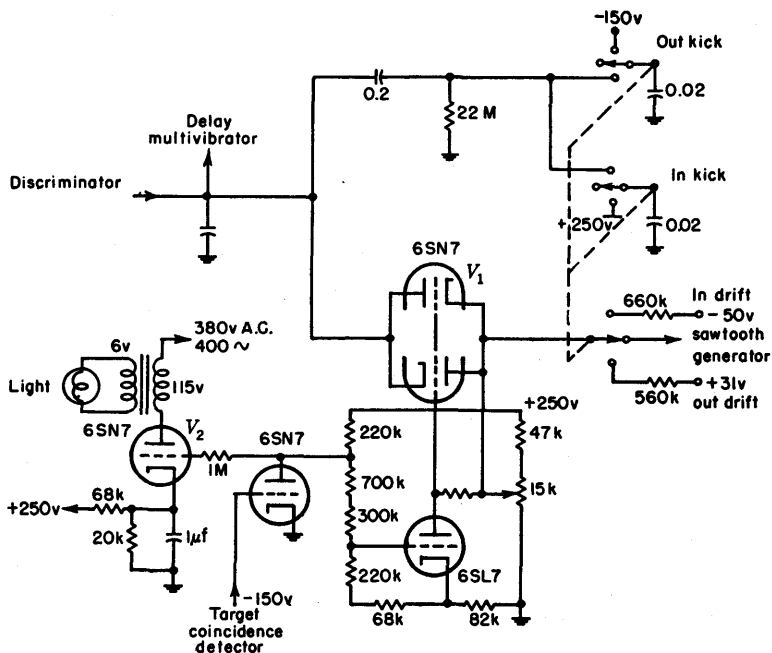


FIG. 8-45—Early ARO automatic search system.

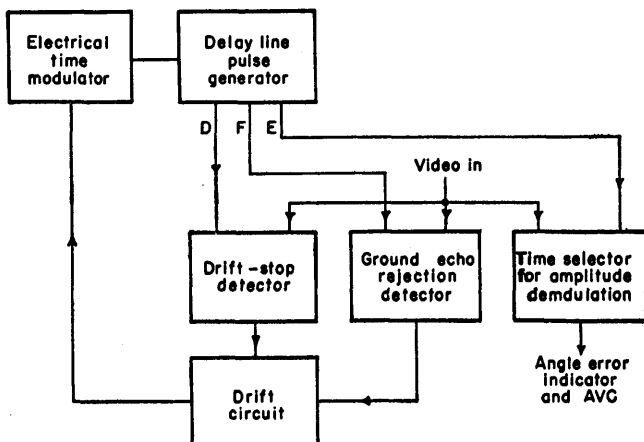


FIG. 8-46.—AI Mark VI automatic target-selection system block diagram.



time constants are restored as soon as the button is released. It has been found desirable to discharge  $C_2$  when the control buttons are depressed. Any desired portion of the range out to greater than 1800 yd can be searched continuously at two or more times per second.

One limitation to the search speed of this system is the time taken for the relay to throw from search to track position, about ten milliseconds. An electronic switch was used in an earlier model as shown in Fig. 8-45. The functions of manual reject, manual drift, automatic search, and automatic tracking are shown. Tube  $V_2$  acts as a variable resistance in series with the primary of a filament transformer to light the target-indicator lamp without a relay or power oscillator.

*A.I. Mark VI.*—The early but excellent British A.I. Mark VI provides an example of an automatic search and track system that uses a

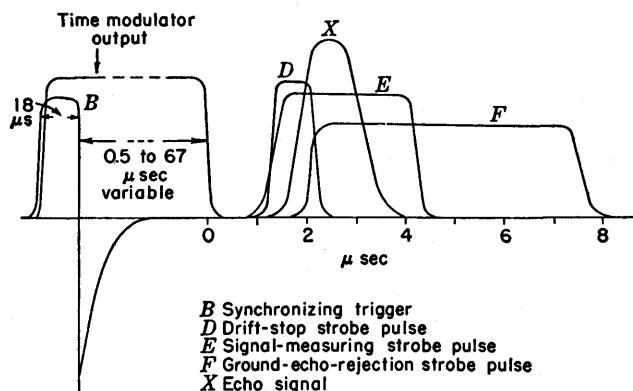


Fig. 8-48—Gating pulses of Mark VI time discriminator and target selector.

single-ended discriminator and that rejects signals of width greater than the transmitted pulse.<sup>1</sup> In this system only qualitative range data were required. The heart of the operation is the standard electronic integrator which provides the search sweep and acts as the function unit integrator, as shown in Fig. 8-46.

An electrically controlled time-modulation circuit triggers a delay-line pulse generator shown in the circuit of Fig. 8-47 as  $V_1$  and  $V_2$ , which supplies the waveforms shown in Fig. 8-48. The three gates  $D$ ,  $E$ , and  $F$  turn on three time demodulators (strobed pentodes) shown in Fig. 8-47, which in turn control the drift circuit to determine whether the gates shall drift out in range, track a signal, or return to minimum range. The operation of the circuit is as follows. The tube  $V_6$  is an integrator whose plate potential determines the range of the gates  $D$ ,  $E$ , and  $F$ . The rate of motion of the plate potential is determined by the input voltage to the

<sup>1</sup> I.E.E. Convention Lecturette, "Automatic Stobes," March 1946.

integrator, which is shown as being +10 volts normally. In the quiescent state, the plate will fall down to +25 volts as in the standard Miller sweep generator at which time the diode  $V_4$  will conduct, driving the grid of  $V_3$  negative which in turn drives the grid of  $V_7$  from its normal value of -20 volts, well below cutoff, to zero; its plate falls and pulls the suppressor of  $V_6$  from +5 volts down to -40 volts to cut off its plate current. The plate then rises, bringing the range gates in, until it is caught by the plate of  $V_{10}$ , whose cathode is held to +125 volts. The plate of the integrator  $V_6$  is coupled to the grid of  $V_7$  through a differentiating network, holding that tube on during the flashback in order to keep the suppressor of  $V_6$  off. Otherwise, the whole drift-return circuit would stop working as soon as the plate of  $V_6$  rose above +25 volts. With this addition, the suppressor is held off until the plate is caught at +125 volts and the grid of  $V_7$  returns to below cutoff. When this happens, its plate rises, bringing the suppressor back to +5 volts, plate current starts to flow in  $V_6$ , the voltage drop in  $R_7$  drives the control grid of  $V_6$  nearly off (-2 volts) through  $C_1$  as in normal phantastron action, after which the grid starts to rise towards +10 volts, and the plate continues its fall from +125 volts to +25 volts, sweeping the range gates from 800 to 33,800 ft. A simpler circuit could be designed using the phantastron or sanatron technique for recycling as described in Chap. 5 of Vol. 19.

The rate of drift or search is determined by the current flowing into the grid side of  $C_1$ , which in turn is determined by the current flowing from the +10 volts tap through  $R_1$ , and the current drawn through  $R_2$ , and the gated pentode rectifier  $V_5$ . The average cathode voltage of  $V_5$  is -10 volts, and its plate is returned to the grid of  $V_6$  which is at -2 volts; hence there is +8 volts from plate to cathode of  $V_5$ . The control grid is normally held at -30 volts except when a 5.5- $\mu$ sec gate ( $E$ ) drives it positive. At that time, the screen current rises sharply, causing a negative step to appear across the 0.45- $\mu$ sec delay line. On reaching the end of the line the pulse cuts off the second control grid, thus allowing plate current to flow for only 0.45  $\mu$ sec of the 5.5  $\mu$ sec that the control grid is gated on. While the screen and control grids are both on, the plate will drop to within 1 volt of the cathode, and with no video signals present, 1.75 ma, (8-1)volts/4000 ohms, will flow. This provides an average current of 1.05  $\mu$ a, which subtracts from the current to 2.4  $\mu$ a flowing through  $R_1$  to give a net current of 1.35  $\mu$ a, which is integrated in  $C_1$  to produce a rate of fall of 27 volts/sec (that is, a range-search period of 4.3 sec). If video signal X appears during the 0.9- $\mu$ sec interval during which  $V_5$  is conducting,  $V_5$  will draw more peak, and hence average current away from the grid side of  $C_1$ ; in fact, if it draws 2.4  $\mu$ a of average current, the plate of  $V_6$  will stop moving and the gates will stand still, thus locking on the signal. To do this a signal of standard

AGC level, namely 25 volts, must overlap pulse *D* by about half its width. If the signal moves, the overlap will change and the gates will automatically track as long as a signal is present. If the signal fades, the current in  $V_5$  will drop to  $1.05 \mu\text{a}$  and the range search will recommence.

If for any reason it is desired to reject a certain echo after the automatic searching has found it and to continue the search to greater range,  $V_5$  may be put out of action long enough for the gate to move past the signal by closing the signal-rejecting switch which causes a negative voltage step to be applied to the outer control grid of  $V_5$ , which then returns to its normal bias as  $C_2$  recharges through the diode  $V_{11}$  and  $R_4$ , a time constant of 0.05 sec, after which the gates can again lock on a signal. This corresponds to a "kick" of about 3000 feet.

On-target indication is given the operator by differentiating the range-search sweep voltage and applying it to the grid of  $V_9$ , which controls the intensity of the angle-error-indicating CRT. When the gates are searching, the derivative is negative and  $V_9$  is cut off. When the gates stop searching,  $V_9$  turns on, bringing the CRT spot intensity up to normal. The CRT is prevented from brightening during the positive-going flashback by the diode part of  $V_8$  and the smoothing network  $R_5$  and  $C_3$ .

Rejection of ground echoes is performed by "integrating" the output of 5.5- $\mu\text{sec}$  time selector. The first ground-return echo from this airborne set was found to be about 6  $\mu\text{sec}$  long; hence the time constant of the "integrating" network was adjusted to discriminate against a 4- $\mu\text{sec}$  signal. The time selector  $V_3$  is a heptode gated on the second control grid by the waveform *F* to select the video signals imposed on the first control grid. The plate potential drops to 10 volts during any coincidence of the gate *F* and the signal, putting a 290-volt drop across the *RC* combination  $R_6$ ,  $C_4$ ,  $C_5$ . After 3.8  $\mu\text{sec}$  the diode  $V_{4a}$  conducts charging  $C_6$  slightly. If the long pulse recurs several times,  $C_6$  charges up enough to start the flashback action described earlier.

The philosophy of this circuit is interesting. It might have been evolved by designing a straightforward balanced (two-gate) time discriminator, to feed an integrator whose quiescent rate is positive rather than zero. As long as the quiescent rate is greater than that which is ever to be encountered from a target, one half of the time discriminator is then contributing nothing, and might as well be omitted. The objection to unbalanced tracking of this type is that the point at which the gate tracks the signal depends upon the signal amplitude and upon the amount of noise present in the single gate. For accurate tracking it would be necessary to have a good AGC circuit or to use a balanced discriminator and an integrator whose quiescent velocity is normally zero, but which would be switched to a positive rate in the absence of a signal. The

unbalanced circuit has two advantages which the AN/APG-5 with its complicated relay switching does not possess: (1) it operates in both track and search functions with no change in circuit connections, and (2) it eliminates the need for a sawtooth scan generator.

#### SUMMARY

**8-18. System Planning.**—The previous sections of this chapter have taken up the various operations to be performed by the automatic time-measuring system and have given practical circuits. Circuit design for the individual operations—time discrimination, target selection, etc.—must be preceded by a block-diagram stage in which the general configuration of the tracking loop and the nature of the several elements are determined.

There are five major configurations of mechanical and electrical elements. These are shown in Fig. 8-49. The other possibilities are numerous, but those illustrated are the ones of greatest interest. It is assumed that velocity memory is required—hence double integration is used, although for most purposes single integration is adequate. For simplicity, the integrators indicated are shown without the necessary stabilizing features without which the loop would be unstable.

Type (a) completely electrical, is typified by the example given in Sec. 8-8 on systems using electrical integrators. An outstanding example of the first type is British Oboe mouse station, which uses both range and range rate as voltages to compute electrically the bomb-release time. Type (b) is identical except for the addition of a servomechanism which converts voltage into shaft rotation for driving mechanical computers or indicators. Examples of this type are numerous, (AN/APG-5, etc.,) principally because of the scarcity of computers taking electrical data. The third type (c) is rather unique in that the mechanical follow-up servo follows time data rather than a voltage. The electronic loop supplies the features of rapid slew and search for target selection, and smooth rate data arising from the inherently high slope accuracy obtainable with electrical time-modulation circuits. These separate time-following mechanical loop offers two advantages—it can be disconnected during search and slew, thus saving wear on itself and the computer which it drives, and it can employ a multiple-scale mechanical time modulator for range precision, while retaining the advantages of an electrical signal-tracking loop. The closest known examples of this type are the automatic range-tracking circuits proposed for the SCR-584 by General Electric Company and the Radiation Laboratory. The first was used in a system called the Automatic Radar produced by General Electric and the second was used in the SCR-784.

Type (d) is fairly conventional for systems that require mechanical



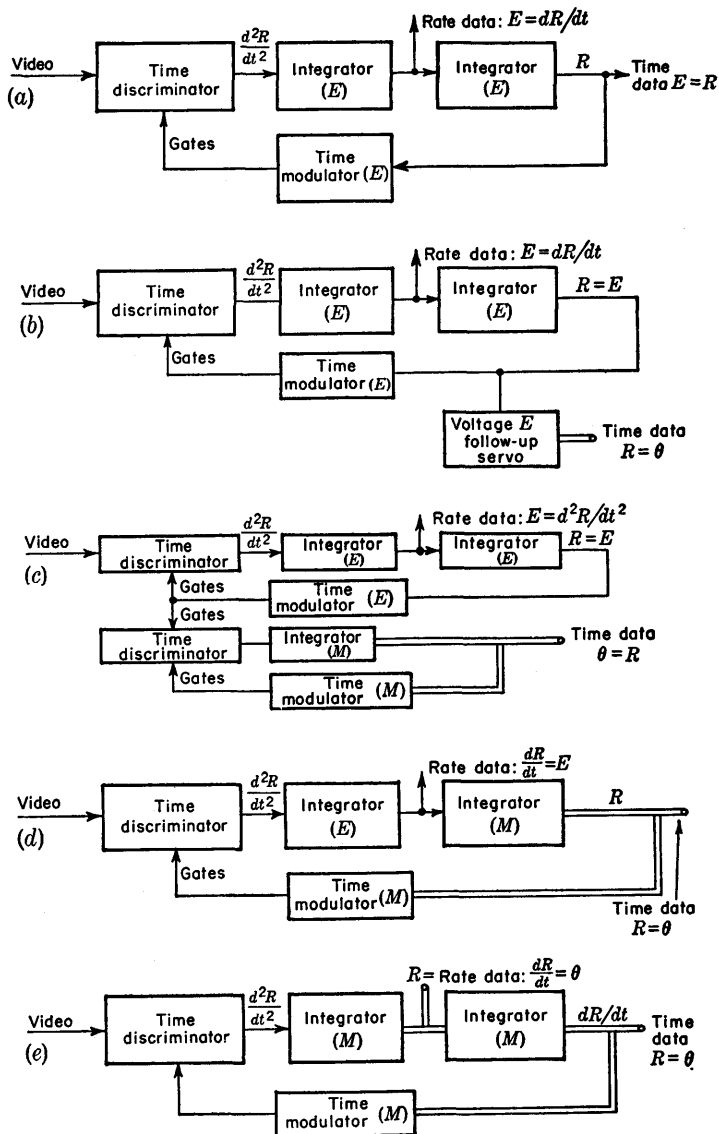


FIG. 8-49.—Five possible configurations of automatic time-measuring systems. The symbols (E) and (M) indicate electrical or mechanical operations.

data outputs. The time modulator may be single- or multiple-scale depending on the accuracy required. A fifth system is proposed as having capabilities of velocity memory limited only by the balance of the time discriminator since the mechanical integrators have no position error.

The process of determining the best configuration for any situation may be illustrated by discussing a hypothetical example.

The requirements might be—

1. Maximum tracking range of 140  $\mu\text{sec}$  with range data accurate to  $\pm 0.05$  per cent, and the rate data accurate to 0.05  $\mu\text{sec/sec}$  for rates of 1  $\mu\text{sec/sec}$ —both range and range-rate data to be in the form of shaft rotations.
2. Provisions for manual, aided, and automatic tracking.
3. Provisions for slewing at greater than 18  $\mu\text{sec/sec}$ .

Since mechanical output data are required, the completely electrical system is ruled out, and the last system is not considered because of the problem of stabilization involved. The accuracy specification in range rules out the electrical system with voltage-to-shaft follow-up since reliable accuracies of 0.05 per cent are not realizable with electrical time modulators. The field is thus reduced to type (c) or (d). The advantages of the type (c) system are that it allows rapid slewing and search, and it provides smooth accurate range-rate data free from periodic errors.<sup>1</sup> The apparent disadvantages are in the complexity and size involved in employing two loops and the fact that with an electrical integrator defining the position of the range gates they would always eventually (in about 10 min) drift to some quiescent point in range and would not remain permanently at any given range without switching to manual operation. For these two reasons, the single-loop mechanical system was often selected and has performed satisfactorily. The reason for rejecting the two-loop system is nevertheless open to question. Although range is stably defined by a mechanical shaft position which is perfectly content to remain fixed indefinitely, the range rate is controlled by the balance of the discriminator and the quiescent point of the electrical integrator. Thus, although there is no preferred position, it is difficult to maintain the quiescent velocity at zero. Furthermore, the range-rate accuracy of the system would only be about 2 per cent, due in part to the cyclic nature of the range errors of a multiple-scale system. Similarly, the two-loop system would be much more suitable for automatic searching. If, however, the radar is to be used under conditions of target confusion and interference, automatic search circuits would be useless and manual

<sup>1</sup> For this application the electrical range-rate data would be followed mechanically in either type of system.

search should be used. Thus the only disadvantage in target selection introduced by the single-loop system is the low slewing speeds obtainable (3000 yd/sec).

From this hypothetical example, the various factors that enter into the conception of a time-measuring system can be seen. A comparison of all five systems on the basis of the most usual requirements is shown in Table 8-2. The column headed "Limiting Factor" reveals two common causes of weakness. One is that a mechanical time modulator must be used to obtain high range accuracy. The development of a highly precise electrical time modulator to replace the currently used capacitance or inductance phase-shifters would open the way to completely electronic precision time-measuring systems. The second weakness arises from the need to supply data as a shaft rotation. The inevitable trend of the future toward electrical computers for high-speed solutions will free time-measuring systems from this additional need for incorporating mechanical elements. But for these two weaknesses, the all-electrical system of Fig. 8-48a would represent the ideal. For the present, the system of Fig. 8-48c comes closest to the ideal in that it has the high range accuracy of the multiple-scale mechanical time modulator, the rate accuracy of the electrical time modulator, the facility at target selection of the electrical loop, and supplies mechanical data with a minimum of wear. Its major disadvantages are cost and weight.

TABLE 8-2.—COMPARISON OF TRACKING SYSTEMS

	<i>a</i>	<i>b</i>	<i>c</i>	<i>d</i>	<i>e</i>	Limiting factor
Range accuracy.....	Poor	Poor	Good	Good	Good	Electrical time modulator (single scale)
Rate accuracy.....	Good	Good	Good	Poor	Poor	Cyclic errors of time modulator
Target acquisition...	Good	Good	Good	Poor	Poor	Mechanical motion
Speed ratio.....	Good	Poor	Poor	Poor	Poor	Mechanical motion
Mechanical data.....	No	Yes	Yes	Yes	Yes	Mechanical motion
Wear.....	Good	Good	Good	Poor	Poor	Slewing done mechanically
Economy.....	Good	Poor	Poor	Poor	Poor	Mechanical elements
Weight.....	Good	Poor	Poor	Poor	Poor	Mechanical elements

## CHAPTER 9

### SYSTEMS FOR AUTOMATIC TIME AND POSITION MEASUREMENT

BY R. I. HULSIZER, J. V. HOLDAM, AND W. B. JONES

#### PRACTICAL SYSTEMS FOR AUTOMATIC TIME MEASUREMENT

BY R. I. HULSIZER

In the light of retrospection, every piece of equipment appears covered with the fingerprints of the designer. There is often as much art as science in the design of practical circuits for performing a particular operation. In addition to this factor, the development during the war was marked by two further diversifying effects. One was the necessity of building useful military equipment before adequate study and experiment had led to satisfactorily systematized theories of design, and the other was the time delay in diffusion of improvements in the theories of design. As a result, the systems for automatic time measurement often show little similarity to each other and less resemblance to design based on any general principles now available.

Although five configurations of systems were presented in the previous chapter, the practical systems to be discussed are divided into only two groups, the simple electrical and the simple electromechanical, for all the more complex forms can be derived from these.

Before a discussion of the more conventional systems, two simple techniques particularly adaptable to laboratory measurements will be mentioned. The simpler involves the simplest method that one can conceive—the “leaning gate” system in which a single time selector is made to drift in range until it intersects enough of a signal to cancel the drift action. This is exemplified by the British systems, AGL-(T) and A.I. Mark VIA, both of which have been mentioned in Chap. 8. These systems perform with a minimum of circuits the functions of search, lock-on, and track. They are limited in accuracy since the single-gated time discriminator is sensitive to signal and noise amplitude.

A second technique which is simple and yet capable of extreme accuracy is that of photographing a circular sweep display with a movie camera and later plotting the data. No tracking circuits are required and systematic errors can be removed from the data. It is, of course, limited to applications where instantaneous data are not required, as in determining the velocity of test models of aircraft.

The demand for instantaneous and accurate data has led to the design of the conventional systems in general use. The first group discussed will be the electrical systems as exemplified by the British Oboe system and the ARO (Automatic Range Only), used in the AN/APG-5, AN/APG-15. The second group are the systems employing mechanical time modulators directly in the tracking loop and will be illustrated later.

**9.1. ARO Electrical System.**—The time discriminator and the automatic search circuits for this system have been discussed in Secs. 8-13 and 8-18 respectively; therefore a brief description will be adequate here. In order to illustrate the design considerations, the chief subject of discussion will be the modifications that were made on the ARO Mark I in a development program aimed at reducing the size, weight, power con-

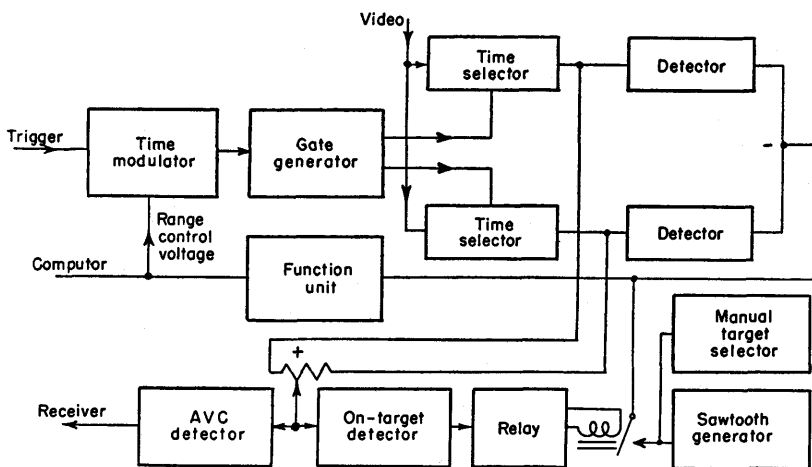


FIG. 9-1.—ARO range system block diagram, Mark I and Mark II.

sumption, and complexity of the circuits. The resultant design was known as the ARO Mark II or Midget ARO.

The block diagram of the circuit remained unchanged and is shown in Fig. 9-1. The schematic diagram of the earlier circuit is shown in Fig. 9-2. The circuit consists of a delay multivibrator as a time modulator, followed by a blocking oscillator to form the early gate and to trigger a similar blocking oscillator that forms the late gate. The time selectors are suppressor-gated 6AC7's. Pulse transformers in the plates of the time selectors invert the gated pulses so that they drive two triode detectors whose difference current produces a net voltage on the large condenser  $C_1$ . A cathode follower with a constant-current pentode as a cathode load provides the range voltage for the delay multivibrator and the range followup servomechanism at low impedance and also

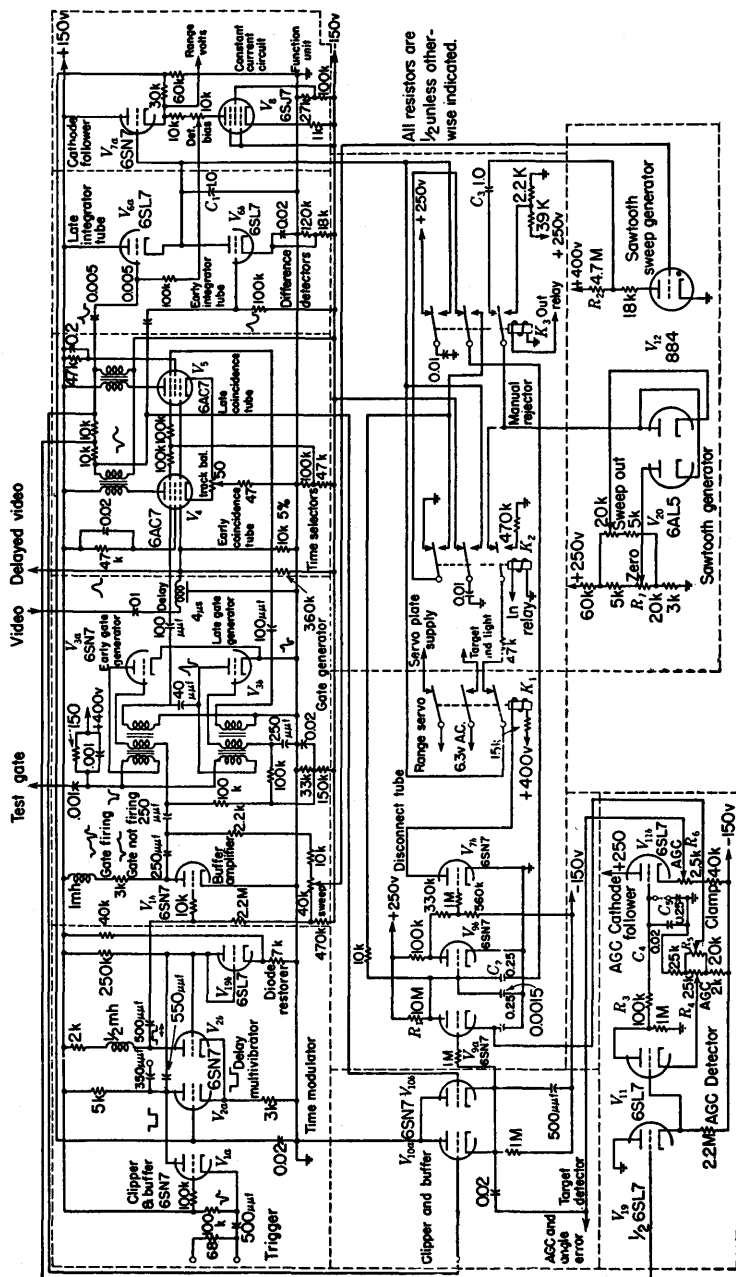


Fig. 9-2.—ARO Mark I range system; dotted lines indicate the functional blocks of the circuit. They are the time modulator, gate generator, time selectors, difference detectors, function unit, on the top row, target detector and range search disconnect in the middle, and AGC and range search in the bottom row.

provides suitable biases for the triode difference detectors. As already described in Sec. 8-17 on-target indication is performed by two "infinite impedance" detectors with a common cathode resistor fed by the two gated signals. The larger signal controls the detector output voltage. If this voltage exceeds the threshold, it closes a relay which connects either a search-sawtooth or manual target-selector control to the range voltage whenever the signal is below the preset threshold. The AGC circuit is a third infinite-impedance detector fed by the sum of the two

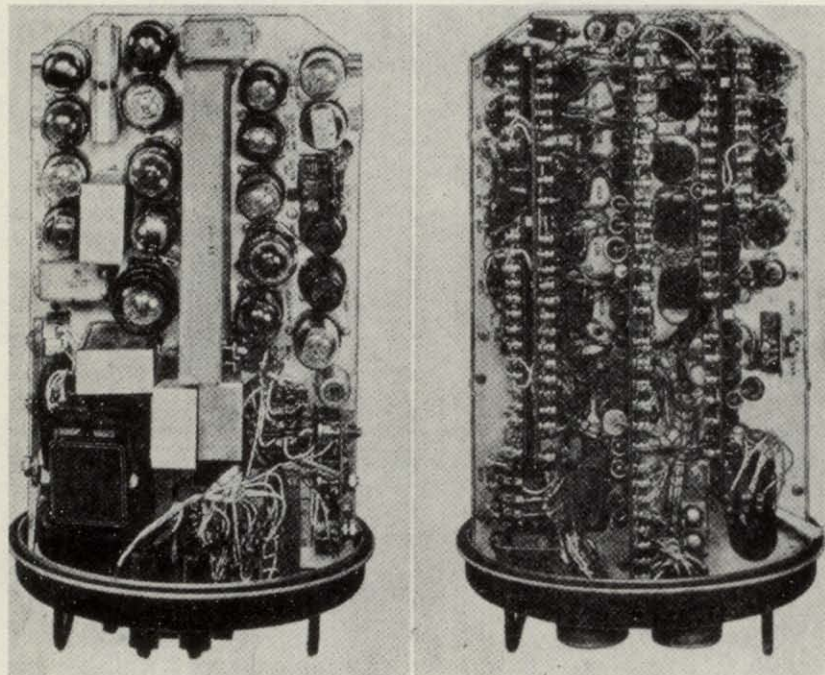


Fig. 9-3.—ARO Mark I range unit (a) top view; (b) bottom view. Dimensions:  $15\frac{1}{2} \times 9\frac{3}{4}$  in.

gated video pulses and operating a d-c amplifier and an output cathode follower.

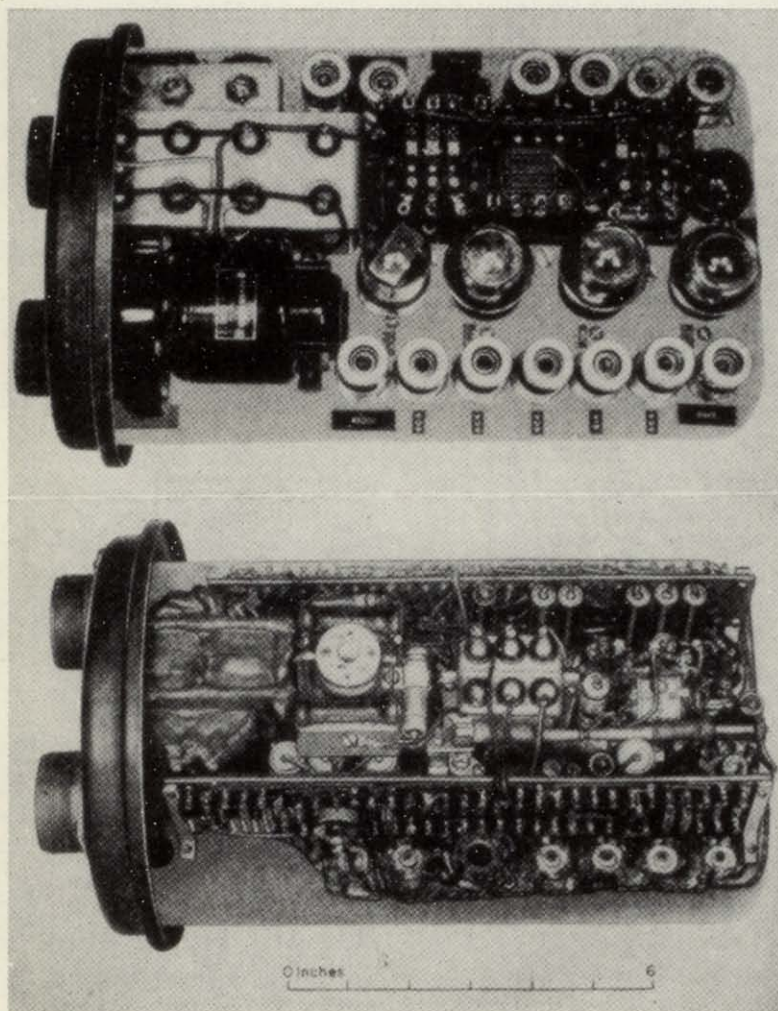
Figure 9-3 shows the completed Mark I ARO chassis. The useful area of the chassis is  $15\frac{1}{2}$  in. by  $9\frac{3}{4}$  in., or 150 in.<sup>2</sup> An estimate of power consumption from the circuit diagram shows about 65 ma from the +400 bus including the regulated current, and 30 ma from the negative bus.

Figure 9-4 shows the schema of the Mark II ARO and Fig. 9-5 shows the constructed chassis. The estimated current drain is 30 ma from the positive supply and 10 ma from the negative supply. The chassis plate has a useful size of  $11\frac{1}{2}$  in. by  $6\frac{1}{2}$  in. or 75 in.<sup>2</sup> The relative densities





of the two constructions give meaning to the size comparison. As pointed out previously, the block diagram remains almost identical. The saving came in simplification of the circuits and use of smaller tubes



(a) top interior; (b) bottom interior. Dimensions are  $11\frac{1}{2} \times 6\frac{1}{2}$  in. Compare with Fig. 9-3 showing earlier unit that performs the same functions as this.

and components. If the development of the Mark II had continued longer, 6AL5 diodes and miniature VR tubes would have been available to replace all the large tubes used except the 5Y3. A feature of note is

the absence of the large 4- $\mu$ sec delay line used in the Mark I to compensate for the large minimum width of the delay multivibrator.

A "bootstrap" self-gating linear-sawtooth generator,  $V_1$ ,  $V_2$ ,  $V_{3b}$ ,  $V_{4a}$ , and a pickoff diode  $V_{4b}$ , replaced the delay multivibrator as the Mark II time modulator, to save 15 ma of current and decrease the minimum range to 50 yd as compared with 400 yd. The bonuses resulting from this change are more accurate range data and elimination of the video delay line. A second modification resulting in appreciable space saving is the use of a single blocking oscillator  $V_6$  with a delay line to form the early and late gates for the time selector. The 0.25- $\mu$ sec delay line can be seen at the right of the underside of the Mark II chassis.

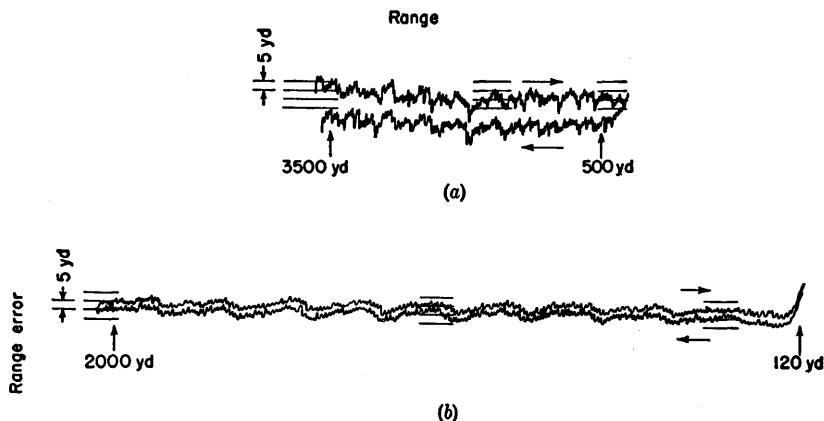


FIG. 9-6.—Range vs. range error of Mark I ARO. (a) represents the 4000-yd range scale. (b) represents the 2000-yd range scale. Note the range error resulting from change in direction of target motion. Rates are  $\pm 25$  yd/sec. Errors cyclic at 200 yd originate in the range-tracking calibrator.

Suppressor-gated 6AS6's are used for the time selectors  $V_8$  and  $V_9$ . The particular improvement here is that the suppressor characteristics of the 6AS6 provide much more of a switch-type gating action than those of the 6AC7. The plate loads of the time selectors are resistors rather than pulse transformers. This saving is made possible by using diode, instead of triode, detectors  $V_{10}$ ,  $V_{11}$  following the time selectors since the diode detectors can accept negative signals.

For the function unit, the Mark II uses an electronic integrator  $V_{17}$ , whereas the Mark I uses only the approximate integration of a high-impedance detector and a large condenser. The integrator is made necessary by the larger range of control voltage of the linear-sweep time modulator. A cathode follower  $V_{18}$  provides a low-impedance output to the computer and convenient feedback path for the 0.01 feedback condenser. The small excursion of the output voltage of the difference detector makes it possible to use fixed biases on the detector diodes.

In the on-target detector circuit, the technique of taking the larger of the two gated signals for the on-target indication is abandoned and a stretched pulse representing the sum of the two gated pulses is amplified at narrow bandwidth in  $V_{12}$  and peak-detected in  $V_{13}$  to drive the relay amplifier  $V_{14}$ . The use of a-c, rather than d-c, amplification results in more stability in the threshold adjustment. The AGC circuit provides an additional stage of pulse amplification  $V_{15}$  after  $V_{12}$  and detects in a diode detector  $V_{16}$ .

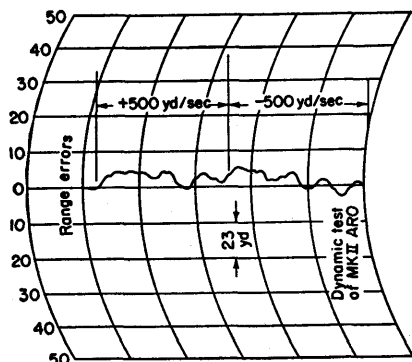


FIG. 9-7.—Range-tracking data of ARO Mark II. Data show range errors due to nonlinearity and velocity. Data obtained from electrical tracking loop only.

The only modifications in the range-search sawtooth generator are the elimination of the limiter and level-setting diodes. The amplitude of the sawtooth wave remains constant, the only variable being the average level adjustment. No change is made in the target-selector relay circuit; it is drawn symbolically in the schema for Mark II merely to decrease the confusion of the circuit.

Figures 9-6 and 9-7 show the dynamic range-tracking data of the Mark I and Mark II systems. The range-tracking calibrator is discussed in Sec. 9-3.

**9-2. British Oboe Electrical System.**—The Oboe Mark IIM<sup>1</sup> is chosen as a second example of an electrical automatic time-measuring system because it illustrates British approach to the problem. The characteristics that it illustrates particularly are the utilization of both range and range-rate output voltages as data for an electrical computer, the incorporation of a multiple-scale time modulator in an all-electrical time-measuring system, an unusual gating technique for obtaining both range-error signal and signal-level indication from two detectors, the use of high-precision electronic integrators in the function unit, and an automatic-coast circuit that provides accurate memory for nearly a minute.

The time-measuring system is part of a British radar-beacon set for precision blind bombing by triangulation. As illustrated in Fig. 9-8, there are two ground stations, "the cat and the mouse," which interrogate

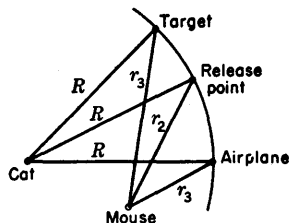


FIG. 9-8.—Geometry of Oboe blind bombing.

<sup>1</sup> IEE Convention Paper, "Oboe," F. E. Jones, March 1946.

a beacon responder in the airplane. The cat station automatically tracks the received signal, compares its range with the distance of the cat from the target and transmits a signal to the pilot to keep him flying on a circular course passing through the target. The mouse station automatically measures the aircraft range and range rate which are compared in a computer to determine the bomb-release point. Reports indicate that the accuracy of range measurement is about five yards, at all ranges out to 350 miles, and bombing accuracy is 12 to 25 circular miles. The high precision of time modulation necessary to produce these results is obtained by the use of a step delay which selects any one of

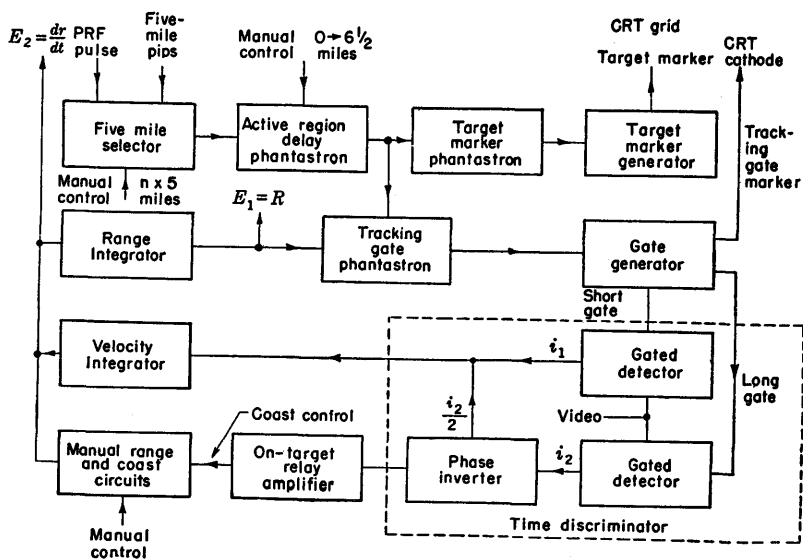


FIG. 9-9.—Oboe range-tracking system block diagram.

70 five-mile crystal-controlled markers to form a trigger for a tracking phantastron that is positioned by the time discriminator and works only over a region of 16 miles centered on the target.

Figure 9-9 shows the block diagram of the system which can operate as either cat or mouse station. The top row of blocks shows the time modulator. The necessary alignment process for supplying standardized data to the computers is described in the remainder of this paragraph. The tracking-gate phantastron control is set at +165 volts, its middle value, and the 5-mile selector and the active-region delay phantastron are adjusted to place the tracking-gate marker at the range of the target as determined from maps. This setting is made with the use of an A-scope display that has accurate 5- and 1-mile intensity markers. The

target-marker phantastron is then adjusted to put out a target marker at the target range. The target-marker phantastron is then left fixed during the operation, its function being to provide on the A-scope a marker which will show the operators the location of the target on the sweep while the tracking-gate phantastron moves about in its operation of tracking the aircraft. From this sweep indication the ground operators estimate roughly the "time to go" before bomb release which they communicate to prepare the bombardier. Except for this convenience the target-marker phantastron is unnecessary. Once the alignment has been completed, the tracking-gate phantastron may be moved from the target range. The departure of the phantastron control voltage from +165 volts indicates to the computer the "residual range," that is, the distance of the aircraft from the target.

As described in Sec. 8-12 the time discriminator generates a current proportional to the misalignment of the gates and the signal. The velocity integrator operates on this current to provide a range-rate voltage. For the computation of bomb-release time in the mouse operation, this is standardized to be at +165 volts when the velocity is zero. The slope of the velocity-control voltage is 0.4 volts/mph. The range integrator integrates the rate voltage to provide range-control voltage centered about +165 volts and having a slope of 33 volts/mile.

Target selection is performed by switching the velocity voltage to a manual control, watching the A-scope for the relative positions of the tracking-gate marker and the aircraft echo, and manually moving the tracking gates to coincide with the echo, whereupon the velocity voltage is disconnected from the manual control and connected to the velocity integrator for automatic tracking.

The current phase inverter in the time discriminator (Fig. 9-14) feeds a relay amplifier which energizes after the signal level has dropped below an arbitrary threshold for more than  $\frac{1}{2}$  sec. The relay disconnects the velocity integrator from all sources of current and connects between plate and grid of the velocity integrator a condenser which has been charged to a "smoothed" velocity voltage. Consequently, the plate (velocity) voltage remains constant at the "smoothed" velocity up to 15 or 20 sec until the echo reappears and automatic tracking recommences.

Figures 9-10 and 9-11 show the timing sequences of the fixed delay (5-mile selector) and the variable delay (tracking-gate phantastron, etc.). Figure 8-29 shows the timing sequence of the tracking gates and the video signals and the circuit schema of the time discriminator.

Following are a few remarks on particular features of circuit design of the Oboe automatic time-measuring system that can be omitted without losing continuity.

The crystal oscillator, whose circuit is not shown, is of the Meacham-

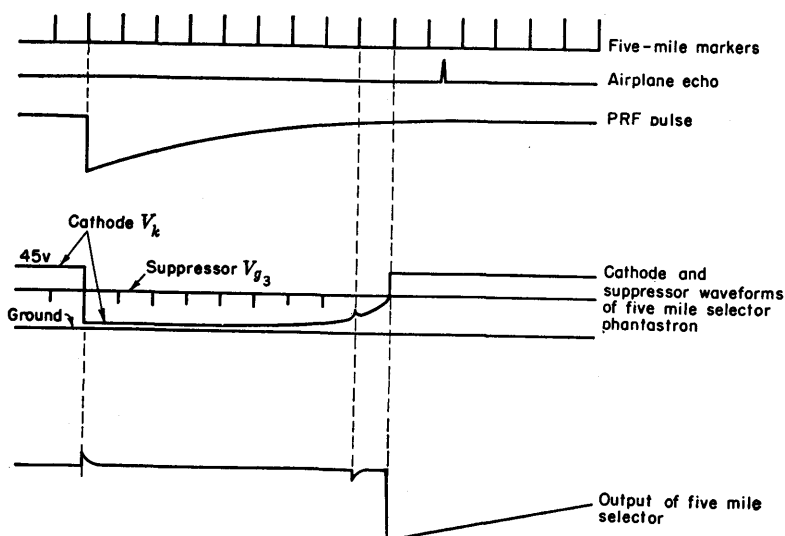


FIG. 9-10.—Oboe 5-mile-selector timing diagram.

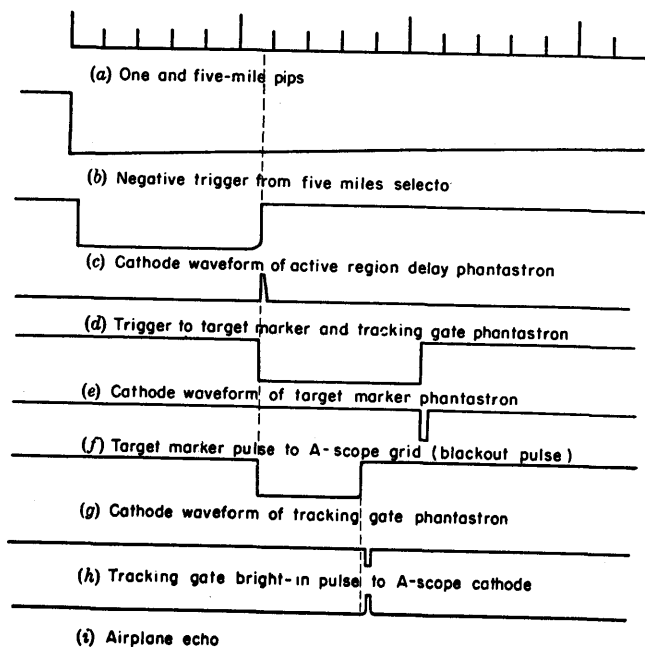
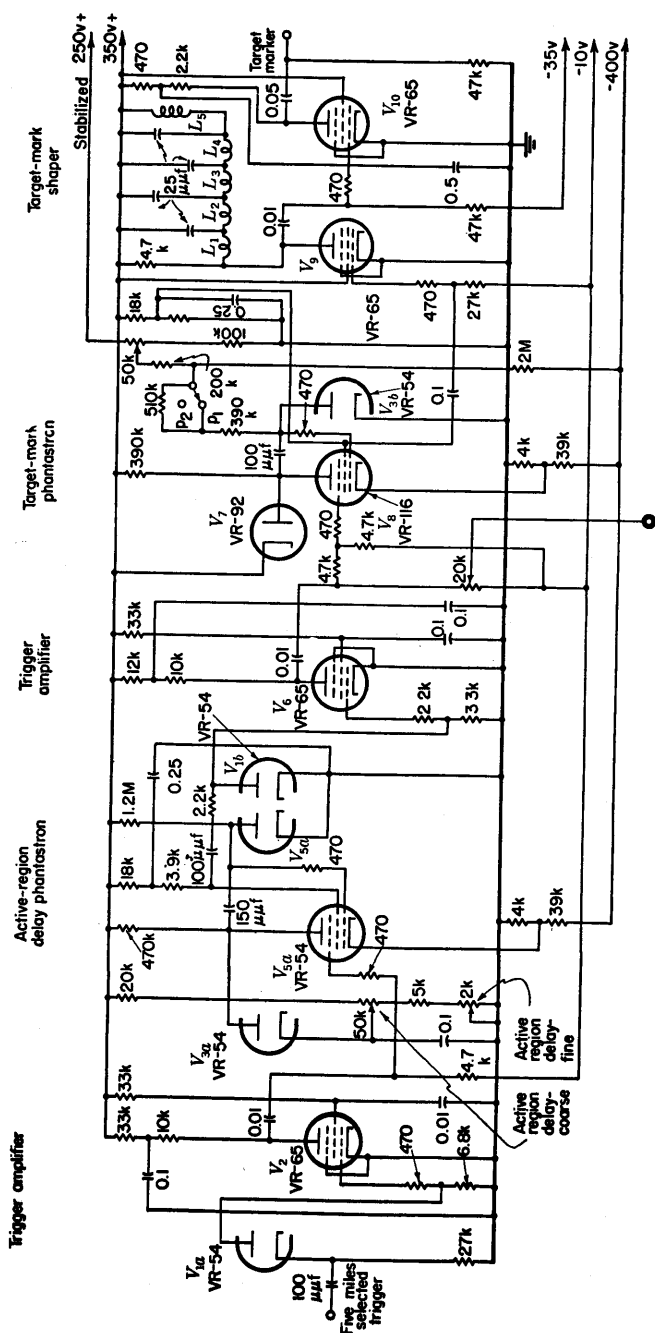


FIG. 9-11.—Oboe active-region timing diagram.





**Fig. 9-13.**—Oboe active-region delay phantastron, target-marker phantastron, and target-marker pulse shaper.



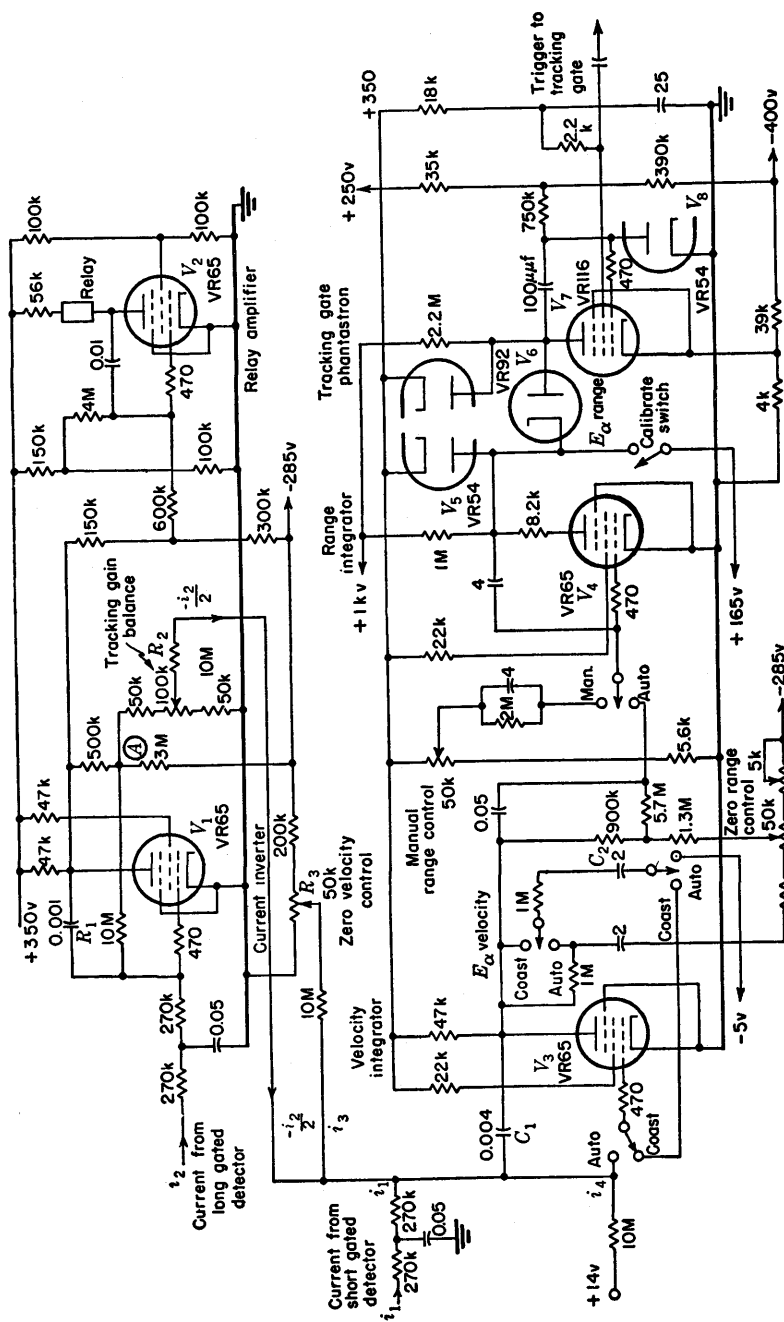


Fig. 9-14.—Oboe tracking-gate phantastron, and function unit, showing specially designed electrical integrators, and coast provisions.

against the crystal pips just before the start of each run so that stability required of the phantastrons is of short duration only.

In Fig. 9-14 is shown the tracking-gate phantastron  $V_7$  that is of conventional type. Its plate-catching diode  $V_6$  is controlled by the range integrator which in turn is controlled either by the velocity tube or by a manual control, depending on the mode of operation. The plate of the phantastron tube is returned to +1000 volts to increase its linearity in the operating range. Insulation breakdown of the tube is prevented by the diode  $V_5$ , which limits the plate swing to +350 volts.

The limitation of having the time modulation continuous over only a short range is tolerable for this particular system and it permits the tracking loop to be completely electrical without reducing the precision of the system.

The rest of the circuits on Fig. 9-14 have to do with the automatic control of the time modulation. The time discriminator is discussed in Sec. 8-12 (Fig. 8-29) and is seen to deliver two currents whose difference is proportional to the misalignment of the range gates and the echo. These currents are indicated as  $i_1$  and  $i_2$ . When the target is correctly located in the gates,  $i_2$  is twice as large as  $i_1$  because its gate is twice as wide as the short gate and extends over the whole echo. Thus  $i_2$  is a true indication of echo intensity and will not change for small motions of the gate with respect to the echo. The tracking loop then compares half the current due to signal level with the current from a gated detector which extends over only the first portion of the signal and time-modulates the gates to make these two quantities equal.

The tube  $V_1$  is a current inverter. If the gain of  $V_1$  is assumed to be infinite, it can be said that the grid of  $V_1$  remains fixed (a virtual ground as discussed in Sec. 8-8) and hence the current flowing in  $R_1$  must be equal to and opposite  $i_2$ . If the voltage at A which produces this equal and opposite current is halved, the current which flows through  $R_2$ , to a potential equal to that of the grid of  $V_1$ , must be equal and opposite to  $i_2/2$  since  $R_1$  equals  $R_2$ . This current  $-i_2/2$  is added to  $i_1$  at the grid of the velocity integrator  $V_3$  which integrates the difference current to supply a velocity voltage  $V_v$ . This voltage is integrated in turn by  $V_4$  to form the range voltage which controls the phantastron. The zero-velocity control  $R_3$  adjusts the grid potential of  $V_3$  so that when  $i_1 = i_2/2$ , the plate of  $V_3$  is at +165 volts, the standard for zero velocity. When  $i_1$  becomes greater or less than  $-i_2/2$ , the plate potential of  $V_3$  must change at a rate which will balance the difference current by an equal and opposite displacement current through  $C_1$ . This unbalance of currents might be due to motion of the target, and the change of the velocity voltage will cause the range voltage to move at a rate which will keep the tracking gates aligned on the target. The zero-range control is

adjusted so that when the velocity voltage equals +165 volts, the plate of  $V_4$  is at +165 volts.

The automatic-coast operation is discussed in the following paragraph. If the signal fades, the velocity voltage will fall to +165 volts with a time constant of several seconds. However, the plate of  $V_1$  will fall and will cause the plate of  $V_2$  to fall with a time constant such that the relay will actuate  $\frac{1}{8}$  sec after the signal fades. When the relay energizes, the three switches around  $V_3$  throw from the automatic position to the coast position. During automatic operation, the velocity voltage charges  $C_2$  through a 2-sec time constant. When the switches throw to coast, this condenser is connected from plate to grid of  $V_3$  and all the sources of current are removed. Since  $C_2$  is charged with respect to the normal grid bias of  $V_3$ , the potential across  $C_2$  is closely equal to the mean potential difference between the plate and grid of  $V_3$  over the preceding two seconds, no current will flow into  $C_2$ , and the plate must stay at the smoothed velocity voltage except for leakage currents. During the  $\frac{1}{8}$ -sec lag before the relay throws, the voltage on  $C_2$  does not change appreciably because of the smoothing effects of the integrator and the smoothing network. The velocity memory under coast conditions is good enough to prevent the introduction of a significant error in bombing under operational conditions if the echo fades 15 sec before bomb release, provided the pilot maintains constant velocity. The advantage of using automatic coast is that unbalance of the time discriminator due to drifts in gain or level of any of the components cannot introduce a false velocity since the time discriminator is disconnected.

It will be recognized, of course, that leakage currents in the range integrator  $V_4$  will have as serious effects as those in  $V_3$ , for it is assumed that by maintaining  $V_0$  constant, the rate of  $V_r$  will remain unchanged. This can only happen if  $V_4$  acts as a true integrator. The most serious source of leakage current in this stage is the 4- $\mu$ f feedback condenser. The specifications call for a condenser having 2000-megohm leakage resistance, and in a later model a mica condenser was used.

There are several suggestions that have been made for revising this circuit. One is to replace the target-marker phantastron and the tracking-gate phantastron with a single linear sawtooth generator and a pair of "multiar" or regenerative amplitude comparators of the type described in Chap. 5. Another is to select the 5-mile pulses in a double-valued time selector rather than by adding them to the phantastron waveform and amplitude selecting as in the present 5-mile pulse selector. It is also felt that 0.1-mile pulses would increase the accuracy of calibration and these could be obtained by multiplying up from the present 1-mile pulses. A time discriminator of the type described in Sec. 8-13 would be used but no improvement in the electrical integrators except the use of

mica condensers can be foreseen since limiting conditions of operation are already employed.

An interesting accessory to the Oboe system is a dynamic tracking tester for testing the automatic-tracking operation and calibrating the slope of  $V_r$  against velocity. It consists of an electronic integrator controlling a phantatron whose output triggers a variable-width variable-amplitude video pulse generator. By varying the input voltage to the integrator, the dummy signal can be made to move at rates from +300 mph to -300 mph over any portion of the 350-mile range. The velocity of the dummy signal can be checked against the accurate range markers with a stop watch and the velocity voltage calibrated.

**9-3. Electromechanical Systems.**—The class of systems in which a mechanical time modulator is employed in the primary signal-following loop may be called "electromechanical" and is exemplified primarily by some of the high-precision automatic range-tracking systems. These systems, like the Oboe, rely on short velocity memory (2 sec) from the first integrator and some sort of coast circuit for long-time velocity memory. The coast circuits often act to keep the rate voltage of the aided-tracking mechanism equal to the rate of the target as measured in automatic tracking. The coast operation then consists of manually or automatically switching to aided-tracking mode where the correct rate is already set up. The single integrator of the function unit consists of the servomechanism employed to drive the mechanical time modulator from the time-discriminator error signal.

Stabilization of a double-integrator electromechanical loop of this type should be a straightforward process for the servomechanism expert. The form of the error signal and the scale factor of the mechanical time modulator are known for each particular circuit. The desired acceleration properties are usually defined on the one hand by the width of the range aperture and the speed with which the target is expected to move through that aperture in the target-selection process, and on the other hand by the necessary lack of response to rapid noise fluctuations. The over-all gain is determined by the maximum tracking speed desired and the velocity error in microseconds permissible at the maximum tracking speed. A treatment of the design of equalizing networks to meet the above requirements with the more complex transfer characteristics of a mechanical servomechanism is presented in Vol. 25 and in Part II of Vol. 22.

An electromechanical system of recent design is shown in Fig. 9-15. The synchronizer originally described in Chap. 4 performs the operation of selecting, once every 330  $\mu$ sec, two of a train of continuously running 163-kc/sec markers. These become the pretrigger and modulator trigger for a system.

The two-scale phase-shifter time modulator employs a condenser phase-shifter for the fine scale and a bootstrapped linear sawtooth generator with diode pickoff for the coarse scale. Its design is conventional

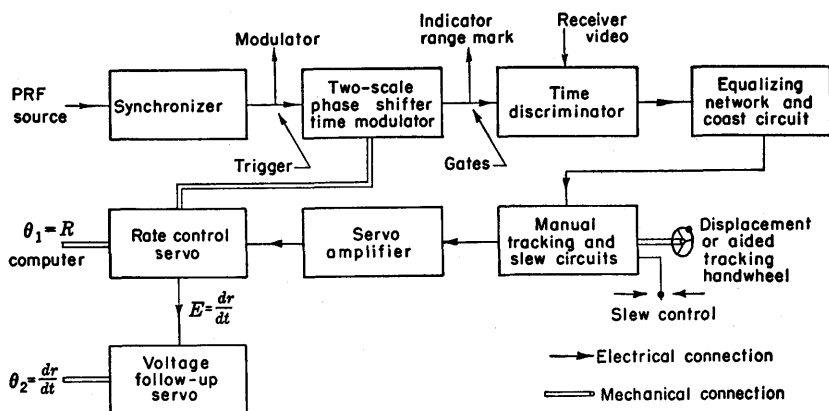


FIG. 9-15.—Block diagram of range-tracking system.

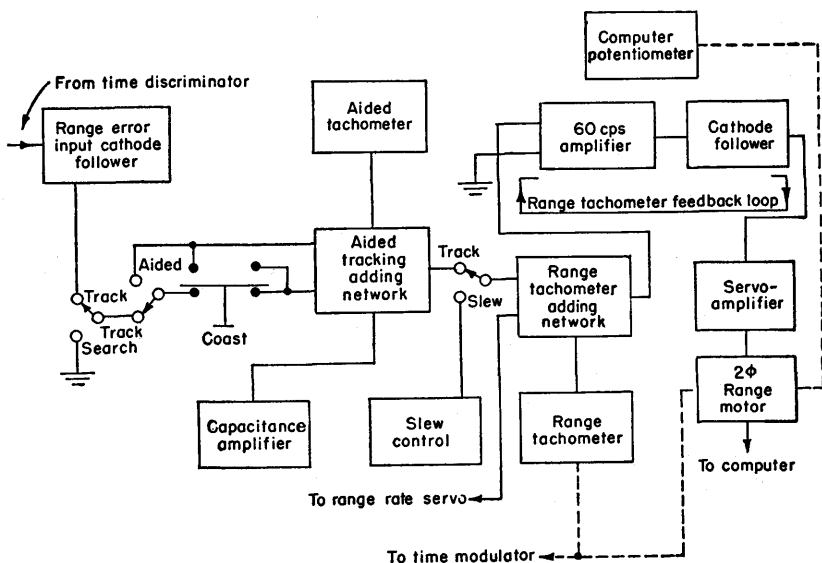


FIG. 9-16.—Function unit block diagram.

and similar to that of Sec. 6-2 and need not be discussed here. The time discriminator whose time-selecting gates are only  $0.12 \mu\text{sec}$  long (70-yd aperture) has been discussed in Sec. 8-12. The time discriminator delivers an error signal of about 1 volt per yard of misalignment.

In Fig. 9-16 is shown the block diagram of the function unit, whose circuit is illustrated in Figs. 9-17 and 9-18. The two unique features are the method of introducing manual displacement during automatic tracking and the method of obtaining aided tracking and coast. The mixing circuits for these two operations are extracted and redrawn in Fig. 9-19. Figure 9-19a shows the automatic-tracking connection where  $R_1$ ,  $R_2$ , and  $C$  form the first branch of the equalizing network and  $R_3$  leads into range servo amplifiers the mixing circuit where the range tachometer voltage is introduced for tachometer feedback. When it is not being turned, the manual-tracking tachometer obviously does not affect the

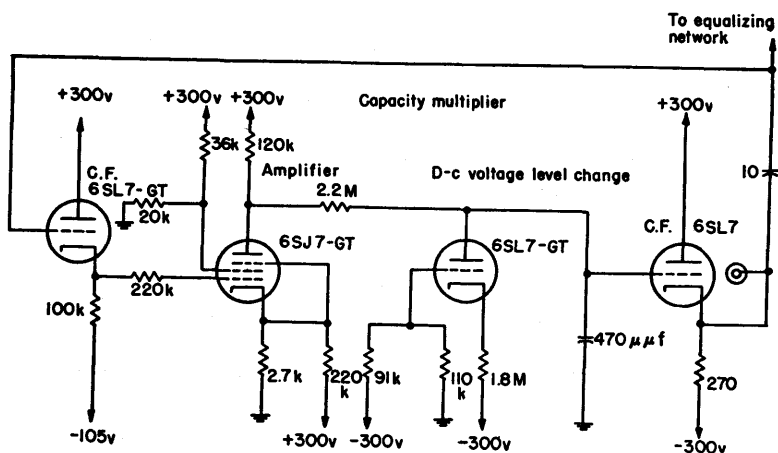


FIG. 9-17.—Equivalent condenser of function unit and memory circuit. This circuit uses plate-to-grid feedback to produce with a  $10\text{-}\mu\text{f}$  condenser a large equivalent condenser  $C'$  by utilizing the well-known Miller effect.

circuit performance, but when it is turned it develops across  $R_3$  a voltage proportional to the rate at which it is being turned. Since the tachometer-feedback servomechanism is an integrator, the range shaft turns in direct proportion to the manual-tracking tachometer and thus gives displacement control. Meanwhile the time discriminator is still operative, and when the gates reach an echo, it will develop a voltage adding to that from the manual-tracking tachometer that will hold the gates on target until the operator stops turning. If he decides the locked-on target is not the correct one, he can pull the gates off the target by a rapid spin of the hand wheel which will overcome the time-discriminator signal. This arrangement, used in conjunction with the slewing control shown in Fig. 9-18, gives excellent performance for target selection. The maximum slewing rate is 5000 yd/sec and the displacement control is 2000 yd/rev.



The connections for aided tracking are redrawn in Fig. 9-19b. There the time-discriminator signal has been disconnected and the tachometer develops for the displacement component a voltage proportional to the rate of turning across the equivalent  $300\text{-}\mu\text{f}$  condenser  $C'$ . The time constant of integration is formed principally by  $R_1$  and  $C'$  to be 300 sec. This gives the time in which an established rate will fall off if the operator makes no further corrections. Since  $C'$  is also charged up to the output voltage of the time discriminator in the automatic-tracking mode, this is the time in which the velocity memory will fall off if the operator pushes the coast button. If the target fades in automatic tracking and the operator does not push the coast button, the established rate will fall off with a time constant of about 2.7 sec, as in Oboe, Sec. 9-2, determined by

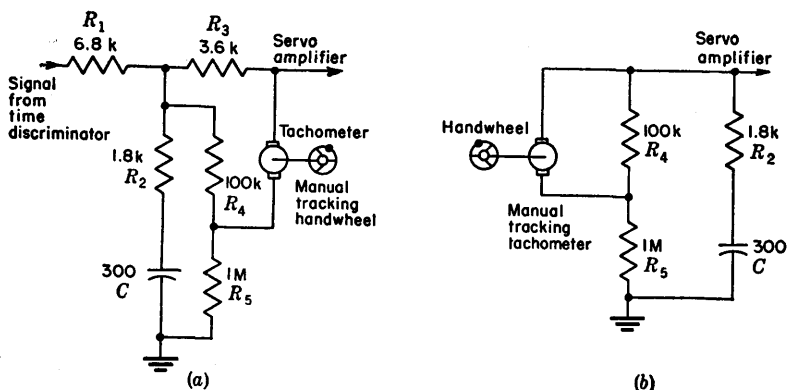


FIG. 9-19.—Equalizing network and manual-control input circuits of range-tracking system, (a) automatic connection with displacement adding, (b) aided tracking connection.

$R_1$  and  $R_2$  and the output resistance of the cathode follower  $V_1$ . Thus reasonable fades are satisfactorily handled since the response speed of the AGC circuit is about  $\frac{1}{800}$  sec. The aided-tracking time constant is  $\frac{1}{2}$  sec, with 100 yd/rev displacement of the handwheel.

It will be noted in Fig. 9-18 that, following the main equalizing network and the tachometer-feedback mixing network, there is a smoothing network consisting of  $R_6$ ,  $R_7$ , and  $C_2$  before the 60-cps switch modulator (Brown Converter). The servoamplifier is a standard small servoamplifier shown in Fig. 9-20. The servomechanism motor is a Diehl FPE-492a two-phase induction motor, and the tachometers are Elinco Type B-44. The motor ratio is 100 yd/rev.

The range-rate followup servomechanism is similar to the range servomechanism except that it is a position, rather than a rate servomechanism.

**Dynamic-tracking Performance.**—One of the most useful aids to the design of automatic-tracking mechanisms of any kind is a dynamic-track-





ing tester which will provide a dummy signal whose range and amplitude variations will simulate those of a real target and which will record directly the difference between the dummy signal range and the range indicated by the automatic range-tracking device. Such a device was

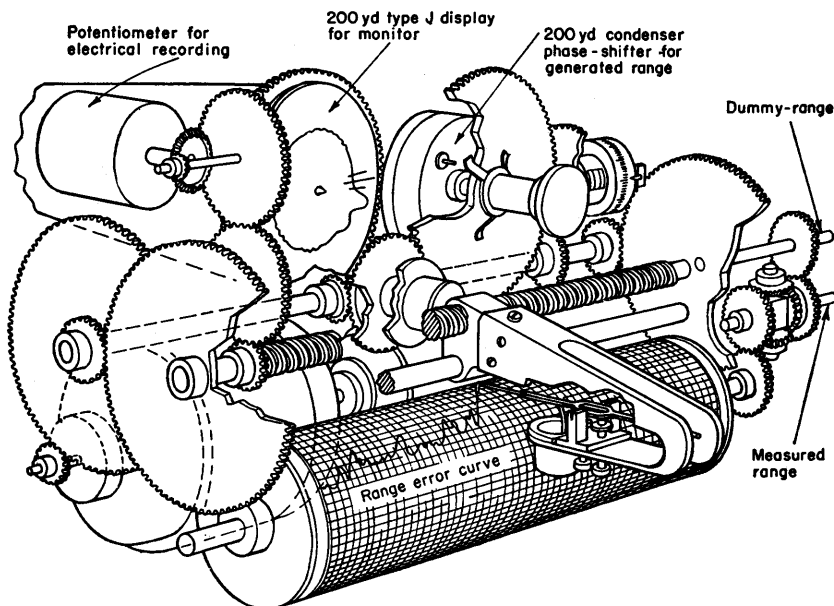


Fig. 9-21.—Dynamic range-tracking tester.

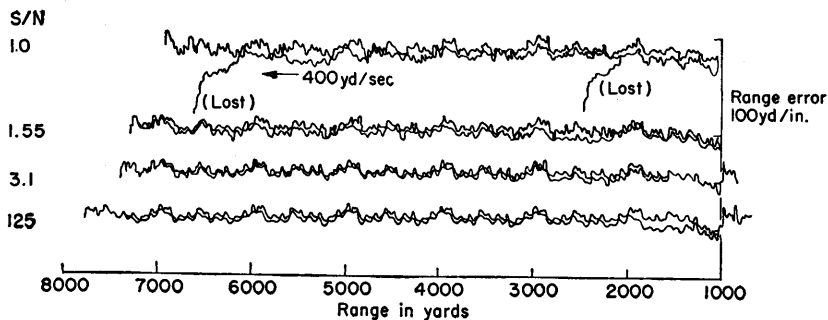


Fig. 9-22.—Velocity errors of range unit on automatic tracking as a function of signal-to-noise ratio  $S/N$ . Video output = 1 volt. Rates = 400 yd/sec out, 200 yd/sec in.

built and is shown in Fig. 9-21. It supplies a time-modulated trigger whose range is related to by the shaft output of a rate servomechanism to within  $\pm 1$  yard. The output shaft drives one input of a differential, whose output shaft is in turn connected to a long cylindrical drum.

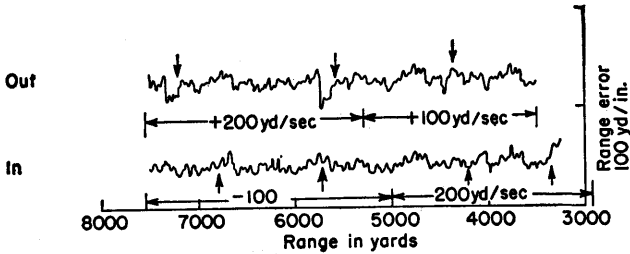


FIG. 9-23.—Short-time velocity memory in automatic tracking of the range system. Effect of fading: signal off sec. AGC level = 1.0 volt.

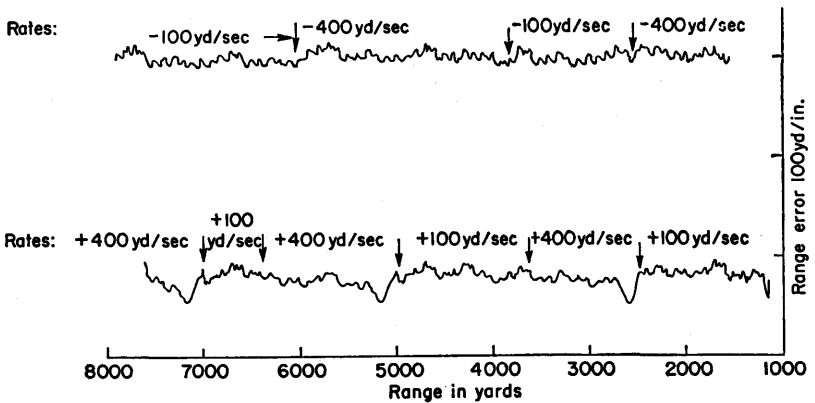


FIG. 9-24.—Response in automatic tracking to velocity step functions. Signal-to-noise ratio = 200. Video level = 1 volt.

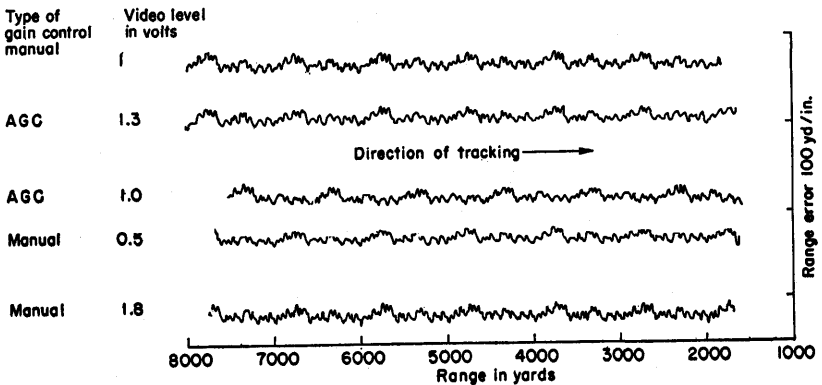


FIG. 9-25.—Automatic tracking performance with varying video level. Signal-to-noise ratio = 25. All curves at rates between -180 and -400 yd/sec.

When the output shaft of the range-tracking unit is connected to the second input of the differential, the rotation of the drum indicates range error. If a pen is made to move along the length of the drum proportionally to range, the resulting trace is a plot of range error vs. range.

Accelerations:

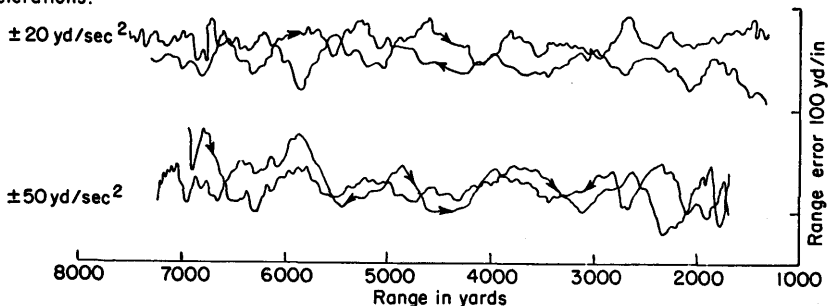


FIG. 9-26.—Aided tracking on accelerating targets with range-tracking controls.

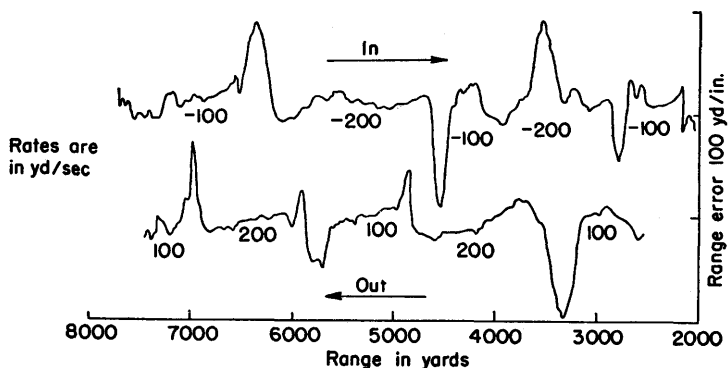


FIG. 9-27.—Response of aided tracker to step functions of velocity.

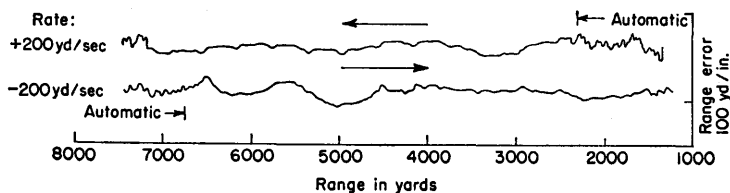


FIG. 9-28.—Aided tracking of a constant-velocity target.

The range rate of the time-modulated trigger is variable from +1200 mph to -1200 mph. Complete reversal of any rate could be made in about  $\frac{1}{8}$  sec. The output trigger is used to fire a pulse generator which gates an i-f oscillator. The oscillator output is amplitude-modulated to simulate antenna scanning and is fed into a receiver i-f strip. Figures

9-22 to 9-29 show the results of testing the above range-tracking system with the dynamic tester. Figure 9-22 shows the velocity errors as a function of signal-to-noise ratio and indicates the period (1000 yd) and the amplitude ( $\pm 5$  yd) of the periodic range errors; no cumulative range error

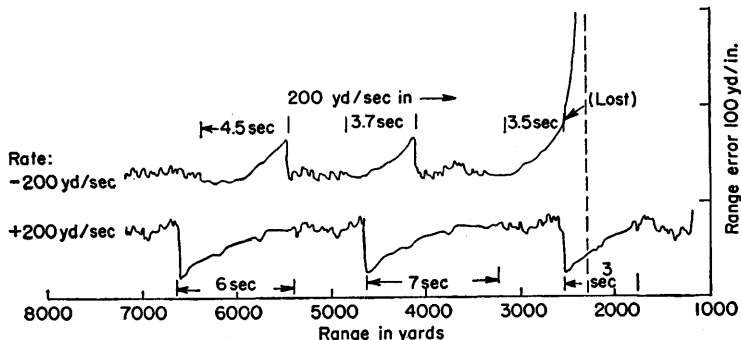


FIG. 9-29.—Coast performance.

is observed. The velocity error is indicated by the separation between traces taken at different speeds for a given signal level. The largest separation seems to be about 10 yd for the indicated speeds with signal-to-noise ratio equal to 1. At this level, the target was lost several times at 400 yd/sec. Since the velocity error prior to losing the target is

much smaller than the range aperture of 70 yd, it is probable that inadequate smoothing of the servomechanism response was responsible for the failure to keep the target. The remainder of the plots show the response to transients under automatic and aided-tracking operation, the effect on automatic tracking of varying the video-signal amplitude, and the effectiveness of the memory and coast provisions. Figure 9-27 indicates that fades of 1 sec can be tolerated without switching to

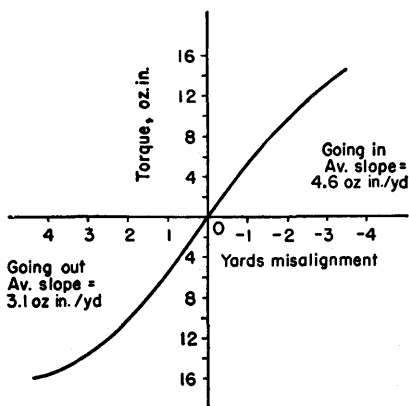


FIG. 9-30.—Mechanical stiffness curve of range-tracking loop.

coast. Under coast conditions the allowable time of fades or interruptions is shown in Fig. 9-29 to vary 3 to 7 sec. The upper curve of Fig. 9-29 indicates that the range of the gates can depart from the range of the target by about 25 yd before the target will be lost on returning to the automatic-tracking mode of operation.

In Fig. 9-30 is shown the static stiffness of the range-tracking loop.

## POSITION ERROR DETECTORS AND INDICATORS

By J. V. HOLDAM

**9-4. General Considerations.**—There are two methods of measuring the angular position of a target with a single radar system in which the dependence of intensity of the received echo on alignment with the beam axis is utilized. One method utilizes continuous circular scan in which a PPI indication is employed. The other employs either conical scanning or lobe-switching with the antenna array pointed continuously at the target. The first method measures the center of the signal on the persistent indicator by means of observing the rate of decrease of signal intensity on either side of center; on fixed targets it provides accuracies of

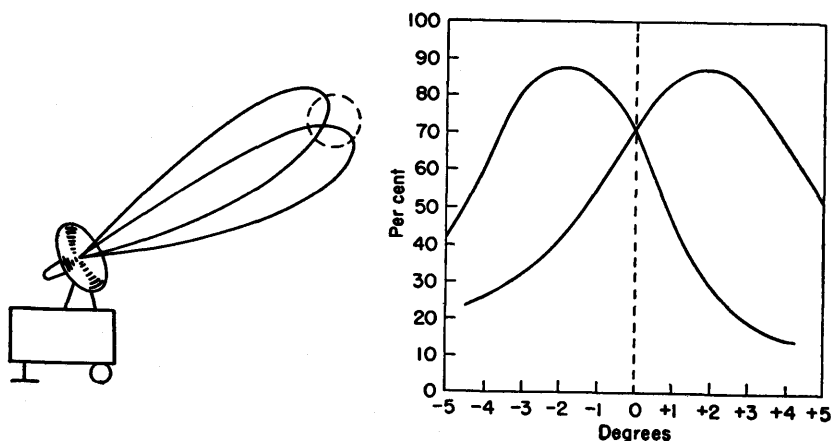


FIG. 9-31.—Conical scanning antenna pattern, SCR-584.

$\frac{1}{20}$  of the beam width. (See discussion of the Precision Ranging Indicator, Chap. 7.) The second method compares continuously the intensity of signal received from two similar positions on opposite sides of the beam where the power is decreasing rapidly with angle. Measurements of similar accuracy have been found with this method. The basic difference between the two systems is that the second provides continuous data with which rapidly moving targets may be followed, whereas the first provides data interrupted at a period equal to the scan period of the antenna, and hence less suitable for moving targets. On the other hand, the first method has the advantage of providing data on many targets at once.

Conical scanning radar systems have thus been used extensively for angular position measurements on moving targets. One of the important techniques used in these systems is the method of obtaining an

error signal that indicates the angular error. The following two sections will describe this technique. The symbol  $\phi$  will be used to represent azimuth angle and  $\theta$  for elevation angle.

A widely used radar employing conical scanning is the SCR-584. Figure 9-31 shows its antenna pattern.

The SCR-584 employs a single-antenna beam, but it is displaced from and rotated about the axis of the parabolic reflector. When the target is off the axis of the reflector, the target echo is modulated at the frequency of rotation of the beam about the axis of the parabola. By a comparison of the phase of the signal modulation with the geometric phase of the antenna beam, the direction of the target from the paraboloid axis is determined, and the amplitude of the signal modulation is a measure of how far the target is off the axis of the parabola. Only if the target lies within a small cone centered on the axis of the reflector is the modulation of the target echo too small to be detected. If the antenna assembly is moved to make the modulation zero, an accurate determination of  $\phi$  and  $\theta$  is made. The beamwidth of the SCR-584 is approximately  $5^\circ$ , but  $\phi$  and  $\theta$  are determined to better than  $\frac{1}{16}^\circ$ .

The type of indication used with precision angle detectors varies with the type of application. The SCR-584 precision angle detector has a closed-loop servomechanism which operates to maintain the parabola axis in coincidence with the target. In other applications the precision angle detector may control a zero-centered meter (British 274) or a type G presentation (AN/APG-15), and the operator becomes a biomechanical link in the servomechanism loop that positions the parabola axis on the target.

**9-5. Design Requirements.**—The design of circuits for the precise determination of  $\phi$  and  $\theta$  is not particularly critical provided the rest of the system is properly designed since the measurement employs the null method of comparing two signals and making them equal. Most systems perform lobe-switching at rates from 30 to 100 cps. It is important that the phase shift be carefully controlled, that overloading be prevented by good AGC action, and that the commutator, or phase discriminator, minimize crosstalk between  $\phi$  and  $\theta$  and be insensitive to harmonics of the switching frequency. Further, the antenna must be designed to minimize harmonics, to minimize false modulation by "pulling" the transmitter as a function of switching phase, and to maintain a fixed relation between the radar axis and some mechanical reference line.

The considerations listed above are in addition to problems confronted in any radar-system design. They are valid only for systems which purport to make precision measurements of  $\phi$  and/or  $\theta$ . They arise from the necessity of making a critical examination of each echo. For

search systems it is sufficient to get an echo—whether it is distorted or whether it overloads the receiver makes little difference.

Most systems that perform lobe-switching by a conical scan (SCR-584, AN/APG-1), offset the lobe from the axis of scan so that the crossover point is approximately 80 per cent power, one way. For antennas whose illumination of the reflector is uniform or varies as  $1/r$  ( $r$  is radial distance on the surface of the reflector measured from the vertex), this crossover provides a compromise between optimum modulation sensitivity and beam broadening. In lobe-switching systems the rate of change of power with angle of the antenna is the limiting factor in the accurate determination of  $\phi$  and  $\theta$ . It is not possible to compensate for small slope at crossover by increased amplification of the modulation since spurious or unwanted modulation is also amplified. Most radar systems employ close coupling between the transmitter and the transmission line,

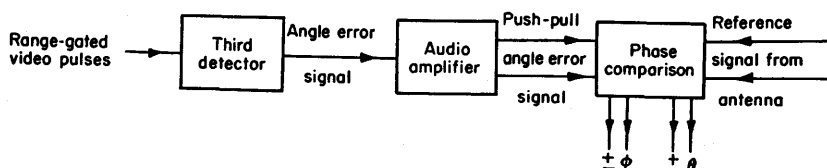


FIG. 9-32.—Block diagram of generalized angle-measuring circuit.

and hence the antenna; therefore it is important that the VSWR in the line be unaffected by the process of lobe-switching.<sup>1</sup>

Figure 9-32 is a block diagram of a generalized angle-measuring circuit. It includes all the components that are discussed and illustrated in detail in the sections that follow.

The requirement on the receiver is that signal modulation must not be distorted. This requirement principally affects the AGC loop design, since it requires that the phase shift due to AGC action to be zero at the modulation frequency. Two essentially different methods have been developed for applying AGC to the receiver. The older method, employed in the SCR-584 and AN/APG-1, AGC voltage is generated from the range-gated video signals and applies this voltage to the receiver after it is operated on by a low-pass filter. Since the filter is designed to eliminate the modulation and higher frequencies, the AGC voltage does not degenerate the desired modulation. A newer and somewhat better way<sup>2</sup> uses a fast-acting AGC that completely degenerates the

<sup>1</sup> Variations in VSWR cause the transmitter to change frequency and power output. If the VSWR varies with switching phase, the net effect is a false modulation on an echo of a target lying on the radar axis. See L. J. Laslett, "Calculation of Conical-scanning Errors," RL Group Report 94-3/43.

<sup>2</sup> See Vol. 23 for a detailed discussion of this circuit.



modulation in the receiver for modulation frequencies up to 300 cps. The modulation for the commutator is taken from the AGC voltage through a bandpass filter. The advantage of the latter method is greater protection of the receiver against overloading from spurious modulations.

Both the AGC voltage and the envelope voltage (demodulated video pulses) are derived in the range unit, or the range gate is cabled to a separate unit where the AGC and error voltages are derived. Systems which measure  $\phi$  and  $\theta$  precisely usually also make a precision measurement of range; hence a narrow range gate is available for the selection of the radar echo of the particular target whose coordinates ( $\phi$ ,  $\theta$ ) are to be measured. It is important that the electronic operations performed on the signal for the determination of range should not distort the signal or the modulation. This is best assured by using a triple-gated video (the early and late gates are used for range tracking and the middle gate for AGC and audio (AN/APG-1), the overlapping gates of AI Mk VI, or a single gate and manual range tracking (SCR-584).

The problem of "detecting" the gated video pulses is difficult.<sup>1</sup> Since all the available information is contained in pulses of very short duration separated by intervals of long duration, the third detector must be designed to make maximum use of the signal while it is available. The most efficient detectors developed for this purpose are the bidirectional detectors.<sup>2</sup> Such circuits have the unusual and desirable characteristic of instantly assuming the average voltage value of each gated signal while it is present, and maintaining it when the signal is not present.

The principal requirements on the audio amplifier following the third detector are constant gain and fixed phase shift. These requirements do not call for special techniques; the only complicating factors are (1) the necessity of filtering the envelope voltage and (2) the change in modulation frequency with speed of the lobe-switching motor. Unless the frequency of lobe-switching is maintained constant, the audio filter must be designed for constant attenuation and phase shift over the range of modulation frequency expected.

The commutator, or phase-discrimination circuit, sorts the audio into  $+\Delta\phi$  and  $-\Delta\phi$  and  $+\Delta\theta$  and  $-\Delta\theta$  components. The requirements on the commutator are linearity at least for small values of audio signal and isolation of  $\phi$  and  $\theta$  components of the audio signal so that the two tracking axes will not interact. The commutation should be full-wave and symmetrical to remove the fundamental frequency from the output and

<sup>1</sup> The circuit which detects video signals to obtain AGC or audio is called the "third" detector.

<sup>2</sup> See Vol. 19, Chap. 14, of this series.

to give minimum response to the large second-harmonic component invariably introduced by dissymmetries in the antenna scanning.

Since the output of the commutator is direct current (superimposed on a strong but useless second-harmonic component), it must be connected to d-c amplifiers if the output is not of the proper voltage or power level for the particular application. Since direct-coupled amplifiers are avoided wherever possible, commutators usually operate at a high level. This has a serious disadvantage (but not so serious as following the commutator with direct-coupled amplifiers) in that it is difficult to operate at high audio levels and maintain a high input impedance at the commutator. Grid current in commutator tubes, whether during an "on" period or an "off" period, tends to react on the final audio driver to cause crosstalk between the  $\phi$  and  $\theta$  axes.

**9-6. Manual Tracking Systems.**—In this section a few systems which provide precise angle measurement on a special indicator are discussed. All the systems discussed are null systems, that is, the antenna-pointing is corrected manually by observing a null indicator. In each system discussed the indicator is a cathode-ray oscilloscope, but some other systems have employed zero-centered meters.

**AN/APG-15.**—Figure 9-33 is a condensed schema of the angle-measuring circuits used in the AN/APG-15 system. This system is a lightweight airborne fire-control system which permits blind fire against enemy aircraft. It employs automatic-ranging equipment described in Sec. 9-1, and presents relative target bearing on a small cathode-ray tube to enable the gunner to position his guns properly.

The envelope of the video representing amplitude modulation is amplified and filtered, and paraphased in  $V_1$  and  $V_2$ . The filter between  $V_1$  and  $V_2$  made up of  $R_5$ ,  $R_6$ ,  $R_7$ ,  $R_8$ ,  $C_3$  and  $C_4$  is broadly tuned to peak at about 30 cps and thus gives good attenuation of the second harmonic at 70 cps. The modulation voltages at the plate and cathode of  $V_2$  are equal in magnitude and differ in phase by 180 electrical degrees. Tubes  $V_3$  and  $V_4$  are full-wave phase-comparison and amplifier tubes for  $\theta$  determination. (The  $\phi$  circuits are not shown but are similar.) The phase comparison takes place by virtue of conduction through  $V_3$  and  $V_4$  when the grid and cathode modulations are in phase. The circuit is essentially a phase-detector: the individual tubes are allowed to conduct only when the resulting differential plate voltage on the two tubes conducting simultaneously is proportional to the  $\theta$  or  $\phi$  component of the pointing error. (This limitation is by virtue of the switch in the cathode circuit mechanically operated by the antenna conical-scan motor.) Network  $R_1C_1$  filters the commutated output and  $V_5$  amplifies it to a level suitable for presentation on a cathode-ray tube. Resistor  $R_2$  serves as a centering control.



In the AN/APG-15 system the conical-scan rate is 36 cps. The AGC filter is designed to have a charge time of  $\frac{1}{10}$  sec and a discharge time of  $\frac{1}{4}$  sec; this enables the AGC to hold the average modulation below saturation in the receiver and not to degenerate the modulation.

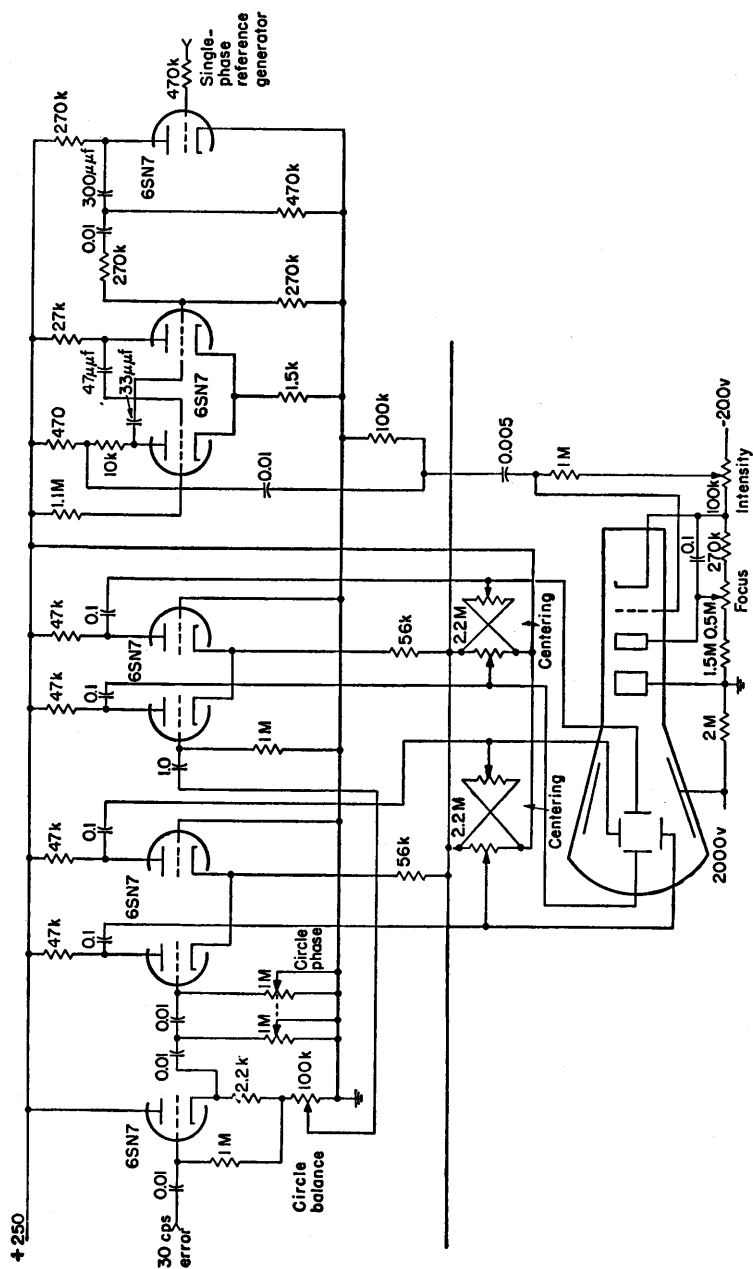
*AGL(-T).*—The British counterpart of the AN/APG-15 employs a phase-comparison circuit as shown in Fig. 9-34. The detected modulation is amplified to a high level, commutated by a mechanical switch driven by the antenna conical-scan motor, and directly connected to the cathode-ray tube. The differential voltage is filtered by  $R_1C_1$ , and  $R_2$  governs the maximum charging rate of  $C_1$ . Resistance  $R_4$  acts as a sensitivity adjustment. The result, in the axis illustrated by Fig. 9-34, is a vertical displacement proportional to the amplitude of the video modulation in phase with the vertical component of the antenna motion.

*SCR-615.*—This is a long-range ground-search system with special circuits for making precise angle measurements. Range tracking is manual, conical scanning is employed only while precise angle measurements are being made, the beamwidth is  $4^\circ$ , and the conical scan rate is 24 cps. Figure 9-35 is a schema of the angle-tracking and AGC circuits. (These exact circuits were not in production before manufacture was stopped by the end of the war.)

The phase-comparing circuit is similar to the one in the AN/APG-15 equipment, but the cathodes are gated by a square-wave generator rather than by a mechanical commutator. The reference voltage comes from a two-phase generator driven synchronously with the antenna. A single video gate is used and it is made to coincide in range with the desired signal by the range-tracking operator. The third detector is of the type mentioned in Sec. 9-5. Positive video signals and a positive range gate are applied to  $V_1$ ; the gated video signal is applied to the grid of the top half of  $V_2$ . Since the lower half is biased beyond cutoff, the 200- $\mu\text{f}$  condenser  $C_1$  charges up to the full value of the signal, and since there is no path for discharge,  $C_1$  maintains the full charge. Immediately preceding the next video signal the "dunking" gate overcomes the bias in the lower half of  $V_2$  and discharges  $C_1$ . The next video signal then charges  $C_1$  to its full value, etc. The net result of this sequence of operation is that  $C_1$  assumes the voltage of each gated video signal in turn.

The function of  $V_3$  is to generate an AGC pulse that will prevent the signal in the range gate from overloading the receiver. The input gate is of constant amplitude and  $V_3$  varies the output-gate amplitude as an inverse function of the potential from the detector. The advantage of gated AGC is that only the signal under examination is operated on. Other signals have the advantage of full receiver gain.





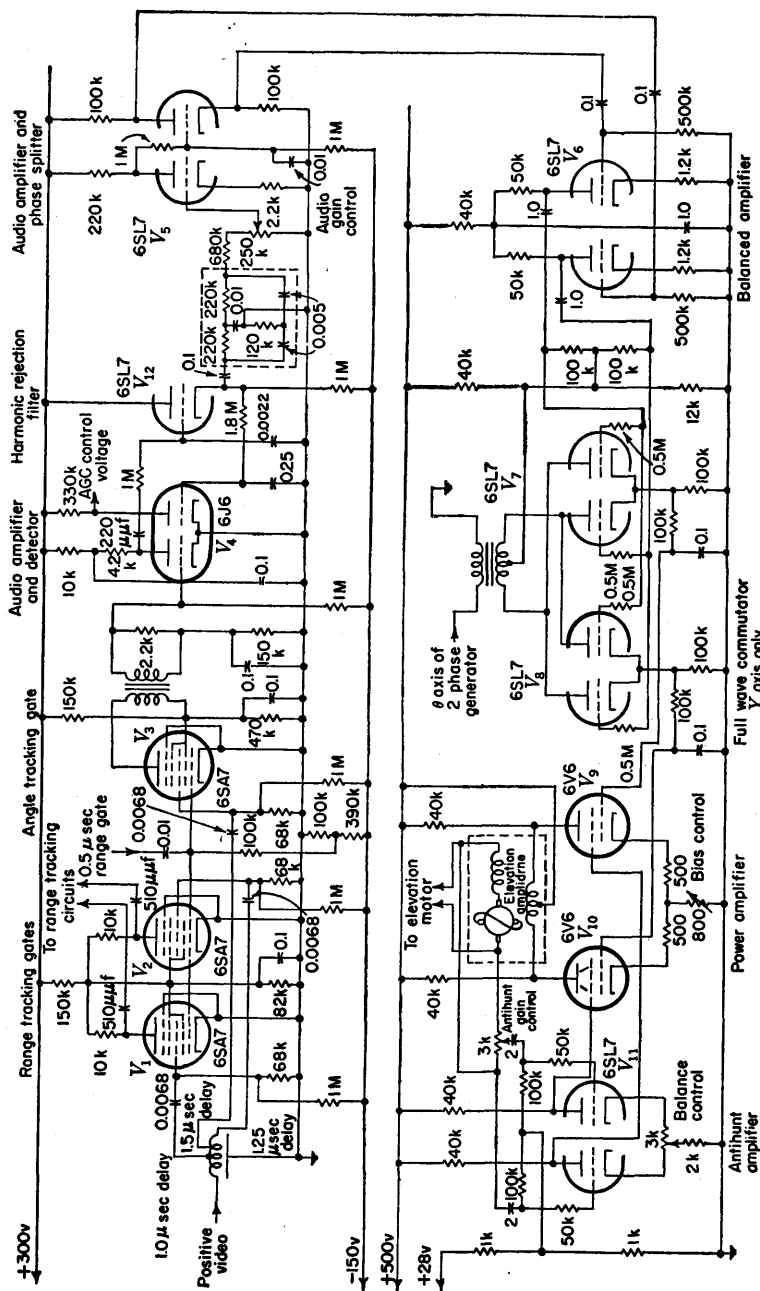
*Phase Comparison on a Circular-trace Cathode-ray Tube.*—This method of phase comparison differs from that of the others in that a cathode-ray tube is used. The conical-scan frequency is 30 cps and is accurately maintained constant by an electronic governor (see Fig. 9-36). The signal being range-tracked is detected and the envelope filtered by a sharp resonant filter (30 cps). It is then divided into four components of equal magnitude and separated in phase by 90 electrical degrees. These quadrature voltages are applied to the four deflection plates of the indicator to make the cathode-ray-tube beam prescribe a circle on the face; the radius of the circle is proportional to the amount of the error, and the phase of the circular sweep (with respect to the phase of the conical scan) is related to the angle between the scan axis and the target. A reference generator on the antenna furnishes a reference voltage which is used to intensify the indicator for a small fraction of the conical scan and which maintains constant phase with the mechanical rotation. Since the error modulation can have all possible phase relations with the reference voltage, the beam intensification can occur at all possible positions of the circular sweep. The net result is a coherent relation between the intensified portion of the circular sweep and the relative target bearing.

The various parts of the circuits in Fig. 9-36 are functionally labeled to facilitate understanding the operation. The advantage of a combined commutator-indicator of this type is the absence of errors due to the drift of d-c amplifiers.

**9-7. Automatic Tracking Systems.**—As with manual tracking systems a few examples of automatic tracking systems are illustrated to point out the variations in design. The differences between manual and automatic operation are obvious; automatic systems are used where the additional weight, size, and power consumption can be tolerated and where the increased accuracy is essential; angle information in automatic systems is used in a servomechanism to correct the position of the scan axis, whereas angle information in manual systems is displayed on a cathode-ray tube.

Figure 9-37 is a schema of the angle-tracking circuits in the AN/APG-1 airborne fire-control system.

Positive video pulses are connected to a delay line which has three output taps and gives video signals delayed by 1, 1.25, and 1.5  $\mu$ sec respectively. The 1- and 1.5- $\mu$ sec delayed video signals are gated in  $V_1$  and  $V_2$  by a single gate, and the outputs of  $V_1$  and  $V_2$  are in the automatic range-tracking circuit. The 1.25- $\mu$ sec delayed video pulse is gated (again by the same gate) in  $V_3$  and supplies the angle error and AGC channels through the common detector  $V_4$ . Network  $R_1$  and  $C_1$  filter the AGC voltage to prevent degeneration of the error signal. The control voltage for the AGC circuits is used to vary the gain of the i-f stages in the pre-

FIG. 9-37.—Angle-tracking circuits in AN/APG-1,  $\theta$  axis only.



amplifier and to control the amplitude of the screen-sensitizing pulse going to the receiver. This latter control is similar to the one used in the SCR-615.

The phase-advance network  $F_1$  assists in stabilizing the servomechanism and is followed by network  $R_2, R_3, C_3$  which filters the output.

Tube  $V_6$  amplifies and paraphases the angle-error signal, and  $V_6$  provides balanced amplification for the two phases. Tubes  $V_7$  and  $V_8$  are full-wave commutators, the  $\pm\Delta\theta$  voltages being generated at their cathodes. The commutator is similar to those previously discussed except for the fact that the reference voltage is injected into the plate circuit and the commutated output is taken from the cathodes. The low-impedance commutated d-c error signal is power-amplified in  $V_9$  and  $V_{10}$  in an amplidyne to control the speed and direction of rotation of the elevation drive motor. Tube  $V_{11}$  is an antihunt amplifier whose connection in the circuit stabilizes the elevation servomechanism.

### TRACKING ON GROUPED OR PERIODICALLY INTERRUPTED DATA

BY W. B. JONES AND R. I. HULSIZER

**9-8. Introduction.**—In the automatic time- and direction-measuring systems that have been discussed, the radar is engaged constantly in obtaining data about a single target. Nevertheless, as discussed in Chap. 7, measurements can be made on a single target while the radar is scanning through  $360^\circ$ . This fact suggests that even while scanning, a radar set might well obtain sufficient information about a particular target to track the target automatically with accuracy. The possibility of this economy in the use of a radar set gave rise to the study of automatic measuring systems using grouped data.

Most search radars scan at a constant rate in azimuth. The radar obtains data on a particular target during the small fraction of the scan that the radar beam is directed toward the target, that is, the data are said to be "grouped." The groups of data are spaced uniformly in time, if the azimuth acceleration (measured by the observer) of the target is small. Consideration has been given to the problem of obtaining data from targets throughout the hemisphere above a ground station or ahead of an airplane. All of the proposed hemispherical scanners interrupt the pulses from a single target for such long periods that tracking is not possible if the target is in motion at all. If a more simple solution were to become available the methods outlined in this section could be extended to three dimensions.

The PPI is an appropriate indicator with an azimuth scan radar. It is of importance that the oscilloscope screen have a long-persistence time constant, for in this way the indicator "remembers" the information derived from the data. The PPI remembers the position of a target

during the time between receptions of groups of data. The ideal measuring system for tracking radar-observed targets (moving with respect to the observer) gives a continuous indication of the displacement of the target. To accomplish this with small error, an automatic tracking system operating from grouped data must be capable of learning and using one or more of the time derivatives of the displacement as well as the displacement in order to anticipate the motion of the target during the periods when no data are being received. The part of the automatic tracking system that measures the time derivatives and predicts the displacement of the target is the function unit. The number of derivatives that the function unit is designed to use is determined by the accuracy desired of the tracking system, the quality of the data, and the accuracy of the measuring reference. In the automatic tracking systems (using grouped data) which have been developed, it has been found useful to measure and use only the first time derivative of the displacement (or velocity) and the displacement of the target. The radar data contain such large errors that employment of any higher derivatives than the first does not improve the operation of a tracking system. The automatic measuring systems to be discussed are, therefore, automatic tracking systems with velocity memory.

There are several applications for automatic tracking systems operating from grouped data. Since the radar set is scanning while collecting data for such a tracking system, it follows that one radar can be used to supply data to many tracking systems and many targets can be tracked automatically and simultaneously. One application of this technique is in airport traffic control where many aircraft flying independently of each other must be tracked. A second is that of tracking the ships in a task force or a convoy where it is of importance to know the relative positions of ships. In these cases, the targets are all of equal interest, and usually no very precise information about any one target is required. A third application is that in which one target in a region is of paramount interest, and precise information is required about this target whereas only rough information is required about other targets in the region. A specific example of this application is the case in which it is desirable to use a search radar for scanning a region and at the same time to use an automatic tracking system operating from the radar data to give precise enough information about a particular target for accurate navigation control. This application may be in conjunction with either a two- or three-dimensional scanning radar. A fourth application is that in which it is desirable to have accurate information about two targets whereas only rough information is needed about other targets in the region scanned. An example of this application is the use of an airborne search radar to obtain data for tracking two responder beacons and thus

accurately determine the location of the airplane. The beacons can be tracked automatically as two targets might be tracked and from the tracking data a continuous indication of the location of the airplane is made available to the navigator.

**9-9. Automatic Time Measurement on Grouped Data.**—The circuits and methods used in automatic timing devices operating on grouped data are very similar to those in automatic timing circuits operating on uniformly spaced data except for certain special restrictions. The special operation of the function unit is to provide continuous position and velocity data in spite of interruptions in the incoming signal. Hence it is often called the “memory device.” If it is assumed that velocity memory is provided by the function unit, there are four constants that must be determined as a function of the length of the data period  $T'$  and the time between data periods  $T$ .

1. Position learning time: If there exists an error in range at the beginning of a particular data period,  $T'_n$  for example, maximum accuracy demands that this error be reduced to zero at least before the end of  $T'_n$ .
2. Position memory: In velocity-memory systems this factor is not always obvious, but as pointed out in the description of the Oboe range-tracking system in Sec. 9-3, it is not only necessary to ensure that the velocity voltage remains constant for velocity memory, but also that the range rate produced by constant velocity voltage remains constant. The integration operation performed on the velocity voltage to produce range voltage must be accurate at least for intervals of time as long as  $T$ .
3. Velocity learning time: If the data are interrupted, there are obviously two methods of obtaining velocity data. The first is to measure rate by the change of range during a data period; the second is to measure rate by the change of range between data periods. The first method is impractical in conventional radar systems because the data periods are so short that the target does not move by an amount comparable to the dynamic range error during the data period. The second method remains if a function unit has velocity memory. Velocity learning implies measuring the difference between the true range and the range which is predicted by the function unit by virtue of its velocity memory and correcting the indicated velocity by an amount proportional to this error. Aided tracking manual with the right time constant is the analogue of this process.
4. Velocity memory: The restriction on velocity memory is that its duration be adequate for time intervals equal to the length of the dataless periods.

The purpose of this section is to examine analytically the dependence of these four constants on the lengths of  $T$  and  $T'$ . A summary of the equations applicable to continuous tracking shows that for a double-integration system providing velocity memory the following equations from Secs. 8-4 and 8-6 define the operations of the time modulation, time discrimination, and double integration:

$$R' = k_1 V \quad (8.3)$$

$$\dot{\epsilon} = k_2(R - R') = k_2 \epsilon \quad (8.2)$$

$$V = \frac{1}{C} \int_0^t i \, dx + \frac{1}{CS} \int_0^t \left[ \int_0^s i \, dx + \text{const.} \right] ds + \text{const.} \quad (8.11)$$

If these three equations are combined and  $k_2$  is assumed to be constant, the result is the equation of motion for the closed tracking loop, in a form, expressing the dependence in different terms than that previously used,

$$p^2 \epsilon + \frac{k_1 k_2 p \epsilon}{C} + \frac{k_1 k_2 \epsilon}{CS} = p^2 R \quad (1)$$

whose solution is

$$\epsilon = a e^{\gamma_1 t} + b e^{\gamma_2 t} + f(p^2 R) \quad (2)$$

where

$$\gamma_1, \gamma_2 = -\frac{k_1 k_2}{2C} \pm \sqrt{\frac{k_1^2 k_2^2}{4C^2} - \frac{k_1 k_2}{CS}} \quad (3)$$

and

$$f(p^2 R) = \frac{1}{\gamma_2 - \gamma_1} \left[ e^{\gamma_2 t} \int_0^t p^2 R(x) e^{-\gamma_2 x} dx - e^{\gamma_1 t} \int_0^t p^2 R(x) e^{-\gamma_1 x} dx \right]. \quad (4)$$

Equation (2) holds when it is assumed that data are continuously available. Now, it is necessary to consider the action of this loop when the data are grouped. Let  $T'$  be the time during which data on  $R$  are available and  $T$  the time between beginnings of the periods measured by  $T'$ , and in all cases of interest here,  $T$  is much greater (20 times or so) than  $T'$ . All analyses will be made assuming that  $T'$  and  $T$  are constant. During the periods measured by  $T'$ , Eq. (1) holds. On the other hand, during the periods measured by  $T - T'$ , no data on  $R$  are received a statement that can be represented by making  $k_2 = 0$  in Eq. (8-2). Thus, for the periods measured by  $T - T'$ ,

$$p^2 R' = 0. \quad (5)$$

Solving this equation:

$$R' = Mt + P \quad (6)$$

where  $M$  and  $P$  are determined by the initial conditions. From Eq. (6), it is evident that  $R'$  changes at a constant rate during the dataless periods,  $M$  is the initial rate of  $R'$ , and  $P$  is the initial value of  $R'$ . This

constant rate of  $R'$  during dataless periods is characteristic of a loop with velocity memory.

The solution of the equation for this tracking loop has been broken into two parts,  $T'$  and  $T - T'$ , for each period  $T$ ; as a result, there are four arbitrary constants in the solution. It would be more desirable to have a single solution which holds for a period  $T$ . Since the periods measured by  $T'$  and  $T$  start coincidentally, a solution for the period  $T$  could be obtained by first letting the initial conditions determine the constants  $a$  and  $b$ . Equation (2) then gives the value of the error if the function  $f(p^2R)$  is known during the period  $T'$ . Thus at the end of the

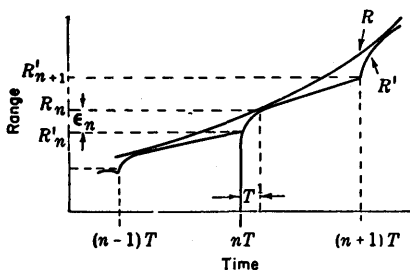


FIG. 9-38.—Time relations of grouped data systems.

period  $T'$ , all the necessary quantities are known for determining  $M$  and  $P$ . This method gives an exact solution for the problem for a period  $T$ . In this way each period  $T$  can be treated separately. A still more useful solution would be one that gives the value of  $R'$  at any time provided the function  $f(p^2R)$  and initial conditions are known. Finding this exact solution would be very laborious by

the method just described. By making some specializing assumptions, however, one can obtain a useful approximate solution.

Since a number of periods  $T$  are to be considered together, it is convenient to number these periods consecutively starting with the period when the boundary conditions are known. Subscripts will then associate quantities with particular periods  $T$  as in Fig. 9-38. Thus  $M_n$  and  $P_n$  are the rate and position of  $R'$  after a time  $T'$  in the  $n$ th period  $T$ . Since  $T'$  is a short time any change in the value of  $R$  during a time  $T'$  is masked by the errors in the data, only the average value of  $R$  during a period  $T'$  is of interest. Let  $R_n$  be the average value of  $R$  during the period  $T'$  of the  $n$ th period  $T$ . Let  $R'_n$  be the value of  $R'$  just before the  $n$ th period  $T$ . Let  $\epsilon_n = R_n - R'_n$ , where  $\epsilon_n$  is treated as the error at the beginning of the data period.

A matter determined by the grouped nature and accuracy of the data is the construction of the memory device in such a way that it can use the data to learn the velocity of the target. As discussed previously, the periods  $T'$  are so short that the only practical method of measuring range is to divide the change in range, given by two successive groups of data, by the time between those two groups. This process can be expressed by the relation

$$M_n - M_{n-1} = \frac{\eta \epsilon_n}{T'} \quad (7)$$

where  $\eta$  is a constant of the order of magnitude of 1 and expresses the practice of allowing the learned velocity to be influenced in a decreasing manner from earlier data periods.

In order to measure the range of a target accurately, the constants  $1/C$  and  $1/CS$  of Eq. (8-11) must be adjusted so that  $\epsilon$  is reduced to a negligibly small value during the periods  $T'$ . Focusing our attention on the  $n$ th data period, Eqs. (8-2) and (8-11) may be combined and written:

$$R' = \frac{1}{C} \int_{nT}^t k_1 k_2 \epsilon \, dx + \int_{nT}^t \left[ \frac{1}{CS} \int_{nT}^s k_1 k_2 \epsilon \, dx + M_{n-1} \right] ds + R'_n. \quad (8)$$

From this equation

$$\frac{dR'}{dt} = \frac{1}{C} k_1 k_2 \epsilon + \frac{1}{CS} \int_{nT}^t k_1 k_2 \epsilon \, dx + M_{n-1}. \quad (9)$$

Now  $k_2 \neq 0$  only for  $nT < t < nT + T'$ . Thus for  $nT + T' > t > (n+1)T$ ,

$$\frac{dR'}{dt} = \frac{1}{CS} \int_{nT}^{nT+T'} k_1 k_2 \epsilon \, dx + M_{n-1} = M_n. \quad (10)$$

In view of Eqs. (7) and (10), it is evident that

$$\frac{1}{CS} \int_{nT}^{(n+1)T} \int_{nT}^s k_1 k_2 \epsilon \, dx \, ds$$

is of the order of magnitude of  $\epsilon_n$ , and since  $T' \ll T$ ,

$$\frac{1}{CS} \int_{nT}^{nT+T'} \int_{nT}^s k_1 k_2 \epsilon \, dx \, ds \ll \epsilon_n. \quad (11)$$

By the approximation  $R = R_n$  for periods  $T'$ , Eq. (8) becomes

$$R_n - R'_n - \epsilon = \frac{1}{C} \int_{nT}^t k_1 k_2 \epsilon \, dx + \int_{nT}^t \left[ \frac{1}{CS} \int_{nT}^s k_1 k_2 \epsilon \, dx + M_{n-1} \right] ds = \epsilon_n - \epsilon. \quad (12)$$

Assuming now that  $M_{n-1}T' \ll \epsilon_n$  and remembering that  $\epsilon$  is to be reduced to a negligibly small value in the time  $T'$ , it is evident that

$$\frac{1}{C} \int_{nT}^{nT+T'} k_1 k_2 \epsilon \, dx \gg \int_{nT}^t \left[ \frac{1}{CS} \int_{nT}^s k_1 k_2 \epsilon \, dx + M_{n-1} \right] ds. \quad (13)$$

Therefore, it is very nearly true that

$$\epsilon_n = \frac{1}{C} \int_{nT}^{nT+T'} k_1 k_2 \epsilon \, dx. \quad (14)$$

Hence, combining Eqs. (9), (10), and (14):

$$C\epsilon_n = \int_{nT}^{nT+T'} k_1 k_2 \epsilon \, dx = CS(M_n - M_{n-1}) = \frac{\eta \epsilon_n CS}{T}$$

or

$$\frac{1}{S} = \frac{\eta}{T}. \quad (15)$$

Equation (15) gives a relation which must hold between the constants of the memory device in order to have the memory device operate as described by Eq. (7). The other condition which has been assumed to be satisfied by the tracking loop is that  $\epsilon$  is reduced to a negligibly small quantity in a time  $T'$  when data on  $R$  are available. How this condition can be satisfied, is seen from examining Eq. (2). Since it has been found convenient to measure  $t$  from the beginning of the zeroth period  $T$ , Eq. (2) may be written

$$\epsilon = a_n e^{\gamma_1(t-nT)} + b_n e^{\gamma_2(t-nT)} + f(p^2 R) \quad (16)$$

where

$$f(p^2 R) = \frac{1}{\gamma_2 - \gamma_1} \left[ e^{\gamma_1(t-nT)} \int_{nT}^t p^2 R(x) e^{-\gamma_2 x} \, dx - e^{\gamma_2(t-nT)} \int_{nT}^t p^2 R(x) e^{-\gamma_1 x} \, dx \right].$$

It has been assumed that  $R$  is very nearly constant during all periods  $T'$ ; thus  $p^2 R$  is small and  $f(p^2 R)$  is negligibly small. With good approximation, therefore, Eq. (16) can be rewritten

$$\epsilon = a_n e^{\gamma_1(t-nT)} + b_n e^{\gamma_2(t-nT)}. \quad (17)$$

It is evident that

$$\epsilon_n = a_n + b_n. \quad (18)$$

The other initial condition can be obtained from Eq. (12). Assuming that  $M_{n-1}$  is small compared with the initial rate of  $\epsilon$  in the  $n$ th period,

$$-\left. \frac{d\epsilon}{dt} \right|_{t=nT} = \frac{k_1 k_2 \epsilon_n}{C}. \quad (19)$$

Thus, from Eqs. (17) and (19),

$$-\frac{k_1 k_2 \epsilon_n}{C} = \gamma_1 a_n + \gamma_2 b_n, \quad (20)$$

and from Eqs. (18) and (20),

$$a_n = \frac{k_1 k_2 + C \gamma_2}{C(\gamma_2 - \gamma_1)} \epsilon_n$$

and

$$b_n = \frac{k_1 k_2 + C \gamma_1}{C(\gamma_1 - \gamma_2)} \epsilon_n.$$

For  $\epsilon_n$  to become small in a time  $T'$ , either  $\gamma_1$  or  $\gamma_2$  (for example,  $\gamma_1$ ) must have a real part which is negative and much smaller than  $-1/T'$ . Since Eq. (15) must be satisfied and since the real part of  $\gamma_1$  must have an absolute value large compared with  $1/T'$ ,  $\gamma_1$  and  $\gamma_2$  are both real because from Eqs. (15) and (3)

$$\frac{k_1^2 k_2^2}{4C^2} \gg \frac{k_1 k_2}{CS} = \frac{k_2 \eta}{CT} \quad \text{or} \quad \frac{k_1 k_2}{C} \gg \frac{\eta}{T}.$$

Therefore,  $|\gamma_1| \gg |\gamma_2|$  and the following equation is a good approximation:

$$\gamma_1 = \frac{k_1 k_2}{C} \quad \text{and} \quad \gamma_2 = -\frac{\eta}{T}.$$

Using these values for  $\gamma_1$  and  $\gamma_2$ , it follows that  $a_n = \epsilon_n$  and  $b_n = 0$  and therefore,

$$\epsilon = \epsilon_n e^{\frac{k_1 k_2}{C}(t - nT)} \quad (21)$$

for  $nT \leq t \leq nT + T'$ . It is apparent that it is desirable to make  $k_1 k_2 / C$  approximately equal to  $10/T'$  or greater. If  $k_1 k_2 / C$  is sufficiently large,  $P_n \cong R'_n + \epsilon_n$ .

The next step is to consider the difference equation. The desired relationships have been found for a grouped data tracking loop:

$$\left. \begin{aligned} \frac{\eta \epsilon_n}{T} &= M_n - M_{n-1} \\ \epsilon_n &= R_n - R'_n \\ R'_n &= R_{n-1} + M_{n-1} T \\ P_n &= R_n + \epsilon_n \\ \gamma_1 &= \frac{k_1 k_2}{C} \approx \frac{10}{T'} \\ -\frac{1}{\gamma_2} &= S = \frac{1}{\eta} T \end{aligned} \right\} \quad (22)$$

From these equations the difference equation is obtained:

$$\epsilon_{n+1} + (\eta - 1)\epsilon_n = R_{n+1} - 2R_n + R_{n-1}. \quad (23)$$

From this difference equation, one can find the maximum error  $\epsilon_n$  in the  $n$ th period, given the maximum error in any other period. In the case in which  $R$  is changing at a constant rate, Eq. (23) becomes

$$\epsilon_{n+1} + (\eta - 1)\epsilon_n = 0.$$

Solving this equation,

$$\epsilon_n = \epsilon_0 (1 - \eta)^n.$$



In order that the tracking loop may be dynamically stable, it is necessary that  $2 > \eta > 0$ . It is significant to note that if  $\eta = 1$ ,  $\epsilon_n = 0$  for  $n > 0$ . This means that the memory device learns the rate of  $R$  as measured in the zeroth period and since  $dR/dT$  is constant in this special case, there will be no error after the zeroth period. Because of errors in the data, it has been found better practice to make  $\eta < 1$ . With  $\eta < 1$ ,  $M_n$  is a weighted average of rates of  $R$  measured in the  $n$  periods.

Criteria have now been established for determining all the constants of a particular automatic measuring system using grouped data. The action of a radar range-tracking loop is different from the system described in an important respect. It was assumed in the foregoing analysis that in the equation  $i = k_2(R - R') = k_2\epsilon$ ,  $k_2$  is a constant when radar data on a tracked target are being received. In most time discriminators, the output is proportional to the strength of the video pulse as well as to the error  $\epsilon$ . This is a good technique because the higher the signal is above noise the more valuable it is as an indication of the target range, and hence the large video pulses should be given greater weight. The two limits on  $k_2$  from the analysis given are that  $k_1k_2/C > 1/T'$ , and that  $k_1k_2/C$  must be small compared with the PRF in order for the assumption of continuous data during  $T'$  to hold.

Function units for performing the operation described in the Eq. (8-11) used in this section have been described in Sec. 8-6. It should be noted that the time constants of the function unit are exactly defined in grouped-data tracking application, according to Eqs. 22. An item of particular interest here is the importance of the disconnecting devices for rendering  $k_2$  equal exactly to zero during the dataless periods.

**9-10. Example of Automatic Range Tracking on Grouped Data.**—The purpose of  $H_3X$  is to track automatically the ranges of two separate fixed radar beacons from an airplane without interrupting the 3 sec PPI scan of a microwave radar. Thus the data are uniformly grouped.

The schematic diagram of Fig. 9-39 shows one of the tracking loops. Tube  $V_1$  is a trigger amplifier and  $V_2$  a blocking oscillator. The first section  $V_3$  of the time discriminator is gated positive by a gate from the grid winding of  $T_1$ . The second section,  $V_4$ , is gated by the positive overshoot from the plate winding. The video is applied to the grids of  $V_3$  and  $V_4$  and the pulses of current which flow while the gates are on charge the stray capacitances in the plate circuits of  $V_3$  and  $V_4$ . The carrier pulses are removed by the 250  $\mu$ sec. R-C smoothers and the two voltages are amplified differently first in  $V_5$  and  $V_6$  and again in  $V_7$  and  $V_8$ . The difference voltage on the plate of  $V_8$  is coupled capacitively to the neon-tube disconnecter and the bootstrap double integrator  $V_{10}$ . Capacitive coupling is permissible since the error signal appears as a modulated signal at the scanning frequency. The output of the

double integrator controls a phantastron time modulator. In the  $H_3X$  system the angular positions of the radar beacons are nearly constant since they are at a great distance and manual adjustments at infrequent inter-

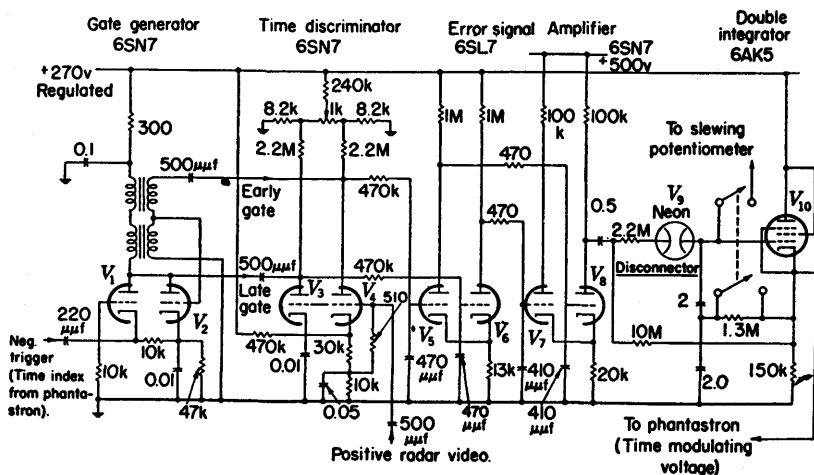


FIG. 9-39.— $H_3X$  tracking loop.

vals suffice for the azimuth tracking. Mechanically operated switches are used to connect the proper tracking loop when the radar is directed toward the radar beacon being tracked.

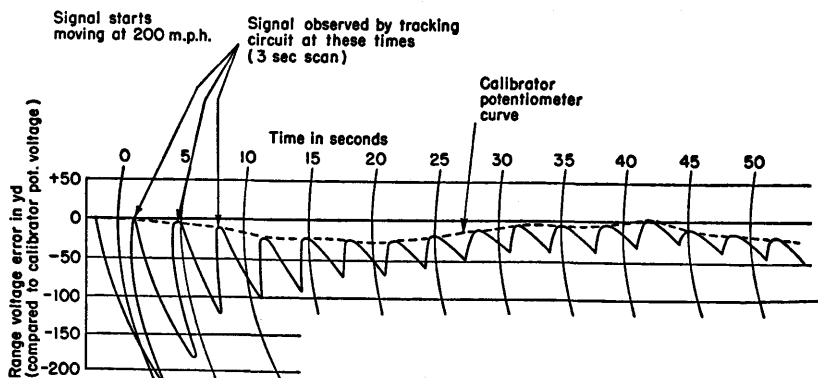


FIG. 9-40.— $H_3X$  tracking data recorded on Esterline-Angus meter.

Figure 9-40 is a graph showing the performance of one tracking loop. For this graph a precision range calibrator Sec. 9.3 was used to supply the video signal. An Esterline-Angus recorder was used to record the error. Thus the graph gives  $\epsilon$  for the tracking loop as a function of time.

To interrupt the data from the calibrator, a mechanically operated switching device was used which switched on the video signal for 0.15 sec ( $T'$ ) every 3 sec ( $T$ ). The automatic loop was started with zero range error and with the range index moving with zero velocity about two seconds before the first data period occurred. The simulated video signal was moving at a rate equivalent to a target with a range rate of 100 yd/sec. It is seen that  $\epsilon$  falls practically to zero for every data period  $T'$ , but the velocity is never correctly learned for the following reasons. For the  $H_3X$  memory circuit,  $\eta = \frac{3}{4}(1.3) = 0.58$ . Since  $\epsilon_1$  in this graph is about 200 yd, it would be expected from the theory that  $\epsilon_2$  would be about 100 yd. In fact it takes three scans for  $\epsilon_n$  to fall to 100 yd and two factors may contribute to this error. One is that the integrator is not perfect; but this explains only a small part of the error because the time constant of the integrator is 125 sec. The major reason is that an oil-impregnated paper condenser was used as the storage condenser in the memory circuit, which because of the dielectric soakage introduced large errors. When its charge is being increased, the condenser appears to discharge in between data periods.

*Mechanical Devices in Measuring Loop.*—Often it is convenient to have a mechanical output from an automatic measuring system. This suggests the use of a mechanically controlled local time modulator with a mechanical memory device. In the cases that have been met in practice, it turns out that  $T'$  is approximately 0.1 sec. As it has been pointed out, the positioning time constant of the tracking loop should be short compared with  $T'$ . It is difficult to make a range-tracking loop containing mechanical devices with a time constant as short as 0.01 sec. Thus, no cases have arisen in which a mechanical memory device would be desirable. Therefore, if a mechanical output from a range-tracking circuit is desired, it is better to have an electric tracking loop and a separate servomechanism device that will follow the electrical range data. An alternative is to treat the range error signals received during the times  $T'$  from the time discriminator as single bits of data recurring at the scanning frequency,  $\frac{1}{T}$ . The mechanical system could then operate on these pulses even as the electrical system operates on pulses at the PRF. Experimental data show that the velocity error can be decreased to 50 per cent within five pulses of the carrier frequency without damaging the loop stability. With  $\eta = 1$ , the electrical tracking loop should be able to remove the velocity error in one period  $T$ , but the  $H_3X$  system tests showed that fluctuations in the data required  $\eta$  to be taken enough smaller that the velocity error was reduced to 50 per cent in three scans. This is not much superior to the performance predicted above for a mechanical tracking system.

**9.11. Automatic Angle-positioning with Grouped Data.**—The photographs of Fig. 9-41 represent the envelope of the video pulses received from a freighter anchored in a calm sea. The bright spots represent a fixed point on the ship as determined optically. The pulses were time selected and demodulated in a two-way switch detector with constant

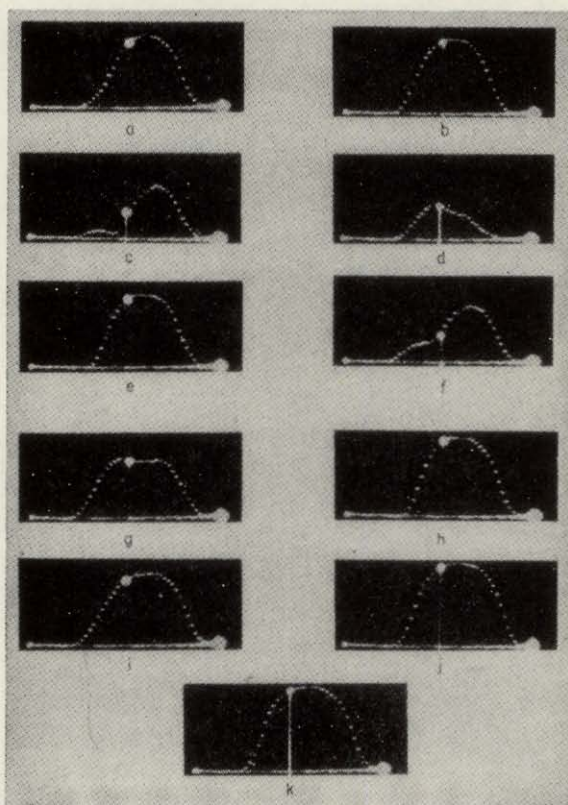


FIG. 9-41.—Azimuth angle envelope of video pulses received from a freighter at anchor in a fairly calm sea. The bright spot represents a fixed point on the ship as determined optically.

output circuit of the type described in Chap. 14, Vol. 19. Two deductions may be made from these pictures. One is that these angular envelope pulses, although occurring on a time scale 1000 times slower than video pulses, can be tracked by the same techniques as those used in range tracking, using adjacent time selectors, etc. The second observation is that the shifts in the center of area of the angular envelope pulse with respect to the optically determined point are so large that smoothing

must be carefully performed. A report on data smoothing<sup>1</sup> indicates that a desirable smoother is the double integrator function unit with one additional *RC* smoothing section. It has also been found that the preferred method of measuring the angular position is to compare first moments of the angular-envelope pulse rather than peak amplitudes or areas.<sup>2</sup>

<sup>1</sup> F. P. Coffin, R. D. Crout, and F. E. Bothwell, "Data Smoothing," RL Report 673, Jan. 23, 1945.

<sup>2</sup> Crout and Bothwell, NDRC Report 14-719.

## CHAPTER 10

### SPECIAL DATA-TRANSMISSION SYSTEMS

BY E. F. MACNICHOL, JR.

#### INTRODUCTION

Data transmission may be defined as the transmission of useful information from point to point. This includes the whole of wire and radio communication, facsimile, and television arts that are beyond the scope of this book. This chapter will confine itself to a brief description of those techniques that are not generally covered in the literature and will discuss several systems in which these techniques have been applied. All the systems discussed are designed for remote control or for telemetering.

There are three fundamental problems involved:

1. The original data, which may be mechanical, optical, chemical, acoustical, thermal, etc., must be converted into electrical components by means of suitable transducers (modulators).
2. The electrical components must be converted into a form suitable for accurate transmission without mutual interference.
3. The original data must be recovered at the receiving end in a form suitable for use.

#### SHORT-DISTANCE WIRE DATA TRANSMISSION

Where distances are short, separate wires may be used for transmitting the electrical components of the data so that Step 2 can be omitted. The problem is simplified to the construction of a suitable transducer at each end.

**10-1. Telemetering.**—Wire data-transmission systems are discussed in Vol. 22 specifically as methods of converting antenna position information of radars into spot displacements on the displays. In this case the cathode-ray tube acts as the output transducer (demodulator). Similar systems are also discussed in Parts I and II of Vol. 21 as computer data input devices and servomechanisms.

The electromechanical modulators and demodulators (transducers) used for data transmission are discussed in Vols. 17 and 19. This chapter will therefore present a summary of general methods of considerable

precision and the specific applications of time-modulation and time-demodulation techniques to data transmission. In addition especial consideration is given the number of circuits<sup>1</sup> necessary for transmission of specific types of information.

A single circuit (pair of wires) can normally transmit a single continuous nonrepetitive quantity such as the rotation of a shaft through an angle of less than  $360^\circ$ . The simplest type of device is shown in Fig.

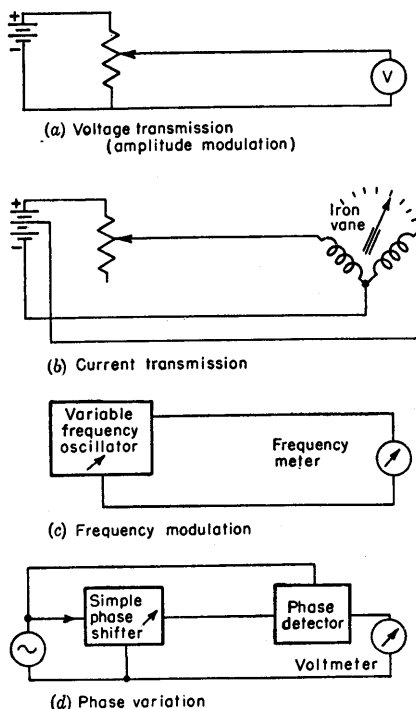


FIG. 10-1.—Simple transmission devices with limited rotation.

10-1a. A potentiometer divides a fixed potential in a ratio determined by the mechanical data; the fraction of the total potential is read by a remotely located voltmeter. This simple device is used to indicate the antenna tilt in the AN/APS-3 radar. It is evident that changes in supply voltage or in the resistance of the circuit will lead to errors in measurement.

A similar device (Fig. 10-1b) is used as a remote gasoline gauge in automobiles. Current from a battery sets up a fixed magnetic field in a coil. Variable current from a variable resistor sets up a varying field

<sup>1</sup> "Circuit" is used here in the sense of a communication system.

in a coil at right angles to the fixed coil. A soft-iron vane indicates the direction of the resultant field. In this case the direction of the vane is indicated by the ratio of two currents so that changes in the battery potential which is common to both circuits are canceled out. In order to achieve this independence of supply potential an extra circuit is necessary. (It is the definition of the volt that permits the transmitting and receiving systems of Fig. 10-1a to be set up independently of one another.)

A general law may be derived from this argument stating that, if a quantity is to be transmitted on an absolute basis and demodulated by means of a device calibrated in terms of absolute magnitude of the quantity, a single pair of wires is needed. If the quantity is to be sent as the ratio between two quantities, a third wire is needed. In this case, however, it is not necessary to have an absolute standard at either end of the transmission link.

Another absolute system that involves only a single circuit is the frequency-modulation system shown in Fig. 10-1c. An oscillator is frequency-modulated (possibly by varying mechanically the capacitance of a tuned circuit). A frequency meter at the receiving end reproduces the input signal. Here the untransmitted datum is time.

The phase of an alternating current can also be used for data transmission as shown in Fig. 10-1d. Phase cannot be transmitted on an absolute basis since phase measurement implies comparison with a reference phase. Two circuits (three wires) must therefore be used.

**10-2. Transmission of Continuous Rotation.**—In order to transmit unlimited rotation two circuits must be used since there is no single quantity that varies continuously and unambiguously with angle. As shown in Fig. 10-2a two currents can be modulated with sine and cosine components of angle by means of two variable resistors attached to an eccentric or to Scotch yokes. These currents can be used to set up orthogonal fields producing a resultant field whose direction can be determined by a suspended magnetic needle. A soft-iron vane cannot be used here as it could line up parallel or antiparallel to the field producing a  $180^\circ$  ambiguity. The magnetic needle will line up only antiparallel to the field. If lined up parallel it would be in a condition of unstable equilibrium and a slight displacement would cause it to swing to the correct position.

For many purposes, especially in synchro systems in which the 3-phase synchro is easier to construct than the 2-phase variety,  $120^\circ$  components are used instead of  $90^\circ$  components. As shown in Fig. 10-2b the  $120^\circ$  components may be transmitted with the same number of wires since if two of the three components are specified the third is automatically determined.



Devices using compass needles are not capable of very great torque output and are easily disturbed by stray d-c fields. To produce large torques efficiently, high magnetic-flux densities are needed. Only iron-core devices can be used for this purpose and on direct current these will suffer from the effects of residual magnetism. Potentiometers or variable resistors do not wear well when used at high speeds and those which will handle large currents require large torques. Certain types of electromechanical modulators and demodulators overcome these objections. They are devices of variable mutual inductance operating on alternating currents. As they are reactive elements they do not dissipate power unless torque is applied as contrasted with variable resistors and d-c-operated electromagnets. Such devices are known generically as synchros and are known under the trade names of Selsyn, Autosyn, Teletorque, Magslip, etc. There are also a-c-operated devices operating on somewhat different principles known as Magnesyns, Telegons, Microsyns, etc. (see Vol. 17 and Part II of Vol. 21). The common synchro generator has a rotor normally excited with alternating current and three stator windings arranged 120° apart. The voltage induced in each stator winding is proportional to the component of the rotor voltage resolved along its axis, and the constant of proportionality is the turns ratio. A synchro motor is identical to the generator except that an eddy-current damping device has been added. If the stator windings of a generator (transmitter) are connected to the stator windings of a motor as shown in Fig. 10-2c, a resultant field will be set up along a direction parallel to the direction of the rotor of the generator. If the rotor of the motor (receiver)

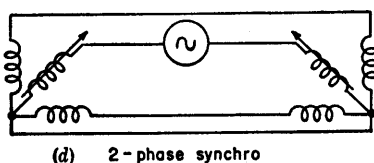
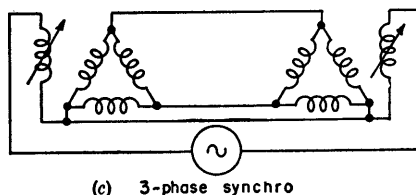
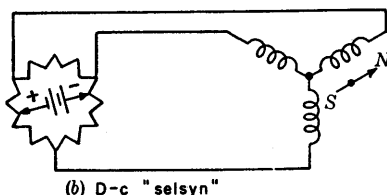
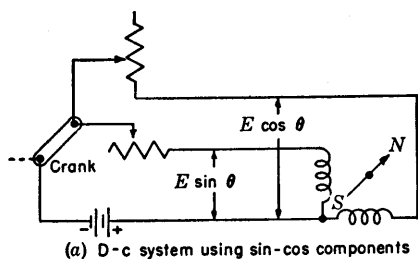


FIG. 10-2.—Devices that transmit 360° rotation.

motor is identical to the generator except that an eddy-current damping device has been added. If the stator windings of a generator (transmitter) are connected to the stator windings of a motor as shown in Fig. 10-2c, a resultant field will be set up along a direction parallel to the direction of the rotor of the generator. If the rotor of the motor (receiver)

are devices of variable mutual inductance operating on alternating currents. As they are reactive elements they do not dissipate power unless torque is applied as contrasted with variable resistors and d-c-operated electromagnets. Such devices are known generically as synchros and are known under the trade names of Selsyn, Autosyn, Teletorque, Magslip, etc. There are also a-c-operated devices operating on somewhat different principles known as Magnesyns, Telegons, Microsyns, etc. (see Vol. 17 and Part II of Vol. 21). The common synchro generator has a rotor normally excited with alternating current and three stator windings arranged 120° apart. The voltage induced in each stator winding is proportional to the component of the rotor voltage resolved along its axis, and the constant of proportionality is the turns ratio. A synchro

is connected to the same source of alternating current as the generator, a torque will be developed which positions the rotor so that the field it produces is antiparallel to the resultant field due to the stator windings. A torque applied to the motor will produce an equal torque at the generator. Thus a synchro system is a sort of electromechanical flexible shaft. All the devices previously shown can transmit power in only one direction. The synchro system is bidirectional. It will be noted that four wires are required in a synchro system because an a-c carrier is used. This extra circuit is necessary to transmit the sign of the rotor's direction. A three-wire system might be designed but there would be a  $180^\circ$  ambiguity. In the d-c system the sign of the rotor position is determined on an absolute basis by the north and south poles of the compass needle.

Synchro systems having two stator windings displaced  $90^\circ$  to one another producing sine and cosine components of the rotor voltage are available. These are frequently used in computation where cartesian components of an a-c voltage are desired but they are rarely used in data transmission. A system using such devices is shown in Fig. 10-2*d*.

It is possible to modulate and demodulate two frequencies, phases, time differences, or other quantities with  $90^\circ$  or  $120^\circ$  components and use them in transmission of continuous rotation but these are usually used in follow-up systems to be described later.

In a synchro system there is an error in the output proportional to the torque supplied by the motor. The torque must also be furnished by whatever drives the generator. In order to minimize the driving torque, amplifiers may be used between the stator windings of the generator and the motor. These amplifiers must have very constant gain to minimize errors. Such amplifiers will not decrease the error due to loading of the motor. The error can be reduced as much as desired by using the synchros as an element in a follow-up system.

**10-3. Follow-up Systems.**—Mechanical data can be most accurately transmitted by having an electromechanical modulator at either end of the wire link. These modulators have identical characteristics. Their outputs are subtracted and the difference amplified to control a motor that drives the input of the second modulator until the difference approaches zero. The follow-up is a servo system and as such is discussed in Part II of Vol. 21.

A simple voltage follow-up is shown in Fig. 10-3; a battery voltage is applied to a potentiometer at the transmitting end. The fraction of the battery voltage at the potentiometer slider is compared with that at the slider of the remote potentiometer. A d-c amplifier drives a motor that moves the slider of the remote potentiometer until the voltages approach equality. The voltages can be made to approach equality within any

specified limits depending upon the gain in the servo loop. If a potential is generated at the receiving end equal to that applied to the transmitting potentiometer a single transmission circuit is needed. Usually an additional circuit is used to transmit the reference potential.

A d-c follow-up for  $360^\circ$  rotation using two  $360^\circ$  potentiometers is shown in Fig. 10-4a. A synchro follow-up is shown in Fig. 10-4b. The synchro used at the receiving end is usually a special type known as a

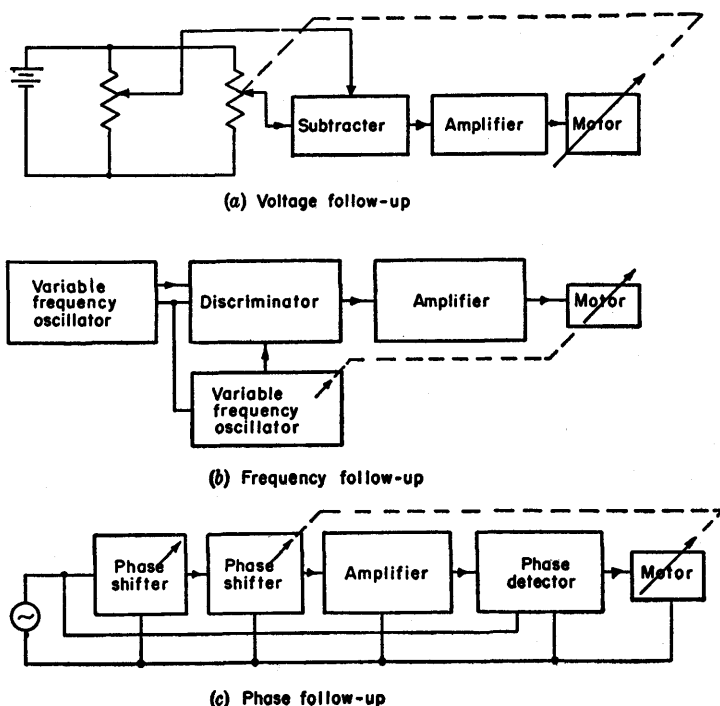


FIG. 10-3.—Simple follow-up devices with limited rotation.

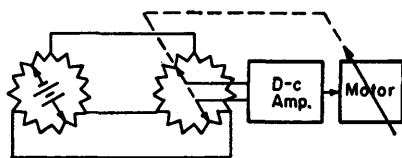
control transformer. Since no torque and very little electrical power is required from it the impedance of all the windings is made very high so that it loads the electrical circuit as little as possible. A very large number of control transformers may be supplied in parallel from a single generator. As in a simple synchro system three circuits (four wires) are needed.

As shown in Figs. 10-3b and 10-3c frequency and phase follow-ups are also possible. As a single frequency will only specify a single component, unlimited rotation is not possible with a single frequency-

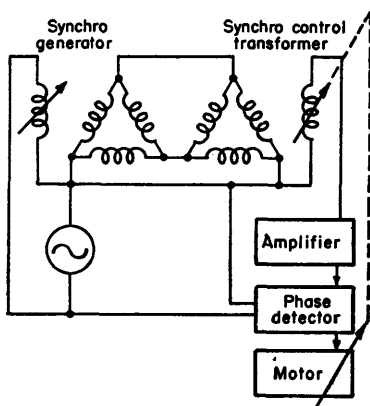
modulated circuit but as frequency is measured on an absolute basis only one circuit is necessary per quantity transmitted. In the phase follow-up, phase may be shifted continuously and unambiguously so that a single phase shift will completely specify a rotation. A reference phase must be transmitted, however, so that only three wires are needed, as in the d-c selsyn system.

**10-4. Characteristics of the Transmission Circuits.**—It is evident that in the systems described above in which amplitude is transmitted on an absolute basis the impedance of the wires must be either negligibly small or constant. Temperature effects would give errors. In the systems in which amplitudes are compared (as in synchro systems) relative amplitudes must be transmitted by the wire lines. As long as the conductors are similar, temperature effects will cancel. The phase shifts in the lines in a-c systems must be identical or correctly compensated since errors will be introduced in attempting to compare the magnitudes of a-c potentials which are not in phase. In the phase follow-up, variation of the amplitudes of the two components will not lead to errors in correctly designed equipment, but the relative phase shifts in the transmission of the components must be constant. The frequency follow-up is unique in that neither amplitude changes nor phase-shift variations (if their period is long compared to the carrier period) will effect the accuracy.

In long lines, direct transmission of synchro or other amplitude-modulated information is usually not feasible due to changes in amplitude and phase down the lines. Carrier systems that are identical with the c-w methods described in radio data transmission may be used satisfactorily. The pulse methods to be described would not usually be operable because of the large bandwidth required. Pulse methods can be used if properly terminated coaxial cables are employed.



(a) D-c follow-up



(b) Synchro follow-up

FIG. 10-4.—Follow-up systems that transmit 360° rotation.

TABLE 10-1.—SUMMARY OF WIRE TELEMETERING SYSTEMS

	No. of circuits for $N$ quantities	Extent of rotation	Is error caused by common level change?	Are errors caused by differential level changes?	Do relative phase shifts cause errors?
Voltage transmission, Fig. 10-1a	$N$	Limited			
Voltage or current comparison...	$N + 1$	Limited	No	Yes	Yes if ac is used
Frequency modulation, Fig. 10-1c	$N$	Limited	No	No	No
Phase modulation, Fig. 10-1d....	$N + 1$	Limited	No	No	Yes
D-c "Selsyn," Fig. 10-2a.....	2 for $> 360^\circ$	Unlimited	No	Yes	.....
D-c sin-cos, Fig. 10-2a.....	2 for $> 360^\circ$	Unlimited	No	Yes	.....
3-phase synchro, Fig. 10-2c....	3 for $> 360^\circ$	Unlimited	No	Yes	Yes
2-phase synchro, Fig. 10-2d....	3 for $> 360^\circ$	Unlimited	No	Yes	Yes
Voltage follow-up, Fig. 10-3a....	$N + 1$ if ref. voltage transmitted	Limited	No	Yes	Yes if ac is used
Frequency follow-up, Fig. 10-3b	$N$	Limited	No	No	No
Phase follow-up Fig. 10-3c.....	$\begin{cases} N + 1 \\ 2 \text{ for } > 360^\circ \end{cases}$	Unlimited	No	No	Yes
Synchro follow-up, Fig. 10-4d...	3 for $> 360^\circ$	Unlimited	No	Yes	Yes

## RADIO DATA TRANSMISSION

**10-5. Introduction.**—If a quantity is to be transmitted accurately by radio it must be converted to a form in which fading and interference do not have a first-order effect. If several quantities are to be transmitted (for example, two quantities specifying shaft position) a separate noninterfering channel must be provided for each component. Frequency-modulated c-w systems and time-modulated pulse systems are both suitable. Both systems permit limiting to minimize the effects of amplitude variations. In c-w systems each component of the electrical information—amplitude, phase, or frequency—modulate an alternating current known as a "subcarrier." Channel separation is achieved by using a different frequency for each subcarrier. The subcarriers are mixed and the output of the mixer frequency-modulates a carrier which is then transmitted. If additional interference rejection is desired, the subcarriers may modulate intermediate carriers that finally modulate the transmitted carrier. In the receiving equipment the subcarriers are recovered by demodulation of the carrier and separated by filtering. They are then demodulated and combined and the original is recovered by the same means used in wire systems. The techniques involve the

TABLE 10-2.—CHARACTERISTICS OF VARIOUS DATA TRANSMISSION SYSTEMS  
Discussed in Chaps. 10 and 11

System	Method of channel separation	Method of transmitting telemetering information	Interference rejection devices
Pulse remote control system	Six or seven different audio tones	On-off relay control by frequency-selective relays, tones transmitted as time-modulated pulse	Five-pulse code
Radiosonde (airborne transmitter, ground receiver)	Time-sequence (determined by altitude)	Frequency-modulated audio tone	None
Omnidirectional beacon (ground transmitter, airborne receiver)	Time-sequence selection	Pulse width and phase modulation	Very accurate PRF selector, pulse-width selector
Time-modulated sine-cosine relay radar system	Time-sequence selection	Time-modulated pulses carrying sine and cosine of antenna direction	Triple-pulse coding, narrow gates
Phase-shifted pulse relay radar system	Time-sequence selection	Phase-shifted pulse train, phase shift directly proportional to antenna direction	Triple-pulse coding
(Ground-to-ground relay) jittered pulse relay radar system	Time-sequence selection	Time-modulated pulse carrier, modulation frequency proportional to antenna speed. Angle marks indicate unique antenna position but synchronization must be achieved by hand	Triple-pulse coding
C-W-FM relay system (airborne transmitter, ship or ground receiver)	Frequency separation of video pulses, c-w subcarrier and audio sub-subcarrier. Triggers and video signals of opposite polarity	Amplitude of two audio tones proportional to sine and cosine of antenna angle. Third tone for level setting	Narrow filters for subcarrier and tones. Insufficient protection for triggers

use of oscillators, amplitude modulators, frequency modulators, frequency converters, amplifiers, filters, and amplitude and frequency demodulators of types conventionally used in the communications art.

In pulse systems each element of the data time-modulates a pulse by varying either its width or its spacing with respect to another pulse. Channel separation is accomplished by transmitting the pulses in sequence. Interference rejection is provided by transmitting each pulse in the form of a multiple-pulse "code" group that is decoded by a sequence of time selectors in the receiving equipment. Pulse systems are composed of PRF oscillators, generators of grouped pulses, time selectors, and time modulators and demodulators as well as the more conventional components. These systems sometimes resemble an artificial radar system in which artificially time-modulated pulses replace the moving echoes.

Relay radar systems are used to transmit video and antenna position signals to remotely located display devices. They contain wideband channels for the transmission of video signals and the sweep triggers (usually coded). The antenna position may be transmitted as a sequence of time-modulated pulses during an unused portion of the pulse-recurrence interval or it may be sent on a separate r-f carrier or subcarrier in the form of pulses or c-w components. To be useful the bearing information must be accurate to  $\pm 5^\circ$  or better so that the telemetering circuits must be carefully designed.

In remote-control systems the information is usually of low precision. It is often confined to switching operations actuated by the presence or absence of a pulse or audio tone. Medium-precision telemetering systems are best illustrated by the radiosonde which is accurate only for a short time after calibration. The British omnidirectional beacon is included as an example of pulse data-transmission system although it is fundamentally a navigational aid.

The characteristics of the data-transmission systems to be described in detail are summarized in Table 10-2.

**10-6. A Pulse Remote-control System.**—The transmitted information consists of five coded pulses at a PRF of 715 pps. The first four pulses are for designating a particular receiver, and the fifth pulse is time-modulated in accordance with one of six audio tones which represent the transmitted data. At the designated receiver, a beacon replies to the fourth pulse provided the fifth pulse is also correctly positioned and is modulated at a frequency corresponding to one of the control tones, thus reporting back to the transmitting station that control has been established. A "neutral" tone is provided to actuate the beacon for checking the communication circuit. Width modulation of the reply pulse on receipt of a control tone is also employed to signify that the control is responding. The pulses are  $0.2 \mu\text{sec}$  wide and their separation is variable





Fig. 10-7. In the explanation that follows, the timing sequence depends upon a PRF generator and, as an example, the SCR-584 has been cited (see Chap. 6). In addition to synchronization, this unit also permits range measurement to facilitate location of the receiving station. To make correct range measurement regardless of the code spacing chosen it is necessary to hold the fourth pulse at a fixed phase with respect to the circular-sweep range unit. This requirement makes it necessary to

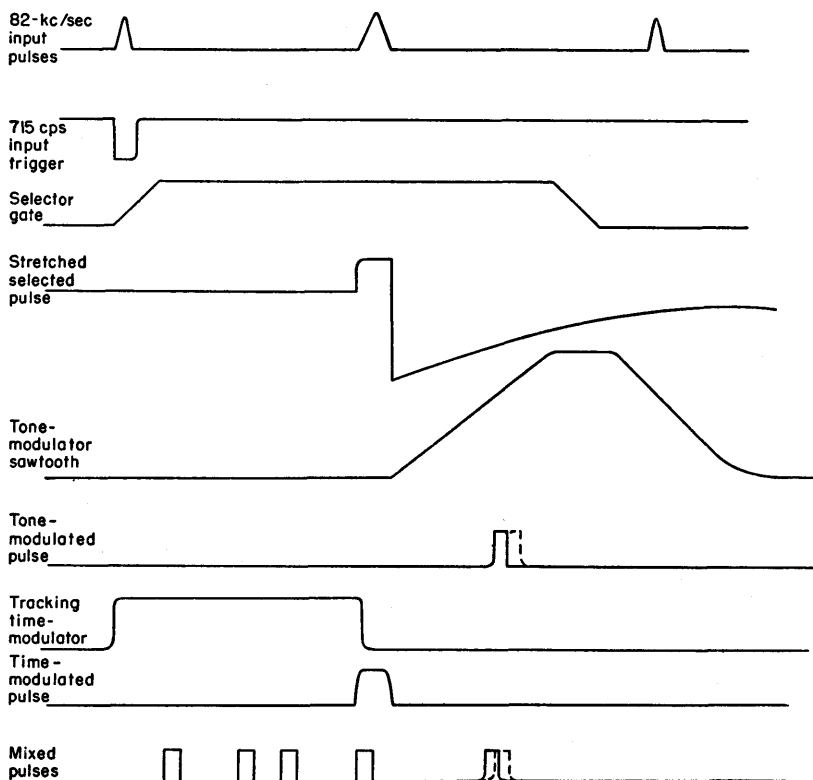


FIG. 10-6.—Timing diagram of remote-control coder.

cause the fourth pulse to coincide with a pulse from the 82-kc/sec oscillator in the range unit in the following manner. The 715-pps trigger from the range unit actuates a monostable multivibrator  $V_2$ , which produces a  $15\text{-}\mu\text{sec}$  pulse. This pulse is applied to a time selector  $V_3$ , which selects the following pulse from the oscillator  $12\text{ }\mu\text{sec}$  after the one that initiates the pulse. The selected pulse is stretched by the diode detector  $V_{4a}$ , which produces a negative step followed by a slow exponential rise. This waveform is taken from the cathode of  $V_{3b}$  and used to generate a

linear sawtooth waveform in the "bootstrap" sawtooth generator  $V_5$ ,  $V_{6a}$ . Time modulation is accomplished by the diode amplitude selector  $V_{6b}$ , which is biased by a d-c potential upon which is superposed an audio control tone. The control tones are generated from conventional Wien bridge oscillators (see Vol. 19 Chap. 4). The outputs of the oscillators are applied through control keys. When no key is depressed the "neutral" tone is automatically applied. The time-modulated sawtooth wave is amplified by  $V_7$  and  $V_{18b}$  and fires the blocking oscillator  $V_{18a}$ , which produces the fifth pulse. The three average positions of the pulse are determined by changing the d-c bias on  $V_{6b}$  by means of the switch  $S_1$ .

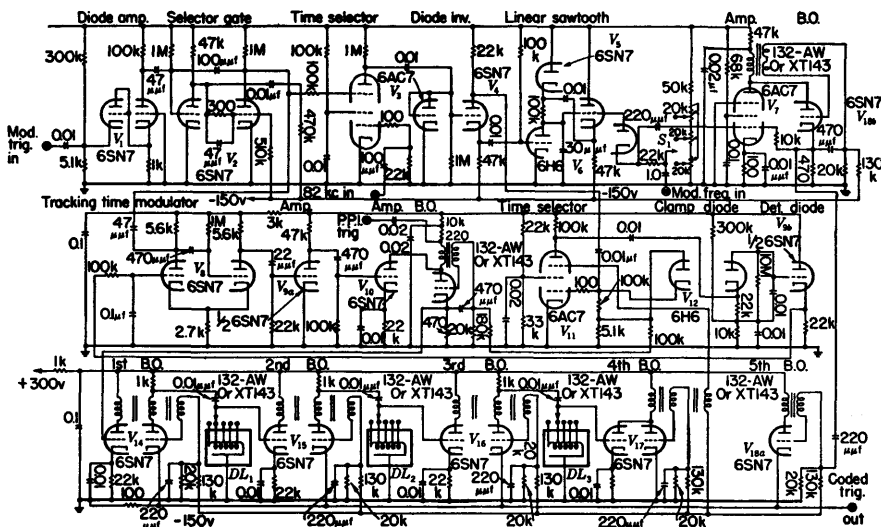


FIG. 10-7.—Remote-control coder.

The leading edge of the rectangle produced by  $V_2$  triggers the time modulator  $V_8, V_9, V_{10}$ . This is a monostable cathode-coupled multivibrator and blocking-oscillator combination. The output of  $V_{10}$  triggers the first-pulse blocking oscillator  $V_{14}$ . The negative current pulse from  $V_{14}$  is passed down the short-circuited delay line  $DL_1$ . The positive reflection from the line triggers the second-pulse blocking oscillator  $V_{15}$ . The third and fourth pulses are similarly formed. The cathodes of all the blocking oscillators are connected and the 0.2- $\mu$ sec pulses mixed across a 100-ohm resistor and applied to the high-power pulse generator of the transmitter.

A positive exponential occurring immediately after the selected pulse from the 82-kc/sec oscillator is taken from the plate of  $V_{4b}$ . This pulse and the fourth code pulse are applied to the time selector  $V_{11}$ . The out-

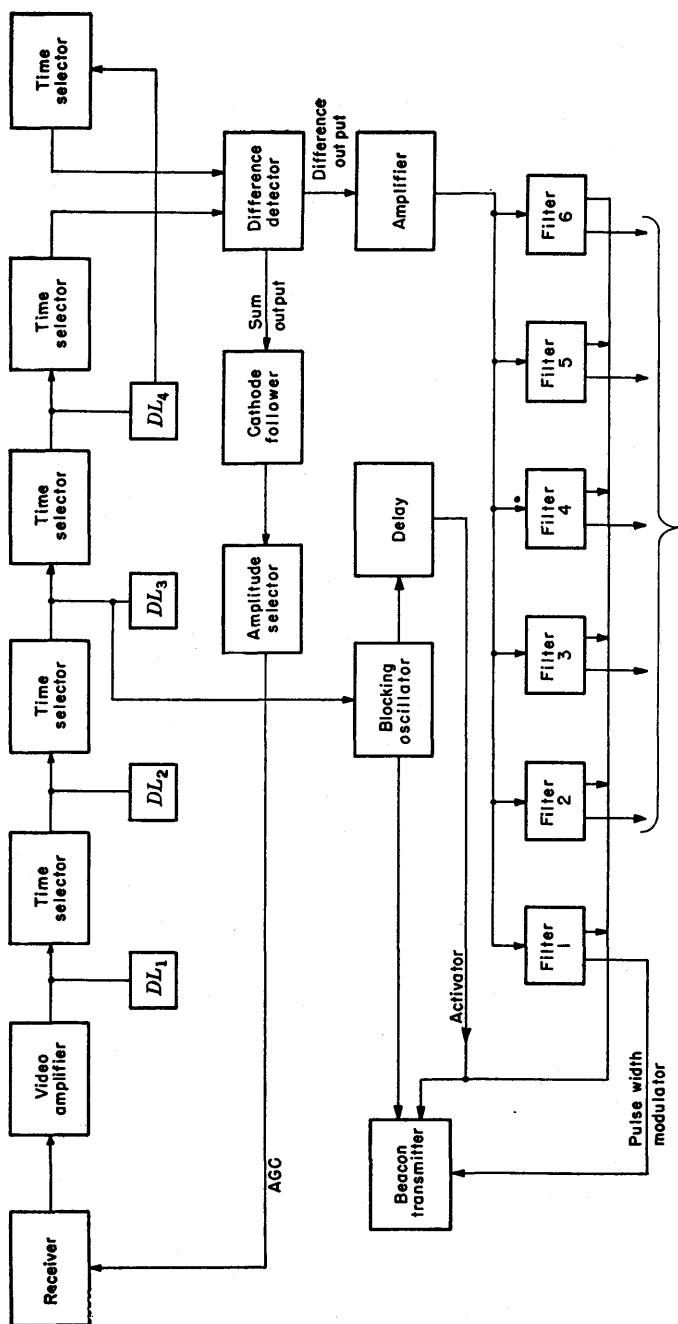


Fig. 10-8.—Block diagram of remote-control receiving system.

put of  $V_{11}$  is integrated by  $V_{12b}$ ,  $V_{9b}$  and applied as bias to  $V_{8a}$ . Since  $V_8$  is a time modulator the time of occurrence of the fourth pulse is controlled by this bias. Conditions are arranged so that the fourth pulse just touches the leading edge of the sawtooth waveform. Since this edge is generated by the rear edge of the selected 82-kc/sec oscillator pulse, the fourth pulse is constrained to coincide with it. No matter what code spacing is selected the time modulator will adjust itself until the condition is fulfilled. (For a complete discussion of automatic range-tracking systems see Chaps. 8 and 9.)

*The Receiving System.*—A block diagram of the receiving system is shown in Fig. 10·8 and circuit diagrams of the decoder and filter circuits

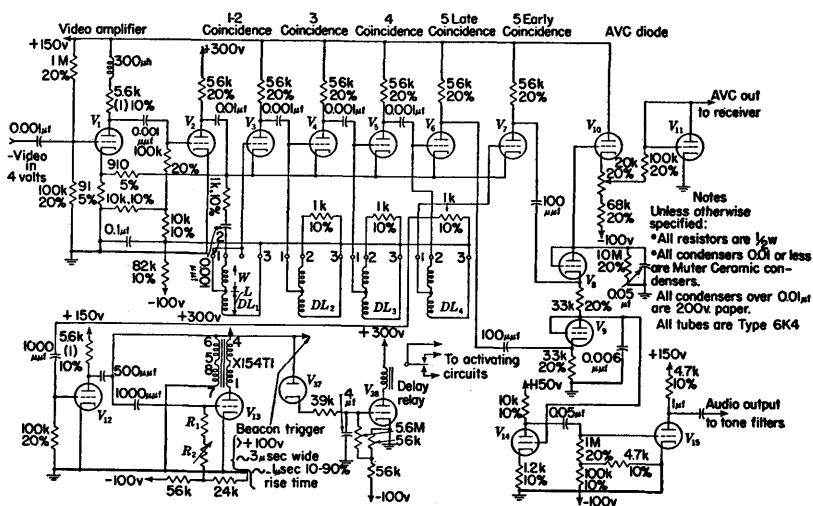


FIG. 10.9.—Decoder for remote control.

in Figs. 10-9 and 10-10. Negative pulses from the receiver (which has a short-time-constant second detector) are applied to the feedback amplifier  $V_1$ ,  $V_2$ . The limit level of the receiver is such that 15-volt pulses appear at the plate of  $V_2$ . The amplifier has a gain of four and an output impedance of about 70 ohms. The negative pulses are applied to the cathodes of the time selectors,  $V_3$ ,  $V_4$ ,  $V_5$ ,  $V_6$ , and  $V_7$ . They are also applied to the delay line  $DL_1$ . The pulses travel down the line and are reflected back until they are absorbed by the 1-k terminating resistor. They appear at the grid of  $V_3$  at a time that is a pulse width less than the total delay time. If the second pulse appears on the cathode of  $V_2$  at the same time that the delayed and inverted first pulse appears on the grid,  $V_3$  will conduct. The grid is connected to a tap rather than to the end of the line because if the negative incoming pulse and the positive

reflected pulse appeared on the grid simultaneously they would cancel. The delay of the line is given by  $D = W + 2L$ , where  $D$  is the effective delay,  $W$  is the delay between the terminals of the line and the tap, and  $L$  is the delay between the top and the short-circuited end of the line.

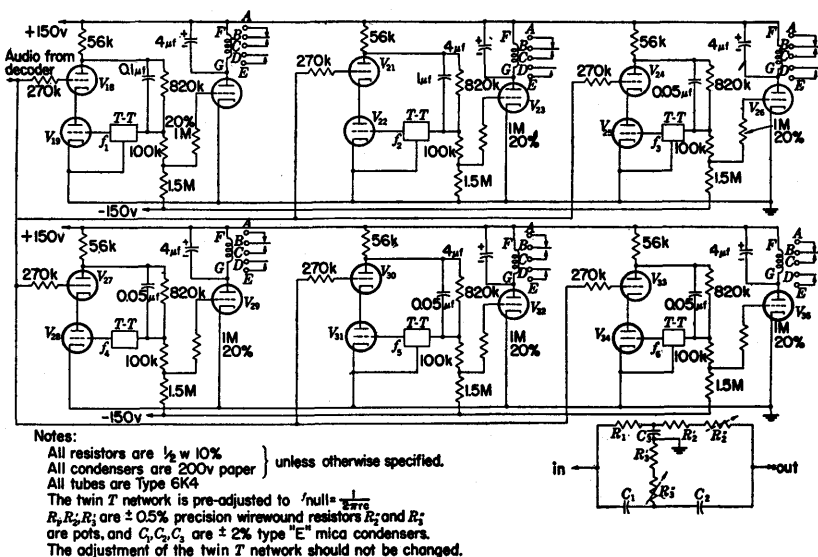


FIG. 10-10.—Tone filters.

The lengths used are given in Table 10-3. All lines are General Electric Type YE4-B and are arranged to plug into the decoding unit. It was

TABLE 10-3.—CHARACTERISTICS OF DECODING LINES

Line No.	Positions that can be used	$D$ , $\mu\text{sec}$	$L$ , $\mu\text{sec}$	$W$ , $\mu\text{sec}$
1	$DL_2, DL_3$ only	0.4	0.2	0
2	All positions	0.8	0.3	0.2
3	$DL_1, DL_2, DL_3$	1.2	0.5	0.2
4	All positions	1.6	0.7	0.2
5	$DL_1, DL_2, DL_3$	2.0	0.9	0.2
6	All positions	2.4	1.1	0.2

found that the transmitter in the SCR-584 could not be made to respond to pulse spacings as close as  $0.4 \mu\text{sec}$ , so Line 1 was omitted, cutting the number of codes from 540 to 375.

The output of  $V_3$  is applied to  $DL_2$  and the positive reflection used as a time-selector pulse for the third input pulse on the cathode of  $V_4$ . The fourth pulse is selected by  $DL_3$  and  $V_5$  in the same manner. The

selected fourth pulse is amplified by  $V_{12}$  and triggers blocking oscillator  $V_{13}$ , which produces a 3- $\mu$ sec 100-volt pulse to trigger the beacon transmitter.

The output of  $DL_4$  appears on the grid of  $V_7$  and 0.2  $\mu$ sec later on the grid of  $V_8$ . The energy in the pulses at the plates of  $V_7$  and  $V_8$  produced by the fifth pulse is dependent upon the duration of the overlap with the delayed selector pulses. The difference between these times is taken by the difference detector  $V_8$ ,  $V_9$ . The signal applied to the grid of  $V_{14}$  consists principally of the time-modulation envelope of the fifth pulse (see Vol. 19, Chap. 14) which is the original audio tone. This tone is amplified by  $V_{14}$  and  $V_{15}$  and applied to the filters.

The circulating current in  $V_7$  and  $V_8$  is proportional to the amplitude of the fifth pulse. It appears as a potential across the 10-megohm resistor and the 0.05- $\mu$ f condenser in the plate circuit of  $V_8$ . It is applied to the diode level-setter (amplitude selector)  $V_{11}$  through cathode follower  $V_{10}$  and then to the grids of the i-f amplifier of the receiver as AVC voltage. The 20-k potentiometer is adjusted so that zero bias is applied to the i-f amplifier for all signals less than 80 per cent of limit level and the gain is rapidly reduced for signals above that level. Thus correctly coded signals are held at 80 per cent of limit level, which insures reliable operation of the decoder while all other signals are limited at a level that is not sufficient to appear in the output in the absence of correct code spacing. Since all five correctly spaced pulses are required to operate the AVC, incorrectly spaced pulses will have no effect.

The tone filters are cascode amplifiers with feedback through a twin-T network to the grid of the bottom tube (see Vol. 18, Chap. 10). The signal is applied through the grid of the top tube. The filters have a gain of about four for the frequency to which they are tuned and have the frequency characteristic of a single-tuned circuit with a  $Q$  of 15. The relays are operated by tubes that are normally cut off and pass current on positive half cycles of the filter output (plate detectors). Condensers of 4  $\mu$ f are used to keep the relays from chattering. In this design only one tone is to be used at a time. The high-voltage pulse generator in the beacon transmitter contains a relay that selects either of two widths for the transmitted pulse. The "neutral" tone operates one pulse width. If any of the control tones are present the pulse width is changed, indicating that the equipment is complying with the order. If no tone is received the transmitter is inactivated. Increased interference rejection and more channels are possible through PRF selection. An elementary type of PRF selection is accomplished by adjusting the time constant in the grid circuit of  $V_{13}$  until the blocking oscillator will not trigger at a PRF higher than 715 pps. In addition, the output of the blocking oscillator is integrated with a time constant of several seconds and the

output applied to a relay which activates the beacon transmitter and the control circuits. Thus, correct signals of the correct PRF and code must be received for a specified length of time before the beacon will reply or control can be established.

**10-7. Radiosonde.**—Probably the simplest and most compact of all radio data transmission devices is the radiosonde. The U.S. Army AN/AMT-1 weighs only 220 g without battery and is designed to be carried aloft by a weather balloon. It transmits temperature, atmospheric pressure, and humidity to the weather station. The position of

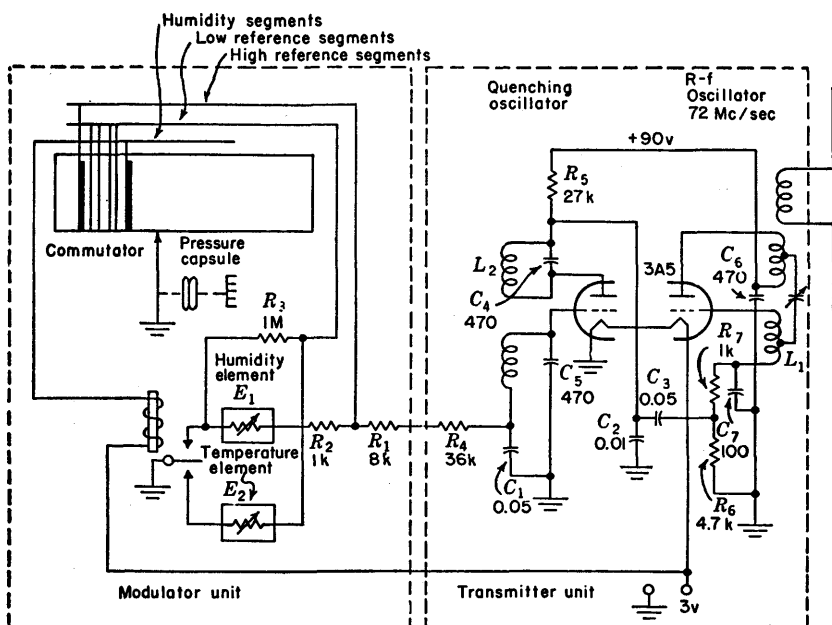


FIG. 10-11.—Radiosonde, AN/AMT-1.

the balloon is determined by radio direction-finding equipment operating on the transmitted signal. A diagram of the AN/AMT-1 is shown in Fig. 10-11. It contains a single 3A5 tube. One section acts as an r-f oscillator at 72 Mc/sec while the other section acts as a quenching (squegging) oscillator which keys the transmitter at an audio-frequency rate. The audio frequency is modulated by changing the grid resistor of the quenching oscillator. The change in grid resistance is accomplished in the modulator unit. Since three quantities must be measured in sequence, some form of channel-switching is needed. Advantage is taken of the fact that as the balloon ascends the atmospheric pressure decreases continuously at a nearly constant rate. The pressure-sensitive

aneroid element moves a slider over a commutator that contains a large number of conducting and insulated segments which are arranged in a definite pattern. The conducting segments are divided into three sets, one of which connects fixed resistances to produce a high-reference tone. The second group connects a larger resistance producing a low-reference tone. The third set of contacts operates a relay which connects the humidity-sensitive element. When the slider is over insulated segments, the temperature element is connected into the circuit. The temperature element is a resistance thermometer. The humidity element is a strip of insulating material with two electrodes between which is a coating, a gelatinous film containing a hygroscopic salt. The conductivity of this film is proportional to the relative humidity.

The receiving equipment contains a recording frequency meter. The pattern with which the high- and low-reference tones occur on the chart indicates the pressure region through which the balloon has passed. The low-reference tone at 190 cps serves as a standard of calibration for the instrument and is repeated often enough to permit corrections to be made if temperature or battery depletion change the characteristics of the transmitter. As quenching oscillators are not too stable this reference is essential.

The quenching oscillator is quite conventional and operates at an intermediate frequency given by

$$f = \frac{1}{A + BR}$$

The accuracy is at best several parts in  $10^2$  since the circuit uses a saw-tooth voltage of about 90 volts, and a tube with a grid base of 5 volts, which may vary at least  $\pm \frac{1}{2}$  volt from tube to tube with aging and with battery voltage. The quantity  $A$  ( $\sim 10^{-3}$ ) corresponds to the time during which oscillation takes place. The quantity  $BR$  ( $B \sim 10^{-7}$ ) is the variable relaxation period. Since  $C_3$  is given as  $0.05 \mu\text{f}$ , it is evident that the portion of the exponential used is  $2.2RC$ .

The r-f oscillator oscillates during the relaxation period and is keyed off when the quenching oscillator oscillates by the plate-current pulse applied to the grid return of the oscillator through  $C_3$ . Loading of the antenna or tuning of the r-f oscillator has negligible effect upon the quenching frequency.

The radiosonde is not a particularly stable device as judged by radar standards. Its ability to make precision measurements depends upon very exacting preflight calibration and maintenance, and upon the fact that it is required to operate for only an hour or two immediately after calibration. The example furnishes an excellent illustration of how extreme economy and simplicity may be achieved if one is willing and able to make frequent calibration.



**10-8. A British Omnidirectional Beacon.**—Pulse time differences may, in certain cases, be used to determine angle.<sup>1</sup> Consider the transmitter shown in Fig. 10-12. Three antennas are placed at the vertices *A*, *B*, *C* of a right isosceles triangle. They are energized in sequence from a transmitter that is pulsed with a 5-kc/sec PRF. The keying sequence is *ABACA*, etc. If pulses were transmitted simultaneously from *A* and *B*, assuming the airplane to be a long way off, the difference in the time of arrival of pulses sent out simultaneously from *A* and *B* is  $(d/c) \sin \theta$ .

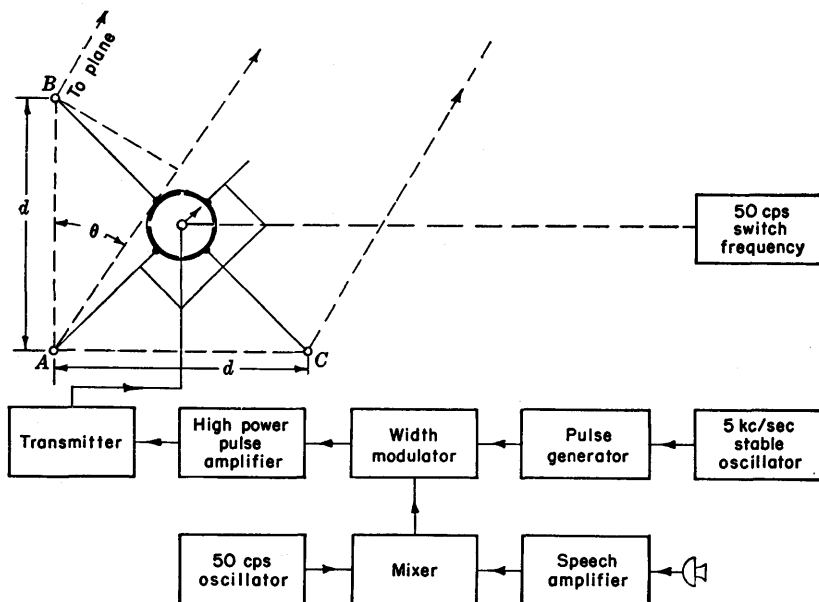


FIG. 10-12.—Transmitter of modified omnidirectional beacon.

From *A* and *C* the time difference is  $(d/c) \cos \theta$ , where *c* is the velocity of propagation. In practice *d* is made 500 ft so that the maximum time difference will be about  $\frac{1}{2} \mu\text{sec}$ . The pulses are also width-modulated between the limits of 1.4 and 1.8  $\mu\text{sec}$  with a 50-cps sinusoid synchronous with the antenna switching frequency which is used for phase comparison in the demodulating equipment. It may be replaced by a voice channel to permit the transmission of weather and landing instruction, etc.

A block diagram of the receiving equipment is shown in Fig. 10-13. A local PRF, which is swept over a frequency range of  $\pm \frac{1}{2}$  per cent by means of an automatic search device, is set up in the receiving equip-

<sup>1</sup> Third Commonwealth and Empire Conference on Radio for Civil Aviation, Summer 1945, British Crown Copyright Reserved.

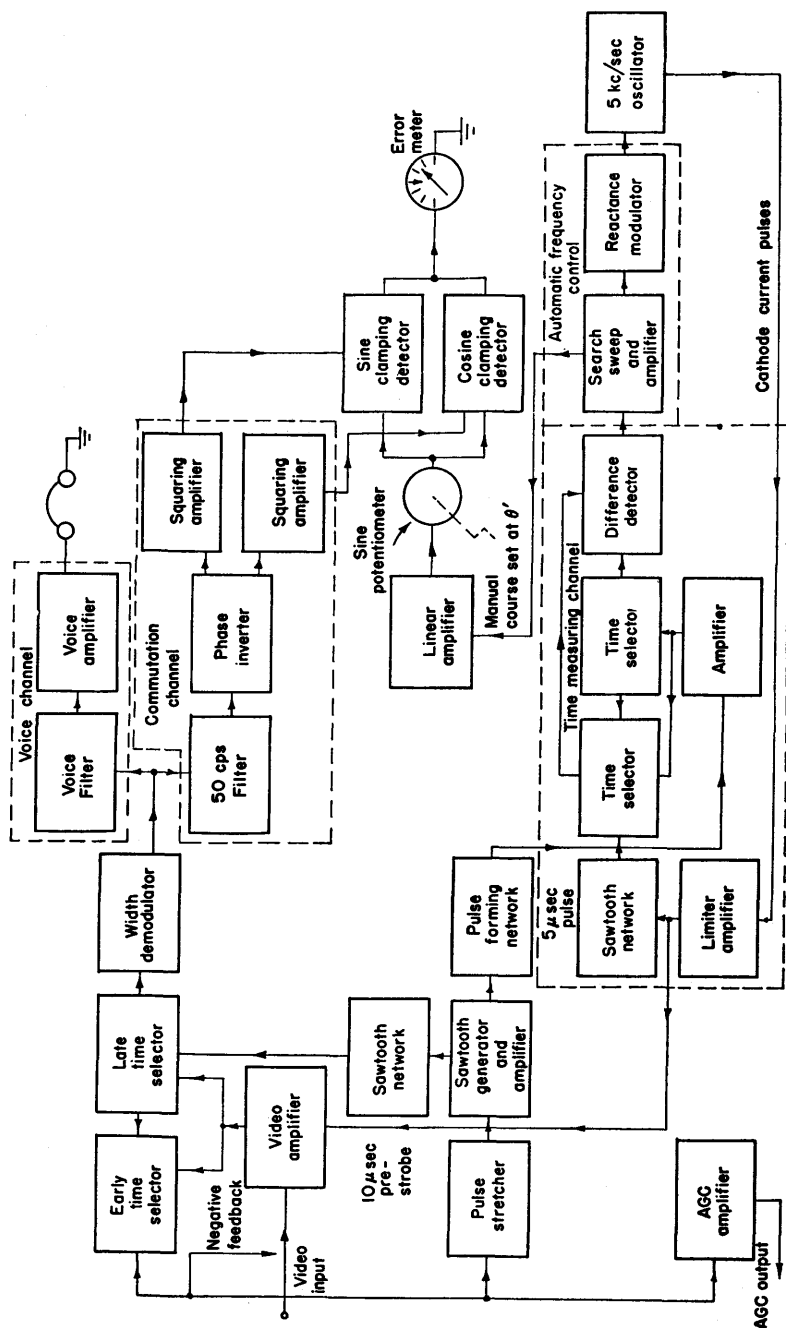


Fig. 10-13.—Block diagram of omnidirectional beacon demodulator.

ment, and 10- $\mu$ sec pulses synchronized with the oscillator are applied to a time-selective video amplifier. If a signal enters during this period it is applied to the early time selector. The output of the early time selector is used to activate a sawtooth generator and a 5- $\mu$ sec pulse generator. After  $\frac{1}{4}$   $\mu$ sec, the sawtooth voltage rises to a potential that switches off the early time-selector and switches on the late time-selector. The 5- $\mu$ sec pulse is synchronous with the leading edge of the signal and is independent of its duration. It is used as the basic time reference. The amplitude of the first  $\frac{1}{4}$   $\mu$ sec of the signal is used for AVC in the receiver. The width of the rear portion of the pulse is demodulated and is applied to the reference sinusoid demodulator and voice channel. The 5- $\mu$ sec pulse is compared in time with a sawtooth wave in a time discriminator. The output of the time discriminator is a voltage that is used to control the frequency of the oscillator. When a 5-kc/sec PRF is received the oscillator is locked in phase by means of this AFC circuit. When antennas are switched there is a phase change in the incoming PRF proportional to  $d \sin \theta$  or  $d \cos \theta$ . The area under the control signal applied to the AFC circuit is proportional to this phase change since phase change is the integral of frequency change. The control signals in the form of pulses recurring with a 200-pps frequency in a pattern which repeats at 50 pps are applied to a sine-cosine potentiometer that is turned to the desired course  $\theta'$ . The sine output is connected to a clamping detector operated by a 90° (of 50 pps) square wave timed to include A-B change-over. The cosine output is similarly selected to include the A-C change-over. The two detected outputs are added and applied to a zero-center course meter. No current will flow through the meter when  $\theta = \theta'$  since then

$$d \sin \theta \cos \theta' + d \cos \theta \sin \theta' = 0.$$

The 5-kc/sec oscillator serves as a phase "memory" to permit the comparison of the phases of the signals from the three antennas since they are not radiating simultaneously.

The positive video signals from the receiver are applied to the control grid of  $V_1$  (see Fig. 10-14). The 10- $\mu$ sec gate is applied to the suppressor, the top of the gate being restored to ground level by  $D_{10}$ . During the quiescent condition and for the initial portion of the signal,  $V_2$  takes all the plate current from  $V_1$  since its grid is held at +100 volts while that of  $V_3$  is held at +80 volts by fixed bias.

Negative feedback is applied from the plate of  $V_2$  to the grid of  $V_1$  to stabilize the gain. The AVC voltage for the screens of the receiver i-f stages is produced from the output of  $V_2$ , which is rectified by  $D_1$  and amplified by  $V_5$ . The grid-plate time-constant of  $V_5$  smooths the AVC information. The output of  $V_2$  is also applied to the cathode of  $D_2$ ,

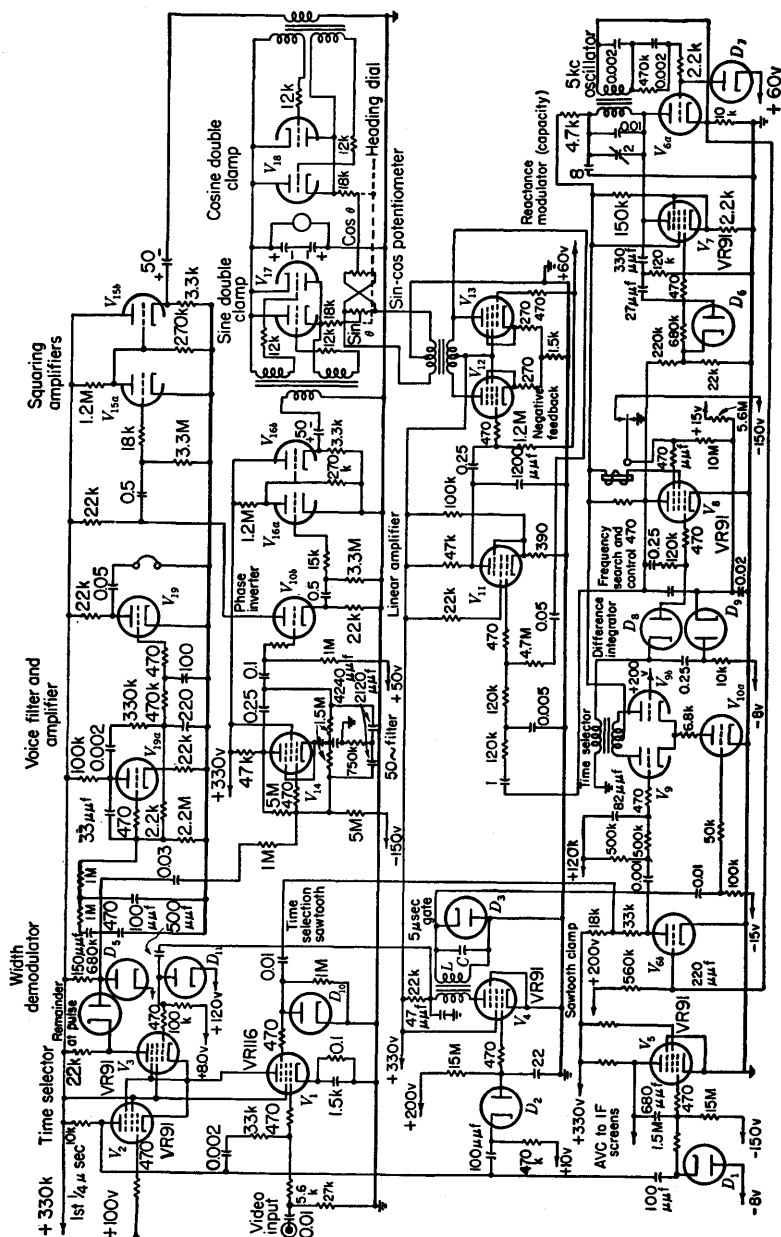


FIG. 10-14.—Modified omnidirectional beacon demodulator.

which produces a negative exponential gate of sufficient duration to cut off  $V_4$  for longer than 5  $\mu$ sec. The sudden interruption of plate current in  $V_4$  by the leading edge of the signal causes shock excitation of the resonant transformer. The diode  $D_3$  absorbs the negative half cycle of the oscillation so that a single positive half cycle of 5- $\mu$ sec duration is produced. The cessation of plate current also causes a 47- $\mu$ f condenser to charge through the 22-k plate load producing a positive-going exponential rise. This sawtooth wave raises the grid of  $V_3$  until it takes all the plate current of  $V_1$ , and  $V_2$  is cut off. As the negative feedback loop is now broken, the full video signal is applied to  $V_1$ , which then limits. The switch-over of current from  $V_2$  to  $V_3$  occurs after the first  $\frac{1}{4}$   $\mu$ sec of pulse. Plate current in  $V_3$  charges a 470- $\mu$ f condenser through  $D_4$ . The final potential reached is determined by the duration of the pulse. The diode  $D_5$  holds the initial potential on the condenser at +225 volts so that 95 volts of signal must be present before any action takes place, and small signals will not operate the width-demodulation channel. The amplitude-modulated sawtooth wave containing the width-modulation envelope is filtered and applied to the voice channel which has a pass band starting above 50 cps and ending below 5 kc/sec but which passes the frequencies necessary for intelligible speech.

The modulated sawtooth wave is also applied to the 50-cps twin-T filter  $V_{14}$ , which has a  $Q$  of three and which rejects the voice frequencies and the 5-kc/sec PRF. The sine-wave output of the filter passes to the phase inverter  $V_{10b}$ ; the outputs are grid-limited by  $V_{15a}$  and  $V_{16a}$ . The coupling time constants and impedances are so chosen that 90° square waves appear in the plate circuits of the tubes. The square waves are applied to cathode followers  $V_{15b}$  and  $V_{16b}$ , which drive the grid transformers of the phase-sensitive detectors. The detectors  $V_{17}$  and  $V_{18}$  operate so that each will pass current only during a quarter cycle of the reference 50-cps waveform, which is centered about the instant of transition between the relevant antennas.

The 5- $\mu$ sec pulse that is initiated by the leading edge of the signal is applied to the grid of  $V_{10a}$  turning on space current. A sawtooth wave is applied to the grid of  $V_{9a}$  and a fixed potential to the grid of  $V_{9b}$ . The proportion of the space current taken by each half of  $V_9$  is determined at any instant by the relative potential of the two grids. As the sawtooth voltage on the grid of  $V_{9a}$  increases, less current will flow in  $V_{9b}$  and more in  $V_{9a}$ . The difference between these currents is taken by the pulse transformer connected between the two plates. This difference takes the form of a positive pulse when current is greater in  $V_{9b}$ , followed by a negative pulse when current is greater in  $V_{9a}$ . The difference in the areas of the two pulses is measured by the difference detector  $D_8$ ,  $D_9$ . (See Vol. 19, Chap. 14.) The normal operating bias of  $D_8$  is -4 volts.

A bias of  $-8$  volts is applied to the plate of  $D_9$ . A Miller integrating circuit is also used with  $V_8$  to provide smoothing of the output and a long memory. The output of  $V_8$  changes the bias on the grid of the reactance modulator  $V_7$ , which controls the frequency of the oscillator by providing a variable reactive load across the tuned circuit. Negative feedback is applied from plate to grid of  $V_7$  through a high-pass network. The network advances the phase on the grid by  $90^\circ$  at the oscillator frequency. Since the plate current is  $180^\circ$  out of phase with the grid potential, a leading component of current is produced in the plate circuit which acts as a capacitance. The a-c voltage applied to the grid of  $V_7$  is limited in amplitude by  $D_6$ , which is biased by the control potential. The grid voltage and plate current are therefore in the form of square waves which produce an accurately linear change in the capacitance shunting the tuned circuit. The  $2.2\text{-k}$  resistance in the cathode of  $V_1$  provides current degeneration which further improves the linearity of the capacitance change.<sup>1</sup>

The oscillator is of the conventional transformer-feedback type with a  $10\text{-k}$  resistor in the cathode circuit. Pulses of cathode current are taken across this resistor for synchronization. The amplitude of the pulses is maintained constant by  $D_7$ , which is biased at  $+60$  volts and which limits the grid rise to  $+60$  volts. The pulses drive the limiter-amplifier  $V_{6b}$  into grid current charging the  $270\text{-}\mu\text{f}$  coupling condenser. At the end of the pulse from the oscillator,  $V_{6b}$  is cut off for the time taken for the condenser to recharge to cutoff bias through a  $560\text{-k}$  resistor taken to  $+200$  volts. A  $10\text{-}\mu\text{sec}$  positive pulse is produced in the plate circuit. Part of this forms the gate applied to the suppressor of  $V_1$ . The gate is converted into a sawtooth wave by an  $RC$ -network. This sawtooth wave is applied to the grid of  $V_{9a}$ .

If the phase of the  $5\text{-}\mu\text{sec}$  pulse is in advance of the time it takes the sawtooth wave to go from  $+120$  to  $+200$  volts (the potential on the grid of  $V_{9b}$ ), the positive pulse produced in the transformer secondary will be larger than the negative one. The grid potential of  $V_8$  will rise so that the plate potential will drop, reducing the current in  $V_7$  and removing capacity from the tuned circuit. This will raise the frequency of the oscillator which advances the phase of the sawtooth wave. The effect of this tracking loop is to keep the  $5\text{-}\mu\text{sec}$  pulse in the center of the rise of the sawtooth wave. The loop is stabilized by the feedback components of  $V_8$ .<sup>2</sup> The constants of the loop are such that it will track out a fluctuation in  $2$  milliseconds.

In the absence of signals the  $5\text{-kc/sec}$  oscillator is caused to search

<sup>1</sup> Williams and Kilburn, "Automatic Strokes and Recurrence Frequency Selector Part II," I. E. E. Convention Paper, March 1946.

<sup>2</sup> See Chap. 8 and F. C. Williams *et al.*, *loc. cit.*

in frequency by a relaxation-oscillator circuit. The grid potential of  $V_8$  rises due to current flowing through a 5.6-megohm resistor returned to +15 volts. The plate runs down linearly to bottom by virtue of the Miller feedback. At bottom, screen current increases, closing the relay in the screen circuit. The suppressor is switched by the relay to -150 volts, cutting off plate current, and the plate rises toward 250 volts. A 10-megohm resistor in the grid circuit is also switched to -150 volts so that when the plate rise is complete the grid potential falls until the relay opens and the cycle recommences. The search circuit sweeps the oscillator frequency from 4975 to 5025 cps in about 10 sec.

The control pulse from the plate of  $V_8$  is filtered and applied to the feedback amplifier  $V_{11}$ ,  $V_{12}$ ,  $V_{13}$ , which is transformer-coupled to the sine-cosine potentiometer. A 60-volt pulse is produced across the potentiometer when a 3-volt input (the maximum value that can be produced by the antenna switching operation) is applied to the input of the amplifier. The sine and cosine outputs of the potentiometer are applied to the triode bidirectional switches  $V_{17}$  and  $V_{18}$ . The difference between the outputs of these switches is applied to the zero-center course meter. A large capacitance is shunted across the meter to reduce fluttering of the needle caused by the pulses.

*Performance.*—Operational tests have demonstrated a mean error of  $1^\circ$  in the bearing of the plane relative to the ground beacon. This error is equivalent to a time-difference error of  $0.01 \mu\text{sec}$ .

## CHAPTER 11

### RELAY RADAR SYSTEMS

By E. F. MACNICHOL JR., W. J. JACOBI, AND F. P. COFFIN

#### TIME-MODULATED SINE-COSINE SYSTEM

By E. F. MACNICHOL JR. AND W. J. JACOBI

**11.1. Principle of Operation.**—This system was designed to relay the PPI picture from an airborne radar to a fixed station by:

1. The production of an azimuth rotation in the remote PPI synchronous with the antenna rotation in the radar system and
2. The transmission of the radar transmitter pulse and receiver video to the remote PPI.

The method of accomplishing (1), is fundamentally a "position" method; that is, the angular position, not the velocity, is reproduced

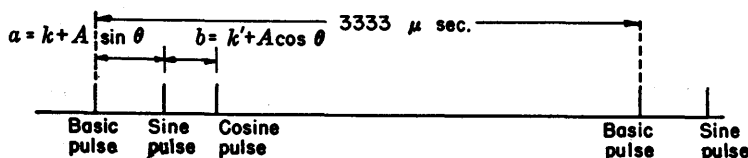


Fig. 11-1.—Time intervals of time-modulated sine-cosine system.

In order to do this, the antenna angle at the sending end (from a fixed zero reference) must be continuously and unambiguously specified. Both the sine and cosine functions of the angle are used for this purpose because either function alone would not give an unambiguous specification. The process of reproducing the angle involves converting angular data to electrical data, transmitting the electrical data to the receiver, and converting the electrical data back to angular data at the receiver. The limiting error of the over-all angular data transmission is approximately  $\pm 3^\circ$  for a maximum angular speed of 6 rpm.

The electrical information transmitted is in the form of a system of pulses. Three pulses are used—the basic pulse, the sine pulse, and the cosine pulse. If  $\theta$  is the angle to be transmitted, the interval between the basic pulse and the sine pulse is made equal to  $K + A \sin \theta$  where  $K$  and  $A$  are constants and  $K > A$  and the interval between the sine pulse and the cosine pulse is made equal to  $K + A \cos \theta$ . These pulses and time intervals are shown in Fig. 11-1. The basic pulse has a con-



stant repetition rate of 300 pps, and the sine and cosine pulses move as shown in Fig. 11-2.

At the sending end, an Arma resolver produces alternating voltages whose peak values are proportional to the sine and cosine, respectively, of  $\theta$ . (A negative value of the function is indicated by a reversal in phase of the voltage.) These voltages are rectified by a phase-sensitive detector, giving output voltages,  $A \sin \theta$  and  $A \cos \theta$ , added to constant voltages to give  $K + A \sin \theta$  and  $K + A \cos \theta$ . These voltages are impressed on linear electrical time modulators. In more detail, the basic pulse generator triggers the sine time modulator (sawtooth); the

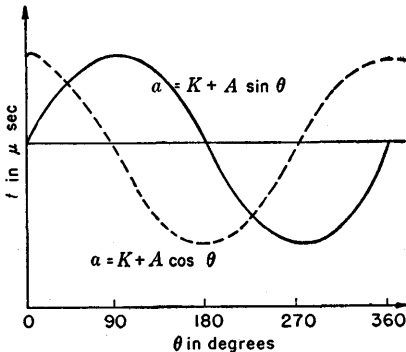


FIG. 11-2.—Sine and cosine pulses.

sine pulse is produced after a time interval proportional to  $K + A \sin \theta$ ; the sine pulse then starts a second delay from which the cosine pulse is evolved. The three pulses are mixed before modulating the radio link transmitter. The device that performs all these functions is known as the "synchronizer."

At the receiving end, the process is essentially reversed in what is known as the "decoder." Here the object is to produce sine- and cosine-modulated carrier voltages which are applied to the stators of an Arma resolver (two-phase synchro). The field thus produced is tracked by rotating the shaft by means of a servomechanism.

The synchronizing pulses received from the relay receiver are separated by a sequence of time selectors, and linear delays are produced corresponding to those in the synchronizer. The sine pulse is automatically tracked by a system of step gates whose position is controlled by a pickoff voltage impressed upon the sine time modulator. The position of the gates is compared with the position of the sine pulse, and the error voltage is used to control an alternating-voltage modulator whose output is the desired sine-modulated carrier,  $(A' \sin \omega't) \sin \theta$ . A bidirectional switch detector, operating from this carrier together with the constant voltage  $K$  produces the pick-off voltage impressed upon the linear delay. Thus the tracking loop is completed. The alternating-voltage carrier adjusts itself until the step gates coincide with the sine pulse, and, since the sine pulse executes a sinusoidal motion, the carrier is modulated in a sinusoidal manner. The cosine pulse is tracked in the same fashion as the sine pulse, using similar circuits, to produce a cosinusoidally-modulated carrier. The two carriers are then

impressed on the 90° stator windings of the Arma resolver and the shaft is rotated by a servomechanism until the rotor pickup voltage is zero. For the pickup voltage to remain zero, the rotor must remain at right angles to the field; since the field follows the transmitted antenna azimuth, the resolver shaft will also follow it. This shaft motion then fulfills requirement (1).

It should be noted that the absolute magnitude of the excursions made by the sine and cosine pulses, and the magnitude of the maximum sine

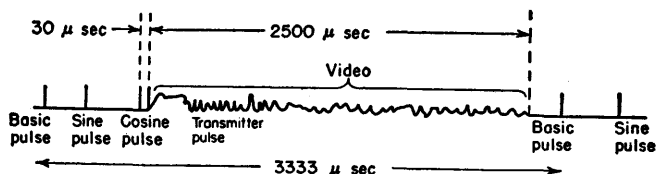


FIG. 11-3.—Signal transmitted over radio link.

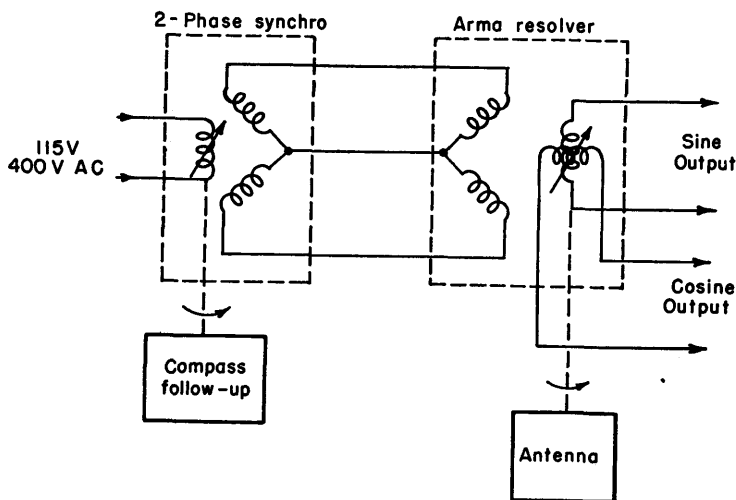


FIG. 11-4.—Synchro schematic diagram.

and cosine carriers in the decoder are not critical; rather, it is the ratio of the sine pulse displacement to the cosine pulse displacement, and the ratio of the sine-modulated voltage to the cosine-modulated voltage that are the important factors. These factors are reasonably easy to control and make possible a stable system.

A few words should be said about the radar transmitter pulse and the radar receiver video pulse, which are transmitted during the time interval between the cosine pulse and the next basic pulse (see Fig. 11-1). The video is time selected so that it will appear only during this interval;

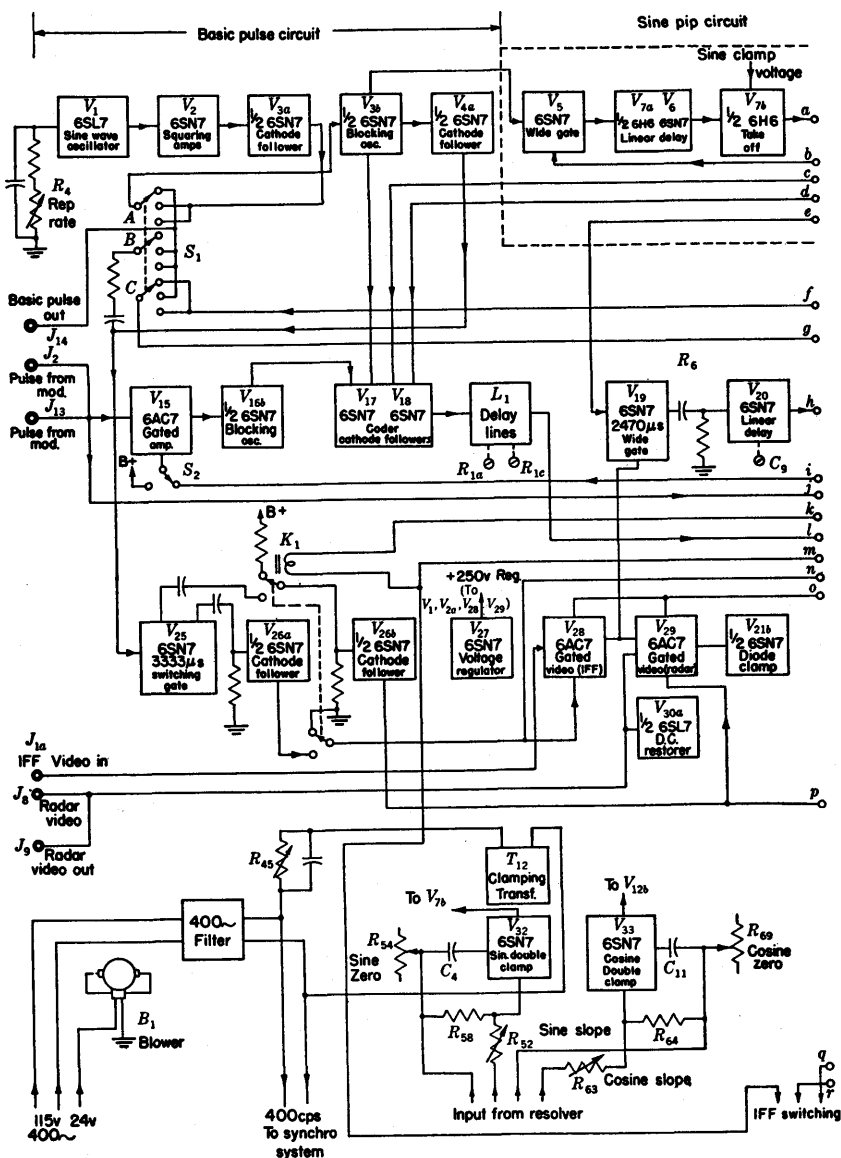
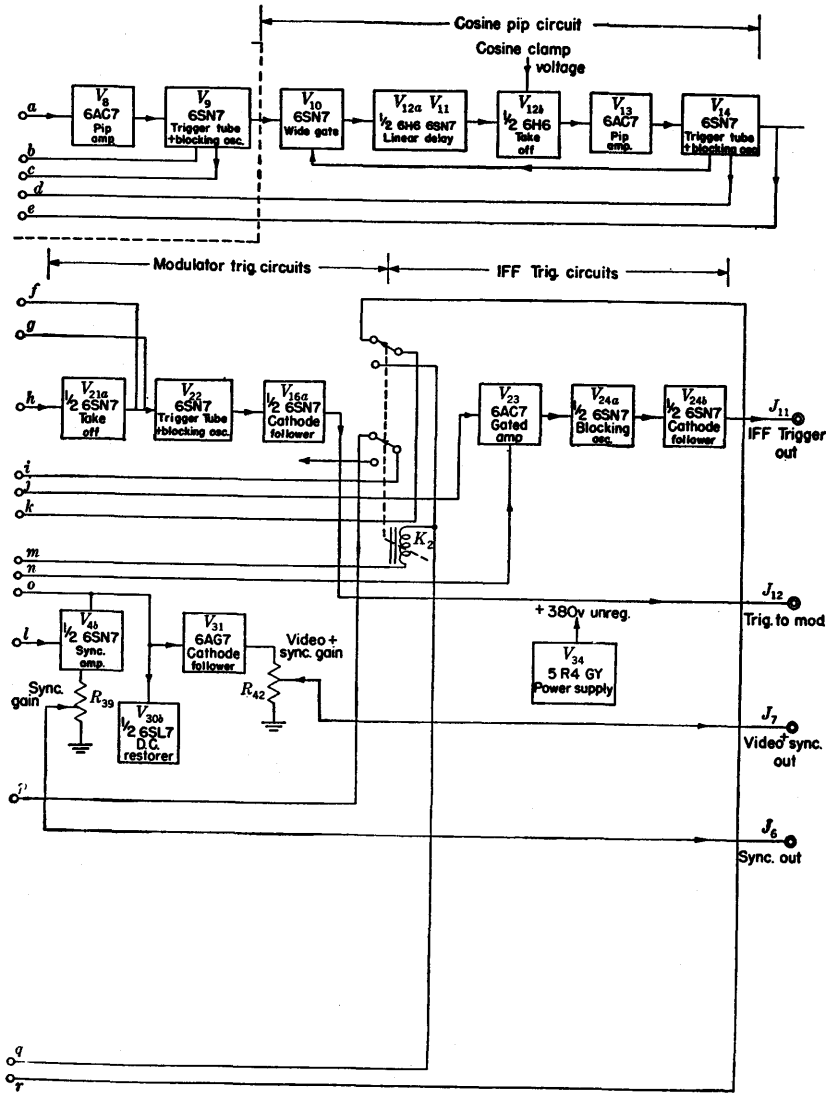


FIG. 11-5.—Block dia-



gram of synchronizer.

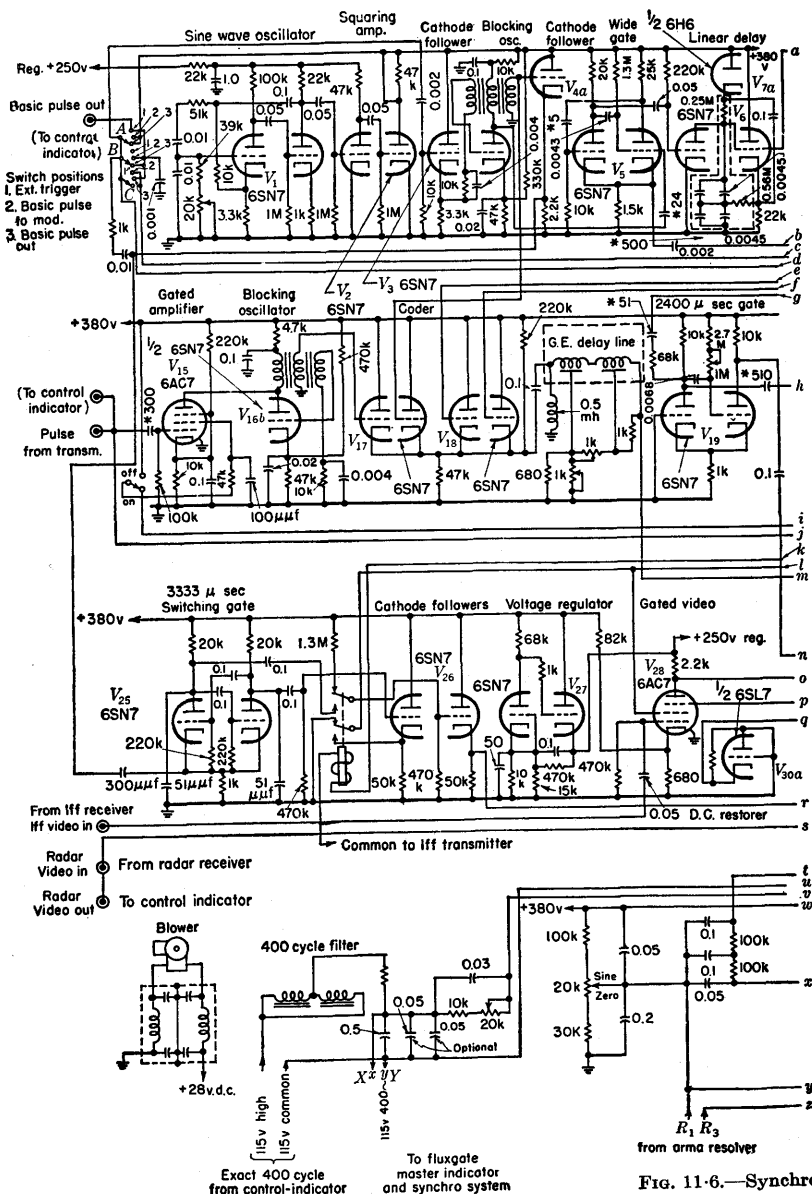
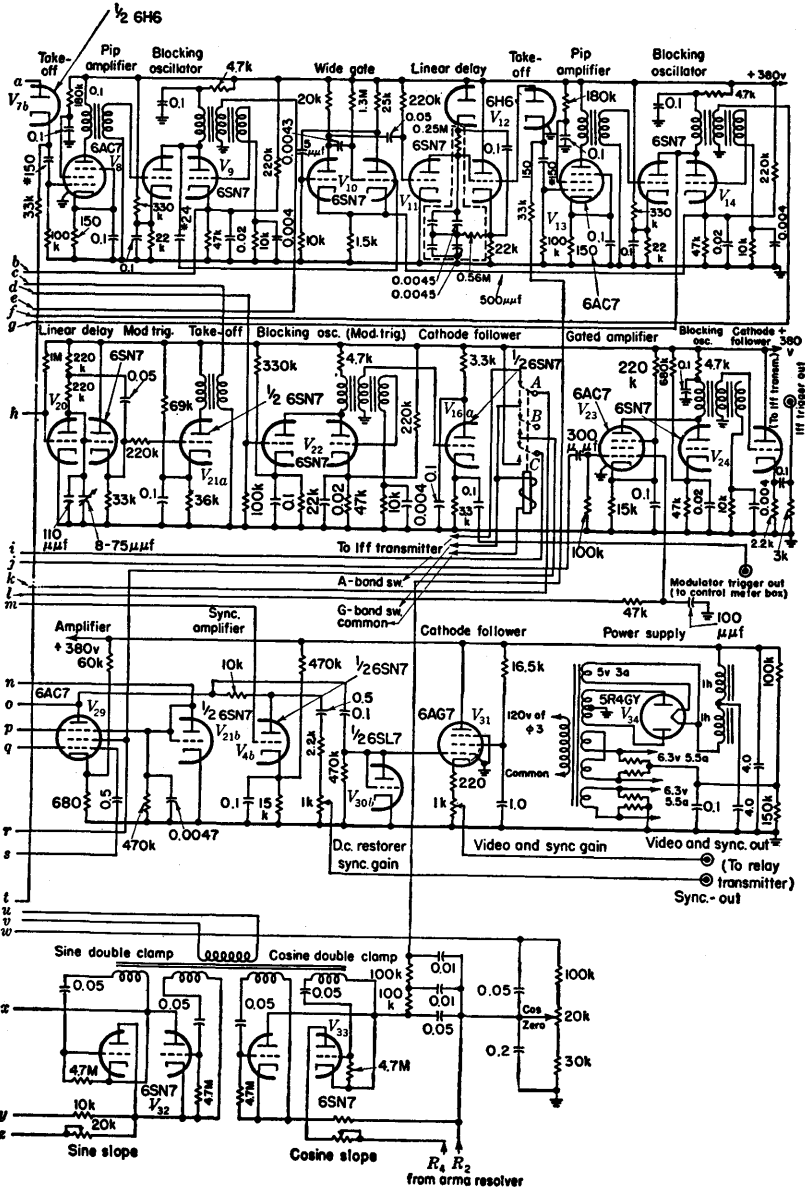


FIG. 11-6.—Synchro-



niser circuit.

otherwise it would mix with the synchronizer pulses (basic pulse, sine pulse, and cosine pulse) and cause displacements of these pulses. The time interval allowed for video corresponds to the maximum range of the radar. Figure 11.3 shows the complete signal transmitted over the radio link.

Provision is made in this system for alternating two types of video pulses (radar and beacon). The radar and beacon pulses are time-selected and applied to their respective indicators. The time-selection process is actuated by the presence or absence of the radar transmitter pulse which is absent when beacon signals are being received.

**11.2. The Synchronizer.**—The first step in angular data transmission is the conversion of angular data to electrical data. In this system the angular information to be transmitted is the position of the radar antenna with respect to true north. An Arma resolver (two-phase to two-phase synchro) mechanically geared to the antenna, acts as a differential while a second synchro (single-phase to two-phase) geared to the fluxgate compass follow-up acts as a generator. The synchros are connected electrically as shown in Fig. 11.4. The 400-cps filter gives the necessary sinusoidal waveform. This voltage is impressed on the single-phase stator of the Diehl Generator. The two-phase rotor of the generator is connected to the two-phase stator of the Arma resolver. The output alternating potentials  $A$  and  $B$  of the stator windings of the resolver consist of the sine and cosine components of the difference between the antenna direction and the compass direction. Expressed mathematically, if  $A \sin \omega t$  is the input potential to the Diehl Generator,  $\theta_1$  the angle through which the generator shaft is turned,  $\theta_2$  the angle through which the resolver shaft is turned, and both synchros have a 1-to-1 ratio throughout, then,

$$\text{Output of } A = (A \sin \omega t) \sin \theta$$

$$\text{Output of } B = (A \sin \omega t) \cos \theta$$

where  $\theta = \theta_2 - \theta_1$ .

The next step in transmitting  $\theta$  consists of phase-detecting the sine and cosine voltages from the Arma resolver and adding a constant voltage to each. This is done in the sine and cosine bidirectional switch detectors (Fig. 11.5) which produce voltages  $A \sin \theta$  and  $A \cos \theta$ . The constant voltage  $K$  is added to each so that the resultant outputs are  $K + A \sin \theta$  and  $K + A \cos \theta$ . These are the voltages that are to be converted to time intervals.

The pulse-forming circuits are the next consideration. Starting at the upper left-hand corner of the block diagram, Fig. 11.5, and the circuit diagram, Fig. 11.6, the basic pulse repetition generator produces a pulse every 3333  $\mu\text{sec}$ . The pulse starts a variable delay, (time modulator), which triggers the sine pulse generator (blocking oscillator) after a time interval

proportional to the voltage  $K + A \sin \theta$ . The sine pulse in turn starts a second variable delay, which triggers the cosine pulse generator at an interval from the sine pulse proportional to the voltage  $K + A \cos \theta$ . A 30- $\mu$ sec fixed delay started from the cosine pulse produces a trigger for the radar modulator. A small portion of the modulator pulse is sent back to trigger the transmitter-pulse blocking oscillator in the synchronizer. The basic pulse, sine pulse, cosine pulse, and transmitter pulse are mixed in the mixer, coded to prevent confusion with interfering pulses on the radio link, and amplified through two channels to give the synchronizing pulse output and the mixed video and synchronizing pulse

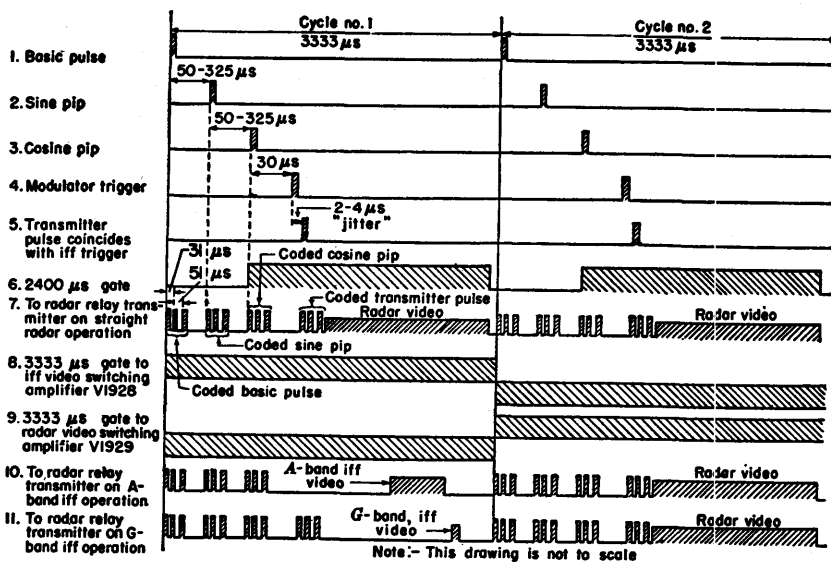


FIG. 11-7.—Synchronizer waveforms.

output. These outputs are respectively used to plate-modulate, and grid-modulate, the radio link transmitter. The two types of modulation are used because the video signal has a high duty ratio and must be sent with low peak power, while the synchronizing pulses have a low duty ratio and may be transmitted with very large peak power.

The video portion of the relay signal is the next consideration. The 2500- $\mu$ sec (200-mile) video gate is triggered from the cosine pulse, but since it has a slow leading edge, it does not reach its maximum value until after the transmitter pulse. This gate (see Fig. 11-7) prevents receiver video pulses from appearing in the relay signal except for 200 miles following the transmitter pulse. This is the interval where useful radar echos will appear. The output signals of the gated video



amplifiers are mixed with synchronizing pulses in only the grid-modulating channel so that the total peak r-f power of the video will be less than that of the synchronizing pulse.

The layout of the detailed circuit diagram follows that of the block diagram and will not be described in detail since it contains no unusual features.

**11.3. Receiving Equipment.**—The receiving equipment for the data-transmission system is known as the “decoder,” although it performs many more functions than simply unscrambling the three-pip “code” used for the synchronizing pulses. The decoder utilizes the signal from the relay receiver, consisting of synchronizing pulses and video signals, to produce a rotation synchronous with that at the transmitter and to distribute the video signals to the indicators in the desired manner.

The decoder may conveniently be divided into six parts:

1. The synchronizing-pulse separator and three-pip decoder.
2. The sequencing circuits and linear delays.
3. The time-discrimination circuits.
4. The sine and cosine modulators and bidirectional switch circuits.
5. The Arma resolver and servoamplifier.
6. The video switching and distribution circuits.

The synchronizing-pulse separator separates the synchronizing pulses from noise and video pulses. The decoder produces single pulses from three-pip-coded synchronizing pulses; these are known as “decoded synchronizing pulses.”

The decoded synchronizing pulses operate a sequence of gates and gated tubes, (time selectors) which separate the pulses and initiate linear sweeps starting with the basic pulse and the sine pulse. These sweeps are similar to those in the synchronizer time modulators at the transmitting end and are used to demodulate the sine and cosine pulses.

To obtain these voltages, some sort of tracking “loop” must be used. It consists of “step gate” tracking circuits, which follow the positions of the sine and cosine pulses and, in the process, produce sine and cosine voltages that are delivered from modulators and drivers to the Arma resolver.

The video switching and distribution circuits provide a low-impedance source of video signals for various indicators and are used to “switch” different types of video signals to the appropriate indicators whenever this type of operation is desired. These circuits will not be discussed in detail. Figures 11-8 and 11-9 are block diagrams of the decoder which may be helpful in following the operation of the circuits.

**11.4. Synchronizing-pulse Decoding Circuits.**—Refer to Fig. 11-10. The positive relay receiver output enters the decoder at a level of 1.5 volts



for video and 3 volts for synchronizing pulses through a short time constant consisting of  $C_1$  and  $R_1$ . Inverter  $V_{1a}$  inverts the signals and provides some limiting because grid current is drawn on strong input signals. The negative output of  $V_{1a}$  is passed through another short time constant ( $C_3$  and  $R_5$ ) to the grid of amplifier  $V_2$ . Positive overshoots resulting from differentiation by the short time constants are suppressed by the grid current drop through  $R_4$ . Negative signals are limited by the cutoff voltage of the tube;  $L_1$  provides some high-frequency peaking to

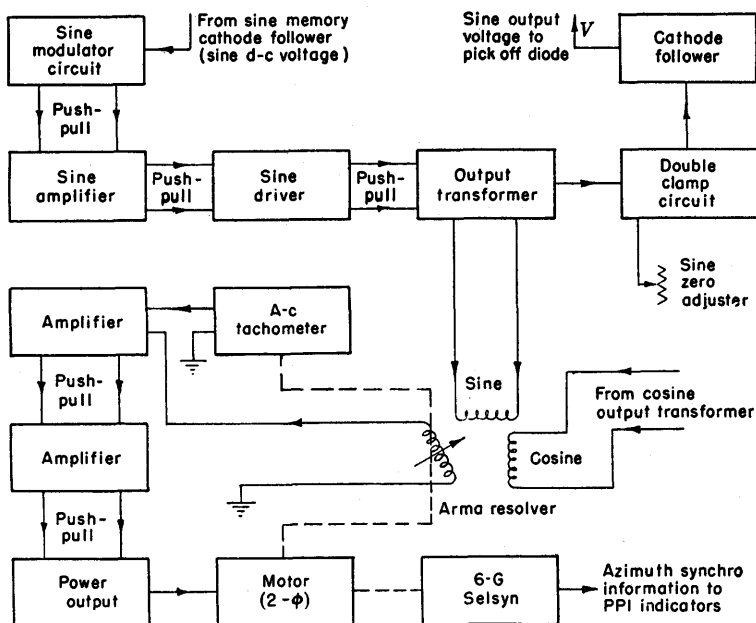


FIG. 11-9.—Sine modulator and servoamplifier circuits.

improve the shape of the synchronizing pulses. The positive limited output of  $V_2$  is impressed upon the grid of the cathode follower  $V_{1b}$ , which drives the decoding delay line.

In the above process, the relay signals have been "differentiated" twice. The purpose of this is to allow only short pulses to be passed; long pulses of interference or video signals are differentiated to form a positive and a negative spike, one of which is later eliminated. The synchronizing pulses are not appreciably affected by this operation. All signals are limited well below their peak value so that variations in signal strength will not affect the decoder operation.

Assuming that a three-pulse-coded synchronizing pulse is present at the output of  $V_{1b}$ , it remains to explain the action of the decoding delay

lines. Note that the *decoder coincidence tube*  $V_3$ , is biased so that positive signals of sufficient amplitude must be impressed simultaneously upon its control and screen grids for the tube to operate. The first pulse of the code is designated  $A$ , the second ( $3\ \mu\text{sec}$  later)  $B$ , and the third ( $8\ \mu\text{sec}$  after  $A$ )  $C$ . (Refer to Fig. 11-11.) At point  $a$ , the screen of  $V_3$ , each pulse appears with no delay. At point  $b$ , across  $R_{13}$  and  $R_{14}$ , each pulse appears delayed  $5\ \mu\text{sec}$ ; this occurs because the winding-to-shield capacitance of the  $3\text{-}\mu\text{sec}$  delay line transmits the pulses that leave the  $5\text{-}\mu\text{sec}$  line. The original pulses appear across the terminating resistor  $R_{12}$  delayed  $8\ \mu\text{sec}$ . The voltage at point  $c$  with respect to ground therefore consists of the sum of the voltage at  $b$  and that across  $R_{12}$ . Thus there is a triple-coincidence arrangement wherein the pulse potentials at  $a$ ,  $b$ , and between  $b$  to  $c$  must coincide for  $V_3$  to conduct. Eight microseconds after the first pulse  $A$  (during the last pulse of the code) a single pulse will be produced at the plate of  $V_3$ . The negative grid bias is adjusted by  $R_{15}$  to provide the proper threshold to discriminate against noncoinciding pulses and against noise. The decoded synchronizing pulses appear at the secondary of the pulse transformer  $T_1$ . Resistor  $R_3$  prevents shock-excited oscillations due to the distributed inductance and capacitance of the transformer.

**11-5. Sequencing Circuits and Linear Delays.**—Refer to Fig. 11-10. The sequencing circuits may be thought of as an endless chain of time selectors that, when operating, separates the various synchronizing pulses from each other. The input to the sequence circuits is the decoded synchronizing pulse output from  $T_1$ ; the output waveform of the sequencing circuits consists of the sine pulse, the cosine pulse, and wide gates, which are used to turn on the sine and cosine linear delays.

The chain begins with the *basic pulse gated tube*  $V_4$ . This tube is biased so that the decoded synchronizing pulses applied to the No. 1 grid will not be effective unless the voltage applied to the No. 3 grid is sufficiently positive. For a moment, let us assume that this is the case and that a positive basic pulse occurs. The plate of  $V_4$  will drop sharply, triggering the monostable multivibrator  $V_5$  which produces the *sine sequence gate*. The positive gate produced at the plate of  $V_{5b}$  is fed to the *cathode follower*  $V_{5a}$ .

This gate, the "sine gate," embraces the period of time in which the sine pulse can be expected. It is applied from the cathode follower to the screen grid of the *sine pulse gated tube*  $V_9$  (time selector) which also has positive decoded synchronizing pulses applied to its No. 1 grid. A special narrow gate is also applied to the No. 3 grid, but this can be disregarded for the moment, the assumption being made that the No. 3 grid has a fixed positive voltage. The cathode of  $V_9$  is biased positively so that the screen voltage must be considerably positive for a synchronizing pulse to be

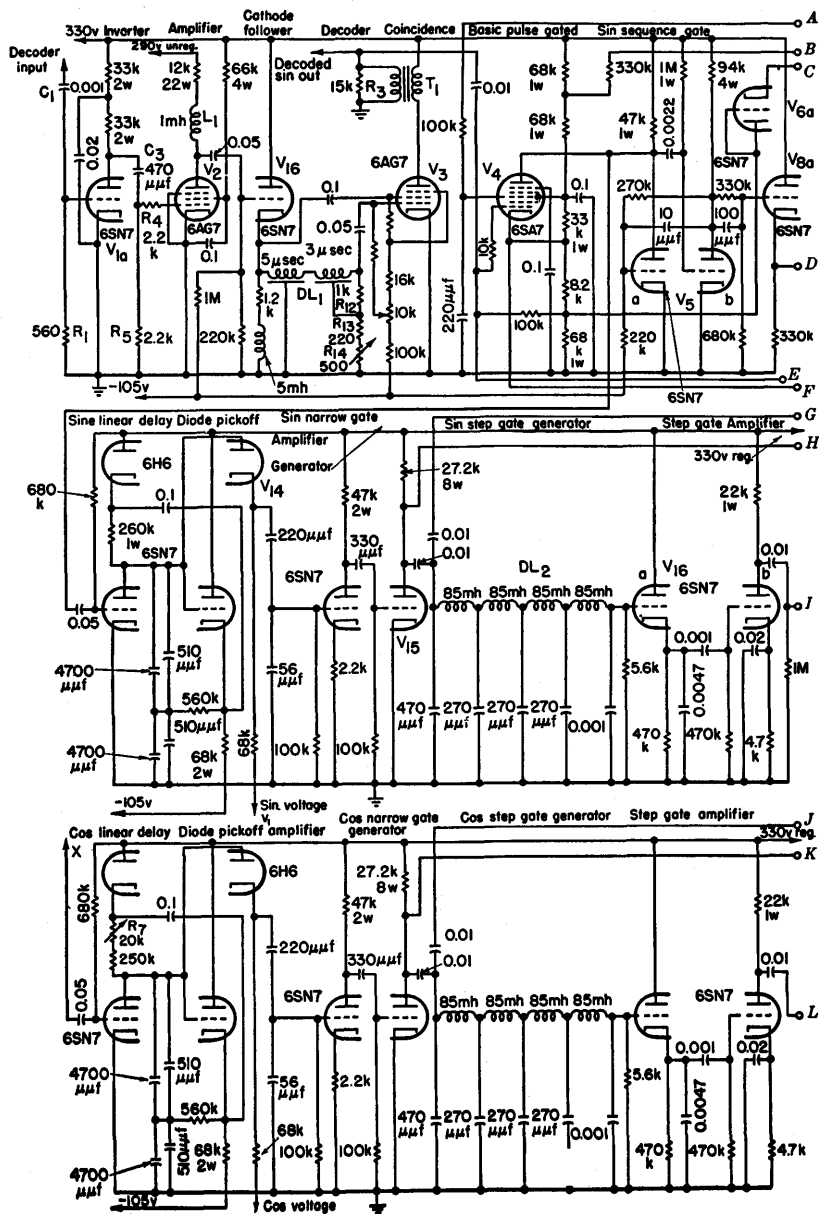


FIG. 11-10.—De-



amplified. Since the screen voltage becomes positive shortly after the basic pulse, the sine and cosine pulses and the transmitter pulse cause conduction of the tube and produce negative pulses at the plate. The sine gate lasts 600  $\mu\text{sec}$  but only the first pulse received is effective.

The first of these pulses, the sine pulse, triggers the *cosine sequence gate*  $V_{10}$ , which is exactly similar to its sine counterpart and operates in conjunction with the *cosine gated tube* to select the cosine and transmitter pulses. Since the first of these is the cosine pulse, it triggers the *video*

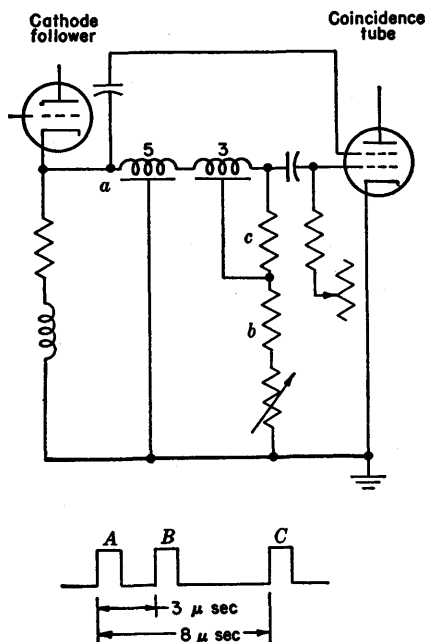


FIG. 11-11.—Decoding delay line.

*blanking gate*  $V_{12}$ , which then lasts for approximately 2500  $\mu\text{sec}$ . This gate is a monostable multivibrator similar to the sine and cosine gates, except that a *restoring cathode follower*  $V_{6b}$  is used between the plate of the "a" section and the grid of the "b" section. This is necessary because of the large duty ratio of the gate (see Chap. 5, Vol. 19 of this series). A negative gate is thus obtained from the cathode of  $V_{6b}$  which starts slightly after the cosine pulse and lasts until approximately 100  $\mu\text{sec}$  before the next basic pulse can be expected. This is equivalent to a positive gate starting 100  $\mu\text{sec}$  before the basic pulse and lasting until the cosine pulse. The gate, therefore, embraces the time interval wherein the basic sine, cosine, and transmitter pulses occur. This positive gate is applied to the

No. 3 grid of the *basic pulse gated tube*  $V_4$ , which was originally assumed to be positive at the time of the basic pulse. Thus the chain has been completed. It is impossible for the chain to operate continuously in any other manner than that just described because of the fixed limits to the motion of the sine and cosine pulses, the fixed length of the sequence gates, and the fixed repetition rate of the basic pulse.

A random interfering pulse could upset the operation for several cycles, but this action is minimized because of the action of the narrow gates, which were neglected in the preceding explanation. These narrow gates are short (50  $\mu\text{sec}$ ) positive gates applied to the No. 3 grids of the sine and cosine gated tubes  $V_9$  and  $V_{11}$ . A pulse entering the No. 1 grids of the gated tubes will not be effective unless it falls within the sine or cosine narrow gates. The method of generating these gates is explained in a later section.

The sine and cosine gates described in the preceding discussion are also used, in their negative form, to initiate *sine and cosine linear delays*. These circuits are of the bootstrap type discussed in Chap. 5 and in Chap. 6, Vol. 19 of this series. The gates, pulses, and linear delays described in this

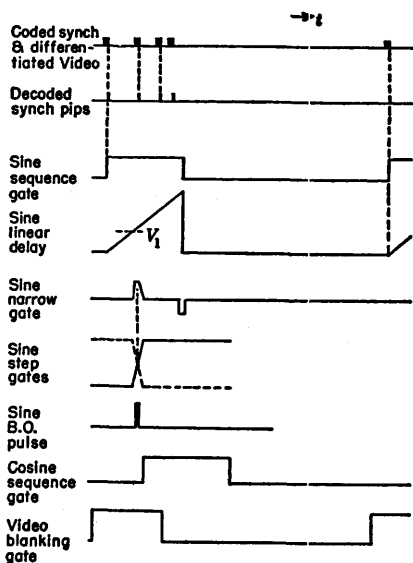


FIG. 11-12.—Timing diagram of receiving equipment.

section are shown in the timing diagram, Fig. 11-12.

**11.6. Step-gate Tracking Circuits.**—The step-gate tracking circuits are used to obtain sine- and cosine-modulated carrier voltages for the Arma resolver. Since they are exactly similar in the sine and cosine channels, only the sine circuits need be described. The production of the narrow gates previously mentioned will also be explained.

The *diode pickoff*  $V_{14b}$  of the sine linear delay is controlled by the *sine linear delay voltage*  $v_1$ . The selected portion of the sawtooth is amplified by  $V_{15a}$  and  $V_{15b}$ , the *sine narrow-gate generator*. The latter tube drives a pulse-forming delay line  $DL_2$ . A positive pulse of length determined by the delay-line constants is produced at the input to the line. This pulse constitutes the sine narrow gate, which is applied to the No. 3 grid of the *sine pulse gated tube*  $V_9$ , as previously explained. The *diode limiter*  $V_{6a}$  limits the negative excursion of the sine and cosine narrow



gates before they are applied to their respective gated tubes. The narrow-gate insertion circuit  $V_7$  is a device for "turning off" the narrow gates whenever too few cosine pulses are obtained, that is, when the narrow gates have become misplaced in time, so that the sequence gating can resume operation. The circuit of  $V_7$  is simply a cathode-follower detector, which raises the potential of the No. 3 grids of  $V_9$  and  $V_{11}$  which permits operation of the gated tubes in the absence of the narrow gates whenever the frequency of cosine pulses from the *cosine blocking oscillator*  $V_{13}$  falls below 300 pps. Since the generation of cosine pulses is dependent upon the basic pulse, sine pulse, and cosine pulse falling within the intervals determined by their selector gates, a control sensitive to improper alignment is achieved.

Since the pulse-forming delay line is terminated in a resistance less than its characteristic impedance, a pulse is produced at its end that has a leading edge halfway between the leading and trailing edges of the narrow-gate pulse, that is, at the time of the sine pulse. This pulse is "stretched"

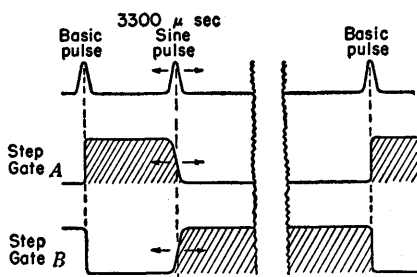


FIG. 11-13.—Timing diagram of sine-pulse step gates.

by the *step-gate generator*  $V_{16a}$ , which is a cathode-follower detector. The stretched pulse is amplified and shaped by the *step amplifiers*  $V_{16b}$  and  $V_{17a}$  to form a "step" gate having a steep edge. The *inverter*  $V_{17a}$  produces a similar gate of opposite polarity. Refer at this point to the timing diagram, Fig. 11-13, for the sine step gates. These gates are characterized by steep linear edges and

flat tops and end shortly after the closing of the sine sequence gate. As previously described the sine pulse, after passing through the sine-gated tube, initiates the cosine selector gate. The rise of the cosine gate triggers the *sine blocking oscillator*  $V_{22b}$ .

Tubes  $V_{18}$ ,  $V_{19}$  and  $V_{20}$  form a time discriminator which determines whether the sine blocking oscillator pulse occurs before or after the transition of the step-gate waveform. The memory cathode follower  $V_{21a}$  is a bootstrap-double integrator<sup>1</sup> accepting the output of the time discriminator, and its output voltage is the sine d-c voltage. It will be remembered that the sine voltage  $v_1$  is controlled by the sine d-c output so that the tracking loop is closed and step-gate transition is held in coincidence with the sine blocking oscillator pulse.

In the normal case of constant velocity rotation, the memory feature of the double integrator enables the receiving Arma resolver to continue

<sup>1</sup> See Chap. 8 and Vol. 19, Chap. 14.

rotating for a considerable time without appreciable error if relay signals are lost temporarily. It is particularly helpful when the relay signals are fluctuating or when bad interference is present. The time constant  $R_{10}$  and  $C_{10}$  is chosen small enough to permit sector scan of the radar, this topic will be discussed in a later section. The cosine time demodulator operates in a similar fashion.

**11.7. Modulators and Bidirectional Switch Detectors.**—So far, a voltage has been produced (the sine d-c voltage) which is somehow indicative of the position of the sine pulse with respect to the basic pulse, that is, of the sine of the angle being transmitted. Also, another voltage ( $v_1$ ) has been assumed, but its production has not been explained.

The end result of the sine tracking loop is the production of a 60-cps alternating voltage modulated in amplitude and reversible in phase by the position of the sine pulse. It is desired that this voltage be zero at the midpoint of the sine pulse excursion ( $185.4 \mu\text{sec}$ ), that it be a maximum at the maximum delay of the pulse ( $321.4 \mu\text{sec}$ ), and that it be a maximum in the opposite direction at the minimum delay ( $49.4 \mu\text{sec}$ ). In other words, an alternating voltage is desired which varies in synchronism with the *sine carrier voltage* from the "A" coil of the transmitting Arma resolver.

The alternating voltage is varied by the sine d-c voltage in the *sine modulator*, shown in Fig. 11-14. This consists of tubes  $V_1$  and  $V_2$ . The 60-cps input to the modulator is obtained from the transformer  $T_1$ , which supplies approximately 100 volts rms. The output signal is taken between the points labeled  $a$  and  $c$ . The grids of both sections of  $V_2$  are held at a fixed voltage determined by a divider consisting of  $R_7$  and  $R_8$ . The grids of  $V_2$  are varied, through an attenuator, by the sine d-c voltage. The actual control voltage of the modulator is the difference between these two voltages; the magnitude and direction of the alternating voltage output are determined by the magnitude and polarity of this difference voltage.

The operation of the modulator is shown in Fig. 11-15. It can be seen that the circuit is a full-wave balanced modulator that depends for its action upon the variation of  $r_p$  with  $E_g$ . It has a large amount of cathode degeneration that allows the operating level of the circuit to vary considerably.

The output current of the modulator is passed through a symmetrical twin- $T$  filter in order to eliminate the second harmonic produced as a result of nonlinear operation of the tubes in the modulator. The *sine amplifier*  $V_3$  is a push-pull voltage amplifier, which drives the *sine driver tube*,  $V_4$ . This push-pull cathode follower has the output transformer  $T_2$  in its cathode circuit. The transformer has two secondaries: one (points 6 and 7) is a low-impedance source for one stator of the receiving Arma resolver. The other winding (points 4 and 5) is a stepup





winding used to complete the tracking loop; it supplies the *sine bidirectional switch detector*  $V_5$ .

This circuit is identical with those used in the synchronizer. It charges the condenser  $C_1$  to the peak value of the sine-wave output of the

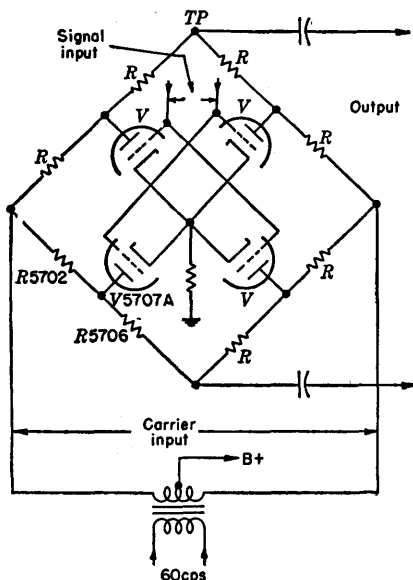


Fig. 11-15.—Simplified diagram of sine modulator.

transformer secondary, the polarity of this charge depending upon the phase of the voltage. One side of  $C_1$  is connected to an adjustable voltage set by  $R_5$ ; this provides the "zero" or base-line setting of the sinusoidal ( $\sin \theta$ ) voltage variation. Thus, we have (the voltage),  $V_1 = K' + A' \sin \theta$  which results from the rectification of the modulator output. The cathode follower  $V_6$  provides a low-impedance source of this voltage, which is returned to the sine linear delay circuit to complete the tracking loop.

It should be noted that the accuracy of modulation of the sine a-c voltage is independent of everything except the *sine zero voltage*, which is set in by  $R_5$  to match the zero value of the sine

a-c voltage with the center of the sine pulse excursion.

The cosine modulator, bidirectional switch, etc., are exactly the same as the sine circuits, the *cosine zero voltage* being set in by  $R_6$ . The slope of the *cosine linear delay*, however, is varied by  $R_7$  (Fig. 11-10) to equalize the effective "slopes" of the over-all sine and cosine loops. It will be recalled that the absolute value of the sine and cosine slopes is unimportant, but the equality of the two is critical.

**11.8. Arma Resolver and Servoamplifier.**—The sine- and cosine-modulated 60-cps voltages are impressed upon the two stator windings of the receiving Arma resolver. The output of the rotor coil is connected to the input of the servo amplifier.

In order to rotate the Arma resolver shaft, an a-c two-phase motor is geared to it through a step-down gearing. The motor is driven by the *servoamplifier*, which has what is known as "tachometer stabilization." An a-c tachometer or drag-cup generator is connected to the shaft of the motor; this device produces a 60-cps voltage having an amplitude directly proportional to the speed of rotation and a phase dependent upon the

direction of rotation. The phase of this voltage is adjusted so that it is the same as that of the error voltage. The tachometer voltage is impressed upon one grid of  $V_7$  (a double triode), and the error voltage is impressed upon the other grid. This stage is a differential amplifier, which drives another stage of voltage amplification employing  $V_8$ . This stage in turn drives the push-pull power output stage ( $V_9$  and  $V_{10}$ ). The motor excitation is taken from the secondary of the output transformer.

For equilibrium conditions to result, the motor must turn at such a velocity that the tachometer voltage will equal the error voltage in magnitude and direction. When the transmitted azimuth is constant, the error voltage is zero and the velocity is zero. The system actually oscillates, or "hunts," slightly to overcome static friction difficulties. When the antenna azimuth is varying at a constant rate, an error voltage is produced sufficient to equal the tachometer voltage produced by the speed of the motor rotation. The gain of the servomechanism is large enough so that the maximum error voltage required will represent a lag less than  $3^\circ$ . Advantages of this type of servomechanism, also known as a "velocity servomechanism," are stated in Vol. 21 Part II.

**11.9. Performance**—In relay systems in which the transmitter or the receiver is mobile a large amount of fading may occur. The receiver contains circuits for decoding the three-pulse code and applying the output on to an AGC circuit so that nearly constant signal strength is maintained. For discussion of the relay link see Vol. 1, Chap. 17, of this series.

The effects of fading are minimized by the double integration in the sine and cosine tracking circuits and by the tachometer feedback in the servo system. The narrow gates that protect the sine and cosine pulse circuits permit false triggering in a very much restricted time interval. The video blanking gate protects the basic pulse in a similar fashion. The triple coding of all synchronizing pulses and of the receiver AGC circuits<sup>1</sup> causes rejection of all single-pulse interference though this interference may overload the receiver and cause the loss of the desired signals. Occasionally several unsynchronized radars will cause interference by accidentally forming the correct code group and this can not be avoided. The effects of interference are to cause rough operation or "spoking" of the PPI. Thermal noise will pass the decoder if the signals are too weak to operate the AGC, though smooth operation has been obtained with synchronizing pulses only twice the RMS amplitude of thermal noise.

<sup>1</sup> The triple code by itself does not give sufficient protection to the AGC in the presence of many strong interfering signals. The AGC time constant must be nearly 1 sec. to prevent degeneration of signals of long duration. Interfering pulses even though they actuate the code only once each second will hold the AGC below the desired level. It has been found that considerable improvement is obtained if the AGC is derived from the cosine pulse only since this pulse is protected by the sequenced gate and its narrow gate in addition to its triple coding.

Long-time-constant smoothing of the servo system markedly reduces "spoking" of the PPI but errors are produced that distort the picture.

A long time-constant also prevents following sector scan of the antenna. A time-constant was chosen that permits  $\frac{1}{2}^\circ$  lag. Every effort was made in the design of the system so that reliable triggering of the PPI sweeps and rotation of the picture would be maintained beyond the point at which the PPI picture is so cluttered with noise and interference that it becomes unusable. The result is a highly complex and unnecessarily cumbersome system. If strong signals and freedom of interference were assured the system could be greatly simplified.

**11-10. Later Developments in Receiving Equipment.**—A significant, but incompletely tested, improvement is the d-c resolver. This unit,

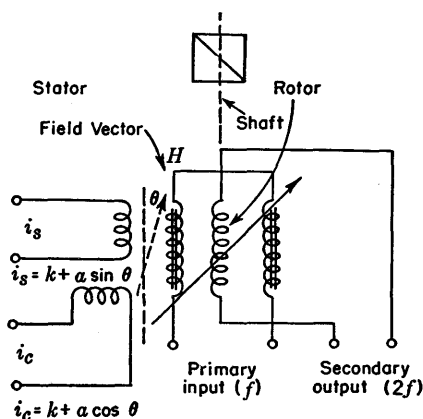


FIG. 11-16.—D-c resolver.

developed to replace the Arma resolver, operates directly from currents proportional to the sine and cosine d-c voltages. A considerable over-all saving in tubes, weight, and power is effected.

As in the Arma resolver, the d-c resolver has two stator coils at right angles to each other, which are supplied by cathode followers whose input signals are the sine and cosine d-c voltages. A resultant d-c field having the angle  $\theta$  with respect to some fixed reference is produced in the resolver. The fields produced by the separate coils vary in proportion to the currents. The vector sum of the two fields is the resultant field, which rotates in synchronism with the stabilized antenna azimuth at the sending end of the data-transmission system.

The rotor of the d-c resolver is constructed as follows. Two coils are wound over straight Permalloy laminations and placed side by side to form the primary. The secondary coil is wound over the primary coils and the complete rotor is mounted on the shaft so that the axes of the coils are

perpendicular to the axes of the shaft (see Fig. 11-16) to produce opposing fluxes and an alternating voltage of frequency  $f$  is impressed across them. The magnetic characteristics of the core are such that the operation is over the nonlinear portion of the B-H curve. Harmonics are therefore induced in the secondary pickup coil, the fundamental frequency being largely suppressed by the "bucking" action of the two primary coils.

Figure 11-17 shows the circuits that rotate the d-c resolver shaft until the secondary rotor voltage is a null. A tuned circuit consisting of the transformer  $T_1$  and  $C_1$  suppresses all frequencies of the secondary output except the second harmonic. Tube  $V_{1a}$  and  $V_{1b}$  comprise a standard

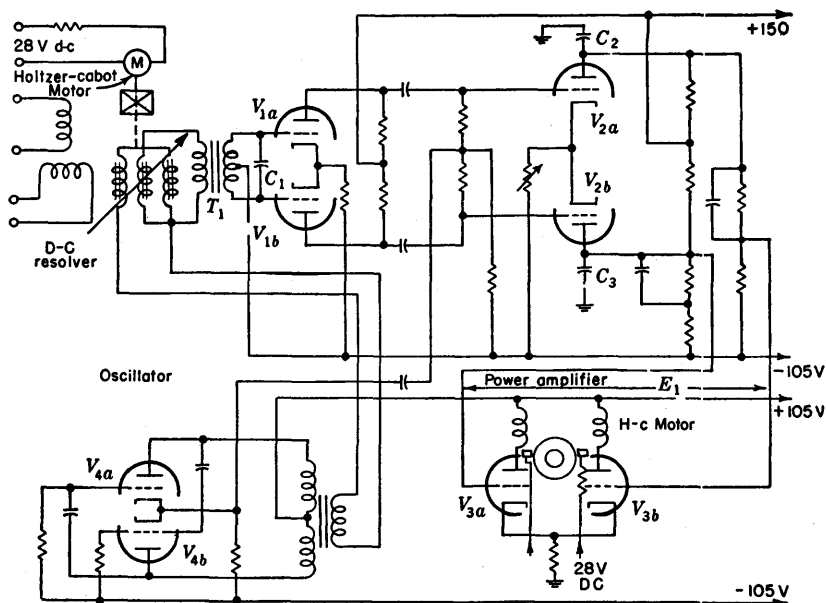


FIG. 11.17.—D-c resolver circuits.

push-pull audio amplifier. Tubes  $V_{2a}$  and  $V_{2b}$  comprise a phase-sensitive detector,<sup>1</sup> which charges the condensers  $C_2$  and  $C_3$  to the peak value of the second harmonic voltage. This detector is really a switch that is turned off and on by a synchronized second harmonic voltage from the same oscillator that supplies the resolver primaries. The switching voltage has the same frequency and phase as the rotor voltage as amplified by  $V_{1a}$  and  $V_{1b}$ . The voltage  $E_1$  is applied to the grids of  $V_{3a}$  and  $V_{3b}$ . These tubes have the split-field windings of a Holtzer-Cabot Type 0803 model B3 motor in their plate circuits (see Vol. 21, Part II). The direction of rotation depends upon the polarity of the difference current.

<sup>1</sup> See Vol. 19, Chap. 14.



The servo design has not been completely tested and the necessary stabilization circuits are omitted.

### PHASE-MODULATED PULSE SYSTEM

By E. F. MACNICHOL JR. AND E. P. COFFIN, JR.

**11.11. Introduction.**—One method of transmitting angular information between two remote stations involves the use of two sine waves having the same frequency but differing in phase.<sup>1</sup> One of the sine waves is used as a reference with respect to which the phase of the other is measured. If the phase of the second sine wave is adjusted in such a manner that the electrical phase angle measured in degrees is made equal to the angle to be transmitted, we have a definite representation of the angle by the use of two sine waves. These two sine waves having been formed at the transmitting station are now transmitted to the receiving station over separate channels by means of a radio or wire link where the phase angle of the phase-shifted sine wave with respect to the reference sine wave is detected and displayed as angular information in an appropriate manner. This method of transmission of angular information forms the basis of the capacity phase-shifter system as will be seen later.

**11.12. Pulse Representation of Phase-modulated Sinusoids.**—It is not necessary to transmit the actual sine waves themselves; instead groups

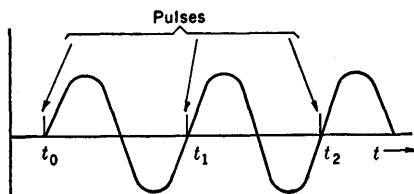


FIG. 11-18.—Simple representation of sine waves by means of pulses.

of pulses can be transmitted from which the sine waves can be reconstructed at the receiving station. The reason for doing this will become apparent later. This representation of sine waves by means of pulses can be accomplished in several ways but perhaps the simplest is shown in Fig. 11-18.

Here very short pulses of about  $1\ \mu\text{sec}$  duration are transmitted at the times  $t_0$ ,  $t_1$ ,  $t_2$ , corresponding to every other zero point of the sine wave. Since there are two zero points in each complete cycle of the sine wave, it is necessary to distinguish between them. The pulses are arbitrarily transmitted at only those zero points at which the slope of the sine wave is positive. Hence, we have a unique representation of the sine wave by

<sup>1</sup> See Chap. 10.

means of these pulses which are separated by equal time intervals. The transmission of pulses that are short compared to their spacing insures that the relative phases of the waveforms are preserved. On the other hand, if sine waves are transmitted any distortion in waveforms during transmission will produce an apparent change in phase.

At the receiving station the original sine wave must be reconstructed from the received group of pulses. One way of doing this is to let one of the pulses trigger off a pulsed oscillator—a device that produces a sine-wave oscillation whose phase with respect to the triggering pulse is always constant (see Vol. 19, Chap. 4 of this series). The frequency of this pulsed oscillator is made equal to the frequency of the original sine wave. Since the phase of the output of the pulsed oscillator is always constant with respect to the triggering pulse, it will also be constant with respect to the original sine wave. Hence, by phase shifting the output of the pulsed oscillator by means of a linear network until the zero points with positive slope of the resultant sine wave coincide with the received pulses, we can produce a sine wave that will be exactly in phase with the original one. Since it is inconvenient to adjust the frequency of the pulsed oscillator to exactly that of the original sine wave, it will be necessary to stop it every few cycles and let the next pulse restart it in order to maintain an accurate phase lock with the original sine wave.<sup>1</sup> The problem of transmitting two separate sine waves over two separate channels has been reduced to that of transmitting two separate groups of pulses over two separate channels. The next section shows these two groups of pulses can be transmitted over a single channel without any confusion.

**11-13. Discussion of Phase-shifter System.**—A timing diagram of the system is shown in Fig. 11-19, and a block diagram in Fig. 11-20.

A “basic” pulse is generated by a blocking oscillator whose repetition period is  $T$ . This pulse triggers off a 16 kc/sec pulsed oscillator. The output sinusoid of this pulsed oscillator is then shifted in phase by means of a phase-shifting condenser<sup>2</sup> by an amount equal to the angle to be transmitted so that any transients have had time to die out, pulses are formed at every other zero point of the phase-shifted sine wave as described above for four complete oscillations. There is now a group of four equidistant pulses. After several more cycles, the pulsed oscillator is turned

<sup>1</sup> If a stable PRF were available at the transmitter the phase-shifted oscillations could be produced at a multiple of this frequency. The comparison with the basic pulse is performed in a manner similar to that used in the British Omnidirectional Beacon (Chap. 10) and in the direct-reading Loran indicator (Chap. 4). Having an accurate PRF at the receiver would permit the use of very narrow gates to protect the basic pulse, indicator trigger, and AGC from interference.

<sup>2</sup> See Chaps. 4, 5, 6, and Vol. 19, Chap. 4.

off and is then retriggered by the next basic pulse and the whole process repeats. These pulses plus the original "basic" pulse are then transmitted over a single channel to the receiving station where they are converted into angular information by the following method.

When the basic pulse is received it triggers a pulsed oscillator that is identical with the one in the transmitter. The output waveform is shifted

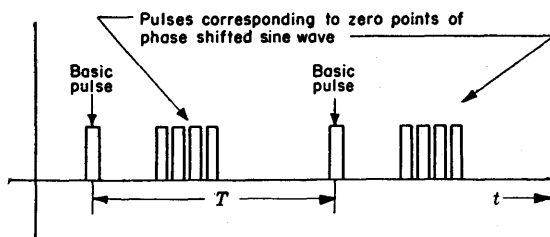


FIG. 11-19.—Operation of phase-shifted pulse system.

in phase as in the transmitter by means of a phase-shifting condenser. The phase-shifted sine wave is then compared with the group of four pulses as they are received and caused to track them in a manner analogous to the process of automatic time demodulation (see Chap. 8).

*Details of the Transmitting Equipment.*—A circuit diagram of the synchronizer is shown in Fig. 11-21. The system trigger is simulated

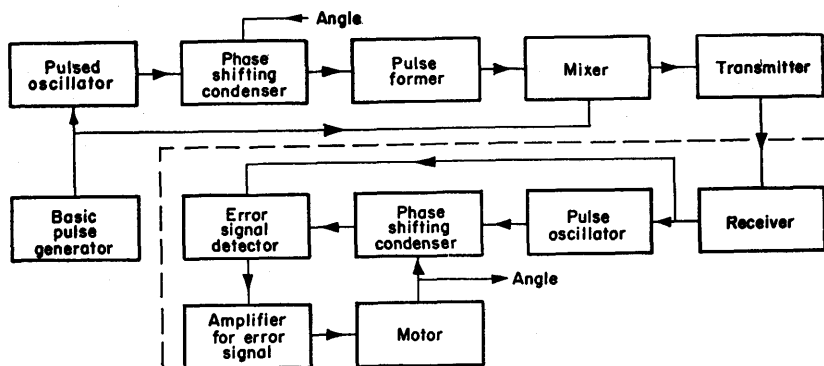


FIG. 11-20.—Block diagram of phase-shifted pulse system.

by the blocking oscillator  $V_{1a}$ . The overshoot of the trigger is applied to the output pulse blocking oscillator  $V_{12a}$  through the amplifier  $V_{12b}$ . A  $1\text{-}\mu\text{sec}$  pulse is formed which is applied to the coding network through the cathode follower  $V_{10b}$ . The network is similar to that used in the sine-cosine system and forms a triple code with  $3\text{-}\mu\text{sec}$  and  $5\text{-}\mu\text{sec}$  spacing. The cathode follower  $V_{13}$  applies the code group to the transmitter through a terminated cable. A negative gate is produced by the gate



multivibrator  $V_2$ . A negative gate is produced which allows the pulsed oscillator  $V_3$  to operate for approximately 8 cycles. The pulsed wave train is applied directly to one plate of a phase-shifting condenser that rotates with the antenna. The wave train is also applied to the phase splitter  $V_4$  thereby advancing the phase  $120^\circ$  and then to  $V_5$ , which advances the phase another  $120^\circ$ . The output wave form of the phase splitters are applied to the other inputs of the phase-shifting condenser so

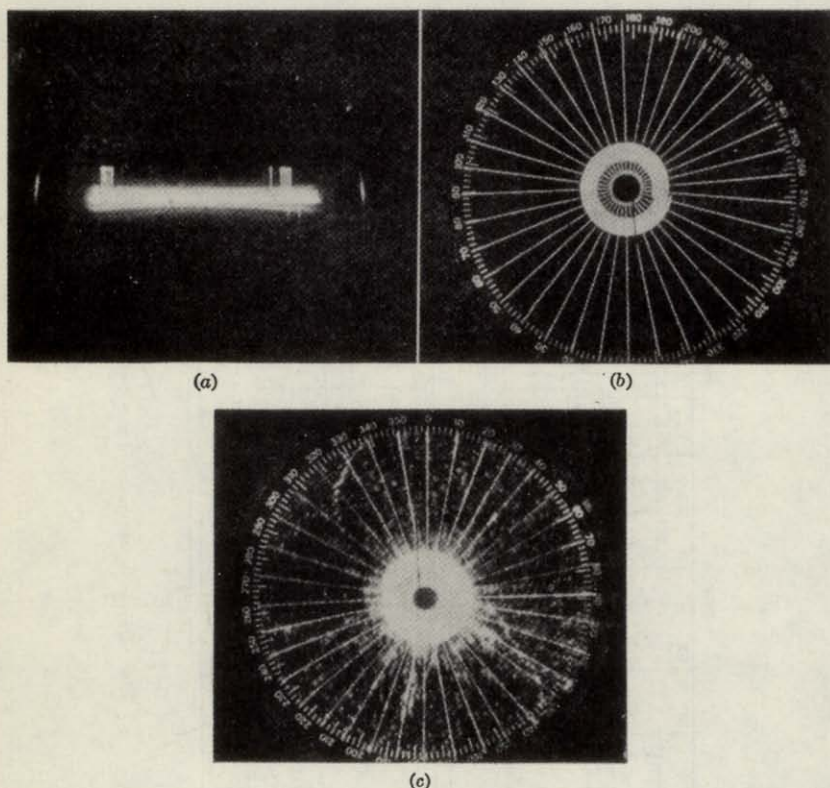


FIG. 11.22.—Phase-shifted pulse system performance.

that a rotating electrostatic field is set up. The phase-shifted output of the condenser is amplified by  $V_6$  and negative half-cycles selected by  $V_{7a}$  are amplified by  $V_{7b}$ , and differentiated by the transformer. The negative gate from  $V_2$  is also applied to  $V_{8a}$ , which initiates a positive sawtooth waveform. The differentiated pulse derived from the phase-shifted wave train is applied to the control grid of  $V_{11}$ . Four pulses are selected by the gate from  $V_9$  which is supplied to the suppressor grid of  $V_{11}$ . The gate is initiated by adding the pulses from the transformer to the sawtooth wave

from  $V_{3a}$  and passing the sum through the amplitude selector,  $V_{3b}$ . The gate is initiated by the third phase-shifted pulse, which, when added to the sawtooth, appears in the output of the amplitude selector. The gate selects the fourth, fifth, sixth, and seventh pulses, which are accurately spaced because the transients have disappeared from the pulsed wave train by the time they are produced. The selected pulses are applied to  $V_{12a}$  and coded in a manner identical to the basic pulse. Figure 11-22<sub>a</sub> shows the appearance of the group of pulses after they have passed through the relay link.

*Details of Receiving Equipment.*—The output of the receiver is taken from a 70-ohm terminated cable at 3 volts peak as shown in Fig. 11-23. It is amplified by  $V_{1a}$  and the video signal is applied to the indicator through  $V_{20}$ . The synchronizing pulses are amplified by  $V_2$  and differentiated by the inductance in the plate circuit. They are further amplified and limited by  $V_3$  and applied to the decoding line. The first two pulses are added on the grid of  $V_4$  and the third pulse drives the screen positive. If the code is correct a pulse appears in the plate circuit and is inverted by the transformer. It is amplified by  $V_5$  which triggers the multivibrator  $V_6$ . Tubes  $V_6$ ,  $V_7$ ,  $V_8$ , and  $V_9$  form a pulsed oscillator phase-shifter circuit which is identical to that in the synchronizer. The output waveform of the phase shifter is amplified by  $V_{10}$  and  $V_{11}$  and applied to the grids of the phase discriminator (phase-sensitive detector)  $V_{12}$ . The pulses that are present in the output of the decoding circuit when the pulsed oscillator is running are selected by  $V_{14}$  and fire the blocking oscillator  $V_{13a}$ . The output of the blocking oscillator is applied to the plates of the phase detector. If the received pulses overlap positive half-cycles of the phase-shifted wave train, the memory circuit of the detector will charge positively. If they overlap negative half-cycles they will charge negatively. The output of the detector is applied as an error signal to the servomechanism, which drives the phase shifter so that the received pulses are always coincident with the zero point of the sine wave. An unusual type of servomechanism is used. With the selector switch  $S_1$  in Position 1 it operates in a conventional manner. The error signal is modulated at 60 cps by a Brown Converter. The modulated carrier is filtered by  $V_{16}$  which is a form of Wien bridge oscillator with gain too low to sustain oscillation. The positive feedback loop of the Wien bridge occurs from the plate of  $V_{16a}$  through a series RC-combination to the grid of  $V_{16b}$ . A shunt RC-combination is in parallel with this grid. The loop is completed back to  $V_{16a}$  through the common cathode resistor. (This selective circuit should be replaced by a twin T feedback selective amplifier. See Vol. 18, Chap. 10.) The filtered output is amplified by  $V_{17}$ ,  $V_{18}$ , and  $V_{19}$  and applied to one phase of a Diehl 2-phase motor. Stabilization is supplied by the "phase advance" circuit  $V_{15b}$  which passes



high-frequency components of the d-c error signal without attenuation and provides large attenuation for the low-frequencies.

When the selector switch is in Position 2 a circuit with the following properties is activated. The servomechanism when presented with information will "learn" the rate at which it must follow that information in a time which is adjustable. If the signal disappears it will "remember" this rate for an adjustable time which can be made very long. In effect this circuit provides smoothing of rotation, which is readily adjustable to fit different operating conditions. The results are achieved qualitatively as follows. Tube  $V_{21a}$  provides a capacitance in the grid circuit which is amplified by the gain of the tube. This capacitance, which is much larger than could be conveniently obtained with a real capacitor having small leakage, constitutes the "memory." Tube  $V_{22}$  provides "phase advance" for stabilization and tachometer feedback is used so that the rate at which the motor turns is proportional to the potential at the cathode of  $V_{22}$ . As the pulses move an error signal is produced across the "memory" circuit. The motor turns at a speed that keeps this small misalignment constant. If the signal fades, charge is stored in the memory circuit causing the motor to continue to turn at the same speed until the signal reappears or until leakage discharges the memory circuit. This is a form of double-integrator system and has basic properties similar to those of Chap. 8.

Competitive tests have indicated that the phase-shifter system operated as well as the sine-cosine system in the presence of noise and interference in spite of the fact that the phase-shifter system was not protected by a PRF selector or narrow gates although these could be added with little difficulty. Also, the number of components is smaller and the construction is simpler than with the sine-cosine system.

It is not necessary for the frequencies of the pulsed oscillators in the transmitting and receiving system to be exactly equal since they are restarted every PRF cycle. Differences as great as 10 per cent appear to have no effect; thus the tuned circuits for these oscillators may be factory preset. The phase-shifting bridges are aligned by means of a dummy condenser, having no rotor plate, which is built into the system. This alignment is the only one that is necessary and corresponds to the zero and slope adjustments of the time modulators in the sine-cosine system.

Typical performance is shown by the photographs of the PPI of the receiving system in Fig. 11-22b. Angle marks of  $10^\circ$  spacing have been transmitted over the link in place of video signals. Comparison of the marks with the illuminated protractor indicates the cyclic error, which has a peak amplitude of  $\pm 4^\circ$ . Figure 11-22c shows the performance of the system in the presence of strong unsynchronized pulse interference.



## SIMPLIFIED RELAY RADAR SYSTEM FOR CONSTANT-SPEED ROTATION

By E. F. MACNICHOL, JR.<sup>1</sup>

**11.14. Introduction.**—The system to be described is suitable for point-to-point operation where fading is not encountered and where the antenna of the radar rotates at nearly constant speed so that it is unnecessary to transmit the antenna position at one-speed. As shown in Fig. 11.24 the radar transmitter pulse initiates a series of synchronizing pulses in the codes. This code group is delayed 10  $\mu$ sec with respect to the transmitter pulse and occupies an interval of 22  $\mu$ sec. The use of this interval by the synchronizing pulses results in the suppression of the first 30  $\mu$ sec of video

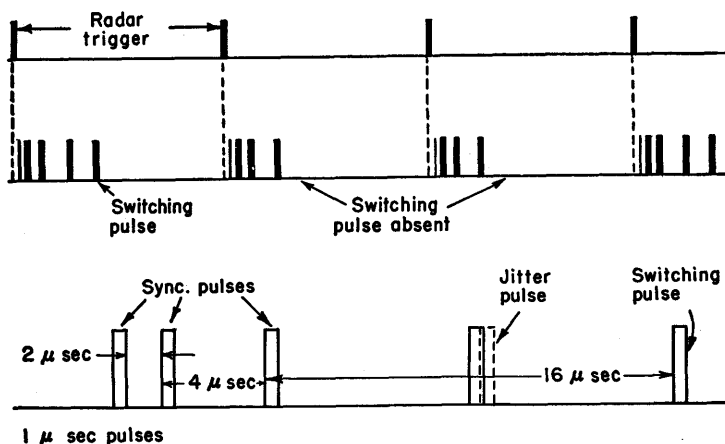


FIG. 11.24.—Information pulses.

signals from the radar. In practice this interval is filled solidly with "ground clutter," thus the loss is not serious. The first three pulses in the group, spaced 2 and 4  $\mu$ sec apart, form a code to protect the indicator trigger and the information pulses. The fourth pulse is jittered its own width by an alternating-current signal derived from an alternator rotating in synchronism with the antenna.

The frequency produced by the alternator is 60 cps when the antenna is turning at 4 rpm. The alternator frequency is therefore proportional to the antenna speed. A switching pulse is produced 16  $\mu$ sec after the occurrence of the third pulse in the code. This pulse, which appears every third cycle of the PRF, operates an electronic switch that inserts video signal from another radar into the relay link. Thus the link can be used to transmit video signals from two separate radar sets. The video signals, synchronizing pulses, and range and angle marks are combined in the

<sup>1</sup> Based on material contributed by L. Bess.

video mixer and transmitted. The received signals are decoded, supplying a trigger for the indicators after the third pulse. The jittered pulse is time-demodulated and the resulting a-c signal is filtered, amplified, and used to drive a synchronous motor, which rotates at the same speed as the alternator driven by the antenna. The motor drives a synchro system through a gear reduction. The synchro system rotates at the same speed as the antenna. Alignment between the radar picture and the relayed picture is accomplished manually with reference to the angle marks that are transmitted along with the video picture. Once alignment has been achieved it is maintained by the system.

**11-15. Details of the System. *Coder.***—Refer to Fig. 11-25. The positive radar system trigger is applied through  $S_1$  and inverted by  $V_{5b}$  to trigger the delay multivibrator  $V_1$ . The 10- $\mu$ sec rectangle produced by  $V_1$  is differentiated by  $T_1$  and the pulse formed by the trailing edge triggers the blocking oscillator  $V_{2a}$  which produces a 0.75- $\mu$ sec pulse. This pulse is delayed by  $L_1$  and retriggers  $V_{2a}$  through  $V_{2b}$  after 2  $\mu$ sec. Blocking bias is built up across  $C_4$  after these two pulses so that  $V_{2a}$  will not retrigger after the second pulse. The output from the cathode of  $V_{2b}$  is delayed by  $L_2$  and triggers  $V_{3a}$  which produces another 0.75- $\mu$ sec pulse. The negative sawtooth voltage in the bias circuit of  $V_{3a}$  operates the switch tube  $V_{3b}$  initiating a positive sawtooth voltage in the plate circuit. The amplitude selector  $V_{4a}$  triggers blocking oscillator  $V_{4b}$  after a delay determined by the cathode bias of  $V_{4a}$  and the slope of the sawtooth waveform. The bias voltage is modulated by the output of the alternator which is geared to the antenna. This alternator is a size-1 synchro with d-c excitation on the rotor. Its output potential is amplified by  $V_{5a}$ . Thus the pulse from  $V_{4b}$  is delayed 8  $\mu$ sec and time-modulated  $\pm 0.5$   $\mu$ sec. The pulse from  $V_{3a}$  synchronizes the 3 to 1 frequency divider  $V_7$  through the cathode follower  $V_{7a}$ . The output of the divider is transmitted to the switching circuits in the video-mixing unit through  $V_{8a}$ . The negative pulse in the plate circuit of  $V_{8a}$  travels down  $L_4$  and is reflected back as a positive pulse after 16  $\mu$ sec when it retriggers  $V_{4b}$  through  $V_{5b}$ . The current pulses from the cathodes of  $V_{2a}$ ,  $V_{3a}$ , and  $V_{4b}$  are mixed and applied to the grid circuit of  $V_6$ , which is a blocking oscillator that produces accurately rectangular pulses of 20 volts amplitude and 1  $\mu$ sec duration with rise and fall times of 0.1  $\mu$ sec across the 75-ohm terminated output cable. This circuit is designed to have very rapid recovery so that it can be triggered by all the pulses in the group. The line  $L_3$  is used to determine the duration of the output pulses that are transmitted to the video mixing unit.

***The Video Mixing Unit.***—Refer to Fig. 11-26. The two video inputs are applied to the "a" section of the mixing tubes  $V_2$  and  $V_3$ . Tubes  $V_{1a}$  and  $V_{1b}$  are d-c restorers. The respective angle marks are applied to the

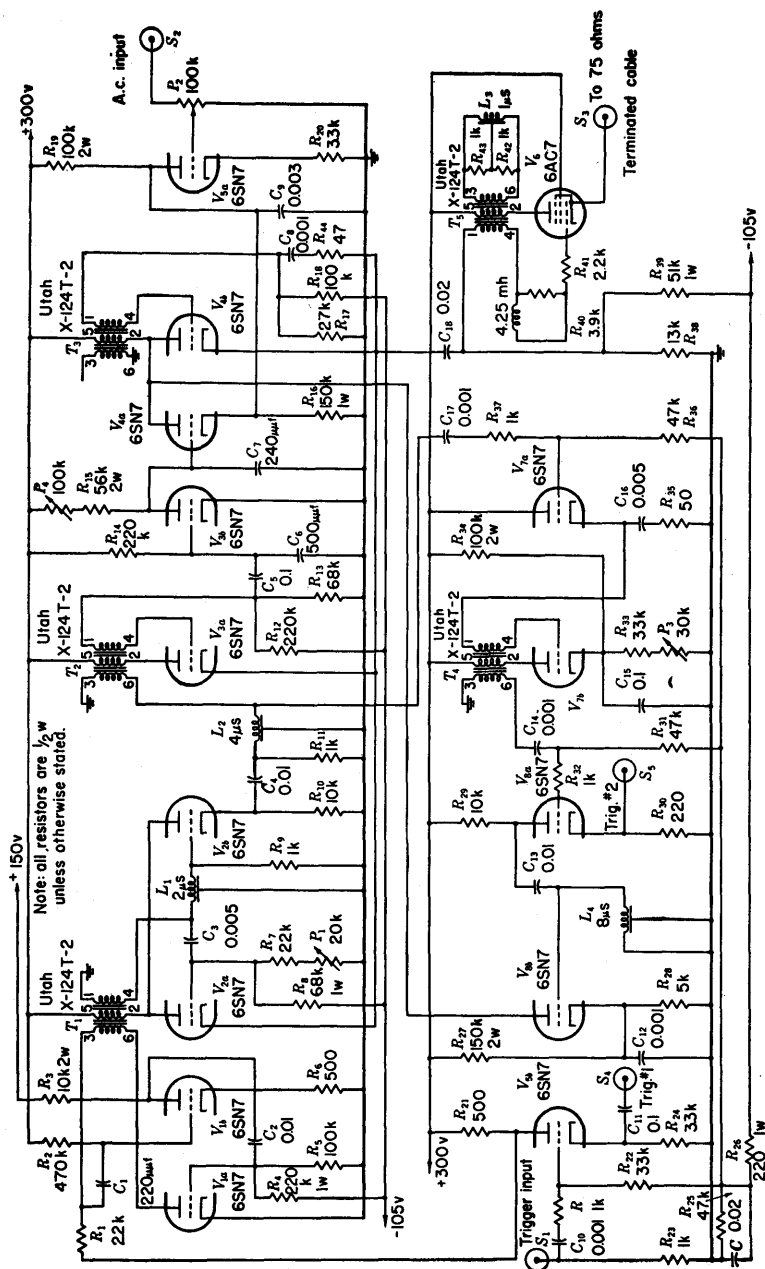


Fig. 11-25.—Coder of simplified relay radar.

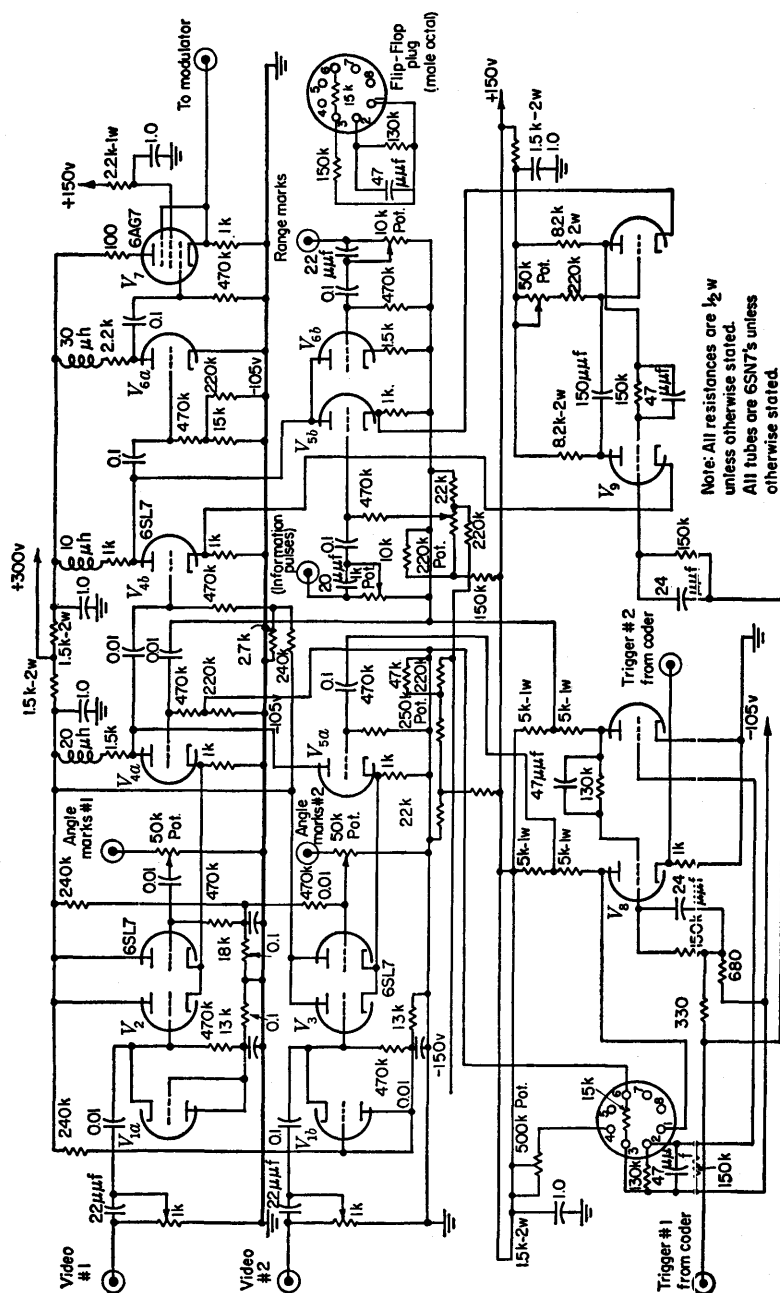


Fig. 11-26.—Video mixing unit of simplified relay radar.

"b" sections. The cathodes of  $V_2$  and  $V_3$  are connected to the cathodes of the time selector tubes  $V_{4a}$  and  $V_{5a}$  respectively. These tubes have a common plate circuit. The bistable multivibrator  $V_8$  (scale of 2) switches the grids of  $V_{4a}$  and  $V_{5a}$  so that video current from one input circuit or the other, but not both, will reach the plate circuit. The multivibrator is triggered on the grid of the "a" section by the trigger pulse from the coder, and on the cathode by the switching pulse. When the switching pulse is present the video signal from input 2 is transmitted; when it is absent the video signal from input 1 is transmitted since the "a" section is held off by trigger 1 applied to the cathode. The common output current of  $V_{4a}$  and  $V_{5a}$  is applied to the grid of  $V_{4b}$ . A time-selective switching circuit is formed by  $V_{4b}$  and  $V_{5b}$  which have a common plate circuit. The synchronizing pulses are applied to the grid of  $V_{5b}$  while the cathodes of  $V_{4b}$  and  $V_{5b}$  are switched by the monostable multivibrator  $V_9$ . A gate, which lasts about 35  $\mu$ sec, is formed after the input trigger and permits synchronizing pulses to reach the output circuit. At all other times the selected video signal is applied to the transmitter. Range marks are mixed with the video through  $V_{6b}$ . The mixed output is applied to the transmitter through the amplifier  $V_{6a}$  and cathode follower  $V_7$ .

*The Decoder.*—Refer to Fig. 11-27. Positive 2-volt signals from the relay receiver are passed through a  $1\frac{1}{2}$ - $\mu$ sec time-constant and applied to the grid of  $V_{1a}$  which is initially conducting since  $V_{11b}$  is cutoff. The short time-constant removes long interfering pulses that would otherwise operate the decoder. The pulses are amplified to 8 volts and applied to the grid of the limiter  $V_2$  which cuts off at -4 volts, yielding an output of +70 volts. The pulses are applied to the grid of  $V_{3a}$  which drives  $L_1$ . Part of each pulse is delayed by  $L_1$  and part appears directly in the output across a 430-ohm resistor. When the correct code group is transmitted the delayed first pulse adds to the undelayed second pulse to overcome the bias on the grid of  $V_3$ . The output pulse of  $V_3$  is delayed by  $L_2$  and appears on the cathodes of  $V_4$ . If the grids of the two sections of  $V_4$  are at the same potential, equal and opposite fluxes are set up in the transformer and no output appears. If  $V_{4a}$  is cut off by the third pulse in the code group appearing in the plate circuit of  $V_{3a}$ , an unbalanced current will be produced in the transformer; and a voltage, induced on the grid of  $V_{5a}$ , will initiate regeneration. This tube acts as a blocking oscillator and produces a trigger for the indicators. The grid-bias waveform cuts off the switch tube  $V_{5b}$  and starts a sawtooth waveform. The amplitude selector  $V_{6a}$  fires the blocking oscillator  $V_{6b}$  after an 8- $\mu$ sec delay. The cathode pulse is delayed by  $L_3$ , amplified by  $V_{7a}$ , and fed back to terminate the pulse. Two 1- $\mu$ sec rectangular gates separated by 1  $\mu$ sec are produced by  $V_{6b}$  and  $V_{7a}$ . These gates are applied to the grids of the time selectors  $V_{8b}$  and  $V_{8a}$  respectively. The "jittered" pulse containing the



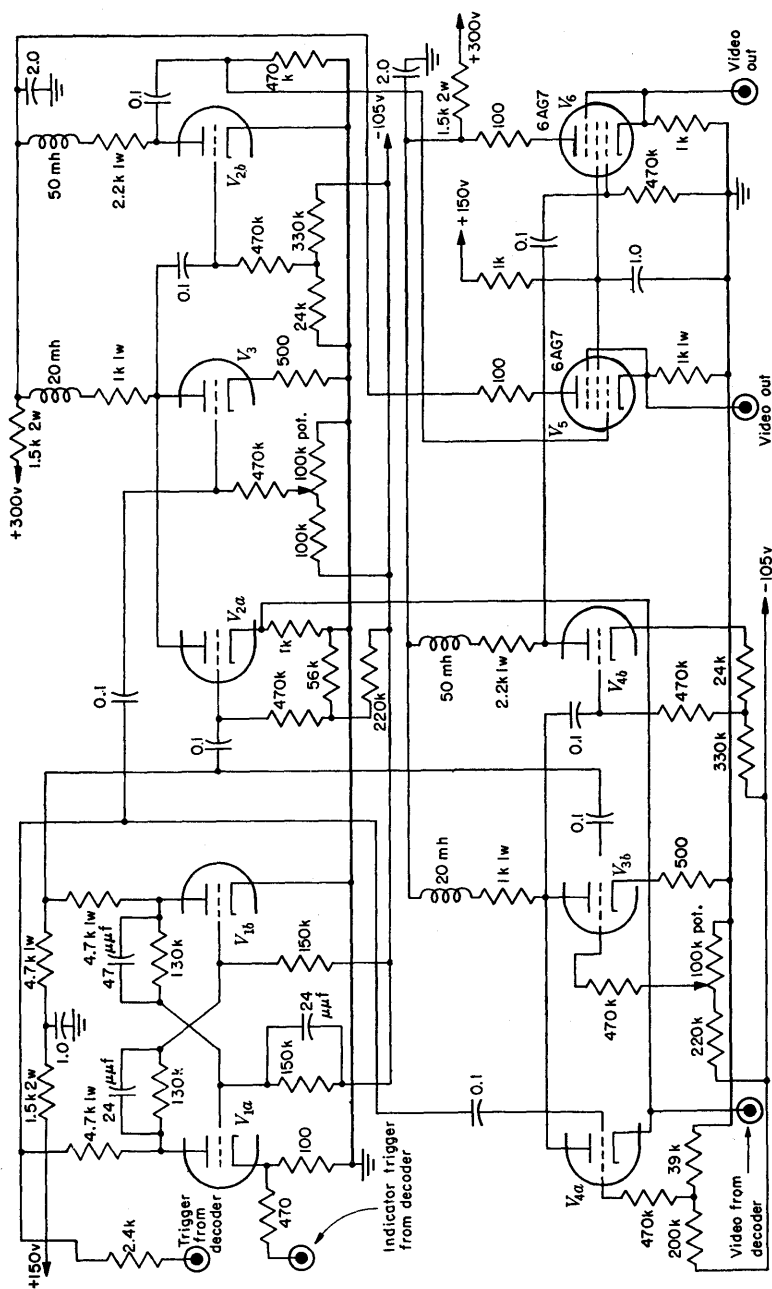


Fig. 11-28.—Video separator of simplified relay radar.

angular information is applied to the cathodes of  $V_8$  from the plate of  $V_{3a}$ . It occurs during the interval occupied by the gates. The output pulses from the plate circuits of  $V_8$  are applied to the difference detector  $V_9$  which reproduces the original waveform of the transmitting alternator. Thus, the original alternating current has been converted to a time-modulated pulse, transmitted, and time-demodulated. The output of  $V_9$  is transmitted to the angle information generator through the cathode follower  $V_{10a}$ .

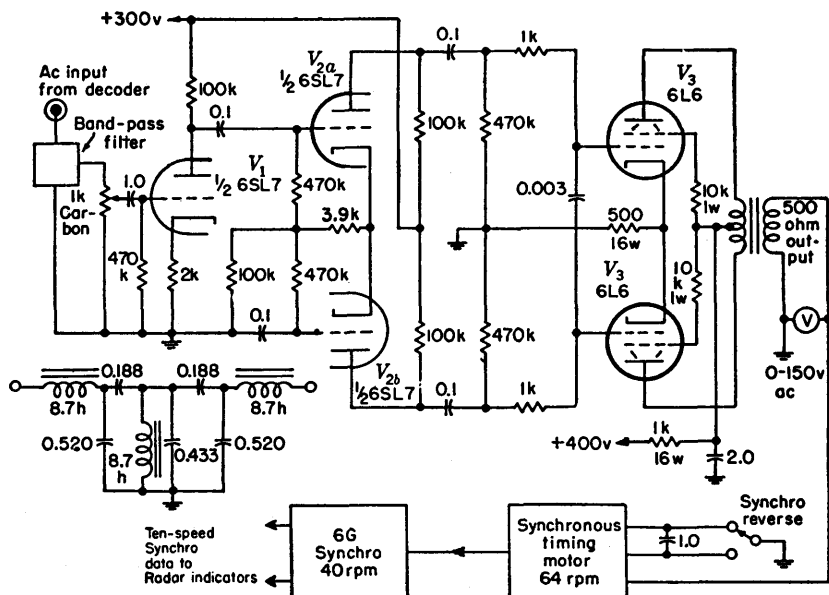


FIG. 11-29.—Angle information generator for simplified relay radar.

In order to prevent video pulses that accidentally have the correct code spacing from actuating the decoder a suppression circuit is used. The decoded pulse from  $V_{3a}$  is applied to  $V_{12a}$ . The negative pulse in the plate circuit travels down  $L_5$ , is inverted by the short circuit, and appears as a positive pulse on the grid of  $V_{10b}$  16  $\mu$ sec later. It is delayed another 2  $\mu$ sec and triggers  $V_{11}$ , a monostable multivibrator, producing a 3000- $\mu$ sec gate, which cuts off  $V_{1a}$  during the video period. Tube  $V_{1b}$  is a pedestal-removing tube that does not appear to be altogether necessary.

The video switching pulse is selected by  $V_{12b}$ . The decoded trigger pulse appears on the grid of the tube after a 16- $\mu$ sec delay. If the switching pulse appears on the cathode it must occur at this time. The output waveform of  $V_{12b}$  is transmitted to the video separator unit.



*The Video Separator.*—Refer to Fig. 11-28. Negative video signals are applied to the cathodes of  $V_{2a}$  and  $V_{4a}$  of the video separator from  $V_{7b}$  in the decoder. The switching waveforms on the grids are derived from the bistable multivibrator  $V_1$  which operates in a manner identical to that in the video mixer. Tube  $V_{1a}$  is turned off by the indicator trigger and turned on by the switching pulse when it appears. Tubes  $V_{3a}$  and  $V_{3b}$  are pedestal-removing tubes, which draw the same quiescent currents as  $V_{2a}$  and  $V_{4a}$ . The output signals of channel 1 is amplified by  $V_{2b}$  and applied to the output line by  $V_5$ . Video 2 is handled similarly by  $V_{4b}$  and  $V_6$ .

*The Angle Information Generator.*—Refer to Fig. 11-29. The demodulated a-c from the decoder is applied to a bandpass filter having a pass band of 30 to 90 cps. This filter permits a variation in antenna speed of 2 to 6 rpm. The output is amplified by a conventional audio amplifier  $V_1$ ,  $V_2$ ,  $V_3$ ,  $V_4$  and applied to a synchronous clock motor which rotates the synchro that drives the indicators.

Tests of the system have shown that it will operate satisfactorily in the presence of a reasonable amount of pulse interference without appreciable drift of the pattern for a period of several hours. It is simpler to align, operate, and maintain than the systems previously described since the wave shape of the output pulse is not critical and slight maladjustment of the time modulator and demodulator has negligible effect due to the fact that data are transmitted at 900-speed ( $\frac{1}{3}^\circ$  per turn).

### C-W RELAY RADAR SYSTEM

By E. F. MacNICHOL, JR.

This relay radar system uses sinusoidally modulated audio-frequency tones for angle data transmission. (It is designated as AN/ART-18 and AN/ARR-17.) In this system three audio sub-subcarriers are used to specify the angular position of the antenna. These frequency-modulate a 2-Mc/sec subcarrier, which is additively mixed with the radar video and synchronization pulses to deviate a carrier of approximately 100 mc/sec. In the receiving system the video pulses and subcarriers are separated into the appropriate channels by filters and demodulated to give d-c voltages proportional to the sine and cosine of the antenna position. These could be used to provide a shaft rotation as in the pulsed sine-cosine system but as the equipment is now designed the voltages are used to modulate linear time base components for a fixed coil ME PPI (see Vol. 22).

**11-16. General Description of Transmitter Functions.**—A block diagram of the transmitting equipment is shown in Fig. 11-30. A synchro having a single-phase rotor and two-phase stator is geared to the antenna at 1-speed. The stator windings are excited by an 885-cps oscillator and a 2250-cps oscillator respectively. The rotor output, therefore, contains a component at 885 cps of amplitude  $E_1 \sin \theta$  and another of

$E_1 \cos \theta$  at 2250 cps, where  $\theta$  is the angle of the synchro rotor. When  $\sin \theta$  or  $\cos \theta$  becomes negative the AC reverses phase (see Vol. 19, Chap. 12 of this series). Since the reversal of phase cannot be demodulated in the receiving equipment unless a reference phase is transmitted, a fixed amount  $E_2$  (larger than  $E_1$ ) of each of the unmodulated tones is added to the synchro output. The output of the voltage divider (adding network) of each frequency is always in phase with its oscillator and is always greater than zero. A fixed output signal is also obtained from a third oscillator at 5090 cps and mixed with the output of the voltage divider. This tone serves as a reference level for  $E_2$  so that it can be subtracted from the demodulated output in the receiving equipment.

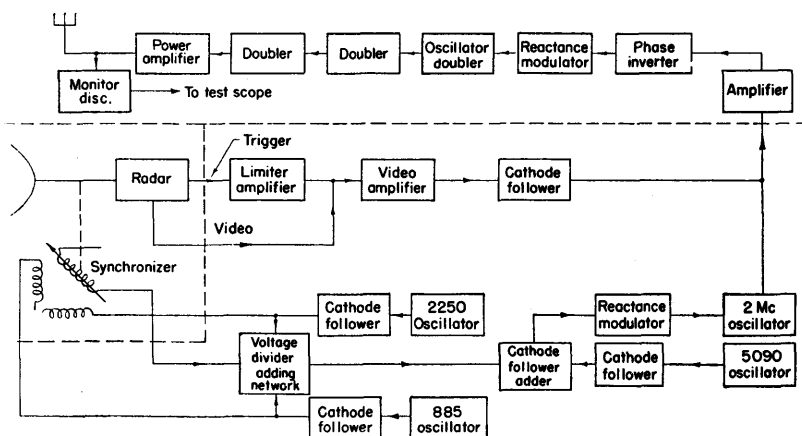


Fig. 11-30.—Transmitting equipment of ART-18 relay radar.

The mixed tones are used in a reactance tube to deviate the 2-Mc/sec subcarrier oscillator.

The PPI sweep trigger is derived from the radar transmitter pulse. It is limited and mixed with the video pulse from the radar receiver but is opposite in polarity. The video signal is also blanked when the trigger pulse is transmitted. The pulse information and the modulated subcarrier are mixed and applied to a reactance modulator to frequency-modulate an r-f oscillator which operates at about 12 Mc/sec. The frequency is doubled three times to give an output of 100 Mc/sec deviated  $\pm 4$  Mc/sec.

The bandwidth of all stages is sufficiently great to pass 1- $\mu$ sec pulses. The identities of the video and trigger pulses are preserved since they deviate the transmitter frequency in opposite directions.

**11-17. General Description of Receiving Equipment.**—A block diagram of the receiving equipment is shown in Fig. 11-31. The receiver

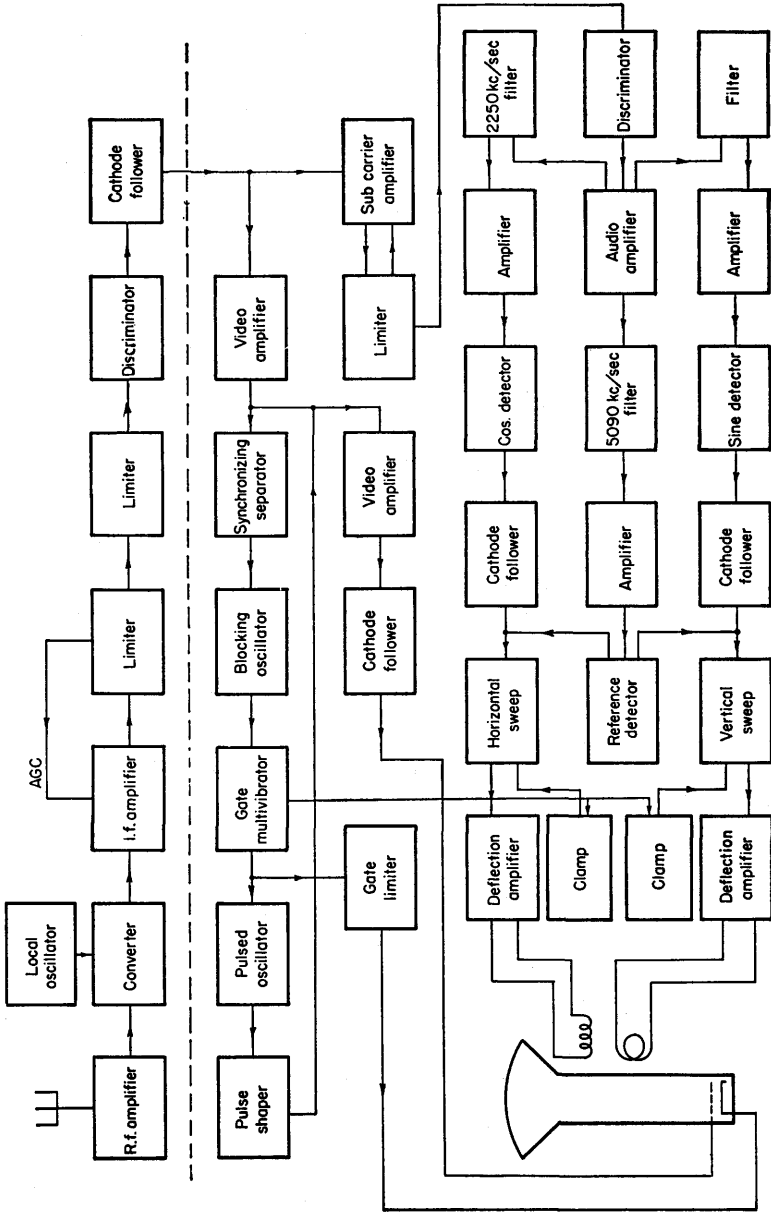


Fig. 11.31.—ARR-17 relay radar receiving equipment.

is a conventional superheterodyne with a pass band of 8 Mc/sec and follows the general principles discussed in Vol. 23 of this series. The output of the receiver consists of the modulated 2-Mc/sec subcarrier and video and trigger pulses. These are sorted out and applied to the indicator tube in the separator unit. The subcarrier is filtered out and amplified in the subcarrier amplifier, limited, and demodulated. The three audio tones are separated by means of bandpass filters. The 885- and 2250-cps modulated tones are demodulated and applied to cathode followers. The 5090-cps tone is filtered and demodulated. The demodulated d-c output of the 5090-cps tone is subtracted from each of the demodulated sine and cosine outputs to remove the level due to the fixed a-c component. The subtracted output potentials are now d-c voltages  $E \sin \theta$  and  $E \cos \theta$  which are symmetrical with respect to ground. These voltages are applied to the charging resistors of the horizontal and vertical sweep generators. The output voltages of these sweep generators are amplified and used to drive the fixed deflecting coils of the PPI. To a first approximation the slopes of the sweeps are proportional to the voltages applied to the charging resistors. The electron beam of the CRT is deflected in the direction of the resultant field produced in the two deflecting coils. The two components of the field are proportional to the amplitudes of the sawtooth waveforms, which are always in the ratio of  $\sin \theta$  and  $\cos \theta$ . Thus the spot will sweep radially outward in the direction  $\theta$ .

The receiver output is also amplified in the video amplifier which has insufficient bandwidth to pass very much of the 2-Mc/sec subcarrier. A biased amplifier and blocking oscillator separates the synchronizing pulse from the video pulse of opposite polarity. The synchronizing pulse operates a wide gate (rectangle generator) that operates the pulsed range-mark oscillator. The pulsed sinusoid generated by this oscillator is limited and differentiated to produce range marks, which are then mixed with the video pulses. These pulses are amplified further and applied to the grid of the indicator. No attempt is made to remove the synchronizing pulse from the video channel since it appears before the sweep has started. The rectangle from the gate multivibrator is limited and used to intensify the CRT during the sweep. It is also used to cut off the clamp tubes producing the sweep components.

**11.18. Details of the System.** *The Mixer Unit.*—Refer to Fig. 11-32. The tone oscillators are of the conventional RC phase-shift variety using 3-section high-pass networks (see Vol. 19, Chap. 4 of this series). They are mounted in an oven whose temperature is thermostatically controlled. The resistor network that adds the fixed a-c level from each stator input is also in the oven since it is extremely important that the ratio of synchro output potential to the fixed component of the audio



carrier<sup>1</sup> be constant. The frequencies of the oscillators are factory adjusted and their stability is such that no controls are provided. Cathode followers are provided to furnish current for the synchro windings and amplitude adjustments are provided for each. A gain control is also provided for the 5090-cps output which is mixed with the modulated tones.

The reactance modulator is of the capacity-feedback type in which a grid voltage is produced in the reactance tube which leads the plate voltage by  $90^\circ$ . The magnitude of this voltage depends upon the  $g_m$  of the tube, which is controlled by grid bias. The effect of the out-of-phase component is to make the reactance tube appear as a variable capacitance. (See any standard text on FM.)<sup>2</sup>

Positive excursions of the modulating signal increase the  $g_m$  and the effective capacitance, decreasing the oscillator frequency. The oscillator is of the electron-coupled variety in which the grid-cathode-screen circuit acts as a Hartley oscillator. The plate tuned-circuit is heavily loaded by the output attenuator so that its pass band is very broad.

Positive video pulses are supplied to the amplifier  $V_8$ , which has a gain less than unity. Bias developed across  $C_{30} R_{41}$  prevents the trigger cathode-follower  $V_9$  from conducting. Negative video signals developed in the plate of  $V_{8a}$  are again inverted by  $V_{8b}$  and applied to the video and trigger cathode follower  $V_{10}$ . The output waveform of this stage is mixed with the 2-Mc/sec subcarrier and sent to the transmitter. The negative trigger from the radar is limited by cutting off  $V_{9a}$ . This pulse raises the cathode of  $V_9$  cutting off  $V_{8a}$ . This action produces a positive pulse on the plate of  $V_{8a}$  and a negative pulse is sent to the transmitter. The cathode of  $V_{8a}$  is raised sufficiently by the trigger pulse to prevent the transmission of video signals.

*The Transmitter.*—Refer to Fig. 11-33. Positive video pulses, negative triggers, and the 2-Mc/sec subcarrier are applied to an additional video amplifier and phase inverter. Signals are applied  $180^\circ$  out of phase to the grids of the reactance tubes. One tube appears as an inductance in parallel with the oscillator tuned-circuit while the other appears as a capacitance. The effects are equal and opposite so that by increasing the  $g_m$  of one tube while decreasing that of the other a linear deviation is obtained over a wide range. The oscillator is of the push-pull electron-coupled type. The plates of both tubes are connected in parallel so that odd harmonics cancel. The second harmonic is selected by the double-tuned coupling transformer. The two doublers are

<sup>1</sup> This system bears a striking similarity to the pulse sine-cosine system. The amplitude of the 885-cps tone is  $K + A \sin \theta$ ; that of the 2250 cps tone in  $K + A \cos \theta$ ; and that of the 5090 cps tone is  $K$ .

<sup>2</sup> A. Hund, *Frequency Modulation*, McGraw-Hill, New York, 1942.



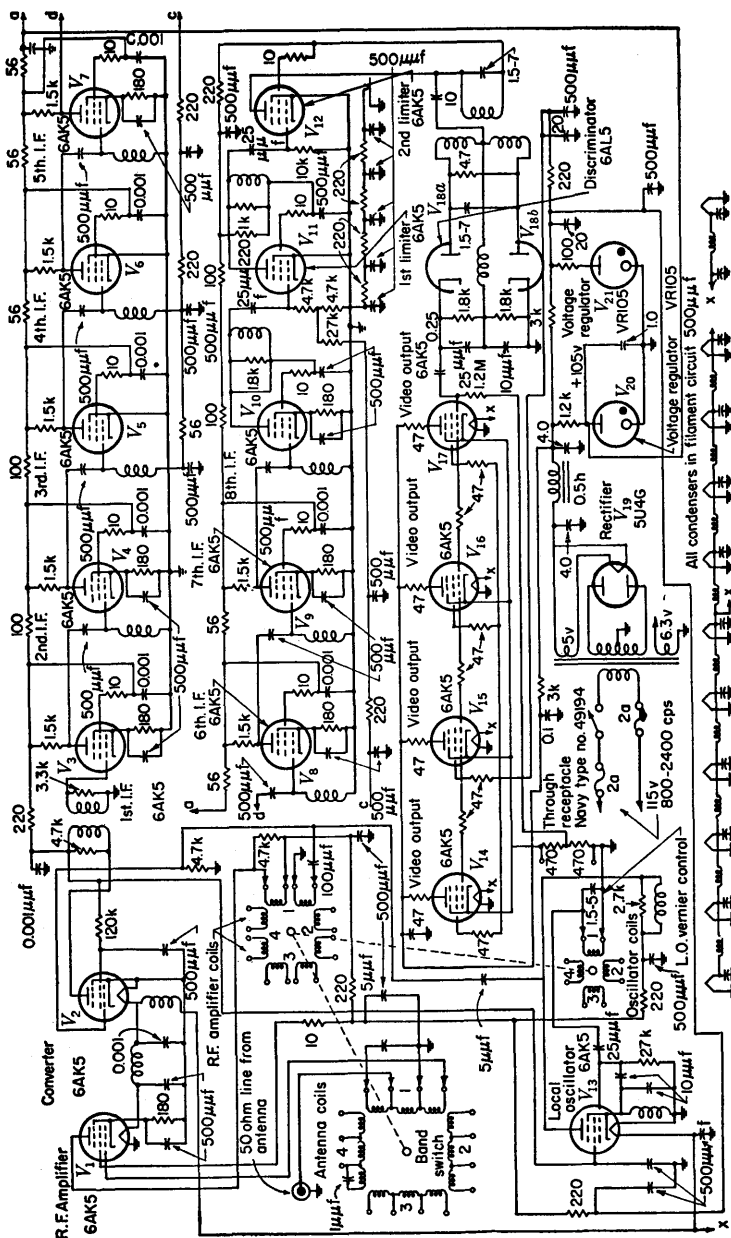


Fig. 11-34.—Receiver of ARR-17 relay radar.



All tuned circuits are overcoupled and  $Q$  values made low to permit the required 8-Mc/sec pass band.

*The Receiver.*—Refer to Fig. 11-34. The preamplifier, converter, and local oscillator use 6AK5's. The antenna and converter tuned circuits are factory preset. A trimmer condenser is provided to control the LO frequency. The LO voltage is mixed with the signal and injected into the grid circuit of the converter. The i-f stages are 6AK5's. Eight are used and are arranged in staggered pairs at 55 and 65 Mc/sec with a gain of 10 each, giving an effective band width of 8 Mc. AGC is applied to the grids of the third and fourth stages.

Two limiters are used. Limiting takes place by rectification in the grid circuit of each tube (see Vol. 19, Chap. 9 of this series). The bias developed decreases the average plate current in each tube. The bias developed by the first limiter is also used as the AGC control voltage. The time constant in the AGC circuit is kept to a minimum so that high-level pulsed interference will suppress the desired c-w carrier for as short a time as possible (much less than the PRF of any pulsed system likely to be encountered).

The discriminator, which follows the second limiter, is of the conventional type (see Vol. 23). Four 6AK5's are used as an output cathode follower to present a 75-ohm output impedance to the cable leading to the separator unit.

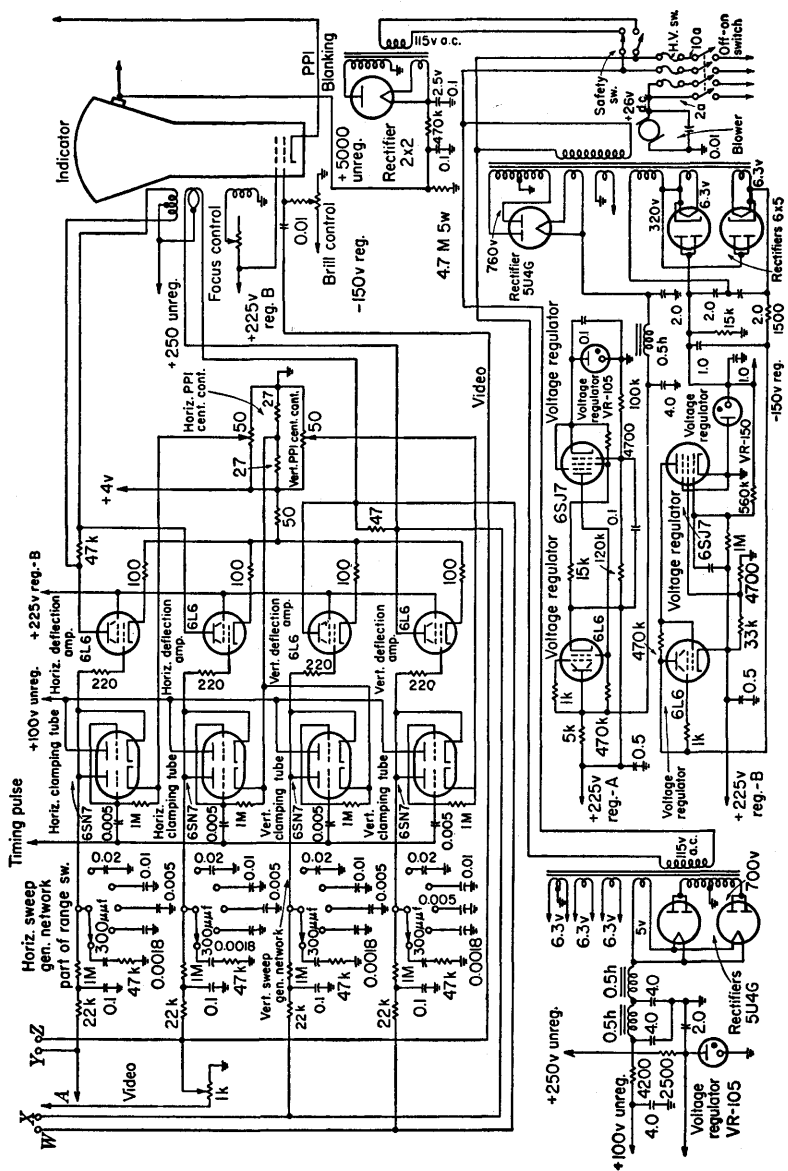
*The Separator Unit.*—Refer to Fig. 11-35. The composite signal from the receiver consists of positive video signal, negative triggers, and the 2-Mc/sec frequency-modulated subcarrier. The subcarrier is selected and amplified by two 6AK5 stages and grid-limited by two additional stages. Bias developed in the first limiter grid circuit is applied to the grids of the preceding amplifier as AGC. A discriminator centered at 2 Mc/sec demodulates the subcarrier. After amplification the mixed audio tones are separated by double-tuned transformers, passed through individual gain controls, and amplified further by 6V6 Class A power amplifiers.

The 885- and 2250-cps tones are demodulated by full-wave peak rectifiers, which are arranged to provide phase inversion to drive the grids of the output cathode followers in opposite directions. The 5090-cps tone is demodulated in a peak half-wave voltage doubler whose output potentials are proportional to the average level of the carrier and are used to subtract a d-c value from the output signal of the 885 and 2250 cps demodulators. Thus d-c voltages are obtained which are proportional to  $\sin \theta$  and  $\cos \theta$  and vary symmetrically with respect to ground. These voltages are applied to each of the four sweep networks and their magnitudes determine the rates of rise of the sweep sawtooth waveforms when the clamp tubes are gated off. The sweep networks

are arranged in pairs, two for the horizontal sweep and two for the vertical sweep. The networks in each pair are supplied with control voltages of opposite phase so that a positive and a negative sawtooth waveform are produced by each pair. They are amplified by the 6L6 GA power amplifiers and applied to the center-tapped deflecting coils. Centering is accomplished by adjusting the voltage to which one of each pair of clamp tubes is returned.<sup>1</sup>

The video and trigger pulses are amplified and inverted by  $V_1$ , yielding positive triggers and negative video pulses. The trigger pulse is applied to the grid of the synchronizing signal pick-off tube  $V_{4a}$ . This amplitude selector is caused to conduct only by positive pulses larger than a value set by the bias divider in the grid circuit. The negative pulse produced in the plate circuit by the trigger is coupled to the plate of the blocking oscillator  $V_{4b}$ . Coupling through the transformer causes  $V_{4b}$  to conduct and initiate regeneration. The blocking-oscillator pulse triggers the gate multivibrator, which is of the conventional divider-coupled type with one stable state. (See Vol. 19, Chaps 5 and 6 of this series for descriptions of the action of the multivibrator and blocking oscillator.) The rectangle initiated by the trigger is slightly longer than the sweep length desired. A gang switch switches the condensers in the multivibrator and the sawtooth generator and the tuned circuits in the range-mark generator so that the gate length, sweep speed, and range-mark spacing are appropriate for the range chosen. The cathode follower  $V_{16b}$  drives the cable to the indicator where the negative gate pulse is applied to the cathode of the CRT. The negative gate is also used to cut off  $V_{14a}$ , producing a train of damped oscillations in the tuned circuit (see Chap. 4 and Vol. 19, Chap. 4 of this series). The positive excursions of the wave train are limited by grid current in  $V_{14b}$ . The negative half-cycles are steepened and inverted by  $V_{14b}$ . Additional squaring is accomplished by  $V_{15a}$  so that the output of this tube is practically a square wave. On the longest range energy is fed back to  $L_4$  from the plate of  $V_{15a}$  to maintain the amplitude of the oscillations of the tuned circuit. Since on the shorter ranges the  $Q$  of the coils is sufficient, the damping is not objectionable. Tube  $V_{15b}$  normally draws grid current through  $R_{35}$ . It is rapidly cut off by the square wave applied to its grids, exciting a critically damped oscillation in  $L_5$ . The peak of this oscillation is selected and further amplified by  $V_{16a}$ . The negative output of this tube is mixed with the video in the grid circuit of the second video amplifier  $V_2$ . The method of producing range marks used in this instrument appears to be extremely wasteful of tubes and current. Five triode sections are used when three or at most four would suffice. All of the tube sections but one draw a large average plate current.

<sup>1</sup> For discussion of the two-way clamp see Vol. 19, Chap. 3 of this series.





Tube  $V_2$  amplifies and inverts the mixed video pulses and range marks, which are applied to the grid of the CRT through the cathode follower  $V_3$ .

**11-19. Remarks and Comments on the System.**—The equipment is well designed and extremely simple to operate, having a minimum of controls. It is not complicated electronically and is light in weight and not bulky. The system performs satisfactorily over land and water and at all times will provide a usable radar picture up to a range of at least 100 miles if the receiving antenna location is 50 ft or higher above the water line and if optical line of sight transmission is maintained.

It was determined that the minimum signal strength that would still provide a usable picture is in the order of 20  $\mu$ v.

"Any interference within about 6 mc of the i-f frequency of the receiver will cause considerable distortion and complete failure of the received presentation.

(This is not an inherent limitation of the system since proper shielding of the i-f circuits would remove such interference.)

"Interference will also be experienced on the operating channels when other (c-w) equipment or ground search radars which operate on the same or adjacent frequencies are operating in the same vicinity as the receiving location.

"Considerable ripple and distortion of the received picture will result if the radar system pulse repetition frequency or harmonics of the pulse repetition frequency are within plus or minus 50 cycles of any of the three audio frequencies."<sup>1</sup> The accuracy is as good as that of the AN/APS-2 Radar that supplied the signals for the system (better than  $\pm 5^\circ$ ).

<sup>1</sup> This section is abstracted from "Final Report on AN/ARR-17 and AN/ART-18 Equipments, Radar Repeat-back Radio Link," Navy Dept. Bu. Aero., July 14, 1945.

## CHAPTER 12

### DELAY AND CANCELLATION OF RECURRENT WAVE TRAINS

BY H. B. HUNTINGTON, W. SELOVE, AND D. GALE

**12.1. Introduction.** *The Function.*—The purpose of these chapters is to discuss a technique whereby a voltage  $V$  which varies with time  $t$  can be delayed by an interval  $D$  and then subtracted from itself. Expressed analytically, the function is  $V(t + D) - V(t)$ . If  $V(t)$  is periodic in  $t$  of period  $D$ , the cancellation is complete; but if the voltage wave train repeats itself only approximately from one interval of duration  $D$  to the next, this technique will indicate the existence of such variations as might otherwise pass unnoticed. In this way small changes in the repetitive voltage, whether in amplitude or in phase, can be separated and amplified to give information concerning their relative size and distribution in time.

In many technical fields the execution of the function described above will be an asset. Quite certainly, considerable use can and will be found for a technique that accomplishes it. It is not feasible, however, to discuss here its general applications and future possible development. Although these techniques were developed for a special purpose, this in no way invalidates their general usefulness. The possibility of cancellation of pulse trains has been mentioned in Chap. 2 as a method for speed determination. In fact, practical application of this technique has been made in the precise measurement of the velocity of propagation for supersonic waves in mercury.

*The Instrument.*—One technique to accomplish delay and cancellation involves the use of storage tubes, a subject that is treated in full in Vol. 19, Chap. 21 of this series. Briefly the action may be described by saying that the storage tubes retain the voltage  $V(t)$  as a pattern of charge laid on the surface of an insulator by a scanning electron beam. The stored information is made available at a later time by a second scanning of the beam. Within this general framework several very different procedures show promise. The device offers considerable intrinsic flexibility in that it can be adapted immediately to any value of the delay  $D$ . The project is as a whole, however, in the developmental stage.

Another technique that employs a supersonic delay device<sup>1</sup> to delay

<sup>1</sup> The use of a supersonic delay device has already been presented in Chap. 4.

the wave train for the interval  $D$  is discussed here. The action of super-sonic delay lines is treated in Vol. 19, Chap. 23. Its relation to the other

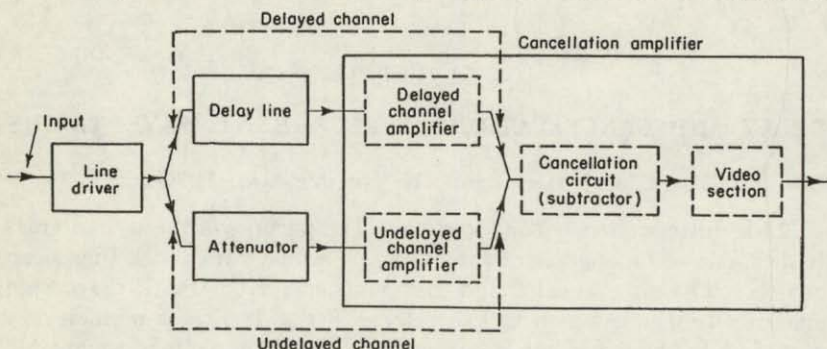


FIG. 12-1.—Delay and cancellation device.

components in the unit that performs delay and cancellation is indicated in the block diagram of Fig. 12-1.

From the block diagram the functional interdependence of the subject matter treated respectively in each of the next four sections becomes

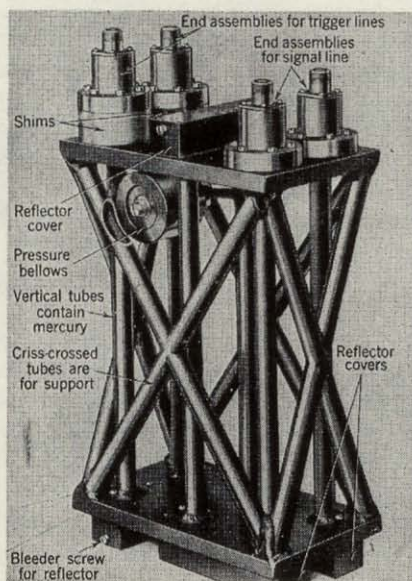


FIG. 12-2.—Delay line completely assembled.

evident. The first treats the delay line; the second, the line driver; the third, the cancellation amplifier; and the fourth, the control of the repetition rate. In the cancellation amplifier provision is made for



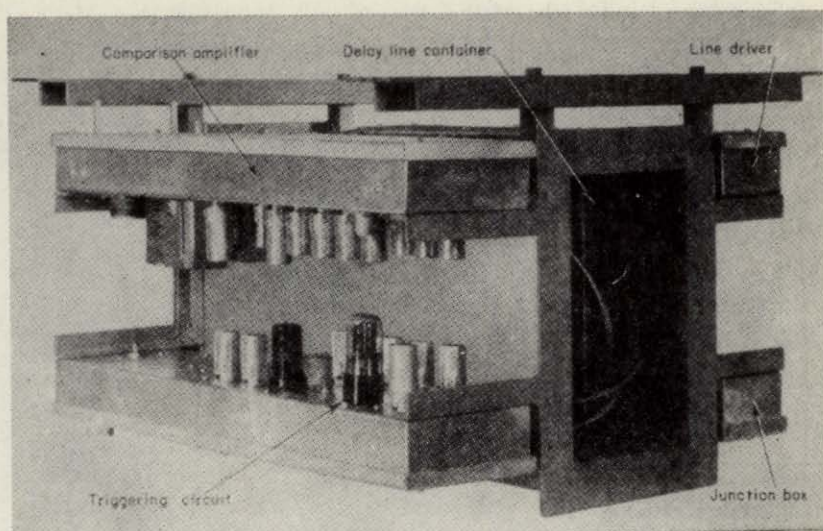


FIG. 12-3.—Delay-line container and associated chassis.

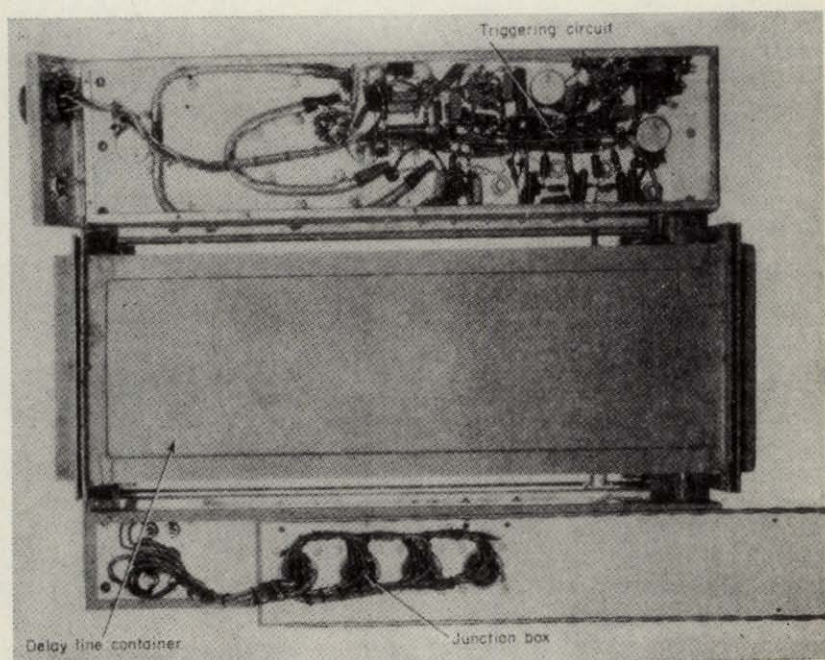


FIG. 12-4.—Triggering circuit and junction box.



matching the bandwidths of the delayed and undelayed channels, and the subtraction is performed. The video section amplifies the uncanceled residue. The repetition rate refers to the repetitive wave trains. It is,

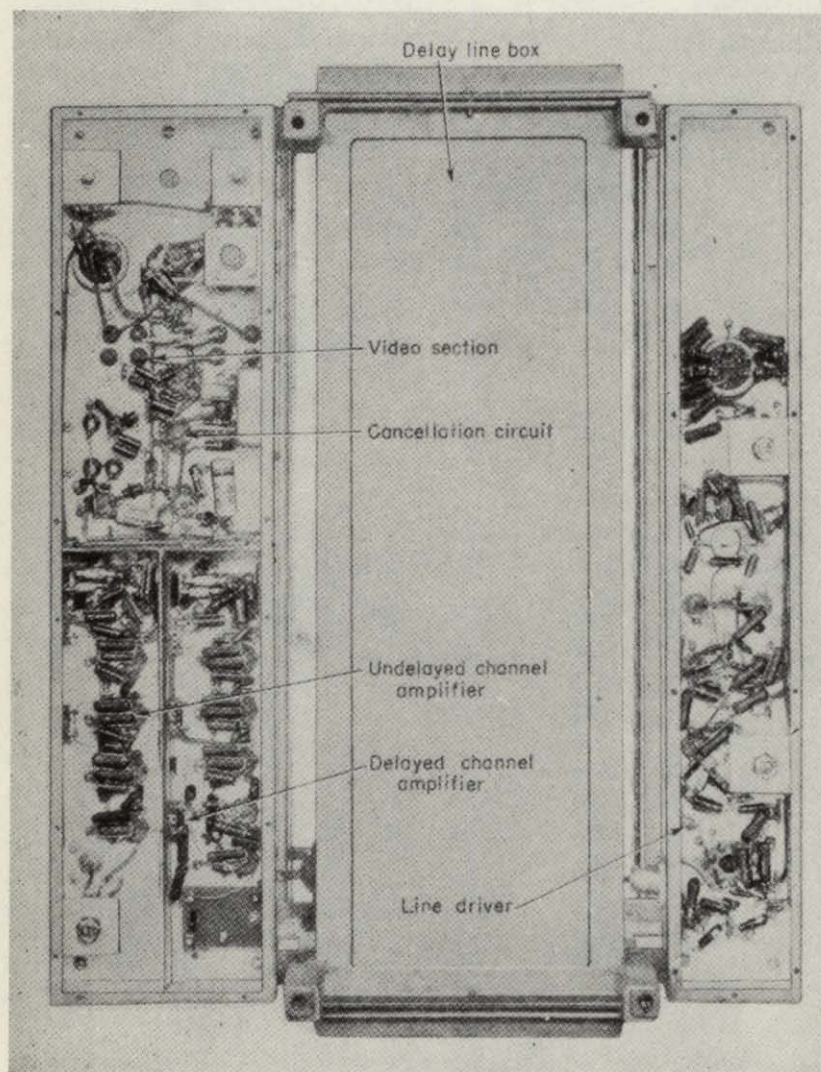


FIG. 12-5.—Cancellation amplifier and line driver.

of course, important to take measures to insure that the repetition interval equals the delay time.

The requirement and limitations of such a system (Fig. 12-1) can be discussed only briefly here and will form the basis for more detailed

treatment in later chapters. In particular, the value of the delay can be as long as several milliseconds, though the delay device for such times as 3 msec or more may become unwieldy. These delays are essentially fixed or only variable over one per cent or so, according to present mechanical design.

The concept of degree of cancellation is an important one for the understanding of subsequent chapters. The quantity is used as a figure of merit for the delay and cancellation unit as a whole. It is obtained by feeding an exactly repetitive wave train (usually a series of single square pulses) into the delay and cancellation unit. The ratio of the amplitude of the cancelled residue to the amplitudes of the wave trains before cancellation gives the degree of cancellation. One per cent or 40 db down represents very good performance and is often arbitrarily chosen as a design goal.

Two important stability considerations are involved in maintaining the delay time equal to the repetition interval, and in keeping the amplitudes in the two channels the same size. The former problem is particularly troublesome since the sonic velocity is a function of temperature. It will be shown later (in Chap. 16) that the two time intervals must agree to about  $1/100$   $\mu$ sec to achieve cancellation of 1 per cent of a pulse with rise time of about one  $\mu$ sec.

Because of the amplifier stability requirements, electronically regulated supplies are generally used for plate and screen voltages throughout. The easiest way to insure that the same degree of cancellation holds throughout the dynamic range of the input signal is to require that both the delayed and undelayed channels be kept accurately linear over the same range. Under these conditions the net uncanceled residues will be proportional to period-to-period changes in nearly repetitive wave trains. For some applications this feature is an advantage.

An example of a device for the delay and cancellation of recurrent waveforms is shown with its components in Figs. 12-2 to 12-5.

## THE DELAY LINE

BY H. B. HUNTINGTON

### DESIGN OF DELAY LINE FOR CANCELLATION

**12-2. Introduction.**—Chapter 23, Vol. 19 of this series on supersonic delay lines explains the fundamental principle of the device and to what uses it has been put. Many of the theoretical and semiempirical considerations which enter into its design have been developed in a recent journal article.<sup>1</sup> In the Components' Handbook, Chap. 7, Vol. 17 of

<sup>1</sup> "Ultrasonic Delay Lines I," H. B. Huntington, A. G. Emslie, and V. W. Hughes; "Ultrasonic Delay Lines II," A. G. Emslie, H. B. Huntington, H. Shapiro, and A. E. Benfield. Part I in the *J. of the Franklin Inst.*, January 1948; Part II to be published.

this series, the important formulas have been collected in abbreviated form and an attempt has been made to show how these relations should be applied to actual delay-line design.

In general, the delay-line engineer has to meet certain specifications of an electrical nature. Usually there will be the delay time, the bandwidth, and the pulse width of the signals. To meet these specifications he has the choice of the following parameters: the transmitting medium, the carrier frequency,<sup>1</sup> the dimensions of the piezoelectric crystal, the line geometry, and the mechanical tolerances. Some of these parameters are already limited by the considerations treated in Vol. 17. There the emphasis was mainly on building lines that would give, for constant bandwidth and given driving conditions, the maximum output. The same considerations also apply here but the associated cancellation introduces additional complications. The new requirements fall mainly into three categories: echo elimination, bandpass shaping, and equalization of delay time with repetition interval. Each of these requirements is discussed in turn in the next three sections.

**12-3. Echo Elimination.**—One very important requirement for a delay device that is employed as part of a cancellation unit is that it gives for every input signal only one output signal at the time of expected delay and no other appreciable signal at any other time. This means that any accessory signals such as can easily arise in a supersonic device from multiple echoes must be kept below a certain relative level—for example, the 40 db down that has been mentioned before as an arbitrary design goal. In particular, consideration must always be given to the possibility that some of the energy in the supersonic pulse may be reflected once from the receiver crystal, once from the transmitter crystal, and return to give an unwanted signal at the receiver crystal. This will be henceforth referred to as the “echo of triple delay,” since it appears at the receiver at a delayed time three times as long as the wanted delay. Actually there may be a series of such echoes appearing at times that are odd multiples of the design delay. There are two fundamentally different approaches to the problem of reducing these echoes.

The first approach is to reduce the reflection at the crystal surface by absorbing energy into the crystal backing. To do this the acoustic impedance of the medium<sup>2</sup> in contact with the back side of the crystal must match the acoustic impedance of the transmitting medium closely enough so that the reflection coefficient is 0.1 or less. The impedances

<sup>1</sup> It has already been pointed out in Vol. 19, Chap. 23 of this series that, from the very nature of the delay line, a carrier frequency is necessary for the faithful preservation of the wave train.

<sup>2</sup> The acoustic impedance of the crystal does not enter if the crystal thickness is an odd number of half wavelengths, which is the condition for resonance.

can be matched exactly by backing the crystal with the same fluid as that used for the transmitting medium, or, in the case of a mercury-filled delay line, the crystals can be soldered to lead or tin, both of which match mercury rather satisfactorily. The constructional and mechanical problems associated with the absorbing backing are treated in Vol. 17, Sec. 7.2 of this series. It should be pointed out that it is not sufficient to transmit the energy into the crystal backing, but the beam must either be absorbed or dispersed in the backing material to prevent its emergence intact at a later time. Because of its greater absorption lead is preferable to tin. From the formulas given in Vol. 17, Sec. 7.2 one notes that the loss arising from mismatch at the crystals is increased from 3 to 6 db when an air-backed crystal (which should be totally reflecting) is replaced by one with a perfectly absorbing backing. A crystal that is supported by a dry metal electrode is in effect air-backed since it is in contact with the metal at only a few points and only a very thin layer of air is needed to afford a complete mismatch.

The second approach to the problem of eliminating the multiple echoes is to rely on the attenuation in transit to reduce the reflected energy to the required level. In this connection it is possible to use reflecting dry electrodes. By its nature this approach is better suited to the lines of longer delay, 1000  $\mu$ sec or more. A loss of about 20 db per transit is needed if the "echo of triple delay" is to be reduced sufficiently. This loss might be contributed from several sources. Actual attenuation in the transmitting medium is made up of two parts, the free-space attenuation and the tubular attenuation. From the formulas given in Vol. 17, Sec. 7.1 of this series one notes that the free-space attenuation varies directly as the square of the frequency and the tubular attenuation directly as the square root of the frequency and inversely as the inner diameter of the tube that contains the transmitting medium.<sup>1</sup> A third source of attenuation will arise for "folded lines" at the reflectors. These reflectors are usually set at right angles to one another and at 45° to the path of the beam. They serve to bend the beam back on itself through a parallel pipe. Even though the material of the solid reflectors is so chosen that the critical angle for transmission into the solid is less than 45°, some loss usually appears at these surfaces (see Vol. 17, Sec. 7.3). Lastly, successive multiple echoes may be reduced by a small degree of misalignment, which has only a minor effect on the direct supersonic signal.

The elimination of multiple echoes by loss in transit then depends on the following combination of design parameters: transmitting medium, carrier frequency, tube diameter, line geometry, and mechanical toler-

<sup>1</sup> The formula for the tubular attenuation holds only when there is good sonic contact between the transmitting medium and the tube wall.

ances. Of these the choice of transmitting medium is likely to be limited by the demand for bandwidth, as discussed in Sec. 12-4. Moreover, many media are ruled out because of excessive attenuation. A paragraph on each of the other parameters is here included to indicate to what extent one is restricted in the respective choices.

Though the carrier frequency also enters into bandwidth considerations, it is important to choose a value that will give about the required attenuation in transit. In connection with the choice of carrier frequency, it should be mentioned that, where the cancellation takes place after rectification of the modulated carrier, the carrier frequency must be high enough to insure a sufficient number of cycles per pulse to reproduce the envelope with adequate accuracy irrespective of carrier phase. Experiments by W. Selove have shown that this number is approximately seven for the degree of cancellation of 40 db with a pulse whose rise time is  $\frac{1}{2}$  the pulse length. As an example, one would not use a 10-Mc/sec carrier to cancel  $\frac{1}{2}$ - $\mu$ sec pulses.

In the choice of the tube diameter, space and weight can be reduced by using a smaller bore. There is also another reason, which will become apparent in the next section on bandwidth, why tubular attenuation is preferable to free-space attenuation. On the other hand,<sup>1</sup> optimum-loss bandwidth results when the capacitance of the active crystal area equals the stray capacitance. (This holds if the load resistors at transmitter and receiver are small compared with the impedance of the transducers, which is generally the case.) Too small a tube bore means too small an active area and, for conditions well removed from the optimum, this causes serious impedance mismatch. Another reason for avoiding too small a tube diameter is that it may introduce velocity dispersion among the frequency components of the pulse with resulting pulse distortion. Such an effect has been observed for delay lines using a 5-Mc/sec beam through 24 ft of mercury inside tubes about a half-inch in diameter. In a delay line using a 10-Mc/sec beam through 16 ft of mercury inside tubes  $\frac{5}{8}$  in. in diameter, no appreciable deterioration of the pulse was observed. The case of propagation down a tube with the boundary conditions of vanishing pressure at the wall has been analyzed<sup>2</sup> and it has been shown that the distortion should depend essentially on a parameter

$$\gamma = \left( \frac{\Delta f}{f} \right)^2 \cdot \frac{\lambda d}{A},$$

where  $\Delta f$  is the pulse bandwidth,  $f_0$  the carrier frequency,  $\lambda$  the wavelength,  $d$  the length of path, and  $A$  the area of the tube cross section.

<sup>1</sup> H. B. Huntington, et al., *op. cit.*; also Vol. 17, Sec. 6-4, of this series.

<sup>2</sup> Information obtained from H. J. McSkimin of the Bell Telephone Laboratories, Murray Hill, N. Y.

In the matter of line geometry the space requirements play an important role in determining into how many sections the path of the beam is to be bent. Once the number of reflectors has been decided, one can expect in general a loss of about one to three decibel per reflection from a fine ground surface in computing the attenuation to be expected in transit. Practically no loss has been observed on reflection from polished surfaces or moderately rough surfaces (see Vol. 17, Sec. 7-3).

To reduce multiple echoes by misalignment involves either extremely precise machining or provision for adjustment after assembly. Neither is to be recommended. Moreover, we have already mentioned that pulse shape often suffers in tubes that are misaligned.

**12-4. Bandpass Shaping.**—To accomplish a high degree of cancellation it is desirable to match closely the pass bands of the delayed and undelayed channels. Consequently, one wishes to reduce to a minimum any distortion in amplitude response introduced by the delay line. It is desirable, therefore, to make the pass band of the delay line as flat as possible in the region of the pass band of the channels.

The response of the crystal, exclusive of the circuit that resonates out the crystal capacity, has been treated in some detail and the case of the crystal in contact with the same medium on both sides is covered by a particularly simple formula.<sup>1</sup> The  $Q$  for this case is given by

$$Q = \frac{n\pi}{4} \times \frac{\text{acoustic impedance of piezoelectric material}}{\text{acoustic impedance of transmitting medium}}$$

where one is using the  $n$ th harmonic of the fundamental frequency of the crystal. In general, to obtain a low  $Q$  one must employ a transmitting medium of high acoustic impedance. For this reason most of our work has been with mercury (though water is perfectly satisfactory for systems of small over-all bandwidth). If mercury is used, the demands of bandwidth allow considerable latitude in the choice of carrier frequency.

As can be seen from the formula quoted above for  $Q$ , the bandwidth for a fixed frequency varies inversely as the harmonic  $n$  that is employed. Also it requires  $n$  times the voltage to produce the same output when the  $n$ th harmonic replaces the fundamental. Harmonic operation is recommended only at those frequencies for which a crystal vibrating in the fundamental would be too thin for convenient manufacture and handling.

The frequency response of the quartz transmitting into mercury is relatively flat in the region of resonance. Theory<sup>2</sup> indicates that, for air-backed quartz, the response should be even slightly flatter than for quartz with mercury on both sides. Considerable use has already been

<sup>1</sup> H. B. Huntington, et al., "Ultrasonic Delay Lines I" Sec. B.

<sup>2</sup> H. B. Huntington, et al., *op. cit.*

made of this flatness to employ crystals whose undamped resonance frequency lay just outside the pass band of the cancellation unit. For example it was possible to use a 26-Mc/sec crystal with a 30-Mc/sec carrier without suffering any appreciable band-pass distortion over a 6-Mc/sec bandwidth. There was an advantage in using such crystals since it had been found that occasionally even heavily damped crystals exhibited peaks or dips in their pass band at the exact frequency of their free resonance. (It is surmised that these effects are perhaps the results of small bubbles or dust particles between the quartz and mercury.) The appearance of either peaks or dips in the pass band of the cancellation unit would cause a marked deterioration in performance.

The delay line, however, does introduce one unavoidable source of bandpass distortion in the frequency dependence of its attenuation. On this score the tubular attenuation, which varies as the square root of the frequency, is easier to compensate than the free space attenuation, which varies as the square of the frequency. The electronic techniques by which this compensation is accomplished are discussed in Sec. 12-19.

**12-5. Equalization of Delay Time with Repetition Interval.**—The purpose of this section is to treat the mechanical complications introduced into delay-line design by some of the methods for equalization of delay time with repetition interval. The complications are of two sorts: those that make it possible to vary line delay over a small range, and those that provide additional delay channels to regulate the period of the trigger that initiates the repetitive wave trains.

At present there are two techniques (Vol. 17, Sec. 7-3 of this series) in use for making variable mercury delay lines that can be used in the field. In one the position of a crystal or reflector is controlled by a mechanical drive. Part of the coupling shaft is actually immersed in the mercury and a packing cell prevents leakage of the fluid. For mercury an effective packing gland is made of linear threads dipped in ceresine wax and tightly compressed around the shaft. The second technique involves a bellows construction that allows the driving mechanism to be completely outside that space occupied by the transmitting medium. Stainless steel bellows are available for use with mercury, but should, perhaps, be internally lacquered to prevent mercury contamination.

The simplest provision for an additional delay channel to regulate the trigger is to supply a nearly duplicate delay line that is placed in the same thermal environment as the signal delay line. This trigger line actually must be shorter by about a microsecond to allow time for amplification and triggering. An advantage of this arrangement is that it involves no additional design. The disadvantages are the increased space and weight demands and the problem of maintaining the transmitting medium in the two lines at the same temperature.

A modification of this scheme has been to use half-length lines for trigger generation and then to count down in frequency by a factor of 2. Another variation of this scheme is to employ a quarter-length line and use the same crystal for transmission and reception. When this was tried, however, the multiple reflections arriving with random phase at nearly the same time as successive triggers gave considerable difficulty. This was cause for some surprise as it had been estimated that the multiple echoes would be 8 to 10 db below their actual value. The estimate had been based on a small reflection coefficient from a steel mirror placed normal to the path of the beam. Apparently the surface-ground steel was not sufficiently smooth to give good acoustic contact over the surface; consequently the simple theory is inapplicable. The half- and quarter-length lines were designed to be part of the same mechanical unit as the signal delay line and were fed from the same mercury reservoir. This feature increased the compactness of the device and facilitated the equalization of temperature between signal and trigger lines.

It is not necessary, however, to use two separate delay lines, and a third crystal (Vol. 17, Sec. 7-2 of this series) for control of repetition rate can be inserted. Here a reflecting block, placed a little in front of the receiving crystal and at  $45^\circ$  to the path of the beam, reflects a fraction of the energy through  $90^\circ$  to a third crystal set in a recess in the tube wall. The position of the reflector block may be varied, if so required, to adjust slightly the trigger delay to insure synchronization. This scheme involves practically no additional space or weight requirements but does complicate the construction of the end assembly. Since the paths for signal and trigger are almost identical temperature, considerations no longer enter. Some provision must be made to prevent large signals from triggering the repetition-rate generator. This can be done in a variety of ways. One possible solution would be to use separate carrier frequencies from a broadband transmitter for signal and trigger on opposite sides of the resonant crystal frequency. The receiving circuit at the third crystal is then maintained narrow enough to exclude signal pulses.

#### EXAMPLES OF DELAY DESIGN

**12-6. Mercury Lines.**—The mechanical and electrical properties of several mercury delay lines have already been treated with considerable detail in Vol. 17, Chap. 7 of this series. The discussion here will be limited to those aspects that have been treated generally in the first part of this chapter.

The delay device introduced in Sec. 12-1 (see Fig. 12-2) operates at a carrier frequency of 15-Mc/sec and gives a delay of 1000  $\mu$ sec. The signal path traverses four sections of tubing (ID of  $\frac{3}{8}$  in.) which are inter-



connected by corner reflectors. The attenuation in transit was designed to be about 20 db but actually exceeds this value, probably because of extra loss at the six  $45^\circ$  reflecting surfaces. As a result, no trouble is experienced with unwanted echoes. Quartz crystals with a resonance frequency of 17.5 Mc/sec were chosen to eliminate the possibility of a peak or dip in the pass band of the delay device. Equalization of delay time with repetition interval was accomplished by incorporating an extra half-length line of two sections to control the time between triggers. Collars were added under the end assemblies to bring the delay up to nearly one half the delay of the signal line. The final adjustment is made with a variable electronic delay (see Secs. 12-29 to 12-30).

Another delay device used for cancellation purposes is shown in Fig. 12-6. This device gives a delay of over 3300  $\mu$ sec with a carrier frequency of 10 Mc/sec. The greater distance of transit makes a lower

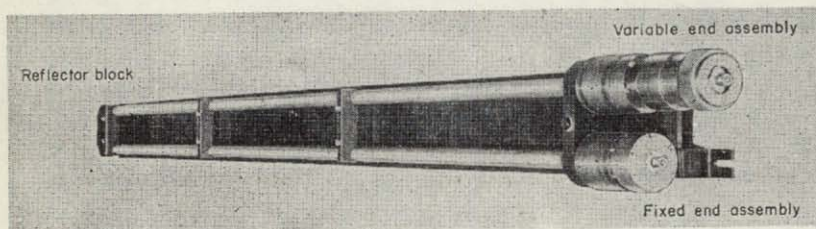


FIG. 12-6.—Assembled delay line.

carrier frequency necessary to avoid excessive attenuation. As can be seen from Fig. 12-6, the line is composed of two parallel sections interconnected by a corner reflector. The end assembly on the tube at the right contains a mechanism for varying the position of the crystal; hence the delay time can be adjusted over a small range. For controlling the repetition interval a duplicate delay line is used placed in the same casket as the signal line, in the same thermal environment as nearly as possible. The lengths are then adjusted to give synchronization.

**12-7. Water Delay Line in System Use.**—The British have made use of a water delay line for cancellation of pulse trains (see Fig. 12-7). The path in water is over 9 ft long, corresponding to a delay of nearly 1700  $\mu$ sec. A 10-Mc/sec carrier is used. The beam is folded once by a brass corner reflector, whose plane can be rotated to give accurate alignment. Accurate machining of the reflector takes care of the adjustment in the other degree of freedom. The beam is confined to pipes that have a line-stretcher feature to allow variation of the delay time. The pipes themselves are immersed in a water tank which is maintained at a temperature of  $72.5^\circ\text{C}$ . At this temperature the sonic velocity of water has its

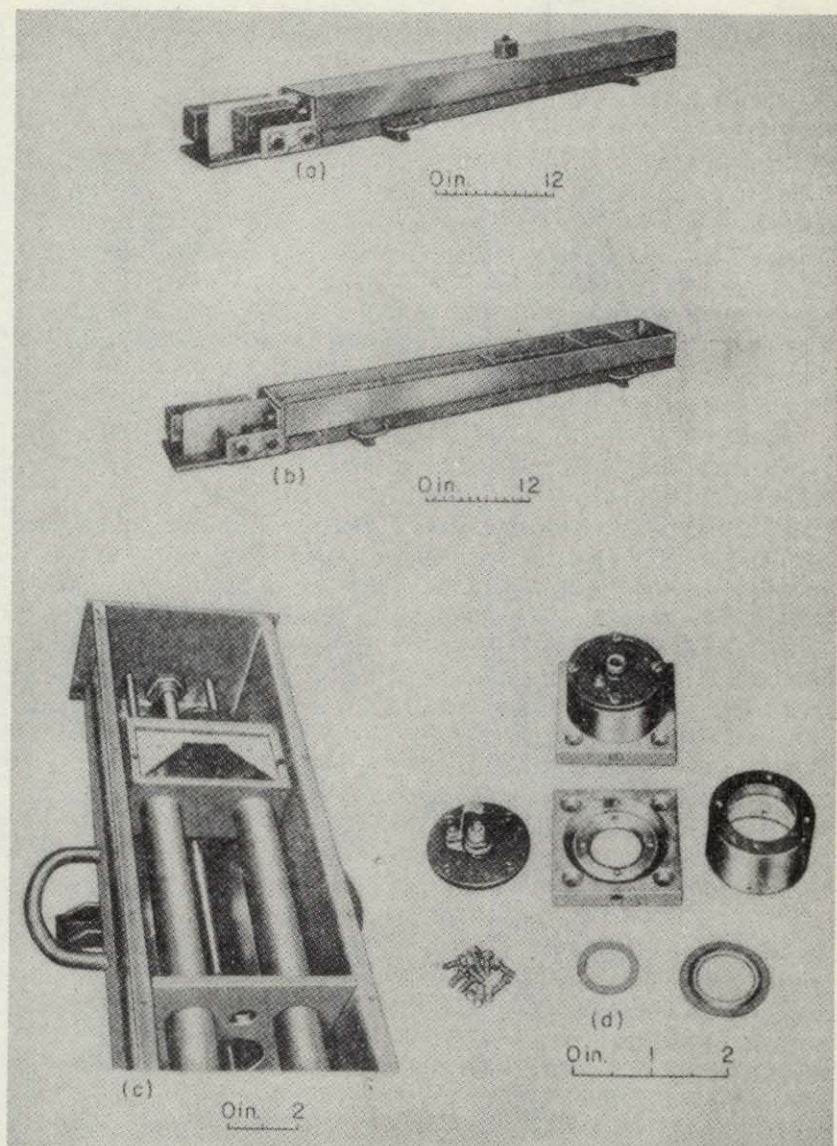


FIG. 12-7.—Water delay line: (a) line assembled; (b) line, cover removed; (c) line-stretcher construction and reflector block; (d) crystal mount, disassembled.

maximum value so that difficulties with conduction currents and refraction effects are greatly reduced. Moreover, the attenuation in water is much lower at higher temperatures than at room conditions. The end assemblies containing the crystal mounts are attached to the wall of the tank.

The attenuation in the water is considerable so that the multiple reflected echoes are completely lost. On the other hand, much better coupling is possible to water than in mercury, which makes up for the increased loss in the transmitting medium. Bandwidth is necessarily much narrower and this limits the discrimination of the system to longer pulses. Within this fundamental limitation the cancellation problem is somewhat simpler. For one thing the pass band is narrow enough so that the variation of attenuation with frequency will have little effect. The line-stretcher adjustment of the guiding tubes allows the operator to set the delay time to agree with the repetition interval. Once synchronization is achieved it should be maintained. At least the constant-temperature delay line can be expected to hold the delay fixed.

**12-8. Possibility of Using Delays in Solids.**—Although liquids have been employed on all actual system application so far, there has been a research program in progress to investigate the possibilities of delays in solids.<sup>1</sup> The use of liquids involves certain mechanical problems, such as leakage, breakage, and air bubbles. With mercury considerable trouble has been experienced with mechanical impurities and metal amalgams which formed slowly. The effects of aging and mechanical shocks and of variations in pressure have been discussed in Vol. 17, Sec. 7-6. Because of these difficulties with liquids it has been thought that a delay in a solid medium would be well worth developing for a cancellation system. The primary intrinsic difficulty with delays in solids arises from the fact that sonic velocities are three to five times that encountered in liquids. This means not only that the delay path must be longer by such a factor, but also that the final beam spread will be increased by the square of this factor. This comes about because the angular spread of the beam is proportional to the wavelength, or the velocity. A secondary intrinsic difficulty arises from the fact that in the solid three sonic modes can be propagated as compared to the single compressional mode in the liquid. As a result the transfer of energy from one mode to the others is a complicating possibility that may occur whenever the beam is incident on a surface across which there is a discontinuity in sonic properties. In addition to these intrinsic difficulties there are several problems in technique and preparation of materials. The method of applying the crystals to the solid in such a way as to secure good acoustic contact is a case in

<sup>1</sup> For complete details on this program at Radiation Laboratory see D. L. Arenberg, "Supersonic Solid Delay Lines," RL Report No. 932.

point. Moreover, supersonic beams of high frequencies are easily scattered in solids (1) by precipitated impurities, (2) by residual stresses, and (3) by the polycrystals of the substance itself. In addition specimens of numerous glasses having none of these defects showed considerable intrinsic attenuation.

Such difficulties as those discussed above are not important in the building of short supersonic solid delays (less than  $25\ \mu\text{sec}$ ), which have already been successfully developed and used (see Vol. 17, Sec. 7-7). Recently the use of a solid delay has been shown to be practical for cancellation application and will be treated here in some detail.

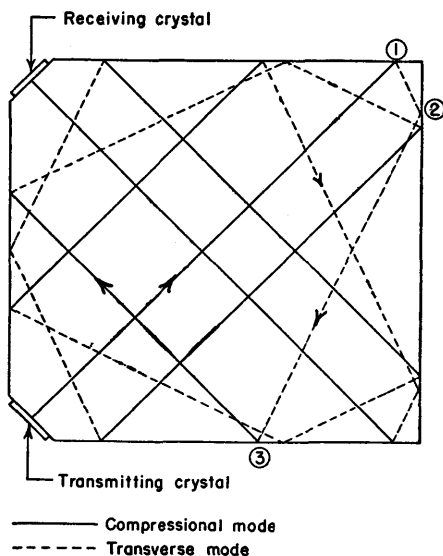


FIG. 12-8.—Two-dimensional sound path in fused quartz block.

By far the most suitable material so far investigated for this purpose is fused silica, or fused quartz as it is commonly called. Its intrinsic attenuation is very low, as might be expected from the high  $Q$  of crystal quartz. It can be procured commercially very pure and relatively strain-free. Usually there are, however, some striae or small bubbles appearing throughout which have undoubtedly some scattering effect. The General Electric Company is equipped to make disks 10 in. in diameter and a few inches thick. When one of these disks is polished and viewed between crossed polaroids, there is some evidence of birefringence, but on the whole these pieces are remarkably homogeneous and isotropic. The attenuation in transit is low enough so that it is difficult to measure accurately. For solids there is reason to believe that attenuation in a region far from any resonance should be linear with frequency.

The present technique is to fix the crystals to the quartz with a thin layer of melted paraffin. If considerable care is exercised to exclude all dirt and bubbles and if all excess wax is pressed out from under the crystal, a faithful reproduction of microsecond pulses can be achieved at 15 Mc/sec. This means the transducer has adequate bandwidth, nearly as large as that obtained by the use of mercury. For a quartz crystal loaded down by fused quartz on one side, one would expect a  $Q$  of about one. Actually, a bandwidth of  $3\frac{1}{2}$  Mc/sec at a carrier frequency of 15 Mc/sec has been measured.

At least two schemes have been conceived to prevent the supersonic beam from being broken up into various modes on reflection. One of these is called the "two-dimensional path." The design calls for cutting the disks into nearly square rectangles with facets at two of the corners cut at  $45^\circ$  to the sides, (see Fig. 12-8). Two or three such designs have already been tried out and one has proved very successful. The second scheme calls for a three-dimensional path for the beam in the quartz and requires considerable explanation for adequate presentation. The design calls for facets on the corners cut at compound angles and requires special equipment. There are excellent prospects that future results with the "three-dimensional path" will be at least as good as those already obtained with the "two-dimensional path."

For every homogeneous solid there is an internal angle of incidence for the compressional beam at which complete transfer from the compressional to transverse mode takes place on reflection. Fortunately, for fused quartz this angle falls at nearly  $45^\circ$ . Direct use of this fact is made in the design of the "two-dimensional paths." Following the path traced in Fig. 12-8 (where the compressional mode is represented by a full line and transverse propagation is shown by dotted lines) we see that the beam starts initially from the  $45^\circ$  facet in the compressional mode as excited by an X-cut crystal, crosses the block, and on striking the quartz-air interface is reflected in the transverse mode. Because of the different velocities in the two modes, the angle of reflection differs from the angle of incidence. On the next reflection the beam strikes outside the critical angle for exciting the compressional mode and the beam is totally reflected. At the third reflection a situation appears that is identical with the first reflection except for reversal in time. Consequently, the beam is transformed from transverse to compressional vibration. This cycle repeats every three reflections and eventually the beam in the compressional mode strikes the receiving crystal at normal incidence. There is then a family of such paths distinguished by the value of  $n$  where  $3n$  gives the number of reflections. The ratio of block length to block width determines which path is used. Figure 12-8 shows the case for  $n = 5$ , and this is the case that has given the most successful results. The delay with such a block is over 400  $\mu$ sec.



In evaluating the possible use of quartz for transmitting medium in a delay and cancellation system, one can say that the bandwidth is adequate, but that accessory signals give considerable trouble in the present state of development. In the most favorable case they are of the order of magnitude of 30 db down.

### CIRCUIT CONSIDERATIONS IN DRIVING LINE

By W. SELOVE

**12.9. Required Nature of Signal.**—The signals to be compared must be applied to the delay line and to the undelayed channel in such a form

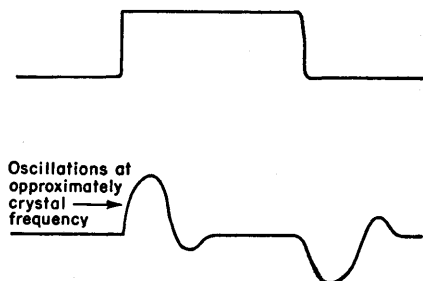


FIG. 12-9.—Response of quartz-mercury line to video signals

that they are transmitted through the channels with the desired fidelity and permit the desired accuracy of cancellation.

**Carrier Frequency.**—Acoustic delay lines that use quartz crystals have a bandwidth proportional to the resonant frequency of the crystals. Video signals, which have a spectrum centered at zero frequency, cannot be transmitted through such a line without severe distortion. This distortion, which is similar to that produced by a “quasidifferentiator” circuit, is shown in Fig. 12-9. By the use of crystals having a resonant frequency approximately equal to the reciprocal of the pulse length, pulses can be transmitted into mercury with satisfactory pulse shape.

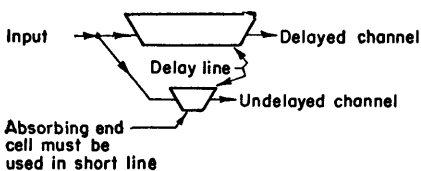


FIG. 12-10.—Method of compensating for video-signal distortion.

Transmission with such comparatively low-frequency crystals has not been thoroughly investigated for practical delay-line tube diameters, and it is difficult to predict whether satisfactory operation can be achieved in this manner for moderately long delays (of more than about 1000  $\mu$ sec). If the primary purpose of the cancellation unit is to indicate the existence of signal changes (from repetition period to repetition period), then video transmission in which some distortion-compensating device is used may be satisfactory, as shown in Fig. 12-10. The apparatus required if video

signals are to be transmitted directly is considerably simpler than the apparatus for the commonly used carrier-frequency signals.

Signals may be delayed without distortion in an electromechanical delay line by transmitting them as carrier-frequency signals and by using a sufficiently high carrier frequency to obtain the necessary bandwidth. (Other factors affecting the choice of carrier frequency are discussed in Sec. 12-2.) This is the method which has been used exclusively.

**Carrier Level.**—Figure 12-11 represents an amplitude-modulated signal

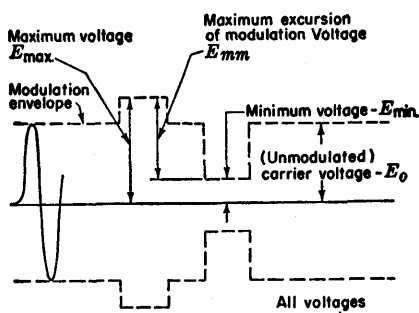


FIG. 12-11.—Modulated-carrier signal.

commonly used for mercury delay-line transmission. This section considers the requirements on the magnitude of the unmodulated carrier level  $E_0$ . Specifically, it must be determined whether  $E_0$  can be so small that the modulation envelope has zero amplitude for some signals or in the absence of signals. This question is of interest because a complex array of equipment may be required to ensure that the modulation envelope

never has zero amplitude. The problem of “adding” a carrier level to signals is treated in Sec. 12-10.

The factor which determines whether the modulation envelope may ever have zero amplitude is the method of cancellation used in the cancellation amplifier. The possible methods are two: “carrier-frequency cancellation” or cancellation of the individual carrier-frequency cycles in the signals, and “envelope cancellation” of the detected modulation envelope of the signals. (These methods are defined in Sec. 12-18.) If carrier-frequency cancellation is used, it is of no consequence whether the modulation envelope ever has zero amplitude; but in envelope cancellation, accurate cancellation requires identical envelope reproduction in the delayed-channel and undelayed-channel detectors. Identical response can be guaranteed only if the minimum voltage  $E_{\min}$  applied to the detector is sufficiently large to avoid the nonlinear response which any detector exhibits for sufficiently small signals. For envelope cancellation, therefore, the carrier level should be somewhat higher than the maximum negative modulation.

Another factor affecting the choice of carrier level, although generally less important than the preceding one, is the interaction of the carrier level with the pulse distortion caused by the variation of delay-line attenuation with frequency. This variation may be great enough in

some cases to distort the pass band of the delayed channel in the manner shown in Fig. 12-12. A pass band such as that of Fig. 12-12c is said to have "semisingle-sideband" transmission. The amount of distortion produced by a semisingle-sideband system depends on the effective percentage modulation; the lower the ratio of  $E_{mm}$  to  $E_0$  (see Fig. 12-11), the lower the distortion.<sup>1</sup> This reason for a high carrier level is not very important, however, since compensation for the delay-line distortion of the pass band is usually introduced for other reasons (see Sec. 12-19). It should also be noted that in many cases the delay-line bandpass

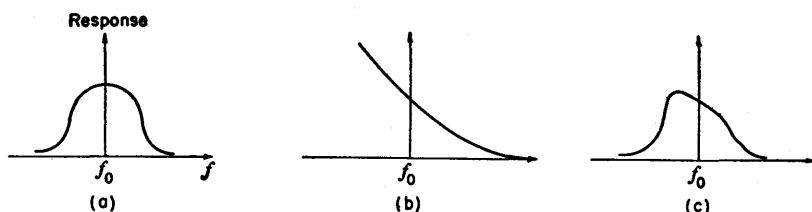


FIG. 12-12.—Distortion of pass band of delayed channel. (a) Typical pass band of delayed channel exclusive of delay line. (b) Possible transmission characteristic of delay line. (c) Combined pass band of (a) and (b).

distortion is so small that the possibility of semisingle-sideband distortion can be neglected.

### 12-10. Method of Obtaining Required Type of Signal. *Video Signals.*

If the signals to be compared are video signals, they must be converted to a carrier frequency. The next several sections of this chapter describe the design considerations for an appropriate converter.

*Carrier-frequency Signals.*—The signals to be compared may be carrier-frequency pulses. It may be possible to apply such signals directly to the delay line as follows:

1. In carrier-frequency cancellation, if the carrier-frequency cycles of unchanging signals have the same phase (i.e., with respect to the timing signal or trigger) in successive repetition periods.
2. In envelope cancellation, if the carrier level is not zero. (If the carrier frequency of the pulses is not suitable for delay-line transmission, a frequency converter may be used, subject to the principles discussed in Sec. 12-12.)

If envelope cancellation is to be used and the carrier level is zero, the signals cannot be applied directly to the line. There are two techniques which may be used to obtain the required signal: the carrier-frequency signals may be detected and the resulting video signals used with a modulated carrier generator, or a carrier may be added. Suitable methods of adding a carrier will now be considered.

<sup>1</sup> See H. E. Kallmann and R. E. Spencer, *Proc. I.R.E.*, **12**, 557-561 (1940).



A carrier from a source independent of the source of signals cannot be added to the signals because such addition will convert nonchanging signals, which should cancel, into changing signals, which will not cancel. This conversion occurs because, even though the amplitude of a pulse may not change in successive repetition periods, a fluctuating signal will result if the phase angle between this pulse and the carrier changes in

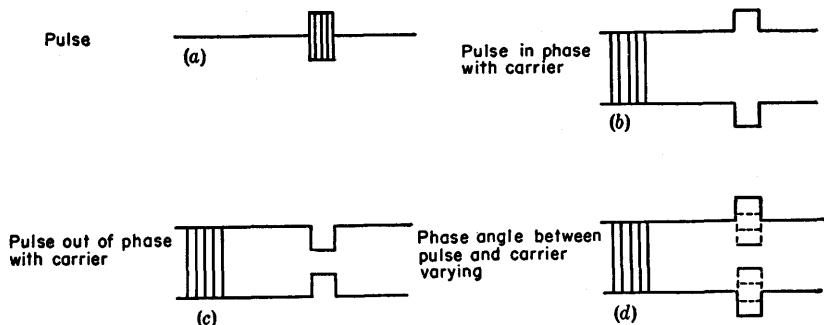


FIG. 12-13.—Fluctuation resulting from addition of noncoherent pulse and carrier.

successive repetition periods, as shown in Fig. 12-13. Figure 12-14 shows the general form of coherent-phase technique—either the c-w generator, which supplies the carrier level, can be made to control the phase of the pulse-signal source or the pulse can be made to control the phase of the c-w generator.<sup>1</sup> The “device” of Fig. 12-14 is the device whose varying characteristics in successive repetition periods are to be investigated by

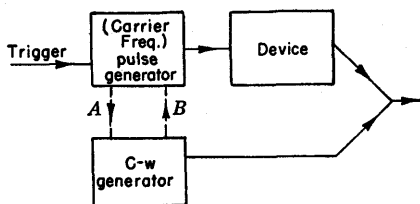


FIG. 12-14.—Coherent-phase technique. Arrow A, coherence of CW by pulse. Arrow B, coherence of pulse by CW.

the cancellation circuit. Because this device generally transmits signals with some delay, the c-w generator must have a certain degree of stability in order that its phase will be coherent even with delayed signals (if they are nonchanging, of course). Correspondingly, addition of the outputs of the phase-coherent, stable c-w generator and the “device” can provide a sensitive means of determining whether the time delay in the latter varies in successive repetition periods.

<sup>1</sup> A typical circuit of a “coherent oscillator” and other pertinent information can be found in Chap. 22, Vol. 23.

### CARRIER GENERATOR AND MODULATOR UNIT

The following four sections are concerned specifically with a unit that converts video signals to modulated-carrier signals suitable for a system using envelope cancellation. Much of the material included, however, is applicable to systems using carrier-frequency cancellation or having information supplied in the form of carrier-frequency signals.

The modulated-carrier-generator unit of the system shown in Fig. 12-4 is referred to frequently for examples of the principles discussed. A circuit diagram of this unit is given in Fig. 12-15.

**12-11. Oscillator.**—The oscillator of a modulated-carrier-generator for envelope cancellation is a simple device. The frequency stability required is only that which will keep signals in the pass band of the following circuits. The amplitude must be stable enough to prevent spurious fluctuations. Satisfactory stability can generally be obtained by the use of a regulated plate- and screen-voltage supply, as is commonly necessary on all tubes affecting signals before cancellation.

Oscillator circuits are discussed in detail elsewhere in this series.<sup>1</sup> Any of the usual circuits is satisfactory. The modulation technique recommended in the next section requires only small oscillator output, although it may be convenient to have push-pull output.

If the stage following the oscillator is the modulator, attention must be given to the problem of preventing the modulating signals from undesirably affecting the oscillator.

**12-12. Modulation.**—Modulation of the carrier must be accomplished in such a way that the modulation envelope (a) is constant for a signal whose amplitude does not change from one repetition to the next, (b) reproduces changes in a modulating signal with the desired linearity of incremental response (usually linearity of better than 10 per cent is unnecessary), and (c) reproduces signals with the desired rise time. Requirement (c) determines the minimum permissible bandwidth of the modulating circuits, and (a) necessitates freedom from any "transient" effects.

*Modulation Transients.*—An undesirable transient effect can occur if the modulating signal contains frequency components in the carrier-frequency region which appear in the modulator output. If such carrier-frequency components are present, a transient signal that has a definite phase with respect to the modulating signal at approximately the carrier frequency will exist. The frequency spectrum of the transient will depend on the frequency spectrum of the modulating signal and on the pass band of the circuits through which the transient passes. If the modulating signal is approximately a step function and if the circuits

<sup>1</sup> Vol. 19, Chap. 4.

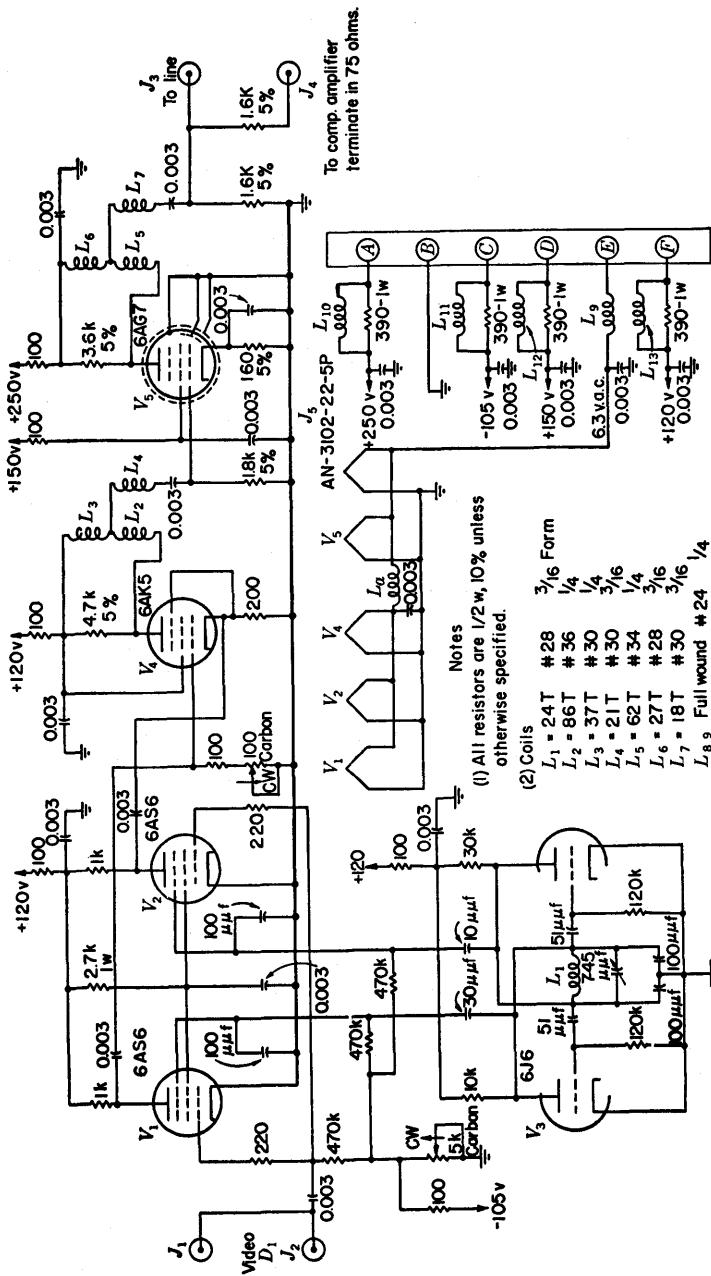


Fig. 12-15.—A 15-Mc/sec carrier generator and signal-balanced modulator.

referred to have a pass band centered at the carrier frequency, then the frequency of the transient will be approximately the carrier frequency. In successive repetition periods, the phase of the carrier will not necessarily be the same at the beginning of the modulating signal. The sum of the transient and the modulated carrier, therefore, will vary in suc-

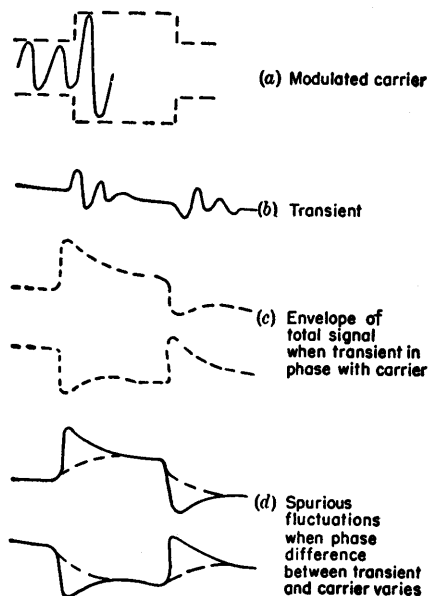


FIG. 12-16.—Effect of modulation transient.

cessive repetition periods even if the modulating signal does not change. The spurious fluctuations which result are illustrated in Fig. 12-16.

Transient effects of modulation can be reduced or eliminated by the use of a “balanced modulator,” in which the output does not contain signal-frequency components (see Vol. 19, Chap. 11). Figure 12-15 shows an example of a signal-balanced modulator in which the single-ended signal is applied to the parallel-connected grids of  $V_1$  and  $V_2$ . The push-pull carrier is applied to the suppressor grids and a push-pull output is taken between the plates. The modulating voltage is applied to grid 1 instead of grid 3. The 100-ohm rheostat in the grid return of  $V_4$  is an adjustment for obtaining balance for transient cancellation. It was

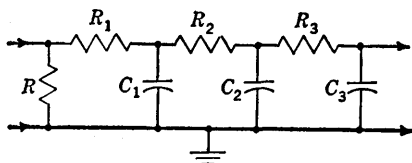


FIG. 12-17.—Simple RC-filter for pulse-smoothing.  $R_1C_1 = R_2C_2 = R_3C_3$ ;  $R_3 > 5R_2$ ;  $R_2 > 5R_1$ .

found possible with this circuit to reduce transient output to about 0.1 per cent of the desired output signal.

Another procedure for reducing transient effects is to employ a pulse-smoothing network. Figure 12-17 shows a simple form of  $RC$ -filter which may be used for pulse-smoothing if an impedance-level change is permissible in the filter.

Pulse-smoothing not only reduces modulation-transient effects, but also eases the bandpass-matching requirements on the cancellation amplifier. The degree of smoothing used is determined by a compromise between these advantages and the loss of pulse definition in time resulting from smoothing.

If the phase of the carrier were always the same at the beginning of an unchanging modulating signal, transients would not cause spurious

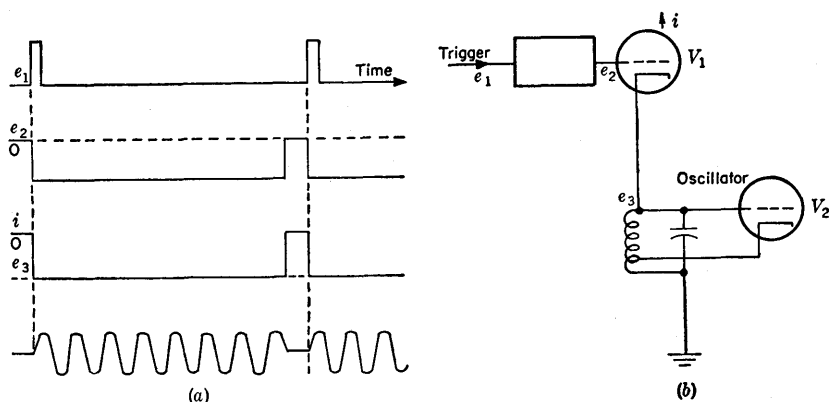


FIG. 12-18.—Pulsed oscillator.

amplitude fluctuations. Such a phase relation can be obtained by setting the phase of the carrier with each trigger, that is, by a pulsed oscillator (see Vol. 19, Chap. 4). The oscillator must have suitable frequency stability so that the carrier phase will be coherent even with modulating signals that occur some time after the trigger. An untried method is outlined below.

In the pulsed oscillator illustrated in Fig. 12-18, the cathode impedance of  $V_1$  during conduction is so low that  $V_2$  is prevented from oscillating; each trigger turns  $V_1$  off and the resulting transient sets the phase of the tank-circuit oscillation.

Modulation transients are objectionable only if the spurious fluctuation in the output has greater amplitude than the smallest fluctuation of interest. Thus, the permissible percentage fluctuation due to transients is inversely proportional to the ratio of the largest modulating signal to the smallest signal of interest—the “dynamic range” of signals. The

relative effect of transients can therefore be reduced by compression of the dynamic range of signals. Range compression is discussed further in Secs. 12-15 and 12-16.

Modulation methods are discussed elsewhere in considerable detail.<sup>1</sup>

**12-13. Amplification.**—Weak signals must be delivered by the delay line at sufficiently high level to prevent their discernibility from being impaired by noise produced in the cancellation amplifier. The maximum voltage required to drive the delay line depends on the line attenuation and the dynamic range of signals transmitted. If an oscillator-modulator combination cannot deliver sufficient output, carrier-frequency amplification must be used.

Amplification may be used between the oscillator and modulator (if they are separate) or following the modulator. The advantages of the former method are that the amplifiers need not be wideband and that isolation is provided between the oscillator and modulator. The possible disadvantages of the method are that if the modulation is performed at "high level" it may be slightly nonlinear owing to cutoff or grid current in the modulator, and amplification of the modulating signal may be required. The possible nonlinearity is generally small, and linearity is necessary for obtaining balanced operation. The unit shown in Fig. 12-15 exemplifies the use of low-level modulation in a signal-balanced modulator followed by wideband amplification.

**12-14. Output Circuit.**—It will often be necessary that the output circuit have the greatest possible gain-bandwidth product (where "gain" is used to mean "transfer impedance") in order to obtain sufficiently high delay-line output signal. The controllable factors which affect the gain-bandwidth product are total shunt capacitance of the output circuit and the complexity of the circuit.

In order to decrease the shunt capacitance of the circuit and to avoid the necessity of a long connecting cable, the output tube should be located physically near the delay-line input terminal. It is assumed here that if high-efficiency coupling is desired, any connecting cable used will act effectively as a pure shunt capacitance because it is short compared with a carrier-frequency wavelength and is not terminated in its characteristic impedance. Operation with characteristic-impedance termination of the cable is not generally used if high-efficiency coupling is desired because such operation, although it has the advantage that an arbitrarily long cable can be used, cannot generally provide so high efficiency as other coupling methods.<sup>2</sup>

The required coupling efficiency determines the complexity of the coupling circuit, which will ordinarily be either a single-tuned or double-

<sup>1</sup> See Vol. 19, Chap. 11 of this series.

<sup>2</sup> A treatment of cable-termination methods is to be found in Vol. 23, Chap. 7.

tuned circuit. The former is simpler to construct and adjust, and is more tolerant of variations in circuit capacitance that may occur when the delay line or output tube is changed, but double-tuned circuits can provide greater gain-bandwidth product. Slight mistuning of this circuit is relatively unimportant because it affects both the undelayed signal and the delayed signal equally.

The signals supplied to the undelayed and delayed channels should be identical. This identity can be guaranteed by obtaining the signal for the undelayed channel from a frequency-insensitive voltage divider at the input crystal of the delay line. The load resistance for the output circuit can be used conveniently as such a divider and the signal transmitted to the undelayed channel through a terminated low-impedance line.

The circuit shown in Fig. 12-15 uses a double-tuned output circuit, loaded on the secondary side only. The voltage divider used to feed the undelayed channel is located in the modulated-carrier-generator chassis rather than at the delay-line crystal. This procedure is satisfactory in this circuit because the cable from the voltage divider to the crystal is very short compared with a wavelength at carrier frequency and therefore acts essentially as a pure shunt capacitance. The output tube and circuit in this unit provide a maximum output of about 10 volts rms, with an output-circuit bandwidth of about 6 Mc/sec for a delay-line crystal capacitance of about 30  $\mu\text{f}$  and a cable capacitance of about 5  $\mu\text{f}$ .

### DYNAMIC-RANGE COMPRESSION

**12-15. Definition and Advantages of Compression.**—It has been stated in Sec. 12-12 that the difficulty of some design problems depends directly on the dynamic range of signals, that is, on the ratio of the largest signal to the smallest signal of interest. This section and the following one are concerned with methods for reducing the dynamic range of signals without appreciably affecting fluctuations from repetition period to repetition period.

The advantages to be gained by the use of compression are as follows:

1. The cancellation quality need not be so high. Cancellation must be so good that uncanceled residues from nonchanging signals are smaller than the smallest desired fluctuations of interest. If the ratio of the largest to the smallest signal is reduced, less accurate cancellation is required.
2. The maximum voltage required to drive the delay line is smaller. For a given maximum available voltage, therefore, the percentage modulation can be reduced, or for a given maximum available voltage, longer delays (with more attenuation) can be used.

3. The cancellation amplifier need not have so good a noise figure since if the maximum modulation voltage is kept fixed and the dynamic range of signals reduced, the weak-signal level delivered by the delay line will be increased.
4. Modulation transients are less important.
5. The bidirectional video amplifier in the cancellation amplifier need not have so much gain since, for a given maximum modulation voltage at the cancellation amplifier detectors, the level of weak signals is increased by a decrease in the dynamic range of the modulation. (This amplifier is often not easy to design, but a reduction in the gain required and in the dynamic range of signals to be handled can considerably simplify the design.)

**12-16. Methods.**—Several methods of dynamic-range compression were suggested. The most promising of the methods, sawtooth com-

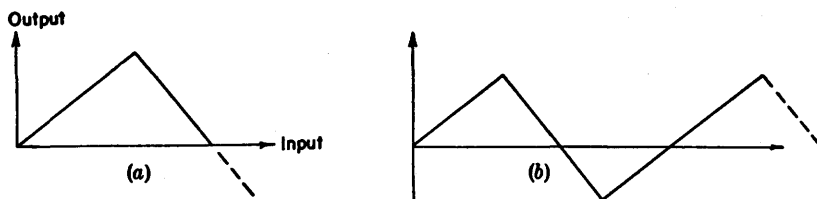


FIG. 12-19.—Sawtooth characteristics for dynamic-range compression.

pression, which operated successfully in preliminary tests, is described briefly in the following paragraph.

The principle of the sawtooth compressor involves the use of an amplitude response characteristic, such as is shown in Fig. 12-19, which has an essentially constant-magnitude slope but which is not monotonic. The efficiency of such a characteristic depends on the sharpness of the "peaks," where fluctuations in the input signal may be compressed. Experimentally, relatively sharp peaks have been obtained by the use of back-biased circuits. Figure 12-20 is a simplified schematic diagram of a circuit that has the response shown in Fig. 12-19a.

The rms noise should be small (20 to 30 db down) relative to the amplitude of the sawtooth waveform. Otherwise the probability of detecting a

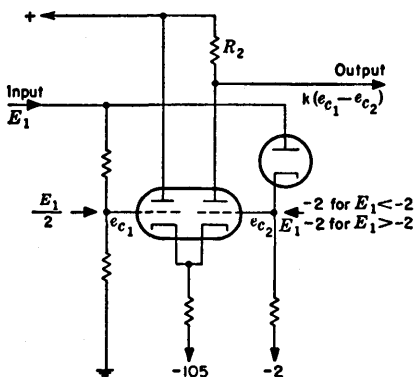


FIG. 12-20.—Circuit to give response shown in Fig. 12-19a.



change in signal amplitude is poor because a shift from one sawtooth wave to another may give an amplitude change that is less than noise.

### CANCELLATION AMPLIFIERS

By W. SELOVE

**12-17. Introduction.**—Subtraction of successive waveforms and, cancellation of their nonchanging parts take place in the cancellation amplifier. This unit usually consists of four principal sections: a carrier-frequency amplifier in the delayed channel and one in the undelayed channel, a subtraction circuit, and a video section for handling the signals remaining after cancellation (see Fig. 12-1).

For perfect cancellation, the delayed and undelayed channels must have identical over-all frequency response and linearity characteristics. Special attention must sometimes be given to securing high-efficiency coupling between the delay line and the cancellation amplifier.

Special requirements are usually imposed on the video section by the nature of the signals to be handled. Noncanceling signals may be bidirectional (see Vol. 19, Chap. 11), and the maximum uncanceled signal may be very much larger than the smallest uncanceled signal of interest. In some cases, efficient utilization of noncanceling signals requires their full-wave rectification.

The cancellation amplifier may also include special features and circuits to provide automatic adjustment of cancellation and gain controls.

**12-18. Cancellation Methods.**—There are two methods of cancellation that may be used (see Sec. 12-9). Even though the cancellation amplifier is very much simpler for the carrier-frequency method, envelope cancellation is the only method that has been used. The reason is to be found in the stability requirements on the repetition rate. For envelope cancellation, the repetition period must be "jitter free" to a fraction of a pulse length (see Sec. 12-28); for carrier-frequency cancellation, it must be jitter-free to a fraction of a carrier-cycle period, which requires a considerably higher degree of stability. At the pulse lengths used, it has been readily possible to obtain the necessary stability for envelope cancellation but not for carrier-frequency cancellation. For future applications, however, carrier-frequency cancellation may be feasible; it is, therefore, appropriate to consider here how the cancellation-amplifier requirements are affected by the cancellation method, even though the circuits treated in detail in the following sections are those suitable primarily for envelope cancellation.

Precision envelope cancellation requires that the envelope be linearly reproduced at the outputs of the delayed and undelayed channels. Since

the output circuits consist of detectors, a moderately high output signal level is necessary to ensure linear envelope reproduction. To obtain a suitably high signal level, considerable gain in the delayed-channel amplifier will usually be required because signals are usually delivered by the delay line at comparatively low level. For carrier-frequency cancellation, however, no gain whatsoever is necessary before cancellation, and passive elements may be used for subtraction. In envelope cancellation, noncanceling signals are bidirectional. In carrier-frequency cancellation, although noncanceling signals can appear with either "positive" or "negative" phase, the detected signals will constitute unidirectional video signals. The difficulties of handling bidirectional video signals are discussed at greater length in Secs. 12-25 to 12-27.

#### CARRIER-FREQUENCY CHANNELS AND CANCELLATION CIRCUIT

**12-19. Pass Band. General Theory.**—For perfect cancellation, the delayed and undelayed channels must affect a signal identically.<sup>1</sup> It will generally become easier to approach this condition as the effect of the channels on the signal is reduced, which is accomplished by increasing the bandwidths of the channels.

The effective shape of the delayed or undelayed signal is determined by the over-all system bandwidth. The delayed and undelayed channels of the delay-and-cancellation unit (see Fig. 12-4) will affect this shape little, and a small unbalance in the channels will therefore not be serious if the channel bandwidths are large compared to the over-all system bandwidth. A factor of 2 will probably be a satisfactory compromise with the number of tubes required.

*Bandpass Compensation.*—In order that the delayed and undelayed channels may have essentially identical frequency response, compensation must often be provided (1) for the frequency response of the delay line, and (2) for the difference in the number of tuned stages of amplification required in the two channels.

The transmission attenuation of a liquid delay line increases with frequency; for a round tube of length  $l$  and diameter  $d$ , the attenuation (db) is given by

$$\alpha = k_1 l f^2 + k_2 \frac{l}{d} \sqrt{f},$$

where  $k_1$  and  $k_2$  are constants for a given medium,  $l$  is the length, and  $f$  is frequency (see Sec. 12-2). In many cases, the variation of delay-line attenuation over the delayed-channel pass band is so great as to distort this pass band severely. For example, for the 1000- $\mu$ sec mercury line

<sup>1</sup> For general information applicable to the design of the carrier-frequency channels, the reader is referred to Vol. 23.

illustrated in Fig. 12-2 the attenuation for frequencies near 15 Mc/sec varies at about 2 db per Mc/sec. Figure 12-21 shows how such rapid variation will distort a pass band from one of 4.0-Mc/sec width centered at 15 Mc/sec, to one of 3.0-Mc/sec width centered at 14 Mc/sec.

Two undesirable effects would result from operation without compensation for the delay-line characteristic. First, at a given carrier frequency, signals would not be transmitted through the delayed and undelayed channels with identical shape; and second, slight changes in carrier frequency would affect the relative amplitude response of the two channels and hence cancellation. This effect is often so serious that compensation must be used.

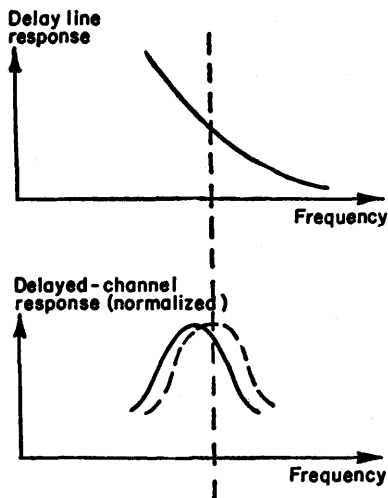


FIG. 12-21.—Effect of delay line on delayed channel pass band.

Compensation for the delay-line characteristic can be achieved by the use of a suitable network in either channel (or networks in both channels)—that is, a network having the same attenuation-vs.-frequency characteristics as the line may be inserted in the undelayed channel, or a network with a reciprocal characteristic may be used in the delayed channel. The latter method is preferable because it results in bandwidths in both

channels greater than would be obtained if a distorting network were used in the undelayed channel.

A compensating circuit consisting of a single-tuned circuit tuned to a frequency higher than the carrier frequency may be used. Such a circuit, with a suitable bandwidth and center frequency, can provide good compensation for characteristics such as those described in the previous paragraph. The procedure for determining the proper values of the parameters is described elsewhere. An example of the use of this type of compensation circuit is the interstage coupling between  $V_3$  and  $V_4$  of Fig. 12-22.

As was stated, compensation must be provided for the difference in the number of tuned stages of amplification required in the two channels. For envelope cancellation, the voltage gain required in the delayed-channel amplifier is often as high as 100, 1000, or more. To obtain the necessary gain with the desirable bandwidth often requires a number of stages of amplification. The over-all pass band of these several stages cannot be exactly matched by a pass band equally "wide" produced by

the smaller number of stages needed to supply the necessary gain in the undelayed channel amplifier. The matching is poorest if the bandwidth of the undelayed channel is reduced by a single "narrowing" circuit to a value approximately equal to the bandwidth of the delayed channel; yet such a simple method of compensation is often satisfactory if highly accurate cancellation is not required, if the numbers of tubes in the channels do not differ by more than one or two, and especially if the channel bandwidths are large compared to the over-all system bandwidth.

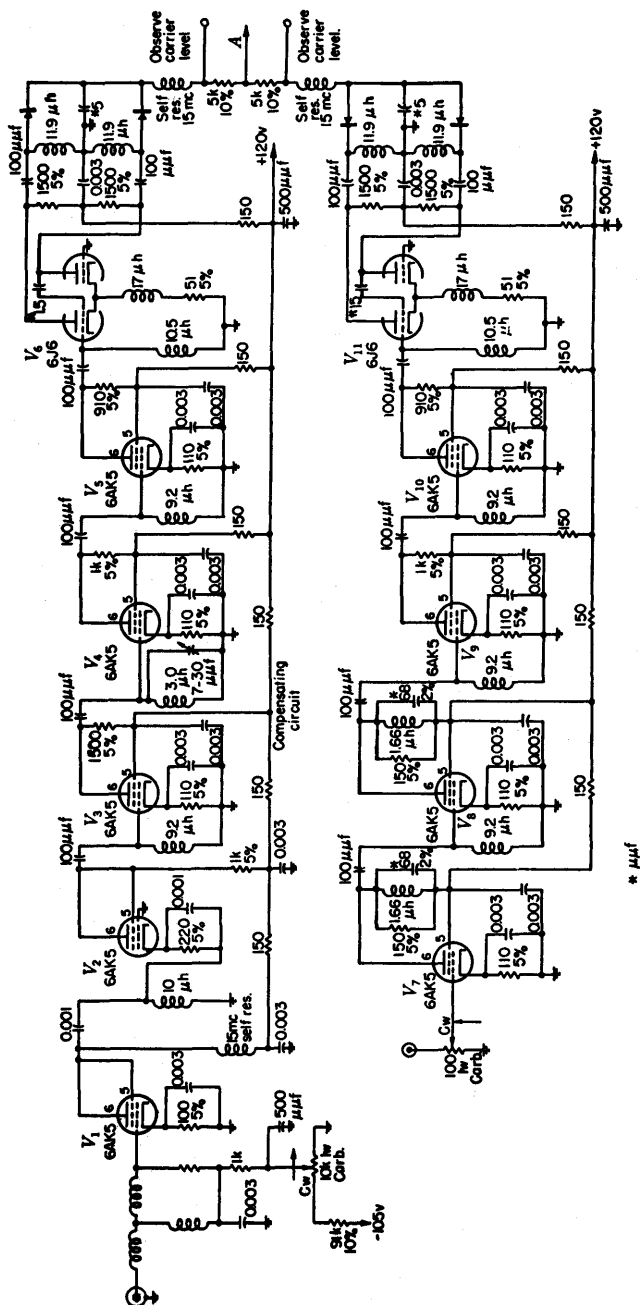
A more intricate method of compensation is to employ additional tuned circuits in the undelayed channel which will help give a more exact duplicate of the over-all frequency response of the delayed channel. The extra circuits required in the undelayed channel may be connected by attenuation units as in Figs. 12-22 and 12-23.

If identical numbers of stages are used in both channels, the undelayed-channel amplifier will have far more available gain-bandwidth product than is necessary. The attenuation units ensure that this amplifier does not have so much gain as to make the noise in its input circuit contribute appreciably to the over-all noise. In the circuit of Fig. 12-22, these measures consist of the reduction of gain in the inter-stage circuits of  $V_{7-8}$  and  $V_{8-9}$ , by the use of what might be called "narrow-band resistors," resistors paralleled by fixed-tuned circuits, with constants chosen to give proper bandwidth.

**12-20. Linearity.**—For accurate envelope cancellation the modulation envelope of signals must be linearly reproduced at the detectors. Figure 12-24 (cf. Fig. 12-11) illustrates how, for linear reproduction, the minimum amplitude of the modulation envelope must not be so small as to fall in the nonlinear response region of the detectors, and how the maximum amplitude of the envelope must not be so large as to cause nonlinear operation of any of the amplifiers. Measures that may be taken to obtain a linear-response region large enough to accommodate the modulation envelope are (1) reduction of the percentage modulation represented by signals and (2) increase of the maximum distortionless output voltage of the carrier-channel output amplifiers.<sup>1</sup> The maximum distortionless output voltage for an output tube may be increased by an increase in the load impedance of the output circuit but at the expense of the bandwidth.

In practice, the signals in the final stages of the carrier-frequency channels may be so large as to make operation not strictly linear. Rough compensation for slight nonlinearity may be obtained by operating the last two stages in one channel under conditions identical with those of the last two stages in the other channel.

<sup>1</sup> Dynamic-range compression, discussed in Secs. 12-15 and 12-16, is useful for reduction of percentage modulation.





**12-21. Gain. Gain Control.**—Gain control is generally required in both channels to accommodate the largest expected variations in tube transconductances and, in the delayed channel, to accommodate variations in delay-line attenuation. This control should be located early in the

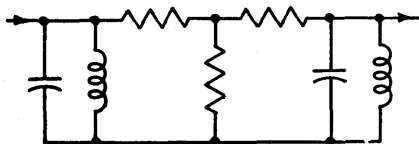


FIG. 12-23.—Isolation of single-tuned circuits by attenuation pad.

amplifiers so that signals do not become large enough, before reaching the gain-controlled stage or stages, to operate tubes nonlinearly.

For the undelayed channel, a simple and satisfactory method of gain control consists of a low-impedance, noninductive potentiometer (preferably carbon), which can serve as both a gain control and an input cable termination. This type of control is illustrated in Fig. 12-22.

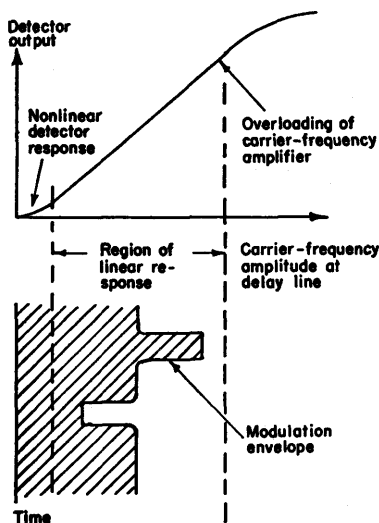


FIG. 12-24.—Modulation envelope conditions for linear reproduction.

For several reasons (see Vol. 23), grid-bias gain control is usually used in the delayed channel, usually on the first two stages. When the delayed-channel amplifier is designed, the required gain should be chosen so that the gain-controlled stages will not be normally operated at such reduced gain as to affect adversely the signal-to-noise ratio of signals passing through this channel. Possible impairment of this signal-to-noise ratio can occur in two ways. First, the gain of the gain-controlled stages may be set so low that noise produced in the following stage produces

an output comparable to that of weak signals. Second, if tube noise in the first stage is comparable to the level there of weak signals, the signal-to-noise ratio will be impaired if this stage is operated at too low gain, because grid-gain control decreases the gain of a tube faster than it decreases its noise. It is for this second reason that it may be desirable to apply gain-control bias to more than one stage.

In practice the gain control of each channel is adjusted to give approximately the correct value of detected-carrier voltage, and then either

control is used to adjust the final balance for best cancellation. For very accurate cancellation it may be necessary to set the gain to within 1 per cent of the correct value; therefore the gain control used for cancellation adjustment must be smoothly and finely adjustable.

*Gain Stabilization.*—Since no advantage was taken of negative-feedback for gain stabilization, stabilization of the relative gains of the two channels depends upon the use of identical numbers of tubes in the two channels. This method is used in the circuit of Fig. 12-22,<sup>1</sup> and has

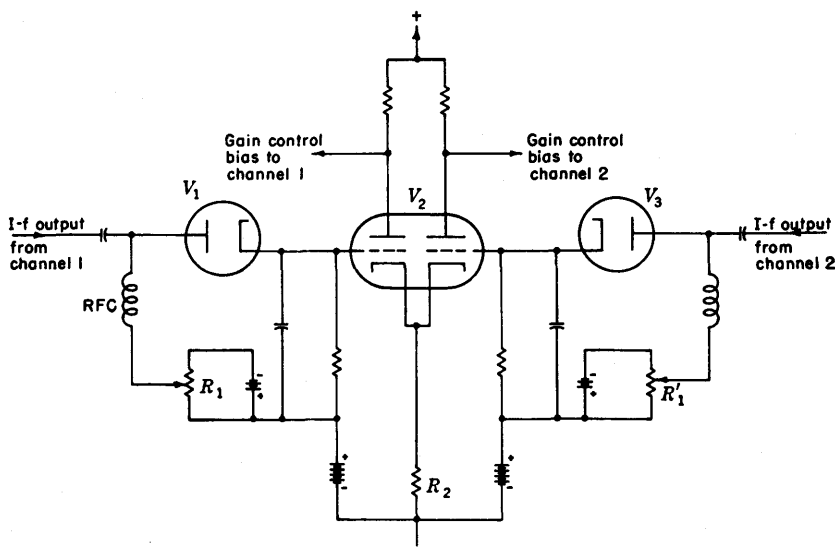


FIG. 12-25.—Gain-stabilization circuit.

proved fairly satisfactory. The gains of the two channels have remained equal for several hours within 2 or 3 per cent over temperature ranges of 30° C.

A stabilization method that can be used alternatively or in addition to the use of identical numbers of tubes is automatic gain control (AGC). Automatic-gain-control voltage can be applied either on the basis of the cancellation-circuit output produced by an unchanging test signal or, in envelope cancellation, on the basis of the output of the detectors corresponding to the carrier amplitude. The first of these methods is generally complicated and will not be discussed here.

<sup>1</sup> It will be seen that there is actually one more tube in the delayed channel than in the undelayed channel. In the circuit used, however,  $V_2$  has a voltage gain of unity, essentially independent of its transconductance; hence stabilization against changes in its transconductance is unnecessary, and for stabilization purposes  $V_2$  is not counted as a tube.



It is clear that any AGC circuit used for carrier-amplitude stabilization should have a response time that is long compared to the pulse length used; otherwise, individual modulation signals will be somewhat demodulated. Even if the AGC circuit has a time constant very long compared to the repetition period, undesirable effects can occur if the AGC tends to keep the average output level of each channel constant. If the carrier is modulated with unidirectional signals obtained, for example, from a radar system, the average voltage level at each detector is likely to vary as the direction of the radar beam is varied; an AGC that tends to keep the average output level of each channel constant would in this case vary the absolute value of comparison-amplifier gain as the beam is moved.

Such a gain variation will not occur if the AGC system tends merely to keep the output levels of the two channels balanced against each other, without regard to their absolute values. Figure 12-25 is a simplified schematic diagram of a proposed AGC circuit which should give level balance stabilization to this type of output. If  $R_2$  is high compared to the cathode impedance of  $V_{2a}$  or  $V_{2b}$ ,  $V_2$  will operate as a differential amplifier (see Vol. 19, Chap. 9), responding only to a difference in the rectified outputs of  $V_1$  and  $V_3$ . The  $R_1$  and  $R'_1$  provide a means for adjusting the channel outputs to the proper value and for initial balance. This AGC circuit operates only as a stabilizer and not as absolute control for cancellation.

**12-22. Detection.**—The detector in each channel must reproduce the modulation envelope as faithfully as possible. In order that the detector output may depend as little as possible on the phase of the carrier cycles within the envelope, full-wave detection is used rather than half-wave.

Detector design is discussed in detail in Chap. 7, Vol. 23 of this series, but a few points will be mentioned here, with the detector circuit in Fig. 12-22 as an example. Germanium crystals are superior to electronic tube rectifiers because of the lower shunt capacitance and lower forward resistance of the crystals. It is advantageous to use a high load-resistance detector to obtain high-efficiency detection and good linearity. The low capacitance of a crystal rectifier not only permits the use of a high load-resistance detector but also makes it possible to obtain a high gain-bandwidth product in the carrier-frequency output circuit, thus reducing the danger of nonlinear operation in the carrier-frequency output amplifier.

The push-pull carrier-frequency output necessary for full-wave detection can be obtained with either a transformer or phase splitter. The former method has the advantage that the balance of the two halves of each detector is not dependent on any amplifiers; the latter method has the advantages that magnetic coupling is not required and that a high degree of symmetry can be obtained for high carrier frequencies

(30 Mc/sec and higher) more easily than with a transformer. The circuit of Fig. 12-22 uses phase splitters for carrier-frequency output amplifiers. The  $1.5\text{-}\mu\text{f}$  condenser used in each of the 6J6 phase splitters is a neutralizing condenser.

**12-23. Cancellation Circuit.**—The signals from the delayed and undelayed channels should be canceled—i.e., subtracted from each other—at the earliest possible point in the cancellation amplifier because, generally, all stages before cancellation must be linear whereas those following cancellation need not be.

For envelope cancellation, the earliest possible point is the output of the detectors. The circuit of Fig. 12-22 uses a simple cancellation circuit or difference detector (see Vol. 19, Chap. 14) which is closely symmetrical for the two channels. A simplified circuit is shown in Fig. 12-26. Rectifiers  $D_1$  and  $D_2$  provide d-c returns for each other. The output of the circuit consists of a

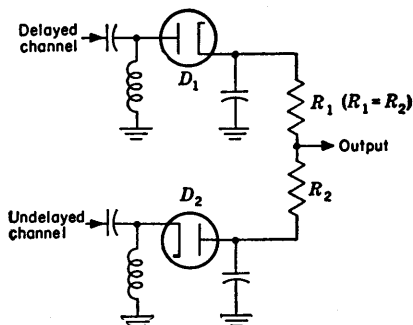


FIG. 12-26.—Simplified cancellation circuit.

a positive rectified component produced across  $R_2$  by the delayed channel, plus a negative rectified component produced across  $R_1$  by the undelayed channel.

**12-24. Coupling to Delay Line.**—In order to obtain delay-line output sufficiently high so that cancellation-amplifier noise is unimportant, the circuit coupling the delay line to the delayed-channel amplifier must have as high a gain-bandwidth product as possible (cf. Sec. 12-14).

As in the case of the circuit at the input end of the delay line, a maximum gain-bandwidth product can be obtained with least complexity by locating the first stage of the delayed channel physically close to the delay-line output terminal and thus eliminating a connecting cable or at least minimizing its length. Any connecting cable, if operated unterminated, should be short compared to a wavelength (i.e., at carrier frequency) not only to minimize shunt capacity but to avoid the introduction of a transfer-impedance characteristic that may not be easy to duplicate in the undelayed channel.

Unlike the situation at the input end of the line, however, not too high a price in fineness of adjustment can be paid for a high gain-bandwidth product because the frequency response of the delayed channel must be kept as nearly as possible like that of the undelayed channel. Thus, a double-tuned circuit loaded only on one side should not be used if satisfactory operation can possibly be obtained with less critical

circuits. This restriction holds even though a circuit loaded on the tube side not only has a higher gain-bandwidth product than a double-tuned circuit loaded on both sides but also presents lower impedance to the tube, thus decreasing noise.

In connection with obtaining delay-line output large compared to the cancellation-amplifier noise, it is appropriate to mention the possibility of reducing this noise to a minimum by the use of a "low noise" input circuit in the delayed channel. In Fig. 12-22  $V_1$  and  $V_2$  comprise such a circuit, the operation of which is discussed in detail in Vol. 23 Chap. 5 of this series.

If the entire cancellation amplifier cannot be placed physically close to the delay-line output, the advantages of having the first stage of the delayed channel so located can be realized by using a preamplifier mounted at the line. Such a preamplifier would in general be connected to the rest of the cancellation amplifier by a low-impedance cable and would have a voltage gain of 2 or 3.

The use of a terminated high-impedance (about 1000-ohm) connecting cable having a suitable amount of time delay (perhaps 0.2  $\mu$ sec) offers the attractive possibility that a particularly simple method of repetition-rate control can be used (see Sec. 12-30). A possible objection to the use of such a cable, however, is that at the usual carrier frequencies of 10 Mc/sec to 30 Mc/sec it might have an objectionable amount of attenuation.

#### VIDEO SECTION

**12-25. Requirements of Video Section.**—In a typical envelope cancellation amplifier, noncanceling signals may produce video outputs at the cancellation point of plus or minus 1 to 100 mv. It is convenient to have a maximum output of one volt or so to a low-impedance line and this is obtained by a video gain of approximately 1000.

As in any video amplifier in which the largest signal occurring is much larger than the smallest signal of interest, care must be taken to prevent large signals from "blocking" the amplifier—that is, from producing a response that would reduce the likelihood that a small signal closely following a large one will be discernible. Methods of designing nonblocking video amplifiers are discussed in detail elsewhere,<sup>1</sup> but some material will be presented. Here, the video signals have a large dynamic range. Moreover bidirectional video is somewhat more difficult to handle than the more common unidirectional video.

**12-26. Amplifier for Bidirectional Video.**—Let us review briefly the cause of the difficulty in the design of a nonblocking video amplifier for signals of large dynamic range and consider the applicability to bidirec-

<sup>1</sup> Vol. 18, Secs. 5-8 and 10-4.

tional signals of the common methods of alleviating the difficulty. (See Fig. 12-27.)

In the final stages of a high-gain video amplifier, it may be possible for a large signal to cause grid current to flow in some stage or stages. Grid-current flow may so bias the coupling condenser, if one is used, as to cause operation at reduced gain or zero gain after the appearance of a large signal, until the condenser discharges. The effect is illustrated in Fig. 12-27*d*. The use of d-c restoration, illustrated in Fig. 12-27*e*, is not applicable to bidirection signals because negative signals cannot be distinguished from overshoots caused by the flow of grid current.

Another attack on the blocking problem with condenser-coupled stages is to prevent the flow of grid current by having such operating

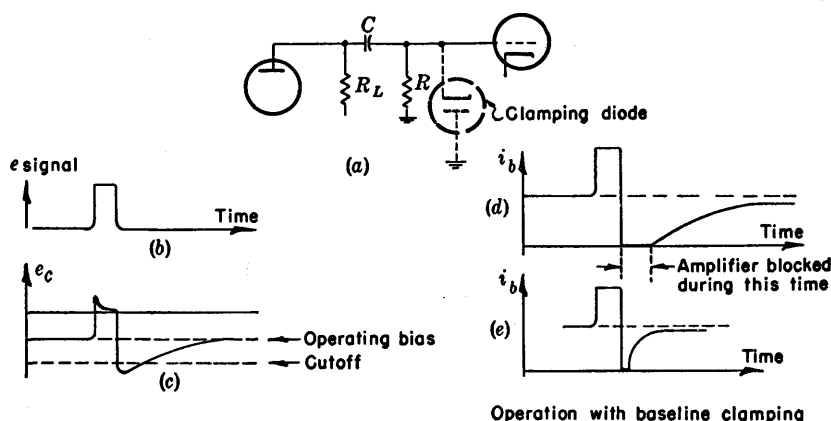


FIG. 12-27.—Amplifier blocking due to grid-current flow.

conditions that no stage can deliver a positive output signal greater than the grid bias on the next stage. For this method to be successful, it is necessary that the "next" stage have reasonably high gain even with suitably high quiescent bias.

Grid-current flow is not harmful if direct coupling is used. The use of direct coupling to prevent blocking is, of course, as effective for bidirectional as for unidirectional signals. In the circuit of Fig. 12-22, direct coupling is used between  $V_{12}$  and  $V_{13}$ . To prevent the application of excessive voltage to the grid of  $V_{13}$  if  $V_{12}$  is removed temporarily,  $V_{17}$  serves as a voltage regulator.

One more blocking-prevention method will be mentioned here—the use of a cathode-coupled amplifier, as exemplified by  $V_{14}$  in Fig. 12-22. From this figure, it can be seen that application of a positive signal to the grid of  $V_{14a}$  results in a negative signal being applied to the grid of  $V_{14b}$ . For increasingly positive signals, the grid of (a) is driven past

cutoff, and the cathode voltage then "follows" the grid of (b) so closely that a very large positive signal is required to make the grid of (b) positive with respect to the cathode. It may be noted that a phase splitter was used in this particular unit as much to provide push-pull output for the following video rectifier as for its nonoverloading characteristic.

A few words about the coupling time constants in the bidirectional video amplifier are appropriate here. Long time constants are unnecessary, because noncanceling signals will not generally produce long unidirectional outputs. Very short time constants are to be avoided because they may cause overshoots of an undesirable nature; in particular, time constants of approximately 5 to 10 pulse lengths can cause multiple overshoots if several cascaded stages have such time constants. Multiple overshoots are particularly undesirable if video rectification is used (see Sec. 12-27). The use of a short time constant, of approximately a pulse length, at the input to the bidirectional video amplifier has the advantage that intermediately long time constants can be used afterwards without trouble from multiple overshoots.<sup>1</sup> If moderately long time constants (of about 50 pulse lengths) are used up to the last interstage circuit and a short time constant is used at the last interstage circuit, the grid-current flow in the last stage can be made unimportant by the use of a grid resistor ( $R$  in Fig. 12-27a), whose value is small compared to the conducting value of the tube grid-cathode resistance.

**12-27. Video Rectification.**—It is often desired to observe the output

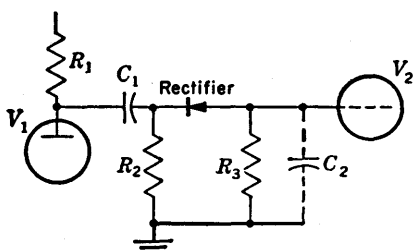


FIG. 12-28.—Elements of video rectifier.

of these devices on an oscilloscope. If the noncanceling output signals are to be presented on a deflection-modulation oscilloscope, the bidirectional form in which these signals are delivered by the cancellation circuit is satisfactory. But if an intensity-modulated oscilloscope is to be used, signals of one polarity will be much more visible than those

of the other; in this case, it will probably be desirable to rectify the bidirectional video signal for unidirectional presentation.

If rectification is to be used, overshoots must be carefully avoided in the bidirectional video amplifier because an overshoot will produce a rectified output identical with that of a signal. Particularly to be avoided are moderately long time-constant overshoots or multiple overshoots.

The push-pull output necessary for full-wave rectification can be obtained with a transformer or a vacuum-tube phase inverter. The

<sup>1</sup> See Chap. 10, Vol. 18.

latter was used in the circuit of Fig. 12-22 because it has excellent non-overloading properties as well as push-pull output.

The elements of a condenser-coupled video rectifier are shown in Fig. 12-28. The following factors determine the circuit constants and operating conditions:

1. The applied signal voltage must be large enough to provide the desired linearity of response to the smallest signals of interest.
2. Resistance  $R_3$  must be small enough to make the time constant  $R_3C_2$  satisfactorily short; the decay time of a signal applied with zero fall-time to the rectifier depends on this time constant.
3. To prevent much rectified voltage from appearing across  $C_1$ ,  $R_2$  should be sufficiently smaller than  $R_3$ . Any such voltage acts as back bias on the rectifier and thus prevents weak signals from being transmitted through the rectifier.
4. In order not to charge up appreciably during a signal,  $C_1$  must be sufficiently large. Any such charging produces blocking of the rectifier—that is, reduces its sensitivity to an immediately following signal.
5. It is necessary that  $R_1$  be as large as is consistent with the required plate voltage on  $V_1$ .

### REPETITION-RATE CONTROL

BY D. GALE

In order to obtain cancellation of wave forms by delay methods, very critical requirements must be met by the recurrence rate of signals. In this chapter these requirements and the various methods of fulfilling them are discussed.

**12-28. Repetition-rate Requirements.**—The block diagram in Fig. 12-29 presents a general picture of a delay and cancellation device (see Fig. 12-1).

A signal will, in general, experience a time delay when passing through any of the blocks of the diagram. Thus  $D_0$  is the delay of the line driver,  $D_1$  that of the delayed-channel amplifier,  $D_2$  that of the undelayed channel, and  $D$  that of the line.

The repetition rate is  $f_r$ , and  $T$ , equal to  $1/f_r$ , is the repetition interval or time interval between signals. Consider a signal at the input terminal at time  $t$ . After passing through the delayed channel it will arrive at the subtractor at the time

$$t_1 = t + D_0 + D + D_1.$$

The next signal, arriving at the input terminal  $t$  seconds later and passing through the *undelayed* channel, will arrive at the subtractor at the time

$$t_2 = t + T + D_0 + D_2.$$

The condition for cancellation is that  $t_1 = t_2$ , or

$$D + D_1 = T + D_2.$$

Hence, for cancellation  $T = D_1 + D - D_2$  and

$$f_r = \frac{1}{D_1 + D - D_2}, \quad (1)$$

which is the basic equation for the repetition rate.

The effect of a difference in the value of  $T$  from its theoretical value will be designated by  $\Delta T$ . Consider two identical voltage pulses whose waveform is given by the equation  $V = f(t)$ . The pulses arrive at the

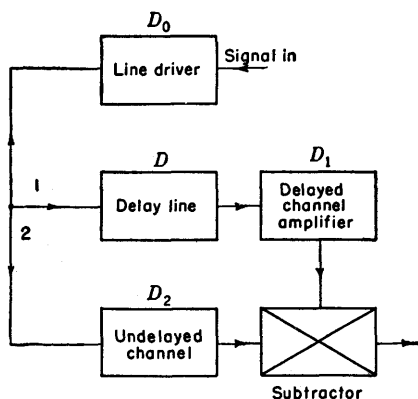


FIG. 12-29.—Delay and cancellation device.

subtractor at times  $t$  and  $t + \Delta T$ ; hence the residue after subtraction is given by

$$R = \text{residue} = f(t + \Delta T) - f(t).$$

For values of  $\Delta T$  which are small compared with the rise time of the pulse the approximation

$$R = f'(t) \Delta T \quad (2)$$

is valid, where

$$f'(t) = df(t)/dt.$$

This is the general equation for the waveform of the residue after cancellation due to an error  $\Delta T$  in time coincidence. The amplitude of the residue will be  $f'(t)_{\max} \Delta T$  and will therefore depend on  $\Delta T$  and the maximum slope of the leading edge of the pulse. The ratio of the residue amplitude to the pulse amplitude is given by

$$\rho = \frac{f'_{\max} \Delta T}{f_{\max}}. \quad (3)$$

What has been said so far applies to the residue immediately after the subtractor. (The subtractor is usually followed by a video amplifier. It is assumed that the ratio of residue to pulse at the output terminal of this amplifier will usually not be the same as the ratio at the subtractor.) Eq. (3) may be simplified by assuming that the pulse rises linearly in a time  $t_r$ ;  $f'(t) = f_{\max}/t_r$ , or  $f'_{\max}/f_{\max} = 1/t_r$ . Hence Eq. (3) becomes  $\rho = \Delta T/t_r$ , or the ratio of residue to pulse amplitude is equal to the ratio of error time to rise time. From this we see that  $t_r$  should be made as large as possible for easy cancellation. The maximum value of  $t_r$  will, of course, depend on the width of the pulse into the delay line. If this width is  $W$ ,  $t_r$  cannot exceed  $W$ . Assume that the receiver bandwidth is so set that

$$t_r = \frac{W}{2} \quad (4)$$

and also that  $\rho$  is to be 1 per cent; that is, the residue is to be down 40 db from the pulse (see Chap. 12). Table 12-1 gives the maximum allowable  $\Delta T$  as a function of  $W$  under the assumption of Eq. (4).

TABLE 12-1.—MAXIMUM ALLOWABLE ERROR AS A FUNCTION OF PULSEWIDTH

Pulsewidth $W$ , $\mu\text{sec}$	Error $\Delta T$ , $\mu\text{sec}$	Repetition-frequency stability for 1000-cps rep. rate
2	$1\frac{1}{2}\mu$	$\frac{1}{10^5}$
1	$3\frac{1}{2}\mu$	$\frac{1}{2 \times 10^5}$
0.5	$4\frac{1}{2}\mu$	$\frac{1}{4 \times 10^5}$

In cases where the area, rather than the amplitude, of the residue is important the following equation applies.

$$2\Delta T \int_0^{\tau} f'(t) dt. \quad (5)$$

To determine the upper limit  $\tau$  refer to diagram Fig. 12-30.

If the output of the cancellation unit is rectified as shown in Fig. 12-30c, the point  $\tau$  will correspond to the value of  $t$  for which  $f(t)$  is a maximum, so Eq. (5) becomes

$$\begin{aligned} \text{Residue Area} &= 2\Delta T[f_{\max} - f(0)] \\ &= 2\Delta T f_{\max}, \end{aligned} \quad (6)$$

since  $f(0) = 0$ .



The striking thing about Eq. (6) is that the residue area is independent of pulse shape,<sup>1</sup> depending only on the maximum amplitude of the pulse, and in particular it is independent of rise time or amplifier bandwidth.

This is mentioned here to illustrate that the 40-db figure for residue amplitude is just an arbitrary value for cancellation. The 40-db criterion of cancellation has meaning only if the rise time is understood to be a definite fraction of pulse length.

There are two ways in which the repetition-interval error can exceed the maximum allowable value for  $\Delta T$ ; by slow drifts in  $f_r$ ,  $D_1$ ,  $D_2$ ,  $D_3$  or  $D$  (see Fig. 12-29) or by jitter, that is, by change of delay time from one repetition cycle to the next in  $f_r$  or the  $D$ 's. Because of the slow drifts as well as because of the tolerances on the sonic-line delay time, it is necessary in all the methods to be discussed, except that explained in Sec. 12-31, to have a time cancellation control that will be a manual adjustment on the repetition frequency or on one of the delays. This control generally forms an essential part of any cancellation system.

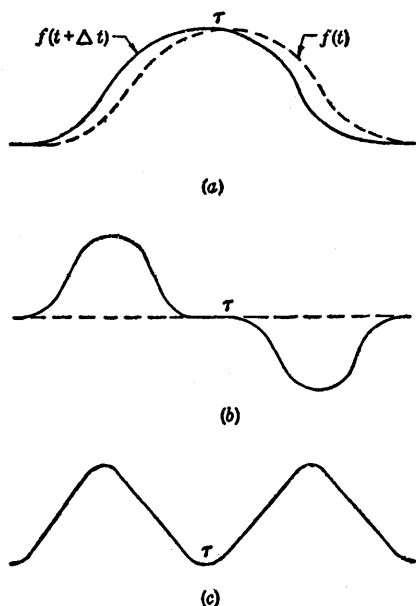


FIG. 12-30.—Pulse cancellation: (a) pulses, (b) residue, (c) rectified residues.

Repetition-rate control systems fall into two categories: stable oscillators and line-synchronized oscillators. The former are oscillators designed with a special view to minimizing the effects of slow drift and jitter. The line-synchronized oscillator is one in which the sonic delay line itself, or a similar line, is used to set the repetition interval.

**12-29. Manual Control of PRF.**—If a crystal-controlled oscillator and frequency divider (see Chap. 4) is used, then mechanical adjustment of the length of the sonic line is necessary, and, in fact, has been used in several practical systems.

An *LC*-oscillator is shown here. The range over which the frequency control must operate will depend on the maximum expected drift in all delays and on oscillator frequency. By far the larger of these effects will

<sup>1</sup> The foregoing analysis is valid only if the original (uncanceled) pulse has a continuous and finite first derivative and only a single maximum. These conditions are generally satisfied.

be the change in the sonic-line delay with temperature. The velocity of sonic waves in mercury varies by 1 part in 3300 for a change in temperature of  $1^{\circ}\text{C}$ , so if a maximum temperature variation of  $50^{\circ}$  is anticipated the total delay time may vary by 1.5 per cent and if an allowance for other drifts is made the oscillator frequency would have to be variable over a range of 2 per cent. The block diagram (Fig. 12-31) illustrates the operation of the circuit, and a detailed circuit diagram is given in Fig. 12-32. The output of a 32-kc/sec *LC*-oscillator is applied to a stable amplitude comparator whose output synchronizes a blocking-oscillator chain which divides by 48 to 300 cps. Time selection is employed to ensure phase stability. (See Chap. 4 and Vol. 19, Chaps. 10 and 16.)

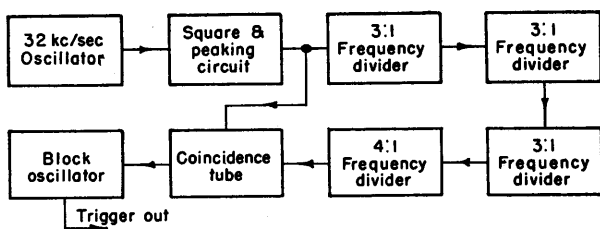


FIG. 12-31.—Stable trigger generator.

**12-30. Line Synchronized Methods.**—A number of methods for repetition-rate control have been proposed in which the delay time of the sonic line itself is used to set the repetition interval and manual control is unnecessary. The principle of operation of such a device involves sending a special timing pulse down the sonic line, amplifying it as it comes out of the line, generating a trigger from the pulse, and once more sending this trigger down the line. This circulating trigger will then act as the recurrence-rate oscillator. The block diagram is given in Fig. 12-33.

The desired repetition interval, from the fundamental formula, is

$$T = D_1 + D_t - D_2,$$

and the period for the circulating trigger is

$$T' = D_t + D_3 + D_4.$$

Thus, for perfect cancellation,

$$T' = T,$$

or

$$D_1 = D_2 + D_3 + D_4. \quad (7)$$

The delay in the trigger pulse amplifier  $D_3$  can be made very small. This delay plus  $D_2$  will usually be of the order of  $D_1$  and will approximately



cancel in Eq. (7). This leaves as a necessary condition for cancellation

$$D_4 = 0.$$

Unfortunately, it is impossible to meet this condition and, indeed, experiments so far have not succeeded in reducing  $D_4$  to less than  $0.1 \mu\text{sec}$ , a considerable error. Therefore, the straightforward procedure illustrated in the block diagram is not practicable and elaborations on the method must be found.

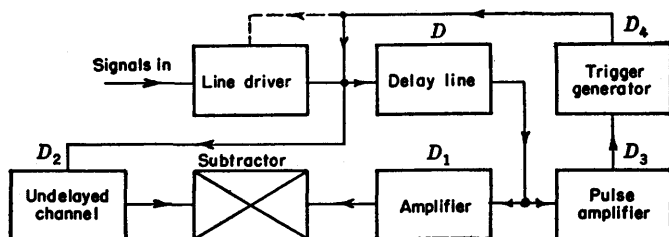


FIG. 12-33.—Line-synchronized repetition rate.

Four approaches to this problem have so far been employed.

1. The delay  $D_1$  may be artificially increased by using an electrical delay line between the signal amplifier and the subtractor.
2. Additional sonic delay may be given to the signals by taking out the trigger somewhere before the end of the line. This involves a third receiving crystal.
3. A second sonic line may be used which receives only the trigger and whose length is set for time cancellation. Each of these three cases will be treated but certain general features common to all three will be discussed first.
4. An electronic frequency tracking has also been used but this method is sufficiently different from the others to warrant separate treatment.

Components common to the first three methods are trigger generators, pulse amplifiers, and cancellation controls, which will be taken up in this order. It is necessary to use some sort of trigger generator in the loop which, when fired by a pulse, will deliver a pulse whose shape and amplitude are independent of the shape and amplitude of the firing pulse. This is necessary to prevent decay of the amplitude of the pulse. Trigger generators are, therefore, either blocking oscillators or thyatrons. With this type of generator, more power can generally be put into the delay line by letting the trigger drive the crystal directly rather than by mixing it with the signals and letting it modulate the line driver.

The trigger generator must have two additional properties. It must be self-starting. That is, it must be capable of free running at some frequency lower than the repetition rate so that an initial pulse will occur. This also ensures that if for some reason the trigger generator fails to fire on a pulse it will eventually fire again automatically. Self-starting is easily achieved with astable circuits (Vol. 19, Chaps. 5 and 6). It is also necessary that only one trigger at a time be allowed to circulate around the loop. As the circuit stands, if an additional pulse should somehow be picked up by the amplifier, it would continue to circulate around the loop. This danger can be avoided if the trigger generator, having once fired, will not fire again for at least half of the desired repetition interval (see

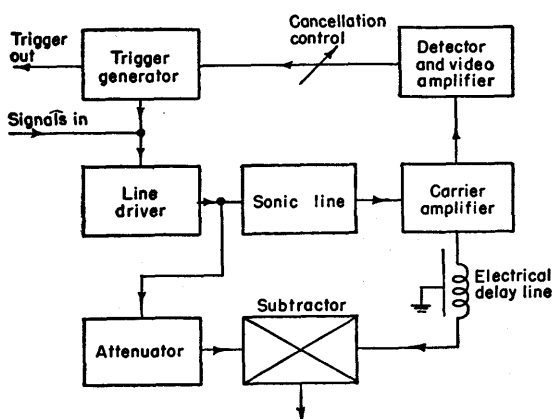


FIG. 12-34.—Proposed system for using electrical delay line.

Vol. 19, Chap. 16). If the amplitude of the triggering signal is limited, then it is possible to adjust the recovery time constant of either of these circuits so that they will not be able to re-fire for a time  $T/2$ . For extreme reliability, however, a blanking gate of duration  $T/2$  should be applied to the pulse amplifier.

The pulse amplifier will generally consist of several stages of gain at the pulse carrier, a detector, and video amplifier. The number of stages needed will vary with the attenuation properties of the line and bandwidth requirements; 40 to 50 db of gain are usually required. If the additional electrical delay line is used in the signal channel, it is desirable to keep the delay as short as possible; hence a broad-band pulse amplifier is used.

The cancellation control may be either mechanical or electronic. In the former case it consists of a means for varying the physical length of the sonic or electrical delay line and will be considered later. The electronic method makes use of some sort of time modulator (see Chaps. 6 and 7).

Of the three methods the simplest and therefore the first to be tried was the electrical line (method 1). There are two possibilities here. The delay can be effected at the carrier frequency or after detection at video frequency. Suitable delay lines for the carrier frequency are not generally available, however, and therefore in the only experiments which were made with this system the video signals were delayed. There were several difficulties encountered. The frequency response of ordinary delay lines was not good enough to permit adequate cancellation. It is possible to obtain a special high fidelity line and to avoid this difficulty to a large extent if the delay line is kept short. In one case there were serious effects of internal reflections in the line giving rise to spurious

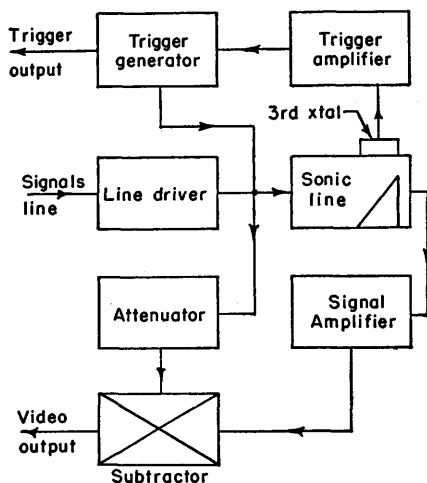


FIG. 12-35.—Three-crystal line.

signals that were well above 1 per cent of the pulse amplitude. This effect was sufficiently serious to make the whole scheme unusable. The difficulty lies entirely in the lines, however, and it should not be impossible to build lines in the future which will be suitable for this use. A possible system is represented by the diagram in Fig. 12-34.

It is seen that, if the carrier amplifier is used both for trigger and signals, there must be some way to distinguish the trigger from the signals in order to keep the trigger generator from firing on signals. Both time selection and amplitude selection are possible (Vol. 19, Chaps. 9 and 10). Another method suitable if the trigger amplifier does not include part of the delayed-channel amplifier is mentioned in the second succeeding paragraph.

In method 2, a three-crystal line (Fig. 12-35) is used (see Sec. 12-5 of this volume and Chap. 7, Vol. 17). Briefly, a 45° reflector is placed in

the line just before the receiving crystal and a second receiving crystal is placed on the wall of the line opposite the reflector. The position of the reflector is adjustable; the delay may, therefore, be varied.

Here, again, one must keep signals from firing the trigger generator and time and amplitude selection may be used as before. Another scheme is that of carrier-frequency discrimination in which the trigger amplifier is tuned to a frequency different from that of the signals. The delay line will generally pass frequency components over such a broad band that satisfactory response can be obtained through the trigger amplifier even if it is tuned 15 or 20 per cent away from the 10-Mc/sec carrier frequency of the signals, for example, at 8 Mc/sec.

In method 3 a separate line is used for setting the repetition rate. Although it is more cumbersome than the three-crystal line this method may have the advantage of mechanical simplicity. It has been used with both mechanical and electrical cancellation control. The lines are placed close to the signal line so that the effects of temperature on both lines will be identical. In practice, a trigger line equal in delay time to the signal line has been used as well as a half length plus a 2-to-1 frequency divider in the trigger circuit (see Sec. 12-5).

A problem that comes up both in connection with this line and with the three-crystal line is that of multiple reflection. Unless absorbing end cells are used, the trigger will be partially reflected at the receiving crystal, transmitted back down the line, and will arrive at almost the same time that the succeeding trigger enters the line. This reflection may be only 10 db down from the new trigger. Since the triggers are approximately pulsed sine waves they may either add or subtract in accordance with their relative phase. This relative phase will depend on the delays in the trigger amplifier and generator, and these delays, particularly with electronic time-cancellation control, will in turn depend on the rate of rise of the pulse, hence the pulse amplitude. The following situation might, therefore, arise. The delay in the trigger generator may increase by a small amount, and thus change the relative phase of trigger and reflection in such a way as to decrease the output trigger amplitude. This, in turn, would slightly increase the trigger generator delay on successive repetitions. This effect could easily produce jitter in the repetition rate sufficient to impair cancellation appreciably. A means of avoiding this difficulty, if absorbing end cells are not used, is to put an additional electrical delay in the trigger loop equal in time to the length of the trigger pulse duration. In this way the second reflection will have been reflected from the transmitting crystal before the succeeding trigger has entered the line, hence they will not occur simultaneously and add together.

Figure 12-36 is a circuit diagram of the unit shown in Fig. 12-5. This trigger generator is used with a trigger delay line separate from, and half

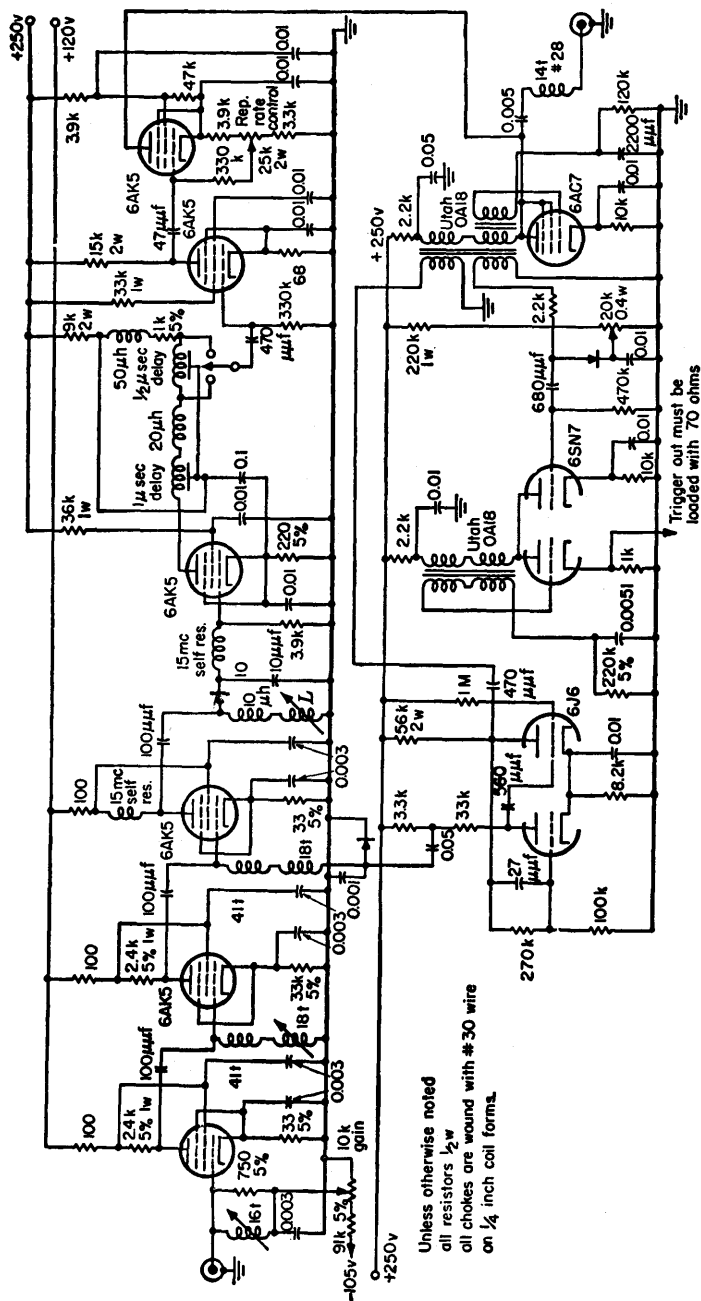


Fig. 12-36.—Supersonic trigger generator.



as long as, the signal delay line. The 6AC7 blocking oscillator thus fires at twice the desired repetition frequency; the 6SN7 blocking oscillator, which triggers the modulator, acts as a frequency divider. The pulse from the 6J6 multivibrator causes conduction in the carrier-frequency amplifier for slightly more than half the 6AC7 period. Cancellation control is by means of variable bias on an amplitude selector, with the range of adjustment extended by means of a switchable short delay line.

Of these three types of line synchronization, the electrical line would perhaps be most satisfactory if adequate electrical lines could be procured. The other two methods perform equally well although the three-crystal line is less cumbersome.

**12-31. Electronic Frequency Tracking.**—This method is similar to the stable-oscillator method in that the recurrence rate frequency is

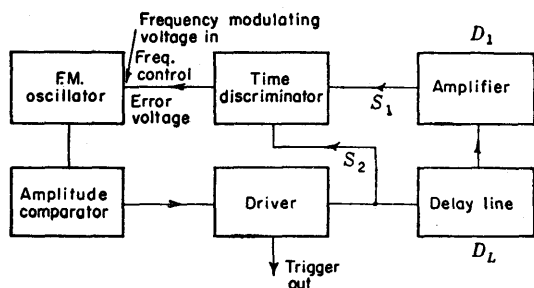


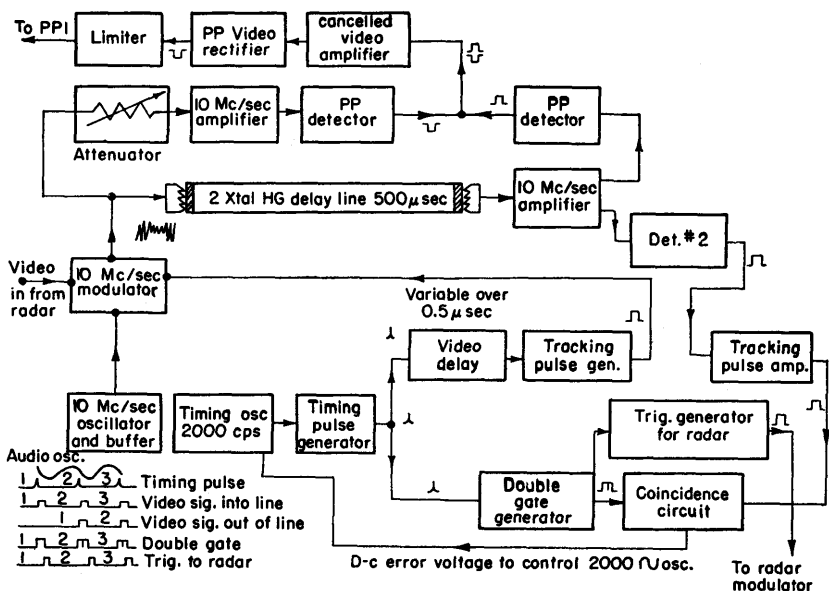
FIG. 12-37.—Electronic frequency tracking.

generated by a purely electronic oscillator. It is also similar to line-synchronized methods in that the frequency of this oscillator is not initially set to the correct value and expected to remain fixed, but is continually and automatically set by the sonic line and associated circuits to maintain the correct value. This is accomplished by the following general technique. A circuit called a time discriminator is used to measure the difference in the time of occurrence of two signals,  $S_1$  and  $S_2$ , occurring at times  $T_1$  and  $T_2$ . In addition a controlled-frequency oscillator whose frequency can be varied over a suitable range by the output of the time discriminator is required. This process is identical with that described in Chaps. 4 and 8. The method is illustrated by the block diagram of Fig. 12-37.

The operation is as follows. The time discriminator is set up so that it compares the time of the  $n$ th pulse from the delay line  $T_1$  with that of the  $(n + 1)$ th pulse into the line  $T_2$ . Let us suppose that an increase in voltage applied to the oscillator will increase its frequency. If  $T_2 - T_1$  is positive, that is, if  $T_2$  occurs after  $T_1$ , the  $(n + 1)$ th signal into the line occurs at too long a time after the  $n$ th signal leaves the line. This means

that the oscillator frequency is too low; hence the time discriminator must develop a positive voltage in order to apply the appropriate correction to the oscillator frequency. Similarly, if  $T_2 - T_1$  is negative, the output of the time discriminator must decrease the oscillator frequency. Provided that the proper dynamic conditions are maintained around the feedback loop (see Chap. 8), the circuit should adjust itself so that  $T_2 - T_1$  equals zero, hence  $T$  equals  $D_L + D_1$ .

**12-32. Practical Circuit Details.**—The design of an actual cancellation unit employing electronic frequency tracking is shown in the block dia-



**FIG. 12-38.**—Cancellation unit using electronic frequency tracking.

gram, Fig. 12-38. Figure 12-39 shows a schematic diagram of the variable-frequency oscillator and associated circuits. The trigger from the timing pulse generator passes through a variable  $0.5\text{-}\mu\text{sec}$  delay to the tracking pulse generator. The modulator, on receiving the tracking pulse, pulses the carrier frequency transversing the delay line. After amplification, detection, and further amplification, this pulse appears at the time discriminator. In the meantime, the succeeding timing trigger has fired the double-gate generator that gives two gates, each about one microsecond in duration with about one microsecond between the gate centers. By virtue of the variable  $0.4\text{-}\mu\text{sec}$  delay, the tracking pulse will fall exactly between the two gates when accurate synchronization is secured. If the pulse falls unequally on the two gates, the time discriminator will give



out an error voltage that will increase or decrease the variable frequency according to the phase difference between the oscillator and the delay-line output. Finally the sine wave from the oscillator controls the timing pulse generator.

The most important component in this timing channel is the variable-frequency oscillator. The oscillator must be very free from jitter if cancellation is to be maintained. In this instance a low-frequency phase-shift oscillator using an RC-feedback was employed (see Vol. 19, Chap. 4). It has the advantages of simplicity and sensitivity to control for a portion of a cycle and grid goes positive and loads down the last network element. By changing the d-c voltage on the grid one can alter the fraction of cycle for which this occurs and thereby control the frequency. A range of  $\pm 1$  volt from the coincidence circuit gives a variation of  $\pm 75$  cps, which is sufficient to make d-c amplification unnecessary. Variation of the resistance  $R_1$  in one of the network branches serves to adjust the oscillator frequency to approximately 2000 cps. Once the system is locked on the tracking signal, its operation can be checked by varying  $R_1$  and observing that the d-c voltage varies accordingly.

The double gate is generated by two blocking oscillators. The action of the second is initiated by the overshoot of the first. Each gate is slightly over 1  $\mu$ sec in duration and roughly of 150 volts amplitude. These gates are applied to the plates of a twin triode in the time-discriminator circuit (see Vol. 19, Chap. 14).<sup>1</sup> When the tracking pulse is equally distributed between the gates, the charge on  $C_1$  remains constant and a steady repetition rate is established.

There are two main advantages to this method of control. The first is that all drifts in any of the delays of the cancellation loop are automatically compensated. The only drift that might disturb cancellation would be drift in the time detector itself. The second advantage of the method is that it involves no additional mechanical parts, as do all the other line synchronized methods discussed. Its disadvantages are the stringent jitter requirements on the oscillator and the relatively large number of tubes required as compared with other methods.

<sup>1</sup> It is not necessary in this cancellation unit to employ any blanking device on the tracking pulse amplifier because the radar echoes are not of sufficient size to affect the timing channel.

## GLOSSARY

- amplitude comparison.**—The process of indicating the instant of equality of the amplitudes of two WAVEFORMS by a sharp pulse or step. It may also be defined as the process of determining the abscissa of a WAVEFORM, given its ordinate.
- amplitude discriminator.**—A circuit which indicates the equality of the amplitudes of two WAVEFORMS or the sense and approximate magnitude of the inequality.
- amplitude selection.**—The process of selection of all values of the input wave greater or less than a given amplitude or lying between two amplitudes.
- astable.**—Referring to a circuit with two quasi-stable states. The circuit generates a continuous train of waves and requires no trigger to execute a complete cycle.
- bistable.**—Referring to a circuit with two stable states. Two triggers are required to put the circuit through one complete cycle.
- blocking oscillator.**—A transformer-coupled feedback oscillator in which the plate current is permitted to flow for one-half cycle, after which bias is generated in the grid circuit to prevent further oscillation.
- bottoming.**—The process of defining the potential at the plate of a pentode by operating below the knee of the  $E_p/I_p$  characteristic. A similar effect exists in triodes with positive grid drive.
- catching diode.**—A diode used to limit the excursion of potential at some point in a circuit. The term is usually used to refer to the termination at a given level of an exponential rise toward a higher potential.
- clamping.**—The process of connecting some point of a network to a desired potential for certain periods of time. This term has been largely replaced by the term SWITCHING.
- clipping.**—AMPLITUDE SELECTION between bounds. The output has a flat top or flat bottom or both.
- d-c restoration.**—A category of the general process of level setting. It refers particularly to bringing either the peak positive or peak negative value of the WAVEFORM to some desired level.
- delay circuit.**—A circuit which is used to delay by a certain time the start of the operation of another circuit.
- delay device.**—A device which accepts as its input a WAVEFORM  $f(t)$  and gives as its output a WAVEFORM  $f(t - \Delta)$  where  $\Delta$  is positive.
- demodulation (or detection).**—The process by which information is obtained from a modulated WAVEFORM about the signal imparted to the WAVEFORM in modulation.
- difference detector.**—A detector circuit in which the output represents the difference of the peak amplitudes or areas of the input WAVEFORMS. The input WAVEFORMS need not be simultaneous.
- flip-flop.**—Colloquialism for MONOSTABLE circuit.
- free-running.**—Colloquialism for ASTABLE.
- frequency discriminator.**—A circuit which indicates the equality of the frequency of two WAVEFORMS or the sense and approximate magnitude of the inequality.
- function unit.**—The unit that controls the external properties of automatic range-tracking equipment and provides the necessary band shaping for stability.

- gating waveform.**—A WAVEFORM (sometimes called the “gate”) applied to the control point of a circuit in such a way as to alter the mode of operation of the circuit while the WAVEFORM is applied.
- jitter.**—Small rapid variations in a WAVEFORM due to mechanical disturbances or to changes in the supply voltages, in the characteristics of components, etc.
- lockover circuit.**—Colloquialism for a BISTABLE circuit.
- microphonics.**—JITTER due to mechanical disturbances, referring especially to tubes.
- Miller circuit.**—A circuit which employs negative feedback from the output to the input of an amplifier through a condenser.
- modulation.**—The process by which some characteristic of a WAVEFORM is varied in accordance with a signal.
- monostable.**—Referring to a circuit with one stable and one quasi-stable state. The circuit requires one trigger to perform a complete cycle.
- multiar.**—A diode-controlled regenerative amplitude comparator. The name refers to a certain circuit configuration.
- multivibrator.**—A two-tube regenerative device which can exist in either of two stable or quasi-stable states and can change rapidly from one state to the other.
- quasi differentiation (integration).**—Approximate differentiation (integration) by a simple circuit.
- phantastron.**—A certain type of one-tube relaxation oscillator employing Miller feedback to generate a linear timing WAVEFORM.
- pulse.**—A WAVEFORM whose duration is short compared to the time scale of interest and whose initial and final values are the same.
- rundown.**—The linear fall of plate voltage in a Miller sweep generator.
- sanaphant.**—A circuit intermediate between SANATRON and PHANTASTRON.
- sanatron.**—A variation of the PHANTASTRON employing a second tube for generating the gating waveform.
- scale-of-two circuit.**—A colloquialism for BISTABLE circuit.
- selector.**—A circuit selecting only that portion of a WAVEFORM having certain characteristics of amplitude, frequency, phase, or time of occurrence.
- selector pulse.**—A pulse used to actuate a time selector.
- shaping.**—The process of modifying the shape of a waveform. The process is called “linear” or “nonlinear” according as the circuit elements are linear or nonlinear.
- signal.**—An electrical or mechanical quantity which conveys intelligence.
- switch detector.**—A detector which extracts information from the input waveform only at instants determined by a selector pulse.
- switching.**—The connection of two points of a network at controllable instants of time. An alternative term is CLAMPING.
- time comparison.**—The process of indicating the amplitude of a WAVEFORM at a given instant.
- time demodulation.**—The process by which information is obtained from a time-modulated wave about the signal imparted to the wave in TIME MODULATION.
- time discriminator.**—A circuit which indicates the time equality of two events or the sense and approximate magnitude of the inequality.
- time modulation.**—Modulation in which the time of appearance of a definite portion of a WAVEFORM, measured with respect to a reference time, is varied in accordance with a signal.
- tracking.**—The process of causing an index to follow the variation of a quantity by means of an inverse-feedback (servo) loop.
- waveform.**—A current or voltage considered as a function of time in a rectangular coordinate system.

# Index

## A

- A-scope, 215
- A-scope presentation, used in British CMH system, 238-243
- Accuracy tests, 129  
(See also Error)
- AFC, 267
- AFC circuit, 96
- AGC, 279  
gated, 373
- AGL-T, British, 330  
phase comparison circuit in, 372
- AGL-(T) discriminator, 278, 310, 322, 330, 341, 373
- AI Mark VI, 334, 370
- AI Mark VI automatic target-selection circuit, 333
- AI Mark VI automatic target-selection system block diagram, 332
- AI Mark VI time discriminator and target selector, 334
- AI Mark VIA, 341
- Altimeter, barometric, 163, 164  
SCR-718, 163, 219
- Amplifiers, cancellation, 498  
pulse-forming, 72  
squaring, 70, 72, 110
- Amplitude comparator, 144  
diode, 73, 151, 173  
regenerative, 73, 74  
with RC-input, 75  
sinusoid, 145
- Amplitude comparison, 71, 75, 76, 107, 110, 142-175  
diode, 108
- Amplitude-comparison circuit, 75, 109
- Amplitude selection, electrical, 221
- Amplitude selector, cathode-ray tube as, 220
- AN/APA-30 ballistic computer, 247
- AN/APG-1, 369, 370  
angle-tracking circuits in, 376, 377
- AN/APG-5 range calibrator, 108, 275, 317, 331, 337, 342  
(See also ARO)
- AN/APG-13A Falcon radar, 223, 224
- AN/APG-15, 317, 327, 331, 342, 368, 371, 373  
time discriminator of, 316
- AN/APN-3, Shoran, 157  
pulse-selection circuits of, 159
- AN/APN-4, 263
- AN/APN-9, 263
- AN/APS-3, 248, 392  
blocking-oscillator PRF generator of, 78
- AN/APS-4, 248
- AN/APS-10 radar, revised model of, 91
- AN/APS-10 synchronizer, 91, 169, 172, 248  
proposed, 92, 94  
timing diagram of, 93
- AN/APS-15 pulse generator, 165
- AN/APS-15 range unit, 120, 164-169, 277  
block diagram of, 164
- AN/APS-15 range-unit waveforms, 165
- AN/APS-15 ten-mile pulse selector, 167
- AN/APS-15 ten-to-one divider, 166
- AN/APS-15 time modulator, 167
- AN/APS-15 twenty-five-to-one divider  
generating PRF pulses, 166
- AN/ARR-17, 458
- AN/ART-18, 458
- Angle-positioning, automatic, with grouped data, 389
- A/R range scope, 256-B, 76
- A/R-scope, 231-238
- Arenberg, D. L., 484
- Arma resolver, 418, 438  
Midget, 342
- ARO (AN/APG-5), 342
- ARO electrical system, 342-348
- ARO Mark I, 342
- ARO Mark I range system, 343

ARO Mark I range unit, 344  
 ARO Mark II, 342, 345  
 ARO radar, 275, 317, 342  
 ARO range system, 342  
 ASB, Navy Radar, 216  
 Automatic angle tracking (*see* Angle-positioning)  
 Automatic range tracking (*see* Tracking)  
 Autosyn, 394

## B

Ballistic computer, 142  
 B-scope, systems using J-scope with, 243-246  
   AN/APA-30, 247  
 BC-1365, Indicator-Tracker Unit, 255  
 Beacon, omnidirectional, 36  
   British, 400, 410-416  
   radar, 33  
 Bell Telephone Laboratories, 142  
 Bendix air-mileage unit, 251  
 Bendix Air-position Indicator, 251  
 Blocking oscillator, 75, 76, 78-80, 151, 167, 317  
   500-yd (328-kc/sec), 110  
   low-impedance, 91  
 Blocking-oscillator dividers, 83, 110, 165  
 Blocking-oscillator PRF generator, 78  
   of AN/APS-3, 78  
 Blocking-oscillator pulse generator, 70, 84  
 Blocking-oscillator voltage pulses, 78  
 Bode, H. W., 282  
 Bootstrap double integrator, 386  
 Bootstrap linear-sawtooth generator, 151, 358  
 Bootstrap self-gating linear-sawtooth generator, 347  
 Bootstrap time-modulation circuit, 128  
 Bootstrap triangle generator, 125-131  
 Bothwell, F. E., 390  
 British AGL-T, 330  
 British Mark II ASV, 216  
 British Oboe, (*see* Oboe)  
 British omnidirectional beacon, 400, 410-416  
 British 274 meter, 368  
 Brown Converter, 361, 447

## C

Calibrator, Model III, 87-89  
 Cathode followers, 130

Cathode-ray tube, as amplitude selector, 220  
 Cathode-ray tube displays, 64  
 Cathode waveform, 105  
 Channel separation, 398, 400  
 Circuit, 392  
 CMH system, British, A-scope presentation used in, 238-243  
 Coast, 278, 304  
 Code group, multiple-pulse, 400  
 Coder, 451  
 Coffin, F. P., 390  
 Coherence, external, 20  
   internal, 18  
 Coil assembly, Helmholtz, 137  
 Cole, A. D., 120  
 Comparator, 135-137  
   amplitude (*see* Amplitude comparator)  
   double-triode, 116  
   cathode-coupled, 116-118  
   multiar (*see* Multiar comparator)  
   regenerative amplitude, 356  
 Comparator circuit, double-triode, 118  
 Component characteristics, 50-62  
 Compression, dynamic-range, 496  
 Condenser phase shifter, 358  
 Condenser system, 3-phase, 172  
 Conical scanning, 367, 368  
 Conical-scanning antenna pattern, SCR-584, 367  
 Continuous-wave system, 7, 16-18  
 Counter dividers, 102  
 Counters, 102  
   scale-of-two, 154  
   step, gas-filled tube, 100  
 Crout, R. D., 390  
 Crystal oscillator, 71, 83, 153  
   Class C, 75  
   80.86-kc/sec, 164  
   pulsed, 238  
   triode, 83  
   80.86-kc/sec, 93  
   tri-tet, 88  
 Crystal rectifier, germanium, 91  
 Crystals, receiving, 135  
   transmitting, 135  
 Current transformer, 316  
 Cursors, 178  
 C-w systems, frequency-modulated, 398  
 Cycle matching, 11



## D

- Data, grouped, or periodically interrupted, tracking on, 378
  - intermittent, 28, 29
    - aided tracking with, 247-251
- Data transmission, phase for, 393
  - radio, 398
  - short-distance wire, 391
- Data-transmission systems, special, 391-416
  - various, characteristics of, 399
- Decca, 34
- Decoder, 426, 454
- Decoding circuits, synchronizing-pulse, 426-429
- Delay lines, supersonic (*see* Supersonic delay lines)
  - variable, 132
- Delay multivibrator, 131, 140, 342, 347
  - coarse-scale, 162
- Delay phantastron, Oboe active-region, 353
- Delay tank, supersonic, 132-135, 140
- Delay-tank time-modulation system, 132
- Delays, linear, 429-433
- Demodulation, time modulation and, 5-7
- Demodulators, 391, 400
- Detectors, position error, 367
- Diehl FPE-492a two-phase induction motor, 361
- Diehl Generator, 424
- Diode amplitude comparator, 71, 125-131, 153
- Disconnector, 304
  - neon tube, 386
- Distance measurement, accuracy of, 32
- Divider circuit, sinusoidal, 158
- Dividers, blocking-oscillator, 83, 110, 165
  - counter, 102
  - phantastron, 104
  - pulse-frequency, multivibrators as, 154
- Doppler, pulsed, 20
- Doppler frequency, 17
- Double-scale system, 49
- Dumont 256-B A/R oscilloscope, 89, 231

## E

- Electromechanical systems, 357-366
- Electronic marks, movable, 222-225

- Elinco Type B-44 tachometers, 361
- Error, cyclic, 141
  - gross, 156
  - limiting, 113
  - probable, 113
  - reset, 192
  - slope, 114
  - of time measurement, 40
  - in time-measurement circuits, 120
  - in usual sanatron circuit, 124
  - zero, 114
- Esterline-Angus recorder, 387

## F

- Falcon radar, AN/APG-13A, 223-231
- Farnborough, 482
- Feedback amplifier, negative, 117
- 4- $\mu$  sec pulses, 78
- 50- $\mu$  sec pulses, 96
- Fink, D. G., 89
- Follow-up systems, 395-397
- Fredrick, A. H., 119
- Frequency dividers, 88, 102, 267
  - amplitude-comparison multivibrator, 147
  - with injection feedback, 100
  - pulse, 83
  - sinusoidal, 160
- Frequency division, 81-87
- Frequency modulation, 5, 393
  - and demodulation, 13-15
- Frequency stability, 77, 78, 80, 110
- Frequency tracking, electronic, 522
- Function unit, 277, 279, 280
  - mechanical, 305-308

## G

- Gate, selecting, 151
- Gate generator, pulse-selecting, 6- $\mu$  sec, 152
- Gate generator multivibrator, 117
- Gee, 34, 261
- Gee-H, 30
- General Electric Automatic Radar, 337
- General Electric Company, 337, 485
- General Electric Type YE4-B lines, 406
- Generators, angle information, 458
  - Diehl, 424
  - of grouped pulses, 400

- Generators, linear-sawtooth, bootstrap,  
     151, 358  
     bootstrap self-gating, 347  
     positive-feedback, 225  
     linear sweep, 153  
     marker (*see* Marker generators)  
     phantastron-gate, 104  
     range-mark, 69  
     triangle, bootstrap, 125-131  
     trigger, multiple-frequency, 81
- Goniometer, 240  
     inductance, 158, 161  
     phase-modulating, 154
- Gostyn, E., 88
- Grayson, H., 482
- Ground track, 23
- Ground, virtual, 294, 295
- Ground-position indicator, 251
- Indices, fixed, 181  
     for manual time measurement, 215  
     movable, 182  
     tracking, 183
- Induction motor, two-phase, Diehl FPE-492a, 361
- Injection feedback divider for Oboe PRF, 103-107
- Integrator, bootstrap, 302, 303  
     difference, 302, 303  
     double, bootstrap, 386  
     electrical, 291-303  
         Oboe, 354  
     electromechanical, 252  
     electronic, 347, 357  
     feedback amplifier, 302, 303  
     mechanical, 305  
     Miller (*see* Miller integrator)
- Interference rejection, 400

## H

- H<sub>2</sub>X, 119  
     (*See also* AN/APS-15)
- H<sub>1</sub>X range phantastron, 122
- H<sub>2</sub>X range unit, 120, 123
- H<sub>2</sub>X time modulator, 121
- H<sub>2</sub>X, 386-388
- Hand Radar Set, 243
- Helmholtz coil assembly, 137
- Hewlett-Packard oscillator, 140
- Hite, G., 125
- Holdam, J. V., 120
- Holtzer-Cabot Type 0808 model B3  
     motor, 441
- HR radar system, 163
- Hughes, V. W., 125
- Huntington, H. B., 478, 479
- Hybrid time and phase discriminator, 97
- Hyperbolic navigation systems, 261

## I

- Indication, on-target, 328
- Indicator, Air-position, Bendix, 251  
     ground-position, 251  
     plan-position (*see* PPI)  
     position error, 367  
     precision type B, 255  
     radar, 108  
     type M, 223
- Indicator-Tracker Unit BC-1365, 255
- Indices, 180-184

## J

- J-scope, 216-219  
     systems using, with B-scope, 243-246  
         with PPI, 243-246
- Jitter, 78
- Jones, F. F., 348
- Jordan, W. H., 323
- Juxtaposition, 186, 188, 190-196

## K

- Kallman, H. E., 489

## L

- Larlett, L. J., 369
- LC-oscillator, 107, 135-137  
     pulsed, 108  
     20-kc/sec, 96  
     328-kc/sec, 110
- LC-stabilization, 83
- Linearity, 114
- Lobe-switching, 367
- Loran, 11, 34, 173, 181, 261
- Loran automatic-frequency-tracking circuit, lightweight, 97
- Loran feedback PRF divider, direct-reading, lightweight, 101
- Loran indicator, circuit details of, 267-274  
     lightweight, direct-reading, 96, 169-174

- Loran PRF generator, direct-reading, lightweight, 100-103
  - Loran repetition frequencies, 264
  - Loran time discriminator, lightweight, automatic-frequency-control circuit, 98
  - Loran time-discriminator timing diagram, 99
  - Loran time modulator, direct-reading, lightweight block and timing diagram of, 169
    - phase modulator of, 170
  - Loran timing sequence, 264-267
- M
- M-scope, 225
  - McGrath, S., 120
  - McSkimin, H. J., 478
  - Magnesyns, 394
  - Magslip, 394
  - Mark I ARO, 344
    - range vs. range error of, 347
  - Mark II ARO, 344
  - Mark II ASV, British, 216
  - Mark IIM, Oboe, 348
  - Mark 36 radar, angle-tracking circuits in, 375
  - Marker generators, grouped, 106
    - single-frequency, 107, 108
    - multiple-frequency, 81
    - single-frequency, 81
    - 20-mile, 85
  - Markers, grouped, multiple-frequency, 109, 110
  - Master station, 261
  - ME PPI, 458
  - Meacham range unit, 142-147
  - Measurements, manual, 176-274
  - Memory, 304
    - position, 282, 380
    - velocity (*see* Velocity memory)
  - Memory time, 278
  - Micro-H, 30
  - Microsyns, 394
  - Mile, nautical, 103
    - statute, 103
    - 2000-yd, 103
  - Miller feedback, 131
  - Miller feedback time modulator, 114
  - Miller integrator, 114-116
    - high-gain, 140
    - multistage, 116-118
    - self-gating, 118-124
  - Miller integrator amplifier, 117
  - Mixer unit, 461
  - Mixing unit, video, 451
  - Model SJ radar range circuit, 134
  - Model III calibrator, 87-89
  - Modulator, electromechanical, 391
    - zero-range trigger for, 95
  - Modulator trigger, 91
  - Multiar comparator, 114-116, 124, 356
  - Multiple-scale systems, 61, 219
  - Multivibrator, 80
    - delay (*see* Delay multivibrator)
    - gate generator, 117
    - monostable, 144
    - 100- $\mu$  sec, 97
    - as pulse-frequency divider, 154
    - scale-of-two, 84
    - symmetrical, 80
      - as PRF generator, 80
    - unsymmetrical monostable, 94
  - Multivibrator PRF generator, 80
- N
- Navy Radar ASB, 216
- O
- O-phase adjustment, 73
  - Oboe, 168, 277, 315, 350, 357
  - Oboe active-region delay phantastron, 353
  - Oboe active-region timing diagram, 351
  - Oboe blind bombing, geometry of, 348
  - Oboe electrical integrators, 354
  - Oboe electrical system, British, 348-357
  - Oboe 5-mile pip selector, 352
  - Oboe ground station, British, 103, 311
  - Oboe Mark IIM, 348
  - Oboe mouse station, 337
  - Oboe PRF, injection feedback divider for, 103-107
  - Oboe PRF divider, 103
  - Oboe range-tracking system block diagram, 349
  - Oboe time discriminator, 311, 312
  - On-target indication, 328

100- $\mu$  sec multivibrator, 97  
 Oscillations, buildup of, 38  
 Oscillator, 107  
   blocking (*see* Blocking oscillator)  
   coherent, 11  
   crystal (*see* Crystal oscillator)  
   crystal-controlled, 141  
   gated, 110  
   Hewlett-Packard, 140  
   instability of, 77  
   LC- (*see* LC-oscillator)  
   pulsed, 107, 109, 142, 144, 145, 148, 229  
   quenching, 79  
     with air-core transformer, 79  
   random, precise synchronization of, 99  
   RC-, 70  
   RC sine-wave, 80  
   relaxation (*see* Relaxation oscillator)  
   SCR-268, 137  
   sine-wave, Class C, crystal-controlled, 81.94-kc/sec, 76  
     crystal-controlled 163.88-kc/sec, 72  
   squegging, 79  
   two independent, precise system of synchronization for, 99  
   variable-frequency, 137-140  
   Wien-bridge, 70, 139  
 Oscillator range circuits, sinusoidal, 135  
 Oscilloscope, Dumont 256-B A/R, 89, 231

## P

Phantastron, 95, 106, 118, 120, 164, 167, 168, 171, 349, 350, 352, 355-357  
   microphonic effects in, 123  
   pulse-selecting, 94, 171, 173  
   temperature compensation of, 123  
 Phantastron accuracy, 122  
 Phantastron cathode waveform, 105  
 Phantastron delay, component variations upon, effect of, 123  
 Phantastron divider, 104  
 Phantastron-gate generator, 104  
 Phantastron operation, 121  
 Phase demodulation, 5  
 Phase-discriminator, 155  
   hybrid time and, 97  
 Phase modulation, 142-175  
   and demodulation, 7-13  
   of timing, 57

Phase-modulation network, 158  
 Phase-modulation range unit, two-scale, 143  
 Phase-modulation system, three-scale, 157-161  
 Phase modulator, 135-137, 145  
   condenser, 142, 144, 150, 151  
   of lightweight direct-reading Loran time modulator, 170  
   mechanical, 168  
   3-phase condenser, 170  
 Phase shifter, 238  
   condenser, 358  
   magnetic, 137  
 Phase-shifter system, discussion of, 443-449  
 Photoelectric cells, 276  
 Position error detectors, 367  
 Position error indicators, 367  
 Position-finding, 29  
 Position learning time, 380  
 Position memory, 282, 380  
 Potentiometer, exponentially tapered, 142, 146, 153  
   linear range, 151  
   sine-cosine, 252  
   360°, 396  
 PPI, ME, 458  
   with mechanical scale, 219  
   pulsed range-mark circuit designed for, 107  
   systems using J-scope with, 243-246  
 PPI range-marker circuit, 108  
 Precision Range Indicator, block diagram of, 148  
   timing diagram of, 148  
 Precision ranging indicator, precise pulsed, range-marker circuit from, 108  
 Precision type B indicator, 255  
 PRF divider phantastron, cathode waveform of, 105  
   screen waveform of, 105  
 PRF dividers, 85  
 Oboe, 103  
 PRF generation, 78  
 PRF generators, 69  
   blocking-oscillator (*see* Blocking-oscillator PRF generator)  
   Loran (*see* Loran PRF generator)  
   multivibrator, 80

PRF generators, symmetrical multivibrator as, 80  
     synchronization by, 45  
 PRF oscillators, 400  
 Propagation-time circuits, 141  
 Pulse divider, ten-to-one, 165  
 Pulse generator, AN/APS-15, 165  
     blocking-oscillator, 70, 84  
     delay-line, 107  
     r-f, synchronization by, 43  
 Pulse remote-control system, 400-408  
 Pulse selection, 87-89, 160  
 Pulse-selection circuits, of AN/APN-3, Shoran, 159  
 Pulse selector, 89-95, 146, 153, 171  
     ten-mile, AN/APS-15, 167  
     time modulator and, 146  
 Pulse system, phase-modulated, 442  
     time-modulated, 398  
 Pulse transformer, 78  
     132-DW, Westinghouse, 317  
 Pulses, 0.12- $\mu$  sec, 317  
     4- $\mu$  sec, 78  
     50- $\mu$  sec, 96  
     grouped, generator of, 400  
     time-modulated, 400

## R

R-gate, 233  
 R-sweep, 233  
 Radar beacons, 33  
 Radar indicator, 108  
 Radar set, British, time discriminator of, 315  
 Radar synchronizer, 71  
 Radar systems, 31  
     HR, 163, 243  
     relay (*see* Relay radar systems)  
 Radiosonde, 408  
 Range, two-scale, 238  
 Range calibrator, AN/APG-5 (*see* AN/APG-5 range calibrator)  
 Range-mark circuit, pulsed, designed for PPI, 107  
 Range-mark generators, 69  
 Range-mark mixer, 83  
 Range-marker circuit, pulsed, precise, from precision ranging indicator, 108  
     pulsed LC, 108  
 Range-marker generation, 78  
 Range marks, fixed, 229  
 Range tracking, automatic, 168  
     on grouped data, 386-388  
 Range-tracking servoamplifier circuit, 362  
 Range-tracking tester, dynamic, 363  
     (*See also* Tracking tester, dynamic)  
 Range unit, Meacham, 142-147  
     phase-modulation, two-scale, 143  
     on radar systems, calibration of universal instrument for, 102  
     two-scale, 143  
     Wurzburg, 163  
 Ranging indicator, precision, 147-153  
 RC-input, regenerative amplitude comparator with, 75  
 RC-oscillator, 70  
 RC-sine-wave oscillator, 80  
 RCA, Industry Service Division, 157  
 Reactance tube, 96, 97  
 Receiver, 466  
     gain control of, 41  
     variation of delay with signal amplitude in, 41  
 Receiver bandwidth, 39  
 Receiver delay time, 40  
 Receiver gate, 163  
 Receiving equipment, 426  
     sequence of time selectors in, 400  
 Recorder, Esterline-Angus, 387  
 Recovery time of circuit, 116  
 Rectangle generator, variable-width, use of, to produce time-modulated tracking index, 222  
 Reed, H. J., 119  
 Relaxation oscillator, 107  
     gas-tetrode, 76, 77  
 Relay radar systems, 400, 417-470  
     c-w, 458  
     performance of, 470  
     performance in, 439  
     simplified, for constant-speed rotation, 450  
 Repetition-rate control, 511  
 Reset error, 192  
 Reset interval, 194  
 Resolver, d-c, 440  
 Response times, 275  
 Rise time, 39

## S

Sanatron, precision, 124  
 simple, 124  
 Sanatron circuit, usual, errors in, 124  
 Scale coordination by frequency division, 153-155  
 Scanning, conical, 367, 368  
 SCR-268 oscillator, 137  
 SCR-268 radar, 135  
 SCR-584 radar, 89, 161, 163, 337, 368-370, 406  
   conical scanning antenna pattern, 367  
 SCR-584 circular-sweep time modulator, 161  
   block diagram of, 162  
 SCR-615, 373, 378  
   angle-tracking circuits in, 374  
 SCR-682A radar, 255  
 SCR-718 altimeter, 163, 219  
 SCR-784 time discriminator, 313-315, 337  
 Screen waveform, 105  
 Search circuits, automatic, 278  
 Selsyn, 394  
 Separator unit, 466  
 Sequencing circuits, 429-433  
 Servoamplifier, 438  
 Servomechanism, range follow-up, 331  
   velocity, 252  
   with velocity memory, 449  
 Shoran, 30, 161  
 Sickles Company, F. W., 88  
 Signal and index, superposition of, 195-198  
 Sine-cosine system, time-modulated, 417  
 Sine-wave tracking, 155-157, 242  
 Single-scale circuits, 111-141  
   comparison of, 140, 141  
 Sinusoids, phase-modulated, pulse representation of, 442  
 Slave station, 261  
 Spacing, 400  
 Specification, 51  
 Speed, blind, 19  
   ground, 21, 24  
 Speed measurements, 16-24  
   accuracy of, 32  
 Spencer, R. E., 489  
 Step interpolation, 168  
 Step-interpolation time modulation, 164

Storage tube, 99  
 Subassembly, 170, 174  
   faulty, 170  
 Subcarrier, 398  
 Supersonic delay lines, mercury, 481  
   solid, 484-487  
   water, 482-484  
 Sweep, circular, 81, 99, 142, 168, 184, 341  
   displays in, 161  
   exponential, 215  
 Sweep generator, exponential, 144  
 Synchro systems, 393  
 Synchronization, 42-47  
   by automatic-frequency tracking, 95-100  
   precise, of random oscillators, 99  
   precise system for two independent oscillators, 99  
   by PRF generator, 45  
   remote control of, 46  
   by r-f pulse generator, 43  
 Synchronizer, 81-83, 87, 90, 424-426  
   AN/APS-10 (*see* AN/APS-10 synchronizer)  
   automatic-frequency-tracking, block diagram of, 96  
   radar, 71

## T

Tachometer feedback, 359  
 Tachometers, Elinco Type B-44, 361  
 Target indication, 326  
 Target indicator, automatic, 278  
 Target selection, 277, 278, 325  
   automatic, 326, 330-337  
   manual, 329  
 Telecommunications Research Establishment, 310  
 Telegons, 394  
 Telemetering, 391-393  
 Teletorque, 394  
 Temperature changes, 141  
 Temperature coefficients, 141  
   delay-line, 108  
 Test oscilloscope, TS-100, 89  
 ZDP-1, 219  
 Time aperture, 277  
 Time demodulation, 62-64  
 Time discrimination, 62-64, 276  
 Time discriminator, 95, 97, 308, 309, 356

- Time discriminator, of AN/APG-15, 316
    - of British radar set, 315
    - Oboe, 311, 312
    - pulse-stretching, 318
    - SCR-784, 313-315, 337
    - with time selectors, pulse stretcher, and narrow-band pulse amplification, 317-321
  - Time-marker generator, delay-line, super-sonic, 108
  - Time markers, 81
  - Time marks, electronic, 219
  - Time measurement, automatic, on grouped data, 380-386
    - error of, 40
    - manual, fixed indices for, 215
    - movable tracking marks for, 220
    - medium-precision, in radars, 141
  - Time-measurement circuits, errors in, 120
  - Time-measuring systems, automatic, five possible configurations of, 338
    - especially accurate, 261
  - Time modulation, 4, 47-50
    - and demodulation, 5-7
    - double-scale, 58-61
    - electrical control of, 168
    - multiple-scale, 48-50
    - single-scale, 47, 55-58
    - step-interpolation, 164
  - Time-modulation circuit, bootstrap, 128
  - Time-modulation circuit, nonlinear, 112
  - Time-modulation system, delay-tank, 132
    - three-scale, 169
  - Time modulator, 146, 171, 400
    - AN/APS-15, 167
    - circular-sweep, SCR-584, 161
    - block diagram of, 162
    - H<sub>2</sub>X, 121
    - linear-sweep, 152
    - Loran (*see* Loran time modulator)
    - Miller feedback, 114
    - multiple-scale, 174
    - and pulse selector, 146
    - two-scale, 71, 170
  - Time selection, 62-64, 321-325
  - Time selectors, 400
    - pentode, 88
    - sequence of, in receiving equipment, 400
  - Timing standards, 50
  - Tracking, aided, 200, 203, 206
    - with intermittent data, 247-251
    - velocity servomechanism for, 250
  - automatic, 202
  - automatic frequency, synchronization by, 95-100
  - direct, 200, 202, 220
  - on grouped or periodically interrupted data, 378
  - with intermittent data, 247
  - linear-time-constant, 201
  - memory-point, 201, 207
  - regenerative, 201, 210, 256
  - sine-wave (*see* Sine-wave tracking)
  - two-coordinate, 251-261
  - velocity, 200, 203
- Tracking circuits, step-gate, 433-435
  - Tracking indices, 183
    - time-modulated, use of variable-width rectangle generator to produce, 222
  - Tracking marks, movable, for manual time measurement, 220
  - Tracking methods, 200
  - Tracking systems, comparison of, 340
    - manual, 371-376
  - Tracking tester, dynamic, 357, 361
  - Transformer, air-core, quenching oscillator with, 79
  - Transmission, of continuous rotation, 393-395
    - 360° rotation, 397
  - Transmission devices, simple, with limited rotation, 392
  - Transmitter, 463
  - Trigger generators, multiple-frequency, 81
  - Triggers, delayed, 78
  - Triode coincidence tube, 95
  - Triodes, baseless subminiature, 91
  - TS-100 test oscilloscope, 89, 218
  - Tube, storage, 107
    - subminiature, 170
    - vacuum (*see* Vacuum tube)
  - Tube changes, 141
  - Tube drifts, 141
  - 274 meter, British, 368
  - Type G presentation, 368
  - Type J display, 180
    - with movable index, 220

Type M display, 180  
Type M indicator, 223  
Type 0808 model B3 motor, Holtzer-  
Cabot, 441  
Type YE4-B lines, General Electric, 406

## U

Uttley, A. U., 306

## V

Vacuum tube, 51  
  effects of mechanical shock on, 52  
  and time, 52  
Velocity learning time, 380  
Velocity memory, 278, 284, 380  
  servomechanism with, 449  
Velocity servomechanism, 252  
  for aided tracking, 250  
Vibrations, 141  
Video mixing unit, 451  
Video separator, 458

Voltage pulses, blocking-oscillator, 78  
Voltage-sawtooth circuits, 141

## W

Wave trains, recurrent, cancellation of,  
  471-527  
  delay of, 471-527  
Westinghouse 132-DW pulse transformer,  
  317  
Width, 400  
Wien-bridge oscillator, 70, 139  
Williams, F. C., 306  
Wurzburg range unit, 163

## Z

Zero adjustment, 73  
Zero calibration, 45  
Zero correction, 46, 93, 94  
Zero-range trigger, for modulator, 95  
Zero-setting, 168



## CATALOGUE OF DOVER BOOKS

## ENGINEERING AND TECHNOLOGY

### General and mathematical

**ENGINEERING MATHEMATICS**, Kenneth S. Miller. A text for graduate students of engineering to strengthen their mathematical background in differential equations, etc. Mathematical steps very explicitly indicated. Contents: Determinants and Matrices, Integrals, Linear Differential Equations, Fourier Series and Integrals, Laplace Transform, Network Theory, Random Function . . . all vital requisites for advanced modern engineering studies. Unabridged republication. Appendices: Borel Sets; Riemann-Stieltjes Integral; Fourier Series and Integrals. Index. References at Chapter Ends. xii + 417pp. 6 x 8½. S1121 Paperbound \$2.00

**MATHEMATICAL ENGINEERING ANALYSIS**, Rufus Oldenburger. A book designed to assist the research engineer and scientist in making the transition from physical engineering situations to the corresponding mathematics. Scores of common practical situations found in all major fields of physics are supplied with their correct mathematical formulations—applications to automobile springs and shock absorbers, clocks, throttle torque of diesel engines, resistance networks, capacitors, transmission lines, microphones, neon tubes, gasoline engines, refrigeration cycles, etc. Each section reviews basic principles of underlying various fields: mechanics of rigid bodies, electricity and magnetism, heat, elasticity, fluid mechanics, and aerodynamics. Comprehensive and eminently useful. Index. 169 problems, answers. 200 photos and diagrams. xiv + 426pp. 5½ x 8½. S919 Paperbound \$2.00

**MATHEMATICS OF MODERN ENGINEERING**, E. G. Keller and R. E. Doherty. Written for the Advanced Course in Engineering of the General Electric Corporation, deals with the engineering use of determinants, tensors, the Heaviside operational calculus, dyadics, the calculus of variations, etc. Presents underlying principles fully, but purpose is to teach engineers to deal with modern engineering problems, and emphasis is on the perennial engineering attack of set-up and solve. Indexes. Over 185 figures and tables. Hundreds of exercises, problems, and worked-out examples. References. Two volume set. Total of xxxiii + 623pp. 5½ x 8.

S734 Vol I Paperbound \$1.85

S735 Vol II Paperbound \$1.85

The set \$3.70

**MATHEMATICAL METHODS FOR SCIENTISTS AND ENGINEERS**, L. P. Smith. For scientists and engineers, as well as advanced math students. Full investigation of methods and practical description of conditions under which each should be used. Elements of real functions, differential and integral calculus, space geometry, theory of residues, vector and tensor analysis, series of Bessel functions, etc. Each method illustrated by completely-worked-out examples, mostly from scientific literature. 368 graded unsolved problems. 100 diagrams. x + 453pp. 5½ x 8½. S220 Paperbound \$2.00

**THEORY OF FUNCTIONS AS APPLIED TO ENGINEERING PROBLEMS**, edited by R. Rothe, F. Ollendorff, and K. Pohlhausen. A series of lectures given at the Berlin Institute of Technology that shows the specific applications of function theory in electrical and allied fields of engineering. Six lectures provide the elements of function theory in a simple and practical form, covering complex quantities and variables, integration in the complex plane, residue theorems, etc. Then 5 lectures show the exact uses of this powerful mathematical tool, with full discussions of problem methods. Index. Bibliography. 108 figures. x + 189pp. 5½ x 8.

S733 Paperbound \$1.35

### Aerodynamics and hydrodynamics

**AIRPLANE STRUCTURAL ANALYSIS AND DESIGN**, E. E. Sechler and L. G. Dunn. Systematic authoritative book which summarizes a large amount of theoretical and experimental work on structural analysis and design. Strong on classical subsonic material still basic to much aeronautic design . . . remains a highly useful source of information. Covers such areas as layout of the airplane, applied and design loads, stress-strain relationships for stable structures, truss and frame analysis, the problem of instability, the ultimate strength of stiffened flat sheet, analysis of cylindrical structures, wings and control surfaces, fuselage analysis, engine mounts, landing gears, etc. Originally published as part of the *CALCIT* Aeronautical Series. 256 illustrations. 47 study problems. Indexes. xi + 420pp. 5½ x 8½. S1043 Paperbound \$2.25

**FUNDAMENTALS OF HYDRO- AND AEROMECHANICS**, L. Prandtl and O. G. Tietjens. The well-known standard work based upon Prandtl's lectures at Goettingen. Wherever possible hydrodynamics theory is referred to practical considerations in hydraulics, with the view of unifying theory and experience. Presentation is extremely clear and though primarily physical, mathematical proofs are rigorous and use vector analysis to a considerable extent. An Engineering Society Monograph, 1934. 186 figures. Index. xvi + 270pp. 5½ x 8.

S374 Paperbound \$1.85

## Catalogue of Dover Books

**FLUID MECHANICS FOR HYDRAULIC ENGINEERS, H. Rouse.** Standard work that gives a coherent picture of fluid mechanics from the point of view of the hydraulic engineer. Based on courses given to civil and mechanical engineering students at Columbia and the California Institute of Technology, this work covers every basic principle, method, equation, or theory of interest to the hydraulic engineer. Much of the material, diagrams, charts, etc., in this self-contained text are not duplicated elsewhere. Covers irrotational motion, conformal mapping, problems in laminar motion, fluid turbulence, flow around immersed bodies, transportation of sediment, general characteristics of wave phenomena, gravity waves in open channels, etc. Index. Appendix of physical properties of common fluids. Frontispiece + 245 figures and photographs. xvi + 422pp. 5½ x 8. S729 Paperbound \$2.25

**WATERHAMMER ANALYSIS, John Parmakian.** Valuable exposition of the graphical method of solving waterhammer problems by Assistant Chief Designing Engineer, U.S. Bureau of Reclamation. Discussions of rigid and elastic water column theory, velocity of waterhammer waves, theory of graphical waterhammer analysis for gate operation, closings, openings, rapid and slow movements, etc., waterhammer in pump discharge caused by power failure, waterhammer analysis for compound pipes, and numerous related problems. "With a concise and lucid style, clear printing, adequate bibliography and graphs for approximate solutions at the project stage, it fills a vacant place in waterhammer literature." WATER POWER. 43 problems. Bibliography. Index. 113 illustrations. xiv + 161pp. 5½ x 8½.

S1061 Paperbound \$1.65

**AERODYNAMIC THEORY: A GENERAL REVIEW OF PROGRESS, William F. Durand, editor-in-chief.** A monumental joint effort by the world's leading authorities prepared under a grant of the Guggenheim Fund for the Promotion of Aeronautics. Intended to provide the student and aeronautic designer with the theoretical and experimental background of aeronautics. Never equalled for breadth, depth, reliability. Contains discussions of special mathematical topics not usually taught in the engineering or technical courses. Also: an extended two-part treatise on Fluid Mechanics, discussions of aerodynamics of perfect fluids, analyses of experiments with wind tunnels, applied airfoil theory, the non-lifting system of the airplane, the air propeller, hydrodynamics of boats and floats, the aerodynamics of cooling, etc. Contributing experts include Munk, Giacomelli, Prandtl, Toussaint, Von Karman, Klemperer, among others. Unabridged republication. 6 volumes bound as 3. Total of 1,012 figures, 12 plates. Total of 2,186pp. Bibliographies. Notes. Indices. 5½ x 8.

S328-S330 Clothbound, The Set \$17.50

**APPLIED HYDRO- AND AEROMECHANICS, L. Prandtl and O. G. Tietjens.** Presents, for the most part, methods which will be valuable to engineers. Covers flow in pipes, boundary layers, airfoil theory, entry conditions, turbulent flow in pipes, and the boundary layer, determining drag from measurements of pressure and velocity, etc. "Will be welcomed by all students of aerodynamics." NATURE. Unabridged, unaltered. An Engineering Society Monograph, 1934. Index. 226 figures, 28 photographic plates illustrating flow patterns. xvi + 311pp. 5½ x 8.

S375 Paperbound \$1.85

**SUPERSONIC AERODYNAMICS, E. R. C. Miles.** Valuable theoretical introduction to the supersonic domain, with emphasis on mathematical tools and principles, for practicing aerodynamicists and advanced students in aeronautical engineering. Covers fundamental theory, divergence theorem and principles of circulation, compressible flow and Helmholtz laws, the Prandtl-Busemann graphic method for 2-dimensional flow, oblique shock waves, the Taylor-Maccoll method for cones in supersonic flow, the Chaplygin method for 2-dimensional flow, etc. Problems range from practical engineering problems to development of theoretical results. "Rendered outstanding by the unprecedented scope of its contents . . . has undoubtedly filled a vital gap." AERONAUTICAL ENGINEERING REVIEW. Index. 173 problems, answers. 106 diagrams. 7 tables. xii + 255pp. 5½ x 8.

S214 Paperbound \$1.45

**HYDRAULIC TRANSIENTS, G. R. Rich.** The best text in hydraulics ever printed in English . . . by one of America's foremost engineers (former Chief Design Engineer for T.V.A.). Provides a transition from the basic differential equations of hydraulic transient theory to the arithmetic integration computation required by practicing engineers. Sections cover Water Hammer, Turbine Speed Regulation, Stability of Governing, Water-Hammer Pressures in Pump Discharge Lines, The Differential and Restricted Orifice Surge Tanks, The Normalized Surge Tank Charts of Calame and Gaden, Navigation Locks, Surges in Power Canals—Tidal Harmonics, etc. Revised and enlarged. Author's prefaces. Index. xiv + 409pp. 5½ x 8½.

S116 Paperbound \$2.80

**HYDRAULICS AND ITS APPLICATIONS, A. H. Gibson.** Excellent comprehensive textbook for the student and thorough practical manual for the professional worker, a work of great stature in its area. Half the book is devoted to theory and half to applications and practical problems met in the field. Covers modes of motion of a fluid, critical velocity, viscous flow, eddy formation, Bernoulli's theorem, flow in converging passages, vortex motion, form of effluent streams, notches and weirs, skin friction, losses at valves and elbows, siphons, erosion of channels, jet propulsion, waves of oscillation, and over 100 similar topics. Final chapters (nearly 400 pages) cover more than 100 kinds of hydraulic machinery: Pelton wheel, speed regulators, the hydraulic ram, surge tanks, the scoop wheel, the Venturi meter, etc. A special chapter treats methods of testing theoretical hypotheses: scale models of rivers, tidal estuaries, siphon spillways, etc. 5th revised and enlarged (1952) edition. Index. Appendix. 427 photographs and diagrams. 95 examples, answers. xv + 813pp. 6 x 9.

S791 Clothbound \$8.00

## Catalogue of Dover Books

**FLUID MECHANICS THROUGH WORKED EXAMPLES, D. R. L. Smith and J. Houghton.** Advanced text covering principles and applications to practical situations. Each chapter begins with concise summaries of fundamental ideas. 163 fully worked out examples applying principles outlined in the text. 275 other problems, with answers. Contents: The Pressure of Liquids on Surfaces; Floating Bodies; Flow Under Constant Head in Pipes; Circulation; Vorticity; The Potential Function; Laminar Flow and Lubrication; Impact of Jets; Hydraulic Turbines; Centrifugal and Reciprocating Pumps; Compressible Fluids; and many other items. Total of 438 examples. 250 line illustrations. 340pp. Index. 6 x 8 1/2. S981 Clothbound \$6.00

**THEORY OF SHIP MOTIONS, S. N. Blagoveshchensky.** The only detailed text in English in a rapidly developing branch of engineering and physics, it is the work of one of the world's foremost authorities—Blagoveshchensky of Leningrad Shipbuilding Institute. A senior-level treatment written primarily for engineering students, but also of great importance to naval architects, designers, contractors, researchers in hydrodynamics, and other students. No mathematics beyond ordinary differential equations is required for understanding the text. Translated by T. & L. Strelkoff, under editorship of Louis Landweber, Iowa Institute of Hydraulic Research, under auspices of Office of Naval Research. Bibliography. Index. 231 diagrams and illustrations. Total of 649pp. 5 1/2 x 8 1/2. Vol. I: S234 Paperbound \$2.00  
Vol. II: S235 Paperbound \$2.00

**THEORY OF FLIGHT, Richard von Mises.** Remains almost unsurpassed as balanced, well-written account of fundamental fluid dynamics, and situations in which air compressibility effects are unimportant. Stressing equally theory and practice, avoiding formidable mathematical structure, it conveys a full understanding of physical phenomena and mathematical concepts. Contains perhaps the best introduction to general theory of stability. "Outstanding." Scientific, Medical, and Technical Books. New introduction by K. H. Hohenemser. Bibliographical, historical notes. Index. 408 illustrations. xvi + 620pp. 5 1/2 x 8 1/2. S541 Paperbound \$2.95

**THEORY OF WING SECTIONS, I. H. Abbott, A. E. von Doenhoff.** Concise compilation of subsonic aerodynamic characteristics of modern NASA wing sections, with description of their geometry, associated theory. Primarily reference work for engineers, students, it gives methods, data for using wing-section data to predict characteristics. Particularly valuable: chapters on thin wings, airfoils; complete summary of NACA's experimental observations, system of construction families of airfoils. 350pp. of tables on Basic Thickness Forms, Mean Lines, Airfoil Ordinates, Aerodynamic Characteristics of Wing Sections. Index. Bibliography. 191 illustrations. Appendix. 705pp. 5 1/2 x 8. S558 Paperbound \$3.25

**WEIGHT-STRENGTH ANALYSIS OF AIRCRAFT STRUCTURES, F. R. Shanley.** Scientifically sound methods of analyzing and predicting the structural weight of aircraft and missiles. Deals directly with forces and the distances over which they must be transmitted, making it possible to develop methods by which the minimum structural weight can be determined for any material and conditions of loading. Weight equations for wing and fuselage structures. Includes author's original papers on inelastic buckling and creep buckling. "Particularly successful in presenting his analytical methods for investigating various optimum design principles." **AERONAUTICAL ENGINEERING REVIEW.** Enlarged bibliography. Index. 199 figures. xiv + 404pp. 5 1/2 x 8 1/2. S660 Paperbound \$2.50

## Electricity

**TWO-DIMENSIONAL FIELDS IN ELECTRICAL ENGINEERING, L. V. Bewley.** A useful selection of typical engineering problems of interest to practicing electrical engineers. Introduces senior students to the methods and procedures of mathematical physics. Discusses theory of functions of a complex variable, two-dimensional fields of flow, general theorems of mathematical physics and their applications, conformal mapping or transformation, method of images, freehand flux plotting, etc. New preface by the author. Appendix by W. F. Kiltner. Index. Bibliography at chapter ends. xiv + 204pp. 5 1/2 x 8 1/2. S1118 Paperbound \$1.50

**FLUX LINKAGES AND ELECTROMAGNETIC INDUCTION, L. V. Bewley.** A brief, clear book which shows proper uses and corrects misconceptions of Faraday's law of electromagnetic induction in specific problems. Contents: Circuits, Turns, and Flux Linkages; Substitution of Circuits; Electromagnetic Induction; General Criteria for Electromagnetic Induction; Applications and Paradoxes; Theorem of Constant Flux Linkages. New Section: Rectangular Coil in a Varying Uniform Medium. Valuable supplement to class texts for engineering students. Corrected, enlarged edition. New preface. Bibliography in notes. 49 figures. xi + 106pp. 5 1/2 x 8. S1103 Paperbound \$1.25

**INDUCTANCE CALCULATIONS: WORKING FORMULAS AND TABLES, Frederick W. Grover.** An invaluable book to everyone in electrical engineering. Provides simple single formulas to cover all the more important cases of inductance. The approach involves only those parameters that naturally enter into each situation, while extensive tables are given to permit easy interpolations. Will save the engineer and student countless hours and enable them to obtain accurate answers with minimal effort. Corrected republication of 1946 edition. 58 tables. 97 completely worked out examples. 66 figures. xiv + 286pp. 5 1/2 x 8 1/2. S974 Paperbound \$1.85

## Catalogue of Dover Books

**GASEOUS CONDUCTORS: THEORY AND ENGINEERING APPLICATIONS**, J. D. Cobine. An indispensable text and reference to gaseous conduction phenomena, with the engineering viewpoint prevailing throughout. Studies the kinetic theory of gases, ionization, emission phenomena; gas breakdown, spark characteristics, glow, and discharges; engineering applications in circuit interrupters, rectifiers, light sources, etc. Separate detailed treatment of high pressure arcs (Suits); low pressure arcs (Langmuir and Tonks). Much more. "Well organized, clear, straightforward," Tonks, *Review of Scientific Instruments*. Index. Bibliography. 83 practice problems. 7 appendices. Over 600 figures. 58 tables. xx + 606pp. 5% x 8. S442 Paperbound \$2.95

**INTRODUCTION TO THE STATISTICAL DYNAMICS OF AUTOMATIC CONTROL SYSTEMS**, V. V. Solodovnikov. First English publication of text-reference covering important branch of automatic control systems—random signals; in its original edition, this was the first comprehensive treatment. Examines frequency characteristics, transfer functions, stationary random processes, determination of minimum mean-squared error, of transfer function for a finite period of observation, much more. Translation edited by J. B. Thomas, L. A. Zadeh. Index. Bibliography. Appendix. xxi + 308pp. 5% x 8. S420 Paperbound \$2.25

**TENSORS FOR CIRCUITS**, Gabriel Kron. A boldly original method of analyzing engineering problems, at center of sharp discussion since first introduced, now definitely proved useful in such areas as electrical and structural networks on automatic computers. Encompasses a great variety of specific problems by means of a relatively few symbolic equations. "Power and flexibility . . . becoming more widely recognized," *Nature*. Formerly "A Short Course in Tensor Analysis." New introduction by B. Hoffmann. Index. Over 800 diagrams. xix + 250pp. 5% x 8. S534 Paperbound \$2.00

**SELECTED PAPERS ON SEMICONDUCTOR MICROWAVE ELECTRONICS**, edited by Sumner N. Levine and Richard R. Kurczok. An invaluable collection of important papers dealing with one of the most remarkable developments in solid-state electronics—the use of the p-n junction to achieve amplification and frequency conversion of microwave frequencies. Contents: General Survey (3 introductory papers by W. E. Danielson, R. N. Hall, and M. Tenzer); General Theory of Nonlinear Elements (3 articles by A. van der Ziel, H. E. Rowe, and Manley and Rowe); Device Fabrication and Characterization (3 pieces by Bakanowski, Cranna, and Uhlir, by McCotter, Walker and Fortini, and by S. T. Eng); Parametric Amplifiers and Frequency Multipliers (13 articles by Uhlir, Heffner and Wade, Matthaei, P. K. Tien, van der Ziel, Engelbrecht, Currie and Gould, Uenohara, Leeson and Weinreb, and others); and Tunnel Diodes (4 papers by L. Esaki, H. S. Sommers, Jr., M. E. Hines, and Yariw and Cook). Introduction. 295 Figures. xiii + 286pp. 6½ x 9¼. S1126 Paperbound \$2.25

**THE PRINCIPLES OF ELECTROMAGNETISM APPLIED TO ELECTRICAL MACHINES**, B. Hague. A concise, but complete, summary of the basic principles of the magnetic field and its applications, with particular reference to the kind of phenomena which occur in electrical machines. Part I: General Theory—magnetic field of a current, electromagnetic field passing from air to iron, mechanical forces on linear conductors, etc. Part II: Application of theory to the solution of electromechanical problems—the magnetic field and mechanical forces in non-salient pole machinery, the field within slots and between salient poles, and the work of Rogowski, Roth, and Strutt. Formerly titled "Electromagnetic Problems in Electrical Engineering." 2 appendices. Index. Bibliography in notes. 115 figures. xiv + 359pp. 5% x 8½. S246 Paperbound \$2.25

## Mechanical engineering

**DESIGN AND USE OF INSTRUMENTS AND ACCURATE MECHANISM**, T. N. Whitehead. For the instrument designer, engineer; how to combine necessary mathematical abstractions with independent observation of actual facts. Partial contents: instruments & their parts, theory of errors, systematic errors, probability, short period errors, erratic errors, design precision, kinematic, semikinematic design, stiffness, planning of an instrument, human factor, etc. Index. 85 photos, diagrams. xii + 288pp. 5% x 8. S270 Paperbound \$2.00

**A TREATISE ON GYROSTATICS AND ROTATIONAL MOTION: THEORY AND APPLICATIONS**, Andrew Gray. Most detailed, thorough book in English, generally considered definitive study. Many problems of all sorts in full detail, or step-by-step summary. Classical problems of Bour, Lotner, etc.; later ones of great physical interest. Vibrating systems of gyrostats, earth as a top, calculation of path of axis of a top by elliptic integrals, motion of unsymmetrical top, much more. Index. 160 illus. 550pp. 5% x 8. S589 Paperbound \$2.75

**MECHANICS OF THE GYROSCOPE, THE DYNAMICS OF ROTATION**, R. F. Delmel, Professor of Mechanical Engineering at Stevens Institute of Technology. Elementary general treatment of dynamics of rotation, with special application of gyroscopic phenomena. No knowledge of vectors needed. Velocity of a moving curve, acceleration to a point, general equations of motion, gyroscopic horizon, free gyro, motion of discs, the damped gyro, 103 similar topics. Exercises. 75 figures. 208pp. 5% x 8. S66 Paperbound \$1.75

## Catalogue of Dover Books

**STRENGTH OF MATERIALS, J. P. Den Hartog.** Distinguished text prepared for M.I.T. course, ideal as introduction, refresher, reference, or self-study text. Full clear treatment of elementary material (tension, torsion, bending, compound stresses, deflection of beams, etc.), plus much advanced material on engineering methods of great practical value: full treatment of the Mohr circle, lucid elementary discussions of the theory of the center of shear and the "Myosotis" method of calculating beam deflections, reinforced concrete, plastic deformations, photoelasticity, etc. In all sections, both general principles and concrete applications are given. Index. 186 figures (160 others in problem section). 350 problems, all with answers. List of formulas. viii + 323pp. 5% x 8. S755 Paperbound \$2.00

**PHOTOELASTICITY: PRINCIPLES AND METHODS, H. T. Jessop, F. C. Harris.** For the engineer, for specific problems of stress analysis. Latest time-saving methods of checking calculations in 2-dimensional design problems, new techniques for stresses in 3 dimensions, and lucid description of optical systems used in practical photoelasticity. Useful suggestions and hints based on on-the-job experience included. Partial contents: strained and stress-strain relations, circular disc under thrust along diameter, rectangular block with square hole under vertical thrust, simply supported rectangular beam under central concentrated load, etc. Theory held to minimum, no advanced mathematical training needed. Index. 164 illustrations. viii + 184pp. 6½ x 9½. S720 Paperbound \$2.00

**APPLIED ELASTICITY, J. Prescott.** Provides the engineer with the theory of elasticity usually lacking in books on strength of materials, yet concentrates on those portions useful for immediate application. Develops every important type of elasticity problem from theoretical principles. Covers analysis of stress, relations between stress and strain, the empirical basis of elasticity, thin rods under tension or thrust, Saint Venant's theory, transverse oscillations of thin rods, stability of thin plates, cylinders with thin walls, vibrations of rotating disks, elastic bodies in contact, etc. "Excellent and important contribution to the subject, not merely in the old matter which he has presented in new and refreshing form, but also in the many original investigations here published for the first time," NATURE. Index. 3 Appendixes. vi + 672pp. 5% x 8. S726 Paperbound \$3.25

**APPLIED MECHANICS FOR ENGINEERS, Sir Charles Inglis, F.R.S.** A representative survey of the many and varied engineering questions which can be answered by statics and dynamics. The author, one of first and foremost adherents of "structural dynamics," presents distinctive illustrative examples and clear, concise statement of principles—directing the discussion at methodology and specific problems. Covers fundamental principles of rigid-body statics, graphic solutions of static problems, theory of taut wires, stresses in frameworks, particle dynamics, kinematics, simple harmonic motion and harmonic analysis, two-dimensional rigid dynamics, etc. 437 illustrations. xii + 404pp. 5% x 8½. S1119 Paperbound \$2.00

**THEORY OF MACHINES THROUGH WORKED EXAMPLES, G. H. Ryder.** Practical mechanical engineering textbook for graduates and advanced undergraduates, as well as a good reference work for practicing engineers. Partial contents: Mechanisms, Velocity and Acceleration (including discussion of Klein's Construction for Piston Acceleration), Cams, Geometry of Gears, Clutches and Bearings, Belt and Rope Drives, Brakes, Inertia Forces and Couples, General Dynamical Problems, Gyroscopes, Linear and Angular Vibrations, Torsional Vibrations, Transverse Vibrations and Whirling Speeds (Chapters on vibrations considerably enlarged from previous editions). Over 300 problems, many fully worked out. Index. 195 line illustrations. Revised and enlarged edition. viii + 280pp. 5% x 8¾. S980 Clothbound \$5.00

**THE KINEMATICS OF MACHINERY: OUTLINES OF A THEORY OF MACHINES, Franz Reuleaux.** The classic work in the kinematics of machinery. The present thinking about the subject has all been shaped in great measure by the fundamental principles stated here by Reuleaux almost 90 years ago. While some details have naturally been superseded, his basic viewpoint has endured; hence, the book is still an excellent text for basic courses in kinematics and a standard reference work for active workers in the field. Covers such topics as: the nature of the machine problem, phoronomic propositions, pairs of elements, incomplete kinematic chains, kinematic notation and analysis, analyses of chamber-crank trains, chamber-wheel trains, constructive elements of machinery, complete machines, etc., with main focus on controlled movement in mechanisms. Unabridged republication of original edition, translated by Alexander B. Kennedy. New introduction for this edition by E. S. Ferguson. Index. 451 illustrations. xxiv + 622pp. 5% x 8½. S1124 Paperbound \$3.00

**ANALYTICAL MECHANICS OF GEARS, Earle Buckingham.** Provides a solid foundation upon which logical design practices and design data can be constructed. Originally arising out of investigations of the ASME Special Research Committee on Worm Gears and the Strength of Gears, the book covers conjugate gear-tooth action, the nature of the contact, and resulting gear-tooth profiles of: spur, internal, helical, spiral, worm, bevel, and hypoid or skew bevel gears. Also: frictional heat of operation and its dissipation, friction losses, etc., dynamic loads in operation, and related matters. Familiarity with this book is still regarded as a necessary prerequisite to work in modern gear manufacturing. 263 figures. 103 tables. Index. x + 546pp. 5% x 8½. S1073 Paperbound \$2.75

## Catalogue of Dover Books

### Optical design, lighting

**THE SCIENTIFIC BASIS OF ILLUMINATING ENGINEERING**, Parry Moon, Professor of Electrical Engineering, M.I.T. Basic, comprehensive study. Complete coverage of the fundamental theoretical principles together with the elements of design, vision, and color with which the lighting engineer must be familiar. Valuable as a text as well as a reference source to the practicing engineer. Partial contents: Spectroradiometric Curve, Luminous Flux, Radiation from Gaseous-Conduction Sources, Radiation from Incandescent Sources, Incandescent Lamps, Measurement of Light, Illumination from Point Sources and Surface Sources, Elements of Lighting Design. 7 Appendices. Unabridged and corrected republication, with additions. New preface containing conversion tables of radiometric and photometric concepts. Index. 707-item bibliography. 92-item bibliography of author's articles. 183 problems. xxiii + 608pp. 5½ x 8½.  
S242 Paperbound \$2.85

**OPTICS AND OPTICAL INSTRUMENTS: AN INTRODUCTION WITH SPECIAL REFERENCE TO PRACTICAL APPLICATIONS**, B. K. Johnson. An invaluable guide to basic practical applications of optical principles, which shows how to set up inexpensive working models of each of the four main types of optical instruments—telescopes, microscopes, photographic lenses, optical projecting systems. Explains in detail the most important experiments for determining their accuracy, resolving power, angular field of view, amounts of aberration, all other necessary facts about the instruments. Formerly "Practical Optics." Index. 234 diagrams. Appendix. 224pp. 5½ x 8.  
S642 Paperbound \$1.65

**APPLIED OPTICS AND OPTICAL DESIGN**, A. E. Conrady. With publication of vol. 2, standard work for designers in optics is now complete for first time. Only work of its kind in English; only detailed work for practical designer and self-taught. Requires, for bulk of work, no math above trig. Step-by-step exposition, from fundamental concepts of geometrical, physical optics, to systematic study, design, of almost all types of optical systems. Vol. 1: all ordinary ray-tracing methods; primary aberrations; necessary higher aberration for design of telescopes, low-power microscopes, photographic equipment. Vol. 2: (Completed from author's notes by R. Kingslake, Dir. Optical Design, Eastman Kodak.) Special attention to high-power microscope, anastigmatic photographic objectives. "An indispensable work," J., Optical Soc. of Amer. "As a practical guide this book has no rival," Transactions, Optical Soc. Index. Bibliography. 193 diagrams. 852pp. 6¼ x 9¼.  
Vol. 1 S366 Paperbound \$3.50  
Vol. 2 S612 Paperbound \$2.95

### Miscellaneous

**THE MEASUREMENT OF POWER SPECTRA FROM THE POINT OF VIEW OF COMMUNICATIONS ENGINEERING**, R. B. Blackman, J. W. Tukey. This pathfinding work, reprinted from the "Bell System Technical Journal," explains various ways of getting practically useful answers in the measurement of power spectra, using results from both transmission theory and the theory of statistical estimation. Treats: Autocovariance Functions and Power Spectra; Direct Analog Computation; Distortion, Noise, Heterodyne Filtering and Pre-whitening; Aliasing; Rejection Filtering and Separation; Smoothing and Decimation Procedures; Very Low Frequencies; Transversal Filtering; much more. An appendix reviews fundamental Fourier techniques. Index of notation. Glossary of terms. 24 figures. XII tables. Bibliography. General index. 192pp. 5½ x 8.  
S507 Paperbound \$1.85

**CALCULUS REFRESHER FOR TECHNICAL MEN**, A. Albert Klaf. This book is unique in English as a refresher for engineers, technicians, students who either wish to brush up their calculus or to clear up uncertainties. It is not an ordinary text, but an examination of most important aspects of integral and differential calculus in terms of the 756 questions most likely to occur to the technical reader. The first part of this book covers simple differential calculus, with constants, variables, functions, increments, derivatives, differentiation, logarithms, curvature of curves, and similar topics. The second part covers fundamental ideas of integration, inspection, substitution, transformation, reduction, areas and volumes, mean value, successive and partial integration, double and triple integration. Practical aspects are stressed rather than theoretical. A 50-page section illustrates the application of calculus to specific problems of civil and nautical engineering, electricity, stress and strain, elasticity, industrial engineering, and similar fields.—756 questions answered. 566 problems, mostly answered. 36 pages of useful constants, formulae for ready reference. Index. v + 431pp. 5½ x 8.  
T370 Paperbound \$2.00

**METHODS IN EXTERIOR BALLISTICS**, Forest Ray Moulton. Probably the best introduction to the mathematics of projectile motion. The ballistics theories propounded were coordinated with extensive proving ground and wind tunnel experiments conducted by the author and others for the U.S. Army. Broad in scope and clear in exposition, it gives the beginnings of the theory used for modern-day projectile, long-range missile, and satellite motion. Six main divisions: Differential Equations of Translatory Motion of a projectile; Gravity and the Resistance Function; Numerical Solution of Differential Equations; Theory of Differential Variations; Validity of Method of Numerical Integration; and Motion of a Rotating Projectile. Formerly titled: "New Methods in Exterior Ballistics." Index. 38 diagrams. viii + 259pp. 5½ x 8½.  
S232 Paperbound \$1.75

## *Catalogue of Dover Books*

**LOUD SPEAKERS: THEORY, PERFORMANCE, TESTING AND DESIGN, N. W. McLachlan.** Most comprehensive coverage of theory, practice of loud speaker design, testing; classic reference, study manual in field. First 12 chapters deal with theory, for readers mainly concerned with math. aspects; last 7 chapters will interest reader concerned with testing, design. Partial contents: principles of sound propagation, fluid pressure on vibrators, theory of moving-coil principle, transients, driving mechanisms, response curves, design of horn type moving coil speakers, electrostatic speakers, much more. Appendix. Bibliography. Index. 165 illustrations, charts. 411pp. 5% x 8. \$588 Paperbound \$2.25

**MICROWAVE TRANSMISSION, J. C. Slater.** First text dealing exclusively with microwaves, brings together points of view of field, circuit theory, for graduate student in physics, electrical engineering, microwave technician. Offers valuable point of view not in most later studies. Uses Maxwell's equations to study electromagnetic field, important in this area. Partial contents: Infinite line with distributed parameters, impedance of terminated line, plane waves, reflections, wave guides, coaxial line, composite transmission lines, impedance matching, etc. Introduction. Index. 76 illus. 319pp. 5% x 8. \$564 Paperbound \$1.50

**MICROWAVE TRANSMISSION DESIGN DATA, T. Moreno.** Originally classified, now rewritten and enlarged (14 new chapters) for public release under auspices of Sperry Corp. Material of immediate value or reference use to radio engineers, systems designers, applied physicists, etc. Ordinary transmission line theory; attenuation; capacity; parameters of coaxial lines; higher modes; flexible cables; obstacles, discontinuities, and junctions; tunable wave guide impedance transformers; effects of temperature and humidity; much more. "Enough theoretical discussion is included to allow use of data without previous background." Electronics. 324 circuit diagrams, figures, etc. Tables of dielectrics, flexible cable, etc., data. Index. ix + 248pp. 5% x 8. \$459 Paperbound \$1.65

**RAYLEIGH'S PRINCIPLE AND ITS APPLICATIONS TO ENGINEERING, G. Temple & W. Bickley.** Rayleigh's principle developed to provide upper and lower estimates of true value of fundamental period of a vibrating system, or condition of stability of elastic systems. Illustrative examples; rigorous proofs in special chapters. Partial contents: Energy method of discussing vibrations, stability. Perturbation theory, whirling of uniform shafts. Criteria of elastic stability. Application of energy method. Vibrating systems. Proof, accuracy, successive approximations, application of Rayleigh's principle. Synthetic theorems. Numerical, graphical methods. Equilibrium configurations, Ritz's method. Bibliography. Index. 22 figures. ix + 156pp. 5% x 8. \$307 Paperbound \$1.50

**ELASTICITY, PLASTICITY AND STRUCTURE OF MATTER, R. Houwink.** Standard treatise on rheological aspects of different technically important solids such as crystals, resins, textiles, rubber, clay, many others. Investigates general laws for deformations; determines divergences from these laws for certain substances. Covers general physical and mathematical aspects of plasticity, elasticity, viscosity. Detailed examination of deformations, internal structure of matter in relation to elastic and plastic behavior, formation of solid matter from a fluid, conditions for elastic and plastic behavior of matter. Treats glass, asphalt, gutta percha, balata, proteins, baker's dough, lacquers, sulphur, others. 2nd revised, enlarged edition. Extensive revised bibliography in over 500 footnotes. Index. Table of symbols. 214 figures. xviii + 368pp. 6 x 9 1/4. \$385 Paperbound \$2.45

**THE SCHWARZ-CHRISTOFFEL TRANSFORMATION AND ITS APPLICATIONS: A SIMPLE EXPOSITION, Miles Walker.** An important book for engineers showing how this valuable tool can be employed in practical situations. Very careful, clear presentation covering numerous concrete engineering problems. Includes a thorough account of conjugate functions for engineers—useful for the beginner and for review. Applications to such problems as: Stream-lines round a corner, electric conductor in air-gap, dynamo slots, magnetized poles, much more. Formerly "Conjugate Functions for Engineers." Preface. 92 figures, several tables. Index. ix + 116pp. 5% x 8 1/2. \$1149 Paperbound \$1.25

**THE LAWS OF THOUGHT, George Boole.** This book founded symbolic logic some hundred years ago. It is the 1st significant attempt to apply logic to all aspects of human endeavour. Partial contents: derivation of laws, signs & laws, interpretations, eliminations, conditions of a perfect method, analysis, Aristotelian logic, probability, and similar topics. xviii + 424pp. 5% x 8. \$28 Paperbound \$2.00

**SCIENCE AND METHOD, Henri Poincaré.** Procedure of scientific discovery, methodology, experiment, idea-germination—the intellectual processes by which discoveries come into being. Most significant and most interesting aspects of development, application of ideas. Chapters cover selection of facts, chance, mathematical reasoning, mathematics, and logic; Whitehead, Russell, Cantor; the new mechanics, etc. 288pp. 5% x 8. \$222 Paperbound \$1.35

**FAMOUS BRIDGES OF THE WORLD, D. B. Steinman.** An up-to-the-minute revised edition of a book that explains the fascinating drama of how the world's great bridges came to be built. The author, designer of the famed Mackinac bridge, discusses bridges from all periods and all parts of the world, explaining their various types of construction, and describing the problems their builders faced. Although primarily for youngsters, this cannot fail to interest readers of all ages. 48 illustrations in the text. 23 photographs. 99pp. 6 1/4 x 9 1/4. \$161 Paperbound \$1.00



## BOOKS EXPLAINING SCIENCE AND MATHEMATICS

### General

**WHAT IS SCIENCE?**, Norman Campbell. This excellent introduction explains scientific method, role of mathematics, types of scientific laws. Contents: 2 aspects of science, science & nature, laws of science, discovery of laws, explanation of laws, measurement & numerical laws, applications of science. 192pp. 5½ x 8. \$43 Paperbound **\$1.25**

**THE COMMON SENSE OF THE EXACT SCIENCES**, W. K. Clifford. Introduction by James Newman, edited by Karl Pearson. For 70 years this has been a guide to classical scientific and mathematical thought. Explains with unusual clarity basic concepts, such as extension of meaning of symbols, characteristics of surface boundaries, properties of plane figures, vectors, Cartesian method of determining position, etc. Long preface by Bertrand Russell. Bibliography of Clifford. Corrected, 130 diagrams redrawn. 249pp. 5½ x 8. T61 Paperbound **\$1.60**

**SCIENCE THEORY AND MAN**, Erwin Schrödinger. This is a complete and unabridged reissue of **SCIENCE AND THE HUMAN TEMPERAMENT** plus an additional essay: "What is an Elementary Particle?" Nobel laureate Schrödinger discusses such topics as nature of scientific method, the nature of science, chance and determinism, science and society, conceptual models for physical entities, elementary particles and wave mechanics. Presentation is popular and may be followed by most people with little or no scientific training. "Fine practical preparation for a time when laws of nature, human institutions . . . are undergoing a critical examination without parallel," Waldemar Kaempfert, N. Y. TIMES. 192pp. 5½ x 8. T428 Paperbound **\$1.35**

**FADS AND FALLACIES IN THE NAME OF SCIENCE**, Martin Gardner. Examines various cults, quack systems, frauds, delusions which at various times have masqueraded as science. Accounts of hollow-earth fanatics like Symmes; Velikovsky and wandering planets; Hoerbiger; Bellamy and the theory of multiple moons; Charles Fort; dowsing, pseudoscientific methods for finding water, ores, oil. Sections on naturopathy, iridiagnosis, zone therapy, food fads, etc. Analytical accounts of Wilhelm Reich and orgone sex energy; L. Ron Hubbard and Dianetics; A. Korzybski and General Semantics; many others. Brought up to date to include Bridey Murphy, others. Not just a collection of anecdotes but a fair, reasoned appraisal of eccentric theory. Formerly titled **IN THE NAME OF SCIENCE**. Preface. Index. x + 384pp. 5½ x 8. T394 Paperbound **\$1.50**

**A DOVER SCIENCE SAMPLER**, edited by George Barkin. 64-page book, sturdily bound, containing excerpts from over 20 Dover books, explaining science. Edwin Hubble, George Sarton, Ernst Mach, A. d'Abro, Galileo, Newton, others, discussing island universes, scientific truth, biological phenomena, stability in bridges, etc. Copies limited; no more than 1 to a customer. **FREE**

**POPULAR SCIENTIFIC LECTURES**, Hermann von Helmholtz. Helmholtz was a superb expositor as well as a scientist of genius in many areas. The seven essays in this volume are models of clarity, and even today they rank among the best general descriptions of their subjects ever written. "The Physiological Causes of Harmony in Music" was the first significant physiological explanation of musical consonance and dissonance. Two essays, "On the Interaction of Natural Forces" and "On the Conservation of Force," were of great importance in the history of science, for they firmly established the principle of the conservation of energy. Other lectures include "On the Relation of Optics to Painting," "On Recent Progress in the Theory of Vision," "On Goethe's Scientific Researches," and "On the Origin and Significance of Geometrical Axioms." Selected and edited with an introduction by Professor Morris Kline. xii + 286pp. 5½ x 8½. T799 Paperbound **\$1.45**

## BOOKS EXPLAINING SCIENCE AND MATHEMATICS

### Physics

**CONCERNING THE NATURE OF THINGS**, Sir William Bragg. Christmas lectures delivered at the Royal Society by Nobel laureate. Why a spinning ball travels in a curved track; how uranium is transmuted to lead, etc. Partial contents: atoms, gases, liquids, crystals, metals, etc. No scientific background needed; wonderful for intelligent child. 32pp. of photos, 57 figures. xii + 232pp. 5½ x 8. T31 Paperbound **\$1.50**

**THE RESTLESS UNIVERSE**, Max Born. New enlarged version of this remarkably readable account by a Nobel laureate. Moving from sub-atomic particles to universe, the author explains in very simple terms the latest theories of wave mechanics. Partial contents: air and its relatives, electrons & ions, waves & particles, electronic structure of the atom, nuclear physics. Nearly 1000 illustrations, including 7 animated sequences. 325pp. 6 x 9. T412 Paperbound **\$2.00**

## Catalogue of Dover Books

**FROM EUCLID TO EDDINGTON: A STUDY OF THE CONCEPTIONS OF THE EXTERNAL WORLD,** Sir Edmund Whittaker. A foremost British scientist traces the development of theories of natural philosophy from the western rediscovery of Euclid to Eddington, Einstein, Dirac, etc. The inadequacy of classical physics is contrasted with present day attempts to understand the physical world through relativity, non-Euclidean geometry, space curvature, wave mechanics, etc. 5 major divisions of examination: Space; Time and Movement; the Concepts of Classical Physics; the Concepts of Quantum Mechanics; the Eddington Universe. 212pp. 5½ x 8. T491 Paperbound \$1.35

**PHYSICS, THE PIONEER SCIENCE,** L. W. Taylor. First thorough text to place all important physical phenomena in cultural-historical framework; remains best work of its kind. Exposition of physical laws, theories developed chronologically, with great historical, illustrative experiments diagrammed, described, worked out mathematically. Excellent physics text for self-study as well as class work. Vol. 1: Heat, Sound; motion, acceleration, gravitation, conservation of energy, heat engines, rotation, heat, mechanical energy, etc. 211 illus. 407pp. 5½ x 8. Vol. 2: Light, Electricity: images, lenses, prisms, magnetism, Ohm's law, dynamos, telegraph, quantum theory, decline of mechanical view of nature, etc. Bibliography. 13 table appendix. Index. 551 illus. 2 color plates. 508pp. 5½ x 8.

Vol. 1 S565 Paperbound \$2.00  
Vol. 2 S566 Paperbound \$2.00  
The set \$4.00

**A SURVEY OF PHYSICAL THEORY,** Max Planck. One of the greatest scientists of all time, creator of the quantum revolution in physics, writes in non-technical terms of his own discoveries and those of other outstanding creators of modern physics. Planck wrote this book when science had just crossed the threshold of the new physics, and he communicates the excitement felt then as he discusses electromagnetic theories, statistical methods, evolution of the concept of light, a step-by-step description of how he developed his own momentous theory, and many more of the basic ideas behind modern physics. Formerly "A Survey of Physics." Bibliography. Index. 128pp. 5½ x 8. S650 Paperbound \$1.15

**THE ATOMIC NUCLEUS,** M. Korsunsky. The only non-technical comprehensive account of the atomic nucleus in English. For college physics students, etc. Chapters cover: Radioactivity, the Nuclear Model of the Atom, the Mass of Atomic Nuclei, the Disintegration of Atomic Nuclei, the Discovery of the Positron, the Artificial Transformation of Atomic Nuclei, Artificial Radioactivity, Mesons, the Neutrino, the Structure of Atomic Nuclei and Forces Acting Between Nuclear Particles, Nuclear Fission, Chain Reaction, Peaceful Uses, Thermocuclear Reactions. Slightly abridged edition. Translated by G. Yankovsky. 65 figures. Appendix includes 45 photographic illustrations. 413 pp. 5½ x 8. S1052 Paperbound \$2.00

**PRINCIPLES OF MECHANICS SIMPLY EXPLAINED,** Morton Mott-Smith. Excellent, highly readable introduction to the theories and discoveries of classical physics. Ideal for the layman who desires a foundation which will enable him to understand and appreciate contemporary developments in the physical sciences. Discusses: Density, The Law of Gravitation, Mass and Weight, Action and Reaction, Kinetic and Potential Energy, The Law of Inertia, Effects of Acceleration, The Independence of Motions, Galileo and the New Science of Dynamics, Newton and the New Cosmos, The Conservation of Momentum, and other topics. Revised edition of "This Mechanical World." Illustrated by E. Kosa, Jr. Bibliography and Chronology. Index. xiv + 171pp. 5½ x 8½. T1067 Paperbound \$1.00

**THE CONCEPT OF ENERGY SIMPLY EXPLAINED,** Morton Mott-Smith. Elementary, non-technical exposition which traces the story of man's conquest of energy, with particular emphasis on the developments during the nineteenth century and the first three decades of our own century. Discusses man's earlier efforts to harness energy, more recent experiments and discoveries relating to the steam engine, the engine indicator, the motive power of heat, the principle of excluded perpetual motion, the bases of the conservation of energy, the concept of entropy, the internal combustion engine, mechanical refrigeration, and many other related topics. Also much biographical material. Index. Bibliography. 33 illustrations. ix + 215pp. 5½ x 8½. T1071 Paperbound \$1.25

**HEAT AND ITS WORKINGS,** Morton Mott-Smith. One of the best elementary introductions to the theory and attributes of heat, covering such matters as the laws governing the effect of heat on solids, liquids and gases, the methods by which heat is measured, the conversion of a substance from one form to another through heating and cooling, evaporation, the effects of pressure on boiling and freezing points, and the three ways in which heat is transmitted (conduction, convection, radiation). Also brief notes on major experiments and discoveries. Concise, but complete, it presents all the essential facts about the subject in readable style. Will give the layman and beginning student a first-rate background in this major topic in physics. Index. Bibliography. 50 illustrations. x + 165pp. 5½ x 8½. T978 Paperbound \$1.00

**THE STORY OF ATOMIC THEORY AND ATOMIC ENERGY,** J. G. Feinberg. Wider range of facts on physical theory, cultural implications, than any other similar source. Completely non-technical. Begins with first atomic theory, 600 B.C., goes through A-bomb, developments to 1959. Avogadro, Rutherford, Bohr, Einstein, radioactive decay, binding energy, radiation danger, future benefits of nuclear power, dozens of other topics, told in lively, related, informal manner. Particular stress on European atomic research. "Deserves special mention . . . authoritative." Saturday Review. Formerly "The Atom Story." New chapter to 1959. Index. 34 illustrations. 251pp. 5½ x 8. T625 Paperbound \$1.60

## Catalogue of Dover Books

**THE STRANGE STORY OF THE QUANTUM, AN ACCOUNT FOR THE GENERAL READER OF THE GROWTH OF IDEAS UNDERLYING OUR PRESENT ATOMIC KNOWLEDGE, B. Hoffmann.** Presents lucidly and expertly, with barest amount of mathematics, the problems and theories which led to modern quantum physics. Dr. Hoffmann begins with the closing years of the 19th century, when certain trifling discrepancies were noticed, and with illuminating analogies and examples takes you through the brilliant concepts of Planck, Einstein, Pauli, de Broglie, Bohr, Schroedinger, Heisenberg, Dirac, Sommerfeld, Feynman, etc. This edition includes a new, long postscript carrying the story through 1958. "Of the books attempting an account of the history and contents of our modern atomic physics which have come to my attention, this is the best." H. Margenau, Yale University, in "American Journal of Physics." 32 tables and line illustrations. Index. 275pp. 5% x 8. T518 Paperbound \$1.50

**THE EVOLUTION OF SCIENTIFIC THOUGHT FROM NEWTON TO EINSTEIN, A. d'Abro.** Einstein's special and general theories of relativity, with their historical implications, are analyzed in non-technical terms. Excellent accounts of the contributions of Newton, Riemann, Weyl, Planck, Eddington, Maxwell, Lorentz and others are treated in terms of space and time, equations of electromagnetics, finiteness of the universe, methodology of science. 21 diagrams. 482pp. 5% x 8. T2 Paperbound \$2.25

**THE RISE OF THE NEW PHYSICS, A. d'Abro.** A half-million word exposition, formerly titled **THE DECLINE OF MECHANISM**, for readers not versed in higher mathematics. The only thorough explanation, in everyday language, of the central core of modern mathematical physical theory, treating both classical and modern theoretical physics, and presenting in terms almost anyone can understand the equivalent of 5 years of study of mathematical physics. Scientifically impeccable coverage of mathematical-physical thought from the Newtonian system up through the electronic theories of Dirac and Heisenberg and Fermi's statistics. Combines both history and exposition; provides a broad yet unified and detailed view, with constant comparison of classical and modern views on phenomena and theories. "A must for anyone doing serious study in the physical sciences." JOURNAL OF THE FRANKLIN INSTITUTE. "Extraordinary faculty . . . to explain ideas and theories of theoretical physics in the language of daily life," *ISIS*. First part of set covers philosophy of science, drawing upon the practice of Newton, Maxwell, Poincaré, Einstein, others, discussing modes of thought, experiment, interpretations of causality, etc. In the second part, 100 pages explain grammar and vocabulary of mathematics, with discussions of functions, groups, series, Fourier series, etc. The remainder is devoted to concrete, detailed coverage of both classical and quantum physics, explaining such topics as analytic mechanics, Hamilton's principle, wave theory of light, electromagnetic waves, groups of transformations, thermodynamics, phase rule, Brownian movement, kinetics, special relativity, Planck's original quantum theory, Bohr's atom, Zeeman effect, Broglie's wave mechanics, Heisenberg's uncertainty, Eigen-values, matrices, scores of other important topics. Discoveries and theories are covered for such men as Alémbert, Born, Cantor, Debye, Euler, Foucault, Galois, Gauss, Hadamard, Kelvin, Kepler, Laplace, Maxwell, Pauli, Rayleigh, Volterra, Weyl, Young, more than 180 others. Indexed. 97 illustrations. ix + 982pp. 5% x 8. T3 Volume 1, Paperbound \$2.25  
T4 Volume 2, Paperbound \$2.25

**SPINNING TOPS AND GYROSCOPIC MOTION, John Perry.** Well-known classic of science still unsurpassed for lucid, accurate, delightful exposition. How quasi-rigidity is induced in flexible and fluid bodies by rapid motions; why gyrostal falls, top rises; nature and effect on climatic conditions of earth's precessional movement; effect of internal fluidity on rotating bodies, etc. Appendixes describe practical uses to which gyroscopes have been put in ships, compasses, monorail transportation. 62 figures. 128pp. 5% x 8. T416 Paperbound \$1.00

**THE UNIVERSE OF LIGHT, Sir William Bragg.** No scientific training needed to read Nobel Prize winner's expansion of his Royal Institute Christmas Lectures. Insight into nature of light, methods and philosophy of science. Explains lenses, reflection, color, resonance, polarization, x-rays, the spectrum, Newton's work with prisms, Huygens' with polarization, Crookes' with cathode ray, etc. Leads into clear statement of 2 major historical theories of light, corpuscle and wave. Dozens of experiments you can do. 199 illus., including 2 full-page color plates. 293pp. 5% x 8. S538 Paperbound \$1.85

**THE STORY OF X-RAYS FROM RÖNTGEN TO ISOTOPES, A. R. Bleich.** Non-technical history of x-rays, their scientific explanation, their applications in medicine, industry, research, and art, and their effect on the individual and his descendants. Includes amusing early reactions to Röntgen's discovery, cancer therapy, detections of art and stamp forgeries, potential risks to patient and operator, etc. Illustrations show x-rays of flower structure, the gall bladder, gears with hidden defects, etc. Original Dover publication. Glossary. Bibliography. Index. 55 photos and figures. xiv + 186pp. 5% x 8. T662 Paperbound \$1.35

**ELECTRONS, ATOMS, METALS AND ALLOYS, Wm. Hume-Rothery.** An introductory-level explanation of the application of the electronic theory to the structure and properties of metals and alloys, taking into account the new theoretical work done by mathematical physicists. Material presented in dialogue-form between an "Old Metallurgist" and a "Young Scientist." Their discussion falls into 4 main parts: the nature of an atom, the nature of a metal, the nature of an alloy, and the structure of the nucleus. They cover such topics as the hydrogen atom, electron waves, wave mechanics, Brillouin zones, co-valent bonds, radio-activity and natural disintegration, fundamental particles, structure and fission of the nucleus, etc. Revised, enlarged edition. 177 illustrations. Subject and name indexes. 407pp. 5% x 8 1/2. S1046 Paperbound \$2.25

## MATHEMATICS, HISTORIES AND CLASSICS

**HISTORY OF MATHEMATICS, D. E. Smith.** Most comprehensive non-technical history of math in English. Discusses lives and works of over a thousand major and minor figures, with footnotes supplying technical information outside the book's scheme, and indicating disputed matters. Vol 1: A chronological examination, from primitive concepts through Egypt, Babylonia, Greece, the Orient, Rome, the Middle Ages, the Renaissance, and up to 1900. Vol 2: The development of ideas in specific fields and problems, up through elementary calculus. Two volumes, total of 510 illustrations, 1355pp. 5¾ x 8. Set boxed in attractive container. T429, 430 Paperbound, the set \$5.00

**A SHORT ACCOUNT OF THE HISTORY OF MATHEMATICS, W. W. R. Ball.** Most readable non-technical history of mathematics treats lives, discoveries of every important figure from Egyptian, Phoenician mathematicians to late 19th century. Discusses schools of Ionia, Pythagoras, Athens, Cyzicus, Alexandria, Byzantium, systems of numeration; primitive arithmetic; Middle Ages, Renaissance, including Arabs, Bacon, Regiomontanus, Tartaglia, Cardan, Stevinus, Galileo, Kepler; modern mathematics of Descartes, Pascal, Wallis, Huygens, Newton, Leibnitz, d'Alembert, Euler, Lambert, Laplace, Legendre, Gauss, Hermite, Weierstrass, scores more. Index. 25 figures. 546pp. 5¾ x 8. S630 Paperbound \$2.00

**A HISTORY OF GEOMETRICAL METHODS, J. L. Coolidge.** Full, authoritative history of the techniques which men have employed in dealing with geometric questions . . . from ancient times to the modern development of projective geometry. Critical analyses of the original works. Contents: Synthetic Geometry—the early beginnings, Greek mathematics, non-Euclidean geometries, projective and descriptive geometry; Algebraic Geometry—extension of the system of linear coordinates, other systems of point coordinates, enumerative and birational geometry, etc.; and Differential Geometry—intrinsic geometry and moving axes, Gauss and the classical theory of surfaces, and projective and absolute differential geometry. The work of scores of geometers analyzed: Pythagoras, Archimedes, Newton, Descartes, Leibniz, Lobachevski, Riemann, Hilbert, Bernoulli, Schubert, Grassman, Klein, Cauchy, and many, many others. Extensive (24-page) bibliography. Index. 13 figures. xviii + 451pp. 5¾ x 8½. S1006 Paperbound \$2.25

**THE MATHEMATICS OF GREAT AMATEURS, Julian Lowell Coolidge.** Enlightening, often surprising, accounts of what can result from a non-professional preoccupation with mathematics. Chapters on Plato, Omar Khayyam and his work with cubic equations, Piero della Francesca, Albrecht Dürer, as the true discoverer of descriptive geometry, Leonardo da Vinci and his varied mathematical interests, John Napier, Baron of Merchiston, inventor of logarithms, Pascal, Diderot, l'Hospital, and seven others known primarily for contributions in other fields. Bibliography. 56 figures. viii + 211pp. 5¾ x 8½. S1009 Paperbound \$1.50

**ART AND GEOMETRY, Wm. M. Ivins, Jr.** A controversial study which propounds the view that the ideas of Greek philosophy and culture served not to stimulate, but to stifle the development of Western thought. Through an examination of Greek art and geometrical inquiries and Renaissance experiments, this book offers a concise history of the evolution of mathematical perspective and projective geometry. Discusses the work of Alberti, Dürer, Pelerin, Nicholas of Cusa, Kepler, Desargues, etc. in a wholly readable text of interest to the art historian, philosopher, mathematician, historian of science, and others. x + 113pp. 5¾ x 8¾. T941 Paperbound \$1.00

**A SOURCE BOOK IN MATHEMATICS, D. E. Smith.** Great discoveries in math, from Renaissance to end of 19th century, in English translation. Read announcements by Dedekind, Gauss, Delamain, Pascal, Fermat, Newton, Abel, Lobachevsky, Bolyai, Riemann, De Moivre, Legendre, Laplace, others of discoveries about imaginary numbers, number congruence, slide rule, equations, symbolism, cubic algebraic equations, non-Euclidean forms of geometry, calculus, function theory, quaternions, etc. Succinct selections from 125 different treatises, articles, most unavailable elsewhere in English. Each article preceded by biographical, historical introduction. Vol. I: Fields of Number, Algebra. Index. 32 illus. 338pp. 5¾ x 8. Vol. II: Fields of Geometry, Probability, Calculus, Functions, Quaternions. 83 illus. 432pp. 5¾ x 8. Vol. 1: S552 Paperbound \$1.85 Vol. 2: S553 Paperbound \$1.85 2 vol. set, boxed \$3.50

**A COLLECTION OF MODERN MATHEMATICAL CLASSICS, edited by R. Bellman.** 13 classic papers, complete in their original languages, by Hermite, Hardy and Littlewood, Tchebycheff, Fejér, Fredholm, Fuchs, Hurwitz, Weyl, van der Pol, Birkhoff, Kellogg, von Neumann, and Hilbert. Each of these papers, collected here for the first time, triggered a burst of mathematical activity, providing useful new generalizations or stimulating fresh investigations. Topics discussed include classical analysis, periodic and almost periodic functions, analysis and number theory, integral equations, theory of approximation, non-linear differential equations, and functional analysis. Brief introductions and bibliographies to each paper. xii + 292pp. 6 x 9. S730 Paperbound \$2.00

**THE WORKS OF ARCHIMEDES, edited by T. L. Heath.** All the known works of the great Greek mathematician are contained in this one volume, including the recently discovered Method of Archimedes. Contains: On Sphere & Cylinder, Measurement of a Circle, Spirals, Conoids, Spheroids, etc. This is the definitive edition of the greatest mathematical intellect of the ancient world. 186-page study by Heath discusses Archimedes and the history of Greek mathematics. Bibliography. 563pp. 5¾ x 8. S9 Paperbound \$2.25

## Catalogue of Dover Books

**THE THIRTEEN BOOKS OF EUCLID'S ELEMENTS**, edited by Sir Thomas Heath. Definitive edition of one of the very greatest classics of Western world. Complete English translation of Heiberg text, together with spurious Book XIV. Detailed 150-page introduction discussing aspects of Greek and Medieval mathematics. Euclid, texts, commentators, etc. Paralleling the text is an elaborate critical apparatus analyzing each definition, proposition, postulate, covering textual matters, mathematical analysis, commentators of all times, refutations, supports, extrapolations, etc. This is the full Euclid. Unabridged reproduction of Cambridge U. 2nd edition. 3 volumes. Total of 995 figures, 1426pp. 5½ x 8.

\$88,89,90, 3 volume set, paperbound \$6.75

**A CONCISE HISTORY OF MATHEMATICS**, D. Struik. Lucid study of development of mathematical ideas, techniques from Ancient Near East, Greece, Islamic science, Middle Ages, Renaissance, modern times. Important mathematicians are described in detail. Treatment is not anecdotal, but analytical development of ideas. "Rich in content, thoughtful in interpretation." U.S. QUARTERLY BOOKLIST. Non-technical; no mathematical training needed. Index. 60 illustrations, including Egyptian papyri, Greek mss., portraits of 31 eminent mathematicians. Bibliography. 2nd edition. xix + 299pp. 5½ x 8.

T255 Paperbound \$1.75

**A HISTORY OF THE CALCULUS, AND ITS CONCEPTUAL DEVELOPMENT**, Carl B. Boyer. Provides laymen and mathematicians a detailed history of the development of the calculus, from early beginning in antiquity to final elaboration as mathematical abstractions. Gives a sense of mathematics not as a technique, but as a habit of mind, in the progression of ideas of Zeno, Plato, Pythagoras, Eudoxus, Arabic and Scholastic mathematicians, Newton, Leibnitz, Taylor, Descartes, Euler, Lagrange, Cantor, Weierstrass, and others. This first comprehensive critical history of the calculus was originally titled "The Concepts of the Calculus." Foreword by R. Courant. Preface. 22 figures. 25-page bibliography. Index. v + 364pp. 5½ x 8.

S509 Paperbound \$2.00

**A MANUAL OF GREEK MATHEMATICS**, Sir Thomas L. Heath. A non-technical survey of Greek mathematics addressed to high school and college students and the layman who desires a sense of historical perspective in mathematics. Thorough exposition of early numerical notation and practical calculation, Pythagorean arithmetic and geometry, Thales and the earliest Greek geometrical measurements and theorems, the mathematical theories of Plato, Euclid's "Elements" and his other works (extensive discussion), Aristarchus, Archimedes, Eratosthenes and the measurement of the earth, trigonometry (Hipparchus, Menelaus, Ptolemy), Pappus and Heron of Alexandria, and detailed coverage of minor figures normally omitted from histories of this type. Presented in a refreshingly interesting and readable style. Appendix. 2 Indexes. xvi + 552pp. 5½ x 8.

S279 Paperbound \$2.25

**THE GEOMETRY OF RENÉ DESCARTES**. With this book Descartes founded analytical geometry. Excellent Smith-Latham translation, plus original French text with Descartes' own diagrams. Contains Problems the Construction of Which Requires Only Straight Lines and Circles; On the Nature of Curved Lines; On the Construction of Solid or Supersolid Problems. Notes. Diagrams. 258pp. 5½ x 8.

S68 Paperbound \$1.60

**A PHILOSOPHICAL ESSAY ON PROBABILITIES**, Marquis de Laplace. This famous essay explains without recourse to mathematics the principle of probability, and the application of probability to games of chance, natural philosophy, astronomy, many other fields. Translated from the 6th French edition by F. W. Truscott, F. L. Emory, with new introduction for this edition by E. T. Bell. 204pp. 5½ x 8.

S166 Paperbound \$1.35

*Prices subject to change without notice.*

*Dover publishes books on art, music, philosophy, literature, languages, history, social sciences, psychology, handicrafts, orientalia, puzzles and entertainments, chess, pets and gardens, books explaining science, intermediate and higher mathematics, mathematical physics, engineering, biological sciences, earth sciences, classics of science, etc. Write to:*

*Dept. catrr.*

*Dover Publications, Inc.*

*180 Varick Street, N.Y. 14, N.Y.*

(continued from front flap)

- Applied Mathematics for Radio and Communications Engineers, Carl Smith. \$1.75
- Fluid Mechanics Through Worked Examples, D. R. L. Smith and J. Houghton. Clothbound \$6.00
- Mathematical Methods for Scientists and Engineers, L. P. Smith. \$2.00
- Teach Yourself the Slide Rule, Burns Snodgrass. Clothbound \$2.00
- An Introduction to the Statistical Dynamics of Control Systems, V. V. Solodovnikov. \$2.25
- Bridges and Their Builders, David B. Steinman and Sara R. Watson. \$2.00
- Rayleigh's Principle and Its Applications to Engineering, George Temple and William G. Bickley. \$1.50
- A History of the Theory of Elasticity and of the Strength of Materials, Isaac Todhunter and Karl Pearson. Clothbound. Three volume set \$17.50
- Basic Theory and Application of Transistors, U. S. Department of the Army. \$1.25
- Basic Electricity, U. S. Navy Bureau of Personnel. \$3.00
- Basic Electronics, U. S. Navy Bureau of Personnel. \$2.75
- The Schwarz-Christoffel Transformation and Its Applications: A Simple Exposition, Miles Walker. \$1.25
- Photometry, John W. T. Walsh. \$3.00
- The Design and Use of Instruments and Accurate Mechanisms: Underlying Processes, Thomas North Whitehead. \$2.00
- Teach Yourself Electricity, C. W. Wilman. Clothbound \$2.00

Paperbound unless otherwise indicated. Prices subject to change without notice. Available at your book dealer or write for free catalogues to Dept. Eng., Dover Publications, Inc., 180 Varick St., N. Y., N. Y. 10014. Please indicate field of interest. Dover publishes over 125 new books and records each year on such fields as mathematics, physics, explaining science, art, languages, philosophy, classical records, and others.



CHANCE  
HULSIZER  
MAC NICHOL  
WILLIAMS

# ELECTRONIC TIME MEASUREMENTS

EDITED BY BRITTON CHANCE  
ROBERT I. HULSIZER  
EDWARD F. MAC NICHOL, JR.  
FREDERICK C. WILLIAMS

ELECTRONIC TIME  
MEASUREMENTS

Highly intensified research activities carried on at government laboratories during World War II resulted in major developments in the radio electronics and high-frequency fields. Classified during the war, much of this information was held to be so valuable that it was written up afterwards by a staff of prominent physicists, mathematicians, and engineers at the Radiation Laboratory of M.I.T. The resulting "Radiation Laboratory Series" is recognized as the most distinguished and comprehensive series on radio engineering ever published.

Precision measurement of very small intervals of time and distance is essential for radar work, television transmission and reception, and in navigational systems such as Loran. Dealing with both manual and automatic methods, the authors of this basic study fully investigate the various problems and techniques of obtaining accurate measurements.

Introducing the book is a survey of techniques for radio distance and speed measurement (time modulation, phase modulation, pulse transmission, and frequency modulation) and a description of speed measurement methods to determine the distance of moving objects (continuous-wave systems and internally- and externally-coherent pulse systems). The material then continues with a survey of basic techniques and methods in pulse time measurement, including the generation of fixed and movable timing markers and their applications to manual and automatic time measurements. How these techniques are used for precision data transmission and for the relaying of the radar PPI to remote points is described next, and the book concludes with a discussion of the use of supersonic delay devices for the cancelling of recurrent waveforms.

Unabridged and unaltered republication of the 1st (1949) edition. Foreword by L. A. DuBridge. Preface by editors. 333 figures. 14 tables. Bibliography in notes. Glossary. Index. xviii + 538pp. 5 $\frac{3}{8}$  x 8 $\frac{1}{2}$ . \$1560 Paperbound \$3.00

A DOVER EDITION DESIGNED FOR YEARS OF USE!

We have made every effort to make this the best book possible. Our paper is opaque, with minimal show-through; it will not discolor or become brittle with age. Pages are sewn in signatures, in the method traditionally used for the best books, and will not drop out, as often happens with paperbacks held together with glue. Books open flat for easy reference. The binding will not crack or split. This is a permanent book.

DOVER

S1560